Food Engineering Series
Series Editor: Gustavo V. Barbosa-Cánovas

Humberto Hernández-Sánchez
Gustavo Fidel Gutiérrez-López *Editors*

Food Nanoscience and Nanotechnology

Springer

Food Engineering Series

Series Editor
Gustavo V. Barbosa-Cánovas, Washington State University, USA

Advisory Board
José Miguel Aguilera, Catholic University, Chile
Kezban Candoğan, Ankara University, Turkey
J. Peter Clark, Clark Consulting, USA
Richard W. Hartel, University of Wisconsin, USA
Albert Ibarz, University of Lleida, Spain
Jozef Kokini, Purdue University, USA
Michael McCarthy, University of California, USA
Keshavan Niranjan, University of Reading, United Kingdom
Micha Peleg, University of Massachusetts, USA
Shafiur Rahman, Sultan Qaboos University, Oman
M. Anandha Rao, Cornell University, USA
Yrjö Roos, University College Cork, Ireland
Jorge Welti-Chanes, Monterrey Institute of Technology, Mexico

Springer's *Food Engineering Series* is essential to the Food Engineering profession, providing exceptional texts in areas that are necessary for the understanding and development of this constantly evolving discipline. The titles are primarily reference-oriented, targeted to a wide audience including food, mechanical, chemical, and electrical engineers, as well as food scientists and technologists working in the food industry, academia, regulatory industry, or in the design of food manufacturing plants or specialized equipment.

More information about this series at http://www.springer.com/series/5996

Humberto Hernández-Sánchez
Gustavo Fidel Gutiérrez-López
Editors

Food Nanoscience and Nanotechnology

Springer

Editors
Humberto Hernández-Sánchez, BSc, MSc, PhD
Escuela Nacional de Ciencias Biologicas
Instituto Politecnico Nacional
Carpio y Plan de Ayala
Distrito Federal
Mexico City
Mexico

Gustavo Fidel Gutiérrez-López, BSc, MSc, PhD
Escuela Nacional de Ciencias Biológicas
Instituto Politécnico Nacional
Carpio y Plan de Ayala
Distrito Federal
Mexico City
Mexico

ISSN 1571-0297
Food Engineering Series
ISBN 978-3-319-13595-3 ISBN 978-3-319-13596-0 (eBook)
DOI 10.1007/978-3-319-13596-0

Library of Congress Control Number: 2015933838

Springer Cham Heidelberg New York Dordrecht London
© Springer Science+Business Media New York 2015
This work is subject to copyright. All rights are reserved by the Publisher, whether the whole or part of the material is concerned, specifically the rights of translation, reprinting, reuse of illustrations, recitation, broadcasting, reproduction on microfilms or in any other physical way, and transmission or information storage and retrieval, electronic adaptation, computer software, or by similar or dissimilar methodology now known or hereafter developed.
The use of general descriptive names, registered names, trademarks, service marks, etc. in this publication does not imply, even in the absence of a specific statement, that such names are exempt from the relevant protective laws and regulations and therefore free for general use.
The publisher, the authors and the editors are safe to assume that the advice and information in this book are believed to be true and accurate at the date of publication. Neither the publisher nor the authors or the editors give a warranty, express or implied, with respect to the material contained herein or for any errors or omissions that may have been made.

Printed on acid-free paper

Springer is part of Springer Science+Business Media (www.springer.com)

This book is dedicated to our families, institute, fellow colleagues and students.

Preface

Food nanoscience and nanotechnology are emergent disciplines that have grown enormously in the last years due to the attractive properties that a number of food-related materials have at the nanoscale. Understanding basic principles of such properties constitutes the basis for building a robust knowledge base for developing products with improved and novel characteristics.

Understanding fundamentals of food nanotechnology represents a huge challenge for universities, industries and the public sector. The complex mechanisms involved in the research, development, production and legislation of food nanoproducts are studied under multi- and inter-disciplinary scopes. Bearing this in mind, this book was conceived.

This book aims to contribute to basic and applied knowledge on these fields by presenting recent advances in selected topics of food nanoscience and nanotechnology, and is divided into a total of 17 chapters. The first chapter presents an overview to the field; the following chapter discusses general techniques for studying food-related nanomaterials, followed by six chapters on specific techniques for preparing food nanomaterials while the next contribution on dispersed systems illustrates this important and vast field. The book continues with three chapters on food nanocomposites, including those for packing purposes, and two chapters on advanced aspects of food nanobiosensors. Finally, three selected case-studied subjects are presented, including food safety aspects.

This book presents a significant and up-to-date review of selected aspects in the field. Distinguished scholars, engineers and technologists from key institutions have contributed chapters that provide a comprehensive analysis of their particular subjects. The premise of this book is that a comprehensive approach to this field requires a deep knowledge of the subject and an effective integration of other disciplines to appropriately convey fundamentals and applications of food nanoscience and nanotechnology.

The book is mainly directed to scholars, industry-related scientists and engineers, as well as to undergraduate and graduate students, who will find a selection of interesting topics.

This work was produced through a National Polytechnic Institute of México effort and the general subjects covered were carefully selected and edited for their

inclusion in this book. It is hoped that it will constitute a valuable addition to the existing literature on food nanoscience and nanotechnology, and that readers will find in it useful and worthy information.

Humberto Hernández-Sánchez
Gustavo F. Gutiérrez-López

Acknowledgements

The editors wish to express their gratitude to the following institutions and persons who contributed to making this book possible:

To Instituto Politécnico Nacional (IPN), Escuela Nacional de Ciencias Biológicas (ENCB) and CONACYT for financial support for carrying out research on nanoscience and nanotechnology that led to conceive this book and to the PhD program in Food Science and Technology of these institutions for providing the academic platform for carrying out this research.

To Dr. Gustavo Barbosa-Cánovas for their continuous support, valuable suggestions and for encouraging editors to produce this volume and also to our graduate students for providing materials for various chapters and proofreading parts of the book.

To our fellow colleagues, all of them professors at IPN-ENCB and to the various contributors who considered this book as appropriate to publishing part of their research.

Contents

1 **Introduction** 1
Humberto Hernández-Sánchez and Gustavo F. Gutiérrez-López

2 **Tools for the Study of Nanostructures** 5
M. Escamilla-García, J.S. Alvarado-González, Georgina Calderón-Domínguez, J.J. Chanona-Pérez, Juan V. Méndez-Méndez, María de Jesús Perea-Flores and R.R. Farrera-Rebollo

3 **Development of Food Nanostructures by Electrospinning** 39
Matteo Scampicchio, Saverio Mannino and Maria Stella Cosio

4 **Polysaccharide-Based Nanoparticles** 59
Erika A. López-López, M. Aurora Hernández-Gallegos, Maribel Cornejo-Mazón and Humberto Hernández-Sánchez

5 **Protein-Based Nanoparticles** 69
Esmeralda Jiménez-Cruz, Izlia J. Arroyo-Maya, Andrés Hernández-Arana, Maribel Cornejo-Mazón and Humberto Hernández-Sánchez

6 **Indentation Technique: Overview and Applications in Food Science** 81
Israel Arzate-Vázquez, Jorge Chanona-Pérez, Germán A. Rodríguez-Castro, Ariel Fuerte-Hernández, Juan V. Méndez-Méndez and Gustavo F. Gutiérrez-López

7 **Lipid Matrices for Nanoencapsulation in Food: Liposomes and Lipid Nanoparticles** 99
Lucimara Gaziola de La Torre and Samantha Cristina de Pinho

8 High Shear Methods to Produce Nano-sized Food Related to Dispersed Systems 145
Cynthia Cano-Sarmiento, Liliana Alamilla-Beltrán, Ebner Azuara-Nieto, Humberto Hernández-Sánchez, Dario I. Téllez-Medina, Cristian Jiménez-Martínez and Gustavo F. Gutiérrez-López

9 Hydrodynamic Characterization of the Formation of Alpha-Tocopherol Nanoemulsions in a Microfluidizer 163
Amor Monroy-Villagrana, Liliana Alamilla-Beltrán, Humberto Hernández-Sánchez and Gustavo F. Gutiérrez-López

10 Role of Surfactants and Their Applications in Structured Nanosized Systems 177
María Ximena Quintanilla-Carvajal and Silvia Matiacevich

11 Food Nano- and Microconjugated Systems: The Case of Albumin–Capsaicin 187
Lino Sánchez-Segura, Evangelina García-Armenta, María de Jesús Perea-Flores, Darío Iker Téllez-Medina, Juan C. Carpio-Pedroza, Humberto Hernández-Sánchez, Liliana Alamilla-Beltrán, Antonio R. Jiménez-Aparicio and Gustavo F. Gutiérrez-López

12 Polymer Nanocomposites for Food Packaging Applications 205
Shyam S. Sablani

13 Nanobiosensors in Food Science and Technology 213
Angélica G. Mendoza-Madrigal, Jorge Chanona-Pérez, Leonor Guadarrama-Fernández, Humberto Hernández-Sánchez, Georgina Calderón-Domínguez, Eduardo Palacios-González and Rubén López-Santiago

14 Carbon Nanotubes and Their Potential Applications in Developing Electrochemical Biosensors for the Detection of Analytes in Food 231
Leonor Guadarrama-Fernández, Angélica G. Mendoza-Madrigal, Jorge Chanona-Pérez, Arturo Manzo Robledo, Georgina Calderón-Domínguez, F. Xavier Rius, Pascal Blondeau and Jordi Riu

15 Safety Studies of Metal Oxide Nanoparticles Used in Food Industry 243
Verónica Freyre-Fonseca, Norma L. Delgado-Buenrostro, Yolanda I. Chirino and Gustavo F. Gutiérrez-López

16 Multiscale and Nanostructural Approach to Fruits Stability 267
Gabriela R. Cáez-Ramirez, Darío I. Téllez-Medina and Gustavo F. Gutierrez-López

17 Modulating Oxidative Stress: A Nanotechnology Perspective for Cationic Peptides 283
Anaid Hernández-Jabalera, Javier Vioque, Manuel Alaiz, Julio Girón-Calle, Cristina Megías, Cristian Jiménez-Martínez and Gloria Dávila-Ortíz

Index 299

Contributors

Manuel Alaiz Instituto de la Grasa, Consejo Superior de Investigaciones Científicas, Sevilla, Spain

Liliana Alamilla-Beltrán Departamento de Graduados e Investigación en Alimentos, Escuela Nacional de Ciencias Biológicas, del Instituto Politécnico Nacional, México, DF, Mexico

J.S. Alvarado-González Departamento de Ingeniería Bioquímica Prolongación de Carpio, Escuela Nacional de Ciencias Biológicas, IPN, Casco de Santo Tomás, C.P., México DF, Mexico

Izlia J. Arroyo-Maya University of Massachusetts Amherst, Amherst, MA, USA

Israel Arzate-Vázquez Centro de Nanociencias y Micro y Nanotecnologías, Instituto Politécnico Nacional, México, DF, Mexico

M. Aurora Hernández-Gallegos Departamento de Graduados e Investigación en Alimentos, Escuela Nacional de Ciencias Biológicas, Instituto Politécnico Nacional, México, DF, Mexico

Ebner Azuara-Nieto Instituto de Ciencias Básicas, Universidad Veracruzana, Xalapa, Veracruz, México

Pascal Blondeau Department of Analytical and Organic Chemistry, Universitat Rovira i Virgili, Tarragona, Catalonia, Spain

Gabriela R. Cáez-Ramirez Facultad de Ingeniería, Universidad de La Sabana, Chia, Colombia

Georgina Calderón-Domínguez Departamento de Ingeniería Bioquímica Prolongación de Carpio, Escuela Nacional de Ciencias Biológicas, IPN, Casco de Santo Tomás, C.P., México DF, Mexico

Cynthia Cano-Sarmiento Departamento de Graduados e Investigación en Alimentos, Escuela Nacional de Ciencias Biológicas, del Instituto Politécnico Nacional, México, DF, Mexico

Juan C. Carpio-Pedroza Instituto Nacional de Diagnóstico y Referencia Epidemiológica, CENAVECE-Secretaria de Salud, México, DF, Mexico

J.J. Chanona-Pérez Departamento de Ingeniería Bioquímica Prolongación de Carpio, Escuela Nacional de Ciencias Biológicas, IPN, Casco de Santo Tomás, C.P., México DF, Mexico

Jorge Chanona-Pérez Departamento de Ingeniería Bioquímica, Escuela Nacional de Ciencias Biológicas, Instituto Politécnico Nacional, México, DF, Mexico

Yolanda I. Chirino Laboratorio 10, Unidad de Biomedicina, Facultad de Estudios Superiores-Iztacala, Universidad Nacional Autónoma de México, Los Reyes Iztacala, Estado de México, México

Maribel Cornejo-Mazón Departamento de Biofísica, Escuela Nacional de Ciencias Biológicas, Instituto Politécnico Nacional, México, DF, Mexico

Maria Stella Cosio Department of Food, Environmental and Nutritional Science, University of Milan, Milan, Italy

Gloria Dávila-Ortíz Depto. Graduados e Investigación en Alimentos, Escuela Nacional de Ciencias Biológicas, Instituto Politécnico Nacional, México, DF, Mexico

Lucimara Gaziola de La Torre School of Chemical Engineering, University of Campinas, Campinas, SP, Brazil

Samantha Cristina de Pinho Food Engineering Department, College of Animal Science and Food Engineering, Universidade de São Paulo, Pirassununga, SP, Brazil

Norma L. Delgado-Buenrostro Laboratorio 10, Unidad de Biomedicina, Facultad de Estudios Superiores-Iztacala, Universidad Nacional Autónoma de México, Los Reyes Iztacala, Estado de México, México

M. Escamilla-García Departamento de Ingeniería Bioquímica Prolongación de Carpio, Escuela Nacional de Ciencias Biológicas, IPN, Casco de Santo Tomás, C.P., México DF, Mexico

R.R. Farrera-Rebollo Departamento de Ingeniería Bioquímica Prolongación de Carpio, Escuela Nacional de Ciencias Biológicas, IPN, Casco de Santo Tomás, C.P., México DF, Mexico

Verónica Freyre-Fonseca Departamento de Graduados e Investigación en Alimentos. Escuela Nacional de Ciencias Biológicas, Instituto Politécnico Nacional, México, DF, México

Norma L. Delgado-Buenrostro Laboratorio 10, Unidad de Biomedicina, Facultad de Estudios Superiores-Iztacala, Universidad Nacional Autónoma de México, Los Reyes Iztacala, Estado de México, México

Ariel Fuerte-Hernández Instituto Politécnico Nacional, México, DF, Mexico

Evangelina García-Armenta Departamento de Graduados e Investigación en Alimentos. Escuela Nacional de Ciencias Biológicas, Instituto Politécnico Nacional, Mexico, DF, Mexico

Julio Girón-Calle Instituto de la Grasa, Consejo Superior de Investigaciones Científicas, Sevilla, Spain

Leonor Guadarrama-Fernández Departamento de Ingeniería Bioquímica, Escuela Nacional de Ciencias Biológicas, Instituto Politécnico Nacional, México, DF, Mexico

Gustavo F. Gutiérrez-López Departamento de Graduados e Investigación en Alimentos. Escuela Nacional de Ciencias Biológicas, Instituto Politécnico Nacional, México, DF, México

Departamento de Ingeniería Bioquímica, Escuela Nacional de Ciencias Biológicas, Instituto Politécnico Nacional, México, DF, Mexico

Andrés Hernández-Arana Departamento de Química, Universidad Autónoma Metropolitana, México, DF, Mexico

Anaid Hernández-Jabalera Depto. Graduados e Investigación en Alimentos, Escuela Nacional de Ciencias Biológicas, Instituto Politécnico Nacional, México, DF, Mexico

Humberto Hernández-Sánchez Departamento de Graduados e Investigación en Alimentos, Escuela Nacional de Ciencias Biológicas-Instituto Politécnico Nacional, Sto. Tomás, México DF, Mexico

Antonio R. Jiménez-Aparicio Centro de Desarrollo de Productos Bióticos, Instituto Politécnico Nacional, Mexico, MOR, Mexico

Esmeralda Jiménez-Cruz Departamento de Graduados e Investigación en Alimentos, Escuela Nacional de Ciencias Biológicas, Instituto Politécnico Nacional,, México, DF, Mexico

Cristian Jiménez-Martínez Departamento de Graduados e Investigación en Alimentos, Escuela Nacional de Ciencias Biológicas, del Instituto Politécnico Nacional, México, DF, Mexico

Erika A. López-López Departamento de Graduados e Investigación en Alimentos, Escuela Nacional de Ciencias Biológicas, Instituto Politécnico Nacional, México, DF, Mexico

Rubén López-Santiago Departamento de Inmunología, Escuela Nacional de Ciencias Biológicas, Instituto Politécnico Nacional, México, DF, Mexico

Saverio Mannino Department of Food, Environmental and Nutritional Science, University of Milan, Milan, Italy

Arturo Manzo Robledo Laboratorio de Electroquímica y Corrosión, Escuela Superior de Ingeniería Química e Industrias Extractivas, Instituto Politécnico Nacional, México City, México

Silvia Matiacevich Departamento de Ciencia y Tecnología de los Alimentos. Facultad Tecnológica, Universidad de Santiago de Chile, Santiago, Chile

Cristina Megías Instituto de la Grasa, Consejo Superior de Investigaciones Científicas, Sevilla, Spain

Juan V. Méndez-Méndez Centro de Nanociencias y Micro-Nanotecnología del IPN, Unidad Profesional Adolfo López Mateos, Col. Zacatenco, C. P., México DF, Mexico

Centro de Nanociencias y Micro y Nanotecnologías, Instituto Politécnico Nacional, México, DF, Mexico

Angélica G. Mendoza-Madrigal Departamento de Ingeniería Bioquímica, Escuela Nacional de Ciencias Biológicas, Instituto Politécnico Nacional, México, DF, Mexico

Amor Monroy-Villagrana Departamento de Graduados e Investigación en Alimentos, Escuela Nacional de Ciencias Biológicas, Instituto Politécnico Nacional, México, DF, México

Eduardo Palacios-González Laboratorio de Microscopía de Ultra Alta Resolución, Instituto Mexicano del Petróleo, México, Mexico

María de Jesús Perea-Flores Laboratorio de Microscopía Confocal-Multifotónica. Centro de Nanociencias y Micro y Nanotecnologías. Unidad Profesional "Adolfo López Mateos", Instituto Politécnico Nacional, México, DF, Mexico

María Ximena Quintanilla-Carvajal Facultad de Ingeniería, Universidad de La Sabana, Chía, Colombia

Jordi Riu Department of Analytical and Organic Chemistry, Universitat Rovira i Virgili, Tarragona, Catalonia, Spain

F. Xavier Rius Department of Analytical and Organic Chemistry, Universitat Rovira i Virgili, Tarragona, Catalonia, Spain

Germán A. Rodríguez-Castro Instituto Politécnico Nacional, México, DF, Mexico

Shyam S. Sablani Biological Systems Engineering, Washington State University, Pullman, WA, USA

Lino Sánchez-Segura Departamento de Graduados e Investigación en Alimentos. Escuela Nacional de Ciencias Biológicas, Instituto Politécnico Nacional, Mexico, DF, Mexico

Matteo Scampicchio Free University of Bozen, Bolzano, Italy

Dario I. Téllez-Medina Departamento de Graduados e Investigación en Alimentos, Escuela Nacional de Ciencias Biológicas, del Instituto Politécnico Nacional, México, DF, Mexico

Javier Vioque Instituto de la Grasa, Consejo Superior de Investigaciones Científicas, Sevilla, Spain

Chapter 1
Introduction

Humberto Hernández-Sánchez and Gustavo F. Gutiérrez-López

Food nanotechnology is rapidly gaining attention in food science and industrial applications. Aspects related to legislation, general acceptance by the consumers as well as the development of fabrication methods to produce competitive nanofoods represent a challenge that has to be framed within a multi- and interdisciplinary scope. Foods are inherently nanostructured materials constituted by the self-assembly of thousands of compounds in different compartments and states of aggregation including amorphous, crystalline, vitreous, and rubbery which have the natural task in the living organism of inducing multiscale functions that are often onset at the nanolevel. FDA regulations (FDA 2014), state that nanofood materials must have at least one dimension in the nanoscale range (1–100 nm), also establish that these products must exhibit properties and phenomena, including physical or chemical properties or biological effects that are attributable to its nanodimension(s). Therefore, particulate systems exhibiting sizes larger than 100 nm but possessing cracks, pores, cavities, etc., in the nanorange, which provide function to the food product such as immobilization of water promoting its preservation as well as of substances such as vitamins and minerals within these structures, are considered in the nanofood field.

Foods are nanostructured materials composed of hundreds of thousands of nanosized particles and molecules assembled in characteristic forms of the living organism. However, these arrangements are not considered within the nanofield unless the isolated materials and particles perform independently as nanomaterials by exhibiting characteristic properties that do not possess at the microscale. Current legislation states that FDA-regulated nanoproducts should meet the requirement to possess at least one dimension in the nanoscale range that allows the product to exhibit properties or phenomena, including physical or chemical properties or biological effects, attributable to its nanodimension(s). A comprehensive report on

H. Hernández-Sánchez (✉) · G. F. Gutiérrez-López
Departamento de Graduados e Investigación en Alimentos, Escuela Nacional de Ciencias Biológicas-Instituto Politécnico Nacional, Carpio y Plan de Ayala s/n, 11340 Sto. Tomás, México DF, Mexico
e-mail: hhernan1955@yahoo.com

© Springer Science+Business Media New York 2015

H. Hernández-Sánchez, G. F. Gutiérrez-López (eds.), *Food Nanoscience and Nanotechnology,* Food Engineering Series, DOI 10.1007/978-3-319-13596-0_1

this matter, including an extensive guide to industry can be found online (FDA 2014).

The number of innovative processes for manufacturing a vast number of nanoproducts is steadily growing such as those related to food preservation by nanostructured materials and by water mobility control as well as those involving novel hardware, tools, and interpretation algorithms directed to the design and preparation of commercially available nanoproducts and to those that are in the pipeline for patenting, and close to the mass production stage such as the vast number of dispersed systems that have been developed, additives, nanopackaging, food biosensors, and biomarkers. In addition, complex and highly specialized pieces of equipment used to produce and appraise these products have been developed in the last years and principles of the standards and regulations in this field are being discussed, including issues related to labeling and ambient-related constrictions and polluting hazards and disposal tasks.

Internet searching indicates that at present there are over 1300 identified nanoproducts that are produced by hundreds of different companies located in many countries, with the USA having the greatest number, a number that has more than quintupled over the past 10 years. Many of these products are available online from noncredited companies and may implicate a risk for the potential consumer.

Recent developments on nanosized materials have been developed in various food-related fields in different fields. In the food–agro sector (Bucheli 2014), it is possible to mention, nanocapsules for the efficient delivery of pesticides, fertilizers, and other agrichemicals; delivery of growth hormone doses in a controlled fashion; nanoparticles for targeted genetic engineering and nanosensors for monitoring soil conditions and crop growth; nanocapsules to improve of nutraceuticals in standard ingredients; nanoencapsulated flavor enhancers; nanotubes and nanoparticles as gelation and thickening agents, nanoparticles bioavailability to selectively bind and remove chemicals or pathogens; nanoemulsions and nanoparticles improving absorption and distribution of nutrients; nanoencapsulation of nutraceuticals for better stability, delivery, and absorption; cellulose nanocrystal composites as nutrient carriers; coiled nanoparticles to efficiently deliver nutrients to cells without affecting color or taste and in food packaging developments including antibodies attached to fluorescent nanoparticles for detecting chemicals or foodborne pathogens; biodegradable nanosensors for temperature and moisture monitoring; and nanoclays and nanofilms as barrier materials to prevent spoilage, electrochemical nanosensors to detect ethylene, surface coatings with nanoparticles of Ag, Mg, Zn, and heat-resistant films with silicate nanoparticles.

Future developments include (Chaudhry and Castle 2011; Bucheli 2014) processed nanostructured or textured food (less use of fat and emulsifiers, better taste); nanocarrier systems for delivery of nutrients and supplements in the form of liposomes or biopolymer-based nanoencapsulated substances; organic nanosized additives for food, supplements and animal feed; inorganic nanosized additives for food, health food, and animal feed; and food packaging applications such as plastic polymers containing or coated with nanomaterials for improved mechanical or functional properties, nanocoatings on food contact surfaces for barrier or antimicrobial

properties, surface-functionalized nanomaterials, nanosized agrochemicals, nanosensors for food labeling, water decontamination and animal feed applications such as nanosized additives that can bind and remove toxins or pathogens.

Evaluating nanomaterials in foods include three main aspects: definition of the type of nanomaterial, its relation to the process/product and appraisal of the end application (Szakal et al. 2014). Potential exposures' risks to nanomaterials include: nanosized or nanoencapsulated ingredients released in food processing, migration from food contact materials, residues from nanoformulated or nanoparticulate agrichemicals, contamination due to nanocompounds released to environment in such a way that the risk assessment and characterization there implies, the hazard identification and characterization, exposure assessment (Aschberger et al. 2011), and regarding physicochemical analysis decision scheme, it is heuristic in nature (Szakal et al. 2014) and once a particular nanomaterial is analyzed for the first time, the methods may change and be more appropriate for the particular nanomaterial in the subsequent analyses until an established method is adopted.

In this book, special interest is given to innovative processes and products such as food preservation by nanostructured materials as well as to novel hardware, tools, and interpretation algorithms involved in the design and preparation of these products and to those that are in the pipeline for patenting, and mass production such as dispersed systems and biosensors. In addition, some of the main complex and highly specialized pieces of equipment used to appraise these products will be mentioned to present and attempt at describing some of the main general trends in this emerging field.

References

Aschberger K, Micheletti C, Sokull-Klüttgen B, Christensen FM (2011) Analysis of currently available data for characterising the risk of engineered nanomaterials to the environment and human health—lessons learned from four case studies. Environ Int 37: 1143–1156

Bucheli T (2014) Agricultural applications of nanotechnology. In: Parisi C, Vigani M, Rodríguez-Cerezo E (eds) Proceedings of a workshop on Nanotechnology for the agricultural sector: from research to the field, Seville, November 2013. European Commission, Joint Research Centre, Institute for Prospective Technological Studies, Luxembourg, p 10–12

Chaudhry Q, Castle L (2011) Food applications of nanotechnologies: an overview of opportunities and challenges for developing countries. Trends Food Sci Technol 22:595–603

FDA (2014) Guidance for industry: assessing the effects of significant manufacturing process changes, including emerging technologies, on the safety and regulatory status of food ingredients and food contact substances, including food ingredients that are color additives. U.S. Department of Health and Human Services Food and Drug Administration, Center for Food Safety and Applied Nutrition. http://www.fda.gov/Food/GuidanceRegulation/GuidanceDocumentsRegulatoryInformation/ucm300661.htm. Accessed 10 Oct 2014

Szakal C, Roberts SM, Westerhoff P, Bartholomaeus A, Buck N, Illuminato I, Canady R, Rogers M (2014) Measurement of nanomaterials in foods: integrative consideration of challenges and future prospects. ACS Nano 8(4):3128–3135

Chapter 2
Tools for the Study of Nanostructures

M. Escamilla-García, J.S. Alvarado-González, Georgina Calderón-Domínguez, J.J. Chanona-Pérez, Juan V. Méndez-Méndez, María de Jesús Perea-Flores and R.R. Farrera-Rebollo

2.1 Introduction

The design of food materials with improved quality characteristics and beneficial effects for humankind is one of the current trends of food industry (Aguilera et al. 2003 and Aguilera 2005) and is in this context that the scientific community have started to design food items with specific properties, and where the structure at micro- and nanoscopic levels has become very important as it plays a crucial role in food functionality (Aguilera and Stanley 1999). Regarding this subject, many of the currently carried out studies have been done using high-resolution microscopy, and spectroscopy techniques, providing basic and fundamental knowledge about structure, and their relation with processing and functionality.

In this chapter, some of the most used microscopy techniques for analyzing the structure of biological materials at the micro- and nanoscale will be presented. These techniques are usually applied looking for the changes that promote the arise of new properties and phenomena that emerge at these scales, hence, the purpose of this chapter is to provide the reader with examples of the application of different types of microscopy techniques usually used to characterize food items.

G. Calderón-Domínguez (✉) · M. Escamilla-García · J.S. Alvarado-González · J.J. Chanona-Pérez · R.R. Farrera-Rebollo
Departamento de Ingeniería Bioquímica Prolongación de Carpio, Escuela Nacional de Ciencias Biológicas, IPN, Plan de Ayala s/n, 11340 Casco de Santo Tomás, C.P., México DF, Mexico
e-mail: gcalderon@ipn.mx

J.V. Méndez-Méndez
Centro de Nanociencias y Micro-Nanotecnología del IPN, Unidad Profesional Adolfo López Mateos, Calle Luis Enrique Erro s/n, 07738 Col. Zacatenco, C. P., México DF, Mexico

M.J. Perea-Flores
Laboratorio de Microscopía Confocal-Multifotónica. Centro DF Nanociencias y Micro-Nanotecnología del IPN, Unidad Profesional Adolfo López Mateos, Calle Luis Enrique Erro s/n, 07738 Col. Zacatenco, C. P., México DF, Mexico

© Springer Science+Business Media New York 2015

H. Hernández-Sánchez, G. F. Gutiérrez-López (eds.), *Food Nanoscience and Nanotechnology,* Food Engineering Series, DOI 10.1007/978-3-319-13596-0_2

2.2 Structure

Food structure is defined as the organization of food constituents at multiple spatial scales that result in the common food properties, mainly textural. Depending on how the product is studied, it can be catalogued in different ways. At one extreme, a food product can be considered at a macroscopic level, where the whole product is evaluated, for example, to obtain some physical or morphometric characteristics, while at the other extreme, when analyzing its molecular composition it will be categorized at a micro- or nanoscale (Ubbink et al 2008). However, this evaluation will depend on the products' constituents and on the dominant length scales that establish the food properties (Fig. 2.1) and it is in this context that microscopy analysis becomes irreplaceable (Aguilera et al. 2003).

The selection of the microscopy techniques to be used, is based on the elements that composed the structure of the sample and that are wanted to be analyzed (Fig. 2.2) and considering the relevant scale as the dimensional level at which the effects of certain phenomena can be observed or explained. A first distinction is required between macrostructure (bulk or macroscopic level) and microstructure (Aguilera 2000). Nowadays structures can be resolved to the atomic level (nanostructure) but the challenge is to identify the relevant scales responsible for the desired functionality, which may vary from molecules at interfaces to visible particles (Aguilera 2000) and decide which microscopy tools can be used to fulfill this purpose. Table 2.1 shows the main characteristics and the resolution range of the different microscopy systems.

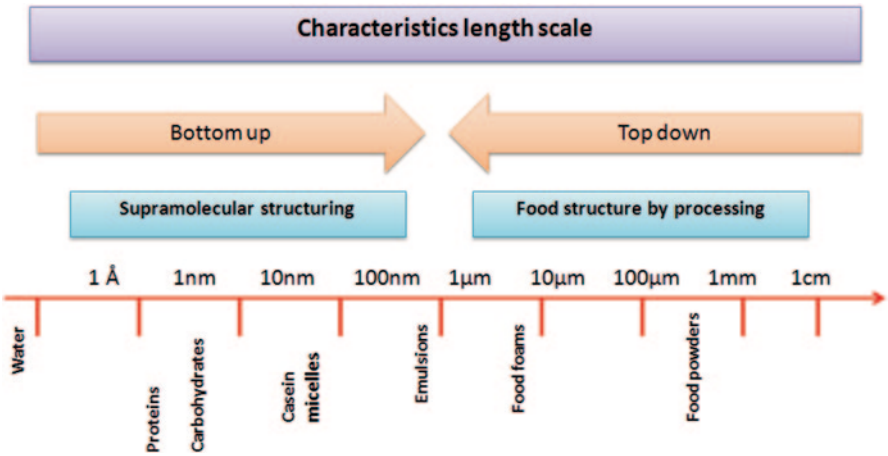

Fig. 2.1 Characteristic length scales in food and examples of representative food ingredients and food structures

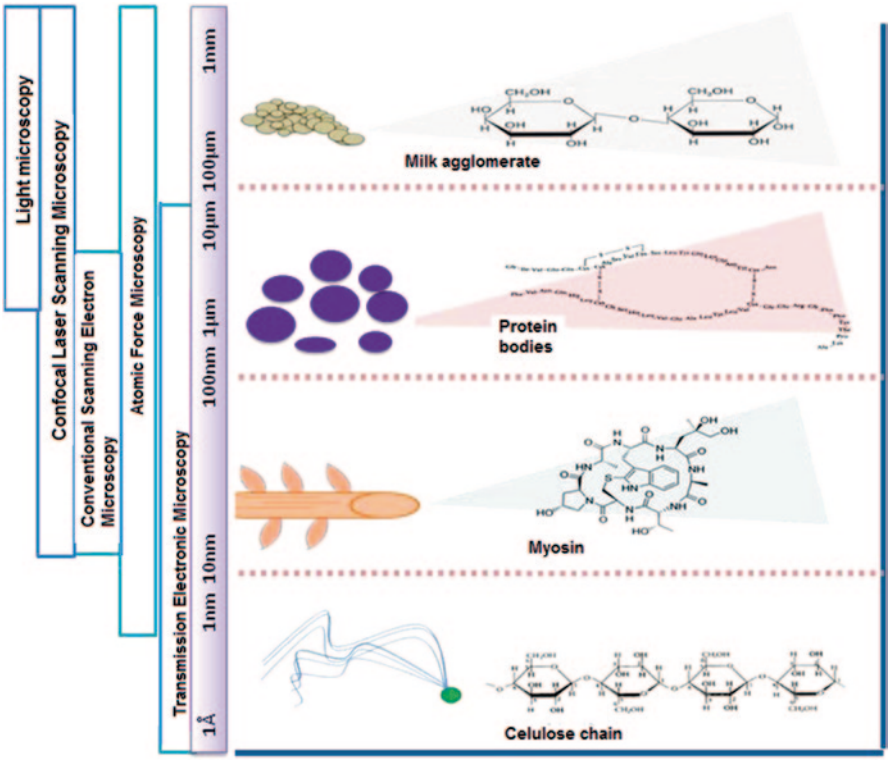

Fig. 2.2 Microscope scales and structural levels used in food science

2.3 Tools for the Study of Micro- and Nanomaterials

2.3.1 Light Microscopy

Optical or light microscopy applied to food items was initially used in order to detect the presence of contaminants, whether accidental or deliberate. This kind of microscopy involves the pass of visible light, either transmitted through or reflected from the sample, through a group of lenses, resulting in the image magnification of the observed samples (Abramowitz and Davidson 2007). Sometimes the specimens under observation, due to their own natural structure, do not need any special treatment to be observed (amplitude specimens), however, others show so little difference in intensity and/or color that their feature details are extremely difficult to discern, requiring the samples a special treatment or a contrast method such as dark field, fluorescence, or confocal microscopy, but even when applying these methods, the resolution that is possible to reach by optical microscopy is low (0.2 µm) giving rise to some modifications.

Table 2.1 Features of microscopy systems used in food science and nanotechnology

Microscopy	Resolution	Uses
Photonic	80 nm–5 cm	Amplitude specimens
Stereo	100 μm–5 cm	Thick or opaque tissues. Overall structure from animal or plant tissues
Fluorescence (FM)	120 nm–1 mm	Fluorescence specimens (natural or added with fluorochromes)
Confocal laser scanning (CLSM)	100 nm–1 mm	Enables the reconstruction of three-dimensional structures from images. To study overall structure and changes during processing. Protein and lipid bodies, components differentiation
Multiphotonic	80 nm–1 mm	Subcellular fluorescence and deep analysis in thick tissue. Ultrastructure and nanometric elements can be observed
Scanning electron microscopy (SEM)	3 nm–500 μm	Superficial or external structural characteristics. Membranes, myosin, cells, particles, and other cellular structures can be studied
Environmental scanning electron (ESEM)	3 nm–500 μm	Low-vacuum microscope for hydrated samples; it is ideal for biological samples
Transmission electron microscopy (TEM)	0.1 Å–1 nm	It is used in biological science for ultrastuctural studies to organelles, cell walls, molecular structure of proteins, lipids, and polysaccharides
Scanning probe (SPM) or atomic force (AFM)	0.1–500 nm	Analytic three-dimensional surface profiles can be observed at nanolevel

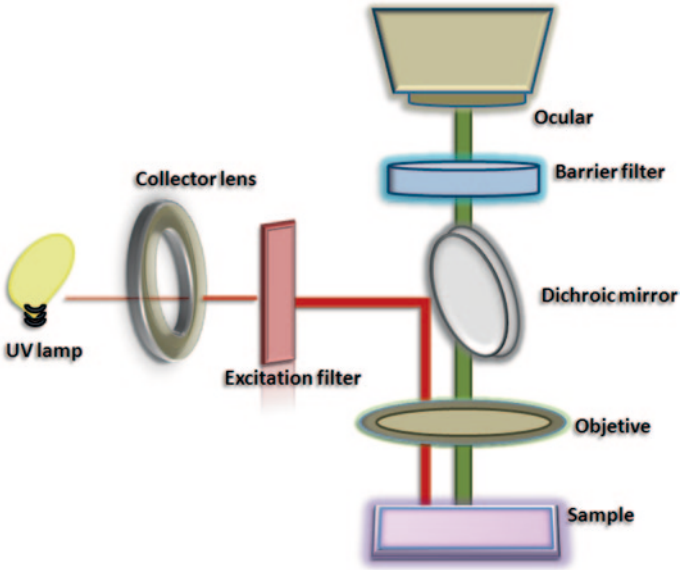

Fig. 2.3 Dark-field microscopy light path

2.3.1.1 Dark-Field Microscopy

Dark-field microscopy creates contrast in unstained transparent specimens such as living cells. This depends on controlling the illumination of the specimen so that the central light that normally passes through and around the specimen is blocked, allowing only oblique rays to illuminate the observed sample (Fig. 2.3). This kind of microscopy has been used to detect metal nanoparticles (Raschke et al 2003) for biomolecular recognition. Kim et al. (2007) demonstrated the usage of dark-field detection with a rather large bead (>2 μm) for stretching DNA or RNA detecting enzymatic activity. The scattering from metal beads was so intense that it could even be used for high speed measurements as was shown for studying the flagella rotary motor at frequencies as high as 300 Hz.

2.3.1.2 Fluorescence Microscopy

Fluorescence microscopy is based on the same common principles applied to optical microscopy (Fig. 2.4), differing in the management related to the generation and transmission of the wavelengths suitable to the fluorochromes to be visualized. Excitation processes usually require short wavelengths in the near UV (quartz, halogen, mercury, etc.).

The basis of the technique lies on the fluorescence properties of some elements or compounds. Usually, fluorochromes are added knowing that they will be bound to the antibodies by a stable chemical bond that cannot be broken during the course

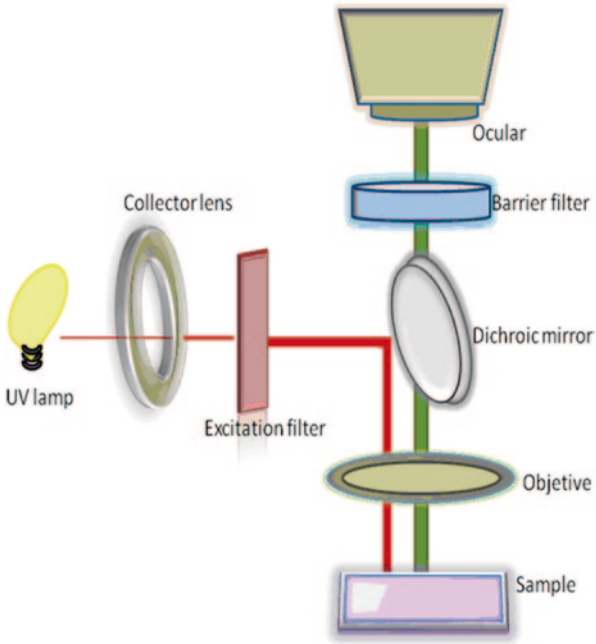

Fig. 2.4 Fluorescence microscopy

of the immunological reaction. Some compounds have natural fluorescence such as some vitamins, steroids, porphyrins, etc. Other fluorescent compounds such as rhodamine, auramine, fluorescein, and acridine orange are used in various staining techniques.

Fluorescence microscopy methods have been developed with improved optical interference filters, dichroic mirrors, epi-illuminators, sensitive films, and electronic imaging devices. For the application of the fluorescence detection systems, four elements must be compatible: an excitation source, a fluorophore, a filter of a particular wavelength that isolates photon excitation, and a detector that registers the emitted photons and produces a recordable output, usually as an electrical signal or a photographic image (Perucho-Lozano 2011).

Fluorescence microscopy has been used in various fields of microbiology, genetic engineering and physiology, and for observing previously invisible processes, including the development of neurons, how cancer cells are disseminated, the development of Alzheimer's disease, the growth of pathogenic bacteria, and the proliferation of the AIDS virus among others (Pérez-Millán and Becú-Villalobos 2009)

2.3.1.3 Confocal Laser Scanning Microscopy (CLSM)

The confocal laser scanning microscopy (CLSM) is a novel technique widely used to characterize the microstructure of the materials related to medical, biological,

and materials sciences. It can be applied to gather the microstructure by a dynamic and nearly noninvasive observation (Dürrenberger et al. 2001; Jekle and Becker 2011).

The confocal laser scanning microscope was first conceived by Minsky in 1955, in order to observe individual nerve cells within a packed central nervous system. He designed a simple instrument in which a pinhole was placed in front of an objective and a condensing lens, promoting by this way effectively discriminated out-of-focus light contributions from the specimen (Pygall et al. 2007).

The CLSM proved to be particularly valuable in improving fluorescence images. The optics reject light from outside the focal plane (out-of-focus flare) resulting in images superior in contrast and clarity and with an improvement in the lateral (*x, y*) resolution over standard optical microscopes. The CLSM image is also a true optical section and this capability allows imaging at depth inside translucent specimens. The slice thickness can be as thin as 0.5–1.5 μm but is dependent upon the numerical aperture of the objective lens (Pygall et al. 2007).

CLSM is one of a suite of fluorescence imaging instruments, which include: scanning confocal, spinning disc, multiphoton, and wide-field microscope. This equipment has a light source with a scanning unit and an aperture or pinhole (the information from the focal plane), which improves the depth of focus limit (Pygall et al. 2007). The confocal system operates by obtaining information from optical sections focus only on one focal plane, where the sample is excited by the impegiment of a specific wavelength laser beam (transmitted or reflected), and where the sample will tend to fluoresce (naturally or induced) (Aguilera and Stanley 1999; Aguilera 2000). This optical section will contain information from one focal plane only, therefore, by moving the focal plane of the instrument by steps of defined distance (range in μm) through the depth of the specimen, a stack of optical sections will be recorded. This property of CLSM is important for solving three-dimensional (3D) microstructures (Fig. 2.5), where the information from regions distant from the plane of focus can blur the image of such object (Dürrenberger et al. 2001; Pygall et al. 2007; Perea et al. 2010, Aguilera and Stanley 1999; Amos and White 2003; Achir et al. 2010; Chassagne-Berces et al. 2009).

The CLSM incorporates two operation modes; the first is by illuminating the sample point-by-point and rejecting the out-of-focus light. The principle is shown in Fig. 2.6, where the excitation laser beam (intense blue excitation light) reflects off the light in a dichroic mirror, directing it to an assembly of vertically (*x*) and horizontally (*y*) scanning mirrors; these motor-driven mirrors scan the laser across

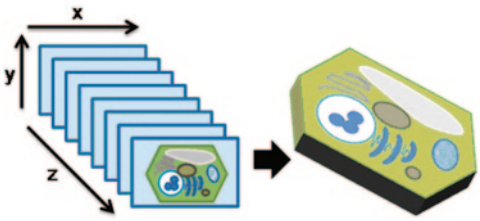

Fig. 2.5 Optical sections of vegetable cell from focal planes (*x, y*) at different depths (*z*) through a cell, which provides a three-dimensional image

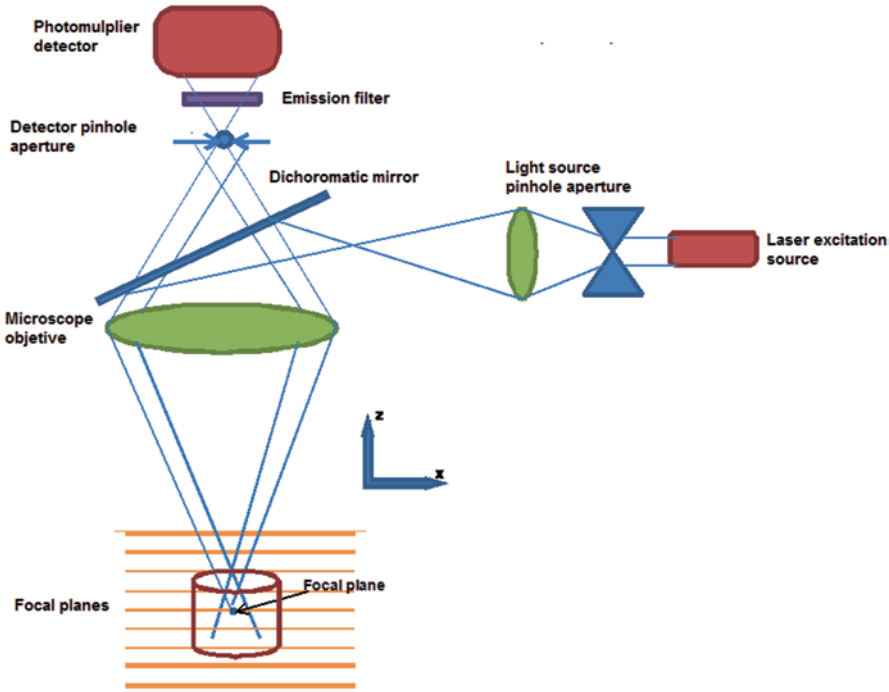

Fig. 2.6 The confocal principle

the specimen through the microscope objective. The fluorescence light emitted by the dye molecules (induced or autofluorescence) passes back through the objective and is descanned by the same mirror through a pinhole placed in the conjugated focal (called confocal) plane of the same; the pinhole thus rejects all out-of-focus light arriving from the sample and the light only from the focal point (plane) can pass the pinhole and be measured. Finally, the emitted light is measured by a detector such as a photomultiplier tube. Then, a computer reconstructs the two-dimensional image plane one pixel at a time (single optical sections), and a 3D reconstruction of the sample can be performed by combining a series of such slices at different depths. This kind of microscopy has been widely used in real time biological experiments applied to living cells and tissue sequences (Prasad et al. 2007; Amos and White 2003; Cox 2002; Semwogerere and Weeks 2005; Dürrenberger et al. 2001; Paddock 2000).

The advantages of the CLSM is the capability to obtain optical sections of different focal planes, providing a larger resolution in a section plane (x, y), and a good resolution between the section plane (>0.25 μm in z-direction).

CLSM Applications

The application of CLSM to study the microstructural characterization of food materials has been particularly fruitful in the area of lipid components because optical sectioning overcomes the tendency of fats to smear and migrate. Lipids are also well suited to fluorescent staining. The possibility of combining CLSM with rheological measurements, light scattering, and other physical analytical techniques in the same experiments with specially designed stages offers the opportunity to obtain detailed structural information of complex food systems. Different examples of CLSM application are shown in Table 2.2.

2.3.1.4 High-Resolution Optical Microscopy Methods

During the last 5 years, super-resolution optical microscopy techniques have emerged marked by the invention of the stimulated emission depletion microscopy (STED) and the stochastic optical reconstruction (STORM/fluorescence) photo-activated localization microscopy (PALM). Both tools have in common the possibility to add to the diffraction limit resolution, at least in theory, a dominator, eliminating the impossibility of resolving images smaller in size than the half of the wavelength of light. This booming resulted in the rapid development of many other high resolution improved microscopy methods, as well as the arise of many new acronyms.

High or super-resolution microscopy techniques have been classified into two groups: one based on spatially patterning the excitation light and the other based on single-molecule localization (Huang 2010). From the first group, STED microscopy is the most successful one. This technique is based on the sharpening of the laser focus with a second laser (STED laser), which suppresses spontaneous fluorescence emission by stimulated emission, as the exited fluorophore is brought to the ground state by emitting light in the same color as the STED laser. The resolution is improved when increasing STED laser intensity. Biological samples resolution has been reported to be in the range from 20 to 30 nm.

Regarding single molecule localization, this methodology is based on the detection of fluorescence of photo-switchable fluorescent probes and STORM/PALM microscopy has become one of the most known methods. This method applies several imaging cycles, where a small, optically resolvable fraction of fluorophores is activated and imaged, repeating the cycles while scanning the sample. The fundamental principle is based on the consecutive emission of sufficient photons to enable precise localization before it becomes deactivated by photo-bleaching. By this way, the resolution of the final image is not limited by diffraction, but by the precision of each localization, being possible to achieve up to approximately 20-nm resolution and with the advantage of only requiring a standard fluorescence microscope, low power continuous wave lasers, and a sensitive CCD camera (Bates et al. 2008), however their use in food materials has not been documented.

Table 2.2 Applications of the CLSM and multiphoton microscopy in organic and inorganic materials

Materials	Description	Reference
Bacteria	*Bacillus cereus* spores germination	Coote et al. 1995
Zein films	Zein films deformation mechanisms. Real time and microtensile stage	Emmambux and Stading 2007
Biopolymer gels	Nature and spatial distribution of protein aggregates and polysaccharides in gel structure	van den Berg et al. 2009
Emulsions	Oil-in-water (O/W) emulsion structure and stability	Calero et al. 2013
Polysaccharides	Localization of polysaccharides in foods, (pectin and carrageenan) by immunological in-situ techniques	Arltoft et al. 2007
Food composite	Separation of phases in a gel during compression	van den Berg et al. 2008
Starch noodle dough	Evaluation of swelling behavior of the broccoli and starch particles in noodles	Silva et al 2013
Starch	Gelatinization behavior of starch granules obtained from different sources (maize, potato, wheat, and barley)	Schirmer et al. 2013
Dough	Wheat dough proteins microstructure and their relation with rheology properties	Jekle and Becker 2011
Foods	Potential and limitations of CLSM to study the microstructure of Yam (*Dioscorea cayenensis rotundata*) parenchyma, bread, and pasta (cereal products)	Dürrenberger et al. 2001
Lacteous	Effect of whey proteins on structural properties of stirred yoghurt systems at different protein and fat content	Krzeminski et al. 2011
Biofilms	Identification of bacteria and extracellular polymeric substances distribution within a biofilm matrix during growth	Wagner et al. 2009
Materials	Proliferation, morphology, and adhesion of fibroblast and epithelial cell lines, on Fe–Pd thin films	Allenstein et al. 2012 (In Press)
Seeds	Three-dimensional (3D) distribution of proteins and lipids in a parenchyma cell from seed, showing green fluorescence from protein bodies and yellow from pectin (middle lamella)	Mosele et al. 2011

Table 2.2 (continued)

Materials	Description	Reference
Food	Changes in distribution of fat globules and bacterial colonies within cheese tprotein matrices	Romeih et al. 2012
Tissue	Microstructure of potatoes (raw and cooked tubers)	Bordoloi et al. 2012
Membrane systems	Multiphoton microscopy apply in Langmuir films (lipid monolayers at the air–water interface)	Brewer et al. 2010
Fibers	3D multiphoton microscopy of elastic fiber system in native porcine and tissue engineered heart valves	Köning et al. 2005
Cell	3D multiphoton microscopy of living cells (chromaffin cells and PC12 cells) to determine the chromatin bovine cells structure and the arrangement of acid organelles	Straub et al. 2000

2.3.2 Electron Microscopy

Electron microscopes were developed due to the limitations of light microscopes which are limited by the physics of light to 500x or 1000x magnification and a resolution of 0.2 μm. In the early 1930s, this theoretical limit had been reached and there was a scientific desire to see the fine details of the interior structures of organic cells (nucleus, mitochondria, etc.). This required 10,000x plus magnification which was just not possible using light microscopes. The transmission electron microscope (TEM) was the first type of electron microscope to be developed while the first scanning electron microscope (SEM) debuted in 1942 but the first commercial instruments arouse in 1965 (Voutou and Eleni-Chrysanthi 2013).

Atomic-scale techniques, such as conventional transmission electron microscopy, although powerful, are limited by the extremely small amounts of material that are examined. However, recent advances in electron microscopy provide a number of new analytical techniques that expand its application in environmental studies, particularly those concerning heavy metals on airborne particulates or water-borne colloids. High angle annular dark-field scanning transmission electron microscopy (HAADF-STEM), STEM-energy-dispersive X-ray spectrometry (EDX), and energy-filtered TEM (EFTEM) can be effectively used to identify and characterize nanoparticles. The image contrast in HAADF-STEM is strongly correlated to the atomic mass: heavier elements contribute to brighter contrast. Gold nanocrystals in pyrite and uranium nanocrystals in atmospheric aerosols have been identified by HAADF-STEM and STEM-EDX mapping and subsequently characterized by high-resolution TEM (HRTEM). (Utsunomiya and Ewing 2003).

The electronic microscopy (EM) is recurrently used in food science (SEM and TEM systems) and the most important technological advances in microscopy have been the developments in these equipments. The general principle is the electrons bombardment to the sample, differing essentially in the way the compartment camera is sealed, treated with different pressure-voltage properties, detectors attached, and modes of the equipments. In the SEM systems, the amount of vacuum discerns these techniques: vacuum SEM, extended pressure SEM, and low vacuum SEM. Furthermore, an extended branch using the cryogenics is the Cryo-SEM devices which is well developed in foodstuffs; in this type, the specimen is frozen with temperatures between −100 and −175 °C maintaining the life-like appearance and allowing the fracture of the sample for long-cross and transversal section study.

2.3.2.1 Scanning Electronic Microscopy (SEM)

The SEM is a microscope that uses electrons to form an image. In this type of microscopy, the specimen is covered with a thin metal layer, usually gold, and it is swept with electrons. A detector measures the signal, displaying 3D figures, reproducing sample's topography and even composition. Electrons are emitted by a cathode of tungsten and passed throughout a column that has a vacuum of about 10^{-7} Torr. Here, the initial beam is focused by electromagnetic lenses decreasing the

beam diameter until it becomes almost punctual. The main parts of an SEM are: the electron source (gun), electron lenses, sample stage, and detectors.

The electron source emits electrons which strike the specimen by creating a magnified image, while magnetic lenses create fields that guide and focus the electron beam as conventional lenses do in optical microscopes. Traditionally, electron microscopes have an electron gun fixed with a tungsten filament cathode or an LaB6 simple crystal in comparison with field emission gun (FEG) which is a pointed tungsten tip (Müller emitter) that could be coated with a layer of zirconium oxide (Schottky emitter); the sharper tip of the FEG provides a small, optically bright, and stable electron source capable of reaching smaller scales, for this reason they are called high resolution (120–3 nm in SEM mode and around 1 nm in TEM mode) (Orloff 2009). In contrast, ultrahigh resolution uses spherical and/or chromatic aberration correctors instead of different tips, reaching Armstrong scales (1–0.4 nm) (Haider et al. 2008).

The vacuum system is a very important part of the electron microscope as electrons can be deflected by air molecules. Also, if oxygen or other molecules are present, the life of the filament will be shortened dramatically, since these molecules in the column will act as specimens, scattering the electron beam. The vacuum of the SEM needs to be below 10^{-4} Torr to operate, although most microscopes operate at 10^{-6} Torr or greater vacuum (Dunlap and Adaskaveg 1997).

SEMs employ one to three condenser lenses to de-magnify the electron-beam diameter to a smaller size. The first and second condenser lenses control the amount of demagnification, while the final lens in the column sometimes inappropriately called "objective" focuses the probe on the sample (Fig. 2.7).

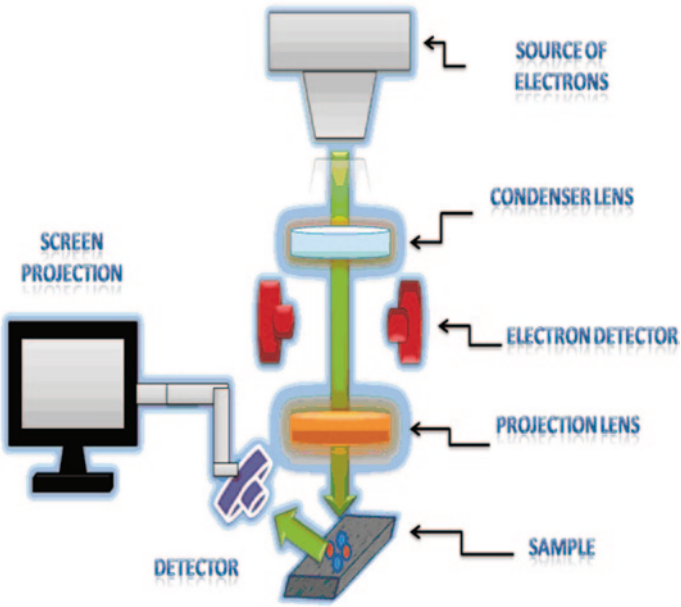

Fig. 2.7 Scanning electronic microscopy

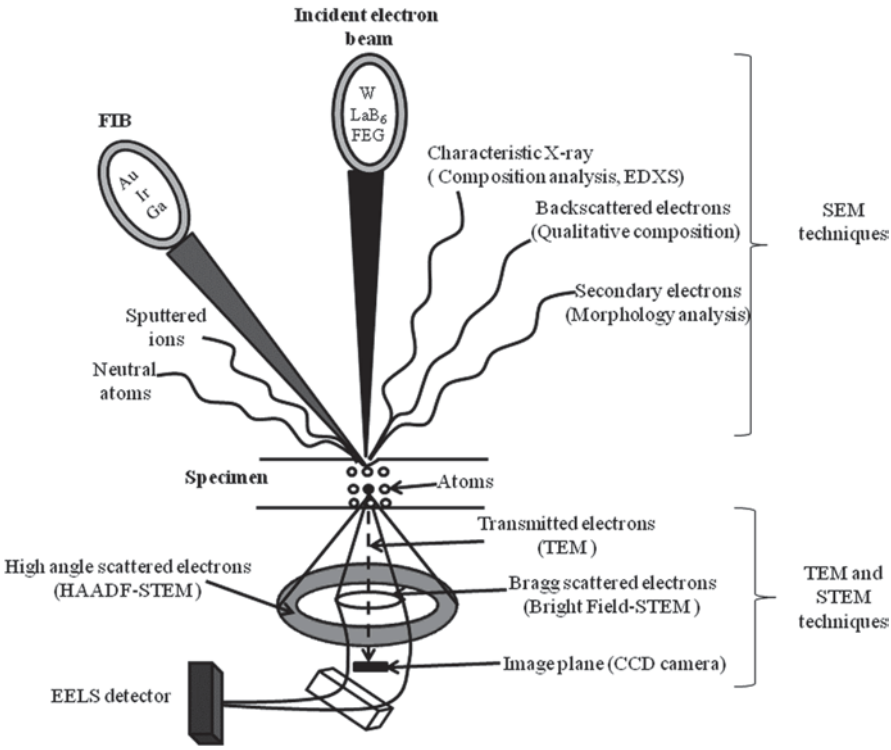

Fig. 2.8 Schematic diagram for electronic microscopy (EM) systems

Signal detection begins when the electron beam, known as the primary electron enters through the specimen. When the primary electron enters it probably travels some distance into the specimen before hitting another particle. After hitting an electron or a nucleus, the primary electron will continue into a new trajectory (scattering). The result of the primary beam interaction with the specimen is the formation of a teardrop-shaped reaction vessel. This reaction vessel by definition is where all the scattering events are taking place (Dunlap and Adaskaveg 1997), and the signals can be collected with several kinds of detectors attached to the equipment and specially design to detect a specific particle and transduce the information into an image or a spectrum (Fig. 2.8).

2.3.2.2 Transmission Electronic Microscopy (TEM)

Transmission electron microscopy (TEM) is a microscopy technique whereby a beam of electrons is transmitted through an ultra-thin specimen, interacting with the specimen as it passes through. An image is formed from the interaction of the electrons transmitted through the specimen; the image is magnified and focused onto an

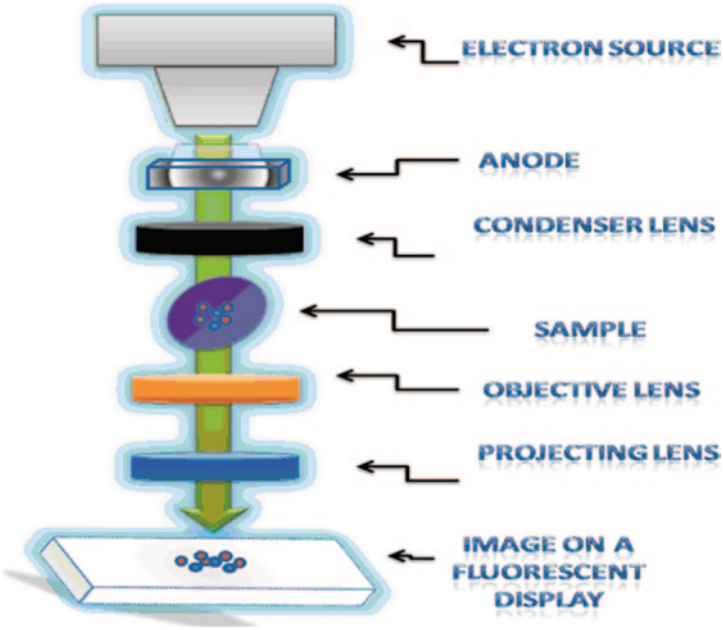

Fig. 2.9 Transmission electronic microscopy (EM)

imaging device, such as a fluorescent screen, on a layer of photographic film, or to be detected by a sensor such as a CCD camera.

The main parts of a TEM are shown in Fig. 2.9:

- Electron gun, which emits electrons that collide or pass through the specimen (depending on type of electron microscope), creating an enlarged image.
- Magnetic lenses to create fields that guide and focus the electron beam as conventional lenses used in optical microscopes do.
- Vacuum system is a very important part of the electron microscope. Because the electrons can be deflected by air molecules, they must make a near-vacuum inside a microscope of this kind.
- Photographic plate or fluorescent screen placed behind the object to be displayed to record the enlarged image.
- System log showing the image that produce electrons, which is usually a computer.

Electron Column of the TEM

The electron column consists of an electron gun and a set of five or more electromagnetic lenses operating in vacuum. It is convenient to divide up the TEM into three components: the illumination system, the objective lens/stage, and the imaging system.

The illumination system comprises the gun and the condenser lenses and its role is to take the electrons from the source and transfer them to the specimen. The electron beam is accelerated to energy in the range 20–1000 keV in the electron gun then the electron beam passes through a set of condenser lenses in order to produce a beam of electrons with a desired diameter. The illumination system can be operated in two principal modes: parallel beam and convergent beam. The first mode is used primarily for TEM imaging and selected area diffraction (SAD), while the second is used mainly for STEM imaging, analysis via X-ray and electron spectrometry, and convergent beam electron diffraction (CBED).

The objective lens and the specimen holder/stage system is the heart of the TEM. Here is where all of the beam–specimen interactions take place and the two fundamental TEM operations occur, namely, the creation of the various images and diffraction patterns (DP) that are subsequently magnified for viewing and recording. The imaging system uses several lenses to magnify the image or the DP produced by the objective lens and to focus these on the viewing screen or computer display via a detector, CCD, or TV camera. Images are recorded on a conventional film positioned either below or above the fluorescent screen or digital capture can be utilized using CCD or TV cameras. (William and Carter 2009).

The illumination system is situated in the top part of microscope and consists of the electron source and then condenser lenses. The illumination system takes the electrons from the source and transfers them to the sample in the form of parallel or convergent beam. Usually the following electron sources are used: thermionic sources like LaB6 or tungsten sources and FEG. All of them have some advantages and disadvantages. However nowadays modern microscopes are normally equipped with FEG, because this source produces very bright electron beam by operating at low temperature and having very long lifetime.

The condenser lenses are used to form the electron beam which illuminates the sample. By changing the focal distance of condenser lenses, parallel or convergent illumination is created. The parallel beam is usually used in traditional TEM, while the convergent beam is typical for STEM mode (scanning TEM). Objective lenses are used for image formation. After propagating through objective lens all electron beams from the sample are focused at the image plane. Here, one uses the objective aperture in order to exclude electrons at high scattering angles. In HRTEM mode, usually no objective apertures are used (Tyutyunnikov 2010).

High-resolution TEM (HRTEM) is one of the most powerful tools used for characterizing nanomaterials, and it is indispensable for nanotechnology. In fact, decades before the national nanotechnology initiative, scientist had started examining small particles by HRTEM. Traditionally, HRTEM has been mainly applied for imaging, diffraction, and chemical analysis of solid materials. Analysis of such tubular structures required extensive development of electron microscopy (Wang 2003).

Modern TEM has three basic operation modes: imaging, diffraction, and spectroscopy analyses. In a transmission electron microscope, the objective lens takes the electrons emerging from the exit surface of the specimen, disperses them to create a DP in the back focal plane, and recombines them to form an image in the image plane (Bai et al. 2013)

The spectroscopy analyses in a modern analytical TEM include energy-dispersive x-ray spectroscopy (EDX) and electron energy-loss spectroscopy (EELS) that allow quick analysis of material chemistry on the nanoscale. With the newly developed EFTEM, quick elemental mapping not relying on the scanning technique is possible (Bai et al. 2013).

TEM has the advantage over SEM that cellular structures of the specimen can be viewed at very high magnifications. However, TEM sample preparation is longer and more difficult than that for SEM and includes additional steps such as postfixation, embedding in a resin, the sectioning of samples, and the staining of semithin and ultrathin sections. Specimen preparation for TEM includes eight major steps: cleaning, primary fixation, rinsing, secondary fixation, dehydration, and infiltration with a transitional solvent, infiltration with resin and embedding, and sectioning with staining. (Stadtländer 2007).

Table 2.3 shows some examples of common electron microscopy applications in food materials.

2.3.3 Atomic Force Microscope

Atomic force microscopy (AFM) is part of a scanning probe microscopy family that is based on the scanning tunneling microscopes (STM) which measure topography of surface using the tunneling current which is dependent on the separation between the probe tip and a highly conductive sample surface. The AFM was invented by Gerd Binnig and Christoph Gerber (1986), and it is able to provides 3D images of the topographic surface of conducting and nonconducting materials (Tortonese et al. 1993) to molecular and in some cases atomic resolution, sensing the forces created due to the interaction of the tip and the surface sample at very short distance of 0.2–10 nm (probe sample separation); this instrument also is able to measure forces at the picoNewton scale at the level of a single atom (Binning et al. 1986). For some materials, few or no preparation is needed and some of the common materials tested are: composites, glasses, metals, polymers, electronics, membranes, films, synthetic ceramics, composites, and biological organisms, in numerous fields such as, automotive, aerospace, chemical, material science, and biology.

The images are acquired by means of a very sharp tip supported on the free end of a flexible cantilever. The AFM tip located above the sample "gently" touches the surface and records the small force between the probe and the surface. The AFM can be used in air and aqueous environments (Florin et al. 1995), with live microorganism such as bacteria and cells, and to perform studies of phenomena such as electrode position (Lu and Zangari 2006), wear resistance (Li et al. 2006), surface roughness (Sudam and Nichols 1994; Ryan 2000), lubrication (Koinkar and Bhushan 1996), corrosion, nanotribology (Tambe and Bhushan 2005), and adhesion. Specifically in biology, it has been used to study nucleic acids, receptor–ligand complex, the molecular interactions determining the stability of single proteins and to understand the elastic and viscous properties of membrane proteins using dynamic modes (Janovjak et al. 2005), and has been extended to probe the dynamics

Table 2.3 Electron microscopy applications in food materials

Food materials	Microscope	Processing or phenomena	Processing conditions	Microstructure examination and results	Reference
Apple	ESEM	Freeze and vacuum drying	−70 °C/48 h 70 °C (store)	Cellular integrity loss and membrane denaturalization	Acevedo et al. 2008
Mango	SEM	Heating (Jam)	190 °C 65–66 °Brix	Network regions, large and small pores as well as dense	Basu and Shivhare 2010
Plum	SEM	Boiling candying	15 min/0.7 m3 60–75 °Brix	Boiled-cell separation. Candied-tissue recovery	Nunes et al. 2008
Mushroom	Cryo-SEM	Air drying rehydration	°C 1–210 min	Vacuum rehydration showed swollen and soft samples	García-Segovia et al. 2010
Chicken	TEM	Apoptosis induction	7 days Ca^{2+}	Increase myofibrillar dissociation and proteolysis	Chen et al. 2011
Pork	SEM	Drying salting	8 weeks glutaminase	Increase of crosslinks during the drying period	Romero de Ivila et al. 2010
Beef	SEM	Cooking	70/4 °C store gellan, salts	Dispersed pores. Intact rods (fibers), filaments (gellan)	Totosaus and Pérez-Chabela 2009
Cheese	SEM	Packing (Turkish)	12 % salt 90 days	Compact and denser protein matrix for the cheese packed	Akalin and Karaman 2010
Yogurt	SEM	Storage fortification	9 weeks, pre-probiotics	Pre-polymerized whey increased protein network	Walsh et al. 2010
Milk (Cow)	SEM	Heating	130 °C 18 s	Chemical cross-linkers improved the casein protein	Ghosh et al. 2009

Table 2.3 (continued)

Food materials	Microscope	Processing or phenomena	Processing conditions	Microstructure examination and results	Reference
Wheat	SEM	Roasting	280–350 °C 45–120 s	Roasted wheat has a porous structure	Venkatesh et al. 2008
Corn	SEM	Extrusion (imitation)	700 rpm 1.2 L h	Fractured particles with small rounded particles on surface	Carvalho et al. 2010
Rice	SEM	Boiling drying	10–12 min −20 °C, 80 °C	Porous surface, some cases slightly deformed	Rewthong et al. 2011

ESEM environmental scanning electron, *SEM* scanning electron microscopy, *TEM* transmission electron microscopy

of single molecules, including polysaccharides. Also it has been used to determine properties such as adhesion and electrostaticity (Lin et al. 2005).

The AFM is limited to surface image but it is possible to prepare the sample embedding it and cutting section to expose the desired internal structure.

2.3.3.1 Principles of the AFM

The AFM has some unique features because it can be used in air or aqueous environments; the only condition is that the environment in which the experiment is carried out allows the laser pass. The AFM differs from other types of microscopes because it can image samples under natural conditions; this is an advantage because the samples are kept in nonstress conditions, such as drying, coating with metal, vacuum, or freezing that can alter the normal characteristics of the sample. This characteristic is especially useful for biological applications. The resolution of the AFM is in the rate of tens of nanometer and the resolution in force rate is in the order of picoNewtons. The AFM is a very versatile instrument because not only it can be used to obtain topography images but also it has been used to study magnetic, electric, Piezo, conductive, and capacitance properties.

AFM topography images can be obtained by scan-raster, where a very sharp tip, mounted on the free end of a cantilever, is perpendicularly in touch with the surface sample. This is controlled by a photo sensor; in Fig. 2.10 the bacterial growth on a flat surface, scanned by a cantilever tip is shown.

Different types of atomic force microscopes are offered by different companies, presenting most of them with slight differences in the design, but in general, the sample is fixed on the scanner (magnetically, clamped, or double-sided tape, etc.), then the scanner moves the sample in *X* and *Y* directions, while this happens the

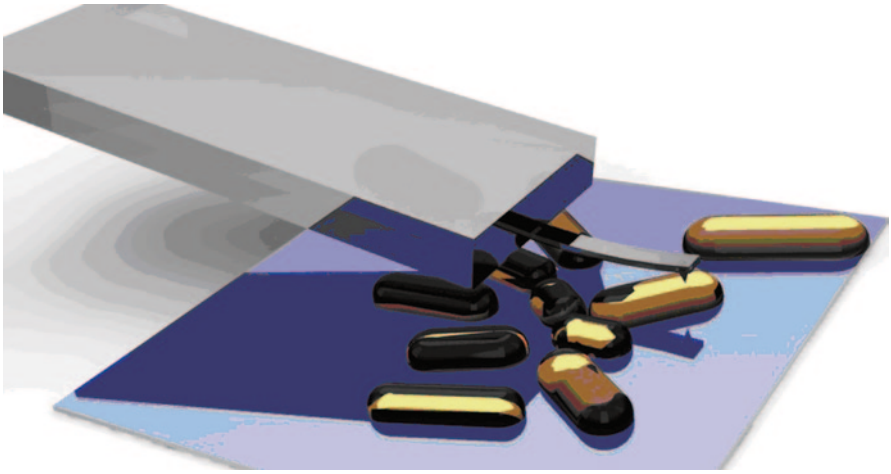

Fig. 2.10 Bacteria scanning

movement of Z is controlled by the scanner which uses the optical signal to sense the interaction between the tip and the sample, keeping it constant, and raising or lowering the sample according to the optical signal. The scan area is defined by the user taking into account the limitations of the scanner. The position of the scanner is recorded constantly to reconstruct 3D images. The AFM is not only used to construct models, but also to study interaction forces and in food process it has found special interest.

2.3.3.2 Components of an AFM

In order to have a more clear idea of the AFM, here we will discuss some of the main components of the MultiMode™ (SPM, Bruker). The multimode is formed by two components, the controller (NanoScope™) and the Microscope. The controller allows the instrument to operate in different modes. This unit is capable of scanning areas according to the scanner used, in the Fig. 2.11, the AFM microscope and the parts that integrated it can be seen.

Some of the main components of the microscope are listed below:

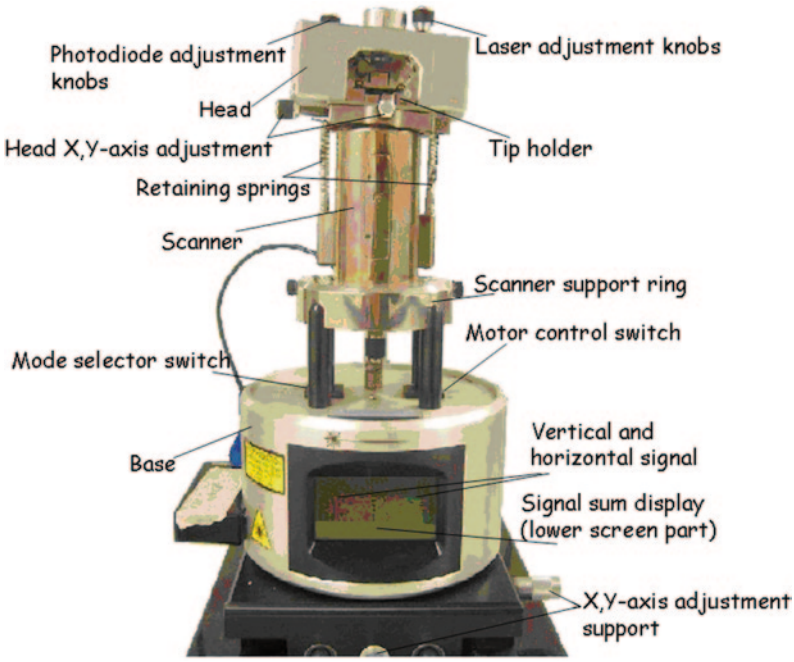

Fig. 2.11 Multimode scanning probe microscopy (SPM)

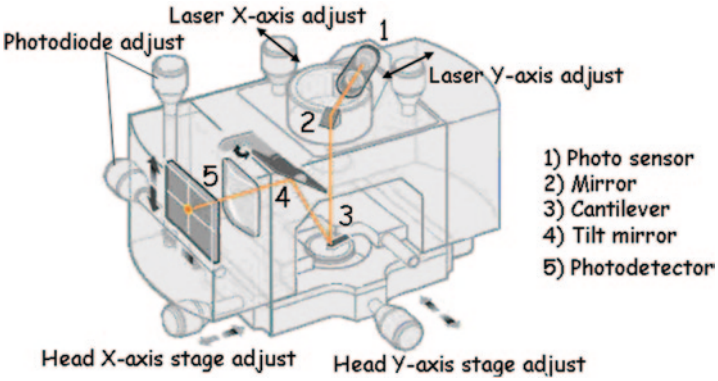

Fig. 2.12 Details of the optical head of the atomic force microscopy (AFM)

The Optical Head

The optical head is a block place on the scanner with the help of tree metallic beads and fixed with two springs. In Fig. 2.12 a picture of the head and the internal and external elements marked with numbers are presented: the laser (1), the mirror (2), cantilever (3), tilt mirror (4), and photosensor. The knobs are used to move the optical head to the desired location (head *X, Y*-axis stage adjust). Both *X, Y*-axis adjust knobs are used to move the laser to obtain the maximum signal and finally, in the upper and back part of the optical head a pair of knobs (photodiode adjust) used to center the laser on the photodetector and to obtain vertical and horizontal signal near cero are located.

Tip

The tip Fig. 2.13 was traditionally made of diamond on a gold film, but nowadays most are made of Si_3N_4 or Si with a radius of approximately 10 nm; however, it is possible to find in the market cantilever with tip radius of approximately 2 nm. The tip is the heart of the AFM, and it is very important for the success of the technique, as it must accurately reflect the surface features of the specimens under investigation. The image is constructed by scanning the sample with the tip, therefore the selection of tip plays an important role in the obtaining of an accurate surface to-

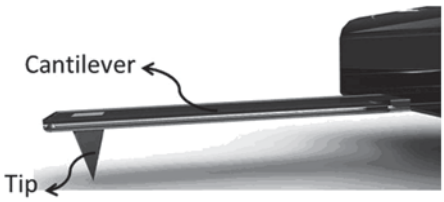

Fig. 2.13 Tip mounted on a side of the cantilever

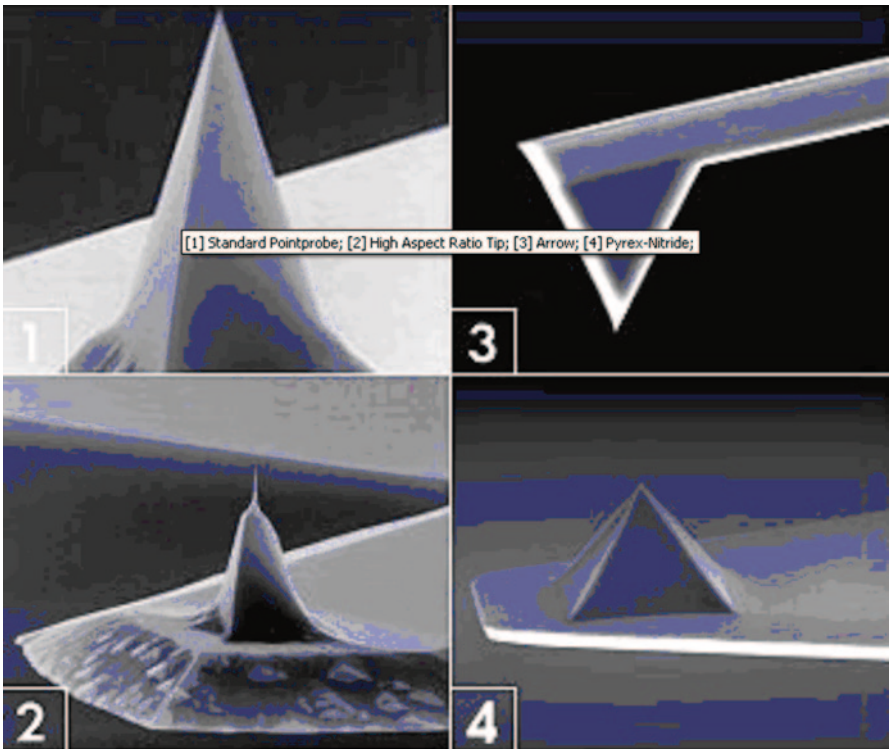

Fig. 2.14 Atomic force microscopy (AFM) cantilever probes, (1) Standard pointprobe®. (2) High aspect ratio tip. (3) Arrow™. (4) Pyrex-Nitride™. Electron micrographs by Jean-Paul Revel, Caltech. Tips from Park Scientific Instruments; super tip made by Jean-Paul Revel. Figure taken from http://www.nanoworld.com

pography. The tip is attached to a cantilever Fig. 2.13, giving the tip freedom of movement. Depending on the topography of the sample; the displacements of the cantilever can be vertical and/or torsional; different cantilever tips can be seen in Fig. 2.14.

The commercial tips available are made using different techniques and materials, including micromachining, lithographic photo-masking, etching and vapor deposition, etc. In addition, the tip can also be one of a number of different shapes, for instance, a parabola, pyramid, truncated pyramid, tilted pyramid, and cylinder, and with a specifically characteristic chemical or biological coating.

Effects of the Tip Diameter

There are still a number of long-standing problems in obtaining consistent high-resolution images using AFM. The radius and shape of the end of the AFM tip can vary resulting in a loss of sharpness (Li et al. 2007; Bykov et al. 2003). Since, in order to

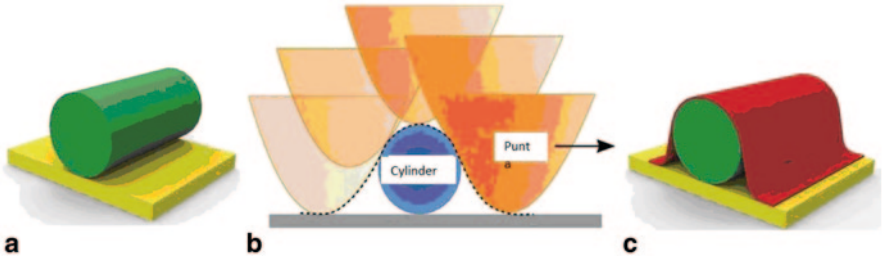

Fig. 2.15 Effect of the tip diameter

obtain high resolution it is important to have a very sharp tip. However, it has some implications; if the diameter of the tip is very small it will be damaged easily, and also it is more complicated to fabricate such tips, on the other hand, if the tip used is not sharp enough the image obtained will not reflect the real sample topography.

In Fig. 2.15 (a) can be observed a cylinder bounded to a flat surface, in (b) the direction of the scan and the tip form are described, while (c) shows the convolution image obtained by the AFM. It is clear from this figure that the cantilever cannot enter to the lower part of the cylinder, this is a phenomenon that has to be taken into account when the images are obtained.

Photosensor

The optical lever is the most common mode of detecting deflection. The laser beam is reflected off the cantilever, striking a photosensitive sensor, which measures the changes in the intensity of the light produced by the deflection and the lateral movements of the cantilever, magnified thousands of times due to the distances between the cantilever and the photodetector. The photosensors used in the AFM are two (double) and four-segmented photosensors made of semiconductor diodes (Fig. 2.16 and 2.17 in that order). The photosensor senses the variations of the optical signal and transforms them into an electrical signal. The double-segmented photosensor is used to sense vertical deflection of the cantilever and the four-segment photodiode performs the same task as the two segments but it has the capability of also measuring the displacement (torsion); normally this photodiode is used in the frictional mode (Kasas et al. 1997).

Scanner

Scanners are made of piezoelectric ceramic materials that are radially polarized. These materials have the characteristic that contract or expand according to the current applied. Electrodes are attached to the piezo-material, and movements are achieved by applying a high voltage over the electrodes located around the material. Three-dimensional positioning is possible by applying the precise voltage to the

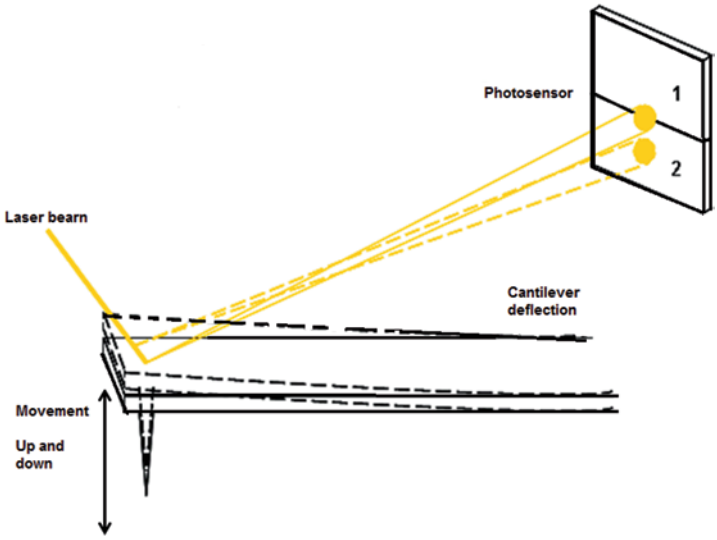

Fig. 2.16 Two segment photosensor

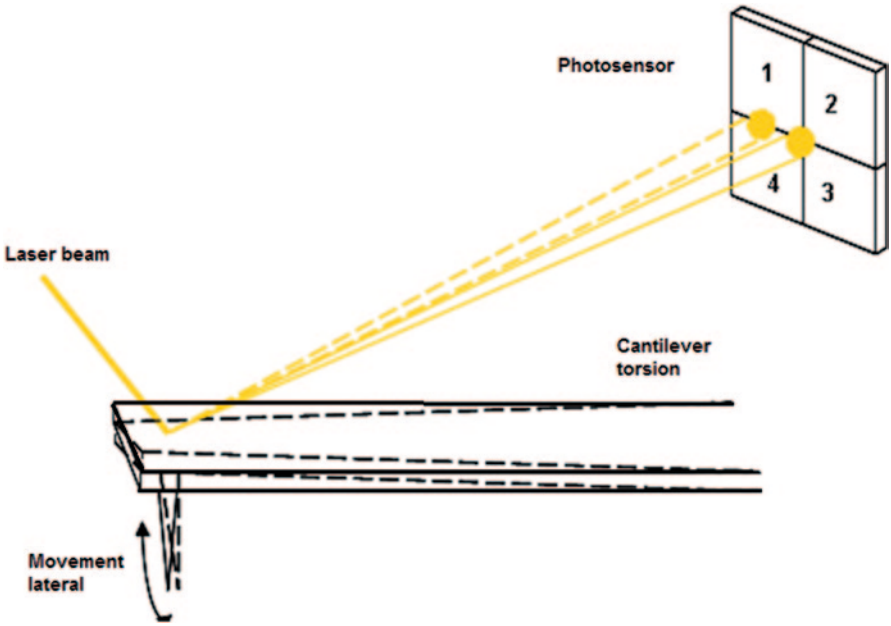

Fig. 2.17 Four segment photosensor

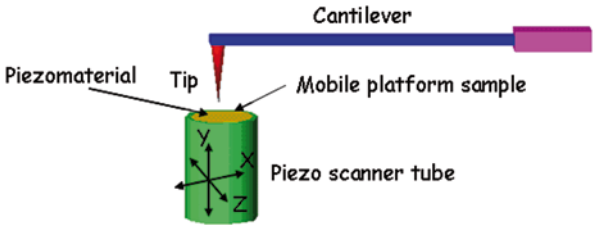

Fig. 2.18 Tube scanner configuration

main axis, *X, Y*, and *Z*. The movement is controlled by the electronic feedback (Fig. 2.18).

2.3.3.3 AFM Operation Modes

Figure 2.19 shows the deflection behavior of the cantilever when it approaches to the surface. Initially, the cantilever is above and moves towards the surface (the cantilever is undeflected), as soon it approaches the surface at a very small distance (about 10 nm) it experiments an attraction force; if the cantilever continues with the movement towards the sample, it experiments at some point a repulsion force switching direction of the deflection; this repulsion force continues until it contacts the surface sample, therefore it can be said that the force experimented by the tip is dependent on the distance between the cantilever and the sample.

Contact Mode

In this mode, the tip "touch" the sample surface, and as presented in Fig. 2.20, when the tip is in contact with the sample it experiments a repulsive force, therefore it can be said that contact mode works in repulsive forces and the force applied to scan

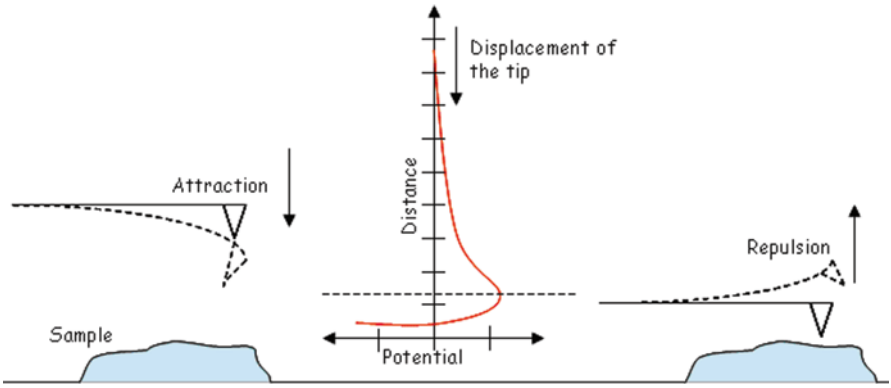

Fig. 2.19 Tip-sample forces in atomic force microscope (AFM)

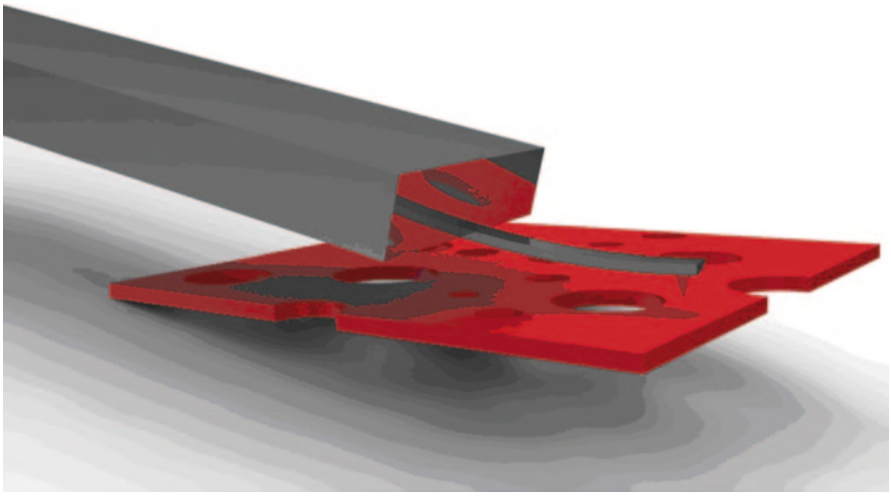

Fig. 2.20 Tip in contact with a surface

Fig. 2.21 Atomic force microdscopy (AFM); tapping mode

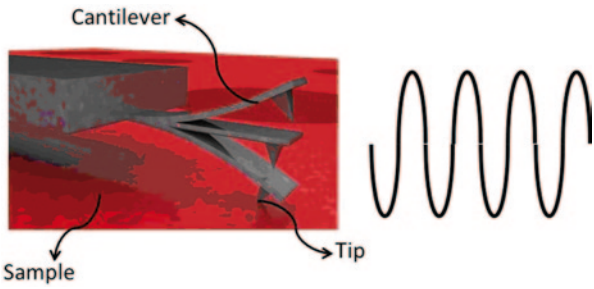

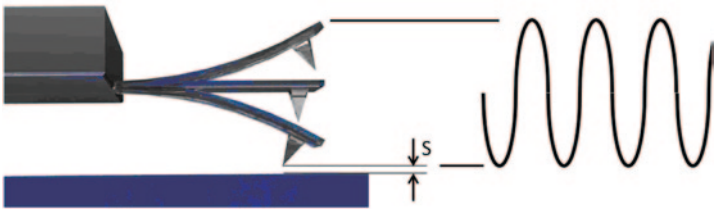

Fig. 2.22 Atomic force microscopy (AFM; noncontact mode

a surface has to be bigger than the repulsion experimented by the tip. Figure 2.18 shows the tip in contact with the surface of a sample.

Tapping Mode

In tapping mode, the cantilever oscillated at or below its resonant frequency and intermittently touch the sample; this technique is used when it is necessary to overcome frictional forces or adhesion, that make the image acquisition difficult. According to Fig. 2.21, tapping mode works in attraction and contact mode.

Noncontact

The cantilever oscillates near to its resonant frequency (almost constant) near the surface of the sample but does not contact it. The interaction of the tip and the sample (Fig. 2.22) induces variations in the amplitude, as a result of different forces such as Van der Waals, electrostatic, chemical magnetic, and drag forces (viscous fluids); these forces decrease the oscillation amplitude, and the controller senses this change to keep a constant distance between the tip and the sample, approximately of the order of 1–10 nm, by the loop control. In order to work with this mode, it is very important to control the environment conditions.

2.3.3.4 Food Applications

In order to prepare food, several industrial process are used such as drying, mixing, evaporation, frying, milling, etc., which promoted changes in the food structure. The AFM has become a useful tool to study nanostructural changes and nanomechanical properties such as stiffness and adhesion in food; also it has been used as sensor to detect microorganism on the food. The AFM has been useful to understand the relation of the structure of food and its relation with function, because the food properties rely upon nano- and microscale, also the nutritional impact is related to its structure (Gunning et al. 2010), In Table 2.4, some examples of AFM applications in the food field are listed.

Table 2.4 Atomic force microscope (AFM) applications

Material	Description	Mode	Parameter	Reference
Starch granules, amylopectin-amylose	Macromolecule and polymer imaging, observation of pectin, study of molecular interactions	—	Topographic image	Hongsshu et al. 2007
Biosensors	AFM cantilevers used as biosensors to detect microorganisms	Tapping	Shift in the resonance frequency due to bacteria growth	Fu et al. 2010
Wheat and potato starch	Study of the structure and the atomic organization of starch	Contact mode	Observation of nodules and general topography	Balwin et al. 1998
Gelatin	Study of the structure mesoscopic and molecular and mechanical properties of gelatin films	SFM (scanning frictional force), contact mode	Topography and friction image were obtained	Haugstad et al. 1994
Fish gelatin	Characterization of the nanostructure of the fish gelatin	Tapping mode	Topographic visualization where structural changes can be seen	Wang et al. 2008
Milk Protein β-casein, β-lactoglobulin y α-lactalbumin	Displacement of proteins in the interface air–water	Contact mode	Acquire images of surface structures formed such as areas covered by proteins and divers formations	Mackie et al.1999
Wheat starch	Visualization of the morphology of the surface and the determination of the size of the starch wheat grains	Contact mode	Obtention of topographic images of starch and visualization of internal structures	Neethirajan et al. 2008
Corn starch	Study of the internal structure of the corn starch	Contact, tapping, lateral force, and friction mode	Image of internal structures of the starch macromolecules and mechanical properties of the corn starch	Baker et al. 2001

Table 2.4 (continued)

Material	Description	Mode	Parameter	Reference
Probiotic bacteria	Determination of adhesion force of the bacterial cell wall	Force volume image	Capturing of adhesion maps and elasticity	Schaer-Zammaretti and Ubbink 2003
Edible films	Characterization of micro-structure of films	Tapping mode	Images of the surface to visual-ize structures and roughness characterization	Arzate-Vázquez et al. 2012

AFM atomic force microscope

References

Abramowitz M, Davidson MW. (2007) Introduction to microscopy. In: Molecular expressions. Florida State University. http://micro.magnet.fsu.edu/primer/anatomy/introduction.html Accesed. 22 Aug 2014

Acevedo NC, Briones V, Buera MP, Aguilera JM (2008) Microstructure affects the rate of chemical, physical and color changes during storage of dried apple discs. J Food Eng 85:222–231

Achir N, Vitrac O, Trystram G (2010) Direct observation of the surface structure of French fries by UV-VIS confocal laser scanning microscopy. Food Res Int 43:307–314

Aguilera JM (2000) Microstructure and food product engineering. Food Technol 54(11):56–64

Aguilera JM (2005) Why food microstructure? J Food Eng 67:3–11

Aguilera JM, Stanley DW (1999) Microstructural principles of food processing and engineering, 2nd edn. Springer, New York

Aguilera JM, Chiralt A, Fito P (2003) Food dehydration and product structure. Trends Food Sci Technol 14:432–437

Akalin AS, Karaman AD (2010) Innfluence of packaging conditions on the textural and sensory characteristics, microstructure and color of industrially produced turkish white cheese during ripenning. J Texture Stud 41:549–562

Allenstein U, Ma Y, Arabi-Hashemi A, Zink M, Mayr SG (2012) Fe-Pd bases ferromagnetic shape memory actuators for medical applications: Biocompatibility, effect of surface roughness and protein coatings. Acta Biomater 9(3):5845–5853

Amos WB, White JG (2003) How the confocal laser scanning microscope entered biological research. Biol Cell 95:335–342

Arltoft D, Madsen F, Ipsen R (2007) Screening of probes for specific localization of polysaccharides. Food Hydrocoll 21:1062–1071

Arzate-Vázquez I, Chanona-Pérez JJ, Calderón-Domínguez G, Terres-Rojas E, Garibay-Febles V, Martínez-Rivas A, Gutiérrez-López GF (2012) Microstructural characterization of chitosan and alginate films by microscopy techniques and texture image analysis. Carbohydr Polym 87(1):289–299

Bai XC, Fernandez IS, McMullan G, Scheres SHW (2013) Ribosome structures to near-atomic resolution from thirty thousand cryo-EM particles. eLife 2:e00461

Baker AA, Miles MJ, Helbert W (2001) Internal structure of the starch granule revealed by AFM. Carbohydr Res 330(2):249–256

Baldwin PM, Adler J, Davies MC, Melia CD (1998) High resolution imaging of starch granule surfaces by atomic force microscopy. J Cereal Sci 27(3):255–265.

Basu S, Shivhare US (2010) Rheological, textural, micro-structural and sensory properties of mango jam. J Food Eng 100(2):357–365

Bates M, Huang B, Zhuang X (2008) Super-resolution microscopy by nanoscale localization of photo-switchable fluorescent probes. Curr Opin Chem Biol 12:505–514

Binnig G, Quate CF, Gerber C (1986) Atomic force microscope. Phys Rev Lett 56(9):930–934

Bordoloi A, Kaur L, Singh J (2012) Parenchyma cell microstructure and tectural characteristics of raw and cooked potatoes. Food Chem 133:1092–1100

Brewer J, Bernardino de la Serna J, Wagner K, Bagatolli LA (2010) Multiphoton excitation fluorescence microscopy in planar membrane systems. Biochim Biophys Acta 1798:1301–1308

Bykov VA, Novikov YA, Rakov AV, Shikin SM (2003) Defining the parameters of a cantilever tip AFM by reference structure. Ultramicroscopy 96(2):175–180

Calero N, Muñoz J, Cox PW, Heuer A, Guerrero A (2013) Influence of chitosan concentration on the stability, microstructure and rheological properties of O/W emulsions formulated with high-oleic sunflower oil and potato protein. Food Hydrocoll 30:152–162

Carvalho CWP, Takeiti CY, Onwulata CI, Pordesimo LO (2010) Relative effect of particle size on the physical properties of corn meal extrudates: Effect of particle size on the extrusion of corn meal. J Food Eng 98:103–109

Chassagne-Berces, S, Poirier C, Devaux M-F, Fonseca F, Lahaye M, Pigorini G, Girault C, Marin M, Guillon F (2009) Changes in texture, cellular structure and cell wall composition in apple tissue as a result of freezing. Food Res Int 42:788–797

Chen L, Feng FX, Lu F, Xu LX, Zhou HG, Li YQ, Guo YX (2011) Effects of camptothecin, etoposide and Ca2 + on caspase-3 activity and myofibrillar disruption of chicken during postmortem ageing. Meat Sci 8(3):165–174

Coote PJ, Billon CMP, Pennell S, McClure PJ, Ferdinando DP, Cole MB (1995) The use of confocal scanning laser microscopy CLSM to study the germination of individual spores of Bacillus cereus. J Microbiol Methods 21:193–208

Cox G (2002) Biological confocal microscopy. Mater Today (Kidlington) 53:34–41

Dunlap M, Adaskaveg JE (1997) Introduction to the scanning electron microscope: theory, practice and procedures. Facility for Advanced Instrumentation. University of California, Davis

Dürrenberger MB, Handschin S, Conde-Petit B, Escher F (2001) Visualization of food structure by confocal laser scanning microscopy CLSM. Lebenson Wiss Technol 34:11–17

Emmambux MN, Stading M (2007) In situ tensile deformation of zein films with plasticizers and filler materials. Food Hydrocoll 21:1245–1255

Florin EL, Rief M, Lehmann H, Ludwig M, Dornmair C, Moy VT, Gaub HE (1995) Sensing specific molecular interactions with the atomic force microscope. Adv Biosens Bioelectron 10(9–10):895–901

Fu L, Zhang K, Li S, Wang Y, Huang TS, Zhang A, Cheng ZY (2010) In situ real-time detection of *E. coli* in water using antibody-coated magnetostrictive microcantilever. Sens Actuators B Chem 150(1):220–225

García-Segovia P, Mognetti C, Andrés-Bello A, Martínez-Monzó J (2010) Osmotic dehydration of *Aloe vera* (*Aloe barbadensis* Miller). J Food Eng 97(2):154–160

Ghosh A, Ali MA, Dias GJ (2009) Effect of cross-linking on microstructure and physical performance of casein protein. Biomacromolecules 10:1681–1688

Gunning AP, Kirby AR, Parker ML, Cross KL, Morris VJ (2010) Utilizing atomic force microscopy in food research. Food Technol 64:32–37

Haider M, Müller H, Uhlemann S, Zach J, Loebau U, Hoeschen R (2008) Prerequisites for a Cc/Cs-corrected ultrahigh-resolution TEM. Ultramicroscopy 108:167–178

Haugstad G, Wladfelter WL, Weberg EB, Weberg RT, Teatherill TD (1994) Probing biopolymer films with scanning force methods. MRS Proc 355: 253. doi:10.1557/PROC-355-253

Hongshun Y, Yifen W, Shaojuan L, Hongjie A, Yunfei L, Fusheng C (2007) Application of atomic force microscopy as a nanotechnology tool in food science. J Food Sci 72 (4): R65–R75

Huang B (2010) Super-resolution optical microscopy: multiple choices. Curr Opin Chem Biol 14: 10–14

Janovjak H, Müller DJ, Humphris ADL (2005) Molecular force modulation spectroscopy revealing the dynamic response of single bacteriorhodopsins. Biophys J 88(2):1423–1431

Jekle M, Becker T (2011) Implementation of a novel tool to quantify dough microstructure. Procedia Food Sci 1: 1–6

Kasas S, Thomson NH, Smith BL, Hansma PK, Miklossy J, Hansma HG (1997) Biological applications of the AFM: from single molecules to organs. Int J Imaging Syst Technol 8(2):151–161

Kim S, Blainey PC, Schroeder CM, Xie XS (2007) Multiplexed single molecule assay for enzymatic activity on flow-stretched DNA. Nat Methods 4(5):397–399.

Koinkar VN, Bhushan B (1996) Microtribological studies of unlubricated and lubricated surfaces using atomic force/friction force microscopy. J Vac Sci Technol A 14(4):2378–2391

Köning K, Schenke-Layland K, Riemann I, Stock UA (2005) Multiphoton autofluorescence imaging of intratissue elastic fibers. Biomaterials 26:495–500

Krzeminski A, GroBhable K, Hinrichs J (2011) Structural properties of stirred yoghurt as influenced by whey proteins. Lebenson Wiss Technol 44:2134–2140

Li ZH, Wang XQ, Wang M, Wang FF, Ge HL (2006) Preparation and tribological properties of the carbon nanotubes-Ni-P composite coating. Tribol Int 39(9):953–957

Li J, Casell A, Dai H (2007) Carbon nanotube tips for MAC mode AFM measurements in liquids application note. Available via Agilent Technologies. http://cp.literature.agilent.com/litweb/pdf/5989-6376EN.pdf. Accessed 04 Sept 2014

Lin S, Chen JL, Lin HW (2005) Measurements of the forces in protein interactions with atomic force microscopy. Curr Proteomics 2:55–81

Lu G, Zangari G (2006) Electrodeposition of platinum nanoparticles on highly oriented pyrolitic graphite. Part II. Morphological characterization by atomic force microscopy. Electrochim Acta 51(12):2531–2538

Mackie AR, Gunning AP, Wilde PJ, Morris VJ (1999) Orogenic displacement of protein from the air/water interface by competitive adsorption, J Colloid Interface Sci 210(1):157–166

Mosele MM, Hansen AS, Hansen M, Schulz A, Martens HJ (2011) Proximate composition, histochemical analysis and microstructural localization of nutrients in immature and mature seeds of marama bean *Tylosema esculentum*—an underutilized food legume. Food Chem 127:1556–1561

Neethirajan S, Thomson DJ, Jayas DS, White NDG (2008) Characterization of the surface morphology of durum wheat starch granules using atomic force microscopy. Microsc Res Tech 71(2):125–132

Nunes C, Santos C, Pinto G, Lopes-da-Silva JA, Saraiva JA, Coimbra MA (2008) Effect of candying on microstructure and texture of plums (*Prunus domestica* L.). Lebenson Wiss Technol 41(10):1776–1783

Orloff J (2009) Handbook of charged particle optics. CRC Press, Rockaway Beach

Paddock SW (2000) Principles and practices of laser scanning confocal microscopy. Molec Biotechnol 16(2):127–149

Perea FMJ, Chanona PJJ, Terrés RE, Calderón DG, Garibay FV, Alamilla BL, Gutiérrez LGF (2010) Microstructure characterization of milk powders and their relationship with rehydration properties. In: Woo MW, Daud WRW, Mujumdar AS (eds) Spray drying technology. TPR Group, Singapore, pp 197–218

Pérez-Millan MI, Becu-Villalobos D (2009) La proteína verde fluorescente ilumina la biociencia. Medicina 69:370–374

Perucho-Lozano, CJ (2011) Optimización de imágenes de muestras biológicas obtenidas por fluorescencia. M Sc dissertation, Universidad Industrial de Santander, Colombia

Prasad VP, Semwogerere D, Weeks ER (2007) Confocal microscopy of colloids. J Phys Condens Matter 19:1–25

Pygall SR, Whetstone J, Timmins P, Melia CD (2007) Pharmaceutical applications of confocal laser scanning microscopy: the physical characterization of pharmaceutical systems. Adv Drug Deliv Rev 59:1434–1452

Raschke K, Shabahang M, Wolf R (2003) The slow and the quick anion conductance in whole guard cells: their voltage-dependent alternation, and the modulation of their activities by abscisic acid and CO_2. Planta 217:639–650

Rewthong O, Soponronnarit S, Taechapairoj C, Tungtrakul P, Prachayawarakorn S (2011) Effects of cooking, drying and pretreatment methods on texture and starch digestibility of instant rice. J Food Eng 103:258–264

Romeih EA, Moe KM, Skeie S (2012) The influence of fat globule membrane material on the microstructure of low-fat Cheddar cheese. Int Dairy J 26: 66–72

Romero de Ivila MD, Ordóñez JA, De la Hoz L, Herrero AM, Cambero MI (2010) Microbial transglutaminase for cold-set binding of unsalted/salted pork models and restructured dry ham. Meat Sci 84:747–754

Ryan GW (2000) Anisotropy of surface roughness on aluminium sheet studied by atomic force microscopy. Microsc Microanal 6(2):137–144

Schaer-Zammaretti P, Ubbink J (2003) Imaging of lactic acid bacteria with AFM—elasticity and adhesion maps and their relationship to biological and structural data. Ultramicroscopy 97(1–4):199–208

Schirmer M, Höchstötter A, Jekle M, Arendt E, Becker T (2013) Physicochemical and morphological characterization of different starches with variable amylase/amylopectin ratio. Food Hydrocoll 32:52–63

Semwogerere D, Weeks ER (2005) Confocal microscopy. In: Wnek GE, Bowlin GL (eds) Encyclopedia of biomaterials and biomedical enginnering. CRC Press, New York, pp 705–714

Silva E, Birkenhake M, Scholten E, Sagis LMC, van der Linden E (2013) Controlling rheology and structure of sweet potato starch noodles with high broccoli poder content by hydrocolloids. Food Hydrocoll 30:42–52

Stadtländer CTKH (2007) Scanning electron microscopy and transmission electron microscopy of mollicutes: challenges and opportunities. In: Méndez-Vilas A, Díaz J (eds) Modern research and educational topics in microscopy, Formatex, Badajoz, pp 122–131

Straub M, Lodemann P, Holroyd P, Jahn R, Hell SW (2000) Live cell imaging by multifocal multiphoton microscopy. Eur J Cell Biol 79:726–734

Sudam BM, Nichols MF (1994) Surface roughness of plasma polymerized films by AFM. In: Proceedings of the 16th Annual International Conference of the IEEE Engineering in Medicine and Biology, Baltimore, 3–6 Nov 1994

Tambe NS, Bhushan B (2005) A new atomic force microscopy based technique for studying nanoscale friction at high sliding velocities. J Phys D Appl Phys 38(5):764–773

Tortonese M, Barrett RC, Quate CF (1993) Atomic resolution with an atomic force microscope using piezoresistive detection. Appl Phys Lett 62(8):834–836

Totosaus A, Pérez-Chabela ML (2009) Textural properties and microstructure of low-fat and sodium-reduced meat batters formulated with gellan gum and dicationic salts. Lebenson Wiss Technol 42:563–569

Tyutyunnikov D (2010) High resolution transmission electron microscopy investigations of FeP t and Au nanoparticles. Dissertation, University Duisburg-Essen. Germany

Ubbink J, Burbidge A, Mezzenga R (2008) Food structure and functionality: a soft matter perspective. Soft Matter 4:1569–1581

Utsunomiya S, Ewing RC. 2003. Application of high-angle annular dark field scanning transmission electron microscopy, scanning transmission electron microscopy-energy dispersive x-ray spectrometry, and energy-filtered transmission electron microscopy to the characterization of nanoparticles in the environment. Environ Sci Technol 37:786–791

van den Berg L, Jan Klok H, van Vliet T, van der Linden E, van Boekel MAJS, van de Velde F (2008) Quantification of a 3D structural evolution of food composites under large deformations using microrheology. Food Hydrocoll 22:1574–1583

van den Berg L, Rosenberg Y, van Boekel MAJS, Rosenberg M, van de Velde F (2009) Microstructural features of composite whey protein/polysaccharide gels characterized at different length scales. Food Hydrocoll 23:1288–1298

Venkatesh MK, Ravi R, Keshava BK, Raghavarao KSMS (2008) Studies on roasting of wheat using fluidized bed roaster. J Food Eng 89:336–342

Voutou V, Eleni-Chrysanthi S (2013) Electron microscopy: the basics. Physics of advanced materials winter school. Available at http://optiki.files.wordpress.com/2013/03/electron-microscopy-the-basics.pdf. Accessed 4 Sept 2014

Wagner M, Ivleva NP, Haisch C, Niessner R, Horn H (2009) Combined use of confocal laser scanning microsopy CLSM and Raman microscopy RM: Investigations on EPS—Matrix. Water Res 43:63–76

Walsh H, Ross J, Hendricks G, Guo M (2010) Physico-chemical properties, probiotic survivability, microstructure, and acceptability of a yogurt-like symbiotic oats-based product using prepolymerized whey protein as a gelation agent. J Food Sci 75:327–337

Wang ZL (2003) New developments in transmission electron microscopy for nanotechnology. Adv Mater 15(18):1497–1514

Wang Y, Yang H, Regenstein JM (2008) Characterization of fish gelatin at nanoscale using atomic force microscopy. Food Biophys 3:269–272

Williams DB, Carter CB (2009) Transmission electron microscopy: a textbook for materials science. Spinger, New York

Chapter 3
Development of Food Nanostructures by Electrospinning

Matteo Scampicchio, Saverio Mannino and Maria Stella Cosio

3.1 Introduction

Among the techniques used to prepare nanostructures, electrospinning is considered one of the most simple, straightforward, cheap, and fast. Most of the advantages and specific features, that are the base of such success, were already described by Rayleigh in 1897 (Burger et al. 2006), studied in more detail by Zeleny in 1914 (Zeleny 1914), and patented for the first time by Formhals in 1934 (Formhals 1934).

In the 1960s, fundamental studies on the jet forming process were initiated by Taylor (Taylor 1969), laying the groundwork of electrospinning. Then, Baumgarten in 1971 and Larrondo and Manley in 1981 revived the technique by electrostatic spinning of respective polyacrylonitrile (PAN) solutions (Baumgarten 1971) and polymer melts (Larrondo and Manley 1981b, Larrondo and Manley 1981c, Larrondo and Manley 1981a). There was a little interest in electrospinning until mid-1990s but, with the growing interest in the field of nano-science and nanotechnology researchers started to realize the huge potential of the process in nano-fiber production (Teo and Ramakrishna 2006). Since then, electrospinning found an increasing use as in different areas, such as high efficiency filter media, protective clothing, catalyst substrates, and adsorbent materials.

S. Mannino (✉) · M. S. Cosio
Department of Food, Environmental and Nutritional Science, University of Milan, Milan, Italy
e-mail: saverio.mannino@unimi.it

M. Scampicchio
Free University of Bozen, Bolzano, Italy

© Springer Science+Business Media New York 2015

H. Hernández-Sánchez, G. F. Gutiérrez-López (eds.), *Food Nanoscience and Nanotechnology,* Food Engineering Series, DOI 10.1007/978-3-319-13596-0_3

3.2 Spun-Fiber Preparation

A spun-fiber is produced via ejection of a jet from a positively charged viscous polymeric solution through a capillary tip to an electrically grounded target. Thus, electrospinning can produce long fiber strands at a comparative low cost and high production rate. Moreover, the simplicity and inexpensiveness of its setup and the ability to produce nano-fibers with a controlled morphology and surface topology from different materials in various fibrous assemblies make it highly attractive to both academia and industry (Ramakrishna et al. 2006).

Many different synthetic polymers, polymer composites, and natural polymers such as collagen and chitin have been electrospun as well as more recently metals, metal oxides, ceramics, and glasses. A multitude of functions such as salts, nanoparticles, biological systems may also be added to the polymer solution and electrospun. Moreover, the nano-fibers can be incorporated into larger units, even into devices. Due to the possibility of electrospinning a wide variety and combination of materials, electrospun nano-fibers are adaptable and usable in diverse applications from bioengineering, human healthcare, and filtration systems to sensing. This versatility has been enhanced by the technological advancement which leaded to develop new and different arrangements of the basic electrospinning setup (Ramakrishna et al. 2006; Sun et al. 2003).

Respect to conventional fiber spinning methods from polymer solutions or melts, electrospinning is not easily scalable. Lab-scale electrospinning systems have generally low productivity due to the low feed rate of the polymeric solution (low flow rates are essential for obtaining ultrafine fibers). To overcome this limitation, Chu and coworkers proposed an array of multiple needles in an electrospinning process (Fang et al. 2006; Srivastava et al. 2007; Theron et al. 2005) This is called multi-jet electrospinning and it is considered a promising way to achieve high productivity and easy scale-up (Zheng et al. 2013; Valipouri et al. 2013; Jiang et al. 2013).

3.2.1 Principle of the Electrospinning Technique

Electrospinning is a technique that allows to obtain, by means of a cold process, polymeric fibers by applying an appropriate electrical field to a concentrated polymeric fluid held in a syringe. The polymer surface at the end of the syringe tip forms a drop if pressure or gravitational force is applied. In the absence of an electric field, the drop surface and shape is maintained by a balance of forces that includes gravitational forces and interfacial forces (surface tension). In electrospinning, the application of an electrical field by means of a high voltage power supply introduces additional forces into the fluid droplet originating different phenomena. First, the surface of the fluid droplet held by its own surface tension at the spinneret tip gets electrostatically charged.

Mutual charge repulsion of polymer and solvent molecules causes a force directly opposite to the surface tension and a contraction of the surface charges to the

grounded collector (Doshi and Reneker 1995). As a consequence, the hemispherical surface of the fluid at the tip of the capillary tube elongates to form a conical shape known as the Taylor cone. The fluid droplet is unstable due to the competition between the electrostatic repulsion and the surface tension. Once the electric field reaches a critical value, repulsive electrostatic force overcomes the surface tension and a fluid jet is formed from the tip of the Taylor cone (Han et al. 2008; Reneker and Yarin 2008; Yarin et al. 2001b). Subsequently, the surface tension causes the droplet shape to relax again, but the liquid stream continues to be ejected in a steady fashion toward the grounded collector. As the jet travels through the electric field, charges accumulate on its surface as a result of the electrostatic repulsion of the different part of the stream. Thus, after traveling linearly for a certain fraction of its path, the fluid jet experiences instabilities in its propagation spiraling or looping. These instabilities are known as bending or whipping instabilities (Yarin et al. 2001b; Reneker et al. 2000; Shin et al. 2001; Yarin et al. 2001a). As a result, while solvent evaporates along the pathway, the fluid jet stream will continuously stretch, extend, and shrink to very small diameter values until dried fibers are deposited onto the collector. The instabilities also cause a strong orientation of the chain molecules in the final fibers. Such orientations cause a significant increase in the strength of the fibers and of the stiffness with values well up to 50 GPa and above (Zuo et al. 2005; Yarin et al. 2001a; Shin et al. 2001; Reneker et al. 2000).

It should be noted that depending on the solution conditions (viscosity, surface tension, polymer concentration) and the process conditions (applied voltage, tip-to-collector distance), instabilities may cause the jet to break up into little droplets and not fibers but particles are deposited on the collector plate. This effect is known as Rayleigh instability and explains what happens in electrospraying or in electrospinning low-viscosity and short-chain molecules (low molecular weight) containing polymer solutions where there are no polymer chains for entanglement (Reneker et al. 2000). During the electrospinning, as the polymer solution is drawn from the capillary, it is the entanglement of polymer chains which prevents the break-up of the electrically driven jet (Ramakrishna et al. 2006). If the conditions of the sample are such that a Rayleigh instability occurs for long-chain molecules that cannot be easily broken up into discrete droplets, e.g., when the polymer concentration is above the overlap concentration, a "pearls-on-a-string" morphology, also known as "beading," can be formed (Fong et al. 1999).

3.2.2 Setup of the Electrospinning Unit

There are basically three components to fulfill the electrospinning process: a syringe, a high voltage power supply, and a collector. A schematic setup of a typical electrospinning unit is shown in Fig. 3.1.

In this setup, a polymer dispersion is placed in the syringe equipped with a blunt ended stainless steel capillary. The syringe is placed in a syringe pump which permits adjustment and precise control of the solution flow rates. The alignment of

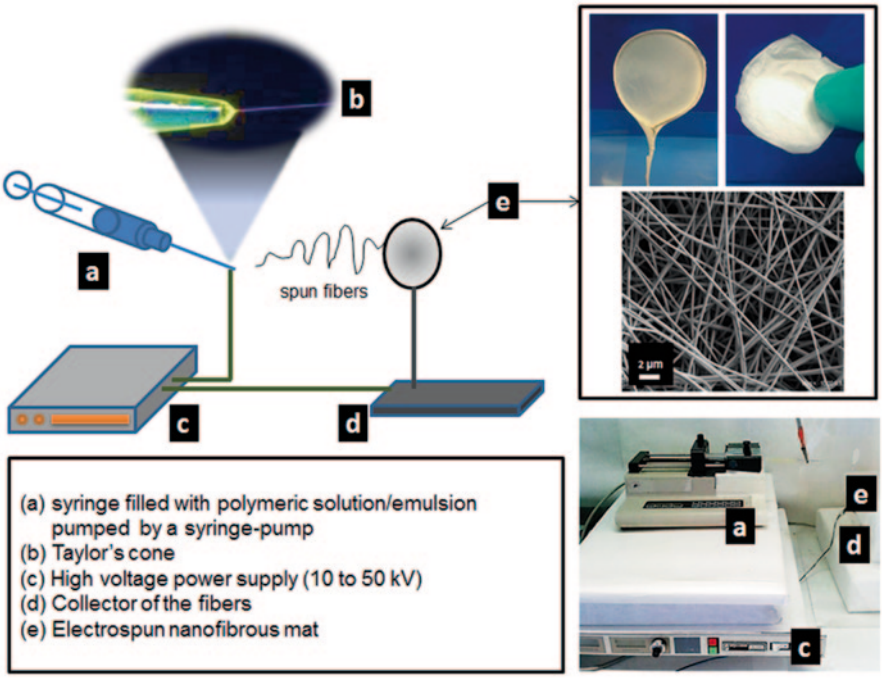

Fig. 3.1 Schematic setup of an electrospinning apparatus

the syringe is usually horizontal although vertical setups have also been described. If the capillary is arranged in a vertical position, the solution may exit the capillary solely due to gravitational forces and a syringe pump may then not be needed (Sahay et al. 2011).

However, this setup allows for much less control than the use of a syringe pump, and consequently the horizontal setup or an arrangement including a syringe pump is preferred. The metallic capillary needle through which the polymeric solution is fed works as a positive electrode and is connected to a high voltage power supply operated in positive DC mode. It represents the high potential difference source capable of producing voltages between 1 and 50 kV. The setup also contains a grounded target collector on which the produced fibers are deposited and which works as the counter electrode. It completes the circuit and allows an electric field to be established between the capillary tip and the target. The involved amperages are typically very low and usually do not exceed a few µAmperes.

Sometimes, it is possible to modify or improve the basic setup of an electrospinning unit, as the aforedescribed one, to further control the electrospinning process and thus to tailor the structures of the resultant fibers (Park et al. 2007; Thorvaldsson et al. 2010). In particular, the majority of modifications reported in literature regards the collectors and the spinneret (Li et al. 2004b; Li and Xia 2004; Li et al. 2004a).

Through the modification of the design or layout of the collector, it is possible to obtain different fiber assemblies or to control the alignment and the orientation of the electrospun fibers. Collectors can be stationary, such as metal plates or parallel electrodes, or rotating-type disks or mandrels (Huang et al. 2003). As the fibers are produced, they are usually spun and collected in a random mat lacking structural orientation. However, collector geometry can influence mat morphology, such as fiber alignment and pattern. For instance, parallel alignment of nano-fibers can be produced by using copper wires spaced evenly in the form of a circular drum as a collector of the electrospun nano-fibers (Katta et al. 2004). Li et al. used a pattern of four electrodes to generate a cross-bar array of aligned nano-fibers (Li and Xia 2004). Using geometric configurations consisting of multiple paired electrodes and their sequentially activating pairs to guide the nano-fiber alignment, one can generate quadratic alignments or more complicated geometries.

Concerning the injection system, instead, a relevant example is the use of a spinneret constituted of two coaxial capillaries. This setup can be used to fabricate polymer nano-fibers with unique core-sheath or hollow structures (Zhang et al. 2006). In addition to the inherent parent polymer properties, nanoparticles, metal salts, and other materials could be added to the polymer matrix to achieve integrated multifunctions (Qu et al. 2013).

Changing also the material of the tip, it is possible to improve the electrospinning process, reducing the applicable voltage and the electrode-to-collector distance. The process is called near-field electrospinning (NFES) and it uses a tungsten electrode as a spinneret by which the polymer solution is supplied in a manner analogous to that of a dip pen (Sun et al. 2006).

In other cases, an electrospinning unit may be enriched by including other components in its arrangement. For instance, an air-blowing module (constituted of an air-blowing assembly and a heating assembly) has been added to an electrospinning setup. It is able to produce a hot air stream around injection system allowing to successfully electrospin polymer solution with an extremely high viscosity. This technique, also known as blowing-assisted electrospinning or electroblowing, has been used to prepare more uniform fibers, as a consequence of the more stable jet achievable compared with that of electrospinning (Burger et al. 2006; Kong et al. 2009; Peng et al. 2008).

3.2.3 Parameters to Consider

To achieve a successful formation of nano-fibers via electrospinning of a polymer solution, the optimal conditions of their spinnability have to be investigated. Polymer spinnability means more precisely the capability of providing fibers with the following features: consistent and controllable diameter; defect-free or defect-controllable surface (controllable morphology).

The key factors influencing the successful outcome of electrospinning are, first, the solution properties, including the viscosity, concentration and molecular weight

of the polymer, elasticity, conductivity, surface tension, electrical conductibility of the solvent, solvent volatility, solubility, glass-transition temperature, melting point, crystallization velocity, and pH value. Second, the processing parameters such as operating voltage, flow rate of the solution, needle-to-collector distance, inner diameter of the needle, hydrostatic pressure in the capillary tube, solution temperature and relative humidity (RH) and temperature, atmospheric pressure, type of atmosphere, and air velocity in the electrospinning chamber (Theron et al. 2004).

3.2.3.1 Solution Properties

One of the principal parameters that impacts the electrospinning process is the viscosity of the polymer solution influencing the resulting fiber morphology and diameter size. Viscosity depends on polymer concentration and molecular weight and the solvent type. Thus, it is possible to say that each parameter under solution properties is connected to each other.

Viscosity is related to the extent of the polymer molecule chain entanglement within the solution. The entanglement of polymers is critical to the formation of fibers. If polymers are not entangled, beads or droplets instead of fibers are typically deposited on the collector plate. Because of this, polymers with higher molecular weight (larger chains) and increasing polymer concentrations favor the formation of fibers. But note that in some cases also a larger fiber diameter (Deitzel et al. 2001; Doshi and Reneker 1995; Fong et al. 1999). For the formation of uniform fibers without beads and/or beaded fibers, the concentration of spinning solution had to be higher than the critical chain entanglement concentration. The critical chain overlap concentration, which is the crossover concentration between the dilute and the semi-dilute concentration regimes, is thus a critical parameter for electrospinning (Tian et al. 2011). In general, higher solution concentration favors the formation of uniform fibers without beads and with higher diameter. Also, an increase in molecular weight of the polymer increases the density of chain entanglements (in solution).

However, increasing the polymer concentration and thus the viscosity of a solution to the point where the flow through the capillary is obstructed may again prevent the formation of fibers (Reneker and Yarin 2008). Moreover, in the case of high polymer concentrations, the drying of the polymer solution at the needle tip may occur leading to the formation of a localized gel, thereby preventing the formation of a proper Taylor cone.

Conversely, at lower viscosities the degree of the polymer chain entanglements is usually lower. Thus, the polymer jets are more likely to break-up and form droplets due to the low viscoelastic force which does not counter-balance the higher Coulombic stretching force. As the electric forces are the main factor responsible for the characteristic jet path, jet instability and stretching of the fibers is one of the main factors responsible for the electrospinning failures of low viscous polymers (Bhattarai and Zhang 2007; Theron et al. 2005).

But low polymer concentrations are often desired as they allow to achieve finer fibers. Unfortunately, this also increases the risk to develop undesirable beaded

structures. This can sometimes be counteracted by increasing the electrical conductivity or decreasing the surface tension (Li and Xia 2004; Li et al. 2004b). About the presence of any defects, such as beads and pores, it is possible to assert that at higher polymer concentration, as at higher viscosity, less is the probability of encounter beads in the final fiber (Fong et al. 1999). The shape of the beads changed from spherical to spindle-like when the polymer concentration varied from low to high levels.

High surface tension of solutions may favor the formation of beads instead of fibers, whereas electrostatic forces (electrical conductivity of the polymer solution) due to charges within the jet have the tendency to elongate and maintain the jet and favor fiber formation (Fong et al. 1999; Doshi and Reneker 1995; Ramakrishna et al. 2006). Thus, solvent with higher dielectric constant and lower surface tension originated fibers with small diameter (Veleirinho et al. 2008).

Factors altering surface tension and/or electrical conductivity may thus influence the electrospinning process. For example, an increase in charges can be obtained by using a solvent with a high dielectric constant or by adding ionic salts or polyelectrolytes. The higher the dielectric constant of solvent, the thinner fiber can be generally obtained, due to the increased charge density in solutions (Son et al. 2004). In this case, more charges are carried along the jet resulting in strong elongation forces due to mutual charge repulsion within the jet. As a consequence the jet is stretched even further, reducing the fiber diameter and the amount of bead formation.

Also the boiling point of the solvent should be low enough such that the evaporation of the solvent occurs under conventional atmospheric conditions. Fiber diameters were found to decrease with increasing density and boiling point of the solvents (Wannatong et al. 2004).

Finally, the formation of chain entanglements is a parameter which affects the stability and formation of fibers during polymer electrospinning. Shenoy has formulated a semi-empirical model to explain the transition from electrospraying to electrospinning. Utilizing entanglement and weight average molecular weights (Me, Mw), the requisite polymer concentration for fiber formation may be determined a priori, eliminating the laborious trial-and-error methodology typically employed to produce electrospun fibers. Complete, stable fiber formation occurs a number of 2.5 entanglements per chain (Shenoy et al. 2005).

In conclusion, polymer solutions must have: a surface tension that is low enough to be overcome by the electrical field; a charge density that is high enough so that the surface tension can be overcome; and a viscosity that is high enough to ensure sufficient chain entanglement to prevent the jet from collapsing into droplets before the solvent has evaporated. Low boiling point clearly speed-up the evaporation. In addition, solvents should enhance the polymer chain interactions by inducing a higher resistance toward disentanglement or orientation by stretching forces applied during the acceleration toward the grounded target thereby increasing the fiber diameter.

3.2.3.2 Processing Parameters

Processing parameters for electrospinning are basically three: a high-voltage supplier, a capillary tube with a pipette or needle of small diameter, and a metal collecting screen (Greiner and Wendorff 2007; Huang et al. 2003). Among the process parameters influencing electrospinning, the applied voltage is the most important one since it determines the degree of electrostatic interaction forces that induce the expulsion of a polymer jet and affects remarkably the fiber diameter (Deitzel et al. 2001). The fibers transport charge across the gap between the charged needle and the electrically grounded target, closing the circuit. At relatively low voltage, electrospray is achieved with the resulting drop formation of the polymer (Jaworek and Sobczyk 2008). As the electrospray voltage is increased smoothly, the measured current undergoes stepwise increments. The charge transport during the passage from electrospray to electrospinning is higher as it reflects the increase in the mass flow rate from the capillary tip to the grounded target (Deitzel et al. 2001).

Usually, operating voltages between 6 and 20 kV are necessary for the formation of the so-called Taylor cone from which the polymer jet is ejected. In certain cases, an increase in the applied voltage will increase the charge density causing the jet to accelerate faster and to stretch more due to greater Coulombic forces in the jet. Lower applied voltages may sometimes cause a decrease in the fiber diameter since a decreased flight speed may allow the jet to split (Zhao et al. 2004). Further, an increase in voltage can cause a broadening of the fiber diameter distribution (Ki et al. 2005).

An increase in the flow rate or a decrease in the syringe tip to the collector distance usually leads to the formation of fibers with larger diameters (Han et al. 2008). In the case of bead formation, increasing flow rates or decreasing the syringe tip to the collector plate distances also increases the size of the beads. High feed rates that exceed a critical value or low tip-to-collector distances can result in the formation of junction zones between the deposited polymer strands or flat ribbon-shaped fibers. This is because there is insufficient time available to allow for all the solvent to evaporate causing the fibers to fuse together. Conversely, at lower feed rates the solvent may have sufficient time to evaporate.

Finally, environmental conditions such as the temperature, the pressure, and the humidity may affect both the solution properties and the rate of the solvent evaporation. For example, increasing the temperature reduces the viscosity allowing for more polymer to be added to the solution. In addition, the solvent may evaporate more rapidly at high temperatures. Conversely at higher humidity, the driving force for solvent evaporation is reduced, resulting again in the formation of junction zones between the deposited fibers or porous surface morphologies. In general, increasing humidity causes an increase in the number, diameter, shape, and distribution of pores located along the surface of electrospun fibers (Casper et al. 2004).

3.2.4 Materials: Electrospun Polymers

Since the discovery of electrospinning, more than 100 different polymers, both synthetic and natural, have been successfully electrospun into nano-fibers, using organic solvents and water or aqueous solutions or from their molten state (Burger et al. 2006).

Among them, the synthetic ones are the most numerous and are considered the most suitable for the fabrication of nano-fibers by electrospinning (Huang et al. 2003, Greiner and Wendorff 2007). They are preferred due to their low cost, high availability, and the wide variety of well-defined molecular and functional characteristics available. Synthetic polymers can be spun in different kinds of solvents more easily than biopolymers. In addition, synthetic polymers may have more well-defined chemical properties (molecular weight, distribution of functional groups along the polymer backbone) that allow for a more uniform behavior during the electrospinning process (Greiner and Wendorff 2007).

Some examples of synthetic polymers successfully electrospun into nano-fibers include PAN, poly(ethylene oxide) (PEO), poly(ethylene terephthalate) (PET), polystyrene (PS), poly(vinyl chloride) (PVC), Nylon-6, poly(vinyl alcohol) (PVA), poly(e-caprolactone) (PCL), polyurethanes (PUs), polycarbonates, polysulfones, poly(vinyl phenol) (PVP), and many others (Burger et al. 2006).

By the way, biopolymer-made fibers are of great interest especially for food industry, because they are nontoxic, edible and digestible, biocompatible or biodegradable, renewable, and sustainable. Unfortunately, electrospinning biopolymers offer many technical challenges: they often require lengthy, complicated, and expensive purification steps prior to electrospinning; they are less soluble in most organic solvents; they have a tendency to form strong hydrogen bonds leading to high solution viscosity or gel formation, which opposes electrospinning; they have poor mechanical properties and processability. A very detailed survey about the recent discoveries of electrospinning of biopolymers is reported in the review of Kriegel et al. (Kriegel et al. 2008).

In addition to the polymer, often more interest is placed on its functionalization. Often, the functionalization step determines in many cases the suitability of use that structures for one or the other application. For instance, one of the most effective strategies to improve the spinnability of polymers with poor features, like low molecular weight, for electrospinning process is to blend them with other spinnable polymers in solution. This is the case for instance of conjugated polymers, which have limited solubility, or most of biopolymers. In fact, the majority of blends electrospun are constituted of biopolymers, difficult to spin, and synthetic ones. For instance, electrospinning of collagen has been possible blending it with PEO (Buttafoco et al. 2006; Huang et al. 2001), PCL (Venugopal and Ramakrishna 2005; Venugopal et al. 2005), or PLA-co-PCL (Lu et al. 2012).

3.3 Applications of Electrospinning in the Food Sector

Food science research has increasingly focused on using polymer nano-fibers in areas such as active packaging and additive encapsulation and process (Perez-Masia et al. 2013). The high surface-to-volume ratio due to the small nano-fiber sizes favors the increased nano-effects, which include increased surface reactivity, high strength-to-weight ratio, and higher thermal conductivity (Yarin et al. 2007).

We previously described how the electrospinning process could yield these nano-fibers through a simple and flexible method. The electrospinning parameters (i.e., applied electric field, solution flow rate, and distance from syringe tip to collector) can be tuned in order to modify fiber properties such as morphology, porosity, and sizes to tailor the fiber mats according to the desired function and application. In the subsequent paragraphs, some applications of electrospun nano-fibers in the food sector and in particular in the encapsulation of bioactive compounds and the filtration process will be described.

3.3.1 Nano-Fibers for Encapsulation and Release of Natural Bioactive Compounds

Promotion of health and prevention of disease through improved nutrition demands the development of food-grade delivery systems, including active packaging and edible structures, to encapsulate, protect, and deliver bioactive components. In particular, volatile substances with antimicrobial features, such as natural essential oils, absolutes, essences, extracts, resins, infusions, etc. are of great interest for the active packaging industry. Their efficient encapsulation and release represent a major challenge, considering their high fugacity and the fact that they are very sensitive to heat, oxygen, and light.

Conventionally, studies involve the dispersion of the active agent in carriers with limited surface areas (e.g., polymer films and layers), with considerable losses during production and storage. Furthermore, the release of active substances from these structures is mainly based on concentration-dependent passive diffusion.

Nano-fibers produced from polymers or biopolymers have shown to be particular promising structures because of their submicron scale and the consequent large surface-to-mass ratios, which allows for more specific triggered releases, yet protecting the active molecules from environmental factors. Furthermore, the kinetics of release can be controlled by adjusting the fiber diameter, morphology, and composition.

As already pointed out, the production of these nanostructured materials by electrospinning, is very simple, cheap, and recently it has been demonstrated that they can overcome several of the problems related to volatiles encapsulation, therefore representing an interesting solution for example to the food-packaging industry. Operating simplicity of the equipment clashes, however, with the complexity of the setup of experimental variables to produce nano-fibers with controlled morphology.

The production on an industrial scale started in the 1990s in various fields including the Life Science. Although nowadays there are several patents about the development of drug delivery systems, the industrial application is limited to niche areas because of the difficulty of monitoring large-scale processes such as the food active packaging sector (Huang et al. 2003).

However, this simple technique allows the production of nano-fibrous polymeric unwoven membranes formed by polymer fibers with diameters ranging from tens to hundreds of nanometers (Greiner and Wendorff 2008; Greiner and Wendorff 2007; Yarin et al. 2007). By virtue of their submicron-to-nanoscale diameter and very large surface area, electrospun fibers may offer a number of additional advantages compared to film and sheet carriers, as they are more responsive to changes in the surrounding atmosphere (e.g., RH and temperature changes), which enables a tunable release of the entrapped compounds (Vega-Lugo and Lim 2009). Moreover, since the electrospinning process takes place at ambient conditions, electrospun fibers are more suitable to encapsulate thermally labile substances than fibers prepared by conventional melt spinning or films produced by extrusion process, or other encapsulation methods, such as spray drying (Qi et al. 2006) and fluid bed coating (de Vos et al. 2010). Furthermore, electrospinning seems suitable to trap aroma compound inclusion complexes (AC-IC) within the meshes of the membrane. This is the case of cyclodextrins inclusion complexes with hydrophobic substances (Koontz et al. 2010; Koontz et al. 2009). Different literature is present on the electrospinning of cyclodextrins with polymer (Uyar et al. 2010; Uyar et al. 2009; Celebioglu et al. 2014; Kayaci et al. 2013; Kayaci and Uyar 2012: Celebioglu and Uyar 2011; Celebioglu and Uyar 2010), but few works are focalized on inclusion of active cyclodextrin in biopolymer, even less on active system bases on complete edible polysaccharides, for food and food-packaging applications. Moreover, in these systems the AC-IC is formed before electrospinning in a multisteps process. Electrospun soy proteins and zein have been used for controlled release of allyl isothiocyanate (Vega-Lugo and Lim 2009) and as carriers for catechins (Li et al. 2009), respectively. However, edible proteic systems, such as the above mentioned, or gelatin and collagen, cannot be electrospun from aqueous solutions due to extensive hydrogen bonding resulting in gel formation, and therefore toxic or aggressive solvents are required to produce these nano-fibers. Casein or wheat proteins have poor electrospinnability and need to be mixed with other polymers such as PEO, PVA, or other synthetic biopolymers like polylactic acid or ε-caprolactone with the use of toxic solvents (Xie and Hsieh 2003; Castro-Enriquez et al. 2012; Montano-Leyva et al. 2011; Selling et al. 2012; Aceituno-Medina et al. 2013). This limits the edibility of the resulting systems.

Edible polysaccharides are commonly used in food applications as coating agents, thickening agents, or additives for technological aims; they are not allergenic and do not need toxic solvents to be electrospun (Schiffman and Schauer 2008; Stijnman et al. 2011; Mascheroni et al. 2013). Pullulan is a natural, water-soluble linear polysaccharide industrially produced by fermentation of starch syrup with a selected strain of *Aureobasidium pullulans*. It consists of maltotriose units (α−1,4 linked glucose molecules) polymerized by α-1,6-glucosidic bonds forming

a stair-step-type structure and has good electrospinnable properties. This polymer however alone is not suitable to encapsulate hydrophobic compounds because of its hydrophilic nature and a linear structure. However, it was shown by Mannino group that it is possible to build a system where β-cyclodextrin crystals, encapsulating the aroma compounds, can be simultaneously fixed to the meshes of pullulan nano-fibers (Mascheroni et al. 2013). This system demonstrates a potential applicability for enhancing microbial safety, in particular of fresh foods at various RH.

Another example is the encapsulation by means of electrospinning of the light sensitive model β-carotene, a colorant and antioxidant molecule widely used in the food industry, in ultrafine fibers of zein prolamine, a sustainable agropolymer. Fiber capsules were in the micro- and nano-range in the cross-section and the encapsulation preserved the fluorescence of the polyene molecules. Observations with confocal Raman imaging spectroscopy showed that the antioxidant was stable and widely dispersed inside the zein fibers but agglomerated in some areas. As a result, electrospinning of zein prolamine shows an excellent outlook for its application in the stabilization of light sensitive added-value food components (Fernandez et al. 2009; Torres-Giner et al. 2008).

The feasibility of producing PVA nano-fibers containing fine-disperse hexadecane droplets by electrospinning a blend of hexadecane-in-water emulsions and PVA was demonstrated by McClemens group (Kriegel et al. 2009; Kriegel et al. 2010). Hexadecane oil-in-water nano-emulsions ($d_{10} = 181.2 \pm 0.1$ nm) mixed with PVA at pH 4.5 yield polymer-emulsion blends containing 0.5–1.5 wt% oil droplets and 8 wt% PVA. Analysis of dry fiber mats and their solutions showed that emulsion droplets were indeed part of the electrospun fiber structures. Depending on the concentration of hexadecane in the initial emulsion-polymer blends, droplets were dispersed in the fibers as individual droplets or in the form of aggregated flocks of hexadecane droplets. Nano-fibers with spindle-like perturbations or nano-fibers containing bead-like structures with approximately five times larger than the size of droplets in the original nano-emulsion were obtained. Remarkably, incorporation of hexadecane droplets in fibers did not alter size of individual droplets, that is, no coalescence occurred. The manufacture of solid matrix containing nano-droplets could be of substantial interest for manufacturers wishing to develop encapsulation system for lipophilic functional compounds such as lipid-soluble flavors, antimicrobials, antioxidants, and bioactives with tailored release kinetics. However, use of an organic solvent is: (a) not feasible if one wants to electrospin hydrophilic polymers and (b) use of organic solvents is generally highly undesirable in the food industry.

Another interesting approach is the preparation of biopolymeric (pullulan and β-cyclodextrin) emulsions in water to be electrospun to fabricate nano-fibrous membranes (NFM) and to encapsulate a bioactive volatile compound (R−(+)−limonene) simultaneously. The morphology of the polysaccharide membranes obtained can be considered as a pullulan nano-fibrous matrix with small crystals homogeneously dispersed. Encapsulation occurs because the conical cavity of the β-cyclodextrin is hydrophobic and able to bind nonpolar molecules in water solutions, combined to the high evaporation rate of the solvent during the electrospinning process. The methodology developed allows encapsulation of the volatile compound in a rapid

and efficient way. Moreover, the release of the limonene from the membranes can be modulated by relative humidity changes, which enables controlled release applications as an active device for food or active packaging.

Electrospinning was also applied to the development of nonmeat food products with an appealing structure. Being able to electrospin proteins in a food-grade way can open a new route toward nutritionally and texturally appealing meat replacers.

Proteins are notoriously difficult to electrospin, mainly because of their complex secondary and tertiary structure and in order to be spinnable, proteins should be well dissolved in a random coil fashion. Globular proteins have too little interaction with each other to entangle during the spinning process. Casein, as a protein with a random coil structure in water, may be a good candidate but electrospinning of pure casein is hard to achieve probably due the clustering of the casein molecules (Xie and Hsieh 2003).

Electrospinning of proteins is possible under conditions in which they dissolve well, in a random coil fashion. Solvents with a good solvent quality disrupt both intra- and inter protein interactions, and solubilize the resulting unstructured protein. However, a few proteins can be spun from solvents acceptable in food industry. One example is zein, the storage protein of maize, which is soluble in 70 % ethanol (Torres-Giner et al. 2008; Yao et al. 2007). In this solvent, the protein is unstructured and behaves similar to a well-soluble polymer.

A second protein, which can be spun from food-grade solvents, is gelatin. Spinning of gelatin solutions from water has long been problematic, because of the gelation at room temperature. However, by using an electrospinning device that includes a temperature control, spinning of gelatin from water is possible (Moon and Farris 2009). The solution should be heated above the melting point making gelatin to behave as a random-coil polymer. Zein or gelatin can be used as carriers for other proteins that cannot be spun by themselves in a way acceptable in the food industry. Hence, using gelatin, zein, or their mixture as carriers for nutritionally complete proteins can yield a controlled way of making fibrous structures for food applications.

3.3.2 Nano-Fibrous Membranes as Filtration Systems

Nanotechnology can greatly enhance filtration systems and overcome the aforementioned drawbacks. One of the main attractive features of nanostructured materials, such as nano-membranes and nano-fibers, is their high surface available. In general, high surface available is desired to enhance reactivity of the materials and speed up adsorption or release mechanisms. But, more interesting is the nanostructured material which contains cavities, pores or, in general, empty volumes, also implies high permeability. This property is fundamental because it means that a membrane which is nanostructured, such as those prepared by electrospinning, also shows a negligible barrier toward diffusion.

Some of the first applications of NFMs as filtration systems were for environmental or product ultra- and nano-filtration. High porosity with small pore size, interconnectivity, microscale interstitial space, high permeability, large surface-to-volume ratio, and low basis weight make nonwoven electrospun nano-fiber meshes an excellent material for filtration of very small particles (less than 100 nm) or even molecules (Bognitzki et al. 2001).

There is a demand of filter structures with improved filtering streams with higher temperature, humidity, flow rates, able to cut off micron, and submicron particulate materials. Today more than 20 companies produce and use electrospun nano-fibers for this purpose because they offer improved physical and chemical stability, they can be fashioned into useful products formats (multilayered filtration structure), and are ease to back-pulsing cleaning. Nevertheless, there are still some challenges in their production such as homogeneity of size distribution, uniformity of structure, and deposition (Barhate et al. 2006; Barhate and Ramakrishna 2007; Kaur et al. 2011).

3.3.3 Application in Environmental Filtration

The control over airborne and waterborne contaminants, hazardous biological agents, allergens, and pollutants is a key issue in food, pharmaceuticals, and biotechnology processes. Particle removal from air and wastewater by a NFM has been studied by Gibson et al. The nano-fiber membrane showed an extremely effective removal (~100 % rejection) of airborne particles with diameters between 1 μm and 5 μm by both physical trapping and adsorption (Gibson et al. 2001). For particle removal from aqueous solution, recent results showed that electrospun membranes can successfully remove particles 3 -10 μm in size (95 % rejection) without a significant drop in flux performance. No particles were found trapped in the membrane, so the membrane could be effectively recovered upon cleaning (Gibson et al. 2001). Desai et al. demonstrated the effective removal of heavy metals such as chromium from water using deaectylated chitosan with NH3 functional group blended in PEO NFM with binding capacity of about 17 μg/mg (Desai et al. 2009; Desai et al. 2008).

Among the applications of nano-fibrous filtering media, the most interesting for applications in food sector are those connected with the production of antimicrobial filter. Antimicrobial nano-fibrous filters may be used to reduce the problems of fouling caused by biofilm during water treatment. A study of Bjorge et al. (Bjorge et al. 2009) for the removal of microorganisms showed that, in the case of non-functionalized membranes, the removal efficiency is not satisfactory. This was explained by the fact that the transmembrane pressure may cause changes in the nonwoven membrane structure which leads to the enlargement of the pores and allows bacteria to pass the membrane. However, functionalization of the membranes with Ag nanoparticles gave a log 4 removal. It is generally known that these particles only have effect on gram-negative bacteria such as *Escherichia coli*, gram-positive bacteria are not affected by these nanoparticles.

Zhang et al. produced nano-fibers from PAN and incorporated silver nanoparticles to create an improved filtration membrane with antibacterial properties effective against gram-positive and gram-negative bacteria (Zhang et al. 2011). Jeong electrospun PU cationomers with quaternary ammonium groups to make fibers inherently antimicrobial (Jeong et al., 2007). Similar results were obtained by Hong incorporating (Hong and Jeong 2011; Jeong et al. 2007) silver nanoparticles on nylon-6 nano-fibers (Hong and Jeong 2011).

3.3.4 Food Filtration

Electrospun NFMs may be a potential alternative tool as affinity or ultrafiltration membrane for highly selectivity separations for scale protein purifications or homogenization membrane for the preparation of emulsion with drop size less than 100 nm. A nano-fibrous affinity membrane was prepared by covalently binding Cibacron Blue F3GA (CB) to the cellulose electrospun nano-fibers. That membrane showed abilities to capture BSA or bilirubin. In addition, the BSA absorbed membrane can be regenerated by rinsing with elution buffer (Ma et al. 2005).

Veleirinho et al. developed an electrospun PET membrane for apple juice clarification (Veleirinho and Lopes-da-Silva 2009). The apple juice obtained from electrospun nano-fiber membrane filtration revealed physicochemical characteristics comparable to those from juice clarified by ultrafiltration or by conventional clarification using filtering aids. Nevertheless, the new process showed a high flux performance and revealed to be much faster, simple, and more economical than the traditional processes. This study introduced a new concept of clarification and opening new approaches for the juice processing industry or even for other food industry fields.

Antimicrobial nano-fibrous filters can be applied to beverages industry to improve their microbial safety. This also will improve the efficiency of the process by completely eliminating thermal treatment steps (e.g., pasteurization) thereby preserving valuable quality attributes such as flavors and vitamins (Kriegel et al. 2008).

Recently, Fuenmayor et al. (2014) developed an electrospun nylon-6 membrane for the filtration of apple juices. The mechanism for the observed filtration behavior was explained in detail with a model based on three resistances in series, respectively, the initial filter resistance, the polarization resistance, and the cake resistance and compared with commercial filtration membrane. Electrospun membranes have initial filter resistance values (as described by the Darcy's law in experiment using distilled water as the liquid flowing through the membrane) much higher than commercial membranes. Furthermore, the concentration polarization resistance of the electrospun nylon-6 membrane was comparable to the commercial polyamide membranes. Polarization resistance values reflect that the accumulation of solute at the membrane interface is responsible to limit the flux, leading to charged chemical species promoting local aggregation and cohesiveness of the fouling layer. However, as the pressure drop increases, the Rp value for the electrospun NFM decreases.

The behavior of commercial membranes was opposite. Apparently, at high pressure, the adsorption of fouling species on the fibers is enhanced and, at the same time, the resistance toward diffusion is reduced. This feature can be explained as at higher pressures, the foulants on the fiber surface are more easily adsorbed on the large surface of the nanostructured membranes, which in turn, reduces the resistance to flow of the overall membrane (Fuenmayor et al. 2014).

Also, Scampicchio et al. reported of the selective adsorption of nylon-6 NFMs toward certain phenol-like species. This selectivity was dependent on the dissociation constant of the phenols (Scampicchio et al. 2008).

References

Aceituno-Medina M, Lopez-Rubio A, Mendoza S, Lagaron JM (2013) Development of novel ultrathin structures based in amaranth (*Amaranthus hypochondriacus*) protein isolate through electrospinning. Food Hydrocoll 31(2):289–298

Barhate RS, Ramakrishna S (2007) Nanofibrous filtering media: filtration problems and solutions from tiny materials. J Memb Sci 296(1/2):1–8

Barhate RS, Loong CK, Ramakrishna S (2006) Preparation and characterization of nanofibrous filtering media. J Memb Sci 283(1/2):209–218

Baumgarten PK (1971) Electrostatic spinning of acrylic microfibers. J Colloid Interface Sci 36:71–79

Bhattarai N, Zhang M (2007) Controlled synthesis and structural stability of alginate-based nanofibers. Nanotechnology 18(45):455601

Bjorge D, Daels N, De Vrieze S, Dejans P, Van Camp T, Audenaert W, Hogie J, Westbroek P, De Clerck K, Van Hulle SWH (2009) Performance assessment of electrospun nanofibers for filter applications. Desalination 249(3):942–948

Bognitzki M, Czado W, Frese T, Schaper A, Hellwig M, Steinhart M, Greiner A, Wendorff J (2001) Nanostructured fibers via electrospinning. Adv Mater 13(1):70–72

Burger C, Hsiao BS, Chu B (2006) Nanofibrous materials and their applications. Annu Rev Mater Res 36:333–368

Buttafoco L, Kolkman N, Engbers-Buijtenhuijs P, Poot A, Dijkstra P, Vermes I., Feijen J (2006) Electrospinning of collagen and elastin for tissue engineering applications. Biomaterials 27(5):724–734

Casper C, Stephens J, Tassi N, Chase D, Rabolt J (2004) Controlling surface morphology of electrospun polystyrene fibers: effect of humidity and molecular weight in the electrospinning process. Macromolecules 37(2):573–578

Castro-Enriquez DD, Rodriguez-Felix F, Ramirez-Wong B, Torres-Chavez PI, Castillo-Ortega MM, Rodriguez-Felix DE, Armenta-Villegas L, Ledesma-Osuna AI (2012) Preparation, characterization and release of urea from wheat gluten electrospun membranes. Materials 5(12):2903–2916

Celebioglu A, Uyar T (2010) Cyclodextrin nanofibers by electrospinning. Chem Commun 46(37):6903–6905

Celebioglu A, Uyar T (2011) Electrospinning of polymer-free nanofibers from cyclodextrin inclusion complexes. Langmuir 27(10):6218–6226

Celebioglu A, Aytac Z, Umu OCO, Dana A, Tekinay T, Uyar T (2014) One-step synthesis of size-tunable Ag nanoparticles incorporated in electrospun PVA/cyclodextrin nanofibers. Carbohydr Polym 99:808–816

Deitzel J, Kleinmeyer J, Harris D, Tan N (2001) The effect of processing variables on the morphology of electrospun nanofibers and textiles. Polymer 42(1):261–272

Desai K, Kit K, Li J, Zivanovic S (2008) Morphological and surface properties of electrospun chitosan nanofibers. Biomacromolecules 9(3):1000–1006
Desai K, Kit K, Li J, Davidson PM, Zivanovic S, Meyer H (2009) Nanofibrous chitosan non-wovens for filtration applications. Polymer 50(15):3661–3669
de Vos P Faas MM Spasojevic M Sikkema J (2010) Encapsulation for preservation of functionality and targeted delivery of bioactive food components. Int Dairy J 20(4):292–302
Doshi J, Reneker D (1995) Electrospinning process and applications of electrospun fibers. J Electrostat 35(2/3):151–160
Fang D, Chang C, Hsiao BS and Chu B (2006) Development of multiple-jet electrospinning technology. Polym Nanofibers, vol 918, p 91
Fernandez A, Torres-Giner S, Lagaron JM (2009) Novel route to stabilization of bioactive antioxidants by encapsulation in electrospun fibers of zein prolamine. Food Hydrocoll 23(5):1427–1432
Fong H, Chun I, Reneker D (1999) Beaded nanofibers formed during electrospinning. Polymer 40(16):4585–4592
Formhals A (1934) Process and apparatus for preparing artificial threads. US Patent 1,975, 504, 10 Feb 1934
Fuenmayor CA, Lemma SM, Mannino S, Mimmo T, Scampicchio M (2014) Filtration of apple juice by nylon nanofibrous membranes. J Food Eng 122:110–116
Gibson P, Schreuder-Gibson H, Rivin D (2001) Transport properties of porous membranes based on electrospun nanofibers RID D-2398-2010. Colloids Surf A Physicochem Eng Asp 187:469–481
Greiner A, Wendorff JH (2007) Electrospinning: a fascinating method for the preparation of ultrathin fibres. Angew Chem Int Ed Engl 46(30):5670–5703
Greiner A, Wendorff JH (2008) Functional self-assembled nanofibers by electrospinning. In: Shimizu T (ed) Self-assembled nanomaterials I: nanofibers. Springer, New York, pp 107–171
Han T, Yarin AL, Reneker DH (2008) Viscoelastic electrospun jets: initial stresses and elongational rheometry. Polymer 49(6):1651–1658
Hong HF, Jeong S (2011) Effect of nano sized silver on electrospun nylon-6 fiber. J Nanosci Nanotechnol 11(1):372–376
Huang L, Nagapudi K, Apkarian R, Chaikof E (2001) Engineered collagen-PEO nanofibers and fabrics. J Biomater Sci Polym Ed 12(9):979–993
Huang Z, Zhang Y, Kotaki M, Ramakrishna S (2003) A review on polymer nanofibers by electrospinning and their applications in nanocomposites. Compos Sci Technol 63(15):2223–2253
Jaworek A, Sobczyk AT (2008) Electro spraying route to nanotechnology: an overview. J Electrostat 66(3/4):197–219
Jeong EH, Yang H, Youk JH (2007) Preparation of polyurethane cationomer nanofiber mats for use in antimicrobial nanofilter applications. Mater Lett 61(18):3991–3994
Jiang G, Zhang S, Qin X (2013) High throughput of quality nanofibers via one stepped pyramid-shaped spinneret. Mater Lett 106:56–58
Katta P, Alessandro M, Ramsier R, Chase G (2004) Continuous electrospinning of aligned polymer nanofibers onto a wire drum collector. Nano Lett. 4(11):2215–2218
Kaur S, Barhate R, Sundarrajan S, Matsuura T, Ramakrishna S (2011) Hot pressing of electrospun membrane composite and its influence on separation performance on thin film composite nanofiltration membrane. Desalination 279(1/3):201–209
Kayaci F, Uyar T (2012) Electrospun zein nanofibers incorporating cyclodextrins. Carbohydr Polym 90(1):558–568
Kayaci F, Ertas Y, Uyar T (2013) Enhanced thermal stability of eugenol by cyclodextrin inclusion complex encapsulated in electrospun polymeric nanofibers. J Agric Food Chem 61(34):8156–8165
Ki C, Baek D, Gang K, Lee K, Um I, Park Y (2005) Characterization of gelatin nanofiber prepared from gelatin-formic acid solution. Polymer 46(14):5094–5102
Kong CS, Yoo WS, Lee KY, Kim HS (2009) Nanofiber deposition by electroblowing of PVA (polyvinyl alcohol). J Mater Sci 44(4):1107–1112

Koontz JL, Marcy JE, O'Keefe SF, Duncan SE (2009) Cyclodextrin inclusion complex formation and solid-state characterization of the natural antioxidants alpha-tocopherol and quercetin. J Agric Food Chem 57(4):1162–1171

Koontz JL, Moffitt RD, Marcy JE, O'Keefe SF, Duncan SE, Long TE (2010) Controlled release of -tocopherol, quercetin, and their cyclodextrin inclusion complexes from linear low-density polyethylene (LLDPE) films into a coconut oil model food system. Food Addit Contam Part A Chem Anal Control Expo Risk Assess 27(11):1598–1607

Kriegel C, Arrechi A, Kit K, McClements DJ, Weiss J (2008) Fabrication, functionalization, and application of electrospun biopolymer nanofibers. Crit Rev Food Sci Nutr 48(8):775–797

Kriegel C, Kit KA, McClements DJ, Weiss J (2009) Nanofibers as carrier systems for antimicrobial microemulsions. Part I: fabrication and characterization. Langmuir 25(2):1154–1161

Kriegel C, Kit KM, McClements DJ, Weiss J (2010) Nanofibers as carrier systems for antimicrobial microemulsions. II. Release characteristics and antimicrobial activity. J Appl Polym Sci 118(5):2859–2868

Larrondo L, Manley JRS (1981a) Electrostatic fiber spinning from polymer melts. III. Electrostatic deformation of a pendant drop of polymer melt. J Polym Sci B Polym Phys 19:933–940

Larrondo L, Manley JRS (1981b) Electrostatic fiber spinning from polymer melts. I. Experimental observations on fiber formation and properties. J Polym Sci B Polym Phys 19:909–920

Larrondo L, Manley JRS (1981c) Electrostatic fiber spinning from polymer melts. II. Examination of the flow field in an electrically driven jet. J Polym Sci B Polym Phys 19:921–932

Li D, Xia Y (2004) Electrospinning of nanofibers: reinventing the wheel? Adv Mater 16(14):1151–1170

Li D, Babel A, Jenekhe S, Xia Y (2004a) Nanofibers of conjugated polymers prepared by electrospinning with a two-capillary spinneret. Adv Mater 16(22):2062–2066

Li D, Wang Y, Xia Y (2004b) Electrospinning nanofibers as uniaxially aligned arrays and layer-by-layer stacked films. Adv Mater 16(4):361–366

Li Y, Lim L, Kakuda Y (2009) Electrospun zein fibers as carriers to stabilize (-)-epigallocatechin gallate. J Food Sci 74(3):C233–C240

Lu L, Wu D, Zhang M, Zhou W (2012) Fabrication of polylactide/poly(epsilon-caprolactone) blend fibers by electrospinning:morphology and orientation. Ind Eng Chem Res 51(9):3682–3691

Ma Z, Kotaki M, Ramakrishna S (2005) Electrospun cellulose nanofiber as affinity membrane. J Memb Sci 265(1/2):115–123

Mascheroni E, Alberto Fuenmayor C, Cosio MS, Di Silvestro G, Piergiovanni L, Mannino S, Schiraldi A (2013) Encapsulation of volatiles in nanofibrous polysaccharide membranes for humidity-triggered release. Carbohydr Polym 98(1):17–25

Montano-Leyva B, Rodriguez-Felix F, Torres-Chavez P, Ramirez-Wong B, Lopez-Cervantes J, Sanchez-Machado D (2011) Preparation and characterization of durum wheat (*Triticum durum*) straw cellulose nanofibers by electrospinning. J Agric Food Chem 59(3):870–875

Moon S, Farris RJ (2009) Electrospinning of heated gelatin-sodium alginate-water solutions. Polym Eng Sci 49(8):1616–1620

Park S, Park K, Yoon H, Son J, Min T, Kim G (2007) Apparatus for preparing electrospun nanofibers: designing an electrospinning process for nanofiber fabrication. Polym Int 56(11):1361–1366

Peng M, Sun Q, Ma Q, Li P (2008) Mesoporous silica fibers prepared by electroblowing of a poly(methyl methacrylate)/tetraethoxysilane mixture in N, N-dimethylformamide. Microporous Mesoporous Mater 115(3):562–567

Perez-Masia R, Lopez-Rubio A, Lagaron JM (2013) Development of zein-based heat-management structures for smart food packaging. Food Hydrocoll 30(1):182–191

Qi H, Hu P, Xu J, Wang A (2006) Encapsulation of drug reservoirs in fibers by emulsion electrospinning: morphology characterization and preliminary release assessment. Biomacromolecules 7(8):2327–2330

Qu H, Wei S, Guo Z (2013) Coaxial electrospun nanostructures and their applications. J Mater Chem A Mater Energy Sustain 1(38) 11513–11528

Ramakrishna S, Fujihara K, Teo W, Yong T, Ma Z, Ramaseshan R (2006) Electrospun nanofibers: solving global issues. Mater Today (Kidlington) 9(3):40–50
Reneker DH, Yarin AL (2008) Electrospinning jets and polymer nanofibers. Polymer 49(10) 2387–2425
Reneker D, Yarin A, Fong H, Koombhongse S (2000) Bending instability of electrically charged liquid jets of polymer solutions in electrospinning. J Appl Phys 87(9):4531–4547
Sahay R, Thavasi V, Ramakrishna S (2011) Design modifications in electrospinning setup for advanced applications. J Nanomater. doi:10.1155/2011/317673
Scampicchio M, Bulbarello A, Arecchi A, Mannino S (2008) Electrospun nanofibers as selective barrier to the electrochemical polyphenol oxidation. Electrochem Commun 10(7):991–994
Schiffman JD, Schauer CL (2008) A review: electrospinning of biopolymer nanofibers and their applications. Polym Rev (Phila Pa) 48(2):317–352
Selling GW, Woods KK, Biswas A (2012) Electrospun zein fibers using glyoxal as the crosslinking reagent. J Appl Polym Sci 123(5):2651–2661
Shenoy S, Bates W, Frisch H, Wnek G (2005) Role of chain entanglements on fiber formation during electrospinning of polymer solutions:good solvent, non-specific polymer-polymer interaction limit. Polymer 46(10):3372–3384
Shin Y, Hohman M, Brenner M, Rutledge G (2001) Experimental characterization of electro spinning: the electrically forced jet and instabilities. Polymer 42(25):9955–9967
Son W, Youk J, Lee T, Park W (2004) The effects of solution properties and polyelectrolyte on electrospinning of ultrafine poly(ethylene oxide) fibers. Polymer 45(9):2959–2966
Srivastava Y, Marquez M and Thorsen T (2007) Multijet electrospinning of conducting nanofibers from microfluidic manifolds. J Appl Polym Sci 106(5):3171–3178
Stijnman AC, Bodnar I, Tromp RH (2011) Electrospinning of food-grade polysaccharides. Food Hydrocoll 25(5):1393–1398
Sun D, Chang C, Li S, Lin L (2006) Near-field electrospinning. Nano Lett 6(4):839–842
Sun Z, Zussman E, Yarin A, Wendorff J, Greiner A (2003) Compound core-shell polymer nanofibers by co-electrospinning. Adv Mater 15(22):1929–1932
Taylor G (1969) Electrically driven jets. Proc R Soc Lond A Math Phys Sci 313(1515):453–475
Teo WE, Ramakrishna S (2006) A review on electrospinning design and nanofibre assemblies. Nanotechnology 17(14):89–106
Theron S, Zussman E, Yarin A (2004) Experimental investigation of the governing parameters in the electrospinning of polymer solutions. Polymer 45(6):2017–2030
Theron S, Yarin A, Zussman E, Kroll E (2005) Multiple jets in electrospinning: experiment and modeling. Polymer 46(9):2889–2899
Thorvaldsson A, Engstrom J, Gatenholm P, Walkenstrom P (2010) Controlling the architecture of nanofiber-coated microfibers using electrospinning. J Appl Polym Sci 118(1):511–517
Tian M, Hu Q, Wu H, Zhang L, Fong H, Zhang L (2011) Formation and morphological stability of polybutadiene rubber fibers prepared through combination of electrospinning and in-situ photo-crosslinking. Mater Lett 65(19/20):3076–3079
Torres-Giner S, Gimenez E, Lagaron JM (2008) Characterization of the morphology and thermal properties of zein prolamine nanostructures obtained by electrospinning. Food Hydrocoll 22(4):601–614
Uyar T, Havelund R, Nur Y, Hacaloglu J, Besenbacher F, Kingshott P (2009) Molecular filters based on cyclodextrin functionalized electrospun fibers. J Memb Sci 332(1/2):129–137
Uyar T, Havelund R, Hacaloglu J, Besenbacher F, Kingshott P (2010) Functional electrospun polystyrene nanofibers incorporating alpha-, beta-, and gamma-cyclodextrins: comparison of molecular filter performance. ACS Nano 4(9):5121–5130
Valipouri A, Ravandi SAH, Pishevar AR (2013) A novel method for manufacturing nanofibers. Fiber Polym 14(6):941–949
Vega-Lugo A, Lim L (2009) Controlled release of allyl isothiocyanate using soy protein and poly(lactic acid) electrospun fibers. Food Res Int 42(8):933–940
Veleirinho B, Lopes-da-Silva JA (2009) Application of electrospun poly(ethylene terephthalate) nanofiber mat to apple juice clarification. Proc Biochem 44(3):353–356

Veleirinho B, Rei MF, Lopes-da-Silva JA (2008) Solvent and concentration effects on the properties of electrospun poly(ethylene terephthalate) nanofiber mats. J Polym Sci B Polym Phys 46(5):460–471

Venugopal J, Ramakrishna S (2005) Applications of polymer nanofibers in biomedicine and biotechnology. Appl Biochem Biotechnol 125(3):147–157

Venugopal J, Ma L, Yong T, Ramakrishna S (2005) In vitro study of smooth muscle cells on polycaprolactone and collagen nanofibrous matrices. Cell Biol Int 29(10):861–867

Wannatong L, Sirivat A, Supaphol P (2004) Effects of solvents on electrospun polymeric fibers: preliminary study on polystyrene. Polym Int 53(11):1851–1859

Xie JB, Hsieh YL (2003) Ultra-high surface fibrous membranes from electrospinning of natural proteins:casein and lipase enzyme. J Mater Sci 38(10):2125–2133

Yao C, Li X, Song T (2007) Electrospinning and crossfinking of zein nanofiber mats. J Appl Polym Sci 103(1):380–385

Yarin A, Koombhongse S, Reneker D (2001a) Bending instability in electrospinning of nanofibers. J Appl Phys 89(5):3018–3026

Yarin A, Koombhongse S, Reneker D (2001b) Taylor cone and jetting from liquid droplets in electrospinning of nanofibers. J Appl Phys 90(9):4836–4846

Yarin AL, Zussman E, Wendorff JH, Greiner A (2007) Material encapsulation and transport in core-shell micro/nanofibers, polymer and carbon nanotubes and micro/nanochannels. J Mater Chem 17(25):2585–2599

Zeleny J (1914) The electrical discharge from liquid points and a hydrostatic method of measuring the electric intensity at their surfaces. Phys Rev 3:69–91

Zhang Y, Wang X, Feng Y, Li J, Lim C, Ramakrishna S (2006) Coaxial electrospinning of (fluorescein isothiocyanate-conjugated bovine serum albumin)-encapsulated poly(epsilon-caprolactone) nanofibers for sustained release. Biomacromolecules 7(4):1049–1057

Zhang L, Luo J, Menkhaus TJ, Varadaraju H, Sun Y, Fong H (2011) Antimicrobial nano-fibrous membranes developed from electrospun polyacrylonitrile nanofibers. J Memb Sci 369(1/2):499–505

Zhao S, Wu X, Wang L, Huang Y (2004) Electrospinning of ethyl-cyanoethyl cellulose/tetrahydrofuran solutions. J Appl Polym Sci 91(1):242–246

Zheng Y, Liu X, Zeng Y (2013) Electrospun nanofibers from a multihole spinneret with uniform electric field. J Appl Polym Sci 130(5):3221–3228

Zuo W, Zhu M, Yang W, Yu H, Chen Y, Zhang Y (2005) Experimental study on relationship between jet instability and formation of beaded fibers during electrospinning. Polym Eng Sci 45(5):704–709

Chapter 4
Polysaccharide-Based Nanoparticles

Erika A. López-López, M. Aurora Hernández-Gallegos, Maribel Cornejo-Mazón and Humberto Hernández-Sánchez

4.1 Introduction

Within the last years, foods enriched with bioactive compounds such as nutraceuticals and nutrients have emerged with great strength in the markets worldwide. The application of nanotechnology includes the use of systems such as micelles, liposomes, nanotubes and nanoparticles for efficient bioactive compounds delivery and improved bioavailability (Kaya-Celiker and Mallikarjunan 2012). Nanoparticles have been developed using mainly proteins and polysaccharides as the biopolymers of choice to be loaded with different bioactive compounds and most authors define them as solid colloidal particles with diameters ranging from 1 to 1000 nm (Tiyaboonchai 2003).

Polysaccharides can be defined as linear or branched macromolecules formed by many monosaccharide units linked by glycosidic bonds. These biopolymers, sometimes also called glycans, can be classified as homopolysaccharides (monosaccharide units are all equal) and heteropolysaccharides (units are of two or more different kinds). The glycosidic bonds can be α or β (1→4, 1→6, 1→3, etc.). Naturally occurring polysaccharides contain from 10 to 250 monose residues and have molecular weights between 2000 and 35,000 Da (Alais et al. 2008). Depending on their function, polysaccharides can also be classified as structural (such as cellulose and chitin) and storage (such as starch, inulin and glycogen). Nanoparticles can be prepared from most of them.

H. Hernández-Sánchez (✉) · E. A. López-López · M. A. Hernández-Gallegos
Departamento de Graduados e Investigación en Alimentos, Escuela Nacional de Ciencias Biológicas, Instituto Politécnico Nacional, México, DF, Mexico
e-mail: hhernan1955@yahoo.com

M. Cornejo-Mazón
Departamento de Biofísica, Escuela Nacional de Ciencias Biológicas, Instituto Politécnico Nacional, 11340 México, DF, Mexico

© Springer Science+Business Media New York 2015

H. Hernández-Sánchez, G. F. Gutiérrez-López (eds.), *Food Nanoscience and Nanotechnology,* Food Engineering Series, DOI 10.1007/978-3-319-13596-0_4

4.2 Starch

All starches are constituted by α-D-glucopyranose units in linear chains linked by α(1→4) bonds in the case of amylose and in branched chains linked by α(1→6) bonds arising from the linear chains in the case of amylopectin. They are ordered in alternating crystalline and amorphous lamellae (9 nm) in the 2–100 μm starch granules (Szymońska et al. 2009). This polysaccharide is a safe, economic, renewable and biodegradable raw material produced by many plants and adequate for the preparation of nanoparticles. The presence of partly crystalline structures in starch allows the production of novel nanoelements: nanocrystals and nanoparticles (Le Corre et al. 2010).

Starch nanocrystals, also known as starch crystallites or microcrystalline starch, are the result of the disruption of the amorphous domains of the granules by acid hydrolysis. By this method, Putaux et al. (2003) were able to obtain platelet nanocrystals from waxy maize starch (with only 1% amylose content) using 2.2 N hydrochloric acid for 6 weeks. The crystals had a length of 20–40 nm. Different lengths have been reported for starch nanocrystals from other sources: 40–70 nm for potato and 30–150 nm for pea (Le Corre et al. 2010). Starch nanocrystals have also been prepared through a complex formation between amylose and a variety of hydrophobic compounds such as n-butanol (Kim et al. 2009). The crystalline complexes are commonly referred as V-amylose, based on their X-ray diffraction pattern. These starch nanocrystals have great potential as nanocarriers for small bioactive compounds, since they have a helical cavity which can host different hydrophobic compounds.

Many protocols are currently available for the preparation of starch nanoparticles (SN). Ma et al. (2008) obtained corn SN by precipitating a gelatinized starch suspension with ethanol. They also prepared citric acid-modified SN using a citric acid solution in ethanol for the derivatization. These modified SN were resistant to heat gelatinization due to the cross linking reaction. Chin et al. (2011) used a similar method for a size-controlled preparation of sago SNs. With the use of adequate surfactants they were able to prepare nanoparticles with average diameters of 150 nm. Tan et al. (2009) prepared starch acetate nanospheres through a simple process of nanoprecipitation, by the dropwise addition of water to an acetone solution of starch acetate. Depending on the procedure conditions, particle sizes between 249 and 720 nm can be obtained. The existence of low polarity microdomains within this kind of nanospheres, suggested the possibility of using these nanoparticles for the encapsulation of hydrophobic bioactive compounds. Szymońska et al. (2009) prepare potato and cassava nanoparticles, with diameters between 50 and 100 nm by passing starch–ethanol suspensions through a vibration mill. Liu et al. (2009) used high-pressure homogenization to generate suspensions of high-amylose corn SNs. In this work, a 5% starch suspension was dispersed through a Microfluidizer for several passes at 207 MPa to obtain highly stable SNs with an average diameter of 100 nm. The viscosity of the suspension decreased with the number of passes through the equipment.

4.3 Dextran

Few reports are available on the preparation of dextran nanoparticles. Dextrans are D-glucose branched polymers. The dextran produced by the bacterium *Leuconostoc mesenteroides* strain NRRL B-512(F) consists of an α(1→6)-linked glucan with side chains connected to the three positions of the backbone glucose units (de Belder 2003). Dextran nanoparticles have been used to stabilize labile bioactive proteins. One of the protocols include incorporation of the protein to a mixture of *L. mesenteroides* dextran (molecular weight 64–76 kDa) and polyethylene glycol in water followed by freezing, phase separation and freeze-drying. After washing with dichloromethane, dextran nanoparticles loaded with the protein of interest can be recovered. The bioactivity of proteins such as β-galactosidase, bovine serum albumin and myoglobin could be preserved by this method (Wu et al. 2013). Dextran-based stable nanoparticles, with an average hydrodynamic diameter of 130 nm and a zeta potential of around −10 mV, have also been prepared by a self-assembly-assisted graft copolymerization of acrylic acid and dextran under the presence of the crosslinker *N,N'*-methylene bisacrylamide. This approach is definitely organic solvent free and surfactant free and therefore environment friendly (Tang et al. 2006).

4.4 Chitin and Chitosan

Chitin, a naturally abundant polysaccharide and the main supporting material of crustaceans and insects is a polymer of *N*-acetyl glucosamine units linked by β(1→4) glycoside bonds. It is relatively water insoluble and has a low chemical reactivity. Chitosan is the *N*-deacetylated derivative of chitin, although this deacetylation is seldom complete (Ravi Kumar 2000). Polysaccharides to be used as bioactive compounds carriers are required to be biodegradable to avoid their accumulation in the body. In the case of chitin, certain chemical modifications must be performed in order to increase its biodegradability. It has been observed, for instance, that carboxymethyl chitin can be degraded faster than chitosan (McConnell et al. 2008) or *N*-succinyl chitosan. Carboxymethyl chitin nanoparticles, with diameters in the range of 200–250 nm, were prepared by cross-linking of a derivatized chitin solution with $CaCl_2$ and $FeCl_3$. These nanoparticles showed antibacterial activity and controlled and sustained release of active compounds at pH 6.8 (Dev et al. 2010). Na Nakorn (2008) prepared chitin nanowhiskers by hydrolysis of chitin with 3 N HCl at 105°C followed by centrifugation and neutralization. The length of the nanowhiskers was 300 nm and they were useful to immobilize proteins such as bovine serum albumin and glucose oxidase.

Chitosan has many interesting properties such as biodegradability, non-toxicity and a good antimicrobial activity against many bacteria, yeasts and fungi (Kong et al. 2010). It has also many important applications in foods such as antioxidant, hypocholesterolemic agent, preservative and thickener (Raafat and Sahl 2009).

Chitosan nanoparticles have been considered by many researchers as very attractive carriers for bioactive compounds. Chitosan is soluble in most diluted organic acids at pH < 6.5 and is obtainable in a wide range of molecular weights. There are five main methods to prepare chitosan nanoparticles: ionotropic gelation, microemulsion, emulsification solvent diffusion and polyelectrolyte complex (Tiyaboonchai 2003).

Ionotropic gelation is based on the electrostatic interaction of the amino groups in chitosan and the negatively charged group of a polyanion. Briefly, this method involves the dissolution of chitosan in acetic acid followed by the addition of a polyanion such as sodium pyrophosphate or tripolyphosphate and a stabilizer such as poloxamer. The nanoparticles are formed under constant stirring at room temperature (Velasco-Rodríguez et al. 2012).

The microemulsion method is based on the generation of chitosan nanoparticles in the water core of reverse micelles which are subsequently cross-linked with glutaraldehyde to produce the final nanoparticles with diameters of around 100 nm (Tiyaboonchai 2003).

Chitosan nanoparticles can also be prepared by the emulsification solvent diffusion method as reported by El-Shaboury (2002). The method is based on the formation of an oil-in-water emulsion after injection of an organic phase into a chitosan HCl solution containing an emulsifier (poloxamer 188 or lecithin) under mechanical stirring followed by high-pressure homogenization according to the technique originally developed by Niwa et al. (1993). The nanoparticles had a size range of 104–148 nm and were suitable to carry highly lipophilic compounds.

The polyelectrolyte complex method is based on the formation of nanoparticles with sizes between 50 and 700 nm by self-assembly of a polycation (such as chitosan) and plasmid DNA under mechanical stirring at room temperature (Erbacher et al. 1998).

Many applications have been reported for chitosan nanoparticles. Na Nakorn (2008) immobilized the enzyme glucose oxidase in chitosan nanoparticles prepared by ionotropic gelation to develop a glucose biosensor. Pulido and Beristain (2010) encapsulated ascorbic acid in chitosan nanoparticles obtained by ionotropic gelation and spray dried afterwards. The vitamin was stable for up to 60 days of storage at a water activity of 0.108 and 35°C. The essential cofactor α-lipoic acid (ALA) is known to be a very strong antioxidant. It is highly unstable when exposed to light or heat; however, it has been stabilized by direct complex formation with chitosan (Kofuji et al. 2008). It has also been encapsulated by spray drying in chitosan microspheres with a diameter of 7.89 μm. Significant retention (75 %) of the antioxidant activity of ALA was obtained when compared to free ALA (Weerakody et al. 2008). Velasco-Rodríguez et al. (2012) prepared ALA-loaded chitosan nanospheres by ionotropic gelation and sodium pyrophosphate or tripolyphosphate as the polyanion and in the presence or absence of poloxamer 188 as stabilizer. Very small nanoparticles (20.3–23 nm) were obtained in the absence of poloxamer 188 and ALA (see Fig. 4.1). The smallest diameters (180 nm) were obtained with sodium pyrophosphate and the poloxamer had the effect of increasing the diameter of the nanospheres. All the preparations showed stability zeta potentials at pH values ≤ 5.3

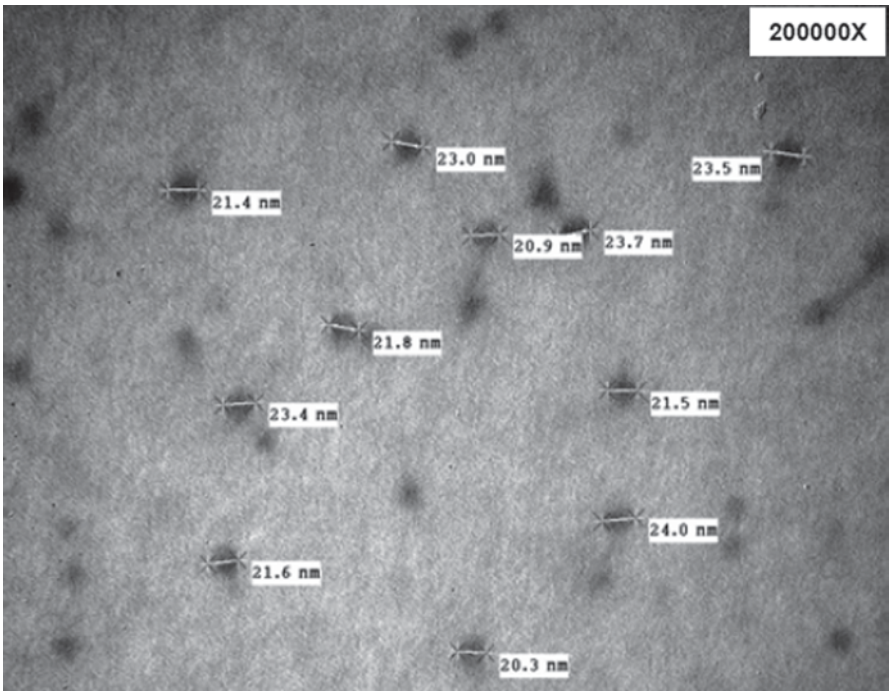

Fig. 4.1 Chitosan nanoparticles formed by ionotropic gelation using sodium tripolyphosphate at pH 5.5 in the absence of poloxamer 188 and α-lipoic acid

indicating a potential use in many acid foods. Using a similar technique, hydrophilic chitosan-polyethylene oxide nanoparticles with a diameter of 200–1000 nm were prepared to be used as protein carriers (Calvo et al. 1997) and chitosan–carbon nanotubes composites have been proposed for use in regenerative medicine and tissue engineering (Olivas-Armendariz et al. 2009).

The preparation of chitosan-based nanoparticles with antimicrobial activity is well studied. These nanoparticles have a good activity against several pathogenic bacteria by themselves since chitosan has a good antimicrobial potential (Raafat and Sahl 2009; Kong et al. 2010), however, the addition of different metal ions enhance this property. Copper-loaded chitosan nanoparticles obtained by ionotropic gelation had good antibacterial activity against *Escherichia coli, Staphylococcus aureus, Salmonella cholerasuis* and *Salmonella typhimurium* (Qi et al. 2004). Du et al. (2009) showed that chitosan nanoparticles loaded with Ag^{+}, Cu^{2+}, Zn^{2+} and Mn^{2+} had a good antimicrobial activity against *S. aureus* and *S. cholerasuis*. This activity was stronger for the nanoparticles than for the free ions and was directly proportional to their zeta potential. Chitosan–silver oxide encapsulated nanocomposite film prepared by solution casting has been proved effective against pathogenic bacteria such as *E. coli, S. aureus, Bacillus subtilis* and *Pseudomonas aeruginosa*. This kind of films has been suggested for food-packaging applications (Tripathi et al. 2011).

4.5 Cellulose

This polysaccharide is the result of the linear condensation of glucose units linked by β(1→4) glycosidic bonds (Alais et al. 2008). Extensive research has been performed on cellulose, cellulose nanoparticles, cellulose whiskers and cellulose-based composites (Moon et al. 2011). Cellulose whiskers have fiber lengths ranging from 100 to several hundred nanometers with diameters of 3–20 nm. They are prepared by acid hydrolysis of cellulose fibers (Zhang et al. 2007). Nanocrystalline cellulose particles can be considered as a new class of cellulosic materials with many applications in food technology, biotechnology and medicine. These nanoparticles are basically prepared by treatment of cellulose fibers with acidic solutions (HCl, H_2SO_4 or a mixture of both) at different temperatures followed by mechanical or ultrasound disintegration (Zhang et al. 2007). Under optimal conditions of sulphuric acid, time and temperature, rod-like nanocrystalline cellulose particles with sizes of 150–200 × 10–20 nm and a yield of up to 75 % can be obtained (Ioelovich 2012). There are many cellulose derivatives which are more soluble than the original polysaccharide which has been used to prepare nanoparticles. Ionic cross-linking with calcium chloride was used to prepare spherical carboxymethyl cellulose nanoparticles with diameters between 150 and 200 nm to encapsulate bioactive compounds (Aswathy et al. 2012). Curcumin, a powerful antioxidant with anti-cancer capacity polyphenol found in turmeric, has been successfully encapsulated in hydroxypropyl methylcellulose (HPMC) nanoparticles. These curcumin-loaded nanoparticles showed maximum anti-cancer activity and induced changes related to cellular apoptosis in prostate cancer cells (Yallapu et al. 2012). There are also some prospects for future applications of cellulose nanoparticle-based polymer composites to increase the competitiveness of green polymers (Pandey et al. 2013).

4.6 Pectin

Pectin is a carbohydrate polymer derived from natural resources and it is the structural component of plant cell walls. Pectin is one of the major constituents of citrus by-products and has good gelling properties to be used in jellies and jams. Chemically, pectin is poly α(1→4) galacturonic acid with varying degree of methylation. Thiolated pectin nanoparticles have been prepared by the ionotropic gelation method using magnesium chloride as ionic crosslinker for encapsulating different bioactive compounds including pharmaceutical drugs (Mishra et al. 2012). Pectin nanoparticles for the encapsulation of highly hydrophobic compounds have been prepared from nanoemulsion templates formed by high-pressure homogenization of pectin–chloroform mixtures (Burapapadh et al. 2012).

4.7 Hydrocolloids

This group includes several kinds of polysaccharides with gelling, thickening and water-binding properties. They are often called gums and are hydrophilic polymers of animal, plant, microbial or synthetic origin that generally contain many hydroxyl groups and may be considered polyelectrolytes. Some of the hydrocolloids most often used in the preparation of nanoparticles are obtained from red and brown algae (Alais et al. 2008). One of the most popular methods to prepare polysaccharide-based micro- and nanoparticles is ionotropic gelation. In this method, the polysaccharides are dissolved in water (sodium alginate or pectin) and added dropwise under constant agitation to a solution containing counterions such as Ca^{2+}, Ba^{2+}, Mg^{2+}, Sr^{2+}, Zn^{2+} or Al^{3+} which will induce ionic gelation and separation of microspheres due to complexation between oppositely charged species (Mørch et al. 2006; Racoviţă et al. 2009). Calcium alginate microbeads (1–3 mm) have been extensively used for the encapsulation of different probiotic bacteria in order to increase the survival of the microorganisms (Lee and Heo 2000). In our laboratory, we have increased this survival by the addition of resistant maltodextrin (Medallion Labs., USA) in the case of *Lactobacillus rhamnosus* GG and *Saccharomyces boulardii* and of trehalose in the case of *Lactobacillus plantarum*. Alginic acid is a naturally occurring heteropolysaccharide extracted from marine brown algae and its structure includes the α-L-guluronic and -D-mannuronic acids in the form of homopolymeric or alternating sequence blocks (Racoviţă et al. 2009). The use of homogenization instead of just agitation is useful in the regulation of the size of the microspheres. Capela et al. (2007) were able to produce beads with an average diameter of 39.2 μm using an Ultra-Turrax benchtop homogenizer at 13,500 rpm for 4 min to encapsulate and increase the survival of different probiotic bacteria. Smaller sizes of around 1000 nm have been obtained with the use of the electrohydrodynamic spraying technique to encapsulate bovine serum albumin in calcium alginate (Suksamran et al. 2009). True nanoparticles with radii < 100 nm have been obtained in the aqueous phase of water-in-oil nanoemulsions using a nonionic oligoethylene oxide surfactant, decane and a 2 % solution of sodium alginate. The ionic gelation of alginate was induced by the addition of a $CaCl_2$ solution with stirring (Machado et al. 2012). Alginate nanoparticles have been used as carriers for different bioactive compounds (Ahmad et al. 2010) including the bacteriocin nisin which has been effectively used in nisin-loaded chitosan/alginate nanoparticles against *S. aureus* in raw and pasteurized milk (Zohri et al. 2010).

Carrageenans are hydrocolloids obtained from red sea algae. They are formed mainly by the potassium, sodium, calcium, magnesium and ammonium sulfate esters of galactose and 3, 6-anhydrogalactose copolymers. These hexoses are alternately linked at the α(1→3) and β(1→4) sites in the polysaccharide (Senthil et al. 2010). The position of the sulfate groups and some inner bonds in the hexoses gives origin to different types of carrageenan such as the κ and λ forms. Oliva et al. (2003) have taken advantage of the ability of λ-carrageenan to spontaneously self-assemble to amphiphilic basic compounds to prepare 50 nm nanoparticles with

dexchlorpheniramine maleate. Ionic gelation between carrageenans and chitosan has been used to prepare nanoparticles with particle sizes ranging from 373 to 803 nm (Senthil et al. 2010).

4.8 Conclusion

Many naturally occurring polysaccharides can be considered as abundant, cheap and adequate raw materials to be used in the preparation of nanoparticles for the encapsulation of different kinds of bioactive and food compounds for their safe delivery in the human body. Several processes have been developed for the preparation of nanoparticles of different shapes and sizes which include chemical reactions or physical treatments and the choice depends on many factors such as safety, economic and environmental considerations, etc.

References

Ahmad Z, Pandey R, Sharma S, Khuller GK (2010) Alginate nanoparticles as antituberculosis drug carriers: formulation development, pharmacokinetics and therapeutic potential. Indian J Chest Dis Allied Sci 48:171–176

Alais C, Linden G, Miclo L (2008) Biochimie alimentaire. Dunod, Paris

Aswathy RG, Sivakumar B, Brahatheeswaran D, Raveendran S, Ukai T, Fukuda T, Yoshida Y, Maekawa T, Sakthikumar DN (2012) Multifunctional biocompatible fluorescent carboxymethyl cellulose nanoparticles. J Biomater Nanobiotechnol 3:254–261

Burapapadh K, Takeuchi H, Sriamornsak P (2012) Novel pectin-based nanoparticles prepared from nanoemulsion templates for improving in vitro dissolution and in vivo absorption of poorly water-soluble drugs. Eur J Pharmaceut Biopharmaceut 82:250–261

Calvo P, Remuñán-López C, Vila-Jato JL (1997) Novel hydrophilic chitosan polyethylene oxide nanoparticles as protein carriers. J Appl Polym Sci 63:125–132

Capela P, Hay TKC, Shah NP (2007) Effect of homogenisation on bead size and survival of encapsulated probiotic bacteria. Food Res Int 40:1261–1269

Chin SF, Pang SC, Tay SH (2011) Size controlled synthesis of starch nanoparticles by a simple nanoprecipitation method. Carbohyd Polim 86:1817–1819

De Belder AN (2003) Dextran. Amersham Biosciences, Uppsala

Dev A, Mohan JC, Sreeja V, Tamura H, Patzke GR, Hussain F, Weyeneth S (2010) Novel carboxymethyl chitin nanoparticles for cancer drug delivery applications. Carbohyd Polym 79:1073–1079

Du WL, Niu SS, Xu YL, Xu ZR, Fan CL (2009) Antibacterial activity of chitosan tripolyphosphate nanoparticles loades with various metal ions. Carbohyd Polym 75:385–389

El-Shaboury MH (2002) Positively charged nanoparticles for improving the oral bioavailability of cyclosporin-A. Int J Pharm 249:101–108

Erbacher P, Zou S, Steffan AM, Remy JS (1998) Chitosan-based vector/DNA complexes for gene delivery: biophysical characteristics and transfection ability. Pharm. Res. 15:1332–1339

Ioelovich M (2012) Optimal conditions for isolation of nanocrystalline cellulose particles. Nanosci Nanotechnol 2:9–13

Kaya-Celiker H, Mallikarjunan K (2012) Better nutrients and therapeutics delivery in food through nanotechnology. Food Eng Rev 4:114–123

Kim JY, Yoon JW, Lim ST (2009) Formation and isolation of nanocrystal complexes between dextrins and *n*-butanol. Carbohyd Polym 78:626–632

Kofuji K, Nakamura M, Isobe T, Murata Y, Kawashima S (2008) Stabilization of a-lipoic acid by complex formation with chitosan. Food Chem 109:167–171

Kong M, Chen XG, Xing K, Park HJ (2010) Antimicrobial properties of chitosan and mode of action: a state of the art review. Int J Food Microbiol 144:51–63

Le Corre D Bras J Dufresne A (2010) Starch nanoparticles: a review. Biomacromolecules 11:1139–1153

Lee KY, Heo TR (2000) Survival of *Bifidobacterium longum* immobilized in calcium alginate beads in simulated gastric juices and bile salt solution. Appl Environ Microbiol 66:869–873

Liu D, Wu Q, Chen H, Chang PR (2009) Transitional properties of starch colloid with particle size reduction from micro- to nanometer. J Colloid Interface Sci 339:117–124

Ma X, Jian R, Chang PR, Yu J (2008) Fabrication and characterization of citric acid-modified starch nanoparticles/plasticized-starch composites. Biomacromolecules 9:3314–3320

Machado AHE, Lundberg D, Ribeiro AJ, Veiga FJ, Lindman B, Miguel MG, Olsson U (2012) Preparation of calcium alginate nanoparticles using water-in-oil (W/O) nanoemulsions. Langmuir 28:4131–4141

McConnell EL, Murdan S, Basit AW (2008) An investigation into the digestion of chitosan (non-crosslinked and crosslinked) by human colonic bacteria. J Pharm Sci 97:3820–3829

Mishra RK, Banthia AK, Majeed BA (2012) Pectin based formulations:a review. Asian J Pharmaceut Clin Res 5:1–7

Moon RJ, Martini A, Nairn J, Simonsen J, Youngblood J (2011) Cellulose nanomaterials review:structure, properties and nanocomposites. Chem Soc Rev 40:3941–3994

Mørch ÝA Donati I Strand BL Skjåk-Bræk G (2006) Effect of Ca^{2+}, Ba^{2+}, and Sr^{2+} on alginate microbeads. Biomacromolecules 7:1471–1480

Na Nakorn P (2008) Chitin nanowhisker and chitosan nanoparticles in protein immobilization for biosensor applications. J Met Mat Min 18:73–77

Niwa T, Takeuchi H, Hino T, Kunou N, Kawashima Y (1993) Preparations of biodegradable nanospheres of water-soluble and insoluble drugs with D, L-lactide/glycolide copolymer by a novel spontaneous emulsification solvent diffusion method, and the drug release behaviour. J. Control Release 25:89–98

Oliva M, Díez-Pérez I, Gorostiza P, Lastra CF, Herrera J, Oliva I, Mariño EL (2003) Preparation and characterization of l-carrageenan nanospheres containing dexchlorpheniramine maleate. In: Libro de Comunicaciones del VI Congreso de la Sociedad Española de Farmacia Industrial y Galénica, Granada, España, 2003

Olivas-Armendáriz I, García-Casillas P, Martel-Estrada A, Martínez-Sánchez R, Martínez-Villafañe A, Martínez-Pérez CA (2009) Preparation and characterization of chitosan/carbon nanotubes composites. Rev Mex Ing Quim 8:205–211

Pandey JK, Nakagaito AN, Takagi H (2013) Fabrication and applications of cellulose nanoparticle-based polymer composites. Polym Eng Sci 53:1–8

Pulido A, Beristain CI (2010) Spray dried encapsulation of ascorbic acid using chitosan as wall material. Rev Mex Ing Quim 9:189–195

Putaux JL, Molina-Boisseau S, Momaur T, Dufresne A (2003) Platelet nanocrystals resulting from the disruption of waxy maize starch granules by acid hydrolysis. Biomacromolecules 4:1198–1202

Qi L, Xu Z, Jiang X, Hu C, Zou X (2004) Preparation and antibacterial activity of chitosan nanoparticles. Carbohyd Res 339:2693–2700

Raafat D, Sahl HG (2009) Chitosan and its antimicrobial potential—a critical literature survey. Microb Biotechnol 2:186–201

Racoviţă Ş Vasiliu S Popa M Luca C (2009) Polysaccharides based on micro- and nanoparticles obtained by ionic gelation and their applications as drug delivery systems. Rev Roum Chimie 54:709–718

Ravi Kumar MNV (2000) A review of chitin and chitosan applications. React Funct Polym 46:1–27

Senthil V, Suresh Kumar R, Nagaraju CVV, Jawahar N, Ganesh GNK, Gowthamarajan K (2010) Design and development of hydrogel nanoparticles for mercaptopurine. J Adv Pharm Technol Res 1:334–337

Suksamran T, Opanasopit P, Rojanarata T, Ngawhirunpat T, Ruktanonchai U, Supaphol P (2009) Biodegradable alginate microparticles developed by electrohydrodynamic spraying techniques for oral delivery of protein. J Microencapsul 26:563–570

Szymońska J, Targosz-Korecka M, Krok F (2009) Characterization of starch nanoparticles. J Phys Conf Ser 146:012027

Tan Y, Xu K, Li L, Liu C, Song C, Wang P (2009) Fabrication of size-controlled starch based nanospheres by nanoprecipitation. ACS Appl Mater Interfaces 1:956–959

Tang M, Dou H, Sun K (2006) One-step synthesis of dextran-based stable nanoparticles assisted by self-assembly. Polymer 47:728–734

Tiyaboonchai W (2003) Chitosan nanoparticles: a promising system for drug delivery. Naresuan Univ J 11:51–66

Tripathi S, Mehrotra GK, Dutta PK (2011) Chitosan-silver oxide nanocomposite film: preparation and antimicrobial activity. Bull Mater Sci 34:29–35

Velasco-Rodríguez V, Cornejo-Mazón M, Flores-Flores JO, Gutiérrez-López GF, Hernández-Sánchez H (2012) Preparation and properties of alpha-lipoic acid-loaded chitosan nanoparticles. Rev Mex Ing Quím 11:155–161

Weerakody R, Fagan P, Kosaraju SL (2008) Chitosan microspheres for encapsulation of a-lipoic acid. Int J Pharm 357:213–218

Wu F, Zhou Z, Su J, Wei L, Yuan W, Jin T (2013) Develoipment of dextran nanoparticles for stabilizing delicate proteins. Nanoscale Res Lett 8:197–204

Yallapu MM, Dobberpuhl MR, Maher DM, Jaggi M, Chauhan SC (2012) Design of curcumin loaded cellulose nanoparticles for prostate cancer. Curr Drug Metab 13:120–128

Zhang J, Elder TJ, Pu Y, Ragauskas AJ (2007) Facile synthesis of spherical cellulose nanoparticles. Carbohyd Polym 69:607–611

Zohri M, Alavidjeh MS, Haririan I, Ardestani MS, Ebrahimi SES, Sani HT, Sadjadi SK (2010) A comparative study between the antibacterial effect of nisin and nisin-loaded chitosan/alginate nanoparticles on the growth of *Staphylococcus aureus* in raw and pasteurized milk samples. Probiotic Antimicro Prot 2:258–266

Chapter 5
Protein-Based Nanoparticles

Esmeralda Jiménez-Cruz, Izlia J. Arroyo-Maya, Andrés Hernández-Arana, Maribel Cornejo-Mazón and Humberto Hernández-Sánchez

5.1 Introduction

Proteins are linear polymers of L-α-amino acids with a wide variety of structures and functions. They can be classified in terms of their solubility, chemical structure, shape, and number of monomeric units.

Protein solubility is determined by a variety of interactions including protein–protein, protein–water, protein–ion, and ion–water interactions (Trevino et al. 2008). These biomacromolecules can be classified, based on their solubility in water-soluble proteins (albumins), salt-soluble proteins (globulins), alcohol-soluble proteins (prolamins), acid- or base-soluble proteins (glutelins), and insoluble in most solvents proteins (scleroproteins). While originally used for wheat and cereals, this adaptation of the Osborne fractionation scheme has been applied to most food proteins (Bean and Lookhart 2000). Taking in consideration the different physicochemical properties, biocompatibility, and degradability of food proteins, they have a potential role in the development of nanoparticles as nutraceutical delivery systems (Sundar et al. 2010). There is a growing interest in the use of nanoparticles for drugs and bioactive compounds delivery vehicles (Mohanraj and Chen 2006; Kreuter 2007). Protein nanoparticles are relatively

H. Hernández-Sánchez (✉) · E. Jiménez-Cruz
Departamento de Graduados e Investigación en Alimentos, Escuela Nacional de Ciencias Biológicas, Instituto Politécnico Nacional,, México, DF, Mexico
e-mail: hhernan1955@yahoo.com

I. J. Arroyo-Maya
University of Massachusetts Amherst, 01003 Amherst, MA, USA

A. Hernández-Arana
Departamento de Química, Universidad Autónoma Metropolitana, Unidad Iztapalapa, México, DF, Mexico

M. Cornejo-Mazón
Departamento de Biofísica, Escuela Nacional de Ciencias Biológicas, Instituto Politécnico Nacional, 11340 México, DF, Mexico

© Springer Science+Business Media New York 2015

H. Hernández-Sánchez, G. F. Gutiérrez-López (eds.), *Food Nanoscience and Nanotechnology,* Food Engineering Series, DOI 10.1007/978-3-319-13596-0_5

easy to prepare and due to their subcellular size they can penetrate into tissues through the capillaries or be taken up by the cells (Chen et al. 2006). Desai et al. (1996) have shown that the efficiency of intestinal uptake of 100 nm nanoparticles is 15–250 times better compared to larger size particles. Encapsulation of hydrophobic bioactive compounds in protein nanoparticles usually increases their water solubility and bioavailability (Huang et al. 2010). Additional protection of some bioactive compounds is achieved through the intrinsic antioxidant activity of proteins (Elias et al. 2008).

Casein micelles are one of the naturally occurring protein-based nanosystems which allow a better and more efficient transport of dairy calcium, phosphate, and protein (Müller-Buschbaum et al. 2007). The micelles are formed by the four main types of caseins (α_{s1}, α_{s2}, β, and κ) and have an average diameter of 150 nm (Kaya-Celiker and Mallikarjunan 2012). However, currently there are several protocols for the preparation of nanosystems based on food proteins such as albumins, dairy proteins, gelatin, and some plant proteins. There are two main methods for the preparation of protein nanoparticles: emulsification and desolvation. In the first method, an aqueous solution of the protein is emulsified with a vegetable oil at room temperature and added to preheated oil dropwise to evaporate the water and form the nanoparticles (Jahanshani and Babaei 2008). In the second method, the dropwise addition under stirring of desolvating agents such as organic solvents or salts separates and coacervates the proteins in the aqueous phase. Finally, the addition of a glutaraldehyde solution will induce intraparticle cross-linking to form the protein nanoparticles (Jun et al. 2011). Self-assembly methods have also been reported.

5.2 Casein

Esmali et al. (2011) described the self-assembling of β-casein in micelles to be used as a nanovehicle for curcumin. This hydrophobic phenolic compound is very important in foods as antioxidant but it has also found important applications as antimicrobial since it has bactericidal activity against bacteria such as *Helicobacter pylori* (De et al. 2009). This self-assembly tendency of bovine caseins has also been used by Semo et al. (2007) to load liposoluble vitamin D2 into reassembled casein micelles. These nanoparticles can easily be included in dairy products without modifying their sensory properties and providing partial protection to the vitamin against UV light. A similar technique was used by Zimet et al. (2011) to load casein micelles with the omega-3 polyunsaturated fatty acid docosahexaenoic acid (DHA). Reassembled micelles prepared at 4 °C in the presence of calcium (50–60 nm) or at room temperature in the absence of it (288.9 nm) were able to protect DHA against oxidation showing good stability at 4 °C. Mohan et al. (2013) showed the ability of unmodified casein micelles to bind hydrophobic molecules such as vitamin A without having to perform the process of reassembling of the caseins. The elaboration of casein nanoformulations by enzymatic cross-linking by transglutaminase for entrapping bioactive molecules have also been reported (Elzoghby et al. 2011).

5.3 β-Lactoglobulin (β-LG)

β-LG is the main bovine whey protein, is a relatively small protein formed by 162 amino acids with a molecular weight of 18.4 kDa (Kontopidis et al. 2004). Nanoparticles with an average diameter of 60 nm have been prepared using a desolvation method which included a preheating at 60 °C of the β-LG solution, the use of acetone as desolvating agent, and glutaraldehyde as the cross-linking agent. The nanoparticles were stable under acidic and neutral conditions showing good potential for encapsulation and controlled delivery purposes (Ko and Gunasekaran 2006; Gunasekaran et al. 2007). The preparation of microparticles composed of a core of aggregated β-LG covered by a shell of carboxymethylcellulose (CMC) has been reported by Carpineti et al. (2014). The first step involves the formation of a core of aggregated β-LG by heating protein solutions at 80 °C for 15 min at pH 7 and then, in a second step, to induce the shell deposition by promoting the electrostatic union of the anionic CMC molecules on the previously formed core. The protein core has an average diameter of 200 nm which increases to 1 μm when the polysaccharide is incorporated.

5.4 α-Lactalbumin (α-LA)

It is quantitatively the second most important protein in whey, has a molecular weight of 14.2 kDa, is able to bind calcium, and is the regulatory subunit of the enzyme lactose synthase (Kamau et al. 2010; Kaya-Celiker and Mallikarjunan 2012). Partial hydrolysis of α-LA with a bacterial protease from *Bacillus licheniformis* was shown to induce the formation of nanotubes by self-assembly of the generated peptides. These are the only food protein nanotubes and are formed in the presence of calcium at neutral pH (Kaya-Celiker and Mallikarjunan 2012). Graveland-Bikker et al. (2009) propose the existence of dimeric building blocks which are able to self-assemble into a 10-start, right-handed helix via β-sheet stacking to form the nanotubes. The kind of self-assembly depends strongly on the protein concentration. At α-LA concentrations >3 % and in the presence of calcium, long tubular structures with diameters of about 20 nm can be obtained. At lower α-LA concentrations, linear fibrils with diameters of 5 nm or random aggregates are produced (Kamau et al. 2010). α-LA nanotubes are very stable and due to their long linear structure can be used as viscosifying agents (Kaya-Celiker and Mallikarjunan 2012). The presence of an 8 nm cavity in these tubes could be useful for the possible encapsulation of nutraceuticals, vitamins, and prebiotics (Kamau et al. 2010). This method is applicable to other proteins as well and has been investigated in the immobilization of enzymes or to prepare analogues to muscle fiber (Weiss et al. 2006). Esmaelizadeh et al. (2011) also used enzymatic hydrolysis to produce very small α-LA nanoparticles. They used the endoproteinase Glu-C (V8 protease) from *Staphylococcus aureus* strain V8 to produce partial hydrolysis of ALA in the

presence of calcium or manganese. The resulting mixture was annealed for 2–4 h in a water bath at 50 °C. Under these conditions, nanospheres with diameters between 3 and 5 nm were formed.

Mehravar et al. (2009) used the desolvation process for the preparation of α-LA nanoparticles. They examined the effect of pH, temperature, and solvent on the size of the nanoparticles. They found that the use of acetone as the desolvating agent produced smaller particles than ethanol and that the use of higher values of pH and lower temperatures generated nanoparticles with larger diameters. In this study, nanoparticles with sizes between 102 and 454 nm were obtained. Mehravar et al. (2011) applied the Taguchi method to optimize the diameter of the nanoparticles. The optimal conditions for the production of particles were pH 2.5, 50 °C, and a stirring speed of 750 rpm for a nanoparticle diameter of less than 220 nm. Arroyo-Maya et al. (2012) studied the effect of several treatments on the capacity of ALA to form nanoparticles by the desolvation method with glutaraldehyde cross-linking. The use of acetone as desolvating agent allowed the authors to obtain nanoparticles with smaller sizes (152.3 nm) as shown in Fig. 5.1. The use of the solvent with a small polarity index (isopropanol) produced the particles with the largest hydrodynamic diameter (293.4–324.9 nm). Ethanol produced intermediate size particles (205.1–246 nm). These results could indicate that by carefully controlling the hydrophobic interactions it is possible to control the size of α-LA nanoparticles. The nanoparticles obtained with ethanol had an isoelectric point of 3.61 and are very stable at pH values > 4.8 (according to their zeta potential values) so they could be useful as bioactive compounds' nanocarriers in different foods. The nanoparticles were degraded by trypsin at pH 2 and pancreatin at pH 8 even after the cross-linking reaction.

5.5 Bovine Serum Albumin (BSA)

BSA is a protein with great potential for the preparation of nanovehicles with possible food applications since it is nontoxic and biodegradable. Many reports have dealt with the production of BSA nanoparticles, generally by the desolvation method using acetone with glutaraldehyde cross-linking (Sailaja and Amareshwar 2012). The preparation of size-controlled BSA nanoparticles is still a challenge for food nanotechnologists and there are different proposals. Sailaja and Amareshwar (2012) indicate that size control of BSA nanoparticles can be achieved by the intermittent addition of acetone. Jun et al. (2011) reported that the size and the surface area-to-volume ratio of BSA nanoparticles can be controlled by varying the protein concentration, pH, and NaCl content. They also indicate that the surface area-to-volume relationship is more useful as a parameter than diameter for comparative studies of nanomaterials. Calcium citrate-loaded BSA nanoparticles with diameters from 260 to 919 nm were prepared with this method.

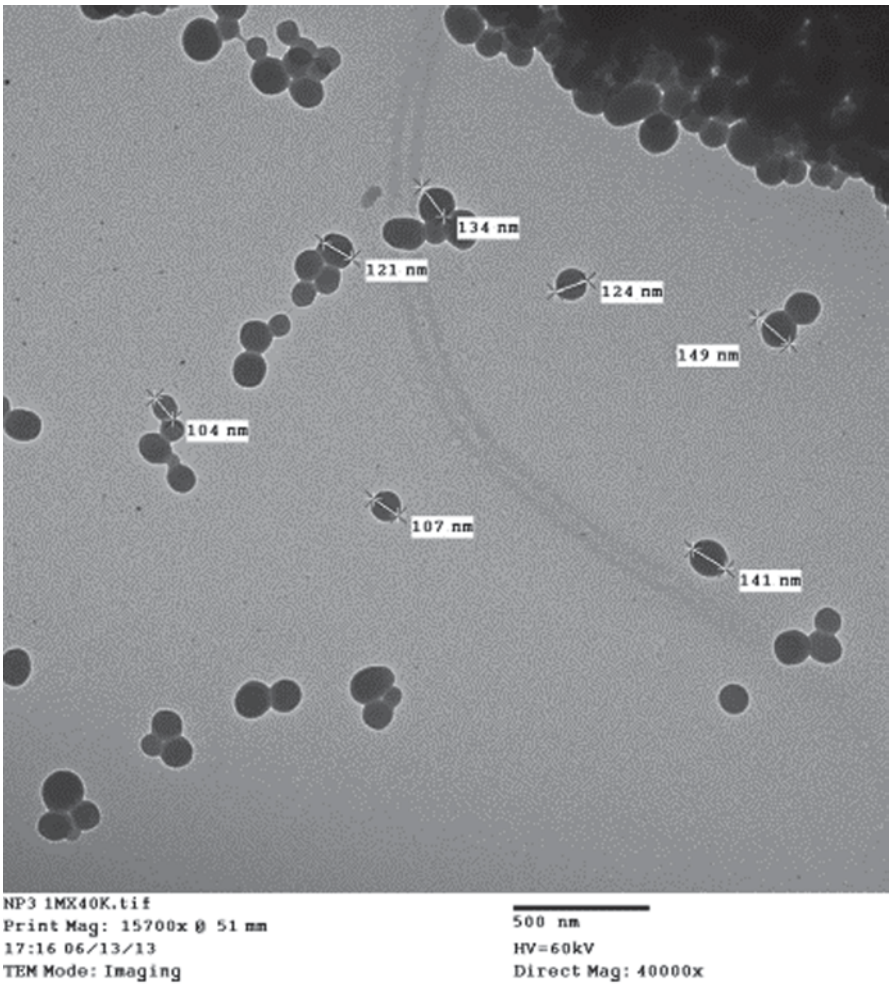

Fig. 5.1 α-Lactalbumin nanoparticles formed by desolvation using acetone as the desolvating agent at pH 3 and cross-linked with glutaraldehyde

Degradation by the enzymes of the gastrointestinal tract is a major factor influencing the efficiency of protein-based nanocarriers. Singh et al. (2010) used poly-L-lysine (PLL) to coat BSA nanoparticles, produced by desolvation with ethanol, to increase the resistance to in vitro enzymatic degradation. They found that the use of lower molecular weight PLL for coating increased the resistance to trypsin degradation and enhanced the stability of the BSA nanoparticles to be used as nutraceuticals nanovehicles.

5.6 Human Serum Albumin (HSA)

HSA, similarly to BSA, has been shown to be biodegradable, safe, easy to purify, and soluble in water, and therefore an ideal protein for nanoparticle preparation (Sebak et al. 2010). These nanoparticles have been usually prepared by the desolvation agent using ethanol as the desolvating agent. The nanoparticles have been stabilized by the addition of glutaraldehyde as a cross-linking agent or by heat denaturation (Weber et al. 2000). As in other cases, HSA nanoparticles have been characterized by sedimentation velocity analysis, dynamic light scattering, size exclusion chromatography, and electron microscopy (Vogel et al. 2002). Several studies have been performed on the parameters of the desolvation process. Results have indicated that the particle size depended on the amount of desolvating agent added (Weber et al. 2000) and on the pH value of the HSA solution prior to desolvation (Langer et al. 2003), but not on the amount of cross-linker of cross-linking procedure (glutaraldehyde or heat). At pH values of 8 and higher low-polydispersity, nanoparticles with average diameters between 200 and 300 nm can be prepared and the higher the pH, the smaller the nanoparticles. An increase in the concentration of glutaraldehyde reduces the surface amino groups decreasing the zeta potential of the nanoparticles (Langer et al. 2008). This kind of particle is degraded in the presence of different proteases such as pepsin and cathepsin B at low pH and trypsin and proteinase K at neutral pH. Arroyo-Maya et al. (2012) have indicated the importance of the dielectric constant and polarity index of the desolvating agent on the nanoparticle size for the case of α-LA. Storp et al. (2012) found something similar for the case of HSA and used a combination of methanol and ethanol as desolvating agent to prepare very small spherical HSA nanoparticles with diameters between 50 and 80 nm.

5.7 Egg Albumin (EA)

EA nanoparticles have also been prepared by the desolvation method using acetone as desolvating agent and cross-linking with glutaraldehyde (Taheri et al. 2012). Size and morphology were studied by photon correlation spectroscopy and atomic force microscopy. The process was optimized using the Taguchi method and the authors were able to obtain nanoparticles with a minimal diameter of 51 nm at 55 °C, 30 mg/ml EA concentration, 500 rpm agitation speed, and pH 4.

5.8 Gelatin

Gelatin is a natural protein prepared from collagen and is commonly used for pharmaceutical, food, and medical applications, because of its biodegradability and biocompatibility in physiological environments (Ramachandran and Shanmu-

ghavel 2010). Nanoparticles with diameters in the range of 112 to 386 nm have been prepared from this macromolecule by a two-step desolvation method using acetone or ethanol as desolvating agents and cross-linking with glutaraldehyde. These nanoparticles showed a good uptake by cells in culture (Azarmi et al. 2006). This method was originally described by Coester et al. (2000) indicating that after the first desolvation step, the low molecular gelatin fractions present in the supernatant are removed by decantation. The high molecular fractions present in the precipitate are resuspended and then desolvated again at pH 2.5 in a second step. The resulting nanoparticles can then be simply purified by centrifugation. Negatively charged gelatin nanoparticles have also been prepared by simple coacervation. These particles are spherical with a diameter of 45 ± 5 nm and are very stable (Mohanty et al. 2005).

5.9 Gliadin

Wheat gliadins are a highly polymorphic group of seed storage proteins which appear to be suitable polymers for the preparation of nanoparticles which are usually able to interact with biological surfaces such as the gastrointestinal mucosa (Jahanshani and Babaei 2008). Gliadin nanoparticles are usually prepared by the desolvation method using an ethanol:water phase (7:3 by vol.) as desolvating agent and cross-linking with glutaraldehyde. The particles so prepared have a diameter of 453 ± 24 nm, a zeta potential of 24.5 ± 0.5 mV, and a yield of 86.8 %. They developed a good bioadhesive interaction with the intestinal mucosa indicating a good potential as a nanovehicle for bioactive compounds (Arangoa et al. 2001). Ezpeleta et al. (1996) used a similar system to prepare all-*trans*-retinoic acid-loaded gliadin nanoparticles. They obtained 500 nm particles with a yield of about 90 % and an entrapment efficiency of about 75 % of the all-*trans*-retinoic acid. This compound has been widely used in the treatment of acne and other skin disorders.

5.10 Legumin

Legumin is one of the most important storage proteins in the pea seeds and is the source of sulfur-containing amino acids in these legumes (Jahanshani and Babaei 2008). Irache et al. (1995) prepared legumin nanoparticles of an average diameter of 250 nm by means of a pH-coacervation method and cross-linking with glutaraldehyde. Coacervates were prepared by mixing one volume of a 0.5 % w/v aqueous solution of legumin (pH 9 with NaOH 0.01 N) with two volumes of a constantly stirred solution of Synperonic™ PE/F 68 in phosphate buffer. The ionic strength and the pH were held constant at 0.103 M and 6.8, respectively. The nanoparticles were stable when the pH was neutral but were quickly degraded at low values of pH. Mirshahi et al. (2002) reported that these nanoparticles are not

able to elicit an immune response when injected intradermally in rats probably due to a reduction in antigenic epitopes of the legumin induced by the glutaraldehyde during cross-linking.

5.11 Zein

Zein, the corn prolamin protein, includes a group of alcohol-soluble proteins which are water insoluble (Gómez-Estaca et al. 2012). Zein nanoparticles are suitable, like gliadin nanoparticles, to incorporate hydrophobic bioactive compounds. There are reports of different methods to prepare this kind of nanoparticles. Zhong and Jin (2009) produced zein nanoparticles by liquid–liquid dispersion. This process takes advantage of the solubility characteristics of zein in ethanol at different concentrations. The particles were prepared by shearing zein solutions into an aqueous phase. The average size of zein nanoparticles was between 100 and 200 nm. This process has been used to encapsulate oregano, thyme, and cassia essential oils. Podaralla and Perumal (2010) produced zein nanoparticles by pH-controlled nanoprecipitation. The particles had an average particle diameter of 460 nm and were successfully used to encapsulate 6,7-dihydroxycoumarin. Gómez-Estaca et al. (2012) used electrodynamic atomization to form the zein nanoparticles. They studied the effects of protein concentration, flow rate, and applied voltage on the size and morphology of the particles. The diameter of the particles ranged from 175 to 900 nm and increased with zein concentration and flow rate. The adequate voltage for the process was 16 kV. Zein nanoparticles with round shapes were produced for zein concentrations from 5 to 15 %, however a sudden change to nanofibers was observed when the concentration reached 20 %. The particles were suitable to encapsulate curcumin. Xu et al. (2011) were able to produce hollow nanoparticles with mean diameters as small as 65 nm and capable of holding larger amounts of bioactive compounds to be carried into cells. In this method, a zein solution in 70 % ethanol was mixed with Na_2CO_3 precipitated in 70 % ethanol to wrap the zein. Water was added to precipitate the zein and to dissolve the carbonate leading to the formation of the hollow zein nanoparticles. Hydrophobic compounds encapsulated in this kind of particles showed a more constant and controlled release than the one in solid zein nanoparticles.

5.12 Soy Protein

Soy protein isolates (SPI) are adequate raw materials for the elaboration of nanoparticles. They consist mainly of the components glycinin and β-conglycinin. Curcumin-loaded SPI nanoparticles have been prepared by the desolvation method using ethanol as the desolvating agent and cross-linking with glutaraldehyde. The mean diameter of the particles was in the range of 220.1 and 286.7 nm and a zeta potential

of −36 mV which guaranteed a good stability. Encapsulation and loading efficiency were 97.2 and 2.7 %, respectively (Teng et al. 2012).

5.13 Conclusion

Protein-based nanoparticles have shown a good potential as bioactive compound delivery systems for foods. So far, nanoparticles from different proteins including water-soluble (albumins, gelatin, SPI) and water-insoluble (zein, gliadin) have been successfully prepared and loaded with several bioactive compounds in order to increase their bioavailability and release. The balance in the composition of hydrophobic and polar or charged amino acids of the protein will have a strong influence in the type of bioactive compound which can be loaded into the nanoparticles. Albumins, for instance, have generally a low content of hydrophobic amino acids and their nanoparticles will be able to hold compounds by hydrogen bonds or electrostatic interactions. The opposite is true for gliadin or zein, and their nanoparticles are suitable for incorporating highly hydrophobic compounds. SPI have a balanced composition and therefore can form nanoparticles which can be loaded with hydrophilic or hydrophobic compounds. It is very likely that in the future chemically or genetically modified proteins with different amino acid balance could be available to prepare nanoparticles which can be loaded with almost any bioactive compound for controlled release to any organ and stable enough to be incorporated in diverse foods. Finally, caution has been suggested in some cases. There are reports indicating that some food processes that involve shear forces may provoke the formation of amyloid fibrils in high protein foods (Raynes et al. 2014). Toxicological testing is suggested in these special cases.

References

Arangoa MA, Campanero MA, Renedo MJ, Ponchel G, Irache JM (2001) Gliadin nanoparticles as carriers for the oral administration of lipophilic drugs. Relationship between bioadhesion and pharmacokinetics. Pharm Res 18:1521–1527

Arroyo-Maya, IJ, Rodiles-López JO, Cornejo-Mazón M, Gutiérrez-López GF, Hernández-Arana A, Toledo-Núñez C, Barbosa-Cánovas GV, Flores-Flores JO, Hernández-Sánchez H (2012) Effect of different treatments on the ability of α-lactalbumin to form nanoparticles. J Dairy Sci 95:6204–6214

Azarmi S, Huang Y, Chen H, McQuarrie S, Abrams D, Roa W, Finlay WH, Miller GG, Löbenberg R (2006) Optimization of a two-step desolvation method for preparing gelatin nanoparticles and cell uptake studies in 143B osteosarcoma cancer cells. J Pharm Pharm Sci 9:124–132

Bean SR, Lookhart GL (2000) Electrophoresis of cereal storage proteins. J Chromatogr A 881:23–36

Carpineti L, Martinez MJ, Pilosof AMR, Pérez OR (2014) β-Lactoglobulin-carboxymethylcellulose core-shell microparticles: construction, characterization and isolation. J Food Eng 131: 65–74

Chen L, Remondetto GE, Subirade M (2006) Food protein-based materials as nutraceutical delivery systems. Trends Food Sci Technol 17:272–283

Coester CJ, Langer K, Von Briesen H, Kreuter J (2000) Gelatin nanoparticles by two step desolvation: a new preparation method, surface modifications and cell uptake. J Microencapsul 17:187–193

De R, Kundu P, Swarnakar S, Ramamurthy T, Chowdhury A, Nair GB, Mukhopadhyay AK (2009) Antimicrobial activity of curcumin against *Helicobacter pylori* isolates from India and during infections in mice. Antimicrob Agents Chemother 53:1592–1597

Desai MP, Labhasetwar V, Amidon GL, Levy RJ (1996) Gastrointestinal uptake of biodegradable microparticles: effect of particle size. Pharm Res 13:1838–1845

Elias RJ, Kellerby SS, Decker EA (2008) Antioxidant activity of proteins and peptides. Crit Rev Food Sci Nutr 48:430–441

Elzoghby AO, El-Fotoh WSA, Elgindy NA (2011) Casein-based formulations as promising controlled release drug delivery systems. J Control Release 153:206–216

Esmaelizadeh P, Fakhroueian Z, Beigi AAM (2011) Synthesis of biopolymeric α-lactalbumin protein nanoparticles and nanospheres as green nanofluids using in drug delivery and food technology. J Nano Res 16:89–96

Esmali M, Ghaffari SM, Moosavi-Movadehi Z, Atri MS, Sharifizadeh A, Farhadi M, Yousefi R, Chobert JM, Haertle T, Moosavi-Movadehi AA (2011) Beta casein-micelle as a nanovehicle for solubility enhancement of curcumin: food industry application. LWT-Food Sci Technol 44:2166–2172

Ezpeleta I, Irache JM, Stainmesse S, Chabenat C, Gueguen J, Popineau Y, Orecchioni AM (1996) Gliadin nanoparticles for the controlled release of all- *trans* -retinoic acid. Int J Pharm 131:191–200

Gómez-Estaca J, Balaguer MP, Gavara R, Hernández-Muñoz P (2012) Formation of zein nanoparticles by electrodynamic atomization: effect of the main processing variables and suitability for encapsulating the food coloring and active ingredient curcumin. Food Hydrocoll 28:82–91

Graveland-Bikker JF, Koning RI, Koerten HK, Geels RBJ, Heeren RMA, de Kruif CG (2009) Structural characterization of α-lactalbumin nanotubes. Soft Matter 5:2020–2026

Gunasekaran S, Ko S, Xiao L (2007) Use of whey proteins for encapsulation and controlled delivery applications. J Food Eng 83:31–40

Huang Q, Yu H, Ru Q (2010) Bioavailability and delivery of nutraceuticals using nanotechnology. J Food Sci 75:R50–R57

Irache JM, Bergougnoux L, Ezpeleta I, Gueguen J, Orecchioni AM (1995) Optimization and *in vitro* stability of legumin nanoparticles obtained by a coacervation method. Int J Pharm 126:103–109

Jahanshani M, Babaei Z (2008) Protein nanoparticle: a unique system as drug delivery vehicles. Afr J Biotechnol 7:4926–4934

Jun JY, Nguyen HH, Paik SYR, Chun HS, Kang BC (2011) Preparation of size-controlled bovine serum albumin (BSA) nanoparticles by a modified desolvation method. Food Chem 127:1892–1898

Kamau SM, Chelson SC, Chen W, Liu XM, Lu RR (2010) Alpha-lactalbumin: its production technologies and bioactive peptides. Comp Rev Food Sci Food Saf 9:197–212

Kaya-Celiker H, Mallikarjunan K (2012) Better nutrients and therapeutics delivery in food through nanotechnology. Food Eng Rev 4:114–123

Ko S, Gunasekaran S (2006) Preparation of sub-100-nm beta-lactoglobulin (BLG) nanoparticles. J Microencapsul 23:887–898

Kontopidis G, Holt C, Sawyer L (2004) β-Lactoglobulin: binding properties, structure, and function. J Dairy Sci 87:785–796

Kreuter J (2007) Nanoparticles—a historical perspective. Int J Pharm 331:1–10

Langer K, Balthasar S, Vogel V, Dinauer N, von Briessen H, Schubert D (2003) Optimization of the preparation process for human serum albumin (HSA) nanoparticles. Int J Pharm 257:169–180

Langer K, Anhorn MG, Steinhauser I, Dreis S, Celebi D, Schrickel N, Faust S, Vogel V (2008) Human serum albumin (HSA) nanoparticles: reproducibility of preparation process and kinetics of enzymatic degradation. Int J Pharm 347:109–117

Mehravar R, Jahanshahi M, Saghatoleslami N (2009) Production of biological nanoparticles from α-lactalbumin for drug delivery and food science application. Afr J Biotechnol 8:6822–6827

Mehravar R, Jahanshahi M, Najafpour GD, Saghatoleslami N (2011) Applying the Taguchi method for optimized fabrication of α-lactalbumin nanoparticles as carrier in drug delivery and food science. Iranica J Energy Environ 2:87–91

Mirshahi T, Irache JM, Nicolas C, Mirshahi M, Faure JP, Gueguen J, Hecquet C, Orecchioni AM (2002) Adaptive immune responses of legumin nanoparticles. J Drug Target 10:625–631

Mohan MS, Jurat-Fuentes JL, Harte F (2013) Binding of vitamin A by casein micelles in commercial skim milk. J Dairy Sci 96:790–798

Mohanraj VJ, Chen Y (2006) Nanoparticles—a review. Trop J Pharm Res 5:561–573

Mohanty B, Aswal VK, Kohlbrecher J, Bohidar HB (2005) Synthesis of gelatin nanoparticles via simple coacervation. J Surf Sci Technol 21:149–160

Müller-Buschbaum P, Gebhardt R, Roth SV, Metwalli E, Doster W (2007) Effect of calcium concentration on the structure of casein micelles in thin films. Biophys J 93:960–968

Podaralla S, Perumal O (2010) Preparation of zein nanoparticles by pH controlled nanoprecipitation. J Biomed Nanotechnol 6:312–317

Ramachandran R, Shanmughavel P (2010) Preparation and characterization of biopolymeric nanoparticles used in drug delivery. Indian J Biochem Biophys 47:56–59

Raynes JK, Carver JA, Gras SL, Gerrard JA (2014) Protein nanostructures in food—Should we be worried? Trends Food Sci Technol 37: 42–50

Sailaja AK, Amareshwar P (2012) Preparation of BSA nanoparticles by desolvation technique using acetone as desolvating agent. Int J Pharm Sci Nanotechnol 5:1643–1647

Sebak S, Mirzaei M, Malhotra M, Kulamarva A, Prakash S (2010) Human serum albumin nanoparticles as an efficient noscapine drug delivery system for potential use in breast cancer: preparation and *in vitro* analysis. Int J Nanomed 5:525–532

Semo E, Kesselman E, Danino D, Livney YD (2007) Casein micelle as a natural nano-capsular vehicle for nutraceuticals. Food Hydrocoll 21:936–942

Singh HD, Wang G, Uludag H, Unsworth LD (2010) Poly-L-lysine-coated albumin nanoparticles: stability, mechanism for increasing *in vitro* enzymatic resilience, and siRNA release characteristics. Acta Biomater 6:4277–4284

Storp B, Engel A, Boeker A, Ploeger M, Langer K (2012) Albumin nanoparticles with predictable size by desolvation procedure. J Microencapsul 29:138–146

Sundar S, Kundu J, Kundu SC (2010) Biopolymeric nanoparticles. Sci Technol Adv Mater doi:10.1088/1468-6996/11/1/014104

Taheri ES, Jahanshani M, Mosavian MTH (2012) Preparation, characterization and optimization of egg albumin nanoparticles as low molecular-weight drug delivery vehicle. Part Part Syst Charact 29:211–222

Teng Z, Luo Y, Wang Q (2012) Nanoparticles synthesized from soy protein: preparation, characterization, and application for nutraceutical encapsulation. J Agric Food Chem 60:2712–2720

Trevino SR, Scholtz JM, Pace CN (2008) Measuring and increasing protein solubility. J Pharm Sci 97:4155–4166

Vogel V, Langer K, Balthasar S, Schuck P, Mächtle W, Haase W, van den Broeck JA, Tziatzios C, Schubert D (2002) Characterization of serum albumin nanoparticles by sedimentation velocity analysis and electron microscopy. Progr Colloid Polym Sci 119:31–36

Weber C, Coester V, Kreuter J, Langer K (2000) Desolvation process and surface characterisation of protein nanoparticles. Int J Pharm 194:91–102

Weiss J, Takhistov P, McClements J (2006) Functional materials in food nanotechnology. J Food Sci 71:R107–R116

Xu H, Jiang Q, Reddy N, Yang Y (2011) Hollow nanoparticles from zein for potential medical applications. J Mater Chem 21:18227–18235

Zhong Q, Jin M (2009) Zein nanoparticles produced by liquid–liquid dispersion. Food Hydrocoll 23:2380–2387

Zimet P, Rosemberg D, Livney YD (2011) Re-assembled casein micelles and casein nanoparticles as nano-vehicles for omega-3-polyunsaturated fatty acids. Food Hydrocoll 25:1270–1276

Chapter 6
Indentation Technique: Overview and Applications in Food Science

Israel Arzate-Vázquez, Jorge Chanona-Pérez, Germán A. Rodríguez-Castro, Ariel Fuerte-Hernández, Juan V. Méndez-Méndez and Gustavo F. Gutiérrez-López

6.1 Indentation Technique

6.1.1 Definition

Indentation technique or instrumented indentation testing (IIT) involves the application of force with a known geometry indenter (tip) on the surface of a material; during the test the force and the depth of the tip into the material surface are constantly monitored (Fischer-Cripps, 2006b). Currently, indentation instruments can control the maximal load applied and the depth of the indenter on the surface. The indentation technique is mainly used for evaluation of mechanical properties such as hardness and elastic modulus, but also can include studies of the fracture resistance of brittle materials, mechanical mapping, dislocation behaviors, yield strength and residual stresses, obtaining information about plastic and elastic deformation, viscoelastic behavior, or performance of time-dependent materials (e.g., polymers and biological materials; Fischer-Cripps 2006b; Lucca et al. 2010).

This technique is very versatile and has some advantages which are mentioned below:

I. Arzate-Vázquez (✉) · J. V. Méndez-Méndez
Centro de Nanociencias y Micro y Nanotecnologías, Instituto Politécnico Nacional, Luis Enrique Erro s/n, Unidad Profesional Adolfo López Mateos, Col. Zacatenco, C.P. 07738 México, DF, Mexico
e-mail: iarzate@ipn.mx, alexfe26@yahoo.com.mx

J. Chanona-Pérez · G. F. Gutiérrez-López
Departamento de Ingeniería Bioquímica, Escuela Nacional de Ciencias Biológicas, Instituto Politécnico Nacional, Carpio y Plan de Ayala s/n, Col. Santo Tomás, C.P., 11340 México, DF, Mexico

G. A. Rodríguez-Castro · A. Fuerte-Hernández
Instituto Politécnico Nacional, SEPI-ESIME, Unidad Profesional Adolfo López Mateos, Col. Zacatenco, C.P., 07738 México, DF, Mexico

© Springer Science+Business Media New York 2015

H. Hernández-Sánchez, G. F. Gutiérrez-López (eds.), *Food Nanoscience and Nanotechnology,* Food Engineering Series, DOI 10.1007/978-3-319-13596-0_6

- It is a quick and nondestructive test.
- The sample size is small.
- It is possible to evaluate mechanical properties of coatings and thin films of micro- and nanometric thickness.
- Measurement is local, allowing the characterization of phases present in the material.
- Mechanical mappings can be performed along the samples.
- Sample preparation is minimal and in the case of metallic materials it is required that the samples are polished just as in the case of bone samples.

Due to the importance and increasing use of the indentation technique in materials science, it was necessary to develop international standards; an example is the international standard ISO 14577 "Metallic materials-instrumented indentation test for hardness and materials parameters," which was published in ISO 2002. The standard consists of three parts, where the part 1 refers to the test method, part 2 to the verification procedures and calibration of testing machines, and part 3 is the calibration of reference blocks. ISO 14577-1 establishes ranges of indentation technique based on the maximum load applied and the maximum depth of penetration (Table 6.1). Subsequently, the Part 4 of the standard was developed that is aimed specifically at the indentation of coatings and thin films, this was called ISO 14577-4 "Test method for metallic and nonmetallic coatings ISO 2007." The development of ISO 14577-4 is currently of great importance because it provides details to consider when applying the indentation technique to characterize coatings and thin films, which are manufactured using nanotechnology tools (e.g., chemical vapor deposition CVD).

As mentioned above, there are great advances in the application of the technique in metallic materials, however recently in biological materials the use of technique is increasing and therefore it is necessary to establish protocols and international standards to consider specific issues in these samples that are more complex due to its multiphasic composition and heterogeneous microstructure.

There are a wide variety of indentation instruments with different features in the market, typically the monitoring of displacement of indenter is done by capacitance or inductance method, while the generation force is done by electrostatic force, magnetic coils, or by piezoelectric element (Ebenstein and Pruitt 2006). Indentation instruments are capable of applying loads in the order of N to μN, which include the three ranges indentation defined by ISO 14577, additionally the instruments count with optical microscopes or heads atomic force microscopy through which the re-

Table 6.1 Ranges of indentation technique as a function of maximum load applied and maximum depth of penetration (based in ISO 14577-1)

Range	Maximum load (Fmax)	Maximum depth (hmax)
Macro	2 N to 30 kN	–
Micro	Less than 2 N	Greater than 200 nm
Nano	–	Less than 200 nm

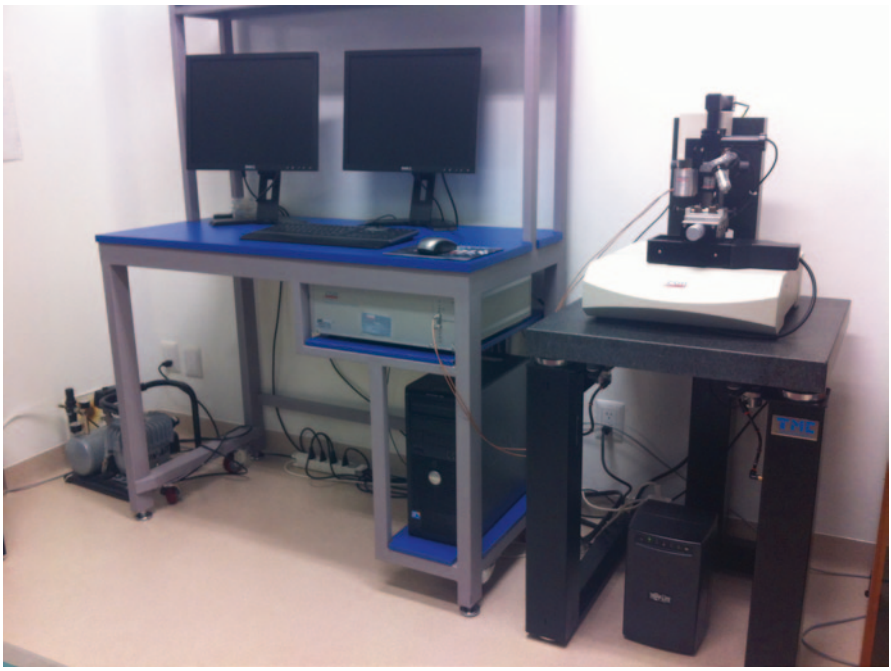

Fig. 6.1 Nanoindentation tester (TTX-NHT, CSM Instruments, Switzerland) located in the Centro de Nanociencias y Micro y Nantecnologías at Instituto Politécnico Nacional, México

sidual footprint after indentation test can be captured. Figure 6.1 shows a nanoindententation tester with optical microscope coupled to a digital camera (NNH-TTX, CSM Instruments, Switzerland).

6.1.2 Measurement Method

Instrumented indentation systems allow the application of a specified force or displacement history, in such a way that force and displacement, P and h, respectively, are controlled and measured simultaneously over a complete loading cycle. The process of IIT involves an indenter tip, normal to the sample surface, which is driven into the sample by applying an increasing load up to a specific value. The indenter is withdrawn gradually and the load decreases until full or partial relaxation occurs in the material. Figure 6.2 illustrates the indentation process steps.

The main purpose of the instrumented indentation technique is to calculate the contact area (A) of the residual footprint as a function of the load applied by the indenter. In order to estimate the size of the contact area (A) it is necessary to know the geometry of the indenter used, because it has to calculate the contact depth (h_c) which is related to the contact area. Therefore, the indenters or tips play an important role in the indentation technique.

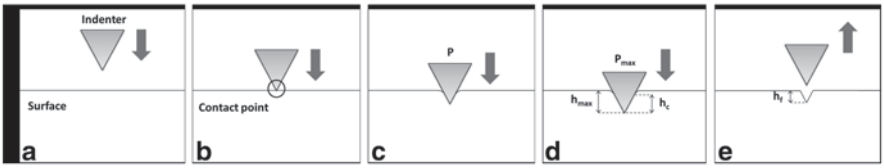

Fig. 6.2 Indentation process steps: approaching the indenter (**a**), contact point between the indenter and surface (**b**), application of the load (**c**), increasing load up to the maximum load (P_{max}) (**d**) and unload the indenter (**e**)

The basic geometries of the indenters include pyramidal and spherical. Berkovich and Vickers are the most pyramidal indenters commonly used. The Berkovich indenter has a pyramidal geometry with triangular base and an angle of 65.03° between the axis of the pyramid and the three faces; on the other hand the Vickers indenter has a pyramidal geometry with square base with an angle of 136° between opposite faces of the pyramid (Fischer-Cripps 2006b, 2011c; Lucca et al. 2010). The pyramidal indenters are mainly used for hard materials (metals and ceramics), but also can be used for biological materials (e.g., bones and teeth) (Ebenstein and Pruitt, 2006; Lucca et al. 2010). The spherical and conical–spherical indenters are recommended for soft materials (e.g., polymers, elastomers, biological materials, and foods) because they minimize plastic deformation and stress concentration and avoid damaging the sample (Ebenstein and Pruitt, 2006). This kind of indenters can be designed in different sizes of 200 μm to 1 μm of diameter. Figure 6.3 shows three-dimensional (3D) representations of the pyramidal (Berkovich and Vickers), spherical, and conical indenters. Another type of indenters that is rarely used is the cylindrical flat punch. Diamond is the material most used for the manufacture of indenters, however they can also be made of tungsten carbide and sapphire (Lucca et al. 2010).

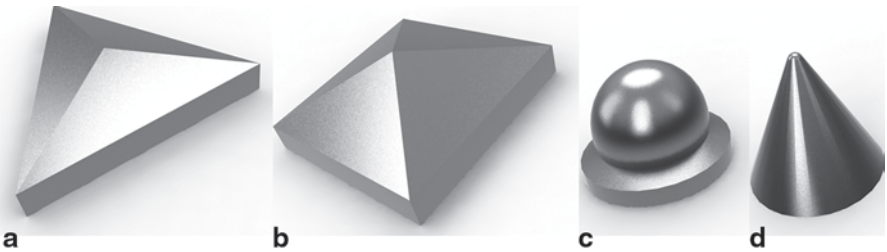

Fig. 6.3 3D representations of the indenters most commonly used in the indentation technique: Berkovich (**a**), Vickers (**b**), spherical (**c**) and conical (**d**)

6.1.3 Analysis of Data (Hardness and Elastic Modulus)

When instrumented indentation test is used to estimate the elastic modulus and hardness of material, it is necessary to obtain load versus depth/displacement measurements. Depth measurement and knowledge of the shape of indenter are used to calculate the contact areas, instead of measurement of the size of impressions. There are different methods to analyze the load-displacement data that are used to compute hardness and elastic modulus of materials. Oliver and Pharr (1992) proposed a method of analysis for the load–displacement curves, known as compliance. Figure 6.4 is a schematic illustration of load–depth indentation measurements, where the deformation during loading is assumed to be both elastic and plastic (Hardness printing form) and the elastic displacement is recovered during unloading. The parameter P is the load and h the displacement relative to the initial surface. From the load–penetration curve, P_{max} is the maximum load, h_{max} is the maximum displacement, S is the contact stiffness determined as the slope of the upper portion of the unloading curve during the initial stages of unloading (dP/dh), and h_f is the permanent depth of penetration after the indenter is fully withdrawn.

Doerner and Nix (1986) determined the hardness (H) and elastic modulus (E) considering that the contact area remains constant as the indenter is withdrawn.

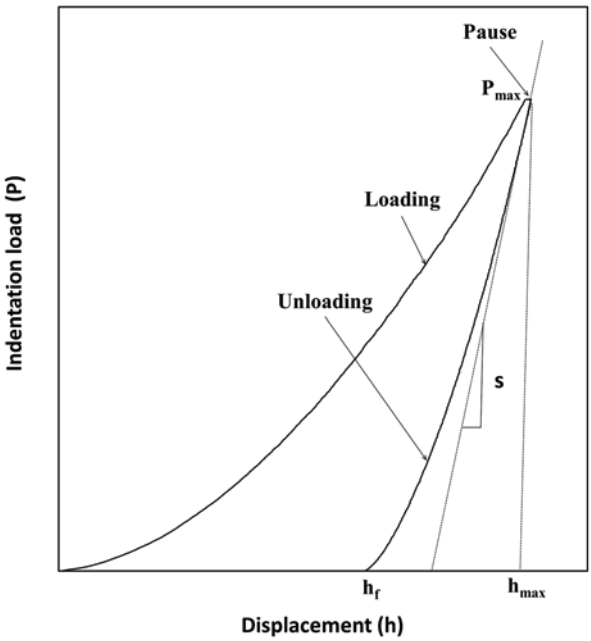

Fig. 6.4 A schematic illustration of load–penetration measurements for an indentation test

However, Oliver and Pharr (1992) showed that unloading curves are distinctly curved and usually well fitted by the power law relation:

$$P = \alpha(h - h_f)^m, \tag{6.1}$$

where α and m are power law fitting constants. From these data, the initial unloading slope (contact stiffness, S) is estimated by analytically differentiating Eq. (6.1) and evaluating the result at the maximum indentation depth:

$$S = \left(\frac{dp}{dh}\right)_{h=h_{\max}} = Bm(h_{\max} - h_f)^{m-1}. \tag{6.2}$$

From Eq. (6.3) is calculated the contact depth h_c (see Fig. 6.5) under the maximum indentation force:

$$h_c = h_{\max} - \varepsilon\frac{P_{\max}}{S}, \tag{6.3}$$

where ε is a constant which depends on the indenter geometry, 0.72 for conical indenters (Hay and Pharr 2000).

The projected contact area, A, under the maximum indentation force considering a sharp conical indenter is obtained by the indenter tip included angle, θ, and the estimated contact depth, h_c, that is

$$A = \left[(h)_c \tan\theta\right]^2. \tag{6.4}$$

According to assumption that the compliances of the specimen and the indenter tip can be combined as springs in series, the effect of a nonrigid indenter on the load–

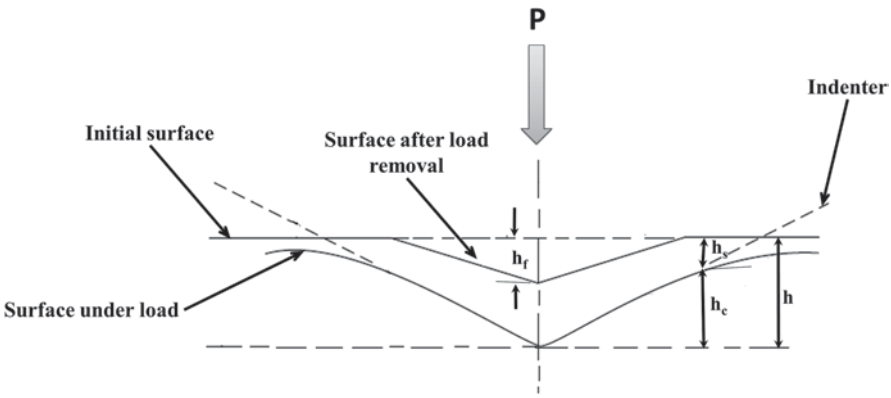

Fig. 6.5 Cross section of an indentation

displacement curve can be accounted for by defining a reduced modulus calculated by

$$E_r = \frac{\sqrt{\pi}}{2\beta}\left(\frac{dP}{dh}\right)\left(\frac{1}{\sqrt{A}}\right) \tag{6.5}$$

and

$$\frac{1}{E_r} = \frac{1-v^2}{E} + \frac{1-v_i^2}{E_i}, \tag{6.6}$$

where v and v_i, E and E_i are Poisson's ratios and elastic modulus of the material evaluated and the indenter material, respectively. Hardness is defined as the ratio of indentation load and projected contact area, as following:

$$H = \frac{P_{max}}{A}. \tag{6.7}$$

This definition of hardness is different from that used in an imaging indentation test. In the latter case, the area is the residual area measured after the indenter is removed, while in the instrumented indentation test the area is the contact area under maximum load. A conventional hardness test with zero residual area would give infinite hardness, while a nanoindentation test would give a finite hardness.

6.1.4 Parameters and Viscoelastic Behavior

Some materials exhibit a time-dependent mechanical behavior or viscoelastic (e.g., glass, metal or ceramics at high temperatures, polymers, plastics, composites; Chena et al. 2013; Lisnyaka et al. 2008); however, most biological materials exhibit different degrees of viscoelasticity (e.g., tissues, organs of plants and animals, food materials; Isaksson et al. 2010). Viscoelasticity is a time-dependent mechanical property of the materials with sensitivity to load rate and deformation applied. Viscoelastic behavior can be quantified in a material by the phenomena occurring in this when loads and deformations are applied, such as modulus of elasticity which is dependent upon the rate of loading, creep, relaxation, and hysteresis.

By indentation technique is possible to determine the viscoelastic properties such as creep and relaxation in different kinds of biological materials (Wu et al. 2011). In order to represent the creep behavior, the sample is subjected to a loading rate until reaching a maximum value, in which the load is kept constant during a certain period of time, and finally applying an unloading rate until this reaches zero. Indenter depth within the period where the load is kept constant represents the creep (Fischer-Cripps 2004a), and is given by the following equation:

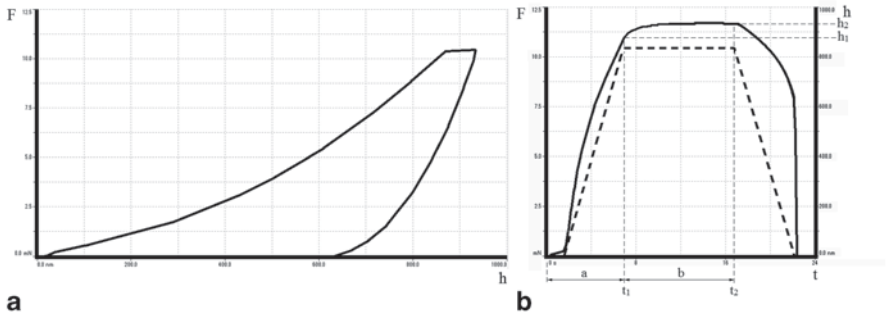

Fig. 6.6 Typical curve of indentation of cortical bone (**a**) and graph of load applied (*segmented line*) and depth indentation (*continuous line*) in function of time (**b**) showing of creep indentation

$$C_{\mathrm{IT}} = \frac{h_2 - h_1}{h_1} \times 100, \tag{6.8}$$

where h_1 is the indentation depth at time t_1 when the force is kept constant, and h_2 is the indentation depth at the time t_2 of holding the constant test force, as shown in Fig. 6.6b.

Figure 6.6a represents the typical curve during a nanoindentation test of cortical bone in osteons lumbar vertebrae pig, showing the relationship between the applied force and the indentation depth. While in Fig. 6b, the segmented line plot represents the application of force and the continuous line plot corresponding indentation depth (creep) both in function of time. The parameters used were: maximum load of 10 mN, loading rate of 120 mN/min, unloading rate of 120 mN/min, and 10 s pause at maximum load.

Otherwise, in order to represent the relaxation behavior, an indentation depth ratio is applied in the sample, to reach a maximum value which is kept constant during a certain period of time and finally applying an unloading rate of the indentation reaching a value of zero. Indenter force is included in the period where indentation depth is kept, represents the relaxation of stresses in the material, and is given by the equation:

$$R_{\mathrm{IT}} = \frac{F_1 - F_2}{F_1} \times 100, \tag{6.9}$$

where F_1 is the force at time t_1 when the indentation depth is kept constant, and F_2 is the force at time t_2 in the moment the indentation depth maintained was removed, as shown in Fig. 6.7b.

Figure 6.7a represents the curve during a nanoindentation test in an annulus porcine lumbar intervertebral disc, showing the relationship between indentation depth and force. Whereas in Fig. 6.7b, segmented line plot represents the indentation depth applied and continuous line plot represents the corresponding force

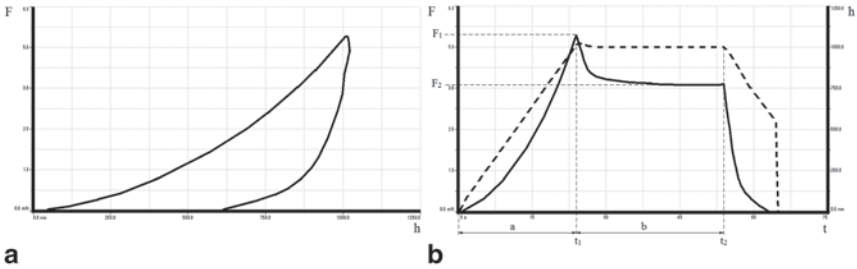

Fig. 6.7 Indentation curve controlling of depth in annulus porcine lumbar intervertebral disc (**a**) and graph of load applied (*continuous line*) and depth indentation (*segmented line*) in function of time (**b**) showing relaxation indentation

(relaxation) both in function of time. The parameters used were: maximum depth of 1000 nm, loading rate of 2500 nm/min, unloading rate of 2500 nm/min, and 30 s pause at the maximum indentation depth.

Therefore, from the above it can be concluded that from indentation curves controlling the applied load and the indentation depth the creep and relaxation indentation can be calculated which are parameters that are associated with viscoelastic behavior. The following briefly describes the term viscoelasticity to have a greater understanding of this behavior present in biological materials.

The two basic components of the viscoelastic behavior are viscosity and elasticity. When sudden load is applied to a viscoelastic material, it exhibits an elastic behavior presenting a deformation, which is represented by a spring in a mathematical model. The elastic behavior is described by Hooke's Law, where the stress is directly proportional to the strain but independent of the strain rate:

$$\sigma = E\varepsilon, \tag{6.10}$$

where σ is the stress, E the elastic modulus, and ε the strain.

Immediately after this, the material behaves as a viscous liquid, which is represented by a dashpot using a mathematical model. This behavior is described by Newton's law, in which the stress is directly proportional to the strain rate but independent of the same strain:

$$\sigma = \eta\left(\frac{d\varepsilon}{dt}\right), \tag{6.11}$$

where σ is the stress, η is the coefficient of viscosity of the fluid, and $\frac{d\varepsilon}{dt}$ is the strain rate.

If a viscoelastic material is subjected to a higher load rate, the slope of the stress–strain curve will be steeper and therefore, the elastic modulus will be higher, this characteristic is typical of viscoelastic materials. In a viscoelastic material, the creep occurs when a sudden load is applied and this is kept constant for a certain time.

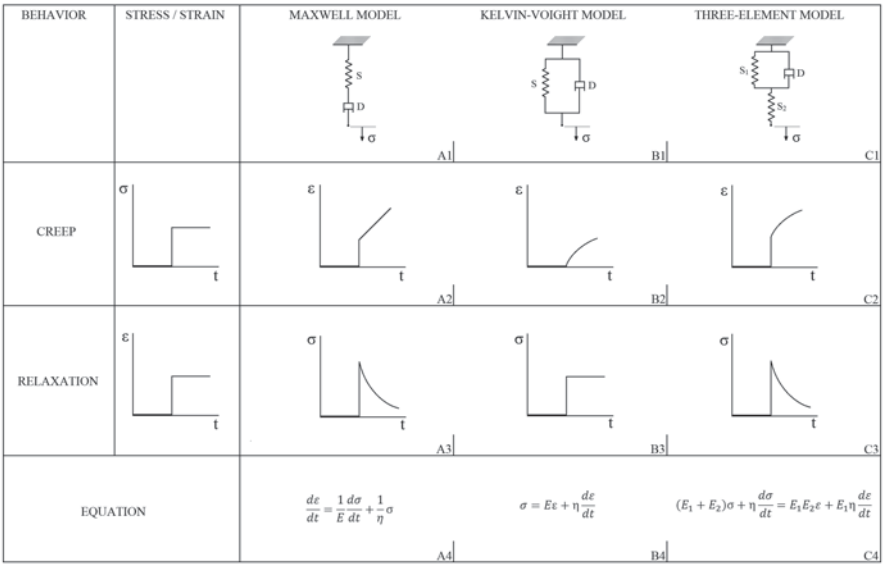

Fig. 6.8 Diagram of different models representing the viscoelastic behavior based in creep and relaxation: Maxwell model (**a**), Kelvin–Voigt model (**b**), and Three-Element Model (**c**)

The typical curve shows a steady state asymptotically (Fig. 6.8, C2). Relaxation occurs when in a previously deformed material, the stresses to which it is subjected decrease asymptotically through a certain time, whereas the deformation is kept constant (Fig. 6.8, C3).

A viscoelastic material also exhibits a phenomenon called hysteresis when subjected to cyclic loading and unloading. During this process, the material presents a loss of energy, which is represented by the area between the loading and unloading curve. Viscoelastic materials can be represented by constructing mathematical models that include arrangements between springs and dashpots. The springs are used to represent the behavior elastic solid, whereas the dashpots represent the behavior of a viscous fluid. From serial and parallel arrangement between these elements, it is possible to construct empirical models that represent more accurate biological materials such as bone, cartilage, tendons, and ligaments.

One of the basic mathematical models is the Maxwell model, which is constructed by a series arrangement of a spring and a dashpot (Fig. 6.8, A1), the governing equation for the model is shown in Fig. 6.8, A4, from which is possible to determine the viscoelastic behavior of the material. In a creep test, this model adequately explains the instantaneous deformation, which is represented by the spring, this being true for biological materials; however, the creep is linear and does not conform to the reality for this type of material (Fig. 6.8, A2), whilst relaxation is exponential, adjusting to the real behavior of biological materials (Fig. 6.8, A3).

Another basic model is the Kelvin–Voigt model which is constituted by a parallel arrangement of a spring and a dashpot (Fig. 6.8, B1), the governing equation for the

model is shown in Fig. 6.8, B4, from which it possible to determine the viscoelastic behavior of the material. In a creep test in this model, the element represented by the spring does not present an instantaneous deformation, which is not true for biological materials; however, the model explains adequately creep behavior within the viscous element (Fig. 6.8, B2), whilst not having a relaxation phenomenon, which is not true for biological materials (Fig. 6.8, B3).

Although these models are useful for understanding, the viscoelastic behavior does not represent any real material known. However, through a combination of these, it is possible to construct more complex models able to represent more efficiently the behavior of different types of biological materials (Yuya et al. 2010; Lukes et al. 2008). One such model is the Three-Element model, which consists of a spring and a Kelvin–Voigt model in series (Fig. 6.8, C1), the governing equation of this model is shown in Fig. 6.8, C4, from which it is possible to determine the viscoelastic behavior of the material. This model is one of the most used to describe the viscoelastic behavior of biological materials, as described more realistically (Fig. 6.8, C2 and C3).

6.2 Mechanical Characterization of Biological Materials by Indentation

During the last decades there has been increasing use of indentation technique of biological materials. This fact is due to the advantages this technique has, which have been mentioned above. In the literature, there are several works in which indentation technique has been employed for evaluating mechanical properties of biological materials to micro- and nanolevels. Table 6.2 has listed some of the published works using indentation technique in biological materials, in the table the aim of the research, the mechanical parameters assessed and type of indenter used can be seen. As seen in Table 6.2, the Young's modulus or elastic modulus is one of the more evaluated parameters due to which the biological materials present elastic or viscoelastic behavior. Additionally, it can be seen that both pyramidal and spherical indenters are used for the examination of samples.

In general, biological tissues that have been characterized by this technique can be grouped into soft tissues (e.g., cartilage, arteries, polymers, hydrogels) and mineralized tissues (e.g., bones, teeth, bioceramics). Some types of samples that have been characterized include bones (Albert et al. 2013), teeth (Fung-Ang et al. 2009), cartilage (Franke et al. 2011), turtle carapace (Achrai and Wagner 2013), black coral skeleton (Juarez de la Rosa et al. 2012) and wings dragonflies (Tonj et al. 2007). The use of indentation technique allows to elucidate and establish correlations of composition-function type, which makes it a powerful and useful tool for the analysis of biological samples.

In the literature, critical review articles are found about the nanoindentation in biologic materials. Ebenstein and Pruitt (2006) reviewed the most important aspects of the technique and cited some examples published. They note that the nanoinden-

Table 6.2 Studies of mechanical characterization of biological materials by indentation technique

Biological material	Objective of work	Mechanical parameters evaluated	Indenter type	References
Articular porcine cartilage	Use of dynamic nanoindentation at different frequency ranges	Storage E' and loss modulus E" (1.9–7.5 MPa)	Berkovich	O. Franke et al. 2011
Poly(dimethyl siloxane) (PDMS), poly(ethylene glicol) (PEG)	Investigate the use of surfactants to eliminate adhesion between the tip and the sample	Young's modulus (0.71–8.34 MPa)	Spherical	Kohn and Ebenstein, 2013
Black coral skeleton	Evaluate the mechanical properties in different zones of the sample	Young's modulus (5.53 to 6.62 GPa) hardness (132.95–157.59 MPa)	Spheroconical	Juárez de la Rosa et al. 2012
Turtle carapace	Correlate the microscale architecture with the mechanical properties	Young's modulus (0.2 to 18.2 GPa) hardness (0.007–0.67 GPa)	Berkovich	Achrai and Wagner, 2013

tation technique has emerged as a powerful tool for the evaluation of mechanical properties at the nano- and microscale in tissues and other biomaterials. Besides, they discuss the operating principle of the technique and mention that most polymers and biomaterials exhibit viscoelastic or time-dependent behavior. A highlight that they deepen is the hydration factor in biological samples, because the evaluated properties depend on the state of hydration of the sample, so it is very important to consider the evaluation of these materials.

In another work, Lucca et al. (2010) presented a review of the measurement method, the instruments used, and the procedures for analysis of results. Also, a section of work allocated to the utility of the indentation in biological materials. They mention that in general the biological materials show small values of the elastic modulus, exhibited viscoelastic behavior, and that the mechanical properties depend of their hydration status. As well they mention some studies that have been conducted in various biological materials.

Moreover, using the indentation technique it is possible to evaluate the fracture toughness in biomaterials and hard tissue such as bones. Kruzic et al. (2009) studied four indentation techniques to evaluate the fracture toughness in cortical bone: the Vickers indentation fracture (VIF) test, the cube corner indentation fracture (CCIF) test, the Vickers crack opening displacement (VOCD) test, and the interface indentation fracture (IIF) test. Among the conclusions of the work indicate that it must take into account the spatial resolution when considering biomaterials and hard biological tissues. Finally, mention that organic component of the hard tissue may influence the evaluation of material properties.

In short, the importance of knowing the articles published and advances in the characterization by indentation technique in biological material, are useful to establish basic considerations that should be taken into account when examining food materials which are likely to have similar characteristics to some biological materials mentioned above.

6.3 Examples of the Use of Indentation Technique in Food Science

There are few reports in the literature regarding the use of the indentation technique to evaluate mechanical properties in foods. Below are discussed some of the works that have been published.

6.3.1 Micromechanical Properties of Hen's Eggshell

Severa et al. (2010) describes the applicability of the indentation method for determining micromechanical properties of hen's eggshell. In methodology, they selected eggshell fragments extracted from different locations and were subsequently embedded in resins. Resin tablets were polished in order to obtain flat surfaces with low roughness values. Roughness has a considerable effect on the measurements of the mechanical properties of the samples evaluated. The elastic modulus was defined as the main parameter for evaluation of the samples. The test variables were: maximum load of 12 mN, loading and unloading rate of 72 mN/min, and pause of 20 s. A Berkovich diamond tip was used in all the experiments. Figure 6.9a shows a typical curve of indentation (force vs. penetration depth) on eggshell. In each sample, the experiment was performed in a matrix of 9 × 24 = 216 indentations in the material cross section as shown in Fig. 6.9b.

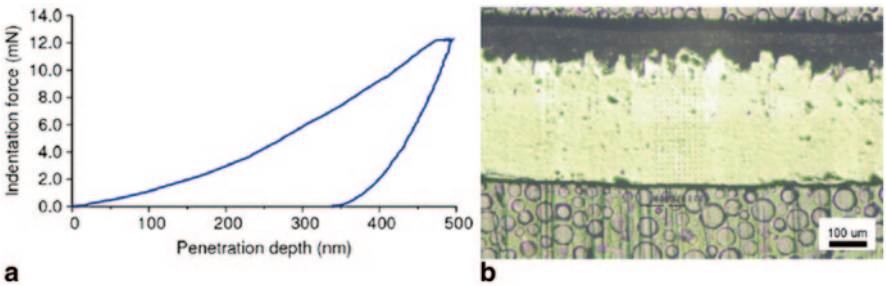

Fig. 6.9 **a** Typical curve of indentation (load vs. penetration depth). **b** Optical image of eggshell cross section shows a matrix of indents (9 × 24 = 216) (Severa et al. 2010)

From the results, high variations in the values of Young's modulus at individual points were found. This fact is attributed to the chemical composition (concentration and crystal orientation of $CaCO_3$). The Young's modulus values were not significantly different and ranged from 47.4 to 53 GPa. They conclude that the indentation technique proved to be appropriate, easy to use, and a powerful tool for local evaluation of mechanical properties of eggshell.

6.3.2 Fracture Behavior in Eggshell

Currently our research group is conducting a study of fracture toughness in eggshell with the purpose of establishing the fracture behavior using a Berkovich indenter. Eggs from a national trademark were randomly selected for the experiment. The eggs were then washed with distilled water to remove dirt. Subsequently, equatorial sections of eggshell were obtained and embedded in epoxy resin. Once the resin was hardened after 24 h, the tablets were polished with sandpaper of different grain sizes and alumina to achieve a mirror finish. Figure 6.10 shows a diagram of eggshell preparation to evaluate the fracture by indentation technique. The surface roughness of the samples was evaluated after polishing with an AFM (diMultimode V, Veeco, USA) and Ra values (arithmetic average roughness) of 6.54 ± 0.45 nm were observed. A nanoindentation tester (TTX-NHT, CSM Instruments, Switzerland) with a Berkovich diamond indenter was used.

Preliminary results showed that high values of maximum loads generated fractures in the cross section of the eggshell. Figure 6.11 shows an optical image of a

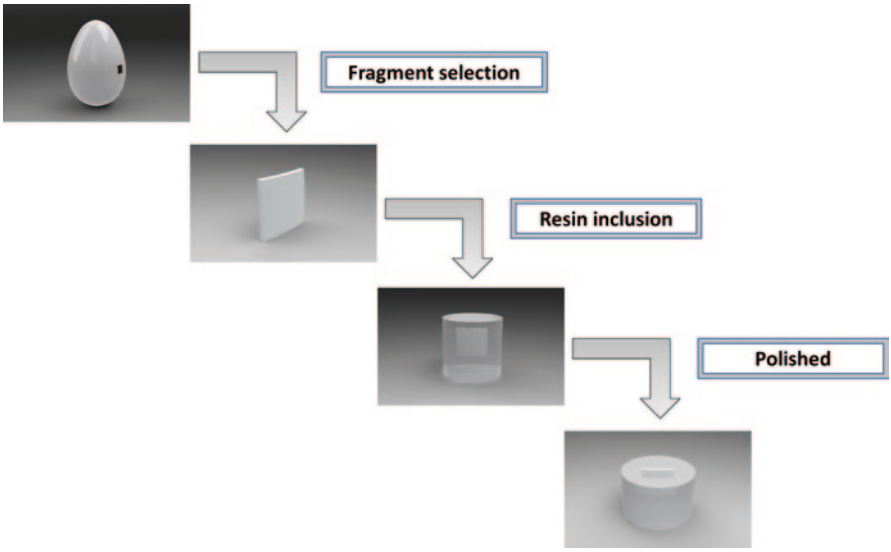

Fig. 6.10 Diagram of eggshell preparation for evaluation by indentation technique

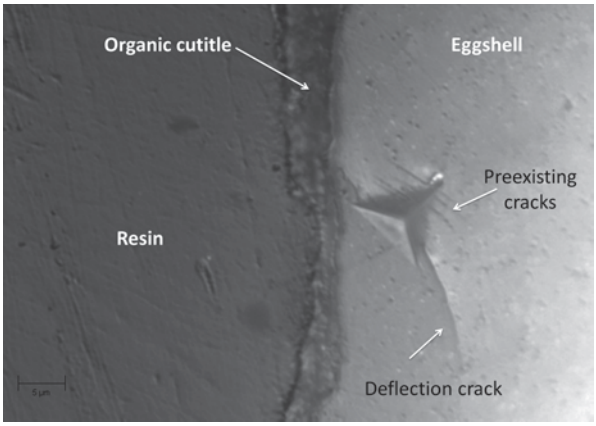

Fig. 6.11 Optical image of residual footprint of indentation on eggshell showing two types of fracture: preexisting cracks and deflection crack

residual footprint indentation showing two types of fracture patterns: preexisting cracks and crack deflection.

It is necessary to continue to conduct more experiments to elucidate properly the fracture pattern and to calculate the fracture toughness by established models in the literature for biomaterials. Another result observed from preliminary results is the presence of the indentation size effect (ISE) which establishes the values of hardness and Young's modulus are based on the maximum load.

6.3.3 Biopolymers and Edible Films

Biopolymer membranes and edible films have been characterized mechanically by indentation technique. Edible films are films made of biopolymers (polysaccharides, proteins, lipids) that act as gas exchange membranes and confer protection to the foods in order to extend their shelf life (Lin and Zhao, 2007) Moreover, due to the growing pollution problem the need to design biodegradable packaging has arisen which incorporates biomolecules (polysaccharides) in their composition significantly reducing the time of biodegradation. Based on the studies published in the literature, this type of membranes are the most evaluated through indentation technique and Table 6.3 shows some of them.

Lower values of elastic modulus are present in these materials seen in Table 6.3. Additionally, the values of the mechanical properties are strongly influenced by the membrane composition and moisture content. The kind of tip that was used in all the work was pyramidal, although, as mentioned above, for this type of materials spherical indenters are recommended.

The advantages of this technique for the characterization of films are obtaining reliable values of hardness and elastic modulus even when the films have small thicknesses and it can carry out localized measurements. When performing the characterization of these materials, the state of hydration should be considered be-

Table 6.3 Studies of mechanical characterization of biopolymer membranes and edible films by indentation technique.

Membranes composition	Objective of work	Young's modulus (GPa)	Indenter type	Reference
Alginate, chitosan, alginate/chitosan	To determinate mechanical properties	0.67–0.76	Berkovich	Arzate-Vázquez et al. 2011
Aloe vera gel/gellan gum	Evaluate differences in edible films based in their composition	0.05–2.02	Berkovich	Alvarado-González et al. 2012
Chitosan	Evaluate the properties of uncross-linked and cross-linked films	1.5 (uncross-linked) and 4.7 (cross-linked)	Vickers	Aryaei et al. 2012
Zein and chitosan	Establish relationship between mechanical and structural properties	0.061–0.088	Berkovich	Escamilla-García et al. 2013
Chitosan, clay, glycerol	Study of the combined effect of both clay and glycerol on the properties	1.70–6.33	Berkovich	Lavorgna et al. 2010

cause the mechanical properties evaluated depend on this variable and also it is important to select the test parameters appropriate for establishing the point of contact between the tip and the material surface. The incorrect contact point location can generate mechanical property values underestimated and overestimated.

6.4 Conclusions

Instrumented indentation technique is an efficient tool for the evaluation of mechanical properties at micro- and nanolevel in materials and biomaterials. This chapter presented an overview of the most important points of the technique. The hardness and elastic modulus are the parameters obtained from the analysis of the indentation curves. Biological and food materials exhibit viscoelastic behavior or time dependence and this topic was discussed. Through discussion of articles related to the use of indentation technique in biological and food materials, the effectiveness of using the technique for the characterization of such materials was demonstrated. Some works in food materials were discussed; however, it is necessary to conduct more studies with other food materials in order to exploit the advantages offered

by the technique. Additionally, it was shown that it is possible to study the fracture behavior in biomaterials. This work aims to establish the basic knowledge of the indentation technique for researchers in the field of food science as well as some points to consider for the effective evaluation of the mechanical properties of foods.

Acknowledgments This research was financed through the project 20131310 provided by Secretaría de Investigación y Posgrado (SIP) at the Instituto Politécnico Nacional (IPN).

References

Achrai B, Wagner HD (2013) Micro-structure and mechanical properties of the turtle carapace as a biological composite shield. Acta Biomater 9:5890–5902

Albert C, Jameson J, Toth JM, Smith P, Harris G (2013) Bone properties by nanoindentation in mild and severe osteogenesis imperfect. Clin Biomech (Bristol, Avon) 28:110–116

Alvarado-González JS, Chanona-Pérez JJ, Welti-Chanes JS, Calderón-Domínguez G, Arzate-Vázquez I, Pacheco-Alcalá SU, Garibay-Febles V, Gutiérrez-López GF (2012) Optical, microstructural, functional and nanomechanical properties of *Aloe vera* gel/gellan gum edible films. Rev Mex Ing Quím 11(2):193–210

Aryaei A, Jayatissa AH, Jayasuriy AC (2012) Nano and micro mechanical properties of uncross-linked and cross-linked chitosan films. J Mech Behav Biomed Mater 5:82–89

Arzate-Vázquez I, Martínez-Rivas A, Méndez-Méndez JJ, Mendoza-Madrigal AG, Ponce-Reyes CE, Chanona-Pérez JJ (2011) Nanoindentation of edible films: a new complementary characterization of nanomechanical properties. In: Proceedings of the 6th International CIGRTechnical Symposium—Towards a sustainable food chain: food, process, bioprocessing and food quality management, Nantes, 18–20 April 2011

Chena Z, Diebelsa S, Peterb NJ, Schneiderb AS (2013) Identification of finite viscoelasticity and adhesion effects in nanoindentation of a soft polymer by inverse method. Comput Mater Sci 72:127–139

Doerner MF, Nix WD (1986) A method for interpreting the data from depth-sensing indentation instruments. J Mater Res 1(4):601–609

Ebenstein DM, Pruitt LA (2006) Nanoindentation of biological materials. Nanotoday 1(3):26–33

Escamilla-García M, Calderón-Domínguez G, Chanona-Pérez JJ, Farrera-Rebollo RR, Andraca-Adame JA, Arzate-Vázquez I, Méndez-Méndez JV, Moreno-Ruiz LA (2013) Physical and structural characterisation of zein and chitosan edible films using nanotechnology tools. Int J Biol Macromol 61:196–203

Fischer-Cripps AC (2004a) A simple phenomenological approach to nanoindentation creep. Mater Sci Eng A Struct Mater 385:74–82

Fischer-Cripps AC (2006b) Critical review of analysis and interpretation of nanoindentation test data. Surf Coat Technol 200:4153–4165

Fischer-Cripps AC (2011c) Nanoindentation. Mechanical Engineering Series, vol 1, 3rd edn. Springer, New York

Franke O, Göken M, Meyers MA, Durts K, Hodge AM (2011) Dynamic nanoindentation of articular porcine cartilage. Mater Sci Eng **C** Mater Biol Appl 31:789–795

Fung Ang S Scholz T Klocke A Schneider GA (2009) Determination of the elastic/plastic transition of human enamel by nanoindentation. Dent Mater 25:1403–1410

Hay JL, Pharr PM (2000) Instrumented indentation testing. ASM Handbook Vol 8. ASM International, Materials Park

Isaksson H, Nagao S, Malkiewicz M, Julkunen P, Nowak R, Jurvelin JS (2010) Precision of nanoindentation protocols for measurement of viscoelasticity in cortical and trabecular bone. J Biomech 43:2410–2417

ISO. (2002) 14577-1,-2,-3. Metallic materials—Instrumented indentation test for hardness and materials parameters- Part 1: Test method, Part 2: Verification and calibration of testing machines, Part 3: Calibration of reference blocks. ISO, Geneve

ISO. (2007) 14577-4. Metallic materials—Instrumented indentation test for hardness and materials parameters- Part 4: test method for metallic and nonmetallic coatings. ISO, Geneve.

Juárez-de la Rosa BA Muñoz-Saldaña J Torres-Torres D Ardisson PL Alvardo-Gil JJ (2012) Nanoindentation characterization of the micro-lamellar arrangement of black coral skeleton. J Struct Biol 177: 349–357

Khon JC, Ebenstein DM (2013) Eliminating adhesion errors in nanoindentation of compliant polymers and hydrogels. J Mech Behav Biomed Mater 20: 316–326

Kruzic JJ, Kim DK, Koester KJ, Ritchie RO (2009) Indentation techniques for evaluating the fracture toughness of biomaterials and hard tissues. J Mech Behav Biomed Mater 2: 384–395

Lavorgna M, Piscitelli F, Mangiacapra P, Buonocore GG (2010) Study of the combined effect of both clay and glycerol plasticizer on the properties of chitosan films. Carbohydr Polym 82:291–298

Lin D, Zhao Y (2007) Innovations in the development and application of edible coatings for fresh and minimally processed fruits and vegetables. Compr Rev Food Sci Food Saf 6:60–76

Lisnyaka VV, Dubb SN, Stratiichukb DA, Stusa NV (2008) Nanoindentation study on viscoelasticity in cesium tungstophosphate glasses. Mater Lett 62:1905–1908

Lucca DA, Herrmann K, Klopfstein MJ (2010) Nanoindentation: measuring methods and applications. CIRP Ann Manuf Technol 59:803–819

Lukes J, Mares T, Nemecek J, Otahal S (2008) Examination of the microrheology disc by nanoindentation. IFMBE Proc 23:1792–1796

Oliver WC, Pharr GM (1992) An improve technique for determining hardness and elastic modulus using load and displacement sensing indentation experiments. J Mater Res 7 (6):1564–1583

Severa L, Nemecek J, Nedomová S, Buchar J (2010) Determination of micromechanical properties of a hen×s eggshell by means of nanoindentation. J Food Eng 101:146–151

Tonj J, Zhao Y, Su J, Chen D (2007) Nanomechanical properties of the stigma of dragonfly Anax Parthenope Julius Brauer. J Mater Sci 42:2894–2898

Wu Z, Baker TA, Ovaert TC, Niebur GL (2011) The effect of holding time on nanoindentation measurements of creep in bone. J Biomech 44:1066–1072

Yuya PA, Amborn EK, Beatty MW, Turner JA (2010) Evaluating anisotropic properties in the porcine temporomandibular joint disc using nanoindentation. Ann Biomed Eng 38:2428–243

Chapter 7
Lipid Matrices for Nanoencapsulation in Food: Liposomes and Lipid Nanoparticles

Lucimara Gaziola de La Torre and Samantha Cristina de Pinho

7.1 Introduction

Food encapsulation systems produced with lipid-based matrices can be considered as good choices for the incorporation of a bioactive molecule, especially when such a molecule is hydrophobic. A high level of hydrophobicity implies in two challenges—the first is of technological nature, and it is related to the difficulty to incorporate a lipophilic bioactive in food formulations, which are often aqueous. The second challenge is related to the low level of absorption of hydrophobic molecules by the gastrointestinal tract. Lipid matrices can help to increase their bioacessibility and bioavailability, as (i) lipids can increase gastric retention time, slowing delivery to the absorption site; (ii) lipids can affect the physical and biochemical barrier function of gastrointestinal tract; and (iii) the presence of lipids can stimulate the secretion of lipid salts and endogenous biliary lipids (Jeong et al. 2007).

Among the colloidal encapsulation systems which can be produced using lipid matrices, suitable to be incorporated in food, there are the emulsions (macroemulsions, microemulsions and nanoemulsions), micelles, hydrogel beads, molecular complexes, liposomes and lipid particles (micro and nano) (McClements and Rao 2011). In this chapter, liposomes and lipid nanoparticles, two systems in which the interest of food scientists and technologists has been increasing in the last 10 years, are described in terms of structure. Also, their various methods of production are shown, as well as their possible utilization in food formulations.

S. C. de Pinho (✉)
Food Engineering Department, College of Animal Science and Food Engineering, Universidade de São Paulo, Pirassununga, SP, Brazil
e-mail: samantha@usp.br

L. G. de La Torre
School of Chemical Engineering, University of Campinas, Campinas, SP, Brazil
e-mail: latorre@feq.unicamp.br

© Springer Science+Business Media New York 2015

H. Hernández-Sánchez, G. F. Gutiérrez-López (eds.), *Food Nanoscience and Nanotechnology,* Food Engineering Series, DOI 10.1007/978-3-319-13596-0_7

7.1.1 Liposomes

Liposomes are colloidal systems, composed by amphipathic lipids that are able to self-assemble into bilayers and in excess of aqueous media aggregate in spherical bilayers with an aqueous interior lumen (Fig. 7.1).

The building blocks for bilayer aggregation are special lipids that basically contain into their molecular structures a polar headgroup and a hydrophobic tale (normally, two fatty acyl chains). This aggregation phenomenon is consequence of a balance between attractive forces form hydrophobic tales to minimize the interactions with water and repulsive forces from the ionic, hydrophilic or steric characteristic of the polar headgroups (Israelachvili 1985). The bilayer aggregation can be predicted by the packing parameter (P) that depends on the optimum surface area (a_0), hydrocarbon chain volume (v) and a critical length (l_c) of molecules [Eq. (7.1)].

$$P = v/a_0.l_c \tag{7.1}$$

If P assumes value between 0.5 and 1, the critical packing shape is a truncated cone allowing the aggregation into bilayers.

Depending on the lipid composition and method of production, liposomes can aggregate in small unilamellar liposomes, where there is only one bilayer and the vesicle size is 100 nm or lower, large unilamellar liposomes with the same number of lamellae, but the size is between 100 nm and 1 μm. If there is more than one lamella these vesicles are considered multilamellar and if there is more than one aqueous nucleus it is named multivesicular. Figure 7.2 presents a schematic representation of the liposome types.

Liposomes resemble biological membranes and depending on the lipid composition, they can be biodegradable and non-toxic (Lasic 1997; Park et al. 2004; Antunes et al. 2009). The common lipids that normally aggregate in bilayers are double-chained lipids with large headgroup areas such as lecithin (phosphatidylcholine, PC), phosphatidylserine, phosphatidylglicerol, phosphatidilinositol, phosphatidic acid among others (Israelachvili 1985). Most of the lipids that aggregate into liposomes are natural and present benefits in nutrition and they can be considered nutraceuticals. The addition of polyunsaturated lipids in diet is beneficial to health (Watkins and German 1998) and is recommended in dietary guidelines (Kritchevsky 1998). As example, phospholipids act as emulsifiers in the gastrointestinal system.

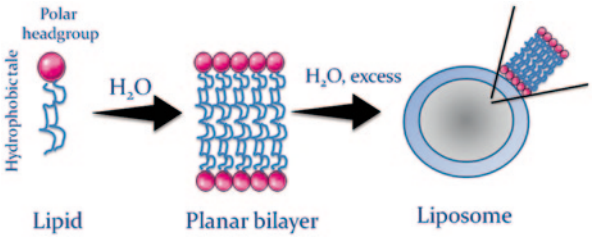

Fig. 7.1 Schematic representation of amphipathic lipid that in presence of aqueous media self-assemble in bilayers and in excess of this media aggregates in liposomes. (Adapted from Vitor et al. 2013)

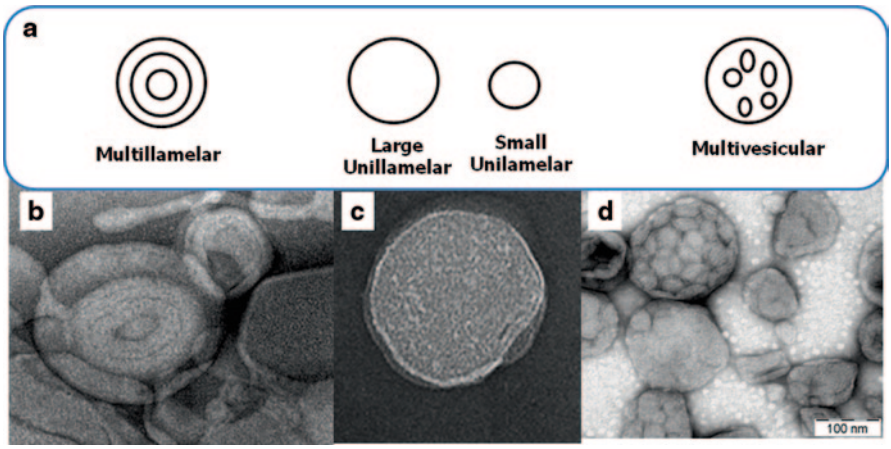

Fig. 7.2 Schematic representation of different types of liposomes (**a**), transmission electron microscopy of multilamellar liposomes (adapted from Rosada et al. 2012) (**b**), small unilamellar liposomes (adapted from Balbino et al. 2012) (**c**) and multivesicular liposomes (**d**)

Specially, PCs are the building blocks of cellular membranes and are fundamental on the replacement membrane mass; phosphatidylserine presents benefits for brain functions (Kidd 2000). Phospholipids with unsaturated carbon chains are prone to oxidation, affecting the bilayer permeability and liposome stability. In this case, the addition of antioxidants (e.g. α-tocopherol, vitamin E) is an alternative to overcome this degradation (Huang and Chung 1998). Another alternative to avoid oxidation is the use of saturated lipids as building blocks for liposome formation and they can easily be found in bulk quantities and food grade for commercial applications.

Other natural font of lipids is the milk fat globule membrane (MFGM) (Thompson and Singh 2006) and since it is a mammalian source the lipids composition is similar to the lipids from the biological membranes, containing basically phospholipids, glycoproteins, neutral lipids among minor other components (McPherson and Kitchen 1983; Ward et al. 2006). The high ratio of sphingolipids and glycosphingolipids to other phospholipids confers benefits to health such as anticarcinogenic properties among others (Dillehay et al. 1994; Schmelz et al. 1996). The ability of MFGM to generate liposomes was demonstrated by Farhang et al. (2012) encapsulating ascorbic acid as molecule model.

One important property of liposomes is the thermal behaviour. Upon heating the phospholipids do not undergo a simple melting process from the solid to the liquid form. Depending on the amount of water, different liquid-crystalline forms can be found (Taylor and Morris 1995). If liposomes composed by only one lipid are heated under controlled pressure, there will be multiple thermotropic transition temperatures that can be detected by differential scanning calorimetry technique. Among these transition temperatures there is one that is reproducible after subsequent cycles of heating and it is the transition from gel to liquid crystalline temperature (T_m). Large entropic changes occur during T_m and the *trans-gauche* rotational

isomerizations of methylene groups about the single C–C bonds along the lipid acyl chains are the most important structural changes (Huang and Li 1999). Sterols (cholesterol, ergosterol, sitosterol, etc.) can also be included and cholesterol presence can affect the bilayer rigidity and permeability, reflecting in a suppression of T_m and also decrease in bioactive release (Taylor et al. 1990; Senior and Gregoriadis 1982; Kirby et al. 1984). In practical terms, T_m is an important parameter for production methods, encapsulation procedures, techniques for size reduction and application of liposomes. Production techniques and downsizing processes (such as extrusion) are normally conducted at temperatures higher than T_m, since membrane fluidity is at its maximum. In addition, some encapsulation procedures and size reduction (Sou et al. 2003) involve temperature variation across T_m in order to control the membrane fluidity and improve the encapsulation of the bioactive compound and freeze and thaw is the name of this conventional method. The lipid supplier can inform the lipid T_m or it can be experimentally determined by using for example differential scanning calorimetry technique. It is fundamental for the knowledge of T_m before the selection of the production method and also the processing temperature. The evaluation of T_m and the thermogram can also be an important parameter in order to investigate the influence of the encapsulated molecule in the thermal behaviour.

Other important parameter to be characterized when liposomal systems are developed is the average diameter and size distribution and the values are mainly associated to the lipid composition and production method (including the sizing procedure). According to the liposome application, the size can be a limit parameter. The size and polydispersity limits are common on pharmaceutical applications (nanoparticles for vaccines, intravenous administration, intracellular delivery) (Eldridge et al. 1991; Gratton et al. 2008; Nagayasu et al. 1999). Despite most of the food application, the rigid control of size and polydispersity are not limiting parameters, its characterization is fundamental regarding safety aspects (Luykx et al. 2008). The dynamic light scattering (DLS) technique is often utilized to determine the mean diameter and size distribution of liposomes (Egelhaaf et al. 1996) and it can be easily adapted for quality control purposes. Asymmetric flow field-flow fractionation coupled with multi-angle static light scattering can also be used to determinate the average diameter and size distribution (Arifin and Palmer 2003).

In terms of liposome visualization, depending on the aggregates characteristic, different techniques can be employed. Light microscopy can be used for multilamellar and giant unilamellar liposomes. However, liposomes in the nanoscale require the use of electron microscopes, such as transmission electron microscope (TEM). TEM technique can be used for enhance detail and morphological investigations at higher resolution imaging as described in an excellent paper by Bibi et al. (2011). These authors investigated different techniques to visualize liposomes. They used TEM to compare the effects of dried-rehydrated vesicle (DRV) liposomes (production of unilamellar liposomes, followed by freeze drying and rehydration steps). According to the authors, the images can be used to support the process effectiveness. Figure 7.2 presents different TEM images of liposomes. The disadvantage is that TEM technique cannot be used to visualize inside the vesicles and cryo-electron microscopy is the alternative. The inner liposomes compartment can be observed

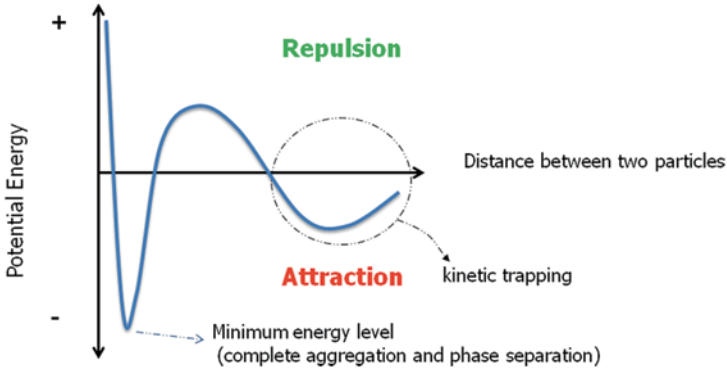

Fig. 7.3 Schematic representation of metastable colloidal system by DLVO theory. By convention, positive values of potential energy correspond to repulsion and negative values to attraction. The kinetic trapping is a minimum of energy, but it is not the lowest minimum of the system. The lowest minimum of energy correspond to irreversible aggregation (complete phase separation)

by and the multilamellar nature can be determinate by this technique (Bibi et al. 2011). Small angle x-ray study can also be used to study structural parameters of liposomes, such as number of bilayers and its thickness (Trevisan et al. 2011; Balbino et al. 2012).

Regarding liposomes stability, these colloidal systems are considered metastable according to the DLVO theory (Derjaguin, Landau, Verwey e Overbeek theory), where the thermodynamic equilibrium (minimum energy level) is complete phase separation (flat bilayers), reflecting on the product's long-term stability. However, metastable systems have a local minimum of energy where there is a kinetic trapping with an energy barrier to complete phase separation, increasing the shelf life (Fig. 7.3) (Islam et al. 1995; Hiemenz 1986).

Different strategies can be employed to increase shelf life stability such as (i) addition of lipids with charged headgroups to increase liposomes repulsion and (ii) addition to polymers that adsorbs on the liposomes surface avoiding aggregation (Antunes 2009; Evans and Wennerstrom 1999). In this last case, it is known as steric stabilization.

Liposomes were initially reported by Alex Bangham in 1965 (Bangham et al. 1965; Bangham, 1992) and the early investigations were concentrated on the use of liposome as cell membrane model or the phase behaviour of lipids under controlled conditions (Ostro and Cullis 1989). Later, the presence of amphipathic domains has led researchers to investigate the potentialities of liposomes as drug and nucleic acid delivery system (Balbino et al. 2012; de la Torre et al. 2009) and diagnostics (Ho et al. 2008). In the field of food engineering, more specifically in nanofoods, it is possible to explore the use of liposomes to deliver vitamins, essential oils, enzymes, probiotics, antioxidants, bioactive peptides and explore their capability to change the pharmacokinetics profile, their ability to increase ingredient solubility, improving ingredient bioavailability and in vitro and in vivo stability (Keller 2001).

7.1.2 Liposome Applications in Food

Liposomes applications have been extensively investigated in the encapsulation of pharmaceutical, cosmetics, anticancer and gene delivery molecules (Vitor et al. 2013, Yang et al. 2007, Balbino et al. 2012). This tendency is not the same regarding applications of liposomes in nanofoods and the development of new products in this area is still in the early stages (Re et al. 2009). However, the interest in using these colloidal systems in food products is increasing (Larivière et al. 1991; Thompson et al. 2009). The major advantages in using liposomes are that the lipids present nutritional characteristics and sustained delivery capability and the ability to release components on demand can be explored (Were et al. 2003). In addition, the conventional encapsulation protects the bioactive from the food matrix or can confine undesirable flavours and tastes (Taylor et al. 2005), enhancing the bioactive molecules stability and efficacy in food applications. It is also possible in the design of liposomes encapsulating more than one bioactive compound in the same lipid vesicle increasing the activities on delivering agents (Mozafari and Mortazavi 2005).

The proper design of liposomes encapsulating bioactive molecules and the success in food applications depends on the well knowledge of the food matrix, such as the colloidal characteristics, the presence of emulsions, nano/microparticles and cells that can probably interact with the liposomes. Normally, after understanding the food matrix, the first step on developing the encapsulation liposomal system is the selection of the lipid or mixture of lipids that will be used as bilayers. The nature of the bioactive molecule, such as hydrophobic or hydrophilic nature and ionic characteristics are key parameters on predicting the possibility of release or strong interaction with the bilayer. As an example, if the bioactive molecule presents cationic characteristics in a certain pH and the liposomes present anionic characteristics, the electrostatic interaction can be so strong that the molecule release will not happen. In this case, if the main design is the protection from the food matrix, the goal will be achieved. However, if it is required gradual release, this goal will not be achieved due to the strong molecule–bilayer interaction. Once the liposome is designed, the proof of concept is an important research step where the use of purified lipids is tested in the ability of encapsulate and release under controlled/simulated conditions of the bioactive compound. After that, in order to make the product feasible to industrial/real applications, the replacement of purified lipids to others that are supplied in industrial quantities for investigation of the influence of bulk lipids on the encapsulation of bioactive compound and the final food matrix is important (Rigoleto et al. 2012). The last step, once the food application has already been proven, the scale up in an additional effort since massive production is required in this field.

As an example of different stages of developing in foods, the antimicrobial activity of nisin, a positively charged, hydrophobic and natural peptide was improved when encapsulated in 100% PC and PC-cholesterol (7:3) liposomes. It was observed as a decrease of 2 log CFU/ml when compared with free nisin when eval-

uated against strains of *Listeria monocytogenes*. This is an important foodborne pathogen that can cause illness or death among members of susceptible populations (pregnant women, infants, and elderly and immunosuppressed individuals) (Were et al. 2004). The same antimicrobial agent was also encapsulated into liposomes containing distearoylphosphatidylcholine (PC) and distearoylphosphatidylglycerol (PG) and the integrity of this colloidal system was assessed after exposition to elevated temperatures (25–75 °C) and a range of pH (5.5–11.0). This study demonstrated the feasibility of nisin-encapsulated liposomes as an antimicrobial-active ingredient in low- or high-pH foods subjected to moderate heat treatments (Taylor et al. 2007). The effect of nisin-encapsulated liposomes composed by partially purified soy lecithin, for bulk supply (with anionic characteristic) demonstrated the effect of encapsulation only at low temperature when compared to free nisin in whole and skim milk (Malheiros et al. 2010). In this case, since the interaction between cells and the nisin is an expected behaviour on the design of nanocarriers for food application, the selection of lipids with appropriate charge and T_m are important parameters to be investigated. Since nisin is cationic peptide, the use of anionic liposomes will increase the electrostatic interaction between molecules and minimize the bioactive molecule release. In addition, if the final liposome containing nisin presents anionic characteristics, the interaction with cells will be avoided due to charge repulsion, avoiding the delivery of nisin inside cells.

The potentiality of bacteriocin-like substance (BLS) from *Bacillus licheniformis* strain P40 as natural biopreservative was also demonstrated after encapsulation into liposomes (PC) (Teixeira et al. 2008). The encapsulation of antioxidants and antimicrobial agents in liposomes is an example of enhancing the properties in the food matrix. Maherani et al. (2012) demonstrated the ability of 1-palmitoyl-2-oleoyl-sn-glycero-3-phosphocholine (POPC), 1,2-dioleoyl-sn-glycero-3-phosphocholine (DOPC) and 1,2-dipalmitoyl-sn-glycero-3-phosphocholine (DPPC) liposomes encapsulate the natural dipeptide antioxidants (L-carnosine), with hydrophilic nature. In this case, the proof of concept on the ability of nanoliposomes encapsulate L-carnosine was demonstrated.

In the field of food fortification, the use of ferrous glycinate (with hydrophilic characteristics) presents superior advantages to iron salts, such as ferrous sulfate (Jeppsen 2001; Layrisse et al. 2000). However, the gastrointestinal environment generates ferrous glycinate instabilities and the encapsulation into liposomes containing egg PC (EPC/cholesterol) protects this molecules. Ding et al. 2011 demonstrated that liposome had stability in simulated gastrointestinal juice at 37°C for 5 h, suggesting the importance of encapsulation for oral administration and the possibility of fortification of food.

Ascorbic acid stabilization was achieved by encapsulation in dipalmitoylphosphatidylcholine (DPPC) and dipalmitoylphosphatidylcholine/cholesterol (DPPC/cholesterol) liposomes with the co-encapsulation of citric acid (Wechtersbach et al. 2012). This study involved challenge tests with catalytic amounts of copper ions and the rate of ascorbic acid oxidation was decreased by up to 300-fold that of free ascorbic acid. Incorporation of cholesterol into the liposomes offered better thermal stability at higher temperatures, but lower stabilization efficacy at room

temperature. Real food matrices were evaluated and the ascorbic acid encapsulation into liposomes was effective in apple juice and fermented milk product, with less stabilization in this last one.

If hydrophobic bioactive compounds are included in the dietary, poor water solubility generates low bioavailability and low stability against gastrointestinal fluids and/or alkaline pH conditions. In this case, the encapsulation in liposomes can overcome these drawbacks. As an example, the encapsulation of polyphenols, such as curcumins can be an alternative towards the development of effective food supplements. In this context, the rhizome of *Curcuma longa L*. (ukon), rich in polyphenols was encapsulated in soybean lecithin. Liposomes containing the ukon extract were in vitro simulated in the gastric and intestinal fluids, demonstrating the ability in partially protecting the curcumin (twofold higher than free curcumin) (Takahashi et al. 2008).

Polyphenol from green tea is also another bioactive substance that can be used in food products (Soriani et al. 1998), presenting antioxidant, antibacterial, anticancer among other properties (Lung et al. 2002; Lambert and Yang 2003; Yamada et al. 2003; Wambura et al. 2011). It can normally be dissolved in ethanol, demonstrating poor water solubility and its sensibility to oxygen and light reduced many of the applications in food products. The encapsulation into lecithin/cholesterol liposomes presented in vitro release process described by a first-order equation and the physico-chemical properties indicate that polyphenol encapsulated liposomes are stable and suitable for different applications (Lu et al. 2011). Moraes et al. (2013) also encapsulated beta-carotene in multilamellar liposomes of hydrogenated soy lecithin, using the technique of proliposomes.

The bioactive beta-carotene can be used as a natural colorant in food and nutraceutical products as an antioxidant agent. However, this molecule is highly hydrophobic and it is prone to initiate a degradation process by the action of oxygen, temperature or light and this susceptibility requires the use of encapsulation techniques and liposomes are one of the possible alternatives. Recently, de Paz et al. (2012) encapsulated beta-carotene in soybean lecithin, generating multilamellar liposomes 1–5μm using novel PGSS (Particles from Gas Saturated Solutions)-drying technique.

Besides the use of liposomes in the food matrix to protect bioactive compounds, another interesting use is the development of rapid assays to detect common food pathogens, such as *Salmonellae, Escherichia coli* O157:H7, *Campylobacter jejuni, Vibrio cholera*, etc. The use of antibody-based assays is a promising alternative to the detection of *Salmonella* and saves time when comparing to conventional culture methods (Valdivieso-Garcia et al. 2001). Ho et al. (2008) developed an immunoassay, which uses immunological reactions to measure the presence of a target substance. These substances provide information about the pathogen presence. In this study, immunoliposomes composed by dipalmitoylphosphatidylcholine (DPPC), dipalmitoylphosphatidylglycerol (DPPG), dipalmitoylphosphoethanolamine (DPPE) and N-((6-(biotinoyl)amino)hexanoyl)-1,2-dihexadecanoyl-sn-glycero-3-phosphoethanolamine triethylammonium salt (Biotin-X-DHPE) were prepared by coupling anti-Salmonella antibody (Ab) (incubation) and encapsulating methyl blue (MB), a visible dye. Immunoliposomes were also evaluated in immunochromatographic test

(ICT) to identify *Staphylococcus* enterotoxin B (SEB), a toxin produced by *Staphylococcus aureus* (Khreich et al. 2008).

Different approaches can be used in order to improve liposome stability and the tendency to lose encapsulated components under storage. The association between polymers and liposomes is a promising alternative. Laye et al. (2008) demonstrated that chitosan-coated liposomes can be prepared by electrostatic deposition method. The authors used soy lecithin, generating liposomes with anionic characteristic. Chitosan is an indigestible cationic polysaccharide, with antimicrobial activity. This biopolymer also present interesting characteristic to reduce fat adsorption in human and animal studies (Filipovic-Grcic et al. 2001; Guo et al. 2003; Baxter et al. 2005; Mun et al. 2006b; Gonzalez-Rodrıguez et al. 2007). The association is possible due to electrostatic interactions and there is a critical range of chitosan concentration that coated liposomes. The presence of an external biopolymer layer can be used to avoid leakage of an active compound or simply for increased colloidal stability. The proper understanding of the mechanism of polymer–vesicle association is an important key in the rational developing of engineered liposomes for application in foods. An excellent review is Antunes et al. 2009 that relates the well-known association between micelles and polymers with the association between liposomes and polymers. Basically, the driving forces for association are the same in both systems. The main forces involved in the association between polymer and vesicles are electrostatic bridging (as explored by Laye et al. 2008), hydrophobic interactions, that allows the penetration of the polymer groups into the vesicle bilayers and hydrogen-bond interactions.

Additional layers can be produced by deposition of different polymers on the liposome surface. As example, Fukui and Fujimoto (2009) prepared chitosan-dextran sulfate (or nucleic acid) layer-by-layer deposition on liposomes. The authors demonstrated the superior stability of multilayered liposome against "free" liposomes against TRITON X-100, an important surfactant normally used to lyse liposomes (Torchillin and Weissig 2003). In addition, 1-hydroxy pyrene-3,6,8-trisulfonic acid (HPTS), alendronate and glucose, molecules with different charges were encapsulated into the liposomes and the multilayered liposomes presented slower release rate. Different polymers, suitable for food industries can be used in this technique. Haidar et al. 2008, prepared layer-by-layer deposition of alginate and chitosan. Bovine serum albumin (BSA) was used as protein model to demonstrate the increase in release time in the liposomes.

Advanced materials can also be explored for food application involving the incorporation of liposomes into nanofibers.

Recently, Yu et al. (2011) produced nanofibers containing the hydrophilic polymer polyvinylpyrrolidone K60 (PVP) and soybean lecithin using electrospinning technique. The authors reported that liposomes could be spontaneously formed after the hydration of the fibers. The size of liposomes could be controlled by varying the content of PC in the nanofibers.

The development of new associations between liposomes and polymers, nanofibers or other materials and nanostructures can be a promising alternative for future

developments for nanofoods, conferring intelligent properties, increasing stability and carrying bioactive compounds.

7.1.3 Methods for Liposome Production

Besides the promising applications of liposomes as carrier for food ingredients, the production method is a special concern since massive production is an important requirement to make the industrial use of this nanostructure feasible. Despite the need to develop techniques for massive production, most of the basic development of liposomes and the proof of concept for its functionalities describe the use of protocols established for laboratorial scale and lipids of high purity are normally used (see Table 7.1).

Regarding the production techniques, the first conventional protocol is the thin film or named as Bangham method (Bangham et al. 1965). Basically, the lipids are solubilized in an organic solvent, such as chloroform or chloroform/methanol. This organic solution is then submitted to drying under nitrogen purge or vacuum, allowing the organization of the lipids in a thin film. Then, the dried film is hydrated with aqueous solution (water or buffer), allowing the lipid hydration. The hydration at small amount of water allows the formation of planar bilayers and the water contained is hydrating the polar headgroups of the lipids (Fig. 7.1). In excess of water, the hydrated lipids are self-assembled into vesicular bilayers, forming the liposomes. This self-assembled process can be considered as a disorganized method, allowing the formation of vesicles with different sizes and lamellarity. Liposomes produced by the thin film method are considered multilamellar, with a broad size distribution (high polydispersity) and an additional step is required for sizing. If the final application requires liposomes with small size or/and low polydispersity, subsequent unit operation is necessary like extrusion (at high pressure), sonication or high-pressure homogenization. The major disadvantage is the use of toxic organic solvents, such as chloroform and methanol, which is not allowed in food industries. The use of thin film method followed by a sizing protocol is a well-accepted protocol in the literature and most of the liposomes presented in Table 7.1 used these techniques.

Other conventional methods are reversed-phase evaporation, involving the formation of O/A emulsion for later removal of the organic solvent (Szoka and Papahadjopoulos 1978), and the Detergent Depletion Method, with the formation of micelles by adding detergents and the liposomes are formed after this detergent removal, using dialysis as separation method (Lasch et al. 2003). The disadvantage of this method is that the final liposome dispersion is very diluted.

The above described methods are mainly used in laboratorial scale. Recent scientific literature reports different efforts in the development of new innovative processes for liposome production aiming at the controlling of average diameter, size distribution and polydispersity. Some of the scalable processes recent developed are described below.

Table 7.1 An overview of recent research articles on liposomes encapsulating bioactives of interest for incorporation in food

Bioactive(s)	Lipid composition	Production method	Reference
L-carnosine	POPC, DOPC, DPPC	Thin film method/freeze and thaw/extrusion	Maherani et al. 2012
Nisin	PC and PC-cholesterol	Thin film method/sonication	Were et al. 2004
Nisin	Distearoylphosphatidylcholine (PC)	Thin film method/freeze and thaw/extrusion	Taylor et al. 2007
Nisin	Partially purified soy lecithin (PC)	Thin film method/freeze and thaw/extrusion	Malheiros et al. 2010
Rhizome of *Curcuma longa L.* (ukon)	Soy lecithin (PC)	Mechanochemical method (homogeneizer/microfluidizer)	Takahashi et al. 2008
Bacteriocin-like substance (BLS) from *Bacillus licheniformis* strain P40	PC	Reversed-phase evaporation	Teixeira et al. 2008
Ferrous glycinate	Egg phosphatidylcholine (EPC/CHOL)	Reversed-phase evaporation	Ding et al. 2011
Ascorbic acid/citric acid	DPPC/cholesterol	Thin film method/freeze and thaw/extrusion	Wechtersbach et al. 2012
Casein hydrolysate	Hydrogenated and purified soy lecithin	Thin film method	Yokota et al. (2012)
Ascorbic acid	Milk fat globule membrane-derived phospholipids	Mechanochemical method (homogeneizer/microfluidizer)	Farhang et al. 2012
Polyphenol from green tea	Lecithin/cholesterol	Thin film method/sonication	Lu et al. 2011
β-carotene	Soybean lecithin (PC)	PGSS (Particles from Gas Saturated Solutions)-drying technique	de Paz et al. (2012)
β-carotene	Hydrogenated and purified soy lecithin	Proliposomes	Moraes et al. (2013)
Methyl blue (MB)/immunoliposome containing anti-Salmonella antibody (Ab)	DPPC, DPPG, DPPE and N-((6-(biotinoyl)amino) hexanoyl)-1,2-dihexadecanoyl-sn-glycero-3-phosphoethanolamine triethylammonium salt (Biotin-X-DHPE)	Reversed-phase evaporation	Ho et al. 2008
Sulforhodamine B	Dipalmitoylphosphatidylcholine, cholesterol, DPPG and DPPE	Reversed-phase evaporation	Khreich et al. 2008

Table 7.1 (continued)

Bioactive(s)	Lipid composition	Production method	Reference
Chitosan-coated liposomes	Soy lecithin (SPC)	High-intensity ultrasonication and high-pressure homogenization	Laye et al. 2008
1-Hydroxy pyrene-3,6,8-trisulfonic acid (HPTS), alendronate and glucose	Dilauroyl phosphatidic acid (DLPA) and dimyristoyl phosphatidylcholine (DMPC) (chitosan-dextran sulfate (or nucleic acid) layer-by-layer deposition on liposomes)	Thin film method/sonication	Fukui and Fujimoto 2009
Bovine serum albumin (BSA)	1,2-dipalmitoyl-sn-glycero-3-phosphocholine (DPPC), cholesterol and a cationic surfactant; dimethyldiocta-decyl-ammonium bromide (DDAB)	Thin film method/extrusion	Haidar et al. 2008
Essential oil of *Eugenia uniflora L.*	Hydrogenated and purified soy lecithin	Thin film method	Yoshida et al. (2010)

CHOL cholesterol; *DOPC* 1,2-dioleoyl-sn-glycero-3-phosphocholine; *DPPC* 1,2-dipalmitoyl-sn-glycero-3-phosphocholine; *POPC* 1-palmitoyl-2-oleoyl-sn-glycero-3-phosphocholine, *DPPG* dipalmitoylphosphatidylglycerol, *DPPE* dipalmitoylphosphatidylethanolamine

Solvent-injection techniques were investigated initially in the 1970s (Batzri and Korn 1973), using ethanol injection method as an example of organic solvent. Isopropanol has already been studied as organic solvent (Gentine et al. 2012) and other organic solvents can be used, although it has to be approved for food applications. Basically, the lipids are solubilized in ethanol (organic phase) and added in a controlled flow rate in a tank with the aqueous phase under controlled stirring (Fig. 7.4a). The immediate mixing between ethanol and water promotes the instantaneous liposome formation (Meure et al. 2008). The process can be developed in a way that ethanol residue is in an accepted range or it can be removed by dialysis (Wagner et al. 2006). If the final application in food requires a thermal operation, the ethanol residue can be minimal. The major process parameters that control the liposome average diameter and size distribution are lipid composition and concentration, type of organic solvent, aqueous phase (type of buffer or water), flow rate of the organic phase injection, the proportion of organic solvent to aqueous phase and also the tank stirring speed (Kremer et al. 1977; Wagner et al. 2002; Pons et al. 1993). This method can be easily adapted in food industries.

Research in the ethanol injection method was continued by different groups demonstrating the feasibility in increasing the lipid concentration in the final liposome (Trevisan et al. 2011) or adapting this technique to microfluidics (Balbino et al. 2013; Jahn et al. 2004, 2007, 2008, 2010). In this case, the organic phase (soluble in water) containing the lipids is pumped into the microchannel and it is hydrodynamic compressed by two aqueous streams. The organic phase diffusion to the aqueous phase allows the liposome aggregation (Fig. 7.4b). Microfluidics is an exciting research area that involves the use of small volumes of fluids (10^{-9}–10^{-18} l) inside channels with dimensions in the order of micrometers (Whitesides 2006). The small volumes can be easily adapted for applications involving point of care, where small amounts are required and also personalized formulation. In terms of production for food industry, massive production is an essential requirement and efforts are still necessary to allow the use of microfluidics in industrial scale.

The membrane contactor technique is another technique derived from the ethanol injection method, with continuous liposome production and considered as a scalable strategy (Jaafar-Maalej et al. 2011). In this case, the lipids are dissolved in the organic phase (ethanol, as example) and pressured across a membrane (tubular porous glass) to the inner tubular direction. The aqueous phase flows in the tangential direction generate the contact between the organic and aqueous phases, allowing the liposomes formation. In this case, the pressure for organic phase permeation, lipid composition, aqueous-phase flow rate and type of membrane are important process parameters. These authors incorporated beclomethasone dipropionate (BDP) and indomethacin (IMC) drugs in egg yolk lecithin with 82 % (bulk supply) and cholesterol using the membrane contactor technique, producing liposomes in nanoscale (60–200 nm) and polydispersity ranging from 0.17 to 0.32. This method can be easily adapted to the food industry.

Another group of techniques involves the use of dense gas (it uses substances that are in the region surrounding the critical point—supercritical fluid) (Meure et al. 2008). CO_2 is the most common solvent used in this technique (conditions to critical

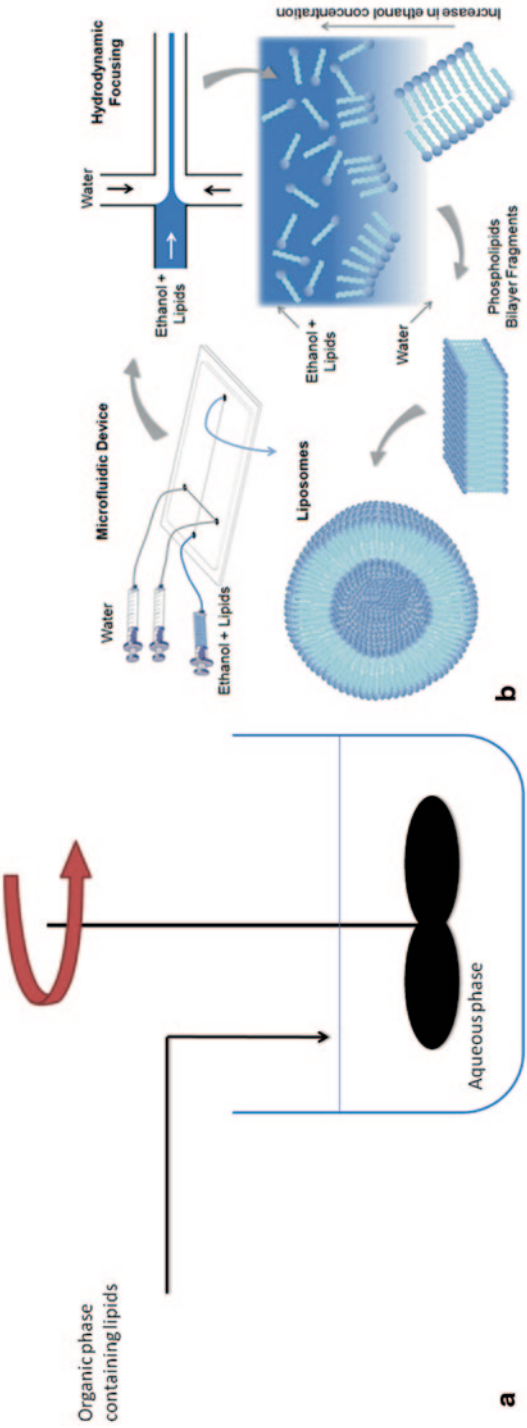

Fig. 7.4 Schematic representation of injection method (**a**) and microfluidic process (Balbino et al. 2013) (**b**) for liposome production

point are 31.1 °C and 73.8 bar) and the solvent removal is facilitated by changing the vessel pressure. Dense gases present solvent properties similar to liquids and mass transport properties similar to gases. However, most of the techniques require the use of organic co-solvent. The first dense gas technique was presented by Castor (1994) using the injection (lipid, co-solvent and gas are compressed and injected into aqueous phase) and decompressing method (lipid, co-solvent, gas and aqueous phase are decompressed into air). There are different variations of the dense gas technique that are well described in Meure et al. (2008) and the major advantage of this method is that CO_2 inactivates bacteria and endotoxins, facilitating the microorganism control in food application (Dillow et al. 1999).

An alternative to remove the use of toxic and hazardous organic solvent is the heating method developed by Mozafari (Mozafari et al. 2002; Mozafari 2005). Basically, the liposome components are hydrated in aqueous phase and heated in the presence of glycerol (3 % v/v) (Mozafari 2005). The process is kept under stirring at high temperatures (60–120 °C) during 45–60 min (Colas et al. 2007). In this case, glycerol is well-accepted water-soluble chemical and it increases the liposome stability. Recent investigations demonstrated that liposomes containing polyunsaturated fatty acids (PUFAs) and produced by the heating method presented higher oxidative stability of PUFAs when compared to conventional Bangham method (Rasti et al. 2012).

If liposomes' production requires size and/or polydispersity reduction, different equipments that are able to process large amount of suspension can be used like extrusion and high-pressure homogenizers. High-pressure homogenizers and microfluidizers apply high shear to the preformed liposomes, due to the use of high pressure imposed by piston pumps. The efficiency in size and polydispersity reduction depends on the applied pressure, equipment concept and also the inner geometry where the liposomes are forced to flow (Mayhew et al. 1987). In practical terms, we can find different equipment with different characteristics and a comparative study is also recommended. Our practical experience in operating high-pressure homogenizers and microfluidizers indicate that the lipid composition and the applied pressure are important parameters that reflect on the final physico-chemical properties. Attention should be focused on the colloidal stability, since the applied high shear can destabilize the physico-chemical properties of liposomes.

When liposomes are used to deliver active molecules, the liposome production and encapsulation method/technology has to be developed considering the hydrophilic/hydrophobic nature of the active compound. If hydrophilic compounds are used, it can be solubilized in the aqueous phase that is used to produce the liposomes and in the case of hydrophobic molecules, it can be solubilized or dispersed in the organic phase. One important parameter to be evaluated is the encapsulation efficiency (EE) and it represents the percentage of active molecules that are really incorporated into the liposomes (anchored on the bilayer or trapped inside the aqueous lumen) when compared with the total amount of active molecule. The EE determination depends on the separation of encapsulated and non-encapsulated active compound from the liposomes (Lasic 1993). Different techniques can be used for separation: centrifugation (in the case of large sizes—particles in micron range),

ultracentrifugation (for small sizes—particles in nano range), size exclusion chromatography (in this case it is important saturate the molecular sieve with lipids prior to use), micro/ultrafiltration among others. The total amount of active compound can be determinate by liposome disruption, to release all the active compounds, using for example organic solvents like ethanol or surfactants like Triton X-100. It is important to notice that in the case of encapsulation of hydrophobic molecules, the maximum encapsulation is limited to its partition into the lipid bilayer (Lasic 1993). The mass relation between active molecules to lipids is another important parameter that can be determinated.

7.2 Lipid Nanoparticles

Lipid nanoparticles are colloidal carrier systems similar to conventional emulsions, but with a nanometric hydrophobic core composed of a lipid solid at room temperature, stabilized by a layer of surfactant (Müller et al. 2002; Mehnert and Mahder 2001). These dispersions can be designed to combine the advantages of polymeric nanoparticles, liposomes and emulsions (Henstchel et al. 2008), presenting extended shelf-life, biocompatibility, a high capacity for incorporating hydrophobic compounds and a good level of protection of sensitive bioactives (Sawant and Dodiya 2008; Müller et al. 2002). Also, they can be engineered to allow the controlled release of the bioactive ingredient and protect the sensitive and labile molecules from degradation, using processes that can be scaled up and that employ no organic solvents (Fathi et al. 2012; Müller et al. 2000). Figure 7.5 shows the scheme of solid lipid nanoparticles (SLN).

Depending on its microstructure, lipid nanoparticles can be classified in two groups: SLN and NLC (nanostructured lipid carriers). SLN are produced when lipids of high purity are employed, whereas NLC are originated when mixtures of lipids, or mixtures of solid and liquid lipids, are used (Müller et al. 2002).

These nanoparticles are an extremely interesting delivery system with multiple potential applications in the food industry, and are of great interest to add hydrophobic bioactives to functional food formulations (Weiss et al. 2008). Such an interest is due to the capacity of the SLN to enhance the dispersibility of lipophilic compounds, as well as their ability to increase the bioavailability of such molecules. In

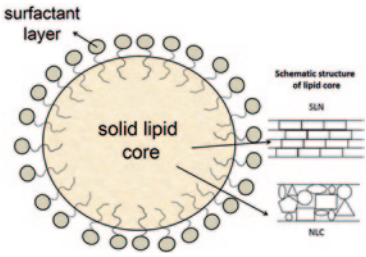

Fig. 7.5 Schematic representation of a lipid nanoparticle and the possible arrangements of core lipid structure

addition, they can increase bioactive stability, have a high payload, are non-toxic, and can be produced without using organic solvents. Another important advantage is that large scale equipments are available for their production.

Therefore, in recent years, the food researchers have started to investigate possible applications of SLN in their area. Several studies can be found in the literature; some of them are shown in Table 7.2.

As can be seen in Table 7.2, several types of surfactants are used in lipid nanoparticles production. Among the food-grade emulsifier systems, suitable for food applications, there are low weight non-ionic surfactants (polysorbates, poloxamers and tyloxapols), phospholipids (egg and soya lecithins) and bile salts, as well as proteins (whey protein isolate, soy protein isolate, beta-lactoglobulin, sodium caseinate, for example, are most used as lipid nanoparticle stabilizers). The choice of the stabilizing system to be used in a particular case of lipid nanoparticle highly depends on the final desired characteristics, as particle size and shelf-life, as well as on the production method to be used. The emulsifier chosen will also be determinant in the polymorphic stability and also in the digestibility extension of the lipid nanoparticles, as well as in the bioacessibility of the encapsulated bioactive.

7.2.1 Microstructure of Lipid Nanoparticles

Crystallinity and polymorphic behaviour are crucial factors of the lipid nanoparticles. The chemical nature of the lipids determines the crystalline structure of the nanoparticle, and it is a key factor in the phenomenon of incorporation or expulsion of the bioactive from the nanoparticles (Müller et al. 2000; Mehnert and Mäder 2001).

SLN are composed of perfect crystals and can be compared to a "brick wall", as shown in Fig. 7.5, and are formed when highly purified lipids are used to produce the lipid particles (Müller et al. 2002; Müller et al. 2000). A high degree of spatial organization, however, can lead to a too low loading capacity for some bioactives, and a more disorganized can be more advantageous. The less crystalline structure is, the higher the particle capacity to incorporate bioactive molecules will be, as microstructural disorganization results in the presence of "voids" capable of accommodating a higher amount of the encapsulated substance. Such a scheme is shown in Fig. 7.5 for the NLC, and the structural disorder can be achieved by mixing solid lipids with liquid lipids, or using non-purified raw materials, instead of highly purified lipids with relatively similar molecules (Müller et al. 2002; Muchow et al. 2008; Sawant and Dodiya 2008).

In the case of NLC, it is possible to distinguish three types: (i) imperfect type; (ii) amorphous type and (iii) multiple type. Figure 7.6 shows a schematic representation of these structures:

The first type—imperfect—is created when different types of lipid molecules are used to build the core of the particle. The imperfect type is crystalline, but there are voids in the structure which are capable to accommodate the bioactive molecules.

Table 7.2 An overview of research articles on solid lipid nanoparticles encapsulating bioactives of interest for incorporation in food

Bioactive(s)	Lipid phase	Surfactant(s)	Production method	Reference
β-carotene	ALDO PGHMS	Tween 80	HPH	Hentschel et al. (2008)
β-carotene	Tripalmitin	Soy lecithin, Tween 80, Tween 60	HPH	Helgason et al. (2008)
β-carotene	Tripalmitin	Tween 20	HPH	Helgason et al. (2009)
β-carotene	Canola stearin	Tween 80, Poloxamer 188	HPH	Malaki-Nik et al. (2012)
β-carotene	Hydrogenated palm kernel oil	Whey protein isolate, sodium caseinate	HPH	Cornacchia and Roos (2011a), Cornacchia and Roos (2011b)
β-carotene	n-hexadecyl palmitate, glyceril stearate, grape seed oil and squalene	Tween 80, Tween 20	High shear homogenization	Lacatusu et al. (2012)
β-carotene	Stearic acid, tristearin, trilaurin, lauric acid	L-a-phosphatidylcholine and dipalmitoyl phosphatidylcholine	High shear homogenization	Triplett and Rathman (2009)
β-carotene + α-tocopherol	Stearilic ferulate	Tween 20	High shear homogenization	Trombino et al. (2009)
β-carotene and tocols	Hydrogenated palm kernel glycerides	Span 40 and Tween 80	HPH	Hung et al. (2011)
α-tocopherol	Palm oil	Whey protein concentrate	HPH	Shukat and Relkin (2011), Shukat et al. (2012)
Catalase	Tripalmitin	Poloxamer 188	Solvent emulsification-evaporation	Qi et al. (2012)
Coenzyme Q10	Compritol 888	Poloxamer 188 and Tween 80	High shear homogenization	Gokce et al. (2012)
Ergocalciferol	Tripalmitin	Tween 20	HPH	Patel and Martin-González (link rid="bib110">2012</link>)
Essential oil of Artemisia arborescens L	Compritol 888	Pluronic F68	HPH	Lai et al. (2006)

Table 7.2 (continued)

Bioactive(s)	Lipid phase	Surfactant(s)	Production method	Reference
Lutein	Glyceryl palmitostearate, palmitinic acid monoglycerides, caprylic/capric triglycerides, lauric acid, myristic acid, palmitic acid and stearic acid	Pluronic F68	ultrasonication	Liu and Wu (2010)
Nisin	Imwitor 900	Poloxamer 188 and sodium deoxycholate	HPH	Prombutara et al. (2012)
Omega-3	Tripalmitin	Tween 20	HPH	Awad et al. (2009)
Quercetin	Glyceryl monostearate	Soy lecithin, Tween 80 and PEG 400	Solvent emulsification-evaporation	Li et al. (2009)
Quercetin	Tristearin	Hydrogenated soybean phosphatidylcholine	High shear homogenization	Scalia and Mezzena (2009)
Resveratrol	Compritol 888 and Mygliol 812	Poloxamer 188 and Tween 80	High shear homogenization	Gokce et al. (2012)

PGHMS propylene glycol high monostearate *HPH* high-pressure homogenization

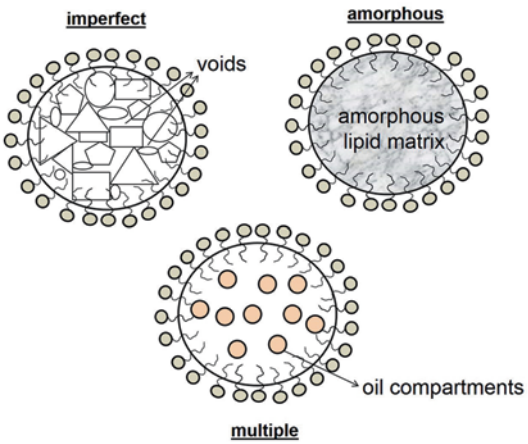

Fig. 7.6 The three types of nanostructured lipid carriers (NLC)

Such a characteristic is important to increase the loading capacity of the lipid particles, and also avoid the drug expulsion that occurs when a highly ordered structure is originated during the crystallization process (Müller et al. 2000).

The second type of NLC can be formed when the particles are cooled but they do not crystallize, remaining in an amorphous state. Therefore, the drug expulsion is minimized, as the transformation from a polymorph form to another does not occur (Bunjes et al. 2007; Jenning et al. 2000; Müller et al. 2002).

The multiple type resembles a multiple emulsion, in which the solid lipid core contains liquid oil compartments. This sort of NLC is a result of the mixture of solid and liquid lipids, being the liquid in a higher amount. At high temperature, complete miscibility can be verified between the solid and the liquid lipid, but, during the cooling process, the solubility of the oil in the solid lipid compound is exceeded. As a result, a precipitation of the oil occurs, in the form of tiny droplets, originating the structure shown in Fig. 7.2. It is important to notice that this process will only occur if the liquid lipid is present in such a concentration much higher than its solubility in the solid lipid at room temperature (Müller et al. 2002; Sawant and Dodiya 2008).

Therefore, the structure of the lipid core of lipid nanoparticles can be engineered in order to control their delivery properties and capacity of protection of the encapsulated bioactives. The mobility of the incorporated and degrading species (like oxidizing species as free radicals, O_2, ions) can be controlled by controlling the physical state of the matrices. The physical state of the lipid matrix is intimately related to their composition; in other words, the choice of the lipids and surfactants are a primordial step in the production of lipid nanoparticles. The lipid composition will determine the type of crystal generated in the cooling step (Weiss et al. 2008; Müller et al. 2000).

The materials used in the production of lipid nanoparticles, which include triglycerides (TAGs), mono/di/triglycerides mixtures, waxes, hard fats (fatty acids) (Severino et al. 2012), exhibit polymorphism. Polymorphism can be defined as the different association configurations the individual lipid molecules can assume in the

lipid state; in other words, the different lattices in which the lipids can crystallize (Weiss et al. 2008; Small 1986).

TAGs are the lipids most often employed in the production of SLN (Severino et al. 2012). The three most commonly encountered forms of crystalline arrangements in these lipids are:

- β(Beta): the most stable, triclinic subcell
- β' (Beta prime): believed to be an orthorhombic perpendicular subcell
- α(Alpha): a more loosely packed configuration in which the chains form a hexagonal lattice

The three polymorphic forms α, β' and β are related to the characteristic and unequivocal packings of the hydrocarbon chains of the TAG molecules (Timms 1984). "Three-legged" structures as medium- and long-chain TAGs pack side by side in separate layers, and the layer thickness ("*d*" spacing) is dependent on the length of the molecule and on the angle of tilt between the chain axes and the basal plane (Timms, 1984; Himawan et al. 2006).

The different polymorphic forms can be identified by X-ray diffraction, where long spacings give information on the repeat distances between crystal planes (chain length packing) and short spacings on subcell structure (interchain distances) (Himawan et al. 2006; Small 1986).

The α-form, the least thermodynamically stable configuration, is a hexagonal structure characterized by one short spacing peak near 0.42 nm. The β'-form is characterized by two strong short spacing peaks at 0.37–0.40 and 0.42–0.43 nm.

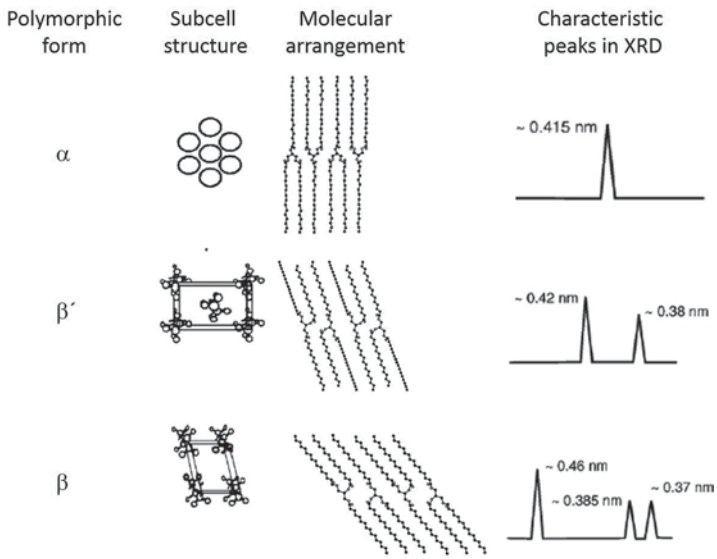

Fig. 7.7 Most common polymorphic forms of the monosaturated triglycerides and their characteristics. (Adapted from Himawan et al. 2006 and Bunjes and Unruh 2007. Copyright 2006, 2007 Elsevier)

The structure is orthorhombic and perpendicular, with a non-close packing, and the chains have an angle tilt between 50 and 70°. The densest and most stable form, β, show in XRD diffractograms a strong lattice spacing line at 0.46 nm and many other strong lines between 0.36 and 0.39 nm. It is a triclinic chain packing, in which a parallel arrangement can be distinguished. The chains, which are closely packed, have an angle tilt between 50 and 70° (Himawan et al. 2006; Timms 1984; Small 1986). Figure 7.7 illustrates the three most common polymorphic forms of TAGs.

It is also possible the identification of sub-forms in the crystalline arrangement of TAGs, especially in the case of raw materials composed of more than one type of TAG. Timms (1984) describes the sub-α form as a β' form which usually melts below an α form and with long spacings unusually large; and a sub-β form, which does not satisfy the criteria for α or β', and shows a strong short spacing at ca. 0.474 nm and several medium strength spacings at ca. 0.45, 0.39 and 0.36 nm.

Highly pure, homogeneous lipids tend to form a platelet-like pattern of β-modification, originating non-spherical lipid nanoparticles (Bunjes 2011; Weiss et al. 2008). A more heterogeneous composition of the lipid-matrix leads to the formation of spherical particles due to the higher percentage of α-crystals in the structure. The shape of the particles is directly related to their colloidal stability and to their rheological characteristics. As an example, Fig. 7.8 shows the microscopical aspect of lipid nanoparticles of tristearin crystallized in both polymorphic forms.

Other factors that determine the polymorphism of SLN are the cooling rate and surfactant type. As for the latter, they play a very important role in controlling the crystallization process of the lipid nanoparticles, due to the small size of the particles. Such a small size means the percentage of lipid molecules interacting with the hydrophobic emulsifier tail groups is large, and, thus, they can modulate the crys-

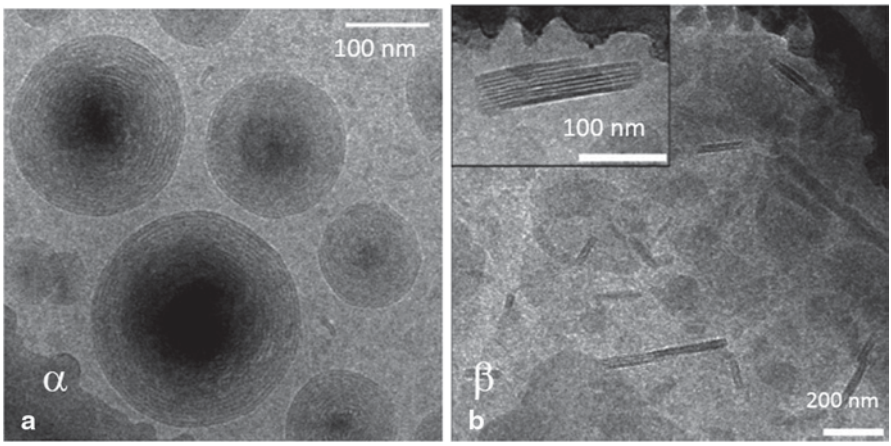

Fig. 7.8 Cryo-electron micrographs of tristearin particles. **a** Dispersion stabilized with purified soy lecithin/sodium glycocholate, crystallized in α-form. **b** Dispersion stabilized with purified soy lecithin/sodium glycocholate mixture, crystallized in β-form. (Adapted with permission from Bunjes and Unruh 2007. Copyright 2007 American Chemical Society)

tallization process. Moreover, the surfactant can change (increase or decrease) the kinetic stability of a generated crystal (Weiss et al. 2008), influencing the polymorphic transitions which can occur during the storage period of the lipid nanoparticles.

In addition, the emulsifiers can impact on the crystallization temperature of the nanoparticles. In the particular case of stabilizers with a chain structure similar to that of the lipidic dispersed material, this effect is especially pronounced (Rosenblatt and Bunjes 2009; Bunjes et al. 2003). The stabilizer chains are responsible for a templating mechanism, leading to the occurrence of the nucleation at higher temperatures (Bunjes and Koch 2005; Westesen and Siekmann 1997; Bunjes et al. 1996). The concentration of emulsifier also influences on the crystallization behaviour of the dispersed lipid phase, as the interfacial tension at the oil–water (o–w) interface can alter the nucleation mechanism (Helgason et al. 2009).

The crystalline arrangement of the lipid nanoparticles is also dictated by the cooling rate during their production (Weiss et al. 2008; Helgason et al. 2008; Jenning et al. 2000). However, it is difficult to find studies which investigate the cooling rate as an isolated parameter, because it acts together with the surfactant type in determining the crystalline arrangement of the particles. An example is given by Bunjes et al. (2003), in which slow and fast cooling rates of tripalmitin nanoparticles originated two slightly different α-forms, with different tendencies to undergo polymorphic transitions during storage.

7.2.2 Stability of Lipid Nanoparticles

The breakdown of a dispersion of lipid nanoparticles is that typically found in colloidal dispersions, as flocculation and sedimentation or creaming and coalescence. According to McClements (2005), an emulsionated system can become unstable due to physical alterations in the spatial distribution or structural conformation of the molecules, and the same is true for solid lipid nanoparticle dispersions. There is a usual classification of the colloidal stability: thermodynamic and kinetic (Hiemenz and Rajagopalan 1997). All lipid nanoparticles are unstable thermodynamically by definition, as their formation relies on a phase separation process, and they will break down if they are left long enough. Therefore, it is the kinetic stability of the system which must be attained in order to produce stable solid lipid nanoparticle dispersions.

The instability phenomena which occur in the lipid nanoparticles can be schematically represented in Fig. 7.9.

Insufficient repulsive forces between particles can lead to the flocculation of the dispersion, during which two or more particles associate with each other but do not merge. Such a reduction in repulsion can be originated by pH, ionic strength, shear forces, temperature, as well as the presence of biopolymers, as all these factors influence on the number and frequency of particle collisions.

Gravitational separation can be caused by flocculation, as the aggregation of the particles changes the density difference between the dispersed and continuous

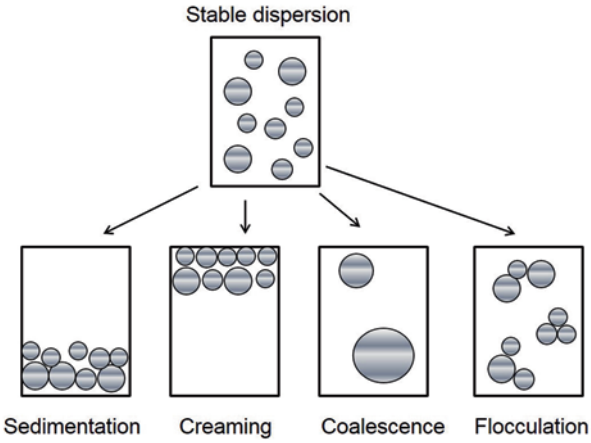

Fig. 7.9 Physical mechanisms of lipid nanoparticles destabilization

phases, and result in creaming or sedimentation. In the case of lipid nanoparticles, both phenomena can occur, depending on the type and amount of crystallized lipid present in the particles' core.

Coalescence, on the contrary of flocculation, occurs when two or more particles merge together to originate a single larger particle. It normally occurs in emulsions, as it requires a liquid matrix, but in lipid nanoparticles a particular case of coalescence may take place. It is named partial coalescence, and occurs when two or more partially crystalline particles join together to form a non-spherical structure (Dickinson and McClements 1996). The solid network of the partially crystalline particles is strong enough to prevent their complete merging, and, instead of a spherical shape, clumps of irregular shape and size are originated (Boode and Walstra 1993), as showed in Fig. 7.10. The fat crystals sticked out through the o–w interface may function as a connection between two particles, as the protruted crystals of the first particle can penetrate into another particle. Then, they remain aggregated because the crystals are wetted better by oil than by water, and the surface area of fat exposed to the aqueous phase can be decreased (Boode et al. 1993; Dickinson and McClements 1996).

The stability of lipid nanoparticles can also be related to their crystalline microstructure. Polymorphic changes can occur in their lipid cores, and such a fact is related to the conditions of storage and also to the type of surfactant present in the stabilizing layer. The possibility to produce lipid nanoparticles in different polymorphic forms stable upon storage for a reasonable period of time, as well as with good properties of bioactive release, is extremely interesting (Rosenblatt and Bunjes 2009). Several studies have observed the emulsifiers affect the crystallization kinetics in lipid nanoparticles, and such a phenomenon is often attributed to the rigidity of the interface formed by the emulsifier; once the lipid crystals have formed it may be more difficult for them to undergo polymorphic transitions when they are part of a rigid surfactant shell (Helgason et al. 2009). Besides, the type of

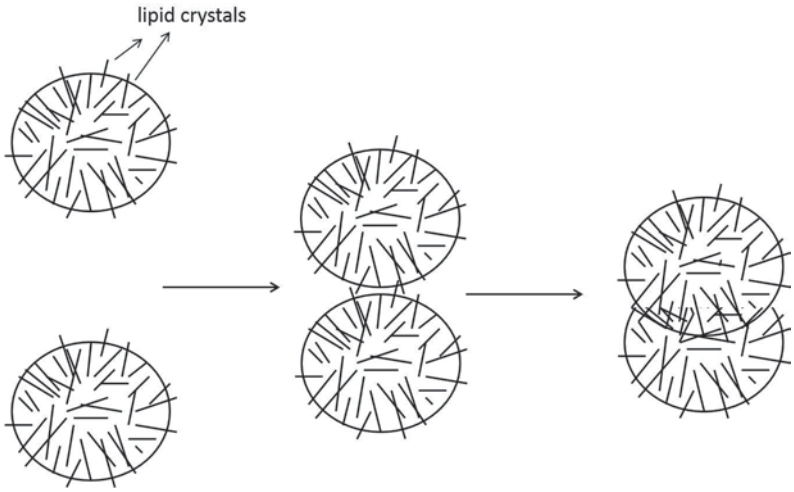

Fig. 7.10 Illustration of the phenomenon of partial coalescence

hydrophobic chain of the emulsifier and its concentration also influence in these polymorphic transitions (Helgason et al. 2008; Rosenblatt and Bunjes 2009; Bunjes and Koch 2005; Bunjes et al. 2003).

A phenomenon which occurs in lipid nanoparticle dispersions is the formation of superstructures and gel. With increasing particle concentration, the viscosity of dispersion increases until a gel-like consistency is obtained (Bunjes, 2011; Illing and Unruh 2004). The type of lipid used to produce the nanoparticles is also a factor which strongly influences on the formation of such a superstructure. Increasing lengths of fatty acid chains of pure triacylglycerols can lead to the formation of more anisometric TAG crystals (platelet-like), and, then, increase the chance of stacked lamellae to occur (Illing et al. 2002). The formation of such stacks results in an increase in the viscosity of the dispersed system, as they are not as mobile as spherical particles.

The type of surfactant used to stabilize the o–w interface of the lipid nanoparticles also influences on the viscosity of the nanodispersions. Lipid nanodispersions stabilized with phospholipids, particularly with monoacid TAG lipid phase, are known to be prone to gel formation. Such a fact is explained by the low mobility of phospholipid molecules in aqueous medium, and, then, they may not be able to immediately cover the newly created interfaces during recrystallization (Westesen and Siekmann 1997). Therefore, a sudden lack of emulsifier can be created locally on the surface of the particles, leading to aggregation and the formation of a gelified structure. The solution for this problem can be the addition of a more mobile co-surfactant, which is able to diffuse in a much shorter time than phospholipids (Bunjes 2011; Helgason et al. 2009; Bunjes et al. 2003).

7.2.3 Methods for Lipid Nanoparticles Production

Lipid nanoparticles can be produced by methods quite well known and explored in the literature, as well as already existent in full scale, as high-pressure homogenization (HPH) and microfluidization. It is important to emphasize the characteristic of lipid nanoparticles highly depend on their method of production, which has a great influence on the bioactive stability, release properties, loading capacity and, of course, on the particle size distribution (Sawant and Dodiya 2008).

The most popular production method used to produce lipid nanoparticles is the HPH. The type of equipment most used is the high-pressure valve homogenizers, which is known as reliable and powerful. Among their advantages, there is the availability of HPH equipments of many sizes and manufacturers, which can be found at reasonable prices (Pardeike et al. 2009; Weiss et al. 2008).

High-pressure valve homogenizers have a pump which pulls the input stream in the case of lipid nanoparticles, a coarse dispersion) into a chamber on its backstroke and then forces it through a narrow valve at the end of the chamber on its forward stroke. Extremely strong disruptive forces cause the breaking down of the particles, and then a fine dispersion is produced (McClements 2005).

Two different techniques can be used in HPH processes—the hot and cold homogenization. Hot homogenization occurs at temperatures above the melting point of the lipid, and the first step is to produce a coarse dispersion by mixing melted lipid, the bioactive to be encapsulated and a hot surfactant solution, using a high speed stirring device. Afterwards, the coarse dispersion is introduced in the high-pressure homogenizer, and the operation must be carried out at controlled temperature. There can be more than one passage through the homogenizer, and the number of passages will be determined by the desired characteristic for the product (normally the particle size). In most cases, three to five homogenization cycles at 500–1500 bar are enough (Mehnert and Mäder 2001). On the other hand, cold homogenization was proposed in order to overcome some problems of the hot homogenization procedure, which are: (i) degradation of the bioactive due to high temperature; (ii) bioactive distribution into the aqueous phase during homogenization and (iii) formation of supercooled melts or complexity of crystallization process of the nanoparticles after homogenization cycles (Mehnert and Mäder 2001; Pardeike et al. 2009). In cold homogenization, the first step is to mix the bioactive and melted lipid, and then such a mixture is cooled and solidified. Then, the solid is milled using a ball or mortar milling, dispersed in a cold surfactant solution, and finally submitted to the HPH step. The particle size of the lipid nanoparticles produced by cold homogenization is, generally, larger than the ones produced by hot homogenization. Figure 7.11 shows a schematic procedure of hot and cold homogenization techniques for lipid nanoparticles production.

Another method of production of lipid nanoparticles which has been becoming very popular is the microfluidization. Such a technique has been used for many years in food industry to produce fine emulsions, and it is also a homogenization process. Then, the general procedure is the same as hot homogenization prior described, though the principle of working of the equipment is different. In micro-

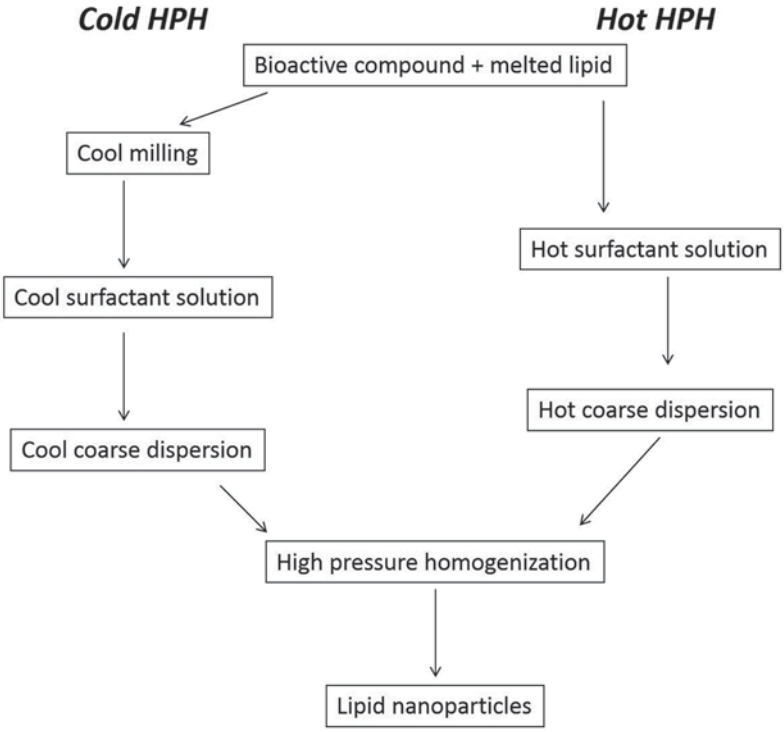

Fig. 7.11 Schematic representation of the cold and hot high-pressure homogenization methods to produce lipid nanoparticles

fluidizers, the inlet fluid is pumped, and the interaction chamber is formed by two channels through the streams flow and interact with each other. After entering the homogenizer, the fluids are accelerated and impinge with each other on a solid surface, generating extremely high disrupting forces due to the collision between the fluid streams (McClements 2005). Another type of microfluidizer operates with separate oil and surfactant solution streams, which interact in the chamber similarly as in the first scheme described (Dickinson and Stainsby 1988).

Microemulsion technique, whose schematic procedure is described in Fig. 7.12, can also be used to produce lipid nanoparticles. Briefly, the lipid material is melted and an o–w surfactant/co-surfactant containing aqueous phase is prepared at the same temperature. Both lipid and aqueous phase are mixed in such a ratio that a microemulsion is produced (ratios vary from 1:2 to 1:100). The systems normally must be kept at high temperatures during the process, as the size of microemulsion is a function of temperature. Afterwards the hot microemulsion is diluted with cold water, causing the breaking of the microemulsion and converting it into a fine emulsion, which recrystallized and formed the lipid nanoparticles (Sawant and Dodiya 2008; Bondi et al. 2007; Souto 2005; Gasco et al. 1992; Cavalli et al. 1993; Cavalli et al. 1997; Migglieta et al. 2000).

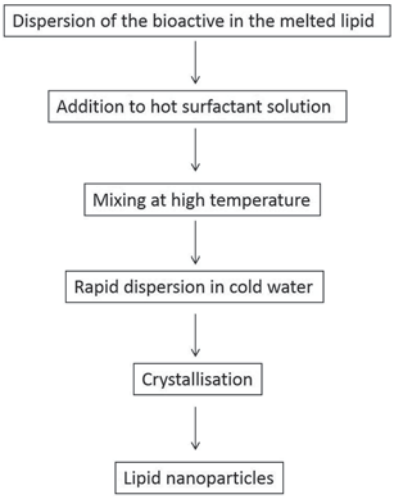

Fig. 7.12 Schematic representation of the microemulsion method to produce lipid nanoparticles

Ultrasonic homogenizers can also be used to produce lipid nanoparticles. This type of equipment creates intense disruptive forces, strong enough to break up lipid and water phases into very small particles (McClements and Rao 2011). Batch and flow-through equipments are available at reasonable prices; however, there is some concern about the possibility of very high temperature spots. The formation of these hot spots could lead to the oxidation of both lipid and bioactive, as well as protein denaturation or polysaccharide polymerization. Another problem which can occur with the use of ultrasonic devices is metal contamination due to probe degradation (Weiss et al. 2008; McClements and Rao 2011).

Low energy methods can also be used to produce lipid nanoparticles. These approaches rely on the spontaneous formation of oil droplets in oil-in-water-surfactant systems when their temperature or composition is changed (Fernandez et al. 2004; Anton and Vandamme 2009; McClements and Rao 2011). Low energy methods lead to the production of nanoparticles due to their capacity to divert the intrinsic physicochemical properties of the surfactants, co-surfactants and excipients in the formulation (Anton and Vandamme 2009; Solans et al. 2010). A common classification of low energy methods divides them in two types: self-emulsification and phase inversion methods. Self-emulsification (or direct emulsification) relies on the chemical energy of dissolution in the continuous phase of the dispersed phase present in the initial system. A common way to prepare o–w nanodispersions by such a method is to dilute into water an o–w microemulsion. Dilution causes a decrease in surfactant concentration, increase the interfacial tension and also both phases to dislocate from their original location. By controlling temperature and mixing conditions, it is possible to produce nanodispersed systems like lipid nanoparticles.

On the other hand, phase inversion methods can be subdivided into phase inversion temperature (PIT) and phase inversion composition (PIC). The PIT method, originally proposed by Shinoda and Saito (1968) is based on the changes in the

curvature (molecular geometry) or relative solubility of non-ionic surfactants with changing temperature (Anton and Vandamme 2009; Solans et al. 2010; McClements and Rao 2011). The phase inversion from o–w to w–o emulsion occurs due to the alteration of HLB of the polyethoxylated non-ionic surfactants with the temperature; as the temperature increases, the POE surfactants dehydrate, decreasing their values of hydrophilic/hydrophobic ratio, or, indirectly, the value of HLB. A nanodispersion can be formed spontaneously by fast cooling an emulsion from a temperature above the PIT to a much more lower temperature, using continuous stirring. In the case of lipid nanoparticles, the step of cooling would also be responsible for the crystallization of the particles. The PIC is similar to the PIT method, but the curvature of the surfactant is altered by changes in the formulation of the systems, rather than the temperature (McClements and Rao 2011; Salager 2006).

Other methods of lipid nanoparticles production found in the literature are solvent emulsification-evaporation (Garcia-Fuentes et al. 2005; Siekmann and Westesen 1996; Sjöström and Bergenståhl 1992), solvent displacement (Hu et al. 2004; Schubert and Müller-Goymann 2003) and emulsification-diffusion techniques (Trotta et al. 2003; Quintanar-Guerrero et al. 2005). However, they are not suitable for food applications as they use organic solvents (not food-grade as cyclohexane, chloroform, ethyl acetate, methylene chloride, isobutyric acid, tetrahydrofuran, for example) in some steps of the process. More recently, microfluidic techniques have also been proposed to produce lipid nanoparticles, but they are still extremely expensive and have no scale-up approaches (Finke et al. 2012).

7.2.4 Characterization of Lipid Nanoparticles

A complete characterization of a lipid nanoparticle dispersion is important to evaluate its suitability for a determined application, and also for its quality control. There are several techniques used to analyze the main characteristics of the lipid nanoparticles, and the most important are summarized in Table 7.3.

In order to determine the average particle size and size distribution, the most used technique is the DLS. Such a technique is based on the measurements of the translational diffusion coefficients (D) of droplets determined by analyzing the interaction between a laser beam and a dispersion (McClements 2005). The DLS is based on the phenomenon of the deflection of the light by the particles. There are many variations of DLS, and the two most commonly used methods in commercial instruments are PCS (photon correlation spectrometry), DSS (Doppler shift spectroscopy) and DWS (dynamic wave spectroscopy). The latter is a type of DLS suitable for analyzing concentrate colloidal dispersions, when multiple scattering is prone to occur (McClements 2005).

As for the measurement of particle surface charge, it is normally carried out by electrophoresis. In commercial instruments, the particle velocity is often determined using sophisticated light scattering measurements, and such velocity is related to its surface charge, as well as to the viscosity of aqueous surrounding medium and dieletric constant of the material (Hiemenz and Rajagopalan 1997; Riley 2005).

Table 7.3 Examples of the most used techniques in the characterization of lipid nanoparticle dispersions

Experimental technique	Measurement
Static light scattering (laser diffraction)	Particle size distribution (diluted dispersions)
Dynamic light scattering (photon correlation spectroscopy, Doppler shift spectroscopy)	
Electrical pulse counting (electrozone sensing or Coulter counter)	Particle size distribution (diluted and concentrated dispersions)
Nuclear magnetic resonance (restricted diffusion measurements of NMR)	
Diffusion wave spectroscopy	Particle size distribution (concentrated dispersions)
Ultrasonic spectrometry	Particle size and concentration of droplets (can be used as an on-line sensor)
Nuclear magnetic resonance (NMR)	Solid content of dispersions (extent of droplet crystallization)
Wide angle X-ray diffractometry (WAXD or XRD)	Polymorphism, crystalline structure
Small angle X-ray scattering (SAXS)	
Neutron scattering	Particle size distribution, thickness of interface layers, spatial distribution of particles in the dispersion
Electroacoustics	Particle size distribution, zeta potential
Electrical conductivity	Disperse volume fraction
Ultrasonics	Phase transitions (melting and crystallization), solid contents
Differential scanning calorimetry	Phase transitions (melting and crystallization)
Particle electrophoresis	Zeta potential
Rheology	Droplet interactions
Transmission electron microscopy	Morphological characteristics
Scanning electron microscopy	
Confocal laser microscopy	
Atomic force microscopy	

The surface charge of lipid nanoparticles, as in any other colloidal systems, is a valuable tool to predict and explain their stability, as high values of surface charges (higher than +30 mV or lower than −30 mV) indicate aggregation of particles is less prone to occur. In addition, the interactions of the particles with other components of food matrix are also influenced by their charge. Also, the digestibility of a lipid nanoparticle is strongly related to its surface charge.

Crystalline microstructure and polymorphic nature of the lipid nanoparticles, as already exposed in this chapter, are extremely important characteristics of this type of colloidal system. Such information is, in most cases, obtained by X-ray techniques (diffraction and scattering) and differential scanning calorimetry (DSC). Among the X-ray techniques, the most used is WAXD (wide angle X-ray diffraction). It detects electron density fluctuations and can relate these fluctuations with the characteristic lengths of the crystalline structure by using Bragg's law [Eq. (7.2)]:

$$2d \sin\theta = \lambda \tag{7.2}$$

where d is the characteristic length (it must be lower than 1 angstrom), 2θ is the scattering angle and is the wavelength of X-ray beam. The directions of the diffracted beams are related to the shape and dimensions of the unit cell of the crystalline lattice (Souto, 2005). A great advantage of WAXD analyses is that they are non-destructive and have high penetration capability for organic systems, as well as is sensitive to small structural changes (Bunjes and Unruh 2007). Figure 7.13 shows examples of WAXD typical diffractograms for lipid nanoparticles.

Another X-ray technique used to characterize the microstructure of lipid nanoparticles is SAXS (small angle X-ray scattering). The main difference between WAXD and SAXS is the range of scattering angles; the denominated WAXD works with angles (2θ) between 5 and 180°, whereas SAXS covers angles between 0.01 and 5° (Bunjes and Unruh 2007). Identification of crystalline structures and their modifications are the most common objectives for the use of X-ray techniques. By using them, it is possible to distinguish crystalline materials from amorphous, as the crystalline show several diffraction bands, whereas amorphous substances do not present a regular baseline. Such a differentiation and characterization is essential for lipid nanoparticle studies aiming food applications, as crystallinity is a key factor in the stability (thus, in the shelf-life) and digestibility of such nanosystems.

DSC is a powerful experimental technique to elucidate the microstructure of lipid nanoparticles. The breakdown of the crystal lattice by cooling or heating the lipid nanoparticle dispersion provides information on crystal ordering and polymorphism (Souto 2005). Modern sensitive DSC equipments can detect crystalline lipid phase transitions at the typical concentrations between 1 and 10 %, or even below (Bunjes and Unruh 2007). It is important, however, to remember DSC is able to detect and quantify thermal events, but it is not capable of identifying the cause of the physical transitions. It is essential to use DSC and another technique in a complementary way (Bunjes and Unruh 2007).

One important point in the thermal behaviour of lipid nanoparticles is the occurrence of a depression in the melting point of the nanoparticles in comparison to the

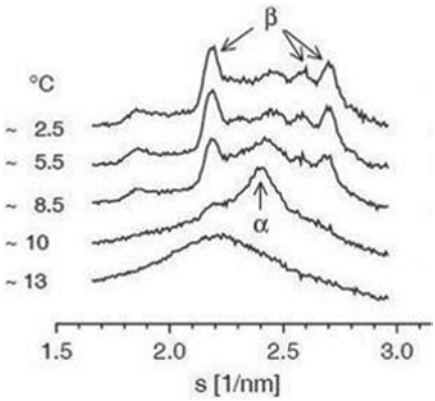

Fig. 7.13 Example of wide angle diffraction patterns of lipid nanoparticles produced with trimyristin and stabilized with purified soy phosphatidylcholine. The polymorphic forms changed with the different temperatures at which the system was submitted ($s = 1/d$). (Adapted with permission from Bunjes and Koch (2005). Copyright 2005 Elsevier)

bulk material. Such a phenomenon is expected for nanodispersions according to the Gibbs–Thomson equation:

$$ln\frac{T}{T_0} = \frac{-2 \cdot \gamma_{SL} \cdot V_S}{r \cdot \Delta H_{fus}} \tag{7.3}$$

where ΔH_{fus} is the specific heat of fusion, T is the melting temperature of a particle with radius r, and T_0 is the melting point of the bulk lipid at the same external pressure. Figure 7.14 shows an example of a comparison of thermograms of the bulk lipid and lipid nanoparticles.

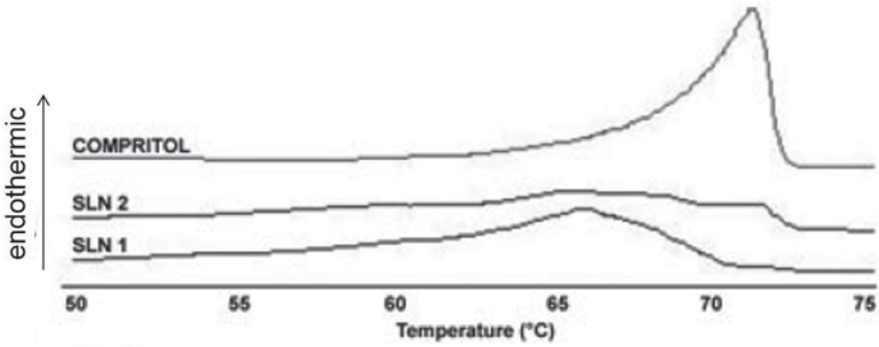

Fig. 7.14 DSC heating curves of bulk lipid (Compritol 888 ATO) and lipid nanoparticle formulations. The lipid nanoparticles were produced with Compritol 888 ATO (9 % mass) and *Artemisia arborescens L.* essential oil (1 % mass) as lipids, and Poloxamer 188 (SLN 1) or Miranol Ultra C32 (SLN 2) as surfactants (2.5 % mass). Melting peaks were altered from 71.2 °C in bulk lipid to 65.7 and 66.7 °C in SLN 1 and SLN 2, respectively, and melting enthalpy decreased from 110 J/g to around 10 J/g in lipid nanoparticles. (Adapted with permission from Lai et al 2006. Copyright 2006 Springer)

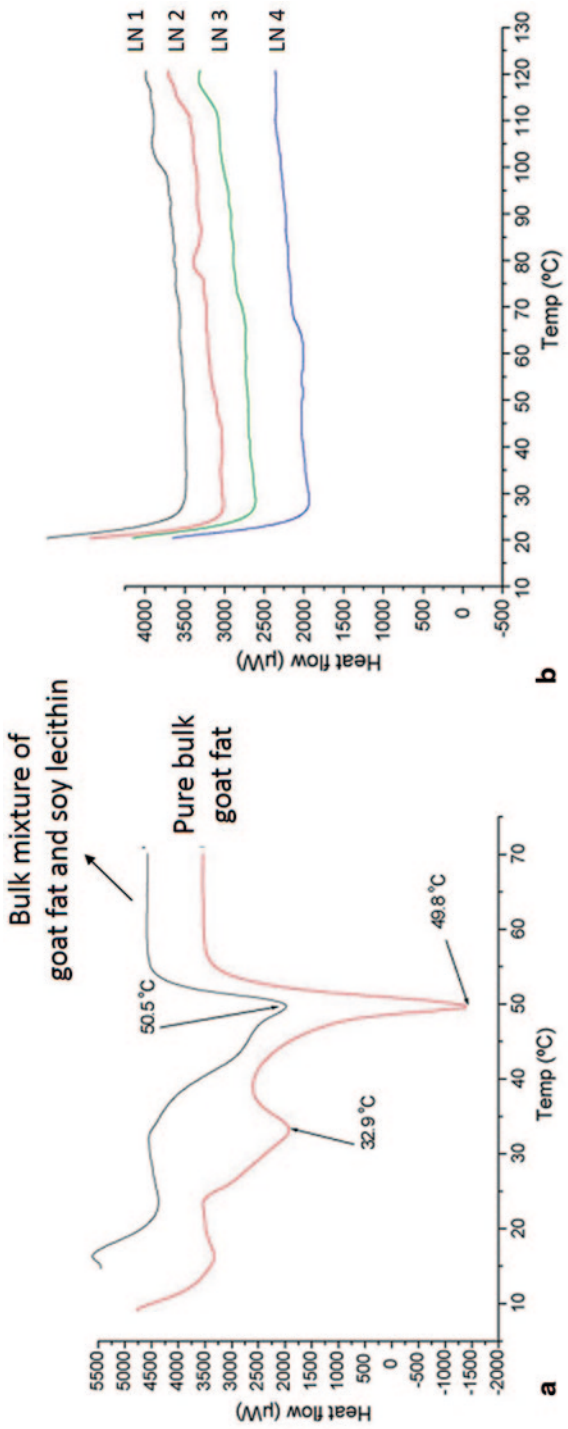

Fig. 7.15 Comparison of thermal behaviour, obtained by DSC, of (**a**) bulk lipids and (**b**)lipid nanodispersions produced with such lipids. The lipid nanoparticles were produced with 5 % of a mixture of goat fat and soy lecithin, and polysorbate 80 as stabilizer (LN1, LN2, LN3 and LN4 contained 1.0, 0,50, 0.10 and 0.0 % polysorbate 80, respectively). (Adapted with permission from Attama and Müller-Goymann 2007. Copyright 2007 Elsevier)

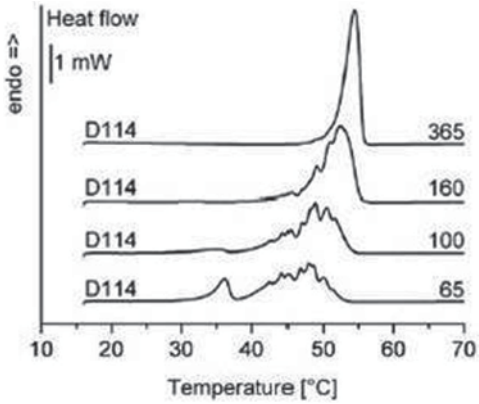

Fig. 7.16 DSC heating curves of trimyristin (Dynasan 114, in the Figure denoted as D114) lipid nanoparticles showing the influence of particle diameter (indicated in nanometers) on the thermal behaviour. The particles were stabilized with 3.2 % soy phospholipid and 0.8 % sodium glycocholate. (Adapted with permission from Bunjes and Unruh 2007. Copyright 2007 Elsevier)

In Fig. 7.15 it is also possible to verify how strong the effect of the nanosizing is in the thermal behaviour of lipid dispersions. The lipid nanoparticles, in the case of the cited study, were around 100 nm of diameter.

The effect of the particle size on the thermal behaviour can be clearly observed in Fig. 7.16. It is evident the influence of particle size becomes more pronounced as the particle size decreases.

Another important aspect which must be observed in thermal analysis of lipid nanoparticles is the heating rate, as metastable polymorphs can transform into more stable ones during the analysis, depending on the conditions set for the analyses (Bunjes and Unruh 2007). The differences in the thermograms for a freshly prepared dispersion of lipid nanoparticles of tristearin can be observed in Fig. 7.17, for the different heating rates applied during the DSC analyses.

High heating rates should be used in DSC analyses of lipid nanoparticles, but a compromise may be necessary in order to not decrease resolution of multiple signals derived from the thermal events (Bunjes and Unruh 2007).

Scanning electron microscopy (SEM), atomic force microscopy (AFM) and transmission electron microscopy (TEM) are extremely useful in determining shape and morphology of lipid nanoparticles. A great advantage of TEM is the possibility of visualizing coexisting structures and microstructure transitions. Conventional TEM, however, can be considered as a preliminary technique to have a first impression of a lipid nanoparticle dispersion. Cryo-TEM and freeze-fractured TEM are certainly the most powerful techniques to investigate lipid nanoparticles visually, since they can provide detailed information about the internal structure of colloidal systems in their native state (Klang et al. 2012). Figure 7.18 shows examples of micrographs of the same sample of lipid nanoparticles, obtained by cryo or freeze-fractured TEM.

Finally, Fig. 7.19 shows the cryo-transmission electron microscopy images of lipid nanoparticles composed of various types of triacylglycerols.

In the micrographs, it can be observed the three-dimensional particles are projected in a two-dimensional way, and it is possible to distinguish deformed hexagonal, elongated circular platelet-like crystalline particles, and dark, “needle”-like

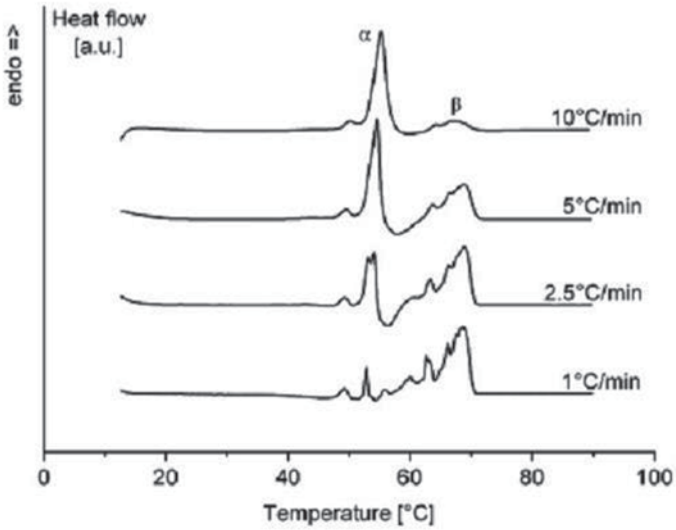

Fig. 7.17 Influence of heating rate on the melting curve of a freshly prepared tristearin (Dynasan 118) nanoparticle dispersion (10% lipid, 2.4% DPPC and 0.6% sodium glycocholate). (Reproduced with permission from Bunjes and Unruh 2007. Copyright 2007 Elsevier)

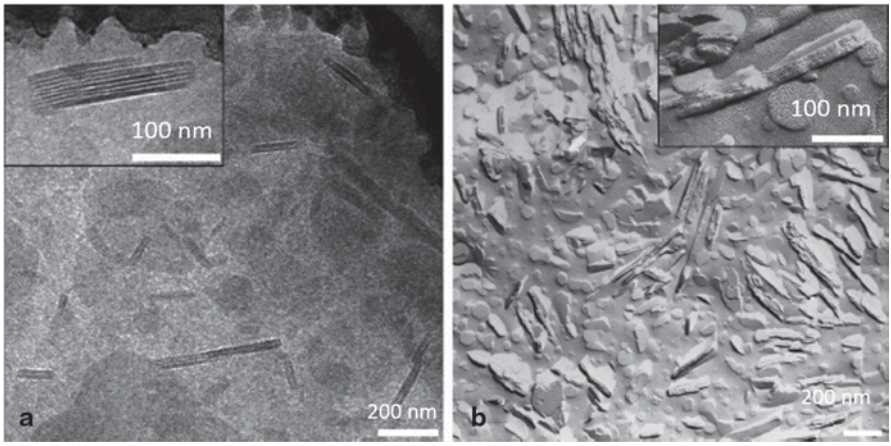

Fig. 7.18 Electron micrographies of a lipid nanoparticle dispersion produced with tristearin (Dynasan 118, 10%) and stabilized with purified soy lecithin (2.4%) and sodium glycocholate (0.6%). **a** Cryo-electron micrograph. **b** Freeze-fractured micrograph. (Adapted with permission from Bunjes and Koch 2005, Copyright 2005 Elsevier)

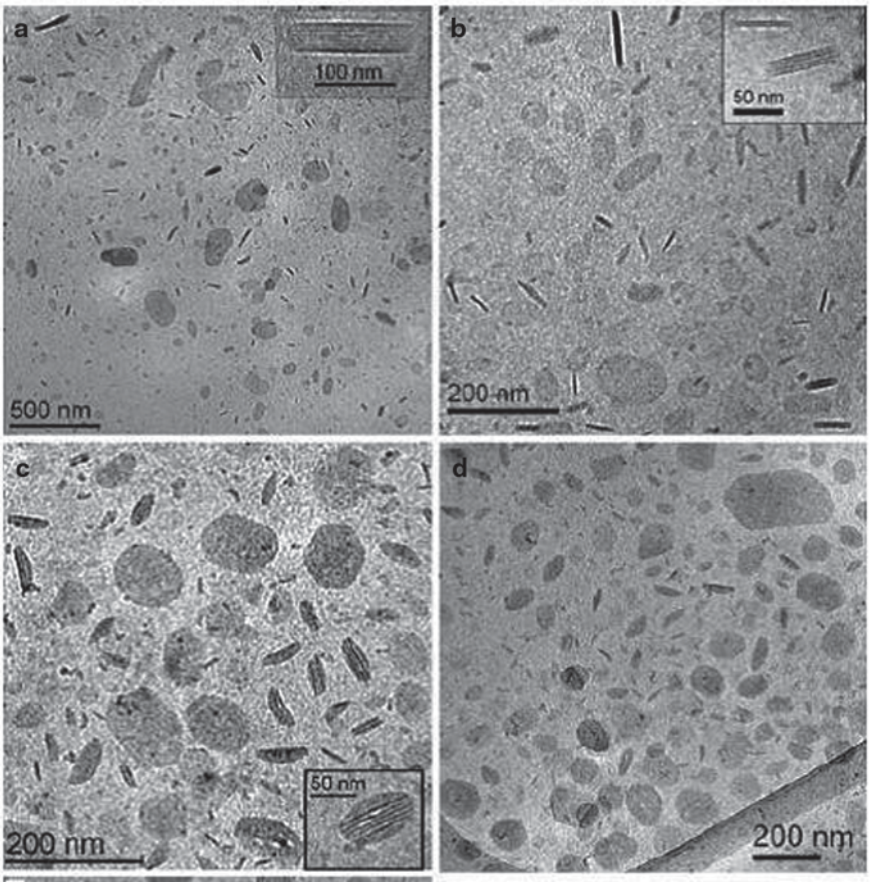

Fig. 7.19 Cryo-TEM images of lipid nanoparticles composed of **a** tristearin; **b** tristearin-monostearin (2:1); **b** tristearin-tricaprin (2:1); **d** tribehenin. The nanodispersions were stabilized with Poloxamer 188. (Adapted with permission of Esposito et al. 2008, Copyright 2008 Springer)

structures (nanoparticles side view) (Esposito et al. 2008). Such morphological observations are typical in lipid nanodispersions systems.

7.3 Conclusions and Future Perspectives

Research to date has demonstrated the excellent potential for the use of liposomes and lipid nanoparticles in the encapsulation of hydrophobic bioactives in food. Their capacity to increase the dispersibility of such compounds and consequently their incorporation in food formulations is a very attractive reason to use them. In terms of processes, the main challenge is to develop scalable production methods,

especially in the case of liposomes, but also for lipid nanoparticles. Besides developing such methods, it is crucial to obtain the process parameters important for the scale-up. In the case of liposomes, the high-pressure methods are not especially interesting for scale-up. In the case of lipid nanoparticles, applications which require a very low particle diameter are many times limited to the use of high energy methods; so, another frontier can be the development of low energy methods in order to produce extremely fine nanodispersions of lipid particles. The use of a wider range of food-grade raw materials is also urgent, as many studies are still based on pharmaceutical paradigms, and they do not present results using different types of lipids (natural butters, for example) or phospholipids (egg phospholipids, or non-purified lecithins), or even other categories of natural surfactants.

A second aspect is related to the evaluation of the digestibility of these lipid-based nanoencapsulation systems. There are many studies in the literature, but most of them do not try to simulate the digestion of the liposomes or lipid nanoparticles in more realistic situations, as if they were incorporated in a more complex food structure.

Finally, the major problem is that there are almost any studies in the scientific literature evaluating the incorporation of liposomes and lipid nanoparticles in food systems. The next challenge is probably prove their theoretical capacity of protection of the hydrophobic bioactives, or improvement of their dispersibility, is good enough to deserve more attention by the food industry as real alternatives for microencapsulation.

References

Anton N, Vandamme TF (2009) The universality of low-energy emulsification. Int J Pharm 377:142–147

Antunes FE, Marques EF, Miguel MG, Lindman B (2009) Polymer-vesicle association. Adv Colloid Interface Sci 147–148:18–35

Arifin DR, Palmer AF (2003) Determination of size distribution and encapsulation efficiency of liposome-encapsulated hemoglobin blood substitutes using asymmetric flow field-flow fractionation coupled with multi-angle static light scattering. Biotechnol Prog 19:1798–1811

Attama AA, Müller-Goymann CC (2007) Investigation of surface-modified solid lipid nanocontainers formulated with a heterolipid-templated homolipid. Int J Pharm 334:179–189

Awad TS, Helgason T, Weiss J, Decker EA, McClements DJ (2009) Effect of omega-3 fatty acids on crystallization, polymorphic transformation and stability of tripalmitin solid lipid nanoparticle suspensions. Crys Grow Des 9:3405–3411

Balbino TA, Gasperini A, Oliveira CLP, Cavalcati LP, Azzoni AR, de la Torre LG (2012) Correlation between physicochemical and structural properties with in vitro transfection of pDNA/cationic liposomes complexes. Langmuir 28:11535–11545

Balbino TA, Aoki NT, Gasperini A, Oliveira CLP, Cavalcanti LP, Azzoni AR, de la Torre LG (2013) Continuous flow production of cationic liposomes at high lipid concentration in microfluidic devices for gene delivery applications. Chem Eng J 226:423–433

Bangham AD (1992) Liposomes—Realizing their promise. Hosp Pract 27:51–56, 61–62

Bangham AD, Standish MM, Watkins JC (1965) Diffusion of univalent ions across lamellae of swollen phospholipids. J Mol Biol 13:238–252

Batzri S, Korn ED (1973) Single bilayer liposomes prepared without sonication. Biochim Biophys Acta 298:1015–1019

Baxter S, Zivanovic S, Weiss J (2005) Molecular weight and degree of acetylation of high-intensity ultrasonicated chitosan. Food Hydrocoll 19:821–830

Bibi S, Kaur R, Henriksen-Lacey M, McNeil SE, Wilkhu J, Lattmann E et al (2011) Microscopy imaging of liposomes: From cover slips to environmental SEM. Int J Pharm 417:138–150

Bondi ML, Azzolina A, Capraro EF et al (2007) Novel cationic solid lipid nanoparticles as non-viral vectors for gene delivery. J Drug Target 15:295–301

Boode K, Walstra P (1993) Partial coalescence in oil-in-water emulsions 1. Nature of the aggregation. Coll Surf A: Phys Eng Asp 81:121–137

Boode K, Walstra PA, de Groot-Mostert EA (1993) Partial coalescence in oil-in-water emulsions 2. Influence of the properties of the fat. Coll Surf A: Phys Eng Asp 81:139–151

Bunjes H (2011) Structural properties of solid lipid based colloidal drug delivery systems. Curr Op Coll Interface Sci 16:405–411

Bunjes H, Koch, MHJ (2005) Saturated phospholipids promote crystallization but slow down polymorphic transitions in triglyceride nanoparticles. J Cont Rel 107:229–243

Bunjes H, Unruh T (2007) Characterization of lipid nanoparticles by differential scanning calorimetry, X-ray and neutron scattering. Adv Drug Del Rev 59:379–402

Bunjes H, Westesen K, Koch MHJ (1996) Crystallization tendency and polymorphic transitions in triglyceride particles. Int J Pharm 129:159–173

Bunjes H, Koch MHJ, Westesen, K (2003) Influence of emulsifiers on the crystallization of solid lipid nanoparticles. J Pharm Sci 92:1509–1519

Bunjes H, Steiniger F, Richter W (2007) Visualizing the structure of triglyceride nanoparticles in different crystal modifications. Langmuir 23:4005–4011

Castor TP (1994) Methods and apparatus for liposomes preparation. World Wide patent WO9427581

Cavalli R, Caputo O, Gasco MR (1993) Solid lipospheres of doxorubicin and idarubicin. Int J Pharm 89:R9–R12

Cavalli R, Caputo O, Carlotti ME, Trotta M, Scarnecchia C, Gasco MR (1997) Sterlization and freeze-drying of drug-free and drug-loaded solid lipid nanoparticles. Int J Pharm 148:47–54

Colas J-C, Shi W, Rao VSNM, Omri A, Mozafari MR, Singh (2007) Microscopical investigations of nisin-loaded nanoliposomes prepared by Mozafari method and their bacterial targeting. Micron 38:841–847

Cornacchia L, Roos YH (2011) Stability of b-carotene in protein-stabilized oil-in-water delivery systems. J Agric Food Chem 59:7013–7020

de la Torre LG, Rosada RS, Trombone APF, Frantz FG, Coelho-Castelo AAM, Silva CL, Santana MHA (2009) Synergy between structural stability and DNA-binding controls the antibody production in EPC/DOTAP/DOPE vesicles and DOTAP/DOPE lipoplexes. Colloids and Surfaces B: Biointerfaces 73:175-184

de Paz E, Martin A, Jose CM (2012) Formulation of beta-carotene with soybean lecithin by PGSS (particles from gas saturated solutions)-drying. J Supercrit Fluids 72:125–33

Dickinson E, Stainsby G (eds) (1988). Advances in food emulsions and foam. Elsevier, London

Dickinson E, McClements DJ (1996). Fat crystallization in oil-in-water emulsions. In: Dickinson E, McClements DJ (eds) Advances in food colloids. Blackie Academic & Professional, Glasgow, p 211

Dillehay DL, Webb SK, Schmelz EM, Merrill AH (1994) Dietary sphingomyelin inhibits 1,2-dimethylhydrazine-induced colon-cancer in CF1 mice. J Nutr 124:615–20

Dillow AK, Dehghani F, Hrkach JS, Foster NR, Langer R (1999) Bacterial inactivation by using near- and supercritical carbon dioxide. Proc Natl Acad Sci U S A 96:10344–10348

Ding B, Zhang X, Hayat K, Xia S, Jia C, Xie M et al (2011) Preparation, characterization and the stability of ferrous glycinate nanoliposomes. J Food Eng 102:202–208

Egelhaaf SU, Wehrli E, Muller M, Adrian M, Schurtenberger P (1996) Determination of the size distribution of lecithin liposomes: a comparative study using freeze fracture, cryoelectron microscopy and dynamic light scattering. J Microsc 184:214–228

Eldridge JH, Staas JK, Meulbroek JA, McGhee JR, Tice TR, Gilley RM (1991) Biodegradable microspheres as a vaccine delivery system. Mol Immunol 28:287–294

Esposito E, Fantin M, Marti M, Dreschsler M, Paccamiccio L, Mariani P, Sivieri E, Lain F, Menegatti E, Morari M, Cortesi R (2008). Solid lipid nanoparticles as delivery systems for bromocriptine. Pharm Res 25:1521–1530

Evans DF, Wennerström H (1999) The colloidal domain where physics, chemistry, biology and technology meet. Wiley-VCH, Canada

Farhang B, Kakuda Y, Corredig M (2012) Encapsulation of ascorbic acid in liposomes prepared with milk fat globule membrane-derived phospholipids. Dairy Sci Technol 92:353–366

Fathi M, Mozafari MR, Mohebbi M (2012) Nanoencapsulation of food ingredients using lipid based delivery systems. Trends Food Sci Technol 23:13–27

Fernandez P, André V, Rieger J, Kühnle A (2004) Nano-emulsion formation by emulsion phase inversion. Coll Surf A:Phys Eng Asp 251:53–58

Filipovic-Grcic J, Skalko-Basnet N, Jalsenjak I (2001) Mucoadhesive chitosan-coated liposomes: characteristics and stability. J Microencapsul 18:3–12

Finke JH, Schur J, Richter C, Gothsch T, Kwade A, Büttgenbach S, Müller-Goymann CC (2012) The influence of customized geometries and process parameters on nanoemulsion and solid lipid nanoparticle production in microsystems. Chem Eng J 209:126–137

Fukui Y, Fujimoto K (2009) The preparation of sugar polymer-coated nanocapsules by the layer-by-layer deposition on the liposome. Langmuir 25:10020–10025

Garcia-Fuentes M, Prego C, Torres D, Alonso MJ (2005) A comparative study of the potential of solid triglyceride nanostructures coated with chitosan or poly(ethyleneglycol) as carriers for oral calcitonin delivery. Eur J Pharm Sci 25:133–143

Gasco MR, Morel S, Carpigno R (1992) Optimization of the incorporation of desoxycortisone acetate in lipospheres. Eur. J Pharm Biopharm 38:7–10

Gentine P, Bubel A, Crucifix C, Bourel-Bonnet L, Frisch B (2012) Manufacture of liposomes by isopropanol injection: characterization of the method. J Liposome Res 22:18–30

Gokce EH, Korkmaz E, Dellera E, Sandri G, Bonferone MC, Ozer, O. (2012a) Resveratrol-loaded solid lipid nanoparticles versus nanostructured lipid carriers: evaluation of antioxidant potential for dermal applications. Int J Nanom 7:1841–1850

Gokce EH, Korkmaz E, Tuncay-Tanrıverdi S, Dellera E, Sandri G, Bonferone MC, Ozer O (2012b) A comparative evaluation of coenzyme Q10-loaded liposomes and solid lipid nanoparticles as dermal antioxidant carriers. Int J Nanom 7:5109–5117

Gonzalez-Rodriguez ML, Barros LB, Palmaa J, Gonzalez-Rodriguez PL, Rabasco AM (2007) Application of statistical experimental design to study the formulation variables influencing the coating process of lidocaine liposomes. Int J Pharm 337:336–345

Gratton SEA, Ropp PA, Pohlhaus PD, Luft JC, Madden VJ, Napier ME et al (2008) The effect of particle design on cellular internalization pathways. Proc Natl Acad Sci U S A 105:11613–11618

Guo J, Ping Q, Jiang G, Huang L, Tong Y (2003) Chitosan-coated liposomes: characterization and interaction with leuprolide. Int J Pharm 260:167–173

Haidar ZS, Hamdy RC, Tabrizian M (2008) Protein release kinetics for core-shell hybrid nanoparticles based on the layer-by-layer assembly of alginate and chitosan on liposomes. Biomaterials 29:1207–1215

Helgason T, Awad TS, Kristbergsson K, McClements DJ, Weiss J (2008) Influence of polymorphic transformations on gelation of tripalmitin solid lipid nanoparticle suspensions. J Am Oil Chem Soc 85:501–511

Helgason T, Awad TS, Kristbergsson K, McClements DJ, Weiss J (2009) Effect of surfactant surface coverage on formation of solid lipid nanoparticles (SLN). J Coll Int Science 334:75–81

Hentschel A, Gramdorf S, Muller RH, Kurz T (2008) b-Carotene-loaded nanostructured lipid carriers. J. Food Sci. 73:1–6

Hiemenz PC (1986) Principles of colloid and surface chemistry, 2nd edn. Marcel Dekker, New York

Hiemenz PC, Rajagopalan R (1997) Principles of colloid and surface chemistry, 3rd edn. Marcel Dekker, New York

Himawan C, Starov VM, Stapley AGF (2006) Thermodynamic and kinetic aspects of fat crystallization. Adv Coll Int Sci 122:3–33

Ho J-aA, Zeng S-C, Tseng W-H, Lin Y-J, Chen C-H (2008) Liposome-based immunostrip for the rapid detection of Salmonella. Anal Bioanal Chem 391:479–485

Hu FQ, Hong Y, Yuan H (2004) Preparation and characterization of solid lipid nanoparticles containing peptide. Int J Pharm 273:29–35

Huang CH, Li SS (1999) Calorimetric and molecular mechanics studies of the thermotropic phase behavior of membrane phospholipids. Biochim Biophys Acta Biomembranes 1422:273–307

Huang YY, Chung TW, Wu CI (1998) Effect of saturated/unsaturated phosphatidylcholine ratio on the stability of liposome-encapsulated hemoglobin. Int J Pharm 172:161–167

Hung LC, Basri, M, Tejo BA, Ismail R, Nang HLL, Hassan HA, May CY (2011). An improved method for the preparations of nanostructured lipid carriers containing heat-sensitive bioactives. Coll Surf B Biointerfaces 87:180–186

Illing A, Unruh T (2004) Investigation on the flow properties of dispersions of solid triglyceride nanoparticles. Int J Pharm 284:123–131

Illing A, Unruh T, Koch, MHJ (2002) Investigation on particle self-assembly in solid-lipid-based colloidal drug carrier system. Pharm Res 21:592–597

Islam AM, Chowdhry BZ, Snowden MJ (1995) Heteroaggregation in colloidal dispersions. Adv Colloid Interface Sci 62:109–136

Israelachvili JN (1985) Intermolecular and surface forces. Academic Press, San Diego

Jaafar-Maalej C, Charcosset C, Fessi H (2011) A new method for liposome preparation using a membrane contactor. J Liposome Res 21:213–220

Jahn A, Vreeland WN, Gaitan M, Locascio LE (2004) Controlled vesicle self-assembly in microfluidic channels with hydrodynamic focusing. J Am Chem Soc 126:2674–2675

Jahn A, Vreeland WN, DeVoe DL, Locascio LE, Gaitan M (2007) Microfluidic directed formation of liposomes of controlled size. Langmuir 23:6289–6293

Jahn A, Reiner JE, Vreeland WN, DeVoe DL, Locascio LE, Gaitan M (2008) Preparation of nanoparticles by continuous-flow microfluidics. J Nanopart Res 10:925–934

Jahn A, Stavis SM, Hong JS, Vreeland WN, Devoe DL, Gaitan M (2010) Microfluidic mixing and the formation of nanoscale lipid vesicles. ACS Nano 4:2077–2087

Jenning V, Thünemann AF, Gohla SH (2000) Characterisation of a novel solid lipid nanoparticle carrier system based on binary mixtures of liquid and solid lipids. Int J Pharm 199:167–177

Jeong SH, Park JH, Park, K (2007) Formulation issues around lipid-based oral and parenteral delivery systems. In: Wasan KM (ed). Role of lipid excipients in modifying oral and parenteral drug delivery, Wiley-Interscience, Hoboken, pp. 32-47

Jeppsen RB (2001) Toxicology and safety of Ferrochel and other iron amino acid chelates. Arch Latinoam Nutr 51:26–34

Keller BC (2001) Liposomes in nutrition. Trends Food Sci Technol 12:25–31

Khreich N, Lamourette P, Boutal H, Devilliers K, Creminon C, Volland H (2008) Detection of Staphylococcus enterotoxin B using fluorescent immunoliposomes as label for immunochromatographic testing. Anal Biochem 377:182–188

Kidd PM (2000) Dietary phospholipids as anti-aging nutraceuticals. In: Klatz RA, Goldman R (eds.) Anti-aging medical therapeutics, vol. IV. Health Quest Publications, Chicago, pp 282–300

Kirby C, Gregoriadis G (1984) Dehydration-rehydration vesicles - a simple method for high-yield drug entrapment in liposomes. Biotechnology 2:979–984

Klang V, Matsko NB, Valenta C, Hofer F (2012). Electron microscopy of nanoemulsions:an essential tool for characterization and stability assessment. Micron 43:85–103

Kremer JMH, Esker MWJ, Pathmamanoharan C, Wiersema PH (1977) Vesicles of variable diameter prepared by a modified injection method. Biochemistry 16:3932–5

Kritchevsky D (1998) Fats and oils in human health. In: Akoh CC, Min DB (eds) Food lipids: chemistry, nutrition and biotechnology. Marcel Dekker, New York, pp 449–462

Lai F, Wissing S, Müller RH, Fadda AM (2006). Artemisia arborescens L. essential oil-loaded solid lipid nanoparticles for potential agricultural application: preparation and characterization. AAPS Pharm 7:E1–E9

Lambert JD, Yang CS (2003) Cancer chemopreventive activity and bioavailability of tea and tea polyphenols. Mutat Res Fundam Mol Mech Mutagen 523:201–208

Lariviere B, El Soda M, Soucy Y, Trepanier G, Paquin P, Vuillemard JC (1991) Microfluidized liposomes for the acceleration of cheese ripening. Int Dairy J 1:111–124

Lasch J, Weissig V, Brandl M (2003) Preparation of liposomes. In: V. Torchilin, V. Weissig (eds) Liposomes: a practical approach. Oxford University Press, New York, pp 3–29

Lasic DD (1993) Liposomes: from physics to applications. Elsevier, Amsterdam

Lasic DD (1997) Liposomes in gene delivery. CRC Press, Boca Raton

Laye C, McClements DJ, Weiss J (2008) Formation of biopolymer-coated liposomes by electrostatic deposition of chitosan. J Food Sci 73:N7–N15

Layrisse M, Garcia-Casal MN, Solano L, Baron MA, Arguello F, Llovera D et al (2000) Iron bioavailability in humans from breakfasts enriched with iron bis-glycine chelate, phytates and polyphenols. J Nutr 130:2195–2199

Li H, Zhao X, Ma Y, Zhai G, Li L, Lou H (2009) Enhancement of gastrointestinal absorption of quercetin by solid lipid nanoparticles. J Contr Rel 133:238-244

Liu CH, Wu CT (2010) Optimization of nanostructured lipid carriers for lutein delivery. Coll Surf A Phys Eng Asp 353:149–156

Lu Q, Li DC, Jiang JG (2011) Preparation of a tea polyphenol nanoliposome system and its physicochemical properties. J Agric Food Chem 59:13004–13011

Lung HL, Ip WK, Wong CK, Mak NK, Chen ZY, Leung KN (2002) Anti-proliferative and differentiation-inducing activities of the green tea catechin epigallocatechin-3-gallate (EGCG) on the human eosinophilic leukemia EoL-1 cell line. Life Sci 72:257–268

Luykx DMAM, Peters RJB, van Ruth SM, Bouwmeester H (2008) A review of analytical methods for the identification and characterization of nano delivery systems in food. J Agric Food Chem 56:8231–8247

Maherani B, Arab-Tehrany E, Kheirolomoom A, Cleymand F, Linder M (2012) Influence of lipid composition on physicochemical properties of nanoliposomes encapsulating natural dipeptide antioxidant L-carnosine. Food Chem 134:632–640

Malaki-Nik A, Langmaid S, Wrigth AJ (2012) Non-ionic surfactant and interfacial structure impact crystallinity and stability of b-carotene loaded lipid nanodispersions. J Agr Food Chem 60: 4126-4135

Malheiros PdS Daroit DJ da Silveira NP Brandelli A (2010) Effect of nanovesicle-encapsulated nisin on growth of Listeria monocytogenes in milk. Food Microbiol 27:175–178

Mayhew E, Conroy S, King J, Lazo R, Nikolopoulus G, Siciliano A et al (1987) High-pressure continuous-flow system for drug entrapment in liposomes. Methods Enzymol 149:64–77

McClements DJ (2005) Food emulsions: principles, practice, and techniques. 2nd ed., CRC Press, Washington

McClements DJ, Rao J (2011) Food grade nanoemulsions: formulation, fabrication, properties, performance, biological fate and potential toxicity. Crit Rev Food Sci Nut 51:285–330

McPherson AV, Kitchen BJ (1983) Reviews of the progress of dairy science—the bovine-milk fat globule-membrane—its formation, composition, structure and behavior in milk and dairy-products. J Dairy Res 50:107–133

Mehnert W, Mäder K (2001) Solid lipid nanoparticles: production, characterization and applications. Adv Drug Del Rev 47:165–169

Meure LA, Foster NR, Dehghani F (2008) Conventional and dense gas techniques for the production of liposomes: a review. Aaps Pharmscitech 9:798–809

Migglieta A, Cavalli R, Bocca C, Gabriel L, Gasco MR (2000) Cellular uptake and cytotoxicity of solid lipid nanoparticles (SLN) incorporating doxorubicin or paclitaxel. Int J Pharm 210:61–67

Moraes M, Carvalho JMP, Silva CR, Cho S, Sola MR, Pinho SC (2013) Liposomes encapsulating beta-carotene produced by the proliposomes method: characterisation and shelf life of powders and phospholipid vesicles. Int J Food Sci Technol 48:274–282

Mozafari MR (2005) Liposomes: an overview of manufacturing techniques. Cell Mol Biol Lett 10:711–719

Mozafari MR, Mortazavi MS (2005) Nanoliposomes: From fundamentals to recent developments. Oxford:Trafford Publishing Ltd.

Mozafari MR, Reed CJ, Rostron C, Kocum C, Piskin E (2002) Construction of stable anionic liposome-plasmid particles using the heating method: A preliminary investigation. Cell Mol Biol Lett 7:923–927

Muchow M, Maincent P, Müller RH (2008) Lipid nanoparticles with a solid matrix (SLN®, NLC®, LDC®) for oral drug delivery. Drug Dev. Ind. Pharm. 34:1394-1405

Müller RH, Mäder K, Gohla S (2000) Solid lipid nanoparticles (SLN) for controlled drug delivery: a review of the state of the art. Eur J Pharm Biopharm 50:161–177

Müller RH, Radtke M, Wissing, SA (2002) Solid lipid nanoparticles (SLN) and nanostructured lipid carriers (NLC) in cosmetic and dermatological preparations. Adv Drug Del Rev 54:S131–S155

Mun S, Decker EA, Park Y, Weiss J, McClements DJ (2006) Influence of interfacial composition on in vitro digestibility of emulsified lipids: Potential mechanism for chitosan's ability to inhibit fat digestion. Food Biophys 1:21–29

Nagayasu A, Uchiyama K, Kiwada H (1999) The size of liposomes: a factor which affects their targeting efficiency to tumors and therapeutic activity of liposomal antitumor drugs. Adv Drug Deliv Rev 40:75–87

Ostro MJ, Cullis PR (1989) Use of liposomes as injectable-drug delivery systems. Am J Hosp Pharm 46:1576–1587

Pardeike J, Hommoss A, Müller RH (2009) Lipid nanoparticles (SLN, NLC) in cosmetic and pharmaceutical dermal products. Int J Pharm 266:170–184

Park JW, Benz CC, Martin FJ (2004) Future directions of liposome- and immunoliposome-based cancer therapeutics. Semin Oncol 31:196–205

Patel MR, San Martin-Gonzalez, MF (2012). Characterization of ergocalciferol loaded solid lipid nanoparticle. J Food Sci 71:N8–N13

Pons M, Foradada M, Estelrich J (1993) Liposomes obtained by the ethanol injection method. Int J Pharm 95:51–56

Prombutara P, Kulwatthanasal Y, Supaka N, Sramala I, Chareonpornwattana S (2012) Production of nisin-loaded solid lipid nanoparticles for sustained antimicrobial activity. Food Control 24:184–190

Qi C, Chen Y, Huang JH, Jina QZ, Wanga, XG (2012). Preparation and characterization of catalase-loaded solid lipid nanoparticles based on soybean phosphatidylcholine. J Sci Food Agric 92:787–793

Quintanar-Guerrero D, Tamayo-Esquivel D, Ganem-Quintanar A, Allémann E, Doelker E (2005) Adaptation and optimization of the emulsification-diffusion technique to prepare lipidic nanopheres. Eur J Pharm Sci 26:211–218

Rasti B, Jinap S, Mozafari MR, Yazid AM (2012) Comparative study of the oxidative and physical stability of liposomal and nanoliposomal polyunsaturated fatty acids prepared with conventional and Mozafari methods. Food Chem 135:2761–2770

Rigoletto, TP; Silva CL, Santana MHA, Rosada RS, de la Torre, LG (2012) Effects of extrusion, lipid concentration and purity on physico-chemical and biological properties of cationic liposomes for gene vaccine applications. Journal of microencapsulation 29, 759-769. DOI:10.3109/02652048.2012.686530

Re MI, Santana MHA, Davila MA (2009) Encapsulation technologies for modifying food performance: new techniques and products. In: Passos ML, Ribeiro CP Jr. (eds) Innovation in food engineering: new techniques and products. CRC Press, Boca Raton. pp 224–275

Riley J (2005). Charge in colloidal systems. In: Cosgrove T (ed) Colloid science:principles, methods and applications. Blackwell Publishing, Oxford

Rosada RS, Silva CL, Andrade Santana MH, Nakaie CR, de la Torre LG (2012) Effectiveness, against tuberculosis, of pseudo-ternary complexes: Peptide-DNA-cationic liposome. J Colloid Interface Sci 373:102–109

Rosenblatt KM, Bunjes H (2009) Poly(vinyl alcohol) as emulsifier stabilizes solid triglyceride drug carrier nanoparticles in the a-modification. Mol Pharm 6:105–120

Salager JL (2006) Emulsion phase inversion phenomena. In Sjöblom J (ed.) Emulsions and emulsion stability. CRC Press, Boca Raton, p 185–226

Sawant KK, Dodiya SS (2008) Recent advances and patents on solid lipid nanoparticles. Rec Pat Drug Del Form 2:120–135

Schmelz EM, Dillehay DL, Webb SK, Reiter A, Adams J, Merrill AH (1996) Sphingomyelin consumption suppresses aberrant colonic crypt foci and increases the proportion of adenomas versus adenocarcinomas in CF1 mice treated with 1,2-dimethylhydrazine: Implications for dietary sphingolipids and colon carcinogenesis. Cancer Res 56:4936–4941

Schubert MA, Müller-Goymann CC (2003) Solvent injection as a new approach for manufacturing lipid nanoparticles—evaluation of the method and process parameters. Eur J Pharm Biopharm 55:125–131

Senior J, Gregoriadis G (1982) Stability of small unilamellar liposomes in serum and clearance from the circulation—the effect of the phospholipid and cholesterol components. Life Sci 30:2123–2136

Severino P, Andreani T, Macedo AS, Fangueiro JF, Santana MHA, Souto EB (2012). Current state of art and new trends on lipid nanoparticles (SLN and NLC) for oral drug delivery. J Drug Del. doi:10.1155/2012/750891

Shukat R, Relkin P (2011) Lipid nanoparticles as vitamin matrix carriers in liquid food systems: on the role of high-pressure homogenisation, droplet size and adsorbed materials. Coll Surf B Biointerfaces 86:119–124

Shukat R, Bourgaux C, Relkin P (2012) Crystallisation behaviour of palm oil nanoemulsions carrying vitamin E. J Therm Anal Calorim 108:153–161

Siekmann B, Westesen K (1996) Investigations on solid lipid nanoparticles prepared by precipitation in o/w emulsions. Eur J Pharm Biopharm 43:104–109

Sjöström B, Bergenståhl B (1992) Preparation of submicron drug particles in lecithinstabilized o/w emulsions. I. Model studies of the precipitation of cholesteryl acetate. Int J Pharm 88:53–62

Small DM (1986) The physical chemistry of lipids. Plenum Press, New York

Solans C, Solé I, Fernandéz-Arteaga A, Nolla J, Azemar N, Gutierrez J, Maestro A, González C, Pey CM (2010) Nano-emulsion formation by low-energy methods and functional properties. In: Hidalgo-Alvarez R (ed) Structure and functional properties of colloidal systems. CRC Press, Boca Raton, pp 457–482

Soriani M, Rice-Evans C, Tyrrell RM (1998) Modulation of the UVA activation of haem oxygenase, collagenase and cyclooxygenase gene expression by epigallocatechin in human skin cells. FEBS Lett 439:253–257

Sou K, Naito Y, Endo T, Takeoka S, Tsuchida E (2003) Effective encapsulation of proteins into size-controlled phospholipid vesicles using freeze-thawing and extrusion. Biotechnol Prog 19:1547–1552

Souto EMB (2005) SLN and NLC for topical delivery of antifungals. Dissertation, Free University of Berlin

Szoka F, Papahadjopoulos D (1978) Procedure for preparation of liposomes with large internal aqueous space and high capture by reverse-phase evaporation. Proc Natl Acad Sci U S A 75:4194–4198

Takahashi M, Kitamoto D, Imura T, Oku H, Takara K, Wada K (2008) Characterization and bioavailability of liposomes containing a ukon extract. Biosci Biotechnol Biochem 72:1199–1205

Taylor KMG, Morris RM (1995) Thermal-analysis of phase-transition behavior in liposomes. Thermochim Acta 248:289–301

Taylor KMG, Taylor G, Kellaway IW, Stevens J (1990) The stability of liposomes to nebulization. Int J Pharm 58:57–61

Taylor TM, Davidson PM, Bruce BD, Weiss J (2005) Liposomal nanocapsules in food science and agriculture. Crit Rev Food Sci Nutr 45:587–605

Taylor TM, Gaysinsky S, Davidson PM, Bruce BD, Weiss J (2007) Characterization of antimicrobial-bearing liposomes by zeta-potential, vesicle size, and encapsulation efficiency. Food Biophys 2:1–9

Teixeira ML, dos Santos J, Silveira NP, Brandelli A (2008) Phospholipid nanovesicles containing a bacteriocin-like substance for control of Listeria monocytogenes. Innov Food Sci Emerg Technol 9:49–53

Thompson AK, Singh H (2006) Preparation of liposomes from milk fat globule membrane phospholipids using a microfluidizer. J Dairy Sci 89:410–419

Thompson AK, Haisman D, Singh H (2006) Physical stability of liposomes prepared from milk fat globule membrane and soya phospholipids. J Agric Food Chem 54:6390–6397

Thompson AK, Couchoud A, Singh H (2009) Comparison of hydrophobic and hydrophilic encapsulation using liposomes prepared from milk fat globule-derived phospholipids and soya phospholipids. Dairy Sci Technol 89:99–113

Timms RE (1984) Phase behaviour of fats and their mixtures. Prog Lip Res 23:1–38

Torchilin V, Weissig V (Eds) (2003) Liposomes: a practical approach. Oxford University Press, Oxford

Trevisan JE, Cavalcanti LP, Oliveira CLP, Torre LGdL, Santana MHA (2011) Technological aspects of scalable processes for the production of functional liposomes for gene therapy. In: Yuan XB (ed) Non-viral gene therapy. InTech, Rijeka, pp 267–292

Triplett II MD, Rathman JF (2009) Optimization of b-carotene loaded solid lipid nanoparticles preparation using a high shear homogenization technique. J Nanop Res 11:601–614

Trombino S, Cassano R, Muzzalupo R, Pingitore A, Cione E, Picci N (2009) Stearyl ferulate-based solid lipid nanoparticles for the encapsulation and stabilization of b-carotene and a-tocopherol. Coll. Surf. B: Biointerfaces 72:181–187

Trotta M, Debernardi F, Caputo O (2003) Preparation of solid lipid nanoparticles by a solvent emulsification-diffusion technique. Int J Pharm 257:153–160

Valdivieso-Garcia A, Riche E, Abubakar O, Waddell TE, Brooks BW (2001) A double antibody sandwich enzyme-linked immunosorbent assay for the detection of Salmonella using biotinylated monoclonal antibodies. J Food Prot 64:1166–1171

Vitor MT, Bergami-Santos PC, Barbuto JAM, De La Torre LG (2013) Cationic Liposomes as Non-viral Vector for RNA Delivery in Cancer Immunotherapy. Recent Pat Drug Deliv Formul 7:99–110

Wagner A, Vorauer-Uhl K, Kreismayr G, Katinger H (2002) The crossflow injection technique: An improvement of the ethanol injection method. J Liposome Res 12:259–270

Wagner A, Platzgummer M, Kreismayr G, Quendler H, Stiegler G, Ferko B et al (2006) GMP production of liposomes - A new industrial approach. J Liposome Res 16:311–3119

Wambura P, Yang W, Mwakatage NR (2011) Effects of sonication and edible coating containing rosemary and tea extracts on reduction of peanut lipid oxidative rancidity. Food Bioprocess Technol 4:107–115

Ward RE, German JB, Corredig M (2006) Composition, applications, fractionation, technological and nutritional significance of milk fat globule membrane material. In: Fox PF, McSweeney PLH (eds) Advanced dairy chemistry: lipids, vol 2, 3rd edn. Springer, New York, pp 213–244

Watkins SM, German JB (1998) Omega fatty acids. In: Akoh CC, Min DB (eds) Food lipids: chemistry, nutrition and biotechnology. Marcel Dekker, New York, pp 463–494

Wechtersbach L, Ulrih NP, Cigic B (2012) Liposomal stabilization of ascorbic acid in model systems and in food matrices. Lebenson Wiss Technol 45:43–49

Weiss J, Decker EA, McClements DJ, Kristbergsson K, Helgason T, Awad T (2008) Solid lipid nanoparticles as delivery systems for bioactive food components. Food Biophys 3:146–154

Were LM, Bruce BD, Davidson PM, Weiss J (2003) Size, stability, and entrapment efficiency of phospholipid nanocapsules containing polypeptide antimicrobials. J Agric Food Chem 51:8073–8079

Were LM, Bruce B, Davidson PM, Weiss J (2004) Encapsulation of nisin and lysozyme in liposomes enhances efficacy against Listeria monocytogenes. J Food Prot 67, 922–927

Westesen K, Siekmann B (1997) Investigation of the gel formation of phospholipid-stabilized solid lipid nanoparticles. Int J Pharm 151:35–45

Whitesides GM (2006) The origins and the future of microfluidics. Nature 442:368–373

Yamada H, Ohashi K, Atsumi T, Okabe H, Shimizu T, Nishio S et al (2003) Effects of tea catechin inhalation on methicillin-resistant Staphylococcus aureus in elderly patients in a hospital ward. J Hosp Infect 53:229–231

Yang T, Cui F-D, Choi M-K, Cho J-W, Chung S-J, Shim C-K et al (2007) Enhanced solubility and stability of PEGylated liposomal paclitaxel: in vitro and in vivo evaluation. Int J Pharm 338:317–326

Yokota D, Moraes M, Pinho SC (2012). Characterization of lyophilized liposomes produced wit non-purified soy lecithin: a case study of casein hydrolysate microencapsulation. Braz J Chem Eng 29:325–335

Yoshida P, Yokota D, Foglio MA, Rodrigues RAF, Pinho SC (2010) Liposomes incorporating essential oil of Brazilian cherry (Eugenia uniflora L.): characterization of aqueous dispersions and lyophilized formulations. J Microencapsul 27:416–425

Yu D-G, Branford-White C, Williams GR, Bligh SWA, White K, Zhu L-M et al (2011) Self-assembled liposomes from amphiphilic electrospun nanofibers. Soft Matter 7:8239–8247

Chapter 8
High Shear Methods to Produce Nano-sized Food Related to Dispersed Systems

Cynthia Cano-Sarmiento, Liliana Alamilla-Beltrán, Ebner Azuara-Nieto, Humberto Hernández-Sánchez, Dario I. Téllez-Medina, Cristian Jiménez-Martínez and Gustavo F. Gutiérrez-López

8.1 Introduction

Nanotechnology comprises the implementation, production, and processing of materials of sizes less than 1000 nm. Nanoscience provides methods and the framework to get an understanding and development of materials and products with new properties due to the formation of nanostructures (Föster and Konrad 2003; Roco 2003). Nano-materials have surprising properties, which are different to their macroscopic counterparts (Wardak et al. 2008; Dresselhaus et al. 2004). Among these properties are physical, chemical, optical, electrical, catalytic, magnetic, mechanical, and biological, which can generate a significant improvement in the performance of products, improve product functionality, create new applications, etc. (Yuan and Zhang 2013). Therefore, nanotechnology has had a significant effect on various industries, including electronics, engineering, telecommunications, medicine, agriculture, cosmetic, and food (Chaudhry et al. 2008; Roco 2003; Sanguansri and Augustin 2006). Nanotechnology has revolutionized the entire food industry, from production to processing, storage, and development of materials, products, and innovative applications. The application of nanotechnology in the food sector has generated innovation in macroscale features of foods, such as texture, flavor, color, workmanship, safety, security, stability as well as the development of a large number of new products (Kuan et al. 2012). Moreover, nanotechnology may also improve the water solubility, thermal stability, and bioavailability of bioactive compounds (McClements et al. 2009; Huang et al. 2010;

G. F. Gutiérrez-López (✉) · C. Cano-Sarmiento · L. Alamilla-Beltrán · H. Hernández-Sánchez · D. I. Téllez-Medina · C. Jiménez-Martínez
Departamento de Graduados e Investigación en Alimentos, Escuela Nacional de Ciencias Biológicas, del Instituto Politécnico Nacional, Carpio y Plan de Ayala s/n. Col. Santo Tomas, CP. 11340 México, DF, Mexico
e-mail: gusfl@gmail.com

E. Azuara-Nieto
Instituto de Ciencias Básicas, Universidad Veracruzana, Xalapa, Veracruz, México

© Springer Science+Business Media New York 2015

H. Hernández-Sánchez, G. F. Gutiérrez-López (eds.), *Food Nanoscience and Nanotechnology,* Food Engineering Series, DOI 10.1007/978-3-319-13596-0_8

Silva et al. 2012; Ezhilarasi et al. 2013). Many of the structural elements of the foods are colloidal in nature and are constructed as a result of self-assembling of nanosize molecules into particulate or interfaces. The ability to control the macromolecules and small components in a food matrix at various length scales has become an integral part of the design of food products. The future development of food requires an understanding of the relationship between the nanostructures, supra-molecular, and higher order with functionality in a physical, nutritional, and physiological level (Sanguansri and Augustin 2006).

8.2 Production of Nanomaterials

In general, nanoscale manufacturing technologies can be classified into three groups: top down, bottom-up, and hybrid technologies of nanomanufacturing (Zhang et al. 2004). From these, the most commonly used approach is the "top down," which involves size reduction by applying a force. The degree of control and refinement in size reduction processes influence the properties of the materials produced. The balance between downsizing at a functional level and exclusively being the things smaller must be clearly understood in order to determine the process that can be used for size reduction. Size usually is related to the functionality of the food materials. A smaller size means a larger surface area and is desirable for some purposes such as improving the water absorption, flavor release, bioavailability, and faster rates of catalysis. Uniformity or narrow size distribution for better control of the functionality and quality of the product is also required. The three types of forces used in the size reduction of food are compression, impact, and shear (Sanguansri and Augustin 2006). One of the most commonly used forces is shear or rupture. The energy intensity required in nanomanufacturing is very high compared to conventional manufacturing technologies (Yuan and Zhang 2013). Some mechanical equipment that can generate intense break forces capable of reducing the size to a nanometer scale are: rotor-stator homogenizer, homogenizer of high-pressure valve, and ultra-high pressure, ultrasonic devices, and microfluidizers (Tadros et al. 2004; Anton et al. 2008; Leong et al. 2009). The nanoparticles can be generated by processes in gaseous or liquid phase. The liquid phase procedures use surface forces to create particles and structures in nanoscale.

8.3 Rotor-Stator Homogenizer

They are also known as high shear devices or high cut due to localized energy dissipation and cutting speeds generated. The distinguishing feature of a rotor-stator homogenizer is the high-speed rotor (movable mixture element) in close proximity to a stator (fixed mixing element). Typical speeds of rotor tip are between 10 and

Table 8.1 Publications using rotor-stator homogenizers

System	Ingredient	Size (nm)	Reference
Nano-emulsion	B-carotene	150	Silva et al. 2011
Nano-emulsion (After spontaneous emulsification)	Avocado oil, jojoba oil and almond oil (with palmitoyl pentapeptide and ceramide IIIB)	233.5 189.7 240.1	Sondari et al. 2010
Nanoparticles	Calcium carbonate	285.90	Hassim and Rachmawati 2010

50 m/s. In a rotor-stator mixer, the cut speed ranges are from 20,000 to 100,000 s^{-1}. The combined action between rotor and stator generate the mixing energy, shearing stresses and elongation, turbulence, and cavitation (in various proportions depending on the speed, viscosity, and other fluid flow parameters), that provide mixing and size reduction. They can be assembled or configured to operate batch, semi-continuously or continuously (Karbstein and Schubert 1995; Atiemo-Obeng and Calabrese 2004; Utomo et al. 2009).

These devices have been widely used in processes such as homogenization, dispersion, emulsification, grinding, dissolving, and cell disruption in fields such as chemistry, agriculture, food manufacturing, chemical reaction processes, etc. Many companies design and supply rotor-stator homogenizers (Silverson®, Omni®, IKA®, etc). Many of the available designs often only differ slightly in geometry, although providers offer different yields. The most used type of this device is the rotor stator for obtaining nanometric sizes of laboratory scale and is manufactured by IKA® (e.g., Ultra-turrax). Table 8.1 shows some research using this equipment.

In the case of laboratory devices, they often are radial which implies that the rotor moves the fluid radially away from the head of the mixer through the slots or holes of the stator; the distributors provide a variety of shapes and sizes of slot or holes. Figure 8.1 shows some examples of the geometries available. Common dispersion technology works by rotor-stator principle. Systems consist of a rotor within a stationary stator. Due to the high circumferential speed, the medium to be processed is attracted axially towards the head of dispersion and then forced to pass through the slots of the rotor stator. The high speed and the minimum gap between the rotor and the stator produce extremely intense cutting forces that achieve a better dispersion.

Utomo et al. (2009) studied the effect of the geometry of the stator in the flow pattern and rate of energy dissipation in these homogenizers. They found that the flow pattern in the openings of stator was very similar for all shapes and sizes of holes and that about 50–60 % of the energy supplied by the rotor is dissipated in the rotor swept region and about 25 % in the jet region. The fraction of the energy dissipated in the region of the hole is 12–15 % for stators with narrow opening and only 8 % for stators with wide opening. The order of magnitude of the rate of energy dissipation in each region (rotor swept region, holes, and jets) is practically the same for all stators.

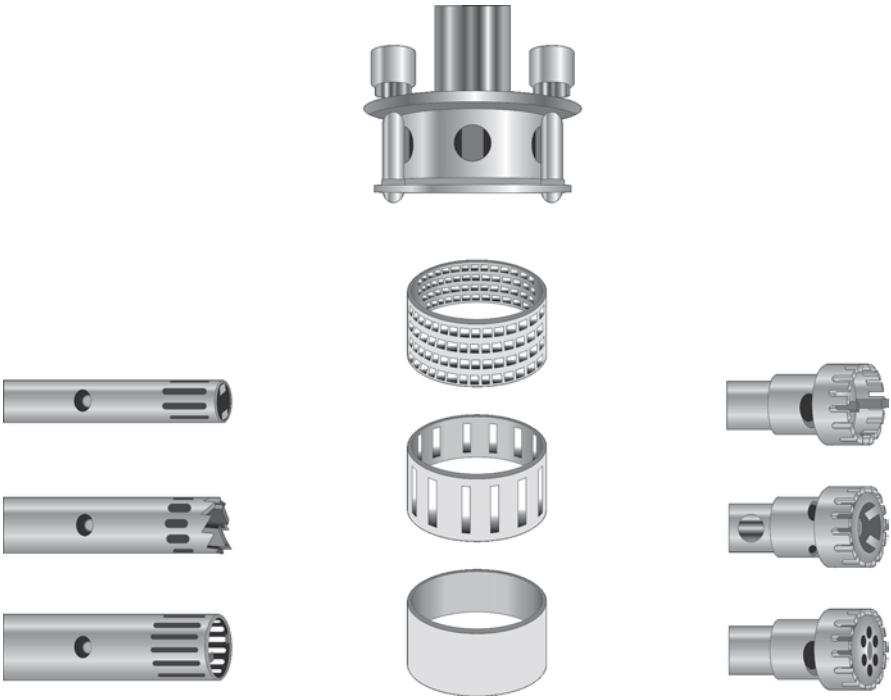

Fig. 8.1 Examples of available geometries for stators

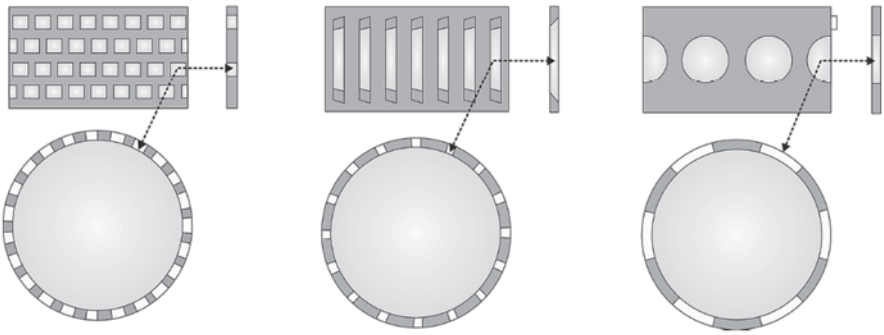

Fig. 8.2 Geometries of the stators used in this study

However, in the case of stators with narrow openings, the distribution of energy dissipation rate in the hole is more uniform. Figure 8.2 shows the stators geometries used in the present study. To set the speed and uptime, the process of development, expansion, and operation of these homogenizers are based mostly on technical evaluations of trial and error, as well as the type of stator to provide system-specific features. The two main forces that can reduce the particle size in these devices are:

the mechanical impact against the wall by the acceleration of the fluid and the shear forces, the intensity of the shear forces can be altered by varying the thickness of the gaps (from 50 to 1000 μm), varying the rotation speed (from 1000 to 25,000 rpm) or by using disks that have toothed surfaces or interlocking teeth (Becher 2001; McClements 2005; Jafari et al 2008).

Although emulsification strength (power) and the time when particles remain in the shear zone are the primary parameters that control the size. In general when compared with other methods of homogenization is considered that these devices do not give a good spread in terms of size and monodispersity, therefore, they often are used as a preliminary process to the main homogenization (Anton et al 2008, Kaltsa et al. 2013).

8.4 High and Ultra-High Pressure Valve Homogenizer

High-pressure homogenization can be profitably applied to reduce the particles and emulsion droplets dispersed in a liquid to finer dimensions, due to the shredding caused by the intense fluid-mechanical stresses generated on the pressurized liquid when flowing at high velocity through a micrometric gap (homogenization valve) (Schultz et al. 2004; Maresca et al. 2011). Recent progress in high-pressure technology and the design of new homogenization valves (ceramic seats and needles) able to withstand pressures up to 400 MPa have indeed opened new opportunities to homogenization processing. By comparison, classical homogenization, the standard industrial process used in the dairy, pharmaceutical, and cosmetic industries to reduce particle sizes operates with an up-stream pressure of about 20 to 60 MPa (Grácia-Juliá et al. 2008). Depending on the nominal pressure level, the technology will be called high-pressure homogenization (HPH, up to 150–200 MPa) or ultra-high-pressure homogenization (UHPH, up to 350–400 MPa). For comparison, the standard homogenization operates with an upstream pressure of ≈20 to 60 MPa, as in dairy industry (Dumay et al. 2013).

A high-pressure valve homogenizer consists of a piston pump and a narrow gap, where the operating pressure is up to 150–200 MPa. Particle break-up occurs within the region of the valve gap and in the jet after the gap. The advantage of this device is that it is scalable for industrial production. It was shown that the flow into the valve gap is elongational with a higher velocity at the passage head wall than at the impact head wall. This acceleration dampens the turbulence and therefore the flow in a laboratory scale homogenizer gap is usually laminar. A jet is formed at the exit of the gap where the majority of the energy dissipates: producing a stable and large eddy that causes the jet to become unstable and attach to a wall. The majority of the particle break-up occurs at the outer regions of the jet, this is because the difference in velocity of the jet and the surrounding fluid produces the highest shearing forces (Innings and Trägårdh 2007; Lee and Norton 2013). As the product passes through the valve, it experiences a combination of intense shear, cavitation, and turbulent flow conditions, which cause the large particles to be broken down into smaller

ones. For a given pump throughput, the homogenizing pressure is determined by the force acting on the axially movable valve plug and the size of the gap resulting from this (Stang et al. 2001; Jafari et al. 2008).

UHPH, also called dynamic high pressure, is a novel technology recently studied in the food, cosmetic, and pharmaceutical areas to fragment particles in dispersions or emulsions, to produce fine and stable emulsions, to modify the viscous properties of fluids due to the particle size reduction, and also to facilitate metabolite extraction as well as to achieve inactivation of microorganisms, enzymes, and even some viruses (Grácia-Juliá et al. 2008). Homogenizers are usually equipped with a high-pressure valve (HP-valve or first-stage) and a low-pressure valve (LP-valve or second-stage). The processing performances importantly depend on the valve design (geometrical characteristics of the needle and seat, height, and shape of the valve gap) but also on the physicochemical characteristics of the fluid (density, viscosity, flow rate). Homogenizers are usually equipped with a HP-valve (or first-stage) and a LP-valve (or second-stage). The processing performances importantly depend on the valve design (geometrical characteristics of the needle and seat, height, and shape of the valve gap) but also on the physicochemical characteristics of the fluid (density, viscosity, flow rate). LP-valve may be used or not during HP-homogenization, depending on the performances of the HP-valve to disrupt particles without or limited particle reaggregation phenomena as usually observed after passing the first-stage in standard homogenization (Dumay et al. 2013).

UHPH delivers the highest potential energy of emulsification (ΔP/volume unit of processed fluid) that is able to create the smallest size of particles below the micron level. In recent years, a growing interest was particularly directed towards the specific innovative functionalities developed from the structural modifications that UHPH could induce. Indeed, the several physical phenomena successively and/or simultaneously involved before (short-time pressure build-up), through (pressure drop, intense shear forces, and elongational stress), and at the outlet (turbulence, cavitation, impacts) of the HP-valve gap, result in modification of particles in the processed fluid. This confers them new structural and physicochemical properties by a top-down (particle size reduction) or bottom-up (particle reassembly) process. Particularly, when the processed fluid is forced through the very narrow HP-valve gap, particles (emulsion oil droplets, fat globules, microorganisms) or polysaccharide macromolecules can be ruptured by the mechanical associated forces inducing a significant reduction of size down to the micron/submicron range (Cortés-Muñoz et al. 2009; Floury et al. 2003, 2004; Paquin 1999; Thiebaud et al. 2003; Dumay et al. 2013). Figure 8.3 shows a comparison between a classic high-pressure homogenizer and an ultra-high pressure one.

The Stansted homogenizing valve technology used here (Fig. 8.3b) consists of ceramic material, which is known to withstand to ultra-high-pressure levels. Moreover, geometry of the valve has been modified compared with a classical one (Fig. 8.3a). Firstly, the flow directions through the valve are reversed: in the classical valve design, the fluid is fed axially into the valve seat, and then accelerates

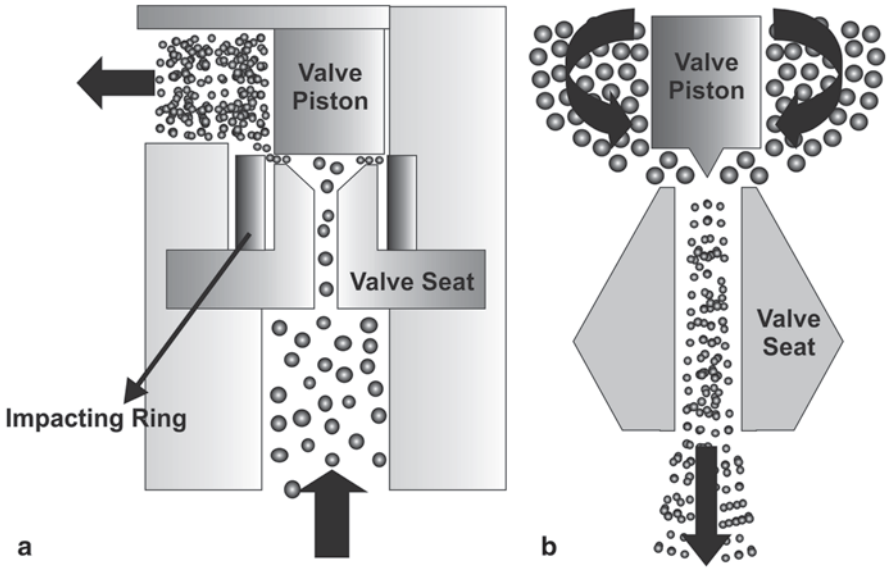

Fig. 8.3 Homogenizing valve geometries: **a** high-pressure homogenizer valve and **b** ultra-high-pressure valve

radially into the small region between the valve and valve seat (Fig. 8.3a). Once the fluid leaves the gap, it becomes a radial jet that stagnates on an impact ring before leaving the homogenizer at atmospheric pressure (Kleinig and Middelberg 1997).

In the Stansted valve (Fig. 8.3b), the fluid is first fed axially along the mobile part of the valve and then accelerates radially through the narrow gap between the valve and valve seat. Numerical simulations revealed that the radial jet leaves the valve seat without impinging on the valve point, but it largely recirculates just downstream the slit of the valve before flowing out of the valve seat. Secondly, the Stansted valve technology is able to reach much higher pressures (350 MPa) than the classical type (70–100 MPa). As operating pressure (ph) is controlled by adjusting the gap (h) between the valve and seat, valve gaps involved in the ultra-high-pressure valve are much narrower ($h \approx 2$–5 μm) than in the classical one (10–30 μm) (Floury et al. 2004). Table 8.2 shows some publications that use this device and the obtained sizes.

8.4.1 Ultrasonic Homogenizer

Ultrasound is defined as sound waves having a frequency that exceeds the limit of human hearing (~20 kHz). It is one of the emerging technologies that have been developed to minimize processing, maximize quality, and ensure the safety of food

Table 8.2 Publications that use high- and ultra-high-pressure valve homogenizers

Matrix	Ingredient	Process parameters	Size (nm)	References
Emulsions	Peanut oil	200 MPa 2–3 steps	138	Cortés-Muñoz et al. 2009
Micelles	Phosphocasein	200 MPa 300 MPa 1 step	130 85	Benzaria et al. 2013
Dispersion	Whey protein aggregates	250–300 MPa 1 step	<100	Grácia-Juliá et al. 2008
Emulsions	Milk	20 and 5 MPa 2 steps	No fat 183, low fat 261	Ciron et al. 2010

products. Ultrasounds have been useful in the inactivation of enzymes and microorganisms, modifying food ingredients, processes of crystallization, extraction of natural compounds, homogenization, and emulsification so as to produce nanoscale materials (Mason et al. 1996 and 2011; Raviyan et al. 2005, Ertugay et al. 2004; Sanguansri and Augustin 2006; Ashokkumar et al. 2008 and 2010; Weiss et al. 2011; Gogate and Pandit 2011; Vilkhu et al. 2008, 2011; Bermúdez-Aguirre and Barbosa-Cánovas 2012; Abbas et al. 2013). Depending on the amplitude of the frequency, ultrasound applications in the processing, analysis and quality control of food can be divided into high and low energy. The low-energy ultrasound (low power or low intensity) have frequencies above 100 kHz and intensities below 1 W/cm^2. They can be used for noninvasive analysis and monitoring of various food materials during processing and storage to ensure high quality and safety. The low-energy ultrasound has been used in a nondestructive way to support cattle breeding programs and to evaluate the composition of raw and fermented meat products, fish, and poultry. In addition, they are also used in the quality control of fresh fruit and vegetables pre- and postharvest, in cheese during processing, commercial cooking oils, bread and cereals, food gels, aerated, and frozen foods (Awad et al 2012).

Other applications include the detection of adulteration of honey and evaluation of the state of aggregation, size, and type of proteins. The high-energy ultrasound (high power or high intensity) that used intensities higher than 1 W cm^2 at frequencies between 20 and 500 kHz, have effects on physical, mechanical, or chemical/biochemical food properties (Mason et al 2011). The ultrasonic generator converts electrical current into ultrasonic energy to power the ultrasonic transducer. The transducer produces an elastic deformation along the alternating voltage, which results in a longitudinal mechanical vibration that produces a cavitation effect in the probe immersed in the solution. Ultrasound propagation through different materials induces compressions and decompressions (rarefactions) of the medium particles, which provide a lot of energy. Probes, as shown in Fig. 8.4, can have different lengths, diameters, and geometries depending on the application (Awad et al. 2012).

The ultrasonic wave causes intense localized heating and this creates gas bubbles that lead to a phenomenon called acoustic cavitation. This cavitation generated violent physical forces including micro-jets, shear forces, turbulence, and shock waves, and results in the high pressure and intense shear forces, which cause the physical

Fig. 8.4 Laboratory ultrasonicator and some probes

disruption of the components and materials of food and can lead and change the rate of chemical reactions (Povey and Mason 1998; Ashokkumar and Mason 2007; Augustin and Sanguansri 2009). When the bubble reaches a critical size, it collapses. The collapse is adiabatic due to high speed of the collapse and does not allow time for a flow of heat, producing a small, localized hot spot. Temperatures are very high (≈ 5000 °C) and so are the pressures (≈ 2000 atm), triggering reactions that generate nanoparticles at the time. Spot size determines the size of the resulting particles (Chaturvedi and Dave 2013).

Table 8.3 Researches that used ultrasonicators

Matrix	Ingredient	Frequency and time	Size (nm)	References
Nanoparticles	Starch	24 kHz 60 min	250	Bel Haaj et al. 2013
Nano-iposomes	Phosphatidylcholine	20 kHz 50 min	150	Pereira-Lachataignerais et al. 2006
Nanocrystals	Curcumin	40 kHz 60 min	166	Moorthi and Kathiresan 2013
Nano-emulsions	Linseed oil	20/24 kHz 5 min	120	Kentish et al. 2008

In some applications, both physical forces and chemical reactions are useful. For example, the stability of the capsules produced by ultrasound for encapsulating active principles and food ingredients of high value can be increased by chemical cross-linking of the protein molecules during the formation process (Cavalieri et al 2008).

Although one of the main problems in the use of ultrasound in the food industry is the controlled modification of the functionality of food ingredients without chemical modification, as the localized high intensities involved in these methods may lead to denaturation of proteins, depolymerization of polysaccharides, or lipid oxidation during homogenization. The ultrasonic processing is influenced by parameters such as amplitude, pressure, temperature, viscosity, and concentration. The results of the processing will be based on: (1) Energy—the energy input per volume treated material (in kWh/L) and (2) Intensity—the actual power output per surface area of the sonotrode (in W/cm^2), where the energy input is the product of power output (kW) and the time of exposure. The time of exposure is directly related to the flow rate through the ultrasonic device (L/h). In the market there are probes of different shapes and sizes depending on the application. Figure 8.4 shows a representation of the more common type of equipment and probes.

Table 8.3 summarizes some researches that used ultrasonicators and the sizes obtained.

Sonication is one of the most popular way to produce nanoscale materials for researching, however, the use of this technology by industry has been limited (Samer and Schork 1999; Anton et al. 2008). The liquid phase reactions based on ultrasound are also one of the most popular forms and prioritized pathways for noncovalent approaches to achieve biological functionalization of nanomaterials (Mason and Lorimer 2002; Awad et al. 2012).

8.5 Microfluidizers

Microfluidization involves transfer of mechanical energy to the particles of high-pressure fluid (Kasaai et al. 2003). It is a form of homogenization that uses micro channel interaction chambers designed to promote cavitation, along with high cutting forces and impact for size reduction, dispersion, or emulsion formation (Kasaai

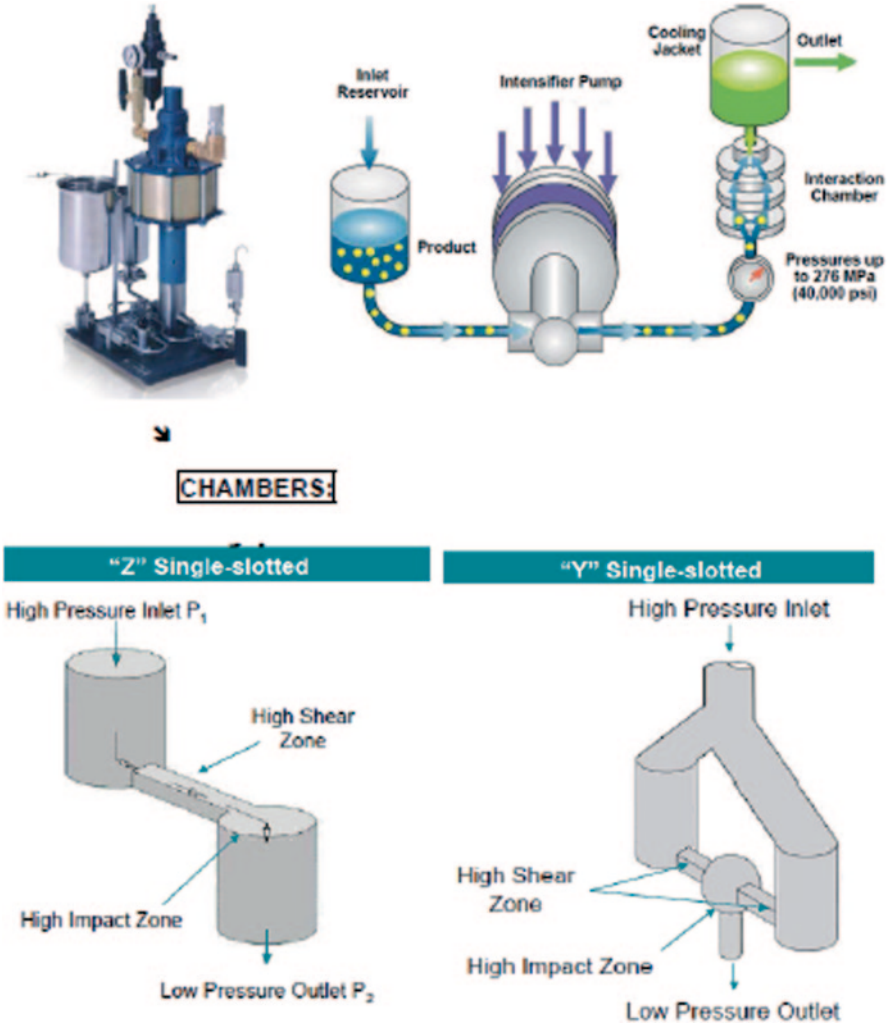

Fig. 8.5 Microfluidizer ® M-110Y showing interaction chambers and schematics of the microfluidization process (Microfluidics Corp.)

et al. 2003; Augustin and Sanguansri 2009). The micro fluidizer contains an intensifier pump that generates high pressure, which is used to force the product to pass through an interaction chamber formed by two micro channels, that will divide the product into two streams when it enters the chamber. Pneumatically powered pump is capable of pressurizing the in-house compressed air (150–650 kPa) up to about 150 MPa (Microfluidics, 2008; Jafari et al. 2007b). Such flows will be accelerated and will end up colliding with each other from opposite directions, creating a high cutting action (Jafari et al. 2006).

Figure. 8.5 shows the equipment M-110Y produced by Microfluidics Corp. The chamber is essentially a continuous microreactor that uses a turbulent mixer,

Table 8.4 Research involving microfluidizers

Matrix	Ingredient	Process parameters	Size (nm)	References
Nanoparticles	Coenzyme Q10	Emulsification-evaporation of solvent 100 MPa 1–4 cycles	40–260	Kwon et al. 2002
Nano-liposomes	Phospholipid-rich fraction derived from MFGM (milk fat globule membrane)	73, 90 and 103 MPa 1–10 cycles	100–150	Thompson and Singh 2006
Nano-fibers	Cellulose of empty fiber from palm fruit	55 MPa 5 cycles	10–30	Ferrer et al. 2012
Nano-emulsions	Lemongrass oil	50, 100 and 150 MPa 1, 2, 3, 4, 5 and 10 cycles	5.8–53.1	Salvia-Trujillo et al. 2014
Nano-emulsions	Milk	150 MPa 1 cycle	Non fat 174, Low fat 194	Ciron et al. 2010

a localized energy dissipation device, and a fixed geometry to generate a uniform pressure profile that creates a precise and repeatable size distribution in the nano-system.

There are two types of chambers: "Y" and "Z." These chambers are of many sizes, ranging from the ones that are used in laboratory to the ones that are used for large-scale production. These chambers can be used in combination with an auxiliary processing module (Microfluidics 2008). Several studies have shown that the homogenization by microfluidization is superior to other types of conventional homogenization. The particle size distribution produced by a microfluidizer appears narrower and smaller than the one obtained in systems produced by traditional methods of homogenization (Jafari et al. 2006, 2007a,b; Perrier-Cornet et al. 2005; Wooster et al. 2008).

If the desired particle size is not achieved after one cycle, it can be attained by increasing the number or cycles, depending on the properties of the sample. The particle size will depend mainly on the pressure, the number of cycles, and the composition of the product. For example, in the case of emulsions it has been shown that microfluidization is unfavourable in specific circumstances such as higher pressures and longer emulsification times, as it leads to "over-processing," which is re-coalescence of emulsion droplets and an increase in droplet size (Jafari et al. 2006, 2007a,b; Olson et al. 2004). Table 8.4 shows some publications that use this device and the sizes reported.

Currently, Microfluidizers are designed with the goal of preventing cavitation. Although it is a strong force that can break particles, it is also harmful to the equipment. By eliminating the presence of cavitation, it is possible to achieve similar levels of particle size reduction while maximizing the life of the equipment. The size of the channels is the same on the laboratory scale as on the production scale. There is a wide range of micro-channel sizes to produce a wide range of shear rates, but for

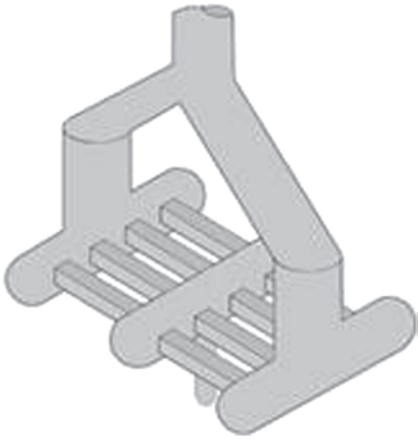

Fig. 8.6 Arrangement of multiple microchannels in parallel in a Y-type interaction chamber

Fig. 8.7 High-pressure laboratory homogenizer for small sample processing

scale-up, rather than increasing the size of the micro-channel, multiple microchannels in parallel are placed such that the same levels of shear on the production scale as the laboratory scale can be achieved. The chambers are shown in Fig. 8.6.

Additionally, Microfluidizer® technology converts fluid pressure more efficiently into shear forces, leading industry performance standards in high-pressure laboratory homogenizers such as the pneumatic instrument called the LM10 (Fig. 8.7),

recommended for small sample processing in applications such as emulsions, dispersions, liposomes, and cell disruption (Microfluidics 2014).

8.6 Conclusions

These methods employ mechanical devices for generating intense disruptive forces required for rupture of macroscopic phases (Abbas et al. 2013). The final structure will depend on how the chemical, physical, and processing interventions are applied to dictate the balance of the intramolecular and intermolecular forces within and between the components in the system (Sanguansri and Augustin 2006).

References

Abbas S, Hayat K, Karangwa E, Bashari M, Zhang X (2013) An overview of ultrasound-assisted food-grade nanoemulsions. Food Eng Rev 5:139–157

Anton N, Benoit JP, Saulnier P (2008) Design and production of nanoparticles formulated from nano-emulsion templates—a review. J Control Release 128(3):185–199

Ashokkumar M, Mason T (2007) Sonochemistry. In: Seidel A (ed) Kirk Othmer encyclopedia of chemical technology. Wiley, New York, pp 1–34

Ashokkumar M, Sunartio D, Kentish S, Mawson R, Simons L, Vilkhu K, Versteeg CK (2008) Modification of food ingredients by ultrasound to improve functionality: a preliminary study on a model system. Innov Food Sci Emerg 9(2):155–160

Ashokkumar M, Lee J, Lida Y, Yasui K, Kozuka T, Tuziuti T, Towata A (2010) Spatial distribution of acoustic cavitation bubbles at different ultrasound frequencies. Chemphyschem 11(8):1680–1684

Atiemo-Obeng VA, Calabrese RV (2004) Rotor–stator mixing devices. In: Paul EL, Atiemo-Obeng VA, Kresta SM (eds) Handbook of industrial mixing: science and practice. Wiley, Hoboken, pp 479–505

Augustin MA, Sanguansri P (2009) Nanostructured materials in the food industry. In: Taylor SL (ed) Advances in Food and Nutrition Research 58. Academic Press, Burlington, pp 183–213

Awad TS, Moharram HA, Shaltout OE, Asker D, Youssef MM (2012) Applications of ultrasound in analysis, processing and quality control of food: A review. Food Res Int 48(2):410–427

Becher P (2001) Emulsions: theory and practice. Oxford University Press, New York

Bel Haaj S Magnin A Pétrier C Boufi S (2013) Starch nanoparticles formation via high power ultrasonication. Carbohyd Polym 92(2):1625–1632

Benzaria A, Maresca M, Taieb N, Dumay E (2013) Interaction of curcumin with phosphocasein micelles processed or not by dynamic high-pressure. Food Chem 138(4):2327–2337

Bermúdez-Aguirre D, Barbosa-Cánovas GV (2012) Inactivation of Saccharomyces cerevisiae in pineapple, grape and cranberry juices under pulsed and continuous thermo-sonication treatments. J Food Eng 108(3):383–392

Cavalieri F, Ashokkumar M, Grieser F, Caruso F (2008) Ultrasonic synthesis of stable, functional lysozyme microbubbles. Langmuir 24(18):10078–10083

Chaturvedi S, Dave PN (2013) Design process for nanomaterials. J Mater Sci 48(10):3605–3622

Chaudhry Q, Scotter M, Blackburn J, Ross B, Boxall A, Castle L, Aitken R, Watkins R (2008) Applications and implications of nanotechnologies for the food sector. Food Addit Contam A 25(3):241–258

Ciron CIE, Gee VL, Kelly AL, Auty MAE (2010) Comparison of the effects of high-pressure microfluidization and conventional homogenization of milk on particle size, water retention and texture of non-fat and low-fat yogurts. Int Dairy J 20(5):314–320

Cortés-Muñoz M, Chevalier-Lucia D, Dumay E (2009) Characteristics of submicron emulsions prepared by ultra-high pressure homogenisation: effect of chilled or frozen storage. Food Hydrocol 23(3):640–654

Dresselhaus MS, Dresselhaus G, Jorio A (2004) Unusual properties and structure of carbon nanotubes. Ann Rev Mater Res 34:247–278

Dumay E, Chevalier-Lucia D, Picart-Palmade L, Benzaria A, Gràcia-Julià A, Blayo C (2013) Technological aspects and potential applications of (ultra) high-pressure homogenisation. Trends Food Sci Technol 31(1):13–26

Ertugay MF, Şengül M, Şengül M (2004) Effect of ultrasound treatment on milk homogenisation and particle size distribution of fat. Turk J Vet Anim Sci 28(2):303–308

Ezhilarasi PN, Karthik P, Chhanwal N, Anandharamakrishnan C (2013) Nanoencapsulation techniques for food bioactive components: a review. Food Bioprocess Technol 6(3):628–647

Ferrer A, Filpponen I, Rodríguez A, Laine J, Rojas OJ (2012) Valorization of residual empty palm fruit bunch fibers (EPFBF) by microfluidization: production of nanofibrillated cellulose and EPFBF nanopaper. Bioresource Technol 125:249–255

Floury J, Desrumaux A, Axelos MAV, Legrand J (2003) Effect of high pressure homogenisation on methylcellulose as food emulsifier. J Food Eng 58(3):227–238

Floury J, Legrand J, Desrumaux A (2004) Analysis of a new type of high pressure homogeniser. Part B. study of droplet break-up and recoalescence phenomena. Chem Eng Sci 59(6):1285–1294

Föster S, Konrad M (2003) From self-organising polymers to nano- and biomaterials. J Mater Chem 13(11):2671–2688

Gogate PR, Pandit AB (2011) Sonocrystallization and its application in food and bioprocessing. In: Feng H, Barbosa-Canovas G, Weiss J (eds) Ultrasound technologies for food and bioprocessing. Springer, New York, pp 467–493

Grácia-Juliá A, René M, Cortés-Muñoz M, Picart L, López-Pedemonte T, Chevalier D, Dumay E (2008) Effect of dynamic high pressure on whey protein aggregation: a comparison with the effect of continuous short-time thermal treatments. Food Hydrocol 22(6):1014–1032

Hassim A, Rachmawati H (2010) Preparation and characterization of calcium carbonate nanoparticles. Paper presented at the AIP Conference Proceedings, Bandung Institute of Technology, Indonesia, 16 June 2010

Huang Q, Yu H, Ru Q (2010) Bioavailability and delivery of nutraceuticals using nanotechnology. J Food Sci 75(1):R50–R57

Innings F, Trägårdh C (2007) Analysis of the flow field in a high-pressure homogenizer. Exp Therm Fluid Sci 32(2):345–354

Jafari SM, He YH, Bhandari B (2006) Nano-emulsion production by sonication and microfluidization-A comparison. Int J Food Prop 9(3):475–485

Jafari SM, He YH, Bhandari B (2007a) Optimization of nano-emulsions production by microfluidization. Eur Food Res Technol 225(5–6):733–741

Jafari SM, He YH, Bhandari B (2007b) Production of sub-micron emulsions by ultrasound and microfluidization techniques. J Food Eng 82(4):478–488

Jafari SM, Assadpoor E, He YH, Bhandari B (2008) Re-coalescence of emulsion droplets during high-energy emulsification. Food Hydrocoll 22(7):1191–1202

Kaltsa O, Michon C, Yanniotis S, Mandala I (2013) Ultrasonic energy input influence on the production of sub-micron o/w emulsions containing whey protein and common stabilizers. Ultrason Sonochem 20(3):881–891

Karbstein H, Schubert H (1995) Developments in the continuous mechanical production of oil-in-water macro-emulsions. Chem Eng Process 34(3):205–211

Kasaai MR, Charlet G, Paquin P, Arul J (2003) Fragmentation of chitosan by microfluidization process. Innov Food Sci Emerg 4(4):403–413

Kentish S, Wooster TJ, Ashokkumar M, Balachandran S, Mawson R, Simons L (2008) The use of ultrasonics for nanoemulsion preparation. Innov Food Sci Emerg 9(2):170–175
Kleinig AR, Middelberg APJ (1997) Numerical and experimental study of a homogenizer impinging jet. AIChE J 43(4):1100–1107
Kuan C-Y, Yee-Fung W, Yuen, K-H, Liong M-T (2012) Nanotech: propensity in foods and bioactives. Crit Rev Food Sci Nutr 52(1):55–71
Kwon SS, Nam YS, Lee JS, Ku BS, Han SH, Lee JY, Chang IS (2002) Preparation and characterization of coenzyme Q10-loaded PMMA nanoparticles by a new emulsification process based on microfluidization. Colloid Surf A 210(1):95–104
Lee L, Norton IT (2013) Comparing droplet breakup for a high-pressure valve homogeniser and a microfluidizer for the potential production of food-grade nanoemulsions. J Food Eng 114(2):158–163
Leong TSH, Wooster TJ, Kentish SE, Ashokkumar M (2009) Minimising oil droplet size using ultrasonic emulsification. Ultrason Sonochem 16(6):721–727
Maresca P, Donsì F, Ferrari G (2011) Application of a multi-pass high-pressure homogenization treatment for the pasteurization of fruit juices. J Food Eng 104(3):364–372
Mason TJ, Lorimer JP (2002) Applied sonochemistry Wiley Online Library
Mason TJ, Paniwnyk L, Lorimer JP (1996) The uses of ultrasound in food technology. Ultrason Sonochem 3(3):S253–S260
Mason TJ, Chemat F, Vinatoru M (2011) The extraction of natural products using ultrasound or microwaves. Curr Org Chem 15(2):237–247
McClements DJ (2005) Food emulsions: principles, practice and techniques. CRC Press, Boca Raton
McClements DJ, Decker EA, Park Y, Weiss J (2009) Structural design principles for delivery of bioactive components in nutraceuticals and functional foods. Crit Rev Food Sci Nutr 49(6):577–606
Microfluidics International Corporation (2008) Manual of 110 Y microfluidizer. Microfluidics Corp, Newton
Microfluidics International Corporation (2014) Digitally controlled lab unit for small sample material processing. http://www.microfluidicscorp.com/images/stories/pdf/lm10.pdf. Accessed 10 Oct 2014
Moorthi C, Kathiresan K (2013) Fabrication of highly stable sonication assisted curcumin nanocrystals by nanoprecipitation method. Drug Invent Today 5(1):66–69
Olson DW, White CH, Richter RL (2004) Effect of pressure and fat content on particle sizes in microfluidized milk. J Dairy Sci 87(10):3217–3223
Paquin P (1999) Technological properties of high pressure homogenizers: the effect of fat globules, milk proteins, and polysaccharides. It Dairy J 9:319–335
Perrier-Cornet JM, Marie P, Gervais P (2005) Comparison of emulsification efficiency of protein-stabilized oil-in-water emulsions using jet, high pressure and colloid mill homogenization. J Food Eng 66(2):211–217
Pereira-Lachataignerais J, Pons R, Panizza P, Courbin L, Rouch J, López O (2006) Study and formation of vesicle systems with low polydispersity index by ultrasound method. Chem Phys Lipids 140(1–2):88–97
Povey MJW, Mason TJ (1998) Ultrasound in Food Processing. Blackie Academic and Professional, London
Raviyan P, Zhang Z, Feng H (2005) Ultrasonication for tomato pectinmethylesterase inactivation: Effect of cavitation intensity and temperature on inactivation. J Food Eng 70(2):189–196
Roco MC (2003) Nanotechnology: Convergence with modern biology and medicine. Curr Opin Biotechnol 14(3):337–346
Salvia-Trujillo L, Rojas-Graü MA, Soliva-Fortuny R, Martín-Belloso O (2014) Impact of microfluidization or ultrasound processing on the antimicrobial activity against Escherichia coli of lemongrass oil-loaded nanoemulsions. Food Control 37(1):292–297
Samer CJ, Schork FJ (1999) The role of high shear in continuous miniemulsion polymerization. Ind Eng Chem Res 38(5):1801–1807

Sanguansri P, Augustin MA (2006) Nanoscale materials development-A food industry perspective. Trends Food Sci Technol 17(10):547–556

Schultz S, Wagner G, Urban K, Ulrich J (2004) High-pressure homogenization as a process for emulsion formation. Chem Eng Technol 27(4):361–368

Silva HD, Cerqueira MA, Souza BWS, Ribeiro C, Avides MC, Quintas MAC, Coimbra JSR, Carneiro-da-Cunha MG, Vicente AA (2011) Nanoemulsions of b-carotene using a high-energy emulsification-evaporation technique. J Food Eng 102(2):130–135

Silva HD, Cerqueira MA, Vicente AA (2012) Nanoemulsions for food applications: development and characterization. Food Bioprocess Technol 5:854–867

Sondari D, Haryono A, Harmami SB, Randy A (2010) Influence of palmitoyl pentapeptide and Ceramide III B on the droplet size of nanoemulsion. In: Mohammed WS, Chung T-Y (eds) Southeast Asian International Advances in Micro/Nano-technology, Thailand, March 2010. Proceings of SPIE, vol 7743. SPIE, Bellingham, p 77430D

Stang M, Schuchmann H, Schubert H (2001) Emulsification in high-pressure homogenizers. Eng Life Sci 1(4):151–157

Tadros T, Izquierdo R, Esquena J, Solans C (2004) Formation and stability of nano-emulsions. Adv Colloid Interface 108–09:303–318

Thiebaud M, Dumay E, Picart L, Guiraud JP, Cheftel JC (2003) High-pressure homogenisation of raw bovine milk. Effects on fat globule size distribution and microbial inactivation. Int Dairy J 13(6):427–439

Thompson AK and Singh H (2006) Preparation of liposomes from milk fat globule membrane phospholipids using a microfluidizer. J Dairy Sci 89(2):410–419

Utomo A, Baker M, Pacek AW (2009) The effect of stator geometry on the flow pattern and energy dissipation rate in a rotor–stator mixer. Chem Eng Res Des 87(4):533–542

Vilkhu K, Mawson R, Simons L, Bates D (2008) Applications and opportunities for ultrasound assisted extraction in the food industry-A review. Innov Food Sci Emerg 9(2):161–169

Vilkhu K, Manasseh R, Mawson R, Ashokkumar M (2011) Ultrasonic recovery and modification of food ingredients. In: Feng H, Barbosa-Canovas G, Weiss J (eds) Ultrasound technologies for food and bioprocessing. Springer, New York, pp 345–368

Wardak A, Gorman ME, Swami N, Deshpande S (2008) Identification of risks in the life cycle of nanotechnology-based products. J Ind Ecol 12(3):435–448

Weiss J, Kristbergsson K, Kjartansson GT (2011) Engineering food ingredients with high-Intensity ultrasound. In: Feng H, Barbosa-Cánovas G, Weiss J (eds) Ultrasound technologies for food and bioprocessing. Springer, New York, pp 239–285

Wooster TJ, Golding M, Sanguansri P (2008) Impact of oil type on nanoemulsion formation and Ostwald ripening stability. Langmuir 24(22):12758–12765

Yuan C, Zhang T (2013) Environmental implications of nano-manufacturing. In: Dornfeld DA (ed) Green Manufacturing. Springer, New York, pp 179–202

Zhang X, Sun C, Fang N (2004) Manufacturing at nanoscale: top-down, bottom-up and system engineering. J Nanopart Res 6(1):125–130

Chapter 9
Hydrodynamic Characterization of the Formation of Alpha-Tocopherol Nanoemulsions in a Microfluidizer

Amor Monroy-Villagrana, Liliana Alamilla-Beltrán, Humberto Hernández-Sánchez and Gustavo F. Gutiérrez-López

9.1 Introduction

The use of nanoemulsions produced by microfluidization as delivery systems of nonpolar functional compounds like bioactive lipids, drugs, flavors, and antioxidants has increasing interest in some industries including food, pharmaceutical, and cosmetics (McClements et al. 2007; Weiss et al. 2009; McClements 2011). One of the advantages (Tadros 2009) presented in these emulsions is that they can be incorporated (Heffernan et al. 2011) into water-based systems and beverages because the particle size is less than the wavelength of visible light (McClements 2011; Weiss et al. 2009) and they can also be considered as a previous step for other processes like spray drying encapsulation (Cao-Hoang et al. 2011; Tan and Nakajima 2005; Yuan et al. 2008). Some approaches made in food industry using this technology include nanoemulsion formulation of several vitamins such as alpha-tocopherol (AT) to improve absorption and bioavailability of this compound (Cheong et al. 2008; Gonnet et al. 2010).

The principle of microfluidization consists in a liquid that is divided into the microchannels of an interaction chamber (IX) and recombined later. The interaction chamber (IX) is a continuous microreactor that uses turbulent mixing, energy dissipation, and a fixed geometry to create a uniform pressure profile and thus obtaining a precise size and distribution of particles. The minimum size of the microchannels can be 50 microns and the rates at which fluids can travel through the chamber are above 500 m/s (Microfluidics 2008).

A. Monroy-Villagrana (✉) · L. Alamilla-Beltrán · H. Hernández-Sánchez · G. F. Gutiérrez-López
Departamento de Graduados e Investigación en Alimentos, Escuela Nacional de Ciencias Biológicas, Instituto Politécnico Nacional, Carpio y Plan de Ayala s/n, CP 11340, México, DF, México
e-mail: amormny@gmail.com

© Springer Science+Business Media New York 2015

H. Hernández-Sánchez, G. F. Gutiérrez-López (eds.), *Food Nanoscience and Nanotechnology,* Food Engineering Series, DOI 10.1007/978-3-319-13596-0_9

Despite the high surface-volume ratio in fluid microchannels, which is beneficial for the higher mass transfer and heat (with the shorter residence time, RT), their small cross-sectional dimensions are a major disadvantage for achieving good mixture (Adeosun and Lawal 2009, 2010; Pipe and McKinley 2009). Since the efficient mixing is a challenge, there are numerous research papers and extensive reviews on micromixers (Hessel et al. 2005; Nguyen and Wu 2005; Adeosun and Lawal 2009, 2010). A commonly used technique to understand and characterize what happens inside this micromixers is the determination of the residence time distribution (RTD) (Levenspiel 1999; Gutierrez et al. 2010). This distribution allows determining the effect of mixing to characterize the behavior of a fluid by knowing the mean RT of molecules within the channels and thus achieving a design process leading to improved product quality (Levenspiel 1999; Gutierrez et al. 2010). This time, in the IX, must be sufficient to allow it to carry out the breakdown of the droplets and absorption of emulsion compounds.

9.2 Nanoemulsions

Emulsions are a class of disperse systems where two immiscible liquids are mixed. The liquid forming the minor proportion is called disperse phase whereas the phase of major proportion is called continuous phase. In the food industry, pharmaceutical, and cosmetics these systems are used for the release of nonpolar functional compounds such as vitamins, antioxidants, antimicrobials, and other types of fatty acids (Bouyer et al. 2011; Bouyer et al. 2013; Pan et al. 2013). According to the particle size, this could be divided into macro-emulsions (0.5–100 μm), miniemulsions (nano) (100–1000 nm), and microemulsions (10–100 nm) (Jafari et al. 2007a; Windhab et al. 2005).

The difference in size of a macro vs. a miniemulsion is that the mini- (nano-) emulsions are less susceptible to gravitational separation (creaming, sedimentation) because the particle size makes the Brownian motion of molecules prevail over the gravitational forces. Moreover, this type of emulsion also exhibits improved stability against flocculation or coalescence because the range of attractive forces between particles decreases with the particle size reduction (Tadros et al. 2004; McClements 2005). Despite of this, there is not a critical size which determines the change in these properties (Weiss et al. 2009).

It has been reported that the bioavailability of nanoemulsions could be up to three times higher than conventional emulsions, increasing the rate of passive diffusion and facilitating the absorption of intestinal lymphatic system (Hatanaka et al. 2010; Lin et al. 2012; Ting et al. 2014). Also, forming nanoemulsions for subsequent encapsulation of bioactive compounds with low solubility in water represents (1) an effective way to increase the bioavailability and improve the dispersion of the bioactive in food products, (2) a way of protection against degradation or interaction with other ingredients, and also (3) a way to reduce the impact on the sensorial properties of food (Donsì et al. 2011; Mayer et al. 2013).

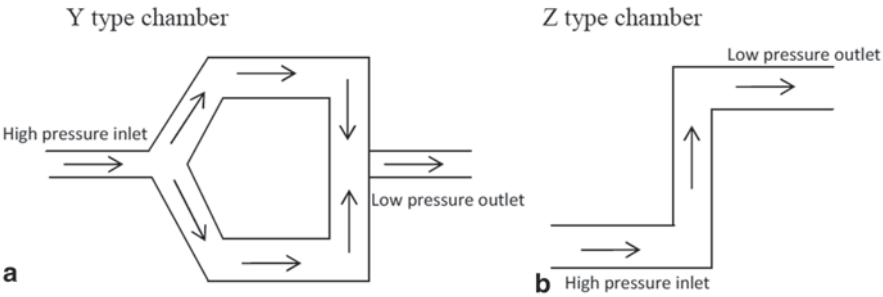

Fig. 9.1 Schematic representation of the interaction chambers (*IX*). **a** Y type chamber. **b** Z type chamber

9.2.1 Nanoemulsion Formation by Microfluidization

Microfluidization is a high-pressure homogenization method commonly used to produce oil-in-water (O/W) micro- and nanoemulsions (Brösel and Schubert 1999; Gramdorf et al. 2008; Schuch et al. 2013). This process involves deformation, collision, and sometimes cavitation to emulsify or disperse a liquid–liquid system or deagglomerate and disperse a solid in to a liquid in an IX (Paquin 1999; Jafari et al. 2007b; Microfluidics 2008), thus producing a particle-size homogeneous distribution (Sanguansri and Augustin 2006; Jafari et al. 2007b). The equipment is a high shear processor that acts as a bomb that forces a coarse emulsion to pass through the IX (Fig. 9.1). The mechanisms involved in to the droplet break-up are deformation and shear forces caused by differences in local pressure (i.e., inertial forces). In laminar flows the deformation is performed only by shear forces, while in turbulent flow the inertial forces also influence the break-up, which is executed by three mechanisms of rupture (Stang et al. 2001):

1. Rupture due to shear forces in laminar flow
2. Rupture due to shear forces in turbulent flow
3. Inertial forces in turbulent flow

The rate of formation of a new interface depends on (1) the hydrodynamic conditions within the break-up zone, the energy dissipation, the viscosity of the two phases; (2) the RT in the break-up zone, type of oil, emulsifier, and concentrations, and (3) the physicochemical properties of each phase such as interfacial tension (Brösel and Schubert 1999; Qian and McClements 2011; Lee and Norton 2013).

9.2.2 Influence of Emulsifier Type on Particle Size

Emulsifiers and stabilizers may influence the results of the emulsification process in different ways: (1) they facilitate the deformation and disruption of the drops by decreasing the interfacial tension, (2) they prevent coalescence by the interface stabilization, or (3) they modify the viscosity of the continuous phase decreasing the

Table 9.1 Food-grade emulsifiers generally used on nanoemulsion production

Oil phase	Emulsifier	Ratio (oil–emulsifier)	Size (nm)	References
β-carotene	Tween 20	1:1.7	60–135	Tan and Nakajima 2005
α-tocopherol	Tween 20	2:1	171	Bouchemal et al. 2004
Orange oil	Starch/ester gum	1:2 > 9 % ester gum	≈200	Lim et al. 2011
Corn oil	β-lactoglubulin	5:2	146	Qian and McClements 2011
Sunflower oil	β-casein	5:2	186	Maher et al. 2011
D-limonene, orange oil	Gum Arabic	10:1	1000	Dickinson et al. 1991

gravitational separation (Brösel and Schubert 1999; Klinkesorn et al. 2004; Tadros 2009).

In systems like microfluidizers, where the contact time between the particles of the emulsion is short, a desirable property of emulsifiers is that they can be easily absorbed by the interface, thus stabilizing the system almost immediately and preventing the re-coalescence (Klinkesorn et al. 2004; Jafari et al. 2007b). An additional challenge is to obtain an emulsion stable enough for further treatments such as spray drying. It has been shown that when biopolymers are used as surface active agents, like Arabic gum or modified starch (Hi-Cap), the stability of the emulsion (and therefore the encapsulation efficiency) is higher in comparison to the emulsions produced with surfactant small molecules (e.g., Tween 20) (Jafari et al. 2008a). Nevertheless, the final particle size will be the sum of the radii of the oil droplet and the layer of the emulsifier around them (McClements 2011). Table 9.1 summarizes food-grade emulsifiers generally used on nanoemulsion production by microfluidization, where appreciable variations in the thickness of layers formed could be found.

9.2.3 Mixing on Microchannels and Residence Time Distribution (RTD)

As mentioned above, to know how the mixing occurs in the IX is essential for the development and implementation of microfluidization for nanoemulsion formulation. Some approaches have been done in reaction technology on microchannels for the synthesis of nanoparticles by Patil et al. (2012). They found that the RTD measurement is a useful tool to characterize the effect of processing parameters on nanoparticle formation, by achieving particles of the size of 4–7 nm.

RTD allows determining the mixing effect to characterize the behavior of a fluid by knowing the mean RT of molecules in the microchannels, and thus achieving a design process to improve product quality (Levenspiel 1999; Gutierrez et al. 2010). For emulsification purposes, the time should be enough to ensure the disruption of

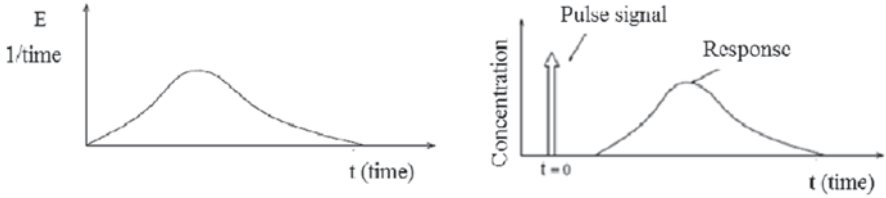

Fig. 9.2 **a** Distributions of the fluid ages in the output (E curve). **b** Distributions of the fluid ages in the output when a pulse of a tracer is introduced

the droplets and the absorption of the components at the interfaces to form the final emulsion.

Some commonly used methods to determine the RTD are the introduction of the tracer (of known concentration) by means of a pulse (E curve), the analysis of their concentration at the exit of this chamber, the effecting of a fluid change or step experiment (F curve), or the introduction of a sinusoidal variation of the concentration of tracer methods. From these, the pulse method is the easiest and most commonly used (Levenspiel 1999; Tayakout-Fayolle et al. 2005). The utilized tracer is often a dye and its concentration is measured on the products by spectroscopy or colorimetry (Apruzzese et al. 2003).

9.2.3.1 E Curve. Distribution of Fluid Age

Determining the RT of each portion of the fluid stream will get the curve of the RTD, also called E curve or C curve (Fig. 9.2) (Levenspiel 1999). Although these curves are equivalent, there are some differences. The E curve represents the distributions of the fluid ages in the output, while the C curve corresponds to the curve of age distribution at the output when a pulse of tracer substance (i.e., dye) is introduced into the fluid stream. To calculate the average residence time (RT) through an E curve the Eq. (9.1) is used, however, in practice this is calculated through a C curve by Eq. (9.2) (Levenspiel 1999).

$$RT = \int_0^\infty tEdt = \frac{\sum_i^n tiEi}{\sum_i^n Ei} \tag{9.1}$$

where

RT = average residence time
t = time
E = distribution of fluid age at the output

$$RT = \frac{\int_0^\infty tC\ dt}{\int_0^\infty C\ dt} = \frac{\sum_i^n tiCi\Delta ti}{\sum_i^n Ci\Delta ti} \tag{9.2}$$

where

RT = average residence time
t = time
C = concentration of the tracer.

The shape of the curve depends on the variation in the distribution or dispersion of the fluid within the microchannels. This will tend to be more or less flattened (leptokurtic, mesokurtic, or platikurtic) according to the deviation from ideal behavior. There are three different types of ideal flow: the plug flow, the completely stirred tank, and the intermittent stream. However, the real flows deviate from ideal flow patterns such as piston flow and completely stirred tank (Pinheiro-Torres and Oliveira 1998; Gutierrez et al. 2010; Levenspiel 1999). In order to assess these changes, there are different models that are derived from ideal flow patterns. Examples of these patterns are: tanks in series, generalized convection and axial dispersion, and the dispersal models, which are the most commonly used (Pinheiro-Torres and Oliveira 1998; Levenspiel 1999; Gutierrez et al. 2010).

9.2.3.2 Dispersion Model

Consider the piston flow of a fluid with some degree of back mixing. In this model, varying in intensities of turbulence or intermixing conditions, flow characteristics may vary from the ideal plug flow to flow stirred tank completely. The dispersion module (D/vL) is the parameter that measures the degree of axial dispersion in the container when:

$\frac{D}{vL} \to 0$ Small dispersion, tends to plug flow,

$\frac{D}{vL} \to \infty$ Great dispersion, tends to completely stirred tank flow.

One way to calculate the dispersion in the equipment is by obtaining the variance of the samples from the average RT. The variance values (Eq. (9.3)) and dimensionless variances (Eq. (9.4)) are obtained by:

$$\sigma^2 = \int_0^\infty (t - RT) * E(t)dt \tag{9.3}$$

$$\sigma\theta^2 = \sigma^2 / RT^2 \tag{9.4}$$

In turn, from the calculated values for the dimensionless variance the dispersion module is calculated by Eqs. (9.5) and (9.6) for closed and open containers, respectively,

$$\sigma\theta^2 = 2\frac{D}{vL} - 2\left[\frac{D}{vL}\right]^2 \left(1 - e^{-\frac{vL}{D}}\right) \tag{9.5}$$

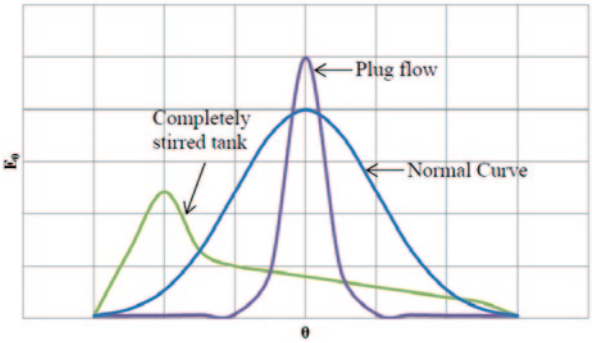

Fig. 9.3 E_θ curve that represents some deviations from normal curves for different levels of mixing in function of dimensionless time (θ) and the dispersion parameter module

$$\sigma\theta^2 = 2\frac{D}{vL} + 8\left[\frac{D}{vL}\right]^2 \tag{9.6}$$

By knowing the dispersion module is possible to construct a dimensionless E_θ curve in function of dimensionless time by the dispersion module (D/vL). Figure 9.3 represents the deviation of the experimental data from the normal curve.

9.2.3.3 Influence of the Energy Density in Pressure Drop and in the Mixing During Microfluidization

Analysis of the RTD is not easy, because the results must be interpreted according to the factors involved in the mixing. For this, we must make an analysis of the fluid path before reaching the IX, the type of flow (laminar or turbulent (number of Re)), the energy loss, and the pressure drop to determine the energy density (energy per volume applied) in the area of maximum deformation (IX). In addition to this, take note that as this is a process where the phenomena of shear, turbulence, and impact occur simultaneously, most of the mechanical energy applied to the IX is dissipated by heat (Stang et al. 2001).

A Case Study on Production of Mini (Nano) Alpha-Tocopherol Emulsions: Effect of Composition and Pressure on Mixing and on Particle Size

1. Although the generalized use of microfluization for nanoemulsion production, no systematic studies have been carried out on the effects of RTD in the size of produced emulsions. For this purpose, a hydrodynamic characterization on the formation of AT nanoemulsions using maltodextrin (MD) and gum Arabic (AG) as emulsifying agents (3:2, respectively) was performed. These emulsions were produced by changing the oil phase concentrations from proportions 1:2 to 1:5 AT/MD-AG and by comparing the hydrodynamics of the emulsion with a red

Table 9.2 Viscosity and density values for water and emulsions

Sample	Viscosity (Pa.s)	Density (kg/m^3)
Water (red tracer)	0.001002	997
1:5	0.0107	1062
1:3.5	0.0126	1057
1:2	0.0121	1053

dye tracer in water (0.05 % w/v red 40 dye). The processing conditions used were 69 and 103 MPa of pressure and one cycle of microfluidization, evaluating also the rheology (viscosity coefficient and density) of the samples.

Rheology

Rheological tests showed that for all emulsions the fluid behavior was Newtonian. Viscosity and density values are presented in Table 9.2.

Pressure Drop and Reynolds Number in Pipes and IX of Microfluidizer

The pressure drop in the microfluidizer before the IX is negligible with values between 0.04 and 0.07 MPa for emulsions and 0.004–0.006 MPa for water (dye). The flow velocities on this area are in the ranges of 0.84–1.3 m/s for the emulsion and 1.15–1.48 m/s for water. At these speeds the Reynolds number for the emulsion were 219–349 indicating that the flow before reaching the IX is laminar while Reynolds numbers for the interaction chamber indicate a turbulent flow with Reynolds values in the range of 138,000–176,000 approximately for water and 8,700–13,500 for emulsions (13–15 times higher in water). The differences in the flow pattern of the emulsion in the pipe and the IX show the dispersion, and the homogenization is carried out mainly in the IX due to the increasing on Reynolds number (25–39 times higher in this area).

RT Distribution and Dispersion Coefficients and Their Effect on Particle Size

Mean RT for each sample, their respective dispersion coefficients values, and the Re for IX are presented in Table 9.3. In Fig. 9.4, the D/vL zone for the emulsion and water obtained for the different pressures (69–103 MPa) is shown. On the E_θ curves (Levenspiel 1999) (data not shown) kurtosis values where negative in all cases (from −1.43 to −0.25), indicating that the curves have a platykurtic distribution, while the asymmetry coefficient values were positive (0.33–1.05) indicating that the curves are asymmetrically positive meaning that the right tail of the distribution is longer than the left side. Comparing these results with those reported by Levenspiel (1999), the curves fall into an area corresponding to intermediate flow in between piston and completely stirred tank (data not shown). Figure 9.5 exhibits the interval of the corresponding values obtained for the dispersion coefficients. Before testing and by the fact of working at pressures ranging from 700 to 1000 atmo-

Table 9.3 Mean residence time (RT), dispersion coefficient (*D/vL*), and Reynolds number for emulsions and water

Pressure (MPa)	Sample	RT	Dispersion coeficient (D/vL)	Re (IX, 75 μm)	Particle size (nm)
69	Water	9.84	0.80	138,206	–
103		4.03	0.91	176,426	–
69	1:5	11.20	0.076	10,110	185
	1:3.5	8.39	0.085	10,975	153
	1:2	7.26	0.052	13,961	138
103	1:5	7.20	0.078	11,199	400
	1:3.5	7.01	0.079	10,930	381
	1:2	3.16	0.150	13,589	367

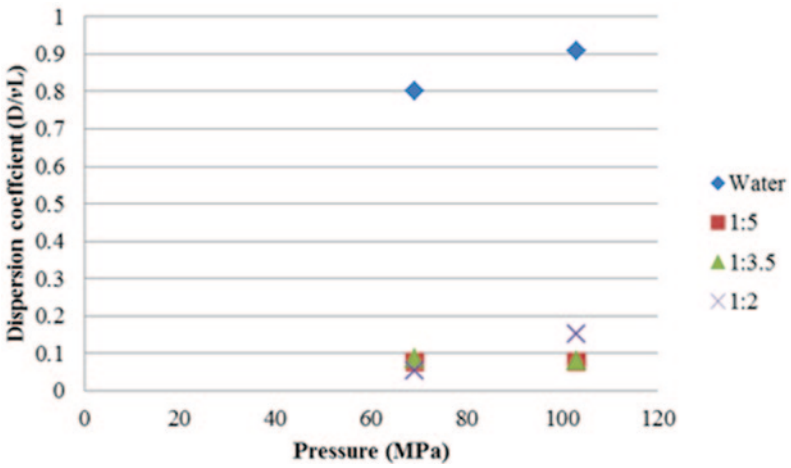

Fig. 9.4 Dispersion coefficient (*D/vL*) in function of pressure (MPa) for water and emulsion samples

spheres (69–103 MPa), the expectations about the flow type were that this will be a completely stirred tank, which was more evident when working with water (dye). While particle size depends on several factors, this will be the result of the speed of stabilization of the emulsion compared to recoalescence (Jafari et al. 2008b). For this evaluation, pressure happens to be the most important factor on the particle size, having 40 % of the influence on this parameter in an inversely proportional manner (Fig. 9.4). Using pressures of 103 MPa or above can result in a higher level of turbulence and collision frequency between particles, decreasing the RT of the emulsion in the IX, and causing a decrement on dispersion making the contact time between AT particles and biopolymers insufficient to stabilize the new interfaces, and this is why a lower pressure must be chosen (69 MPa) that warrants an increase on the RT. According to several reports, the particle size of the emulsion provided

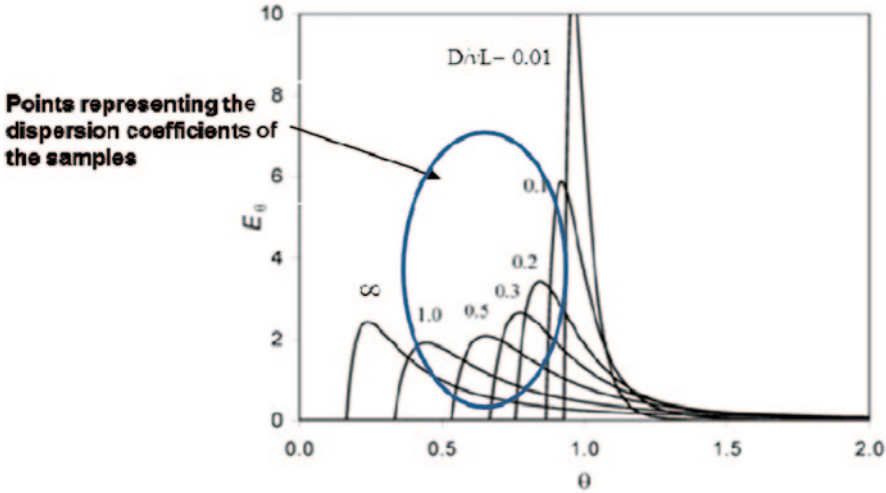

Fig. 9.5 E_θ curves for the different values obtained for the dispersion coefficient

by the microfluidizer is affected by pressure. Qian and McClements (2011) found that when they increased the pressure from 42 to 138 MPa, the particle size decreased from 231 to 165 nm. However, these sizes strongly depend on the type of surfactant employed (Rao and McClements 2012). In this case, MD/GA where elected as core materials for emulsifying purposes. These biopolymers are one of the main polysaccharides used in the food industry and have important applications in spray drying as carriers of bioactive lipids, such as AT (McClements 2009; Gomes et al. 2010). Nevertheless, because of the high molecular mass of the GA, which is responsible of the stabilization of the interfaces and final particle size, it takes longer times to reach the interfaces (Bouyer et al. 2011) so a longer RT provided by low pressure could be effective to reach a lower particle size.

9.3 Conclusions

Production of nanoemulsions by microfluidization was carried out. The optimum conditions were found at 69 MPa and AT/MD-AG proportions of 1:2.5. Under this pressure, the RTD (7.26–11.2) was enough to allow the biopolymers reach the interfaces and achieve a smaller particle size (138–185). Also, the proportion of oil/biopolymer plays an important role on this parameter, finding that increasing the oil phase results in a decrease of particle size, because the layer surrounding the AT interfaces results thinner. It was also observed that the forces acting to carry out the emulsification process are primarily inertial forces in a turbulent regime. The microfluidizer use causes an intermediate level of dispersion in between a completely mixed tank and plug flow, despite the high shear applied. For systems that

use biopolymers with surface properties, as GA, it is possible to achieve small particles in the range of nanoemulsion by varying the proportion of oil/emulsifier and increasing the RT on the IX. The RTD behavior of microchannels was successfully analyzed by employing a pulse input to microchannels at different flow rates of fluid.

References

Adeosun JT, Lawal A (2009) Numerical and experimental studies of mixing characteristics in a T-junction microchannel using residence-time distribution. Chem Eng Sci 64(10):2422–2432. doi:10.1016/j.ces.2009.02.013

Adeosun JT, Lawal, A. (2010) Residence-time distribution as a measure of mixing in T-junction and multilaminated/elongational flow micromixers. Chem Eng Sci 65(5):1865–1874. doi:10.1016/j.ces.2009.11.038

Apruzzese F, Pato J, Balke ST, Diosady LL (2003) In-line measurement of residence time distribution in a co-rotating twin-screw extruder. Food Res Int 36(5):461–467. doi:10.1016/S0963-9969(02)00193-X

Bouchemal K, Briançon S, Perrier E, Fessi H (2004) Nano-emulsion formulation using spontaneous emulsification: solvent, oil and surfactant optimisation. International Journal of Pharmaceutics 280(1–2):241–251. doi:10.1016/j.ijpharm.2004.05.016

Bouyer E, Mekhloufi G, Le Potier I, de Kerdaniel TDF, Grossiord JL, Rosilio V, Agnely F (2011) Stabilization mechanism of oil-in-water emulsions by β-lactoglobulin and gum arabic. J Colloid Interf Sci 354(2):467–477. doi:10.1016/j.jcis.2010.11.019

Bouyer E, Mekhloufi G, Huang N, Rosilio V, Agnely F (2013) β-Lactoglobulin, gum arabic, and xanthan gum for emulsifying sweet almond oil: formulation and stabilization mechanisms of pharmaceutical emulsions. Colloid Surface A 433:77–87. doi:10.1016/j.colsurfa.2013.04.065

Brösel S, Schubert H (1999) Investigations on the role of surfactants in mechanical emulsification using a high-pressure homogenizer with an orifice valve. Chem Eng Process 38:533–540.

Cao-Hoang L, Fougère R, Waché Y (2011) Increase in stability and change in supramolecular structure of β-carotene through encapsulation into polylactic acid nanoparticles. Food Chem 124(1):42–49. doi:10.1016/j.foodchem.2010.05.100

Cheong JN, Tan CP, Man YBC, Misran M (2008) a-Tocopherol nanodispersions: preparation, characterization and stability evaluation. J Food Eng 89(2):204–209. doi:10.1016/j.jfoodeng.2008.04.018

Dickinson E, Galazka VB, Anderson DMW (1991) Emulsifying behaviour of gum arabic. Part 1: effect of the nature of the oil phase on the emulsion droplet-size distribution. Carbohyd Polym 14(4):373–383

Donsì F, Sessa M, Mediouni H, Mgaidi A, Ferrari G (2011) Encapsulation of bioactive compounds in nanoemulsion-based delivery systems. Procedia Food Science 1:1666–1671. doi:10.1016/j.profoo.2011.09.246

Gomes JFPS, Rocha S, do Carmo Pereira M, Peres I, Moreno S, Toca-Herrera J, Coelho MAN (2010) Lipid/particle assemblies based on maltodextrin-gum arabic core as bio-carriers. Colloids Surf B Biointerfaces 76(2): 449–455. doi:10.1016/j.colsurfb.2009.12.004

Gonnet M, Lethuaut L, Boury F (2010) New trends in encapsulation of liposoluble vitamins. J Control Release 146(3):276–290. doi:10.1016/j.jconrel.2010.01.037

Gramdorf S, Hermann S, Hentschel A, Schrader K, Müller RH, Kumpugdee-Vollrath M, Kraume M (2008) Crystallized miniemulsions: influence of operating parameters during high-pressure homogenization on size and shape of particles. Colloid Surface A 331(1–2):108–113. doi:10.1016/j.colsurfa.2008.07.016

Gutierrez CGCC., Dias EFTS., Gut JAW (2010) Residence time distribution in holding tubes using generalized convection model and numerical convolution for non-ideal tracer detection. J Food Eng 98(2):248–256. doi:10.1016/j.jfoodeng.2010.01.004

Hatanaka J, Chikamori H, Sato H, Uchida S, Debari K, Onoue S, Yamada S (2010) Physicochemical and pharmacological characterization of alpha-tocopherol-loaded nano-emulsion system. Int J Pharm 396(1–2):188–193. doi:10.1016/j.ijpharm.2010.06.017

Heffernan SP, Kelly AL, Mulvihill DM, Lambrich U, Schuchmann HP (2011) Efficiency of a range of homogenisation technologies in the emulsification and stabilization of cream liqueurs. Innovative Food Science & Emerging Technologies 12(4):628–634. doi:10.1016/j.ifset.2011.07.010

Hessel V, Holger L, Muller A, Kolb G (2005) Chemical micro process engineering: processing and plants, 1st edn. Wiley, New York

Jafari SM, He Y, Bhandari B (2007a) Effectiveness of encapsulating biopolymers to produce sub-micron emulsions by high energy emulsification techniques. Food Res Int 40(7):862–873. doi:10.1016/j.foodres.2007.02.002

Jafari SM, He Y, Bhandari B (2007b) Production of sub-micron emulsions by ultrasound and microfluidization techniques. J Food Eng 82(4):478–488. doi:10.1016/j.jfoodeng.2007.03.007

Jafari SM, Assadpoor E, Bhandari B, He Y (2008a) Nano-particle encapsulation of fish oil by spray drying. Food Res Int 41(2):172–183. doi:10.1016/j.foodres.2007.11.002

Jafari SM, Assadpoor E, He Y, Bhandari B (2008b) Re-coalescence of emulsion droplets during high-energy emulsification. Food Hydrocolloid 22(7):1191–1202. doi:10.1016/j.foodhyd.2007.09.006

Klinkesorn U, Sophanodora P, Chinachoti P, McClements D (2004) Stability and rheology of corn oil-in-water emulsions containing maltodextrin. Food Res Int 37(9):851–859. doi:10.1016/j.foodres.2004.05.001

Lee L, Norton IT (2013) Comparing droplet breakup for a high-pressure valve homogeniser and a microfluidizer for the potential production of food-grade nanoemulsions. J Food Eng 114(2):158–163. doi:10.1016/j.jfoodeng.2012.08.009

Levenspiel O (1999) Chemical reaction engineering, 3rd edn. Wiley, New York

Lim SS, Baik MY, Decker EA, Henson L, Michael Popplewell L, McClements DJ, Choi SJ (2011) Stabilization of orange oil-in-water emulsions: A new role for ester gum as an Ostwald ripening inhibitor. Food Chemistry 128(4):1023–1028. 1023 -1028. doi:10.1016/j.foodchem.2011.04.008

Lin Y-H, Chiou S-F, Lai C-H, Tsai S-C, Chou C-W, Peng S-F, He, Z-S (2012) Formulation and evaluation of water-in-oil amoxicillin-loaded nanoemulsions using for *Helicobacter pylori* eradication. Process Biochem 47(10):1469–1478. doi:10.1016/j.procbio.2012.05.019

Maher PG, Fenelon MA, Zhou Y, Kamrul Haque M, Roos YH (2011) Optimization of β-casein stabilized nanoemulsions using experimental mixture design. J Food Science 76(8). C1108 -17. doi:10.1111/j.1750-3841.2011.02343.x

Mayer S, Weiss J, McClements DJ (2013) Behavior of vitamin E acetate delivery systems under simulated gastrointestinal conditions: lipid digestion and bioaccessibility of low-energy nanoemulsions. J Colloid and Interface Science 404:215–222. doi:10.1016/j.jcis.2013.04.048

McClements DJ (2005) Food emulsions: principles, practice and techniques. CRC Press, Boca Raton

McClements DJ (2009) Biopolymers in Food Emulsions. MODERN BIOPOLYMER SCIENCE (First Edit, pp. 129–166). Elsevier Inc. doi:10.1016/B978-0-12-374195-0.00004-5

McClements DJ (2011) Edible nanoemulsions: fabrication, properties, and functional performance. Soft Matter 7:2297–2316. doi:10.1039/c0sm00549e

McClements DJ, Decker EA, Weiss J (2007) Emulsion-based delivery systems for lipophilic bioactive components. J Food Sci 72(8):R109–24. doi:10.1111/j.1750–3841.2007.00507.x

Nguyen NT, Wu Z 2005. Micromixers—a review. J Micromech Microeng 15(2):R1–R16

Pan Y, Tikekar RV, Nitin N (2013) Effect of antioxidant properties of lecithin emulsifier on oxidative stability of encapsulated bioactive compounds. Int J Pharm 450(1–2):129–137. doi:10.1016/j.ijpharm.2013.04.038

Paquin P (1999) Technological properties of high pressure homogenizers: the effect of fat globules, milk proteins, and polysaccharides. Int Dairy J 9:329–335

Patil GA, Bari ML, Bhanvase BA, Ganvir V, Mishra S, Sonawane SH (2012) Continuous synthesis of functional silver nanoparticles using microreactor: effect of surfactant and process parameters. Chem Eng Process 62:69–77. doi:10.1016/j.cep.2012.09.007

Pinheiro-Torres A, Oliveira FAR (1998) Residence time distribution studies in continuous thermal processing of liquid foods: a review. J Food Eng 36:1–30

Pipe CJ, McKinley GH (2009) Microfluidic rheometry. Mech Res Commun 36(1):110–120. doi:10.1016/j.mechrescom.2008.08.009

Qian C, McClements DJ (2011) Formation of nanoemulsions stabilized by model food-grade emulsifiers using high-pressure homogenization: factors affecting particle size. Food Hydrocolloid 25(5):1000–1008. doi:10.1016/j.foodhyd.2010.09.017

Rao J, McClements DJ (2012) Impact of lemon oil composition on formation and stability of model food and beverage emulsions. Food Chem 134(2):749–757. doi:10.1016/j.foodchem.2012.02.174

Sanguansri P, Augustin MA (2006) Nanoscale materials development—a food industry perspective. Trends Food Sci Technol 17(10):547–556. doi:10.1016/j.tifs.2006.04.010

Schuch A, Wrenger J, Schuchmann HP (2013) Production of W/O/W double emulsions. Part II: Influence of emulsification device on release of water by coalescence. Colloids and Surfaces A: Physicochemical and Engineering Aspects. doi:10.1016/j.colsurfa.2013.11.044

Stang BM, Schuchmann H, Schubert H (2001) Emulsification in High-pressure Homogenizers. Engineering in Life Sciences 1(4):151–157

Tadros TF (2009) Emulsion science and technology: a general introduction. Emulsion science and technology. Wiley-VCH, Weinheim, Germany 1–56

Tadros T, Izquierdo R, Esquena J, Solans C (2004) Formation and stability of nano-emulsions. Adv Colloid Interfac 108–109:303–318

Tan C, Nakajima M (2005) β-Carotene nanodispersions: preparation, characterization and stability evaluation. Food Chem 92(4):661–671. doi:10.1016/j.foodchem.2004.08.044

Tayakout-Fayolle M, Othman S, Jallut C (2005) A new technique for the determination of contact time distribution (CTD) from tracers experiments in heterogeneous systems. Chem Eng Sci 60(16):4623–4633. doi:10.1016/j.ces.2005.03.014

Ting Y, Jiang Y, Ho C-T, Huang Q (2014) Common delivery systems for enhancing in vivo bioavailability and biological efficacy of nutraceuticals. J Funct Foods 7:112–128. doi:10.1016/j.jff.2013.12.010

Weiss J, Gaysinsky S, Davidson M, Mcclements J (2009) Nanostructured encapsulation systems: Food Antimicrobials. In: Barbosa-Cánovas GV, Mortimer A, Lineback D, Spiess W, Buckle K, Colonna P (eds) Global issues in food science and technology. Academic Press, New York, p 425–479

Windhab EJ, Dressler M, Feigl K, Fischer P, Megias-Alguacil D (2005) Emulsion processing—from single-drop deformation to design of complex processes and products. Chem Eng Sci 60(8–9):2101–2113. doi:10.1016/j.ces.2004.12.003

Yuan Y, Gao Y, Zhao J, Mao L (2008) Characterization and stability evaluation of β-carotene nanoemulsions prepared by high pressure homogenization under various emulsifying conditions. Food Res Int 41(1):61–68. doi:10.1016/j.foodres.2007.09.006

Chapter 10
Role of Surfactants and Their Applications in Structured Nanosized Systems

María Ximena Quintanilla-Carvajal and Silvia Matiacevich

10.1 Introduction

In recent years, nanotechnology has found innumerable applications in different food industries. Nanotechnology involves the characterization, fabrication and/or manipulation of structures, devices or materials that are approximately 1–100 nm in length. When particle size is reduced below this threshold, the resulting material exhibits physical and chemical properties that are significantly different from the properties of macro-scale materials composed of the same substance (Quintanilla-Carvajal et al. 2010; Duncan 2011). The physicochemical properties (such as colour, solubility, viscosity and diffusivity) and biological properties of structures and systems at nanoscale are substantially different than the macro-scale counter parts owing to the interactions of individual atoms and molecules thereby offering unique and novel functional applications (Neethirajan and Jayas 2011). The potential benefits for application of nanotechnologies in food include packaging materials, formulations with improved bioavailability (Chaudhry et al. 2008) and Delivery Systems (Tamjidi et al. 2013) being these ones, one of the most important applications in the food industry. Delivery Systems are defined as one in which a bioactive material is entrapped in a carrier to control the rate of bioactive release. Nanocarriers can protect a bioactive component from unfavourable environmental conditions, e.g. oxidation and pH and enzymes degradation (Fang and Bhandari 2010). However, the stability of these structures, especially those that are applied in food and pharmaceutical fields, has to be generated and stabilized by emulsifiers or surfactants.

M. X. Quintanilla-Carvajal (✉)
Facultad de Ingeniería, Universidad de La Sabana, km 7 vía autopista Norte, Chía, Colombia
e-mail: maria.quintanilla1@unisabana.edu.co

S. Matiacevich
Departamento de Ciencia y Tecnología de los Alimentos. Facultad Tecnológica, Universidad de Santiago de Chile, Santiago, Chile

© Springer Science+Business Media New York 2015

H. Hernández-Sánchez, G. F. Gutiérrez-López (eds.), *Food Nanoscience and Nanotechnology,* Food Engineering Series, DOI 10.1007/978-3-319-13596-0_10

Many nano-food products use emulsifying agents present in the food themselves. Food emulsifiers, more correctly referred as surfactants, are molecules, which contain non-polar and polar regions. In most of the cases, the non-polar groups are aliphatic, alicyclic and aromatic hydrocarbons. On the other hand, the polar functional groups contain heteroatoms such as oxygen, nitrogen and sulphur. Detailed knowledge of the physical chemistry of emulsions is best obtained when pure oil, water and surfactants are used. These substances are regulated by different entities in the world; in the USA, food emulsifiers, along with other additives, are regulated by the Food and Drug Administration, and in Europe by the European Economic Community. As with any other totally new food additive, the need to prove safety of the product in foods at high levels of consumption requires extensive toxicity studies and enormous documentation (Hasenhuettl 2008).

10.1.1 Surfactants or Emulsifiers

In the food industry, the main types of emulsifiers are small molecule surfactants, phospholipids, proteins and polysaccharides. Proteins and polysaccharides have the advantage of being natural ingredients that are often considered more "label-friendly" (Tamjidi et al. 2013). Since food emulsifiers do more than simple stabilize emulsions, they are more accurately termed surfactants (Hasenhuettl 2008). Surfactants or emulsifiers are surface-active molecules that consist of a hydrophilic head group and a lipophilic tail group. The functional performance of the surfactants depends on the molecular characteristics of its head and tail groups. Food-grade surfactants present different molecular structures because their head groups may vary in physical dimensions and electrical charge, while their tail groups may vary in number and degree of saturation. The selection of a particular surfactant depends on the type of the structure that need to be formed, as well as its legal status, cost, usage levels, ingredient compatibility, stability and ease of utilization (McClements 2009).

Several structures' nanosized formulations were already stabilized only by surfactants or rarely by a combination of surfactants and biopolymers (Liu et al. 2012; Zheng et al. 2013) rather than by biopolymers individually. This is mainly because of the ability of surfactants to spontaneously form nanoemulsions by low-energy methods, and because of their ability to rapidly adsorb to droplet surfaces and reduce the interfacial tension in high-energy methods (such as high-pressure homogenization) (McClements and Rao 2011).

10.1.1.1 Surfactants and Emulsifiers Structures

Surfactants can be classified knowing the polar functionality groups: anionic, that contain a negative charge on the bulk molecule associated with a small positive counterion; cationic, that have a positive molecule with a negative charge on the same molecule; amphoteric, that contains both, positive and negative charges on

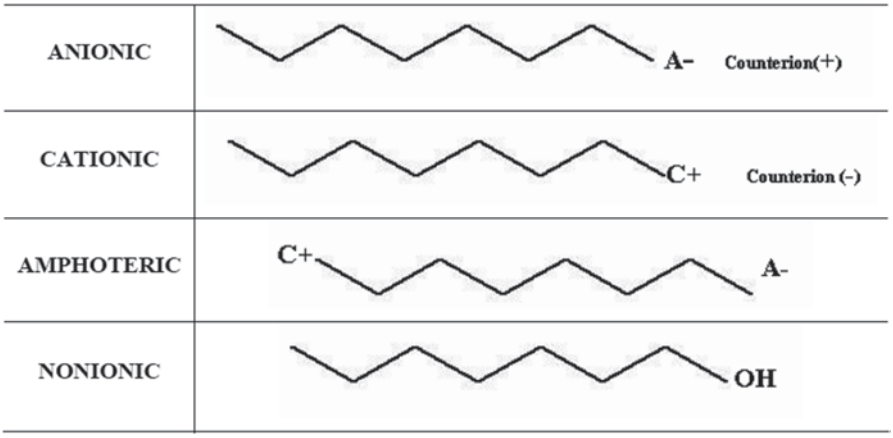

Fig. 10.1 Structure anionic, cationic, amphoteric and nonionic surfactants

the same molecule; and the nonionic, that contain no formal positive or negative charge, but a polar heteroatom can produce a dipole with an electron-dense and electron-depleted region. Figure 10.1 presents the structure of them.

Food surfactants are useful in the design of nanosized systems because the structure and number of heads and tails may be independently varied. Hasenhuettl (2008) described in a simple way a very useful technique to choose the correct emulsifier: the hydrophilic–lipophilic balance (HBL). The number and polarity of the polar heads in the structure of the surfactant determine if it is water or oil soluble. This concept is applied by the calculation of the HBL. High HLB values are associated with easy water dispensability and are useful to prepare oil-in-water emulsions. In contrast, low HBL surfactants are useful to prepare water-in-oil emulsions.

Surfactants may generate bilayer structures described as mesophases or liquid crystals, these structures can adopt different geometric forms as is shown in Fig. 10.2.

10.1.1.2 Surfactants and Emulsifiers Functionality

Their major function, as was mentioned before, is producing and stabilizing emulsions and off course, structured nanosized systems. However other important functions contribute to the development of food technology (Hassenhuettl 2008):

- Foam aeration
- Dispersion
- Strengthening
- Clouding
- Crystal inhibition
- Anti-sticking
- Viscosity modification

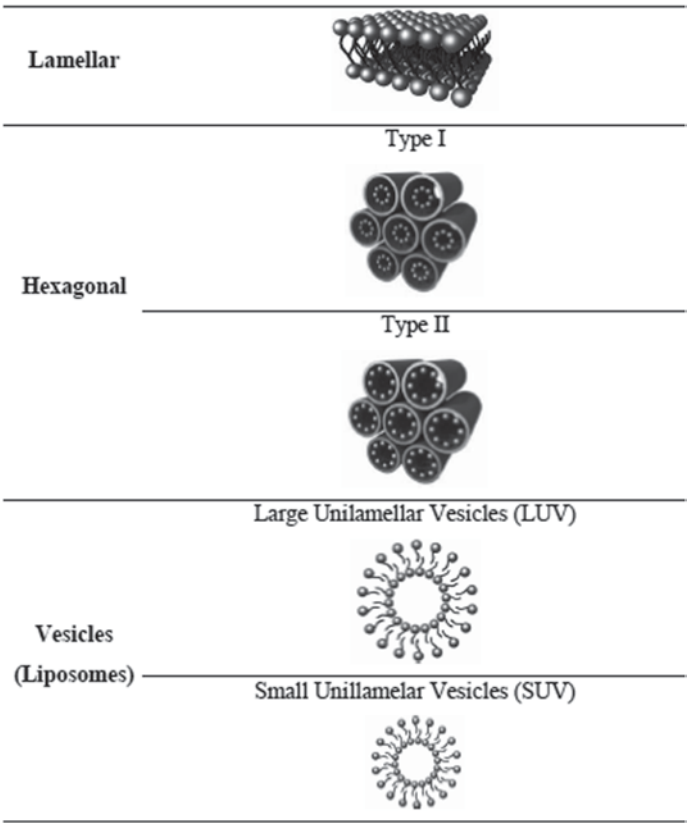

Fig. 10.2 Different geometric forms that a surfactant can adopt

- Controlled fat agglomeration
- Freeze-thaw stabilization
- Gloss enhancement

The characteristic property of all surfactant or emulsifier is their surface activity. This characteristic is the ability to form a surface excess at interfaces. The formation of adsorbed layers at interfaces is displayed in a change of a range of easily observable and technically important properties, specially reducing the surface tension (Bergenstahl 2008). The gain of entropy is very large at low concentrations. If the surfactant displays surface activity and adsorbs at an interface, the system loses entropy, which has to be balanced by a gain in free energy due to the adsorption.

10.1.1.3 Most Important Surfactants Used in the Formulation of Structured Nanosized Systems

A complete list of food surfactants and their Legal Status is published by Hasenhuettl (2008), however, the most used surfactants reported in the literature for preparation

of structured nanosized systems are polyoxyethylene sorbitan monooleate (trade names: Polysorbate® 80, Tween® 80), lecithin and Poloxamer 188.

- Tween 80 is an oleate ester of sorbitol and its anhydrides copolymerized with approximately 20 mol of ethylene oxide for each mole of sorbitol and sorbitol anhydrides (Qiu et al. 2013). This surfactant is a water-soluble and nonionic synthetic surfactant with HLB number ~15. Tween 80 is allowed for certain specific foods by FDA (21CFR172.840).
- Lecithins are naturally occurring surface-active components that can be extracted from soybean, rapeseed and egg (Faergemand and Krog 2003). Natural lecithins are a complex mixture of different phospholipids and other lipids in which phosphatidylcholin, phosphatidyletanolamine and phosphatidylinositol are the most common phospholipids (Faergemand and Krog 2003). Natural lecithins are essentially hydrophobic molecules with intermediate HLB numbers (~umbers (~umbers (~holin, phosphatidyletanolamintanolamintanolaminace excess at interfacesnanosized systems.
- Poloxamer 188 is a nonionic surfactant with HLB number ~29 and is included in the FDA Inactive Ingredients Database (Rowe et al. 2009). Poloxamer 188 is a copolymer based on poly(ethylene oxide)-block-poly(propylene oxide)-block-poly(ethylene oxide) structure. Poloxamers are stable at high temperatures; they are commonly used in industrial, pharmaceutical, natural health product and cosmetic applications, but they are not food-grade (Wulff-Perez et al. 2009; Trujillo and Wright 2010).

Other emulsifiers can be used in the stabilization of structured nanosized systems such as: monoglycerides of hydrogenated palm oil (Martini and Herrera, 2008), Tween 20 (Xin et al. 2013) and Gelucires (Shimpi et al. 2009; Tsai et al. 2012)

10.2 Molecular Interactions to Assemble Nanosized Systems

Knowledge of the various molecular forces that act between food components is important for understanding how to assemble nanosized systems with specific structures. Most of these interactions are modulated by surfactants and the relative importance of them in a particular system depends on three principal factors (i) the types of food components involved such us their molecular weight, charge density, pH profile, flexibility and hydrophobicity, (ii) the solution composition as pH, ionic strength and dielectric constant, and (iii) the environmental conditions like temperature or shearing rate.

- Electrostatic interactions are important for food components that have an electrical charge under the utilization conditions, also, may be either attractive or repulsing depending on whether the charge groups involved have opposite or similar signs. The sign and magnitude of the charge usually depends on the pH

of the solution. The strength and range of these types of interactions decreases when increasing ionic strength due to electrostatic screening effects. Commonly, electrostatic interactions are used to assemble food components.

- Hydrophobic interactions are important in those structures that include considerable amounts of non-polar groups. These interactions can be controlled by modifying the temperature or changing the polarity of an aqueous solution.
- Other important interaction is the hydrogen bonding, characteristic in food components that have polar groups and are capable for forming relatively strong hydrogen bonds with other polar groups on the same or different molecules.
- Steric exclusion is a type of interaction that has important effects in food components that occupy large volumes within a system altering the configurational and/or conformational entropy of the system.

10.3 Structural Design Principles

Some of the structural design principles that can be observed in nanosized systems to assemble novel structures from food components are highlighted:

- Phase separation: when two different substances are mixed, they may be completely miscible and form a continuous phase or they may separate in different non-miscible phases depending on the relative strength of the interactions between the types of molecules present in the mixture. The typical example of this phenomenon is an emulsion that implies strong thermodynamically unfavourable interactions between the different types of biopolymers and surfactants used in the emulsification process.
- Spontaneous self-assembly: under specific and desirable conditions, some components spontaneously assemble into well-defined structures since this minimizes the free energy of the system. The driving force of this phenomenon is system dependent, but often involves hydrophobic attraction, electrostatic interactions and/or hydrogen bond formation. In most of the cases the self-assembly process begins with the hydrophobic attraction that causes the system to adopt a specific molecular organization that minimizes the unfavourable contact area between the non-polar tails of the surfactant molecules and water.
- Directed self-assembly: this process does not happen spontaneously if all the components are mixed simply together. Instead, the order of mixing, temperature, pH or ionic strength-time profiles, must be carefully selected and controlled to direct the different components so that they are assembled into particular metastable structure. The driving force of this process is also system dependent but again hydrophobic attraction, electrostatic interactions and/or hydrogen bond formation are also involved, and the principal actors are the surfactants.
- Directed assembly: it is also possible to create structures by binding molecules together in well-defined ways by micro-manipulation methods; however these types of processes require expensive equipment and are not applied to industrial scales yet.

10.4 Structured Nanosized Systems that Imply the Use of Surfactants

Major structural design principles require the use of surfactants to stabilize themselves; some of them are described in this section.

- Conventional emulsions: in most of the cases these are oil-in-water emulsions (o/w) that consist of emulsifier-coated lipid droplets dispersed in an aqueous continuous phase. They are formed by emulsifying an oil phase in water in presence of a hydrophilic emulsifier. Nanoemulsions (also known as miniemulsions or submicron emulsions) are nanoscale droplets of multiphase colloidal dispersions formed by dispersing of one liquid in another immiscible liquid by physical share-induced rupturing. Different size ranges have been reported in the literature for nanoemulsions (Fathi et al. 2012). Unlike the micro-emulsions that are thermodynamically stable and form spontaneously, nanoemulsions are kinetically stable (Henry et al. 2010). An interesting feature of nanoemulsions in contrast to micro-emulsions is that, they are metastable and can be diluted with water without change in the droplet size distribution (Gutink rid=" al. 2008). However, these particular characteristics depend on the nature and amount of the used surfactants.
- Multiple emulsions: these could be water-in-oil-in-water emulsions (w/o/w) that consist of small droplets of water contained in larger oil droplets that are dispersed in an aqueous continuous phase. First the o/w emulsions are obtained by homogenizing water, oil and oil-soluble emulsifier, and later the w/o/w is then produced by homogenizing the w/o with an aqueous solution containing a water soluble emulsifier (Davidov-Pardo and McClements 2014).
- Multilayer emulsions: Multilayer oil-in-water (M-o/w) emulsions consist of small oil droplets dispersed in aqueous medium, with each oil droplet being surrounded by a nanolaminated interfacial layer, which usually consists of emulsifier. They are normally formed using multistep procedures. First o/w emulsion is prepared by homogenizing an oil and aqueous phase together in the presence of an ionized water soluble emulsifier. Second, an oppositely charged polyelectrolyte is added to the system so that it adsorbs to the droplet surfaces and forms a two-layer coating around the droplets. This procedure can be repeated adding more layers to the droplets using surfactants that modified the interfaces with opposite charges.
- Solid Lipid Nanoparticles (SLNs): are similar to conventional emulsions consisting of emulsifier-coated lipid droplets dispersed in an aqueous continuous phase. However, the lipid phase is either fully or partially solidified, and the morphology and packing of the crystals within the lipid phase may be controlled. The structures are formed by homogenizing and oil and water phase together in the presence of a hydrophilic emulsifier at a temperature above the melting point of the lipid phase. The emulsion is then cooled (usually in a controlled manner) so that the lipids within the droplets crystallize (McClements 2009). Compared to nanoemulsions and liposomes, SLNs have some distinct advantages: (i) having

high encapsulation efficiency, (ii) avoiding use of organic solvents in their preparation, (iii) possibility of large-scale production and sterilization, (iv) providing high flexibility in controlling the release profile due to solid matrix, (v) slower degradation rate allows bioactive release for prolonged times and (vi) the solid matrix can (but need not) protect the incorporated bioactive ingredients against chemical degradation (Fathi et al. 2012).

- Nanostructured lipid carriers (NLC): these structures could be obtained by mixing very different lipid molecules i.e. solid lipids with liquid lipids (oils) based on preparation methods described for SLN. The produced matrix of the lipid particles demonstrates a melting point depression compared to the original solid lipid. In fact by giving the lipid matrix a certain nanostructure, the encapsulation load of bioactive ingredient is enhanced and expulsion phenomenon during storage is limited by preventing the formation of perfect crystals (Chen et al. 2010).
- Nanoliposomes: these structures consist of at least one closed vesicle composed of bilayer membranes which are made of lipid molecules, such as phospholipids and cholesterol. They form when phospholipids are dispersed in aqueous media and exposed to high shear rates by using homogenization techniques. The underlying mechanism for the formation of liposomes is basically the hydrophilic–hydrophobic interactions between phospholipids and water molecules. Active agent can be entrapped within their aqueous compartment at a low yield, or within or attached to the membrane at a high yield (Zuidan and Shimoni 2010).

In support of above advantages, it should be mentioned that bioactive ingredient release from nanoemulsions, which takes place based on the partitioning coefficient and the phase ratios of oil and water phases, is too fast (Washington 1998). Longer release times can be achieved with liposomes. However, it is not yet appropriate for delivery of bioactive food ingredients. Compared to these carriers, release period for SLN is longer because of increase of degradation time of solid matrix. Solid matrices are able to provide more protection against chemical reactions such as oxidation (Müller et al. 2000).

10.5 Theoretical Mathematical Model to Determine the Optimal Value of Surfactant Concentration

Wulff-Perez et al. (2009) reported that destabilization of the nanoemulsions takes place above certain surfactant concentration. This phenomenon can be described as a depletion-flocculation effect caused by non-adsorbed micelles. They presented a theoretical mathematical model based on experimental parameters to determine the optimum value of surfactant concentration. In this section, the model is presented as a useful tool to determine the concentration of surfactants in structured nanosized systems.

The authors developed a theoretical treatment related to the attraction, repulsion and depletion potential using their own experimental parameters. The total interac-

tion energy (V_T) as a function of the shortest distance between the droplet surfaces (H), when they are completely covered by a specific surfactant: Pluronic F68, was assumed to be the sum of all attractive and repulsive potentials:

$$V_T(H) = V_A(H) + V_R(H) + V_{\text{dep}}(H). \tag{10.1}$$

References

Bergenstahll B (2008) Physicochemical aspects of an emulsifier functionality. In: Hasenhuettl G, Hartel R (eds) Food emulsifiers and their applications. Springer, New York, pp 173–193

Chaudhry Q, Scotter M, Blackburn J, Ross B, Boxall A, Castle L, Aitken R, Watkins R (2008) Applications and implications of nanotechnologies for the food sector. Food Addit Contam 25(3):241–258

Chen CC, Tsai TH, Huang ZR, Fang JY (2010) Effects of lipophilic emulsifiers on the oral administration of lovastatin from nanostructured lipid carriers: physicochemical characterization and pharmacokinetics. Eur J Pharm Biopharm 74:474–482

Davidov-Pardo G, McClements DJ (2015) Nutraceutical delivery systems: resveratrol encapsulation in grape seed oil nanoemulsions formed by spontaneous emulsification. Food Chem 167:205–212

Duncan TV (2011) Applications of nanotechnology in food packaging and food safety: barrier materials, antimicrobials and sensors. J Colloid Interface Sci 363(1):1–24

Faergemand M, Krog N (2003) Using emulsifiers to improve food texture. In: McKenna BM (ed) Texture in foods: vol 1: semi-solid foods CRC Press, Boca Raton, pp 216–274

Fang Z, Bhandari B (2010) Encapsulation of polyphenols—a review. Trends Food Sci Technol 21:510–523

Fathi M, Mozafari MR, Mohebbi M (2012) Nanoencapsulation of food ingredients using lipid based delivery systems. Trends Food Sci Technol 23:13–27

Gutiérrez JM, González M, Sole I, Pey CM, Nolla J (2008) Nano-emulsions: new applications and optimization of their preparation. Curr Opin Colloid Interface Sci 13:245–251

Hasenhuettl G (2008) Overview of food emulsifiers. In: Hasenhuettl G, Hartel R (eds) Food emulsifiers and their applications. Springer, New York, pp 1–10

Henry JVL, Fryer PJ, Frith WJ, Norton IT (2010) The influence of phospholipids and food proteins on the size and stability of model sub-micron emulsions Food Hydrocoll 24:66–71

Liu GY, Wang JM, Xia Q (2012) Application of nanostructured lipid carrier in food for the improved bioavailability. Eur Food Res Technol 234(3):391–398

Martini S, Herrera ML (2008) Physical properties of shortenings with low-trans fatty acids as affected by emulsifiers and storage conditions. Eur J Lipid Sci Technol 110(2):172–182

McClements J (2009) Structural design principles for improved food performance: nanolaminated biopolymer structures in foods. In: Huang Q, Given P, Qian M (eds) Micro/Nanoencapsulation of active food ingredients. American Chemical Society, Washington, pp 3–34

McClements DJ, Rao J (2011) Food-grade nanoemulsions: formulation, fabrication, properties, performance, biological fate, and potential toxicity. Crit Revs Food Sci Nutr 51(4):285–330

Müller RH, Mäder K, Gohla S (2000) Solid lipid nanoparticles (SLN) for controlled drug delivery—a review of the state of the art. Eur J Pharm Biopharm 50:161–177

Neethirajan S, Jayas DS (2011) Nanotechnology for the food and bioprocessing industries. Food Bioprocess Technol 4(1):39–47

Qiu S, Liu Z, Hou L, Li Y, Wang J, Wang H, Qin Y, Lui Z (2013) Complement activation associated with polysorbate 80 in beagle dogs. Int Immunopharmacol 15(1):144–149

Quintanilla-Carvajal M, Camacho-Díaz B, Meraz-Torres S, Chanona-Pérez J, Alamilla-Beltrán L, Jimenéz-Aparicio A, Gutiérrez-Lopéz G (2010) Nanoencapsulation: a new trend in food engineering processing. Food Eng Revs 2:39–50

Rowe RC, Sheskey PJ, Quinn ME (2009) Handbook of pharmaceutical excipients. Pharmaceutical Press and American Pharmacist Association, London

Shimpi SL, Mahadik KR, Paradkar AR (2009) Study on mechanism for amorphous drug stabilization using Gelucire 50/13. Chem Pharm Bull 57(9):937–942

Tsai MJ, Wu PC, Huang YB, Chang JS, Lin CL, Tsai YH,Fang JY (2012) Baicalein loaded in tocol nanostructured lipid carriers (tocol NLCs) for enhanced stability and brain targeting. Int J Pharm 423(2):461–470

Tamjidi F, Shahedi M, Varshosaz J, Nasirpour A (2013) Nanostructured lipid carriers (NLC): a potential delivery system for bioactive food molecules. Innov Food Sci Emerg Technol 19:29–43

Trujillo CC, Wright AJ (2010) Properties and stability of solid lipid particle dispersions based on canola stearin and Poloxamer 188. J Am Oil Chem Soc 87(7):715–730

Wulff-Pérez M, Torcello-Gómez A, Gálvez-Ruíz MJ, Martín-Rodríguez A (2009) Stability of emulsions for parenteral feeding: preparation and characterization of o/w nanoemulsions with natural oils and Pluronic f68 as surfactant. Food Hydrocoll 23:1096–1102

Xin X, Zhang X, Xua G, Tana Y, Zhang J, Lv X. Influence of CTAB and SDS on the properties of oil-in-water nano-emulsion with paraffin and span 20/Tween 20. Colloids Surf A Physicochem Eng Asp 418:60–67

Zheng K, Zou A, Yang X, Liu F, Xia Q, Ye R, Bozhong M (2013) The effect of polymeresurfactant emulsifying agent on the formation and stability of a-lipoic acid loaded nanostructured lipid carriers (NLC). Food Hydrocoll 32(1):72–78

Zuidan NJ, Shimoni E (2010) Overview of microencapsulates for use in food products or process and methods to make them. In: Zuidan N, Nedovic V (eds) Encapsulation technologies for active food ingredients and food processing. Springer, New York, pp 3–30

Chapter 11
Food Nano- and Microconjugated Systems: The Case of Albumin–Capsaicin

Lino Sánchez-Segura, Evangelina García-Armenta, María de Jesús Perea-Flores, Darío Iker Téllez-Medina, Juan C. Carpio-Pedroza, Humberto Hernández-Sánchez, Liliana Alamilla-Beltrán, Antonio R. Jiménez-Aparicio and Gustavo F. Gutiérrez-López

11.1 Introduction

The microencapsulation is the process in which bioactive substances, i.e. flavour, vitamins, antioxidants, antimicrobial essentials oils, are introduced into a relatively small matrix or wall material (Lekago and Dunford 2010; Viveros-Contreras et al. 2013). The main objective of microencapsulation is reducing volatility, hygroscopicity and reactivity, thus increasing product stability under adverse environmental conditions (Favaro et al. 2010). The scales of structuration are nano- and microencapsulates since they are difficult to produce when common techniques are used (Jun et al. 2011). The nanostructuring of macromolecules may allow specific applications and functions in the system in which they will be used. In food science, the development of nano- and microencapsulates has been applied to bioactive in-

G. F. Gutiérrez-López (✉) · L. Sánchez-Segura · E. García-Armenta · D. I. Téllez-Medina · H. Hernández-Sánchez · L. Alamilla-Beltrán
Departamento de Graduados e Investigación en Alimentos. Escuela Nacional de Ciencias Biológicas, Instituto Politécnico Nacional, Carpio y Plan de Ayala S/N. Col. Santo Tomás, C.P, 11340 Mexico, DF, Mexico
e-mail: gusfl@gmail.com

A. R. Jiménez-Aparicio
Centro de Desarrollo de Productos Bióticos, Instituto Politécnico Nacional, Carretera Yautepec-Jojutla, Km. 6, Calle Ceprobi No. 8, Col. San Isidro, Yautepec, Apartado Postal 24, 62731 Mexico, MOR, Mexico

J. C. Carpio-Pedroza
Instituto Nacional de Diagnóstico y Referencia Epidemiológica, CENAVECE-Secretaria de Salud, Francisco de P. Miranda No. 177, Col. Unidad Lomas de Plateros C. P., 01480 México, DF, Mexico

M. d. J. Perea-Flores
Laboratorio de Microscopía Confocal-Multifotónica. Centro de Nanociencias y Micro y Nanotecnologías. Unidad Profesional "Adolfo López Mateos", Instituto Politécnico Nacional, Luis Enrique Erro S/N, Zacatenco C. P., 07738 México, DF, Mexico

© Springer Science+Business Media New York 2015

H. Hernández-Sánchez, G. F. Gutiérrez-López (eds.), *Food Nanoscience and Nanotechnology,* Food Engineering Series, DOI 10.1007/978-3-319-13596-0_11

gredients, such as nutrients, phytochemicals and nutraceuticals (Robert et al. 2010; Munin and Edwards-Lévy 2011; Jun et al. 2011). The microencapsulates provide resistance to processing and packaging conditions in order to improve acceptability features such as appearance, flavour, odour and nutritional value (Viveros-Contreras et al. 2013). The self-assembly and functionalisation of this type of structures have shown inherent problems on the size reduction of particles and their physical, chemical and biological properties (Moghimi et al. 2001).

In biological materials, the self-assembly can be defined as the spontaneous organisation of individual components into an ordered structure without human intervention (Zhang et al. 2002) or indirect human intervention such as the change of pH, osmolarity and temperature. The composition of the wall material plays an important role on microencapsulation since it promotes the self-assembly and the molecular arrangement of the nanostructure. The incorporation of low quantities of proteins in the composition of wall material has been an alternative and novel way to minimise the stickiness problem and modify the surface properties of the nano- and microencapsulates (Adhikari et al. 2009a; Adhikari et al. 2009b). Fang and Bhandari (2012) found a novel and alternative use of protein in spray drying of bayberry juice which reduces adhesive behaviour (stickiness) between particles and dryer wall due to the migration of protein molecules to the particle surface. On the other hand, Pascual-Pineda et al. 2013 developed encapsulates of carotenoids prepared by the coacervation method with a nanostructured (alginate/zeolite valfor 100) and a non-nanostructured (alginate at 2 %) wall material. In the alginate/zeolite encapsulates, the zeolite particle embedded in the solid matrix showed micropores of 0.4 nm diameter (ultramicropores), in contrast to the alginate where the macropores were larger than 90 nm diameter; thus, alginate/zeolite encapsulates showed an ability to retain water molecules in the nanocavities. The nanostructuration can establish the relation between the function–structure and morphology of encapsulates, and this relation allows defining specific applications.

11.2 The Albumin-Group Proteins as Wall Material for Encapsulation

Albumin is emerging as a versatile protein carrier for drug targeting and for improving the pharmacokinetic profile of peptide or protein-based drugs (Gelamo et al. 2002; Kratz 2008). The group of albumin proteins has been used for the preparation of nanoparticles, microparticles and encapsulates due to its well-defined primary structure combined with the advantage of enabling surface modifications with dyes, antibodies, antigens, polysaccharides and proteins under stoichiometric conditions which provide stability to the structure (Weber et al. 2000a; Lewis et al. 2006; Zhang et al. 2008, 2009; Gebregeorgis et al. 2013).

Bovine serum albumin (BSA; MW 66,000) and cationised BSA (cBSA) are highly water-soluble containing numerous functional groups suitable for conjugation (Hermanson 2008). BSA is stable at a pH range of 4–9, is soluble in 40 % etha-

nol and can be heated to 60 °C for up to 10 h without deterioration effects (Kratz 2008). BSA possesses in the primary structure a single chain of 580 amino acid residues (Gelamo et al. 2002), a total of 59 lysine -amine groups (with only 30–35 of these typically available for derivatization). Their secondary structure is formed by 67 % of α-helix of six turns and 17 disulphide bridges (Ferrer et al. 2001; Huang and Kim 2004), the protein in solution behaves as a compact spheroid-ellipsoidal shape (Ferrer et al. 2001) with the major axis being 14 nm and the minor axis 4 nm (Honda et al. 2000).

Several studies of BSA and human serum albumin (HSA) involving binding of small molecules, particularly fatty acids and surfactants, based on different spectroscopic techniques have been reported (Choi et al. 2002; Xu et al. 2009; Bourassa et al. 2010); when these molecules bind to a globular protein, the intramolecular forces responsible for maintaining the secondary structure can be altered, producing conformational changes.

11.3 Methods for Nanostructuration of Protein Particles

Basically, three different methods for the nanostructuration of protein particles have been described, based on emulsion formation, pH-coacervation or desolvation (Langer et al. 2003). The emulsification method is based on the partial miscibility of an organic solvent with water. An oil-in-water (O/W) emulsion is obtained upon the injection of an organic phase into a disperse phase containing a stabilizing agent, under mechanical stirring, followed by high-pressure homogenisation (Sailaja et al. 2011). Polymer precipitation occurs as a result of the diffusion of organic solvent into water, leading to the formation of nanoparticles (Jahanshahi and Babaei 2008). However, the most common technique in the preparation of nanoparticles is the desolvation method. A desolvation process derived from the coacervation method is microencapsulation (Jahanshahi and Babaei 2008). Kaibara et al. (2000) described the coacervation as a process in which a homogeneous aqueous solution undergoes liquid–liquid phase separation giving rise to a dense protein-rich phase. The unique characteristics of the coacervate phase suggest it as a model for proteins in cytoplasm-like environments. Regarding the desolvation process, the disadvantage in comparison with emulsion methods for particle preparation is the need for applying organic solvents to remove both the oily residues of the preparation process and the surfactants required for emulsion stabilisation (Langer et al. 2003). The main modification in the pH-coacervation method to elaborate nanoparticles, microparticles and encapsulates is the removal of a surfactant (Lin et al. 1997). Moreover, the addition of acetone or ethanol to an aqueous solution of HSA or BSA produces conformational changes in the protein at pH values between 7 and 9 (Weber et al. 2000a, 2000b; Rahimnejad et al. 2012). Langer et al. (2003) found that stabilisation by the addition of glutaraldehyde solution produces particle cross-linking. The desolvation process can be divided into two parts: a first part where an increase in desolvating agent leads to an increase in the particle size (PS) and a second part

above a 1.5-fold ethanol volume addition where the PS remains constant, but the particle concentration is still increasing (Weber et al. 2000b).

The critical stage in the process or preparation of nanostructured particles is the polycondensation of albumin or cross-linking reaction. Some research works have been focused in the effect of cross-linking on the particle properties (PS, ζ-potential (ζ), percentage of dissolved albumin and available amino groups on the surface of particles; Weber et al. 2000b). Amino groups on protein surface may react with glutaraldehyde through the formation of Schiff bases to form activated derivatives able to cross-link with other proteins (Hermanson 2008). The reaction mechanism is as follows: One of the aldehyde ends can form a Schiff base linkage with ε-amines or α-amines on proteins leaving the other aldehyde terminal available to conjugate with another molecule (Wine et al. 2007; Wang et al. 2008). The concentration of added cross-linker varies according to the protein concentration. For instance, Langer et al. (2003) found that 8 % of glutaraldehyde concentration in water promoted the particle cross-linking process (in HSA, between 0.235 and 1.175 μL/mg). Subsequently, Langer et al. (2008) found that 117.6 μL of 8 % glutaraldehyde in water induced particle cross-linking. This volume corresponds to 200 % of the theoretical amount that is necessary for the quantitative cross-linking of the 60 amino groups present in the HSA molecules of the particle matrix. The cross-linking process influences the physicochemical characteristics such as PS, surface charge and amount of free amino groups on the particle surface (Weber et al. 2000b; Langer et al. 2008).

11.4 Methods for Characterization of the Nano-, Micro- and Macroparticles

11.4.1 Particle Size

The PS generally is controlled by concentration and adjusting BSA, pH, NaCl content and agitation speed, which affect the coagulation of the BSA molecules. The pH is the most important factor when controlling the coagulation of the BSA molecules during the desolvation process. The isoelectric point (pI) of BSA is about 4.9. When the pH shifts toward the pI, the enhanced protein–protein interactions increase coagulation among BSA molecules; as a result, larger BSA particles could be formed (Jun et al. 2011). The techniques most used for determining the PS are photon-correlation spectroscopy (PCS) or dynamic light scattering (DLS). PCS is the industrially preferred method of sub-micron PS analysis (Walther 2000).

Another unusual technique to measure the PS is the digital image analysis (DIA) which is a computer vision-based image method with algorithms developed in order to simultaneously evaluate several parameters such as PS and morphology distribu-

tions. There are many software packages that carry out this method such as ImageJ, Sigma Scan and MATLAB with specialised image processing toolboxes (Igathinathane et al. 2008). Yu et al. (2009) found that the PS distribution of sediments in wastewater can be controlled by DIA, and it described the morphology in an easier way in comparison with a typical laser PS analyser. On the other hand, changes in microstructure and viscosity (measured as PS distribution) of emulsions have been studied by means of DIA (Martínez et al. 2003). As well, morphological changes in *Aspergillus niger* treated with talc micro particles have been evaluated through DIA techniques (Wucherpfennig et al. 2012).

Therefore, DIA has been a useful tool to analyse these parameters in nanostructural systems. Phromsuwan et al. (2013) characterised magnetic nanoparticles from transmission electron microscope (TEM) images and compared the PS results with the one-by-one inspection method, finding that DIA gives more accurate diameter measurements.

11.4.2 Determination of the ζ-potential

The ζ-potential is a measure of the stability of an emulsion or colloidal suspension which is controlled by the layer of ions adsorbed on the surface of oil droplets or colloid particles (Hunter 2001). For instance, in the particles of protein, the prediction and design of molecular folding of proteins could be helpful for better understanding the stabilising mechanism at the oil–water interface by the adsorbing protein (Song and Forciniti 2000; Wiącek and Chibowski 2002). Some features that structure and strengthen the adsorbed protein are of a crucial importance in preventing coalescence of particles, that is, breaking of the emulsion structure; this is known as stability. The adsorbed layer, especially of proteins, is important in aggregation and deposition processes of a dispersed solid phase (Wiącek and Chibowski 2002). In some systems, it has been described that small amounts of the adsorbed protein can promote flocculation by bridging forces to peptides, drugs, ions and other additives (Fan et al. 2014).

Some proteins such as HSA and BSA, at large concentrations, can produce a greatly enhanced stability by an effect known as steric stabilisation (Xiong et al. 2014). The size of the particles affect the stability of emulsion or colloidal suspension; when the particles are small, the dispersion is more stable because the proteins usually change their conformation state after adsorption at the oil–water interface, and the adsorption is strong (Sontum and Christiansen 1997). The ζ-potential is a partial characterisation of the molecular behaviour of the nanostructured particles; however, a complete characterisation should include molecular interactions (biochemical analysis), interfacial behaviour (spectroscopy, microscopy, tensiometry) and bulk properties (dispersion formation, stability and rheology; Sathiya and Akilandeswari 2014).

11.5 Case of Study: Nanostructuration of Particles of BSA and BSA–Capsaicin

The chilli pepper (*Capsicum* spp.) is one of the most important cultivated vegetables and spice crops worldwide (Bosland and Votava 2005; Wang and Bosland 2006). Capsaicin (CAP; (*E*)-*N*-(4-hydroxy-3-methoxybenzil)-8-methyl-*trans*-6-nonanamide) and dihydrocapsaicin ((*E*)-*N*-(4-hydroxy-3-methoxybenzil)-8-methyl-nonanamide) are the main chemical compounds responsible for the spiciness (pungency) of chilli pepper (Kosuge and Furuta 1970); they are synthesised from intermediates of phenylpropanoid pathway and are chemically classified as alkaloids (Perucka and Oleszek 2000). CAP has been applied in the food and pharmaceutical industry (Reyes-Escogido et al. 2011). It has a wide variety of biological and physiological activities which provide some functions such as antioxidant (Antonious et al. 2009), antitumour agent (Lu et al. 2010), inhibitor of the growth of the gastric pathogens (Zeyrek and Oguz 2005) and anti-inflammatory agent (Kim and Lee 2014). Furthermore, different potential applications of these molecules in foods include their use as inhibitors of the growth of food-borne pathogenic bacteria and as additives or flavours (Dorantes et al. 2000); however, they are limited by the irritation caused due to their pungency, and their efficiency decreases because of their quick release properties in some environments. Wanga et al. (2013) developed microcapsules containing CAP which were prepared by the solvent evaporation method via O/W emulsion. Microencapsulates of CAP demonstrated that polylactic acid is a potentially useful biodegradable polymer for making controlled-release microcapsules by the solvent evaporation method. However, its use has not been approved in foods. The encapsulation of CAP may represent an alternative to manipulate and administrate it in the form of microparticles. The authors of the present chapter have developed nanostructurated microparticles of BSA by desolvatation methods and conjugated those microparticles with molecules of CAP at the particle surface, characterising the physicochemical properties of these interactions.

The BSA used in the referred process was molecular biology grade free of DNase, RNase and proteases (Research Organics, USA), and glutaraldehyde 25 % (Sigma Aldrich, Germany) and salts were analytical grade (Merck, Germany). CAP ((*E*)-*N*-(4-hydroxy-3-methoxybenzil)-8-methyl-*trans*-6-nonanamide) was ≥95 %, from *Capsicum* sp. (Sigma Aldrich, Germany). BSA particles were prepared by a desolvation technique as described earlier (Langer et al. 2003). While for the BSA–CAP particles, CAP was diluted in ethanol; 40 mg of CAP was dissolved in 3 mL of 100 % ethanol under shaking for 5 min at 8 °C. A similar process for the preparation of BSA particles was carried out. The desolvation agent was the ethanol-CAP solution. Particles were transformed by the continuous addition (1.0 mL/min) of 3 mL of the ethanol-CAP solution under stirring (160 rpm) at room temperature. After the desolvation process, 5 mL of glutaraldehyde 4 % in a sodium chloride 10 mM solution was added, inducing the cross-linking for 30 min at room temperature. In both treatments, the purification was carried out by centrifugation (3,648 × g, 30 min) and dispersion of the pellet in 10 mM NaCl at pH 9, respectively.

In this case of study, the non-particulated BSA and BSA–CAP were calculated by the solid fraction remaining after the desolvation which was recovered and stored in tubes of 2-mL capacity. Both samples were freeze dried and subsequently weighed. Also, the total protein (TP) content of BSA and BSA–CAP was determined by a monochromator spectrophotometer, EPOCH (Biotek, USA), based on UV-Vis with wavelength selection at 280 nm by the Gen5 Data Analysis software interface (Biotek, USA).

On the other hand, the size of BSA and BSA–CAP particles was measured by using a PS analyser CILAS 1090 (CILAS, France), operating at the following conditions: deionised water as dispersing agent and DLS for polydispersed samples in liquid mode. An aliquot of the particle suspension (200 μL) was added in the chamber for liquid samples. No dilutions were used in this measurement. As mentioned above, ζ-potential is an important parameter to define the stability of the BSA and BSA–CAP particles in suspension. This parameter was measured by using a Zetaplus Analyser (Brookhaven Instruments, USA). For the analysis, 100 μL of the particles suspension was diluted with 9900 μL of deionised water, and the dispersion was achieved by shaking with a vortex mixer for 2 min. The ζ-potential of the particles was calculated by complete electrophoretic mobility distributions in a wide range of −220 to 220 mV dependent on the sample; the pH was determined by using an electrode for aqueous systems.

For the analysis of morphology of the BSA and BSA–CAP particles, 100 μL of the particle suspension was diluted with 9900 μL of deionised water, and the dispersion was achieved by shaking with a vortex mixer for 2 min. The particle suspension was mounted on glass slides and viewed under confocal laser scanning microscopy (CLSM) (LSM 710 NLO, Carl Zeiss, Germany) and magnification of 20x/0.8 M27 Plan-Apochromat. The fluorescence images of particles were acquired in RGB colour, stored in TIFF format at 8 bits and 512 × 512 pixels. Furthermore, a completely randomised experimental design and analysis of variance (ANOVA) were performed for evaluating the significance of the response variables: PS, ζ-potential (ζ), TP, pH, wet protein (WP), dry protein (DP) of BSA and BSA–CAP particles, with CAP content as the only factor.

For this study, the BSA is the main matrix that conjugates with other low weight molecules. The preparation of BSA particles provided conditions to obtain a well-established desolvation method. These properties were used to add CAP in the desolvation agent and establish a process to elaborate the BSA–CAP particles.

The hypothetical scheme of the formation of BSA and BSA–CAP microparticles is depicted in Fig. 11.1. First, an aqueous solution containing freeze-dried BSA was diluted at high stirring. The second step is the desolvation process which was carried out by the constant-velocity addition of ethanol to the BSA batches; for the case of BSA–CAP, CAP was diluted in ethanol solution; this process was carried out at low stirring. The final step was the addition of the cross-linked agent; in this step, the stabilisation of the particles should be carried out. The changes of pH play an important role in the conformational changes of proteins, exposing highly hydrophobic regions of BSA, to capture molecules of CAP.

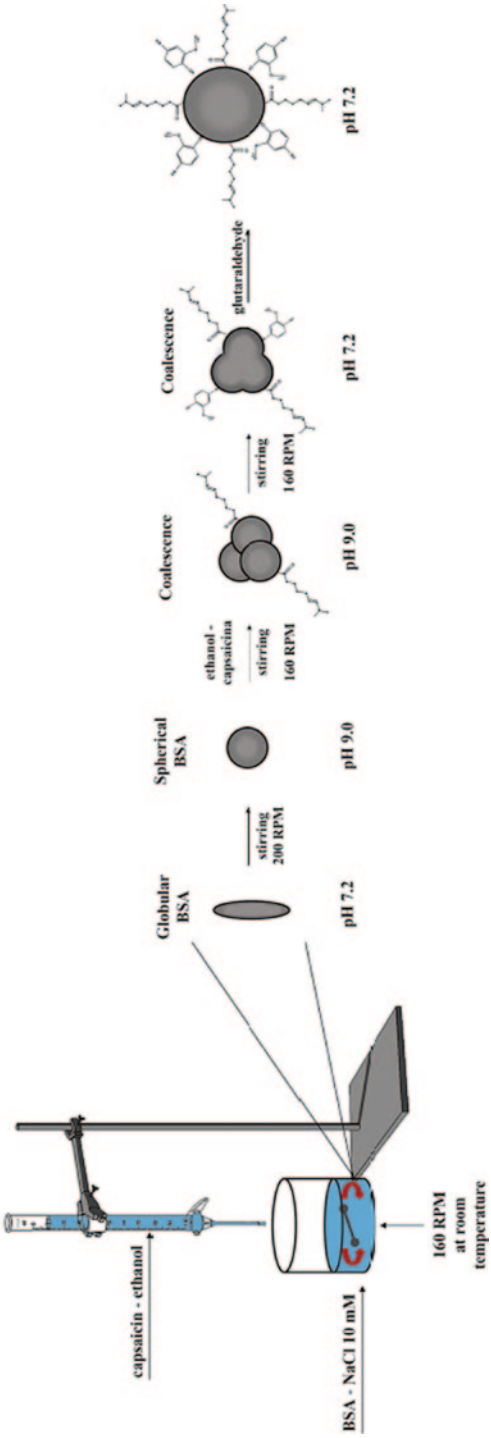

Fig. 11.1 Hypothetical scheme of the formation of BSA–CAP particles

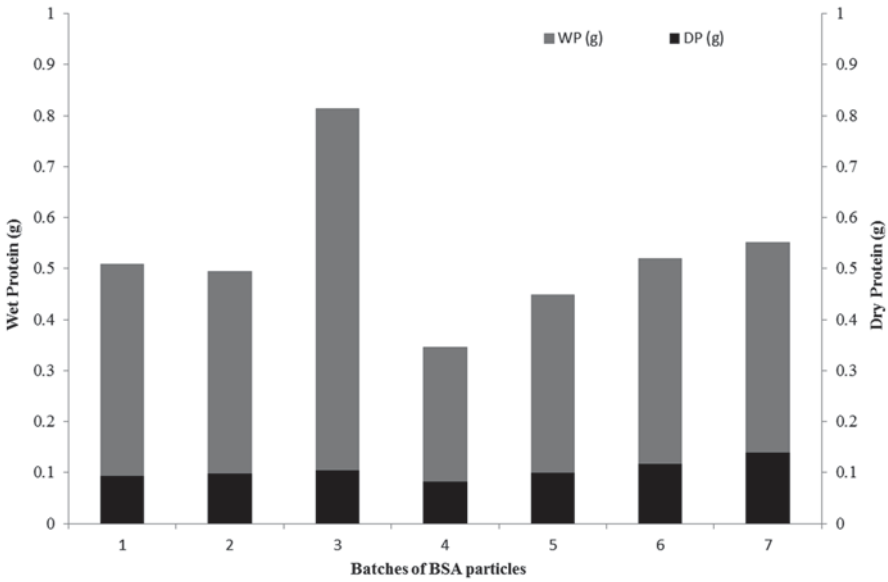

Fig. 11.2 Gravimetric differences between wet and dry weights of bovine serum albumin (*BSA*) protein, non-particulated, for *BSA* treatment. *DP* dry protein, *WP* wet protein

The effect of CAP addition in the desolvation method showed differences between batches of BSA and BSA–CAP (Fig. 11.2 and 11.3). In the treatment of BSA, the average recovery of dried BSA after the process was 50 % (0.10 ± 0.02 g). Therefore, half of the protein was converted to particles; the rest was precipitated in amorphous protein. The capacity of adsorption of the BSA was observed as accumulation of water (0.43 g of water, on average). Figure 11.2 shows the trend in batches of BSA particles and low variability in the wet BSA.

On the other hand, in batches which were added CAP, the average of dry BSA recovered after the process was 40 % (0.08 ± 0.02 g; Fig. 11.3). Therefore, 60 % of the protein was converted to particles; the rest was precipitated in amorphous protein. Jun et al. (2011) found that high concentrations of BSA increase the probability of coagulation. Consequently, larger hydrophobic interactions of BSA increased coagulation of the molecules and produced large particles. The increase in the PS of BSA–CAP batches might be explained by their surface charge and surface hydrophobicity. The surface hydrophobicity dictates the susceptibility to bind non-polar amino acid groups to a part of such surface (Arroyo-Maya et al. 2011).

CAP conjugated with BSA increased the hydrophobic interactions; probably, those electrostatic interactions occurred between the carbon chain region of CAP and binding sites of high affinity of BSA molecules. Choi et al. (2002) found that saturated fatty acids bind with increasing affinity as their chain length increases, at least between chain lengths of eight (octanoic) and 18 (stearic) carbons, due to an increase in hydrophobic interactions (Van der Vusse 2009).

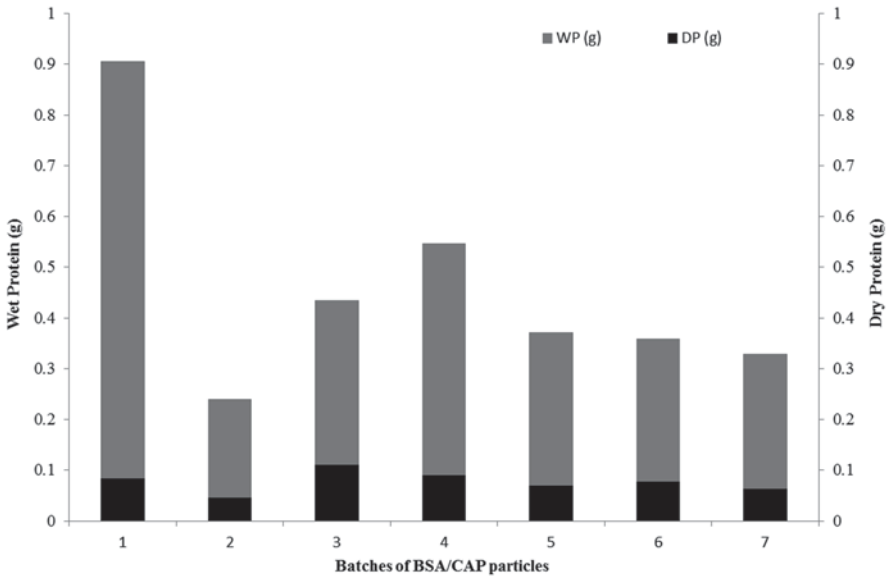

Fig. 11.3 Gravimetric differences between wet and dry weights of bovine serum albumin (*BSA*) protein, non-particulated, for *BSA*–capsaicin (*CAP*) treatment. *DP* dry protein, *WP* wet protein

The main characteristics of BSA particles are summarised in Table 11.1. The PS of BSA–CAP particles was significantly ($p<0.05$) higher than the PS of BSA particles. The BSA PS distribution showed low variability, but this distribution is probably attributed to the agglomerates of particles in small subunits around to a big particle. Finding particles in the range of nanometres is possible, but washing and centrifugation removed all particles of diameter below 1 μm.

The same desolvation process described for BSA particles was used for the preparation of particles with CAP (BSA–CAP). Results of seven batches of independent particle samples are summarised in Table 11.1. In comparison with BSA particles prepared under the same conditions, particles with CAP were larger, approximately 51 times, and showed a low variability in size. Langer et al. (2008) found an opposite behaviour in HSA particles respect to recombinant human serum albumin (rHSA) particles and attributed this effect to the aggregation during protein purification.

On the other hand, the stability and electrical behaviour of the particle surface were evaluated by means of ζ-potential and pH, showing no significant differences ($p>0.05$) for both treatments. In deionised water, BSA particles showed negative ζ-potential values and physiological pH. It means that BSA and BSA–CAP particles were stable; this feature was inherent to BSA because of physiological pH conditions (7.4); the ζ-potential depends on the composition and microstructural arrangement in the surface of the particles; this determines the interaction between electrical charges; while in alkaline conditions, the ζ-potential depends only slightly on the pH, and in acidic region (3–6), the dissociation of amine and carboxyl groups

Table 11.1 Physical-chemical characterisation of BSA particles

	BSA particles	BSA–CAP particles						
Batches	PS (μm)	ζ (mV)	TP (mg/mL)	pH	PS (μm)	ζ (mV)	TP (mg/mL)	pH
1	31.95	−26.11	0.376	6.75	116.41	−16.39	0.7125	7.31
2	5.74	−18.69	0.403	7.34	29.03	−25.36	0.822	7.45
3	4.14	−23.26	0.409	7.57	184.07	−17.63	0.575	7.56
4	6.08	−17.27	0.438	7.49	75.48	−27.51	0.595	7.62
5	5.05	−20.65	0.305	7.36	150.15	−24.61	0.228	7.14
6	27.22	−25.11	0.177	7.26	78.49	−4.46	0.6125	7.5
7	9.3	−26.14	0.154	7.49	24.17	−21.54	0.545	7.6
Mean	12.78	−22.46	0.32	7.32	657.80	−19.64	0.58	7.45
SD	11.67	3.63	0.12	0.27	59.79	7.83	0.18	0.17

PS particle size; ζ ζ-potential; *TP* total protein; *SD* standard deviation

determines the surface charge and the ζ-potential (Wiącek et al. 2014). Wiącek and Chibowski(2002) found that in a pH range of 7–10, the negative charge of freshly formed droplets is constant as a result of the total dissociation of –COOH groups. Moreover, the hydroxyl ions may interact with the protein molecules as well as they influence on the carboxyl group –COOH dissociation. The slight difference between ζ-potential values of BSA and BSA–CAP might be attributed to the interaction of CAP in the surface of particles of BSA–CAP. Therefore, the stability of particles was often higher than expected with respect to ζ-potential measurements. This caused that particles in suspension were stable and their resuspension was carried out by shaking after weeks of storage.

The TP quantified between batches of BSA and BSA–CAP showed difference ($p<0.05$) in the protein transformed in particles (see Table 11.1). The TP for both particles showed significant differences ($p<0.05$) being higher contents of protein for BSA–CAP particles. This difference was observed due to the size of particles in BSA–CAP that were larger and needed more protein in order to stabilise the spherical shape. The characterisation of BSA and BSA–CAP was carried out through the laser excitation wavelengths which were 405, 488, 561 and 633 nm with 4.0 % capacity for 405 nm and 2.0 % for 488–633 nm. This scanning allowed establishing the wavelengths of the BSA and CAP and the conjugate BSA–CAP. The spectrum of the CAP was established from 400 to 550 nm (Fig. 11.4a), for the crystals of

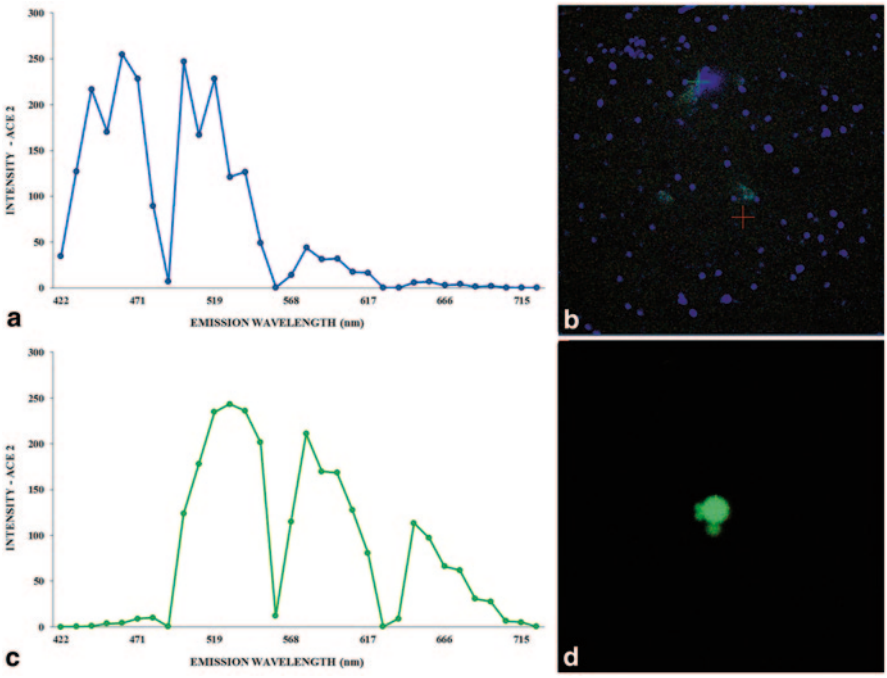

Fig. 11.4 **a** Emission spectrum of capsaicin, from 400 to 550 nm. **b** Crystals of capsaicin (standard). **c** Emission spectrum of BSA particles, from 490 to 625 nm. **d** Isolation of BSA particles (standard)

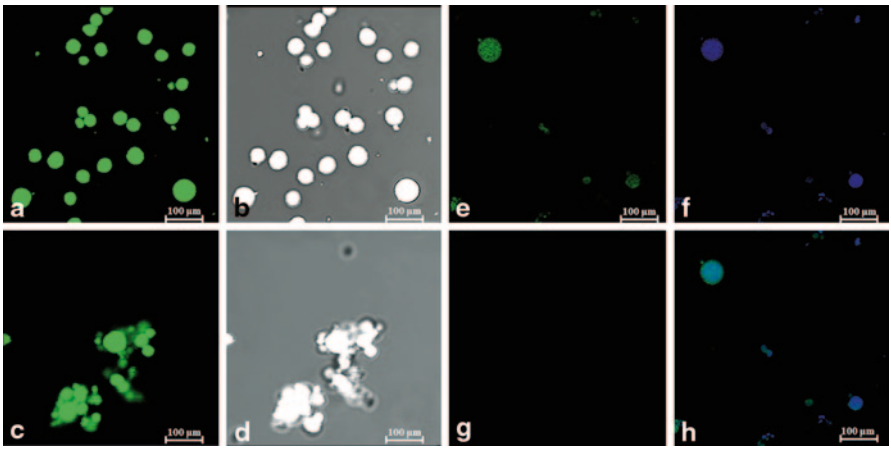

Fig. 11.5 Images of microparticles of BSA and BSA–CAP. **a** Fluorescent image of the spherical microparticles of BSA. **b** Complementary image in phase-contrast microscopy. **c** Agglomeration of BSA microparticles. **d** Complementary image in phase-contrast microscopy. **e** Fluorescent image of microparticles of BSA–CAP in signal of BSA. **f** Fluorescent image of the microparticles of BSA–CAP in signal of CAP. **g** Emission-excitation off. **h** Merge of BSA–CAP signal

CAP (Fig. 11.4b) in ethanol solution. The spectrum of BSA was found from 490 to 625 nm (Fig. 11.4c); this spectrum was constant in all samples and was measured in the particles (Fig. 11.4d), since the polymer of BSA showed different wavelength spectra.

The morphology of the BSA microparticles was spherical. This shape is due to the self-assembly of BSA molecules in the aqueous desolvating condition resulted in the spherical shape (Fig. 11.5a and b), and the fluorescent spectrum was found in the range between 400 and 550 nm in CLSM. However, the main observed size in the samples of microparticles of BSA ranged from 90 to 10 µm; these observations do not discard the possibility of finding nanoparticles in the sample. On the other hand, it was observed agglomeration of BSA microparticles (Fig. 11.5c and d). These agglomerates were composed by small-sized particles (below 1 µm).

In the samples of BSA–CAP, the microparticles were also spherical (Fig. 11.5e and f). This morphology showed similar behaviour in the self-assembly process of BSA molecules in the aqueous desolvating condition; however, the CAP-ethanol solution accelerates the process of the coacervation. CAP (molecule conjugates) was incorporated into the albumin microspheres and nanospheres cross-linked on the surface of the newly formed albumin particles; a similar process was found by Lin et al. (1997) in the preparation of surface-modified albumin nanospheres. The fluorescent spectrum was found in the range from 480 to 700 nm in CLSM. Both spectra, from CAP and BSA, are overlapped. This process formed a new BSA–CAP conjugate which is structurally inserted, forming a homogeneous surface in the protein particles (Fig. 11.5h). The size of microparticles observed in the BSA–CAP samples ranged from 50 to 5 µm; these observations do not discard the possibility of finding nanoparticles in the sample.

11.6 Conclusions

An alternative method for conjugating microparticles of BSA with CAP was proposed. These particles have wide potential applications, mainly related to the attenuation of pungent activity of CAP and biocompatibility and biodegradation of BSA. The role of CAP in the formation of BSA–CAP seems to be related to the PS. Evidence for the association of CAP with BSA in the complex BSA–CAP and the stability of the particles was obtained through measurements of ζ-potential as a function of pH. These values showed a slight increase in the surface electric charges. Nowadays, there are no studies that describe the kinetics and nanostructuration mechanism of materials that constitute nano-, micro- and macroparticulates. This work is a contribution to the description of an alternative method for developing carrier microparticles coupled to a short-chain lipid (CAP), as well as to the structuring mechanism.

References

Adhikari B, Howes T, Bhandari BR, Langrish TAG (2009a) Effect of addition of proteins on the production of amorphous sucrose powder through spray drying. J Food Eng 94:144–153

Adhikari B, Howes T, Wood BJ, Bhandari BR (2009b) The effect of low molecular weight surfactants and proteins on surface stickiness of sucrose during powder formation through spray drying. J Food Eng 94:135–145

Antonious FG, Lobel L, Kochhar T, Berke T, Jarret RL (2009) Antioxidants in *Capsicum chinense*:variation among countries of origin. J Environ Sci Heal B 44:621–626

Arroyo-Maya IJ, Rodiles-López JO, Cornejo-Mazón M, Gutiérrez-López GF, Hernández-Arana A, Toledo-Núñez C, Barbosa-Cánovas GV, Flores-Flores OJ, Hernández-Sánchez H (2011) Effect of different treatments on the ability of a-lactalbumin to form nanoparticles. J Dairy Sci 95:6204–6214

Bosland PW, Votava EJ (2000) Peppers: vegetable and spice *Capsicum*. CABI Publishing, New York

Bourassa P, Kanakis DC, Tarantilis P, Pollissiou GM, Tajmir-Riahi AH (2010) Resveratrol, genistein, and curcumin bind bovine serum albumin. J Phys Chem B 114:3348–3354

Choi K-J, Ho J, Curry S, Qin D, Bittman R, Hamilton AJ (2002) Interactions of very long-chain saturat fatty acids with serum albumin. J Lipid Res 43:1000–1010

Dorantes L, Colmenero R, Hernandez H, Mota L, Jaramillo ME, Fernandez E, Solano C (2000) Inhibition of growth of some foodborne pathogenic bacteria by *Capsicum annum* extracts. Int J Food Microbiol 57:125–128

Fan YH, Nazari M, Raval G, Khan Z, Patel H, Heerklotz H (2014) Utilizing zeta potential measurements to study the effective charge, membrane partitioning, and membrane permeation of the lipopeptide surfactin. BBA-Biomembranes 1838(9):2306–2312

Fang Z, Bhandari B (2012) Comparing the efficiency of protein and maltodextrin on spray drying of bayberry juice. Food Res Int. 48:478–483

Favaro C, Santana A, Monterrey E, Trindade M, Netto F (2010) The use of spray drying technology to reduce bitter taste of casein hydrolysate. Food Hydrocoll 24:336–340

Ferrer LM, Duchowicz R, Carrasco B, Torre GJ, Acuña UA (2001) The conformation of serum albumin in solution: a combined phosphorescence depolarization-hydrodynamic modeling study. Biophys J 80:2422–2430

Gebregeorgis A, Bhan C, Wilson O, Raghavan D (2013) Characterization of Silver/Bovine Serum Albumin (Ag/BSA) nanoparticles structure: morphological, compositional, and interaction studies. J Colloid Interf Sci 389:31–41

Gelamo LE, Silva PTHC, Imasato H, Tabak M (2002) Interaction of bovine (BSA) and human (HSA) serum albumins with ionic surfactants: spectroscopy and modelling. Biochim Biophys Acta 1594:84–99

Hermanson TG (2008) Bioconjugate techniques, 2nd ed. Academic Press, San Diego

Honda C, Kamizono H, Samejima T, Endo K (2000) Studies on thermal aggregation of bovine serum albumin as a drug carrier. Chem Pharm Bull 48:464–466

Huang BX, Kim H-Y (2004) Probing three-dimensional structure of bovine serum albumin by chemical cross-linking and mass spectrometry. J Am Soc Mass Spectr 15:1237–1247

Hunter JR (2001) Measuring zeta potential in concentrated industrial slurries. Colloid Surface A 195:205–214

Igathinathane C, Pordesimo LO, Columbus EP, Batchelor WD, Methuku SR (2008) Shape identification and particles size distribution from basic shape parameters using ImageJ. Comput Electron Agr 63:168–182

Jahanshahi M, Babaei Z (2008) Protein nanoparticle: a unique system as drug delivery vehicles. Afr J Biotechnol 7:4926–4934

Jun YJ, Nguyen HH, Paik S-Y-R, Chun SH, Kang B-C, Ko S (2011) Preparation of size-controlled bovine serum albumin (BSA) nanoparticles by a modified desolvation method. Food Chem 127:1892–1898

Kaibara K, Okazaki T, Bohidar HB, Dubin PL (2000) pH-induced coacervation in complexes of bovine serum albumin and cationic polyelectrolytes. Biomacromolecules 1(1):100–107

Kim Y, Lee J (2014) Anti-inflammatory activity of capsaicin and dihydrocapsaicin through heme oxygenase-1 induction in raw264.7 macrophages. J Food Biochem 38(4):381–387

Kosuge S, Furuta M (1970) Studies on the pungent principle of *Capsicum* part XIV chemical constitution of the pungent principle. Agric Biol Chem 34:248–256

Kratz F (2008) Albumin as a drug carrier: design of prodrugs, drug conjugates and nanoparticles. J Control Release 132:171–183

Langer K, Balthasar S, Vogel V, Dinauer N, Briesen von H, Schubert D (2003) Optimization of the preparation process for human serum albumin (HSA) nanoparticles. Int J Pharm 257:169–180

Langer K, Anhorn GM, Steinhauser I, Dreis S, Celebi D, Schrickel N, Faust S, Vogel V (2008) Human serum albumin (HSA) nanoparticles: reproducibility of preparation process and kinetics of enzymatic degradation. J Pharm 347:109–117

Lekago J, Dunford NT (2010) Effect of spray nozzle design on fish oil-whey protein microcapsule properties. J Food Sci 75:94–97

Lewis W, Keshavarz-Moore E, Windust J, Bushell D, Parry N (2006) Construction and evaluation of novel fusion proteins for targeted delivery of micro particles to cellulose surfaces. Biotechnol Bioeng 94:626–632

Lin W, Coombes A, Davies M, Davis S, Illum L (1997) Preparation of sub 100 nm human serum albumin nanospheres using a pH-coacervation method. J Drug Target 1:237–243

Lu F-H, Chen L-Y, Yang S-J, Yang Y-Y, Liu Y-J, Hsu C-S, Lai C-K, Chung G-J (2010) Antitumor activity of capsaicin on human colon cancer cells *in vitro* and colo 205 tumor xenografts in vivo. J Agric Food Chem 58:12999–3005

Martínez I, Partal P, Muñoz J, Gallegos C (2003) Influence of thermal treatment on the flow of starch-based food emulsions. Eur Food Res Technol 217:17–22

Moghimi MS, Hunter CA, Murray CJ (2001) Long-circulating and target-specific nanoparticles: theory to practice. Pharmacol Rev 53:283–318

Munin A, Edwards-Lévy F (2011) Encapsulation of natural polyphenolic compounds; a review. Pharmaceutics 3:793–829

Pascual-Pineda LA, Flores-Andrade E, Alamilla-Beltrán L, Chanona-Pérez JJ, Beristain CI, Gutiérrez-López FG, Azuara E (2013) Micropores and their relationship with carotenoids stability: a new tool to study preservation of solid foods. Food Bioprocess Technol 7:1160–1170

Perucka I, Oleszek W (2000) Extraction and determination of capsaicinoids in fruit of hot pepper *Capsicum annuum* L. by spectrophotometry and high-performance liquid chromatography. Food Chem 71:287–291

Phromsuwan U, Sirisathitkul C, Sirisathitkul Y, Uyyanonvara B, Muneesawang P (2013) Application of image processing to determine size distribution of magnetic nanoparticles. J Magn 18:311–316

Rahimnejad M, Najafpour G, Bakeri G (2012) Investigation and modeling effective parameters influencing the size of BSA protein nanoparticles as colloidal carrier. Colloid Surfac A 412:96–100

Reyes-Escogido LM, Gonzalez-Mondragon GE, Vazquez-Tzompantzi E (2011) Chemical and pharmacological aspects of capsaicin. Molecules 16:1253–1270

Robert P, Gorena T, Romero N, Sepulveda E, Chavez J, Saenz C (2010) Encapsulation of polyphenols and anthocyanins from pomegranate (*Punica granatum*) by spray drying. Int J Food Sci Tech 45:1386–1394

Sailaja KA, Amareshwar P, Chakravarty P (2011) Different techniques used for the preparation of nanoparticles using natural polymers and their application. Int J Pharm Pharm Sci 3:45–50

Sathiya KC, Akilandeswari S (2014) Fabrication and characterization of silver nanoparticles using *Delonix elata* leaf broth. Spectrochim Acta Mol A 128:337–341

Song D, Forciniti D (2000) Effects of cosolvents and pH on protein adsorption on polystyrene. J Colloid Interf Sci 221:25–37

Sontum CP, Christiansen C (1997) Photon correlation spectroscopy applied to characterisation of denaturation and thermal stability of human albumin. J Pharm Biomed Anal 16:295–302

Van der Vusse JG (2009) Albumin as fatty acid transporter. Drug Metab Pharmacok 24:300–307

Viveros-Contreras R, Téllez-Medina DI, Perea-Flores MJ, Alamilla-Beltrán L, Cornejo-Mazón M, Beristain-Guevara CI, Azuara-Nieto E, Gutiérrez-López GF (2013) Encapsulation of ascorbic acid into calcium alginate matrices through coacervation coupled to freeze-drying. Rev Mex Ing Quím 12:29–39

Walther T (2000) Photon correlation spectroscopy in particle sizing. In: Meyers AR (ed) Encyclopedia of analytical chemistry. Wiley, Chichester, pp 5469–5485

Wang D, Bosland PW (2006) The genes of *Capsicum*. HortScience 41:1169–1187

Wang F, Feng J, Gao C (2008) Manipulating the properties of coacervated polyelectrolyte microcapsules by chemical crosslinking. Colloid Polym Sci 286:951–957

Wanga J, Donga X, Chena S, Loub J (2013) Microencapsulation of capsaicin by solvent evaporation method and thermal stability study of microcapsules. Colloid J 75:26–33

Weber C, Reiss S, Langer K (2000a) Preparation of surface modified protein nanoparticles by introduction of sulfhydryl groups. Int J Pharm 211:67–78

Weber C, Coester C, Kreuter J, Langer K (2000b) Desolvation process and surface characterisation of protein nanoparticles. Int J Pharm 194:91–102

Wiącek EA, Chibowski E (2002) Zeta potential and droplet size of n-tetradecane/ethanol (protein) emulsions. Colloid Surface B 25:55–67

Wiącek EA, Anitowskaa E, Delgado VA, Hołysz L, Chibowski E (2014) The electrokinetic and rheological behavior of phosphatidylcholine-treated TiO2 suspensions. Colloid Surface A 440:110–115

Wine Y, Cohen-Hadar N, Freeman A, Frolow F (2007) Elucidation of the mechanism and end products of glutaraldehyde crosslinking reaction by X-Ray structure analysis. Biotechnol Bioeng 98:711–718

Wucherpfennig T, Lakowitz A, Driouch H, Krull R, Wittmann C (2012) Customization of Aspergillus niger morphology trough addition of talc micro particles. J Vis Exp 61:4023.

Yu RF, Chen HW, Cheng WP, Chu ML (2009) Simultaneously monitoring the particle size distribution, morphology and suspended solids concentration in wastewater applying digital image analysis (DIA). Environ Monit Assess 148:19–26

Xiong C, Zhou X, Zhang N, Zhan L, Chen S, Wang J, Peng W-P, Chang H-C, Nie Z (2014) Quantitative assessment of protein adsorption on microparticles with particle mass spectrometry. Anal Chem 86(8):3876–3881

Xu H, Liu Q, Zuo Y, Bi Y, Gao S (2009) Spectroscopic studies on the interaction of vitamin C with bovine serum albumin. J Solution Chem 38:15–25

Zeyrek Y, Oguz E (2005) *In vitro* activity of capsaicin against *Helicobacter pylori*. Ann Microbiol 55:125–127

Zhang S, Marini DM, Hwang W, Santoso S (2002) Design of nanostructured biological materials through self-assembly of peptides and proteins. Curr Opin Chem Biol 6:865–871

Zhang Y-Z, Dai J, Zhang P-X, Yang X, Liu Y (2008) Studies of the interaction between Sudan I and bovine serum albumin by spectroscopic methods. J Mol Struct 888:152–159

Zhang Y-Z, Zhou B, Zhang X-P, Huang P, Li C-H, Liu Y (2009). Interaction of malachite green with bovine serum albumin:Determination of the binding mechanism and binding site by spectroscopic methods. J Hazard Mater 163:1345–1352

Chapter 12
Polymer Nanocomposites for Food Packaging Applications

Shyam S. Sablani

12.1 Introduction

Over the past few decades, the use of polymer-based packaging for food has grown due to favorable properties, including low density, resistance to breakage and moisture, food ingredient resistance, fabricability into various shapes, transparency, colorability, and availability in a wide range of grades (Arora and Padua 2010). The most common polymers used for food packaging applications are polyolefins, copolymers of ethylene, substituted olefins, polyesters, polyamides (PAs; nylon), and polycarbonates.

These polymers provide a range of chemical and physical properties to the packages fabricated from them. The chemical composition, molecular structure, molecular weight, and degree of crystallinity of polymer determine the physical and chemical properties of packaging (Robertson 2006). Owing to their amorphous nature, polymers are inherently permeable to gases and vapors, including oxygen, carbon dioxide, organic volatiles, and water vapor. The finite oxygen gas-barrier property of polymers limits their application to the packaging of oxygen-sensitive foods.

During the past few decades, nanocomposites based on polymers and inorganic clay minerals consisting of silicate layers have been investigated (Ray et al. 2006, de Abreu et al. 2007; Arora and Padua 2010). Currently, interest is growing in the development of high oxygen-barrier polymeric structures for food packaging applications. In addition to improved gas-barrier properties, these polymer nanocomposites exhibit superior physical properties. This chapter presents a brief review on the preparation and characterization of polymer nanocomposites with emphasis on their gas barrier properties. The potential applications of such structures for in-package sterilization technologies are also highlighted.

S. S. Sablani (✉)
Biological Systems Engineering, Washington State University, Pullman, WA 99164-6120, USA

© Springer Science+Business Media New York 2015

H. Hernández-Sánchez, G. F. Gutiérrez-López (eds.), *Food Nanoscience and Nanotechnology,* Food Engineering Series, DOI 10.1007/978-3-319-13596-0_12

12.2 Preparation of Nanocomposites

Research on polymer nanocomposites has mostly focused on synthetic polymers such as polyethylene, polypropylene (PP), polystyrene, polycaprolactone, polycarbonate, PAs, ethylene vinyl alcohol (EVOH), polyethylene terephthalate (PET), and many others (Nguyen and Baird 2006). Most researchers have used layered silicates known as phyllosilicates to prepare polymer nanocomposites. Montmorillonite clay is the most common form of phyllosilicate used for the preparation of composites; however, other layered silicates such as hectorite, saporite, mica, talc, and vermiculite have also been investigated (Nguyen and Baird 2006). Montmorillonite clay has a plate-like structure and consists of magnesium aluminum silicate. The platelet structure and high aspect-ratio morphology lead to an improved permeation barrier through a tortuous path mechanism. The layer thickness of each platelet is on the order of 1nd chemical propertiedimension varies from 100 to 1000 nm. A clay platelet concentration varying from 1 to 5 % has been employed to investigate improvement in the gas-barrier and physical properties of polymer films. Nanoclay platelets have a very large surface area per unit mass, >750 at^2/g. These silicate platelets form layered structures and stacks, with a gap between them called the "interlayer" or the gallery (Ray et al. 2006).

These silicate platelets are dispersed in the polymeric matrix with a possible arrangement in one of the three forms: (1) nonintercalated or tactoid, (2) intercalated, and (3) exfoliated or delaminated structure (Carrado 2003; Ray et al. 2006; Fig. 12.1). Exfoliated arrangement of nanoclay platelets provides the maximum improvement in the gas barrier and physical properties. The dispersion of nanoclay platelets in the polymer matrix is difficult and often results in phase separation and agglomeration. In order to improve the dispersion of nanoclay in polymer matrix,

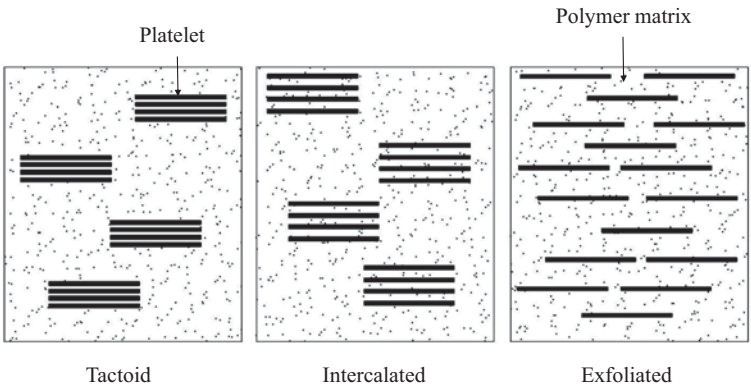

Fig. 12.1 Illustrations showing the tactoid, intercalated, and exfoliated state of the platelets dispersed in the polymer matrix. *Small dots* and *long black bars* represent the polymer matrix and nanoplatelets, respectively. (Adapted from Bhunia et al. 2012)

the platelets are chemically modified to render their surfaces more hydrophobic. The dispersion of nanoparticles in polymer liquid have been explained with a thermodynamic model that views entropic and enthalpic contributions as driving forces for intercalation and exfoliation of particles in long-chain polymer matrices (Vaia and Giannelis 1997; Arora and Padua 2010). Mackay et al. (2006) showed that the thermodynamically stable dispersion of nanoparticles into a polymeric liquid is enhanced when the radius of gyration of the linear polymer is greater than the radius of the nanoparticles.

Polymer nanocomposites are prepared using three common methods: (1) in situ polymerization, (2) intercalation of polymer from solution, and (3) polymer melt intercalation. The in situ polymerization method involves swelling of the layered silicate in monomer solution, followed by polymerization within the intercalated sheets. In the second method, both polymer and layered silicates are solubilized separately in a suitable solvent. The layered silicate solution is then dispersed in the polymer solution, allowing for polymer chain intercalation within the gallery of the silicate. The solvent is then evaporated to obtain exfoliated polymer composites. The polymer melt intercalation method is a solvent-free method and is widely used by the industry to produce polymer nanocomposites. In this method, layered silicates are incorporated into the molten polymer, either in a batch or in a continuous system. The polymer chains diffuse into the silicate galleries to form either intercalated or exfoliated structures, depending upon the degree of penetration (Nguyen and Baird 2006; Ray et al. 2006).

12.3 Characterization of Nanocomposites

The degree of exfoliation in a polymer nanocomposite determines the level of improvement in its physical and barrier properties. Several techniques are used to characterize the morphology of polymer nanocomposites. The most common techniques are wide-angle X-ray scattering (WAXS), small-angle X-ray scattering (SAXS), and transmission electron microscopy (TEM) (Arora and Padua 2010; Sedlakova et al. 2009; Nguyen and Baird 2006). WAXS can provide information on the interlayer spacing of the silicate layers in intercalated nanocomposites. However, this technique cannot provide information on the spatial distribution of the silicate layer in nanocomposites. SAXS is useful when silicate layer spacing exceeds 6–7 nm in intercalated or exfoliated nanocomposites. TEM facilitates the information on spatial distribution of silicates through direct visualization. TEM is a very time-consuming method and provides only qualitative information on selected regions of the polymer nanocomposite. Together, WAXS, SAXS, and TEM offer very valuable information on the polymer nanocomposite morphology.

12.4 Barrier Properties

Polymer nanocomposites can offer improved gas barrier properties to reduce the diffusion of oxygen, water vapor across, and aroma through the matrix and to maintain food quality, thereby increasing the shelf life. Gas permeation through polymer nanocomposites follows a mass transport mechanism similar to that in a semicrystalline polymer matrix. During gas permeation, gas molecules are initially adsorbed on the surface of the polymer and then diffuse through the polymer. In a nanocomposite, the polymer phase is considered to be permeable, and silicate platelets are considered to be nonpermeable to gases (Choudalakis and Gotsis 2009). The barrier property of a polymer material can be described in terms of permeability, which is dependent on the diffusion coefficient of gas and the solubility coefficient of that gas in the polymer matrix. However, research has mostly focused on the estimation of the diffusion and permeability coefficients for nanocomposites, rather than modeling the solubility coefficient (Bhunia et al. 2012). The diffusion of gases in the nanocomposite is influenced by the structural parameters of platelets, including the volume fraction, aspect ratio, orientation angle, and, most importantly, the degree of exfoliation in the polymer nanocomposite (Bhunia et al. 2012; Choudalakis and Gotsis 2009; Gusev 2001; Bharadwaj 2001).

Mathematical studies have shown that polymer nanocomposites with exfoliation configuration exhibited better gas-barrier properties compared with intercalation. The mathematical simulation showed a strong dependence of gas diffusion through composites on aspect ratio, volume fraction, and intercalation width of platelets. Gas-barrier properties showed great improvement, with increasing aspect ratios and volume fractions of nanoparticles (Bhunia et al. 2012; Choudalakis and Gotsis 2009; Gusev 2001; Bharadwaj 2001; Gusev and Lusti 2001). However, no significant improvement in barrier properties was found beyond the platelet volume fraction of 0.05 and the aspect ratio of 500 for exfoliated configuration. A computer model using the commercial software COMSOL Multiphysics illustrated that the gas diffusivity of nanocomposites increased as the rotational angle of platelet increased, gradually diminishing the influence of platelets. Gas diffusivity increased dramatically, as θ changed from 15 to 30°. In fact, the relative increment in relative diffusivity was almost 3.5 times larger (Bhunia et al. 2012). Using a simulated case study, Bhunia et al. (2012) showed that the total amount of oxygen ingress can be reduced by 97 % by incorporating platelets with an aspect ratio of 1000 and a volume fraction of 0.07, dispersed in exfoliated form in the composites. This may improve the shelf life of food stored in a polymer nanocomposite-based packaging. Mathematical models provide a valuable tool for the design and manufacturing of an ideal nanocomposite with improved gas barrier properties for industrial applications.

Several experimental studies have demonstrated significant improvement in gas barrier properties after incorporation of silicates in polymer matrix. Gupta et al. (2006) reviewed the physical and barrier properties of PA-6-clay nanocomposites. They highlighted the work of Liang et al. (2001), which shows that PA-6/

montmorillonite prepared with in situ polymerization reduced the oxygen transmission rate (OTR) of neat PA from 2.2 to 0.45 cc mil/100 in.^{2} day, when 8 % of the silicates were incorporated into the nanocomposites. Akkapeddi et al. (2003) found a significant reduction in the OTRs of nylon-6-based nanocomposites in which the silicate plates of high aspect ratio were incorporated. The polymer nanocomposites were prepared using in situ polymerization process. The OTRs were further reduced by incorporating oxygen scavengers into the matrix. Cabedo et al. (2004) developed EVOH-kaolinite nanocomposites using a melt intercalation process. A proper chemical modification of the natural kaolinite helped improve the degree of exfoliation, increasing the basal spacing from 0.72 nm to values over 3 nm. The researchers also noted an increase in the thermal resistance, glass transition temperature, crystallinity, and oxygen barrier properties. De Abreu et al. (2007) reported that 5 % of Cloisite 15 A nanoparticles in PP- and low-density polyethylene (LDPE)-based composites reduced the OTR from 480 to 374 and from 240 to 210 cc/m^2 day, respectively. Multilayer packaging films incorporating montmorillonite layered silicate and MXD6 nanocomposite as the oxygen barrier layer and LDPE as the moisture resistant layer were developed by the US Army Natick Soldier Research Center using a coextrusion process (Thellen et al. 2009). Silicate concentration at 3.3–3.6 % reduced the OTR of neat film from 3.7 to 1.1 cc/m^2 day. Frounch and Dourbash (2009) developed nanocomposites of PET and two different montmorillonite platelets using a polymer melt intercalation process. They used a corotating twin screw extruder to produce the films and found the lowest oxygen permeability with 1 wt.% nanolin/PET nanocomposite. The Cloisite 15 A exhibited optimal barrier properties, at 2 wt.% (Table 12.1). Results show that the permeability decreased with an increasing degree of exfoliation.

In addition to improving gas-barrier properties, adding 1–5 wt.% of nanoclay has been shown to improve the mechanical properties of polymer films (Chaudhary et al. 2008; Ray et al. 2006; Cho and Paul 2001). Cho and Paul observed a significant improvement in modulus and yield strength of composites after incorporation of 5 % of montmorillonite in nylon-6. Ray et al. (2006) have shown an increase of 100 % in Young's modulus of nylon-6 and LDPE-based nanocomposites (Ray et al. 2006). Incorporation of nanoparticles into polymers has been shown to improve thermal performance, e.g., temperature resistance, flame resistance, thermal decomposition behavior, and linear dimensional changes (Chaudhary et al. 2008; Ray et al. 2006).

12.5 Food Packaging Applications

Polymer nanocomposites with improved oxygen, carbon dioxide, water vapor, and aroma barrier properties are attractive and highly desirable for food packaging applications. High-oxygen barrier films are useful for the packaging of processed cheese and meats. Advanced food-processing technologies, including microwave-

Table 12.1 Oxygen permeability or oxygen transmission rate of polymer nanocomposites

Polymer	Nanoparticles	Method of preparation	Oxygen transmission rate or oxygen permeability		Reference
			Neat film	Composite film	
Polyamide-6	Montmorillonite	–	2.2[a]		Liang et al. (2001)
	2 %			1.4	
	4 %			0.95	
	6 %			0.80	
	8 %			0.45	
Ethylene vinyl alcohol	Kaolinite 2 to 8 %	Compression molding	0.35[b] 45 °C dry condition	–	Cabedo et al. (2004)
Polypropylene	Cloisite 15 A 5 %	Extrusion	480[b]	374	de Abreu et al. (2007)
Low-density polyethylene	Cloisite 15 A 5 %	Extrusion	240[b] 30 °C	210	
Nylon MXD6	Silicate 3.3–3.6 %	5-layer multilayer co-extruded film	3.7[b] 60 % RH	1.1	Thellen et al. (2009)
Polyethylene terephthalate	Cloisite	Corotating twin screw extruder	0.223[c]		Frounchi and Dourbash (2009)
	1 %			0.179	
	2 %			0.157	
	3 %			0.187	
	Nanolin				
	1 %			0.123	
	2 %			0.157	
	3 %			0.155	

[a] OTR, cc mil/100 in.^{2} day
[b] OTR, cc/m^2 day
[c] Permeability, cm^3 cm/m^2 day bar

assisted thermal sterilization (MATS) and pressure-assisted thermal sterilization (PATS) processes, also require enhanced oxygen-barrier polymer packaging for shelf-stable foods. Both the MATS and PATS processes require food to be processed inside its packaging. This exposes the packaging material to temperature, radiation, and pressure extremes that are required for the production of shelf-stable foods. Food packages are required to have very low gas transmission rates in order to protect shelf-stable food against oxygen and water vapor entry. Increases in oxygen permeation into food packaging may severely affect the sensory properties of lipid-containing foods due to rancidity reactions. Water loss or gain during storage can cause moisture-sensitive foods to spoil quickly. Polymer nanocomposite-based multilayer packaging is a promising option for replacing metal and glass-based rigid packaging.

Significant industrial efforts are being made for the design and development polymer nanocomposites. In a joint venture with Mitsubishi Gas Chemical, Nanocor has developed EVOH and MXD6 aromatic nylon-based nanocomposites for multilayer packaging films for moisture and oxygen-sensitive foods. A new family of Aegis nylon-6 nanocomposites has been developed by Honeywell Polymers for use in high-barrier PET beer bottles and is also being considered as a replacement for EVOH in films and pouches. Nanocor and Eastman Chemical have researched nanocomposites of PET and polyethylene (Ray et al. 2006). The ColorMatrix Corporation currently supplies ultra high-barrier nylon composites Imperm® for oxygen-sensitive products and exceptional CO_2 retention for carbonated soft drinks, waters, beers, and flavored alcoholic beverages. Imperm® is most useful in multilayer bottles, films, and thermoformed containers. Durethan KU-2601 (Bayer AG), composed of nylon and layered silicate barriers, has been developed for use in the coatings of paperboard juice containers (Chaudhary et al. 2008).

12.6 Final Remarks

A higher level of fully dispersed nanoclay must be achieved in order to increase the order of magnitude in the gas-barrier properties of polymer nanocomposites. A mathematical framework has been developed for the effective design of nanocomposite structures with superior gas-barrier properties. The melt intercalation technique is widely accepted for the preparation of polymer nanocomposites. A better understanding of clay modification, dispersion, and polymer-clay interaction is needed for the development of exfoliated nanocomposite structures. A limited number of polymer nanocomposites are available in some countries, and it is widely anticipated that the applications of such composites will emerge on the global packaging market. As the applications of polymer nanocomposites for food grows rapidly, the safety and regulatory aspects related to the nanocomposites as food contact materials will need to be addressed.

References

Akkapeddi K, Socci E, Kraft T, Facinelli J, Worley D (2003) A new family of barrier nylons based composites and oxygen scavengers. In: Proceedings of the 61st annual technical conference—society of plastics engineers, Vol 3, Nashville, 4–8 May, pp 3845–3848

Arora A, Padua GW (2010) Review: nanocomposites in food packaging. J Food Sci 75:43–49

Bharadwaj RK (2001) Modeling the barrier properties of polymer layered silicate nanocomposites. Macromolecules 34:9189–9192

Bhunia K, Dhawan S, Sablani SS (2012) Modeling the oxygen diffusion of nanocomposite-based food packaging films. J Food Sci 77:29–38

Cabedo L, Gimenez E, Lagaron JM, Gavara R, Saura JJ (2004) Development of EVOH-kaolinite nanocomposites. Polymer 45:5233–5238

Carrado KA (2003) Synthetic organo and polymer-clays: preparation, characterization, and minerals applications. Appl Clay Sci 17:1–23

Chaudhary Q, Scotter M, Blackburn M, Blackburn J, Ross B, Boxall A, Castle L, Aitken R, Watkins R (2008) Applications and implications of nanotechnologies for the food sector. Food Addit Contam 25:241–258

Cho JW, Paul DR (2001) Nylon 6 nanocomposites by melt compounding. Polymer 42:1083–1094

Choudalakis G, Gotsis AD (2009) Permeability of polymer/clay nanocomposites: a review. Eur Polym J 45:967–984

de Abreu DAP, Losada PP, Angulo I, Cruz JM (2007) Development of new polyolefin films with nanoclays for application on food packaging. Eur Polym J 43:2229–2243

Frounchi M, Dourbash A (2009) Oxygen barrier properties of poly(ethylene terephthalate) nanocomposites films. Macromol Mater Eng 294:68–74

Gupta B, Lacrampe MF, Krawczak P (2006) Polyamide-6/clay nanocomposites: a critical review. Polym Polym Compos 14:13–38

Gusev AA (2001) Numerical identification of the potential of whisker- and platelet-filled polymers. Marcomolecules 34:3081–3093

Gusev AA, Lusti HR (2001) Rational design of nanocomposites for barrier applications. Adv Mater 13:1641–1643

Liang Y, Omachinski S, Logsdon J, Cho W, Lan T (2001) Nano-effect in in-situ nylon-6 nanocomposites. In: Proceedings of the ANTEC 2001 plastics: the lone star, Vol 2, Dallas, 6–10 May, p 2218

Mackay ME, Tuteja A, Duxbury PM, Hawker CJ, Van Horn B, Chen GH, Krishnan RS (2006) General strategies for nanoparticle dispersion. Science 311:1740–1743

Nguyen QT, Baird DG (2006) Preparation of polymer-clay nanocomposites and their properties. Adv Polym Technol 25:270–285

Ray S, Quck SY, Easteal A, Chen XD (2006) The potential use of polymer clay nanocomposites in food packaging. Int J Food Eng. doi:10.2202/1556-3758.1149

Robertson GL (2006) Food packaging. principles and practices, 2nd edn. CRC Press, Boca Raton

Sedlakova Z, Plestil J, Baldrian J, Slouf M, Holub P (2009) Polymer-clay nanocomposites prepared via in situ emulsion polymerization. Polym Bull (Berl) 63:365–384

Thellen C, Schirmer S, Ratto JA, Finnigan B, Schmidt D (2009) Co-extrusion of multilayer poly(m-xylylene adipimide) nanocomposite films of high oxygen barrier packaging applications. J Memb Sci 340:45–51

Vaia RA, Giannelis EP (1997) Polymer melt intercalation in organically-modified layered silicates: model predictions and experiments. Macromolecules 30:8000–8009

Chapter 13
Nanobiosensors in Food Science and Technology

Angélica G. Mendoza-Madrigal, Jorge Chanona-Pérez, Leonor Guadarrama-Fernández, Humberto Hernández-Sánchez, Georgina Calderón-Domínguez, Eduardo Palacios-González and Rubén López-Santiago

13.1 Introduction

Nanotechnology is playing an increasingly important role in the development of biosensors (Vo-Dinh et al. 2001; Haruyama 2003). The sensitivity and performance of biosensors are being improved by using nanomaterials for their construction. The use of these nanomaterials has allowed the introduction of many new signal transduction technologies in biosensors. Because of their submicron dimensions,

J. Chanona-Pérez (✉) · L. Guadarrama-Fernández
H. Hernández-Sánchez · G. Calderón-Domínguez
Departamento de Ingeniería Bioquímica, Escuela Nacional de Ciencias Biológicas, Instituto Politécnico Nacional, Plan de Ayala y Carpio s/n, Col. Santo Tomás, C.P., 11340 México, DF, Mexico
e-mail: jorge_chanona@hotmail.com

A. G. Mendoza-Madrigal
Universidad Autónoma del Estado de Morelos, Escuela de Nutrición, Calle Río Iztacihuatl s/n, Col. Vista Hermosa C. P. 62350, Morelos, México
e-mail: gabrielamenmad@gmail.com

L. Guadarrama-Fernández
e-mail: leonorgf_ibq@hotmail.com

H. Hernández-Sánchez
e-mail: hhernan1955@yahoo.com

G. Calderón-Domínguez
e-mail: gcalderon@ipn.mx

E. Palacios-González
Laboratorio de Microscopía de Ultra Alta Resolución, Instituto Mexicano del Petróleo, Eje Central Lázaro Cárdenas 152, Col. San Bartolo Atepehuacan, C.P., 07730 México, Mexico
e-mail: lameuar@imp.mx

R. López-Santiago
Departamento de Inmunología, Escuela Nacional de Ciencias Biológicas, Instituto Politécnico Nacional, Plan de Ayala y Carpio s/n, Col. Santo Tomás, C.P., 11340 México, DF, Mexico
e-mail: rlslennon@gmail.com

© Springer Science+Business Media New York 2015

H. Hernández-Sánchez, G. F. Gutiérrez-López (eds.), *Food Nanoscience and Nanotechnology,* Food Engineering Series, DOI 10.1007/978-3-319-13596-0_13

nanosensors, nanoprobes, and other nanosystems have allowed simple and rapid analyses in vivo. Biosensors, which are devices that integrate a biological probe and a transducer, have been receiving increasing interest for environmental, industrial, and biomedical diagnostics.

In the food sector, one of the most important problems is the time-consuming and laborious process of food quality-control analysis. Innovative devices and techniques are being developed to facilitate the preparation of food samples and their precise and inexpensive analysis. From this point of view, the development of nanosensors to detect microorganisms and contaminants is a particularly promising application in food nanotechnology (Sozer and Kokini 2009).

Biosensors have recently been defined as analytical devices incorporating a biological material (e.g., tissue, microorganisms, organelles, cell receptors, enzymes, antibodies, nucleic acids, natural products), a biologically derived material (e.g., recombinant antibodies, engineered proteins, aptamers), or a biomimetic (e.g., synthetic catalyst, combinatorial ligands, and imprinted polymers) intimately associated with or integrated within a physicochemical transducer or transducing microsystem, which may be optical, electrochemical, or mass based (Lazcka et al. 2007).

13.2 Biosensors

Figure 13.1 shows a schematic diagram of a biosensor where the bioreceptor recognizes the target analyte, and the corresponding biological responses are then converted into equivalent electrical signals by the transducer. The amplified signal is

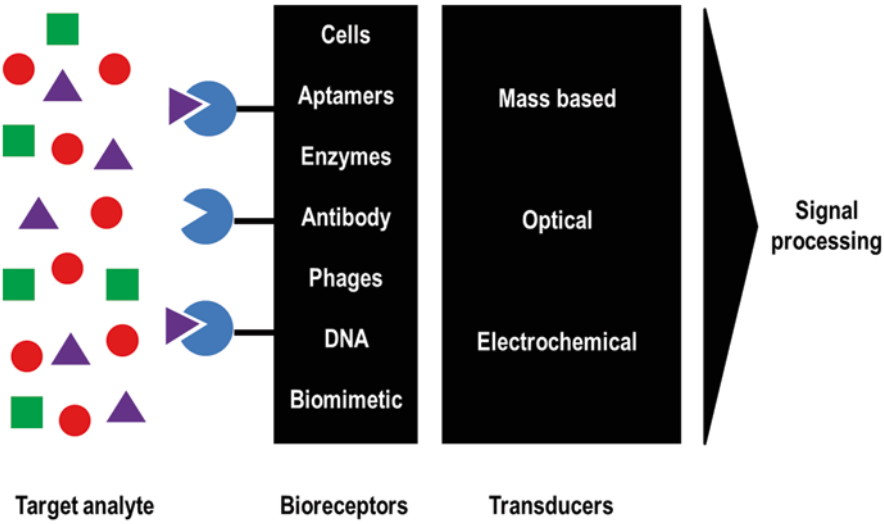

Fig. 13.1 Schematic diagram of a biosensor where the operating principle is shown. It consists of a target analyte, bioreceptors (cells, aptamers, enzymes, antibody, phages, DNA, biomimetic compounds), and a transducer (electrochemical, optical, and mass based)

then processed by the signal processor where it can later be stored, displayed, and analyzed. Biosensors have seen a wide variety of applications primarily in biological monitoring, food safety, and environmental sensing.

13.2.1 Classification

There is a wide variety of bioreceptors such as cells, enzymes, DNA, phages, and antibodies that can be detected by different transduction methods which are electrochemical, optical, and mass based; therefore, biosensors can be classified by their bioreceptor or detection method (Kim et al. 2009; Velusamy et al. 2010; Waggoner and Craighead 2007).

13.2.1.1 Bioreceptors

Biosensors can also be classified according to the type of bioreceptors or the recognition element which are the key to specificity for biosensor technologies. A bioreceptor is a molecular species that utilizes a biochemical mechanism for recognition. They are responsible for binding the analyte of interest to the sensor for the measurement. Bioreceptors can generally be classified into seven different major categories. These categories include enzymes, cellular structures/cells, antibody/antigen, nucleic acids/DNA, and bacteriophage (phage; Velusamy et al. 2010).

Enzymes were the first recognition elements included in biosensors (Clark and Lyons 1962). Enzymatic biosensors measure the selectivity inhibition or the catalysis of enzymes by a specific target; this kind of biosensors for the detection of contaminants in food and environmental samples has been extensively described (Li et al. 2009; Van Dorst et al. 2010). Another frequently used recognition element is whole cells such as bacteria, fungi, yeast, or animal cells. These whole-cell biosensors detect responses of a cell after exposure to a sample, which are related to its toxicity. Microorganisms or whole cell offer an alternative in the fabrication of biosensors because they can be massively produced through cell culturing. Even though metabolisms of the microorganisms are nonspecific, highly selective microbial biosensors can be potentially achieved by blocking the undesired or inducing the desired metabolic pathway and by adapting the microorganisms to an appropriate substrate of interest (target) through selective cultivation conditions. Cells provide sensitivity to a wide range of biochemical stimuli since they contain many highly evolved biochemical pathways; also, cells provide a functional assay for biochemical agents. Close et al. (2009), Nugaeva et al. (2005), and Su et al. (2011) described whole-cell biosensors for food and environmental applications.

Antibodies have been the most popular affinity-based recognition elements. The main advantage of the use of antibodies as recognition elements is their sensitivity and selectivity; they may be polyclonal, monoclonal, or recombinant, depending on their selective properties and the way they are synthesized. In any case, they are generally immobilized on a substrate, which can be the detector surface (Oh et al.

2005), its vicinity (Radke and Alocilja 2005), or a carrier (Ivintski et al. 2000). An antigen-specific antibody fits its unique antigen in a highly specific manner, so that the three-dimensional structures of antigen and antibody molecules are matching. Due to this three-dimensional shape fitting, it is possible to find an antibody that can recognize and bind to any one of a large variety of molecular shapes (Byrne et al. 2009; Velusamy et al. 2010).

On the other hand, phages and nucleic acids are the novel innovative affinity-based recognition elements that are becoming increasingly important for food and environmental sensors, because of their exceptional characteristics, such as their high affinity and specificity for their targets, their fast and cheap production, stability, and their ease to be modified (Van Dorst et al. 2010). Due to their wide range of physical, chemical, and biological activities, nucleic acid-based biosensors have been reported by many researchers for the detection of food pathogen such as *Escherichia coli* O157:H7 (Chen et al. 2008) and *Salmonella* spp. (Lermo et al. 2007). DNA hybridization microarrays have been suggested as a platform for the parallel detection of multiple pathogenic microorganisms in food in a relatively short time.

Recently, bacteriophages have been employed as biorecognition elements for the identification of various pathogenic microorganisms. Bacteriophages are viruses that bind to specific receptors on the bacterial surface in order to inject their genetic material inside the bacteria. Phages recognize the bacterial receptors through its tail spike proteins. Since the recognition is highly specific, it can be used for the typing of bacteria and hence opened the path for the development of specific pathogen detection technologies. There has been reported the application of phage as a biorecognition element for the detection of various pathogens such as *E. coli* (Singh et al. 2009).

13.2.1.2 Transductors

Biosensors can also be classified based on the transduction methods they employ. The transducer plays an important role in the detection process of a biosensor. The main fundamental transduction modes could be categorized as electrochemical, optical, and mass based (Fig. 13.2; Table 13.1). However, there are certain compounds used to improve the detection (label based); in other cases, a label is not required (label free).

Biomolecules such as proteins and nucleic acids often cannot be recognized directly due to their small size. To track these biomolecules and their activity, probes for these target molecules or the target biomolecules themselves can be labeled by conjugation with a detectable agent, commonly a fluorophore or an enzyme which has unique detectable properties such as radioactivity, chromogenicity, fluorescence, or magnetism (Kim et al. 2009). Some of these tags are fluorescent labels (Li et al. 2007), nanomaterials such as gold nanoparticles (Huo and Worden 2007), magnetic nanoparticles (Hsing et al. 2007), and quantum dots (QDs; Jamieson et al. 2007).

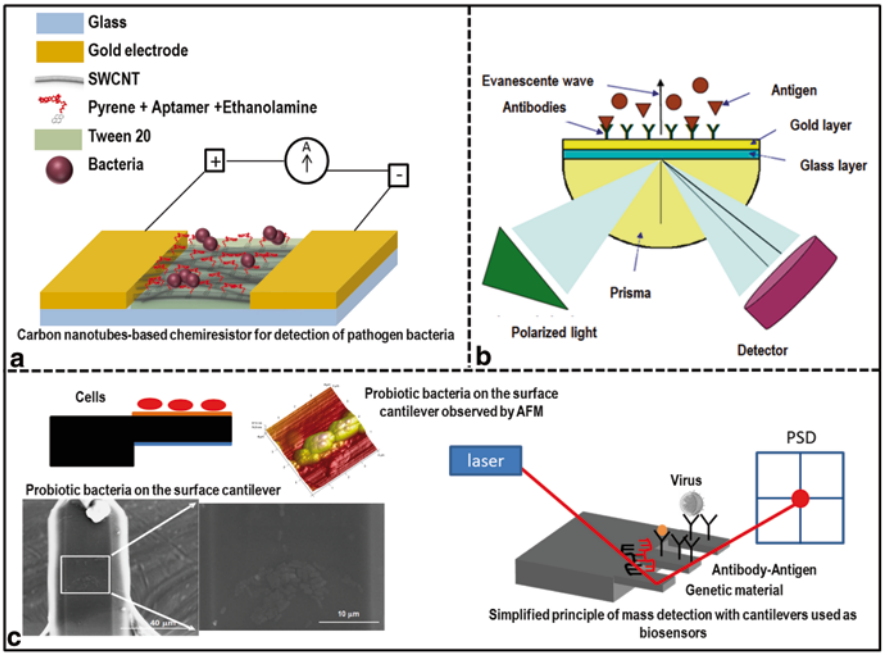

Fig. 13.2 Transduction methods. **a** Electrochemical-based transductor: carbon nanotube-based chemiresistor for the detection of pathogen bacteria. **b** Optic-based transductor for the detection of antigen–antibody. **c** Mass-based transductor for the detection of probiotic bacteria on the surface of a cantilever. Scanning electron microscope (SEM) and atomic force microscope (*AFM*) images with bacterial growth are shown as well as the detection by means of a position sensitive detector (*PSD*) using different bioreceptors

Nanotechnology is playing an increasingly important role in the development of biosensors (Vo-Dinh et al. 2001; Haruyama 2003). Sensitivity and other attributes of biosensors can be improved by using nanomaterials in their construction. Nanomaterials (matrices with at least one of their dimensions ranging in scale from 1 to 100 nm) display unique physical and chemical features (Jianrong et al. 2004). Functional nanoparticles (electronic and optical) bound to biological molecules (e.g., peptides, proteins, nucleic acids) have been developed for use in biosensors to detect and amplify various signals. Gold nanoparticles have been used as new class fluorescence quenchers to develop an optical biosensor for recognizing and detecting specific DNA sequences (Maxwell et al. 2002). Metal nanoparticles can be used to enhance the amount of immobilized biomolecules in the construction of a sensor. Because of its ultrahigh surface area, colloidal Au has been used to enhance the DNA immobilization on a gold electrode, to ultimately lower the detection limit of the fabricated electrochemical DNA biosensor (Cai et al. 2001). Metal nanoparticles have been used to facilitate the electron transfer in nanoelectronic devices. Gold nanoparticles can greatly improve electron transfer across the monolayer molecules self-assembled on the surfaces of electrodes (Zhang et al. 2008). Most biological

Table 13.1 Transduction modes employed for the detection of food importance analytes

Type of biosensor	Analyte	Detection mode	Sensitivity	Reference
Electrochemical- based detection				
Type of biosensor	Analyte	Detection mode	Sensitivity	Reference
Electrochemical- based detection				
Immunosensor based on electrochemical sandwich immunoassay	*E. coli* O157:H7	Amperometric	78 CFU/ml	Muhammad-Tahir and Alocija 2003b
Electrochemical sandwich immunoassay using polyaniline	*E. coli* and *Salmonella* spp.	Conductometric	79 CFU/ml	Muhammad-Tahir and Alocija 2003a
Biosensor based on the attachment of bacteria to platinum surfaces	*E. coli*	Impedimetric	101–107 CFU/ml	Munoz-Berbel et al. 2008
Optical-based detection				
Optical detection by means of protein chip	*E. coli* O157:H7, *S. typhimurium, Y. enterocolitica*, and *L. pneumophila*	Fluorescence microscopy surface plasmon resonance, and imaging ellipsometry	10^2 CFU/ml	Choi and Oh 2008
Quantum dots composed of CdSe/ZnS core/shell using flow cytometry	*E. coli* O157:H7	Quantum dots	10^6 cells/ml	Hahn et al. 2008
Multiplexed sandwich chemiluminescent enzyme immunoassay	*E.coli* O157:H7, *Y. enterocolitica, S. typhimurium*, and *L. monocytogenes*	Chemiluminiscent innmunoassay	104–105 CFU/ml	Magliulo et al. 2007

Table 13.1 (continued)

Type of biosensor	Analyte	Detection mode	Sensitivity	Reference
Electrochemical- based detection				
Type of biosensor	Analyte	Detection mode	Sensitivity	Reference
Electrochemical- based detection				
Mass-based detection				
Magnetoelastic cantilever	*B. anthracis*	Magnetic	10^5 CFU/ml	Li et al. 2009
Cantilever with a nutritive layer	*E. coli*	Photodetection	~ 140 pg/Hz	Gfeller et al. 2005
Gold microcantilevers functionalized with antibodies	*Vibrio cholerae* O1	Atomic force microscope	~ 1×10^3 CFU/ml and m/f~ 146.5 pg/Hz	Sungkanak et al. 2010
Nanocantilevers with very high frecuency characteristics	Evaluation of metallic layer frequencies	Thermo-mechanic displacement	39 fg $Hz^{-1/2}$	Li et al. 2007

CFU colony-forming unit

molecules can be labeled with metal nanoparticles without compromising their biological activities.

Furthermore, nanowires, nanotubes, nanofibers, and nanoprobes have been reported to create highly sensitive, real-time electrically based sensors for biological and chemical species. On the other hand, nanotubes have nanodimensions, graphitic surface chemistry, and electronic properties that make them an ideal material for use in chemical and biochemical sensing. Both single-wall carbon nanotubes (SWCNTs) and multiwall carbon nanotubes (MWCNTs) have been used in biosensors (Davis et al. 2003; Jianrong et al. 2004).

According to the detection principle, electrochemical techniques (transduction method) can be divided into amperometric (Akyilmaz et al. 2007), potentiometric (Ercole et al. 2003), conductimetric (Muhammad-Tahir and Alocija 2003a), and impedimetric (Munoz-Berbel et al. 2008); these techniques are widely used in the development of microbial biosensors.

Carbon nanotubes (CNTs) have been used in diverse devices to detect several biomolecules and microorganisms, more specifically single-wall carbon nanotubes (SWCNTs) because of their electrical properties, and the high surface area because they are highly reactive. Most of the sensor's performance are based on the change in the electrical conductance due to the binding of the interest molecule with the recognition molecule which is attached to the CNT network; here the CNTs are acting as the transducer element. The immobilization method of the biomolecules is the critical step on the biosensor construction, and it has to be chosen considering the recognition element and the sample nature. Most of the sensor's performance are based on the change in the electrical conductance due to the binding of the interest molecule with the recognition molecule which is attached to the CNT network; here the CNTs are acting as the transducer element. The immobilization method of the biomolecules is the critical step on the biosensor construction, and it has to be chosen considering the recognition element and the sample nature. Figure 13.2a shows a scheme of a biosensor which detects E. *coli* by means of antibodies (recognition element), the sensing platform used for the biodetection are gold microelectrodes where the SWCNTs are aligned in the microelectrode gap. The functionalization step is performed in situ. Then, a voltage is applied in the gold electrodes, and the conductance/resistance is measured; this conductance is highly sensitive to any change in the environment which is an advantage for this kind of biosensors because it allows the device miniaturization and the power requirement is low. There are several studies that have been reported for the detection of bacteria (Villamizar et al. 2009), viruses (García-Aljaro et al. 2010), and small molecules such as ATP (Basanta et al. 2011). The detection and identification of pathogenic microorganisms or molecules have great importance in health and food safety, the development of biosensors for an early detection with higher sensitivity is needed. Research in the area of biosensor is necessary to become a real alternative, and the integration of nanostructured materials in the construction of these is a promising option.

On the other hand, optical-based detection consists on the shift measurement of the optical properties after the interaction between the analyte and the recognition element; these properties are based on absorption, reflection, refraction, dispersion,

infrared, Raman diffusion (also surface-enhanced Raman scattering), chemiluminescence, fluorescence, and phosphorescence (Kim et al. 2007). The selection of the optical techniques depends on the analyte characteristics, desired sensitivity, and final application of the biosensor. The most commonly employed techniques of optical detection are surface plasmon resonance (SPR; Fig. 13.2b; Ponmozhi et al. 2012; Willets and Van Duyne 2007) and fluorescence (Ko and Grant 2006) due to their sensitivity. Using the SPR technique, the affinity of biomolecules has been measured, such as nuclear receptor–DNA interactions, DNA hybridization, small molecule–DNA interactions, quantitative immunoassays, drug–protein interactions, protein–ligand interactions, and antibody–antigen interactions (Englebienne et al. 2003; Nguyena et al. 2007).

The mass-based biosensors are suitable for very sensitive detection, in which the transduction is based on the small changes in mass (Fig. 13.2c). The principal means of mass analysis depends on the use of piezoelectric crystals, which can be made to vibrate at a specific frequency with the application of an electrical signal of a specific frequency. When a piezoelectric sensor surface, which has been coated with an antibody, is placed in a solution containing pathogens, the attachment of the agent to the antibody-coated surface results in an increase in the crystal mass, and this gives rise to a corresponding frequency shift. Mass-based detection is relatively easy to use and cost effective and offers direct label-free analysis with increased sensitivity and specificity (Länge et al. 2008; Vaughan et al. 2001).

Cantilever sensors, a class of acoustic-based sensors, are highly sensitive devices capable of label-free quantitative measurement of biomolecular interactions. They are a platform technology and adaptable for various diverse biosensing applications (Johnson and Mutharasan 2012). Nanocantilevers are another innovative class of biosensors. Their detection principle is based on their ability to detect biological-binding interactions, such as between antigen and antibody, enzyme and substrate or cofactor, and receptor and ligand, through physical and/or electromechanical signaling (Hall 2002). Nanocantilever devices have already had tremendous success in studies of molecular interactions and in the detection of contaminant chemicals, toxins, and antibiotic residues in food products (Ramirez-Frometa 2006). Pathogen detection is based on their ability to vibrate at various frequencies in dependence on the biomass of the pathogenic organisms. The silicon surface of nanocantilevers can be modified to attach antibodies, resulting in a change of the resonant frequency depending on the attached mass. Gupta et al. (2004) presented the microfabrication and application of arrays of silicon cantilever beams as microresonator sensors with nanoscale thickness to detect the mass of individual virus particles, and they demonstrated the detection of a single vaccinia virus particle with an average mass of 9.5 fg.

In Table 13.1, more examples of transduction modes employed for the detection of food importance analyte are summarized. Muhammad-Tahir and Alocija (2003b) developed a biosensor based on an electrochemical sandwich immunoassay using polyaniline for detecting foodborne pathogens, such as *E. coli* O157:H7. The biosensor is composed of two types of proteins: capture protein and reporter protein. After adding the sample, the target protein binds to the reporter protein and forms

a sandwich complex with the capture protein. The conductive polymer that is attached to the reporter protein serves as a messenger, reporting the amount of target protein captured in the form of an electrical signal. The architecture of the biosensor utilizes a lateral flow format, which allows the liquid sample to move from one pad to another by capillary action. Results show that the biosensor could detect approximately 7.8×10^1 colony forming unit per milliliter of *E. coli* O157:H7 in 10 min. The same research group (Muhammad-Tahir and Alocija 2003a) developed a conductometric biosensor for detecting food-borne pathogens. The biosensor provides a specific, sensitive, low volume, and near real-time detection mechanism. Results are presented to highlight the performance of the biosensor for enterohemorrhagic *E. coli* O157:H7 and *Salmonella* spp, which are of concern to biosecurity. The lower limit of detection is approximately 7.9×10^1 colony forming units per milliliter within a 10 min process. Another electrochemical-based detection biosensor was developed by Munoz-Berbel et al. (2008), where an approach for quantifying low concentrations of bacteria is described, particularly *E. coli*, based on the measurement of the initial attachment of bacteria to platinum surfaces, using impedance spectroscopy. The value of the interface capacitance in the preattachment stage (before 1 min of attachment) showed correlation with suspended concentration of bacteria from 10^1 to 10^7 CFU/ml. This method was found to be sensitive to the attachment time, to the applied potential, and to the size of the counter electrode.

On the other hand, Table 13.1 also shows optical-based detection biosensors. Choi and Oh (2008) developed an optical detection method based on protein chips for the detection of the various pathogens such as *E. coli* O157:H7, *Salmonella typhimurium, Yersinia enterocolitica,* and *Legionella pneumophila* in contaminated environments. Gold (Au) surface was modified with 11-mercaptoundecanoic acid, and the protein G was immobilized on the Au surface. The responses of the various pathogens such as *E. coli* O157:H7, *S. typhimurium, Y. enterocolitica,* and *L. pneumophila* to the protein chip were investigated by SPR, fluorescence microscopy, and imaging ellipsometry (IE). The lowest detection limit of the fluorescence-based protein chip was 10^2 CFU/ml, and the protein chip using IE could successfully detect the pathogens in concentrations varying from 10^3 to 10^7 CFU/ml. Hahn et al. (2008) utilized QDs to label *E. coli* O157:H7 in cell mixtures which results in greater accuracy and more closely approaches the ideal fluorophore for the pathogen detection using flow cytometry; the biosensor sensitivity was 10^6 cells/ml. A simple and rapid multiplexed sandwich chemiluminescent enzyme immunoassay has been developed by Magliulo et al. (2007) for the simultaneous detection of *E. coli* O157:H7, *Yersinia enterocolitica, Salmonella typhimurium*, and *Listeria monocytogenes*. When the samples were added to the main wells, the bacteria able to specifically bind to the corresponding monoclonal antibody were captured in one of the four subwells. Subsequently, a mixture of peroxidase-labeled polyclonal antibodies against the four bacteria was added, and the peroxidase activity of the bound polyclonal-labeled antibodies in each well was measured by an enhanced luminol-based chemiluminescent cocktail using a low-light charge-coupled imaging device. The assay was simple and fast, and the limit of quantification was in the order of

10^4–10^5 CFU/ml for all bacterial species. This method can be used as a screening test to evaluate the presence of these pathogen bacteria in different foodstuffs.

Finally, Table 13.1 shows mass-based detection biosensors as well. Li et al. (2007) described the fabrication and operation of self-sensing nanocantilevers with fundamental mechanical resonances up to very high frequencies (VHFs). These devices use integrated electronic displacement transducers based on piezoresistive thin metal films, permitting straightforward and optimal nanodevice readout. This nonoptical transduction enables applications requiring previously inaccessible sensitivity and bandwidth, such as fast Scanning Probe Microscopy (SPM) and VHF force sensing. The detection of 127 MHz cantilever vibrations is demonstrated with a thermomechanical noise-limited displacement sensitivity of 39 fm $Hz^{1/2}$. This enables chemisorption measurements in air at room temperature, with unprecedented mass resolution less than 1 ag. Gfeller et al. (2005) were able to detect *E. coli*, which is an indicator of fecal pollution of water and food products, with the help of a cantilever coated with agarose; the use of nanomechanical sensing device was able to detect active growth of *E. coli* cells within 1 h which is significantly faster than any conventional plating method which requires at least 24 h (Sozer and Kokini 2009). Sungkanak et al. (2010) demonstrated a cantilever-based *cholera* sensor; atomic force microscope (AFM) was used to measure the cantilever's resonance frequency shift due to mass of cell bound on microcantilever surface; the microcantilever-based sensor has a detection limit of 1×10^3 CFU/ml and a mass sensitivity of 146.5 pg/Hz, which is at least two orders of magnitude lower than other reported techniques.

13.3 Nanosensors in Food

Science and technology have many challenges in the food and bioprocess field due to the need to produce and manufacture high-quality products; this can be solved by means of nanotechnology. For instance, pathogen detection, food quality, encapsulation, delivery of bioactive compound, packing systems, and food storage are few examples of developing applications of nanotechnology that could improve production processes in order to provide products with better characteristics and functionalities in the food industry. In Table 13.2, some examples, outlooks, and applications are described.

Food quality is very important because the consumers request safe food, as well as pathogen free; in order to accomplish this, alternative may be the use of biosensors for the rapid detection of contaminants. On the other hand, encapsulation has been used for the controlled release of beneficial components that improve the host health, such as probiotics and antioxidants. The delivery of bioactive compounds is important because through nanotechnology, the bioavailability, solubility, and stability of the interest compounds can be improved. Regarding packing systems and food storage, through nanotechnology developments, longer shelf-life, safer packaging, better traceability of food products, and healthier food can also be improved.

Table 13.2 Applications of nanosensors in foods

Description	Advantages	Technology	Reference
Sensors for the grain storage conducting polymer nanoparticles which respond to analyte and volatiles in food storage environment and thereby detect the source and the type of spoilage	Thousands of nanoparticles can be placed on a single sensor to accurately detect the presence of insects or fungi inside stored grain bulk in bins	Food quality	Neethirajan and Jayas 2007, 2011
Systems for the rapid detection of spoilage of product components, for quality control caused by microorganisms at source and during production chain	Nanosensors can provide quality assurance by tracking microorganisms, toxins, and contaminants for automatic control. Nanotechnology also enables to implement low cost	Microorganism identification	Gfeller et al. 2005; Sungkanak et al. 2010; Van Dorst et al. 2010
Encapsulation has been used for the protection and controlled release of beneficial live probiotic species to promote the healthy gut function. The viability of probiotic organisms within freeze-dried yogurt can be improved by nanoencapsulation with calcium-alginate	Ease of handling, enhanced stability, protection against oxidation, retention of volatile ingredients, taste masking, moisture-triggered controlled release, pH-triggered controlled release, consecutive delivery of multiple active ingredients, change in the flavor character, long-lasting organoleptic perception, and enhanced bioavailability and efficacy	Encapsulation	Shefer 2008
Nanotechnology has shown greater potential in improving the efficiency of delivery of nutraceuticals and bioactive compounds in functional foods to improve human health	Nanotechnology can enhance solubility, improve bioavailability, and protect the stability of micronutrients and bioactive compounds during processing, storage, and distribution	Delivery of bioactive compounds	Neethirajan and Jayas 2007, 2011
Packaging systems include adding an antimicrobial nanoparticle into the package, dispersing bioactive agents in the packaging, and coating bioactive agents on the surface	Food packing nanotechnology offers longer shelf-life, safer packaging, better traceability of food products, and healthier food	Packing systems	Buonocore et al. 2005; Coma 2008

Table 13.2 (continued)

Description	Advantages	Technology	Reference
Active packaging films for the selective control of oxygen transmission and aroma affecting enzymes has been developed	Nanotechnology can effectively produce oxygen scavengers for sliced processed meat, beer, beverages, cooked pastas, and ready-to-eat snacks; moisture absorber sheets for fresh meat, poultry, and fish; and ethylene-scavenging bags for packaging of fruits and vegetables	Food storage	Rivett and Speer 2009

Food spoilages by pathogen microorganisms can be detected with nanosensors from days to hours or even minutes. Such nanosensors could be placed directly into the packaging material, where they would serve as "electronic tongue" or "noses" by detecting chemicals released during food spoilage (García et al. 2006). Other types of nanosensors are based on microfluidic devices (Baeummer 2004) and can also be used to detect pathogens efficiently in real time and with high sensitivity. A major advantage of microfluidic sensors is their miniature format and their ability to detect compounds of interest rapidly in only microliters of required sample volumes, which has already led to widespread applications in medical, biological, and chemical analysis; these devices are called lab on a chip (Vo-Dinh et al. 2001).

Nanoelectromechanical system (NEMS) technology is already in use, and these systems contain moving parts ranging from nano- to millimeter scale, which might serve as developing tools in food preservation. NEMS could be used in food quality control devices because they consist of advanced transducers for the specific detection of chemical and biochemical signals. The use of these systems has several advantages for food technology, such as portable instrumentation with quick response, low costs, and smart communication through various frequency levels. In the area of food safety and quality, nanotechnologies are particularly suitable because they are able to detect and monitor any adulteration in packaging and storage conditions. Nanotechnologies are also enabling the development of smaller, cheaper sensors, which will have a wide range of applications from monitoring the pollution in the environment, the freshness of food, or the stresses in a building or a vehicle, among other applications (Sozer and Kokini 2009).

Nowadays, the development of nanotechnology-based biosensors is expected to move in various directions, such as toward a progressive reduction of biosensors taken as advantage the nanoengineering advances, low cost of nanobiosensors, a tendency toward a high sensitivity and inexpensive sensing platforms for use in point of care diagnostics, and low-cost systems for use in remote, marginal areas where medical care is deficient, and full-scale labs are not available or where biodetection in real time is difficult. Thus, an example of nanobiosensor of low

cost is shown in Fig. 13.3a–d, where a chemiresistor based on single-wall carbon-nanotubes for the detection of *Staphylococcus aureus* was mounted in a microscope slide, and their resistance was evaluated with microtips by means of an electrical tests station. Other systems are the lab on a chip, but they may have different goals than single biosensors, such as the need for taking one sample and measuring many things about it, as will likely occur in analysis laboratories. These devices can be implemented by developing new assays with few steps than can be visually understood or by developing instruments that remove the complexity from the user and provide a digital or quantitative readout. These tendencies are being rapidly pursued at the present time. For which the nanobiosensors can reach their real potential, they must be integrated with appropriate packaging techniques, which are usually based on nano/microfluidics. Packaging is focused on how the nanosensor is interfaced to the real world, which may include how the nanosensor receives samples, how it is protected from the outside world, and how the outside world is protected from the nanosensor. Many nano-biosensor concepts have been invented, but the commercial applications have been limited, primarily by limitations in packaging and interfacing. To maximize the value of nanotechnology-based biosensors, it is necessary to integrate these sensors with appropriate micro/nanofluidic systems that can deliver appropriate samples to the sensing platform. Micro/nanofluidic approaches provide one of the most promising strategies to interface nanoengineered biosensors in a wide spectrum of food and biomedical applications (Erickson et al. 2008; Kim et al. 2009). Appropriate microfluidic delivery systems can be used to eliminate contamination, minimize analysis times, and enable portable systems. In any case, the impact of nanoscale sensors will have a profound effect on medical, food, and environmental testing.

Currently, the biosensing systems are wholly portables taking the advantages of the advances on micromachining, microelectronics, microfluidics, microseparation processes, biosensing with genomics, and proteomics techniques. Thereby, the final aim of nanotechnology integrates all stages in a single device involved in the biosensing process, such as the sample handling, preparation, mixing, separation, cell lysing, and biodetecting. Figure 13.3e shows a schematic example of an integrated microfluidic device with nanocomponents for the detection of pathogen microorganisms; in the initial stages, isolating, selecting, and concentrating the sample or eliminating other components that might interfere with the detection are required. These steps could be done by micro or molecular sieves, filtration membranes, and dielectrophoresis, among other purification tools. Then, in a following step separating the pathogenic species can make by selective separation, for instance, by means of antibody bioconjugation. It is also required to see which cells are viable, can be used for fluorescence labeling techniques, or alternatively electrochemical techniques. Subsequently, for the detection of intracellular components, cellular lysing is needed; this can be carried out by thermic, chemical, mechanical, or electrical agents to release the target analyte, which leads to the next block to perform the biodetection. On-chip methods, polymerase chain reaction (PCR), cantilever, and nanosensors-made nanotubes or nanowires are some of the techniques that can be used for this purpose. The transport process consists in the sample passing through

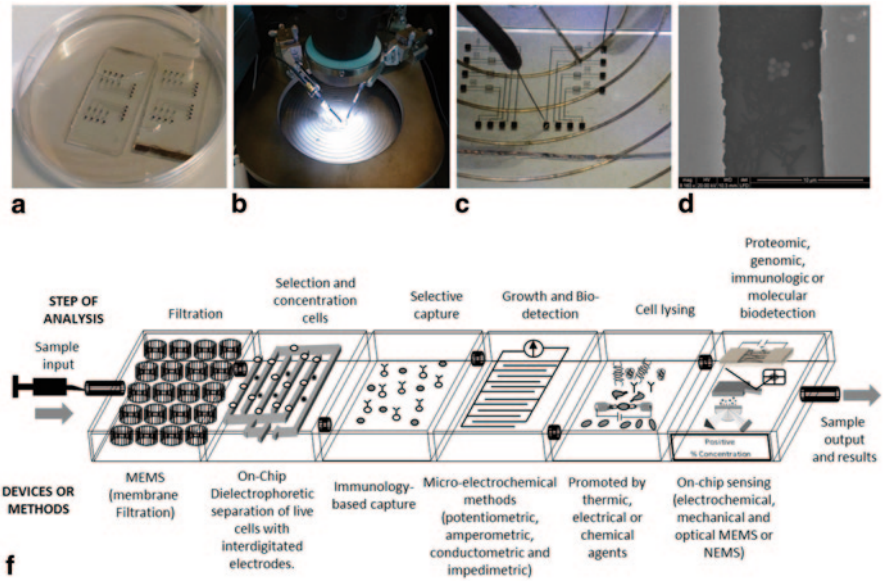

Fig. 13.3 **a** Chemiresistor based on single-wall carbon nanotubes for the detection of *Staphylococcus aureus*. **b** and **c** Resistance evaluation of the nanobiosensor with microtips in a electrical tests station. **d** Environmental scanning electron microscope (ESEM) image of the microelectrode after bacteria detection. **e** Integrated microfluidic devices with nanocomponents for the detection of pathogen microorganisms

an integrated micro-fluidic device which can perform osmotic gradients, electric, or pressure differential (Bashir 2004; Sósol-Fernández et al. 2012). In the end of lab on a chip, the user nonexpert on biodetection techniques receives the results of the test on a liquid crystal display.

13.4 Conclusions

Some advantages of the biosensors are their high sensitivity, selectivity, rapid detection time, and less solvent use; however, one of the main advantages is their versatility because they can be used in different areas such as food, environmental, pharmaceutical, and medical industries, among others. Different configurations or type of biosensors can be created, for instance, there can be chosen different kinds of bioreceptors that can be labeled or not, with gold nanoparticles, QDs, chromophore agents, depending on the transduction method which will be used. Among the transduction methods, the mass-based biosensor has as a major advantage, that a label is not always required to obtain higher specificity; the electrochemical transduction methods allow using fluid samples and the optical transductors to make real-time detections. The outlook regarding biosensors is the use of microfabrica-

tion techniques which has allowed the size reduction, mass production, less costs, feasibility in order to get a lab on a chip for the development of portable biosensors.

Thus, nanotechnology will have a significant impact on food safety for specific detection of a single cell, applying novel technologies that offer the nanotechnology for diagnosis and preventing disease associated to food contamination allows avoiding time consuming on several steps used in the traditional analysis of laboratory to provide faster results and smart solutions to food security.

Acknowledgments Angelica Gabriela Mendoza Madrigal wishes to thank *CONACyT* and *COFAA* for the scholarships provided. This research was supported through the projects 20110627 and 20121001 at the *Instituto Politécnico Nacional* (SIP-IPN), as well as "*Cátedra Coca-Cola para jóvenes investigadores 2011"* (Coca-Cola CONACyT).

References

Akyilmaz E, Erdogan A, Öztürk R, Yasa I (2007) Sensitive determination of L-lysine with a new amperometric micriobial biosensor based on *Saccharomyces cerevisiae* yeast cells. Biosens Bioelectron 22(6):1055–1060

Baeummer A (2004) Nanosensors identify pathogens in food. Food Technol 58:51–55

Basanta KD, Tlili C, Badhulika S, Cella L, Chen W, Mulchandani A (2011) Single-walled carbon nanotubes chemiresistor aptasensors for small molecules: picomolar level detection of adenosine triphosphatew. Chem Commun 47:793–795

Bashir R (2004) BioMEMS: state-of-the-art in detection, opportunities and prospects. Adv Drug Deliv Rev 56:1565–1586

Buonocore GG, Conte A, Corbo MR, Sinigaglia M, Del Nobile MA (2005) Mono- and multilayer active films containing lysozyme as antimicrobial agent. Innov Food Sci Emerg 6:459–464

Byrne B, Stack E, Gilmartin N, O'Kennedy R (2009) Antibody-based sensors: principles, problems and potential for detection of pathogens and associated toxins. Sensors 9:4407–445

Cai H, Xu C, He P, Fang Y (2001) Colloid Au-enhanced DNA immobilization for the electrochemical detection of sequence-specific DNA. J Electroanal Chem 510:78–85

Chen SH, Wu VCH, Chuang YC, Lin CS (2008) Using oligonucleotide-functionalized Au nanoparticles to rapidly detect food borne pathogens on a piezoelectric biosensor. J Microbiol Meth 73:7–17

Choi J-W, Oh B-K (2008) Optical detection of pathogens using protein chip. In: Kim YJ, Platt U (eds) Advanced environmental monitoring. Springer, New York, pp 348–362

Clark Jr LC Lyons C (1962) Electrode systems for continuous monitoring in cardiovascular surgery. Ann NY Acad Sci 102:29–45

Close DM, Ripp S, Sayler GS (2009) Reporter proteins in whole-cell optical bioreporter detection systems, biosensor integrations, and biosensing applications. Sensors 9:9147–9174

Coma V (2008) Bioactive packaging technologies for extended shelf life of meat-based products. Meat Sci 78(2):90–103

Davis JJ, Coleman KS, Azamian BR, Bagshaw CB, Green MLH (2003) Chemical and biochemical sensing with modified single walled carbon nanotubes. Chem-Eur J 9:3732–3739

Englebienne P, Hoonacker AV, Verhas M (2003) Surface plasmon resonance: principles, methods and applications in biomedical sciences. Spectroscopy 17:255–273

Ercole C, Del Gallo M, Mosiello L, Baccella S, Lepidi A (2003) *Escherichia coli* detection in vegetable food by a potentiometric biosensor. Sens Actuator B-Chem 91:163–168

Erickson D, Mandal S, Yang AHJ, Cordovez B (2008) Nanobiosensors: optofluidic, electrical and mechanical approaches to biomolecular detection at the nanoscale. Microfluid Nanofluid 4:33–52

Garcia M, Aleixandre M, Gutiérrez J, Horrillo MC (2006) Electronic nose for wine discrimination. Sensors Actuator B-Chemical 113:911–916

García-Aljaro C, Lakshmi C, Dhamanand S, Miso P, Muñoz JF, Yates V, Ashok M (2010) Carbon nanotubes-based chemiresistive biosensors for detection of microorganisms. Biosens Bioelectron 26:1437–1441

Gfeller KY, Nugaeva N, Herner M (2005) Micromechanical oscillators as rapid biosensor for the detection of active growth of *Escherichia coli*. Biosens Bioelectron 21:528–533

Gupta A, Akin D, Bashir R (2004) Single virus particle mass detection using microresonators with nanoscale thickness. Appl Phys Lett 84:1976–1978

Hahn MA, Keng PC, Krauss TD (2008) Flow cytometric analysis to detect pathogens in bacterial cell mixtures using semiconductor quantum dots. Anal Chem 80:864–872

Hall RH (2002) Biosensor technologies for detecting microbiological food borne hazards. Microbes Infect 4:425–432

Haruyama T (2003) Micro- and nanobiotechnology for biosensing cellular responses. Adv Drug Deliver Rev 55:393–401

Hsing IM, Xu Y, Zhao W (2007) Micro and nano magnetic particles for applications in biosensing. Electroanalysis 19:755–768

Huo Q, Worden JG (2007) Monofunctional gold nanoparticles: synthesis and applications. J Nanopar Res 9:1013–1025

Ivintski D, Abdel-Hamid I, Atanasov P, Wilkins E, Stricker S (2000) Application of electrochemical biosensors for detection of food pathogenic bacteria. Electroanalysis 12:317–325

Jamieson T, Bakhshi R, Petrova D, Pocock R, Imani M, Seifalian AM (2007) Biological applications of quantum dots. Biomaterials 28:4717–4732

Jianrong C, Yuqing M, Nongyue H, Xiaohua W, Sijiao L (2004) Nanotechnology and biosensors. Biotechnol Adv 22:505–518

Johnson BN, Mutharasan R (2012) Biosensing using dynamic-mode cantilever sensors: a review. Biosens Bioelectron 32:1–18

Kim S, Kim KC, Kihm KD (2007) Near-field thermometry sensor based on the thermal resonance of a microcantilever in aqueous medium. Sensors 7:3156–3165

Kim J, Junkin M, Kim DH, Kwon S, Shin YS, Wong PK, Gale BK (2009) Applications, techniques, and microfluidic interfacing for nanoscale biosensing. Microfluid Nanofluid 7:149–167

Ko SH, Grant SA (2006) A novel FRET-based optical fiber biosensor for rapid detection of *Salmonella typhimurium*. Biosens Bioelectron 21:1283–1290

Länge K, Rapp BE, Rapp M (2008) Surface acoustic wave biosensors: a review. Anal Bioanal Chem 391:1509–1519

Lazcka O, Del Campo FJ, Muñoz, FX (2007) Pathogen detection: a perspective of traditional methods and biosensors. Biosens Bioelectron 22:1205–1217

Lermo A, Campoy S, Barbe J, Hernandez S, Alegret S, Pividori M (2007) In situ DNA amplification with magnetic primers for the electrochemical detection of food pathogens. Biosens Bioelectron 22:2010–2017

Li M, Tang X, Roukes ML (2007) Ultra-sensitive NEMS-based cantilevers for sensing, scanned probe and very high-frequency applications. Nature Nanotechnol 2:114–120

Li H, Liu S, Dai Z, Bao J, Yang X (2009) Applications of nanomaterials in electrochemical enzyme biosensors. Sensors 9:8547–8561

Magliulo M, Simoni P, Guardigli M, Michelini E, Luciani M, Lelli R et al (2007) A rapid multiplexed chemiluminescent immunoassay for the detection of *Escherichia coli* O157: H7, *Yersinia enterocolitica, Salmonella typhimurium, and Listeria monocytogenes* pathogen bacteria. J Agric Food Chem 55:4933–4939

Maxwell DJ, Taylor JR, Nie S (2002) Self-assembled nanoparticles probes for recognition and detection of biomolecules. J Am Chem Soc 124:9606–9612

Muhammad-Tahir Z, Alocilja EC (2003a) A conductometric biosensor for biosecurity. Biosens Bioelectron 18:813–819

Muhammad-Tahir Z, Alocilja E. C (2003b) Fabrication of a disposable biosensor for *Escherichia coli* O157: H7 detection. IEEE Sens J 3:345–351

Munoz-Berbel X, Vigues N, Jenkins AT, Mas J, Munoz FJ (2008) Impedimetric approach for quantifying low bacteria concentrations based on the changes produced in the electrode-solution interface during the pre-attachment stage. Biosens Bioelectron 23:1540–1546

Neethirajan S, Jayas DS (2007) Sensors for grain storage. In: Abstracts of the 2007 ASABE Annual International Meeting, Minneapolis, 17–20 June 2007

Neethirajan S, Jayas DS (2011) Nanotechnology for the food and bioprocessing industries. Food Bioprocess Technol 4:39–47

Nguyena B, Taniousa FA, Wilson WD (2007) Biosensor-surface plasmon resonance: quantitative analysis of small molecule–nucleic acid interactions. Methods 42:150–161

Nugaeva N, Gfeller KY, Backmann N, Lang HP, Düggelin M, Hegner M (2005) Micromechanical cantilever array sensors for selective fungal immobilization and fast growth detection. Biosens Bioelectron 21:849–856

Oh B-K, Lee W, Chun BS, Bae YM, Lee WH, Choi J-W (2005) The fabrication of protein chip based on surface plasmon resonance for detection of pathogens. Biosens Bioelectron 20:1847–1850

Ponmozhi J, Frias C, Marques T, Frazao O (2012) Smart sensors/actuators for biomedical applications: a review. Measurement 45:1675–1688

Radke SM, Alocija EC (2005) A high density microelectrode array biosensor for detection of *E. coli* O157:H7. Biosens Bioelectron 20:1662–1667

Ramirez-Frometa N (2006) Cantilever biosensors. Biotechnol Appl Biochem 23:320–323

Rivett J, Speer DV (2009) Oxygen scavenging film with good interplay adhesion. US Patent 75141512

Shefer A (2008) The application of nanotechnology in the food industry. http://bionanotech.uniss.it/?p=703. Accessed 28 Sep 2014

Singh A, Glass N, Tolba M, Brovko L, Griffiths M, Evoy S (2009) Immobilization of bacteriophages on gold surfaces for the specific capture of pathogens. Biosens Bioelectron 24:3645–3651

Sósol-Fernández RE, Marín-Lizárraga VM, Rosales-Cruzaley E, Lapizco-Encinas BH (2012) Análisis de células en dispositivos microfluídicos. Rev Mex Ing Quím 11(2):227–248

Sozer N, Kokini JL (2009) Nanotechnology and its applications in the food sector. Trends Biotechnol 27:82–89

Su L, Jia W, Hou C, Lei Y (2011) Microbial biosensors: a review. Biosens Bioelectron 26:1788–1799

Sungkanak U, Sappat A, Wisitsoraat A, Promptmas C, Tuantranon A (2010) Ultrasensitive detection of Vibrio cholerae O1 using microcantilever-based biosensor with dynamic force microscopy. Biosens Bioelectron 26:784–789

Van Dorst B Mehta J Bekaert K Rouah-Martin E De Coen W Dubruel P Blust R Robbens J (2010) Recent advances in recognition elements of food and environmental biosensors: a review. Biosens Bioelectron 26:1178–1194

Vaughan RD, O´Sullivan CK, Guilbault GG (2001) Development of a quartz crystal microbalance (QCM) immunosensor for the detection of *Listeria monocytogenes*. Enzyme Microb Technol 29:635–638

Velusamy V, Arshak K, Korostynska O, Oliwa K, Adley C (2010) An overview of foodborne pathogen detection: In the perspective of biosensors. Biotechnol Adv 28:232–254

Villamizar R, Maroto A, Rius F (2009) Improved detection of Candida albicans with carbon nanotube field-effect transistors. Sens Actuator B-Chem 136:451–457

Vo-Dinh, T, Cullum, B. M, Stokes, D. L (2001) Nanosensors and biochips: frontiers in biomolecular diagnostics. Sens Actuator 74:2–11

Waggoner P, Craighead H (2007) Micro- and nanomechanical sensors for environmental, chemical, and biological detection. Lab Chip 7:1238–1255

Willets KA, Van Duyne RP (2007) Localized surface plasmon resonance spectroscopy and sensing. Annu Rev Phys Chem 58:267–297

Zhang G-J, Zhang G, Chua JH, Chee R-E, Wong EH, Agarwal A, Buddharaju KD, Singh N, Gao Z, Balasubramanian N (2008) DNA sensing by silicon nanowire: charge layer distance dependence. Nano Lett 8:1066–1070

Chapter 14
Carbon Nanotubes and Their Potential Applications in Developing Electrochemical Biosensors for the Detection of Analytes in Food

Leonor Guadarrama-Fernández, Angélica G. Mendoza-Madrigal, Jorge Chanona-Pérez, Arturo Manzo Robledo, Georgina Calderón-Domínguez, F. Xavier Rius, Pascal Blondeau and Jordi Riu

14.1 Introduction

Nanoscience is the study, understanding, and control of materials at the nanoscale, which is at the level of atoms, molecules, and quantum dots. Nanotechnology considers techniques and structures of size below 100 nm such as carbon nanotubes (CNTs), nanocrystals, and nanoparticles (Aqel et al. 2012). Carbon is the most versatile element that exists. In the form of graphite, it was discovered in 1779 and, 10 years later, in the form of diamond. In 1985, Kroto et al. discovered fullerenes and proved their stability in the gas phase. Afterwards research on structures made of graphitic sheets has increased, leading to the discovery of CNTs by Iijima (1991). He observed that the tubes obtained by the arc-discharge evaporation method have at least two layers, and the size of their outer diameter ranged from 4 to 30 nm, and their length was as high as 1 μm. In 1993, a new type of CNT was discovered with only one layer and a

J. Chanona-Pérez (✉) · L. Guadarrama-Fernández · G. Calderón-Domínguez
Departamento de Ingeniería Bioquímica, Escuela Nacional de Ciencias Biológicas, Instituto Politécnico Nacional, Plan de Ayala y Carpio S/N, Colonia Santo Tomas, CP 11340 México City, México
e-mail: jorge_chanona@hotmail.com

A. G. Mendoza-Madrigal
Universidad Autónoma del Estado de Morelos, Escuela de Nutrición, Calle Río Iztacihuatl s/n, Col. Vista Hermosa, C.P. 62350, Morelos, México
e-mail: gabrielamenmad@gmail.com

A. Manzo Robledo
Laboratorio de Electroquímica y Corrosión, Escuela Superior de Ingeniería Química e Industrias Extractivas, Instituto Politécnico Nacional, Edif. Z-5, 3er. Piso. UPALM-Zacatenco, CP 07738 México City, México

F. X. Rius · P. Blondeau · J. Riu
Department of Analytical and Organic Chemistry, Universitat Rovira i Virgili, Campus Sescelades, C/Marcel·lí Domingo s/n, 43007 Tarragona, Catalonia, Spain

© Springer Science+Business Media New York 2015

H. Hernández-Sánchez, G. F. Gutiérrez-López (eds.), *Food Nanoscience and Nanotechnology,* Food Engineering Series, DOI 10.1007/978-3-319-13596-0_14

diameter of 1–2 nm. Although CNTs were synthesized and described before 1991, the report of Iijima pointed to a potential research field (Aqel et al. 2012).

14.2 CNT Types

There are two main types of CNT, single and multiwalled. Single-walled CNTs (SWCNTs) are formed when a single layer of graphite (graphene) is rolled into a seamless cylinder. They have diameters in the range of 0.70 –1.60 nm (Iijima 1993) but usually are close to 1 nm. They have two regions with different physical and chemical properties, one is the sidewall and the other is the end cap. Their importance lays down on their electrical properties making them excellent conductors (Aqel et al. 2012).

Multiwalled CNTs (MWCNTs) can be considered as a group of concentric SWCNT with different diameters. They can have from 2 to 50 sheets of graphene; the interlayer distance is near to the distance between graphene layers in graphite. Their lengths and diameters differ from those of SWCNT; therefore, their properties are also quite different (Aqel et al. 2012; Iijima 1991).

14.3 CNT Structure

SWCNT can be described by a single vector $\vec{C}$ (chiral vector). Two atoms in a planar graphene sheet are chosen, and one is used as the origin of the vector. The chiral

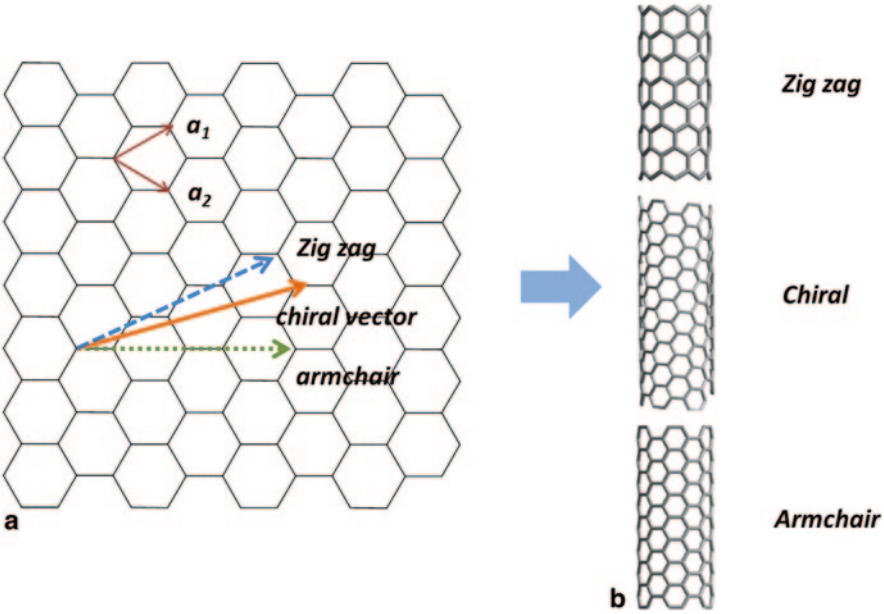

Fig. 14.1 **a** Graphene sheet diagram showing a chiral vector structure classification used to define CNT structure. **b** CNT types

vector $\vec{c}$ is pointed from the first atom toward the second one (Fig. 14.1a) and is defined by the equation:

$$C = \vec{n}_{a1} + \vec{m}_{a2}, \tag{14.1}$$

where n and m are integers and a_1 and a_2 are the unit cell vectors of the two-dimensional lattice formed by the graphene sheets. The direction of the nanotube axis is perpendicular to this chiral vector. The length of its chiral vector gives the circumference of the nanotube. Graphene sheets can be rolled in three different ways depending on the chiral $\vec{c}$. For $m = 0$ and $\theta = 30°$, zig-zag tubes are formed; for $n = m$ and $\theta = 0°$, armchair tubes are formed; and for $n \neq m$ and $0° < \theta < 30°$, the chiral tubes are formed (Fig. 14.1b). Chiral vector affects the optical, mechanical, and electrical properties of CNT (Aqel et al. 2012; Belin and Epron 2005; Dresselhaus et al. 1995).

An MWCNT structure is more complex than SWCNT, and thus they are mostly used as a bulk material in applications where the ordered structuring of the system is not of great importance. Varying the structure of CNT allows for control of their electric properties, such as electrical conductivity or electron emission properties. It is difficult to control the geometric structure of CNT by conventional synthetic methods, but recent techniques have been developed to generate CNT with controlled shapes and properties (Katz and Willner 2004).

14.4 CNT Synthesis

CNTs are produced mainly by three methods: arc discharge, laser ablation, and chemical vapor deposition (CVD) (Aqel et al. 2012). Arc discharge method is the most use for CNT production and is the same method used for fullerene synthesis. The principle of arc discharge technique is the formation of vapor by an arc discharge between two carbon electrodes under an inert atmosphere of helium or argon, using or not catalysts. CNTs are self-assembled from the carbon vapor produced by the high temperatures between the electrodes (Ebbesen and Ajayan 1992). The quantity and quality of CNT will depend on the experimental conditions as inert gas pressure, geometry of the system, carbon, and metallic catalyst ratio (Journet and Bernier 1998).

Laser ablation technique consists of vaporized graphite by irradiation with a high-power laser. Carbon is vaporized from the surface of a graphite piece that is in the middle of a quartz tube in a temperature-controlled oven and in an inert atmosphere. The laser vaporization produces carbon species, which are swept by the flowing gas from the high-temperature zone and deposited on a conical water-cooled copper collector. CNTs are formed when the laser beam gets the surface (Journet and Bernier 1998).

CVD methods utilize the pyrolytic decomposition of hydrocarbon gases at elevated temperatures in the range of 600–1200 °C. CVD technique has become one of the preferred methods for fabricating CNT. The reacting gas used can be acetylene, ethylene, or ethanol, and the metal catalysts used are cobalt, nickel, iron, or a

mix of them. The catalytic method can be widely used for the nanotube production; however, there is a big influence of various parameters such as the nature of the support, the size of active metal particles, and the reaction conditions on the formation of nanotubes (Aqel et al. 2012; Journet and Bernier 1998; Qin 1997).

There are studies in other methods for the CNT production using solar furnace or by electrolysis; also CNT can be synthesized by chemical reactions using polymers or by low-temperature solid pyrolysis (Journet and Bernier 1998). Each technique has some advantages or disadvantages. Which synthesis method is used will depend on the potential use of CNT. Some of the CNT preparation methods are more effective than others, but a problem that all methods face is the ability of the CNT to self-align.

Arc discharge allows the production of SWCNT and MWCNT at the same time. These tubes often covered with amorphous carbon may also contain metallic particles. The yield of CNT is not very high. With the laser ablation method, the yield is much higher, but the quantities are smaller. The CNTs obtained are very clean. And with the CVD method, only MWCNT can be formed and is covered by a thick layer of amorphous carbon. It is possible to get a higher yield of CNTs by optimizing the method for the decomposition of almost all carbon in the form of tubular filaments. Figure 14.2 shows the most important methods for synthesizing CNT.

A large problem with CNT application is the large-scale synthesis and also the purification. In all the CNT preparation methods, the CNT comes with a number of impurities whose type and amount depend on the technique used. The most common impurities are carbonaceous materials as graphite (wrapped up) sheets, amorphous carbon, and smaller fullerenes, whereas metals are the other types of impurities generally observed. These impurities will interfere with most of the de- sired properties of the CNT (Aqel et al. 2012; Ebbesen and Ajayan 1992).

The main objective of purification process is to remove amorphous carbon from the CNT, but it also has some other effects such as increasing or decreasing the

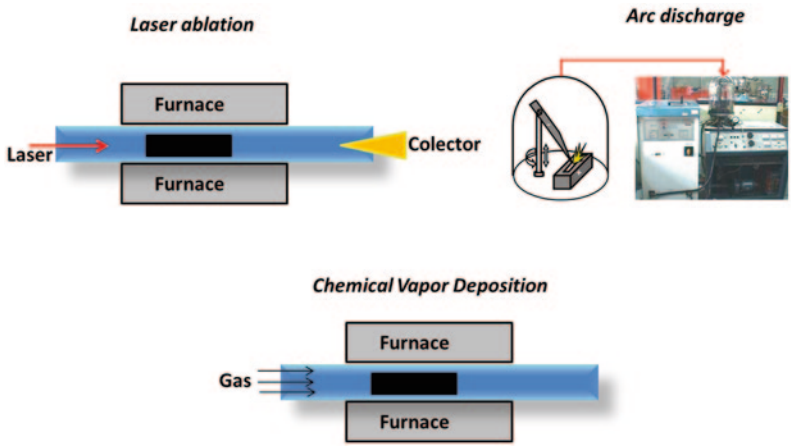

Fig. 14.2 The most important methods of CNT synthesis

volume of the pores, improvement of the surface area, and formation of functional groups. There are several techniques used for the purification process, and it is common to combine them in order to improve the CNT purification. The techniques that are most often used are oxidation treatment, acid treatment, sonication, thermal treatment, and filtration. The typical treatments involve the use of oxidative methods with nitric acid. The caps at both ends of the CNT are removed, and defects such as carboxylic acid groups on the surface are promoted. The properties of the nanotubes are influenced by these defect sites on the walls and at the ends (Aqel et al. 2012; Belin and Epron 2005; Hu et al. 2001, 2003). The techniques should only tear down the carbon impurities and the metals, without changing the CNT, but only few of them fulfill this requirement.

14.5 Characterization

To study the morphology and the structure of CNT, microscopic and spectroscopic techniques could be used. However, only few techniques are able to characterize CNT at the individual level such as scanning tunneling microscopy (STM) and electron microscopy (EM). X-ray photoelectron spectroscopy (XPS) is helpful in order to determine the chemical structure of nanotubes while neutron and X-ray diffraction, infrared (IR), and Raman spectroscopy are mostly global characterization techniques.

The techniques of EM that include transmission electron microscopy and scanning electron microscopy (TEM and SEM) are essential instruments to characterize nanomaterials such as CNT. It gives direct observation of shape, size, and structure. SEM is commonly used to overall observation of CNT morphology, while TEM is useful to measure outer, inner radius and number of layers. The determination of the structures of CNT within the bundles can be obtained using TEM coupled with electron diffraction. Various (Aqel et al. 2012; Iijima 1991, 1993) STM images give directly the three-dimensional morphology of tubes and are consistent with the structure inferred from SEM. It can resolve atomic structure and allows to predict the electronic behavior of CNTs (Sattler 1995).

Raman spectroscopy is one of the most powerful tools for the characterization of CNT. Without sample preparation, a fast and nondestructive analysis is possible. All allotropic forms of carbon are active in Raman spectroscopy (Arepalli et al. 2004), and the position, width, and relative intensity of bands are modified according to the carbon forms (Ferrari and Robertson 2000). The most characteristic features are as follows: a low-frequency peak at <200 cm^{-1} characteristic of the SWNT, called radial breathing mode (RBM), whose frequency depends essentially on the diameter of the tube; a large structure (1340 cm^{-1}) assigned to residual unorganized graphite, called D-line; and a high-frequency bunch (between 1500 and 1600 cm^{-1}), called G band, also characteristic of nanotubes, corresponding to a splitting of the E_{2g} stretching mode of graphite (Mamedov et al. 2002). XPS can provide information about the actual composition and chemical state of surfaces and interfaces that

dominate properties of nanostructured materials (Baer and Engelhard 2010); thus, it is used to study the structural modification and the presence of reactive groups onto CNT walls due to the chemical interaction with organic compounds or gases adsorption (Porro et al. 2007; Droppa et al. 2002).

Due to their electronic structure, CNT and specially SWCNT have discrete optical absorptions that do not occur in other graphitic nanocarbon structures. Absorption spectroscopic technique is very useful as a relative purity measurement of CNT. The are around 7–9 IR actives modes in SWCNTs which depend on the chiral, zigzag, and armchair symmetries (Kuhlmann et al. 1998). IR spectroscopy is often used to determine impurities remaining from the synthesis or molecules capped on the nanotube surface, exhibits all the modification of the CNT structure, and reveals the nature of compounds added to the CNT (Belin and Epron 2005). Figure 14.3 summarizes the most important characterization techniques and shows some examples of images and spectra.

14.6 Functionalization

The chemical reactivity of a CNT is, compared with a graphene sheet, enhanced as a direct result of the curvature of the CNT surface. CNT reactivity is directly related to the pi-orbital mismatch caused by an increased curvature. Therefore, a

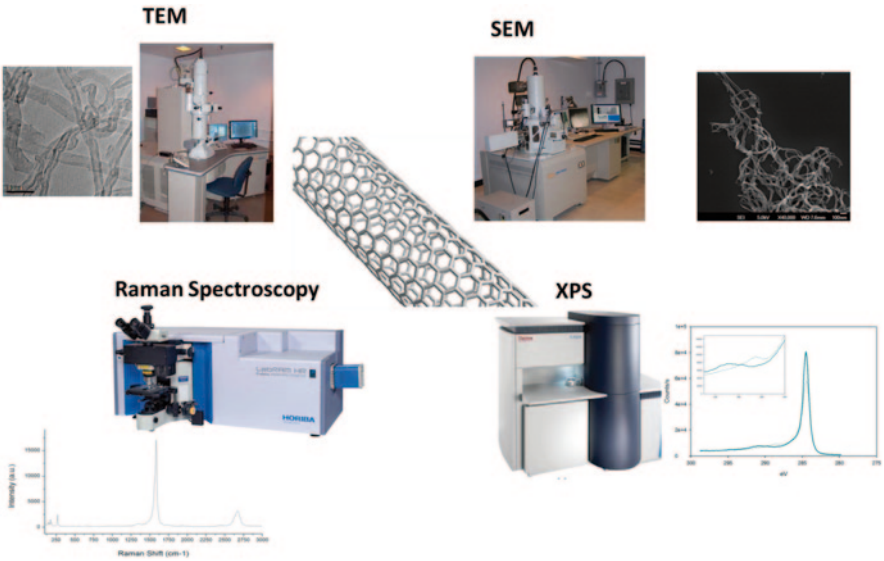

Fig. 14.3 Characterization techniques with some examples of images and spectra that can be obtained in each one. *TEM* transmission electron microscopy, *SEM* scanning electron microscopy, *XPS* X-ray photoelectron spectroscopy

distinction must be made between the sidewall and the end caps of a nanotube. For the same reason, a smaller nanotube diameter results in increased reactivity. Covalent chemical modification of either sidewalls or end caps has shown to be possible. For example, the solubility of CNT in different solvents can be controlled this way. However, direct investigation of chemical modifications on nanotube behavior is difficult as the crude nanotube samples are still not pure enough. Surface modification and functionalization can be performed to selectively immobilize biological molecules. Functional groups such as carboxyl, hydroxyl, carbonyl, alcohol hydroxyl, ester, amine, thiol, and fluorine can be created by wet and dry chemical modification methods such as acid reflux and plasma treatment. Basically, functionalization is a process that creates defects or oxides on the ends and sidewalls of the nanotubes, which will eventually lower their electrical conductivity since it changes the sp^2 hybridization of nanotubes to sp^3 hybridization (Yun et al. 2007).

The main approaches for the modification of CNT can be grouped into three categories: (a) the covalent attachment of chemical groups through reactions onto the π-conjugated skeleton of CNT, (b) the noncovalent adsorption or wrapping of functional molecules, and (c) the endohedral filling of their inner empty cavity (Tasis et al. 2006). Chemical strategies to tune the nanotube electronic properties have been developed. The selective functionalization of SWCNTs (e.g., with thiol groups) and their attachment to preorganized surfaces (e.g., gold) allow the assembly of CNT in devices and, most importantly, provide low-resistance contacts of CNT to other electronic components. With such techniques in hand, CNT should find applications in the development, construction, and use of nanoscale devices such as biosensors (Katz and Willner 2004).

CNTs can be functionalized with various biomolecules without their covalent coupling. Open-ended CNTs provide internal cavities that are capable of accommodating organic molecules and biomolecules such as small proteins (cytochrome C) and DNA (Ito et al. 2003; Davis et al. 1998).

Covalent coupling of biomaterials to CNT is highly important. Based on the specific requirements demanded by potential applications, such as the biocompatibility of nanotube-based biosensors or implantable devices, the chemical modification of CNT is essential. The edges of CNT are more reactive than their sidewalls, thus allowing the attachment of functional groups to the nanotube ends (Katz and Willner 2004). Methods for the immobilization of biological species to nanotubes can be separated into covalent bonding and noncovalent bonding or physical adsorption. Once nanotubes are oxidized and defects are created, moieties such as carboxylic groups and biomolecules can be bonded covalently to the defect sites (Banerjee et al. 2005). Many different conjugation strategies can be applied to immobilize biomolecules with the use of proper coupling agents such as 1-ethyl-3-[3-dimethylaminopropyl] carbodiimide hydrochloride (EDC), *N*-hydroxysulfosuccinimide (NHS), and *N,N′*dicyclohexyl carbodiimide (DCC) for activated amidation (Yun et al. 2007).

Characterization of nanotubes for each of the processes, such as functionalization and bioconjugation, is the key to get quantitative results. SEM and TEM with

energy dispersive X-ray analysis (EDX) are the best methods to observe individual nanotubes. The chemical structure of nanotubes can be determined using XPS, Fourier transform infrared spectrometry (FTIR), Raman spectroscopy, fluorescence imaging, atomic force microscopy (AFM), and STM (Yun et al. 2007).

14.7 Applications

CNTs have properties that give them great application potential in molecular biology. Among these properties are their chemical stability, high electrical conductivity, and high superficial area. Besides, the nanometric scale suggests favorable interactions for their application as biosensors without the use of reagents or labeling (Gooding 2007). As electrode materials, CNTs show better behavior than traditional carbon electrodes and demonstrate catalytic activities toward many electrochemical reactions including O_2 reduction, which is important for catalytic cathodes in fuel cells (Sherigara et al. 2003; Qu et al. 2004).

Enzyme electrodes consist of two parts: a conductive part for electroanalytical purposes and a specific enzyme layer that provides the selectivity. Enzymes provide biological affinity for a particular substrate molecule and catalyze specific reactions of given substrates such as glucose, lactate, cholesterol, urate, pyruvate, glutamate, insulin, amino acids, homocysteine, organophosphate, nerve agents, and neurotransmitters (Yun et al. 2007). Lawrence et al. (2004) have reported that there are 200 dehydrogenases and 100 oxidases. Thus, there are a number of biomolecules and chemicals that can be detected using enzyme biosensors. Figure 14.4 shows an example of the first stage of the construction of an enzymatic sensor. This figure summarizes the characterization techniques that are possible to use in the functionalization process with a biomolecule, in this case an enzyme (amyloglucosidase). In order to prove that this immobilized enzyme can have a potential appli-

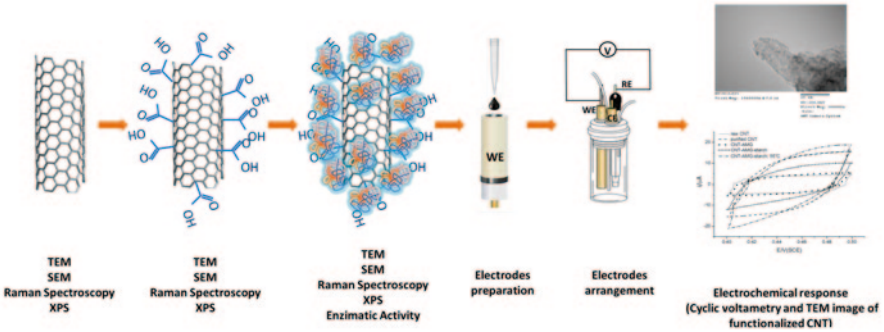

Fig. 14.4 Functionalization pathway of carbon nanotube (*CNT*) with an enzyme with the characterization techniques that can be used in each step of the process. *TEM* transmission electron microscopy, *SEM* scanning electron microscopy, *XPS* X-ray photoelectron spectroscopy

cation as a biosensor, the capacitance of CNT in each step of the functionalization process was determined using cyclic voltammetry. The changes in the capacitance values show that this functionalization process allows having an active enzyme immobilized onto the CNT surface that can be used in the construction of a sensor (Guadarrama-Fernández et al. 2014).

There are studies relating to the development of an electrochemical immunosensor based on carboxylated multiwalled CNTs (c-MWCNTs) electrophoretically deposited onto indium tin oxide (ITO) glass. This c-MWCNTs/ITO electrode surface has been functionalized with monoclonal aflatoxin-B1 antibodies (anti-AFB1) for the detection of aflatoxin-B1 using electrochemical technique. EM, X-ray diffraction, and Raman studies suggest successful synthesis of c-MWCNTs, and the FTIR studies reveal its carboxylic functionalized nature (Singh et al. 2013).

In another work, a new method was developed for the determination of aluminum (Al) in traditional Jordanian foods (Mansaf, Kofta, Tabboola, Hummous, bread), tea, Arabian coffee, and water samples. The method involved solid-phase extraction (SPE) of Al^{3+} from the digested samples after complexation with *D*-mannitol using CNTs as the extractive sorbent. The formation of the Al^{3+}-*D*-mannitol complex was confirmed by IR spectroscopy. Optimization of the SPE method involved sample pH, *D*-mannitol-to-Al mole ratio, sample loading and elution flow rates, adsorbent mass, eluent concentration, and volume. The equilibrium, thermodynamic, and kinetic adsorption studies of Al^{3+}-*D*-mannitol on CNT revealed that adsorption was spontaneous, exothermic, preferred, of physical nature, and followed second-order rate kinetics. Pore diffusion was not the only rate-controlling step (Sweileh et al. 2014).

Another group was working on the detection of staphylococcal enterotoxins (SEs); traditionally, SEs assayed immunologically with an enzyme-linked immunosorbent assay (ELISA). They investigated if CNT could improve the sensitivity of ELISAs and developed an optical CNT immunosensor for the detection of staphylococcal enterotoxin B (SEB) in food. Anti-SEB antibodies were immobilized onto a CNT surface through electrostatic adsorption, and then the antibody–nanotube mixture was bound onto a polycarbonate film. SEB was then detected by a "sandwich-type" ELISA assay on the polycarbonate film. The use of CNT increased the sensitivity of the immunosensor by at least sixfold, lowering the detection limit of SEB. The CNT immunosensor was also able to detect SEB various foods, suggesting the utility of CNT for this and other optical-based immunological detection methods (Yang et al. 2008).

Zhao et al. (2011) developed a novel electrochemical method using multiwalled nanotube (MWNT) film-modified electrode for the detection of quinoline yellow. The effects of pH value, amount of MWNT, accumulation potential, and time were studied on the oxidation peak current of quinoline yellow. It was applied to the detection of quinoline yellow in commercial soft drinks, and the results consisted with the value that obtained by high-performance liquid chromatography (Zhao et al. 2011).

Because of their stiffness, CNTs are ideal candidates for structural applications. For example, they may be used as reinforcements in high strength, low

weight, and high performance composites. The main problem in this area is to create a good interface between nanotubes and the polymer matrix, as nanotubes are very smooth and have a small diameter, which is nearly the same as that of a polymer chain. Secondly, nanotube aggregates, which are very common, behave different to loads than individual nanotubes do. Limiting factors for good load transfer could be sliding of cylinders in MWNTs and shearing of tubes in SWNT ropes. To solve this problem, the aggregates need to be broken up and dispersed or cross-linked to prevent slippage (Endo et al. 2008). This could be an application for the application on the development of food packaging films. Nevertheless, it is important to have more studies about the toxicity of CNT before using them in the food industry. Also there is the possibility of implementing low-cost nanosensors in food packaging to monitor the quality of food during various stages of the logistic process to guarantee product quality up until consumption (Neethirajan and Jayas 2010).

The peculiar toxicity associated with nanomaterials that are different from bulk materials of the same chemical composition has been a concern. In particular, tubular materials with a high aspect ratio such as CNT are suspected of showing asbestos-like toxicity because of their similarity in shape. CNTs focus the attention of many scientists because of their huge potential of industrial applications, but there is a paucity of information on the toxicological properties of this material. Muller et al. (2005) characterized the biological reactivity of purified multiwall CNTs in the rat lung and in vitro. Multiwall CNTs or ground CNTs were administered intratracheally to Sprague–Dawley rats, and they estimated lung persistence, inflammation, and fibrosis biochemically and histologically. Pulmonary lesions induced by CNT were characterized by the formation of collagen-rich granulomas protruding in the bronchial lumen, in association with alveolitis in the surrounding tissues. These lesions were caused by the accumulation of large CNT agglomerates in the airways. Ground CNTs were better dispersed in the lung parenchyma and also induced inflammatory and fibrotic responses. These results suggest that CNTs are potentially toxic to humans and that strict industrial hygiene measures should to be taken to limit exposure during their manipulation.

Because the toxicity of carbon nanomaterials has not been deduced or disproven, these materials should be handled like any other hazardous materials under precautionary principles, and unnecessary exposure to humans and the environment should be avoided (Uo et al. 2011).

Acknowledgments Leonor Guadarrama Fernández wishes to thank CONACyT and PIFI-IPN for the scholarship provided. This research was financially supported through the projects 20131864, 20130333, 20140387, and Red-SIP-NTC-FET at the Instituto Politécnico Nacional (IPN-Mexico) and from CONACyT 161793 and 133102. The TEM images were obtained with the project supported by a grant from the National Institute on Minority Health and Health Disparities (G12MD007591) from the National Institutes of Health.

References

Aqel A, El-Nour KMMA, Ammar RAA, Al-Warthan A (2012) Carbon nanotubes, science and technology part (I) structure, synthesis and characterisation. Arab J Chem 5(1):1–23. doi:10.1016/j.arabjc.2010.08.022

Arepalli S, Nikolaev P, Gorelik O, Hadjiev VG, Holmes W, Files B, Yowell L (2004) Protocol for the characterization of single-wall carbon nanotube material quality. Carbon 42(8–9):1783–1791. doi:10.1016/j.carbon.2004.03.038

Baer DR, Engelhard MH (2010) XPS analysis of nanostructured materials and biological surfaces. J Electron Spectrosc 178–179:415–432. doi:10.1016/j.elspec.2009.09.003

Banerjee S, Hemraj-Benny T, Wong SS (2005) Covalent surface chemistry of single-walled carbon nanotubes. Adv Mater 17:17–29

Belin T, Epron F (2005) Characterization methods of carbon nanotubes: a review. Mater Sci Eng B 119(2):105–118. doi:10.1016/j.mseb.2005.02.046

Davis JJ, Green MLH, Allen H, Hill O, Leung YC, Sadler PJ, Sloan J, Xavier AV, Tsang SC (1998) The immobilisation of proteins in carbon nanotubes. Inorg Chim Acta 272:261–266

Dresselhaus MS, Dresselhaus G, Saito R (1995) Physics of carbon nanotubes. Carbon 33(7):883–891. doi:10.1016/0008-6223(95)00017-8

Droppa R Jr, Hammer P, Carvalho ACM, dos Santos MC, Alvarez F (2002) Incorporation of nitrogen in carbon nanotubes. J Non-Cryst Solids 299–302:874–879

Ebbesen TW, Ajayan PM (1992) Large-scale synthesis of carbon nanotubes. Nature 358:220–222

Endo M, Strano MS, Ajayan PM (2008) Potential applications of carbon nanotubes. Top Appl Phys 111:13–62

Ferrari AC, Robertson J (2000) Interpretation of Raman spectra of disordered and amorphous carbon. Phys Rev B 61:14095–14107

Gooding J (2007) Toward the next generation of enzyme biosensors: communication with enzymes using carbon nanotubes. In: Vo- Dinh T (ed) Nanotechnology in biology and medicine. Methods, devices and applications. CRC Press, Boca Ratón, pp 409–419

Guadarrama-Fernández L, Chanona-Pérez J, Manzo-Robledo A, Calderón-Domínguez G, Martínez-Rivas A, Ortiz-López J, Vargas-García JR (2014) Characterization of functionalized multiwalled carbon nanotubes for use in an enzymatic sensor. Microsc and Microanal 20:1479–1485

Hu H, Bhowmik P, Zhao B, Hamon MA (2001) Determination of the acidic sites of purified single-walled carbon nanotubes by acid–base titration. Chem Phys Lett 345:25–28

Hu H, Zhao B, Hamon MA, Kamaras K, Itkis ME, Haddon RC (2003) Sidewall functionalization of single-walled carbon nanotubes by addition of dichlorocarbene. J Am Chem Soc 125(48):14893–14900. doi:10.1021/ja0356737

Iijima S (1991) Helical microtubules of graphitic carbon. Nature 354:56–58

Iijima SIT (1993) Single-shell carbon nanotubes of 1-nm diameter. Nature 363:603–605

Ito T, Sun L, Crooks RM (2003) Observation of DNA transport through a single carbon nanotube channel using fluorescence microscopy. Chem Commun 13:1482–1483

Journet C, Bernier P (1998) Production of carbon nanotubes. Appl Phys A-Mater 67(1):1–9. doi:10.1007/s003390050731

Katz E, Willner I (2004) Biomolecule-functionalized carbon nanotubes: applications in nanobioelectronics. Chemphyschem 5(8):1084–1104. doi:10.1002/cphc.200400193

Kroto HW, Heath JR, O'Brien SC, Curl RF, Smalley RE (1985) C60: Buckminsterfullerene. Nature 318:162–163

Kuhlmann U, Jantoljak H, Pfänder N, Bernier P, Journet C, Thomsen C (1998) Infrared active phonons in single-walled carbon nanotubes. Chem Phys Lett 294:237–240

Lawrence NS, Deo RP, Wang J (2004) Detection of homocysteine at carbon nanotube paste electrodes. Talanta 63:443–449

Mamedov AA, Kotov NA, Prato M, Guldi DM, Wicksted JP, Hirsch A (2002) Molecular design of strong single-wall carbon nanotube/polyelectrolyte multilayer composites. Nat Mater 1:190–194

Muller J, Huaux F, Moreau N, Misson P, Heilier JF, Delos M, Arras M, Fonseca A, Nagy JB, Lison D (2005) Respiratory toxicity of multi-wall carbon nanotubes. Toxicol Appl Pharm 207(3):221–231

Neethirajan S, Jayas DS (2010) Nanotechnology for the food and bioprocessing industries. Food Bioprocess Technol 4(1):39–47. doi:10.1007/s11947-010-0328-2

Porro S, Musso S, Vinante M, Vanzetti L, Anderle M, Trotta F, Tagliaferro A (2007) Purification of carbon nanotubes grown by thermal CVD. Physica E 37(1–2):58–61. doi:10.1016/j.physe.2006.07.014

Qin LC (1997) CVD synthesis of carbon nanotubes. J Mater Sci Lett 16:457–459

Qu J, Shen Y, Qu X, Dong S (2004) Preparation of hybrid thin film modified carbon nanotubes on glassy carbon electrode and its electrocatalysis for oxygen reduction. Chem Commun 2004:34–35

Sattler K (1995) Scanning tunneling microscopy of carbon nanotubes and nanocones. Carbon 33(7):915–920

Sherigara BS, Kutner W, D'Souza F (2003) Electrocatalytic properties and sensor applications of fullerenes and carbon nanotubes. Electroanalysis 15:753–772

Singh C, Srivastava S, Ali MA, Gupta TK, Sumana G, Srivastava A, Malhotra BD (2013) Carboxylated multiwalled carbon nanotubes based biosensor for aflatoxin detection. Sensor Actuat B-Chem 185:258–264. doi:10.1016/j.snb.2013.04.040

Sweileh JA, Misef KY, El-Sheikh AH, Sunjuk MS (2014) Development of a new method for determination of aluminum (Al) in Jordanian foods and drinks: solid phase extraction and adsorption of Al^{3+}-d-mannitol on carbon nanotubes. J Food Compos Anal 33(1):6–13. doi:10.1016/j.jfca.2013.10.002

Tasis D, Tagmatarchis N, Bianco A, Prato M (2006) Chemistry of carbon nanotubes. Chem Rev 106(3):1105–1136. doi:10.1021/cr050569o

Uo M, Akasaka T, Watari F, Sato Y, Tohji K (2011) Toxicity evaluations of various carbon nanomaterials. Dent Mater J 30(3):245–263

Yang M, Kostov Y, Rasooly A (2008) Carbon nanotubes based optical immunodetection of Staphylococcal enterotoxin B (SEB) in food. Int J Food Microbiol 127(1–2):78–83. doi:10.1016/j.ijfoodmicro.2008.06.012

Yun Y, Dong Z, Shanov V, Heineman WR, Halsall HB, Bhattacharya A, Schulz MJ (2007) Nanotube electrodes and biosensors. Nanotoday 2(6):30–37

Zhao J, Zhang Y, Wu K, Chen J, Zhou Y (2011) Electrochemical sensor for hazardous food colourant quinoline yellow based on carbon nanotube-modified electrode. Food Chem 128(2):569–572. doi:10.1016/j.foodchem.2011.03.067

Chapter 15
Safety Studies of Metal Oxide Nanoparticles Used in Food Industry

Verónica Freyre-Fonseca, Norma L. Delgado-Buenrostro, Yolanda I. Chirino and Gustavo F. Gutiérrez-López

15.1 Introduction

The development of nanotechnology has led us to an exponential usage and the fabrication of nanoparticles (NP) useful to improving the characteristics of different products. A global increase of 5000 % has been reported in patents related to nanotechnology; from 224 new patents granted in 1991 to 12,776 new patents in 2008 (Dang et al. 2010). In 2009 only, the USA invested US$ 1.7 million in nanotechnology R&D (GAO 2010), and in 2015, it is expected a global investment of US$ 1 billion in nanotechnology products (Roco 2005).

The developed NP has been grouped into four types: (1) materials based on carbon and fullerenes, such as shungita, i.e., the most stable carbon form; (2) materials that contain a metallic base such as titanium dioxide (TiO_2) and zinc oxide (ZnO); (3) dendrimers or polymers, such as polyamidoamine dendrimers and polypropyleneimine dendrimers; and (4) the composites of metals, such as platinum with silica cover and layers of Al_2O_3-TiO_2. Such materials have mainly been used by eight industrial areas: automotive, aerospace, electronic and computing, energy and environment, food and agriculture, construction, medicine and pharmacy, and personal care (GAO 2010).

G. F. Gutiérrez-López (✉) · V. Freyre-Fonseca
Departamento de Graduados e Investigación en Alimentos. Escuela Nacional de Ciencias Biológicas, Instituto Politécnico Nacional, Carpio y Plan de Ayala, s/n, CP 11340 México, DF, México
e-mail: gusfgl@gmail.com

V. Freyre-Fonseca · N. L. Delgado-Buenrostro · Y. I. Chirino
Laboratorio 10, Unidad de Biomedicina, Facultad de Estudios Superiores-Iztacala, Universidad Nacional Autónoma de México, Av. De los Barrios No. 1, CP 54059 Los Reyes Iztacala, Estado de México, México

© Springer Science+Business Media New York 2015

H. Hernández-Sánchez, G. F. Gutiérrez-López (eds.), *Food Nanoscience and Nanotechnology,* Food Engineering Series, DOI 10.1007/978-3-319-13596-0_15

15.1.1 Characterization of NP

NP are not used as primary particles but as aggregates and agglomerates with different sizes within the same system (polydispersity). The variety of sizes of aggregates and agglomerates provides NP with different properties which depend on the ionic interactions, pH, and the physicochemical properties of the medium that they were dispersed in. In this regard, NP having greater internalization are highly reactive and have a large surface area and quauntum properties (Kalpana et al. 2012). Also, due to their size, NP allow the use of less material, with new and more efficient effects than with the materials used at a larger scale.

When the use of NP is applied to the production and supply chain of agrofoods, the properties of NP open up new ways to study and promote changes on intra- and intermolecular levels, besides generating catalysis and chemical reactions, muscle contractions, cell transportation, DNA replication, and transcription, among others (Kalpana et al. 2012). All of these functions depend on the physicochemical characteristics of the particles such as their surface area, size, shape, zeta potential, and affinity for a number of different compounds forming the protein corona (Zahoxia et al. 2010). Such a layer modifies the physicochemical characteristics of primary NP and admits agglomerates whose surface reacts with the system in which the NP are dispersed and induce intracellular changes such as structure's modification, cellular cascade induction, and cell cycle deregulation, among others. Consequently, before performing any study of NP toxicity, it is necessary to characterize them in the medium to be used (Fig. 15.1).

In general, the surface area of the aggregates/agglomerates is measured by the Brunauer–Emmett–Teller (BET) method (Lisinger et al. 2013), which consists in measuring the absorption of gas molecules on the surface of the particles, while the hydrodynamic size of the aggregates/agglomerates is measured through dynamic light scattering (DLS). By transmission electronic microscopy (TEM) and scanning electron microscopy (SEM), we can obtain two-dimensional (2D) and three-dimensional (3D) images used in morphology evaluation through digital image analysis (DIA) and by using zeta potential evaluations; we can measure the stability of suspension of the particles in the medium (Tiede et al. 2008).

15.1.2 Security of NP in Health

The accelerated process of elaboration and the increase in use of the new NP have not allowed evaluating or predicting the environmental and human health risks. On the other hand, the exposition to these NP is increasing and tends to accumulate in a variety of systems like, for example, in the aquatic media, soil, air, plants and animals, and humans (Arnall 2003; Cheng et al. 2004; Baun et al. 2008; Brausch et al. 2010). Due to the small size and big surface of the NP, the latter could penetrate the human cells, provoking diseases such as asthma, bronchoalveolar and cardiovascular disorders (BaoYong et al. 2013), Parkinson (Smith and Wayne 2007), Alzheimer (Sompol et al. 2008), and cancer (IARC 2010), among others.

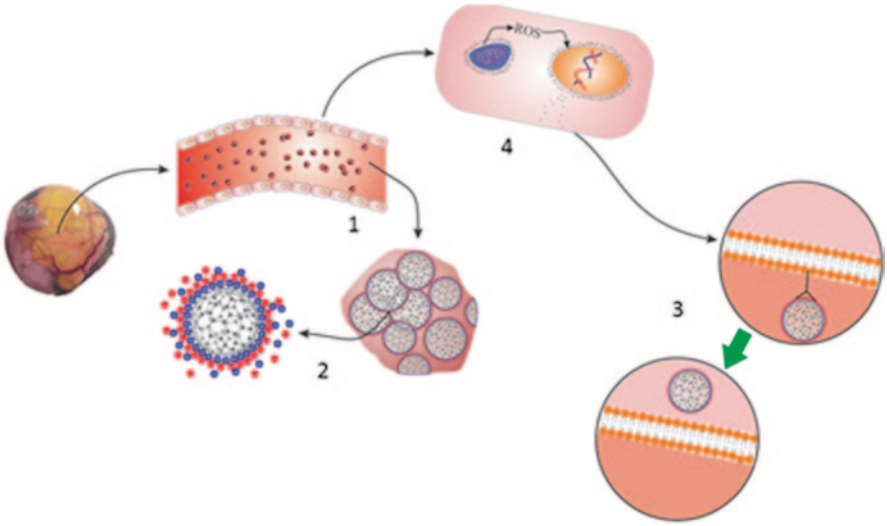

Fig. 15.1 Model of endothelial NP internalization. *1* After exposure, for example, inhalation, dermic wound contact, or oral consumption, NP could reach the bloodstream and interact with blood components; *2* modifying NP properties such as charge, size, and zeta potential, among others; *3* some NP can be internalized by endothelial cells through receptors; and *4* after uptake, it can cause reactive oxygen species to increase and DNA damage

15.2 Exposition Pathways of NP in Humans

There are three pathways of exposure of NP for the latter to get into the human. One of them is inhalation in occupational settings, when the concentration of NP in the air is greater than the recommended by the National Institute for Occupational Safety and Health (NIOSH). The recommended concentration will depend on the type of NP to which it relates but is usually less than 10 g/m^3. Another exposure pathway to NP is the dermal contact through the use of personal care products such as creams, toothpastes, and makeup, among other products containing NP. The third predominant pathway of exposure to NP inside the human is through ingestion of contaminated water or foods that contain within them or who had contact with the NP, such as in packaging (Wang et al. 2013).

Once they get into the human through inhalation, the NP form agglomerates of various sizes that can be deposited on the bronchoalveolar area, and if the NP agglomerates are small enough (<25 nm), they can be translocated to the circulatory system (Bao Yong et al. 2013). On the other hand, if the NP agglomerates in cosmetics come by chance into contact on a skin wound, these NPs could also reach the bloodstream (Gentile et al. 2008). And finally, when NPs are orally ingested, the transport through the gastrointestinal (GI) tract deposits them in the small and thick intestine where, through microvilli, some of these NPs pass to the Peyer's patches and many others pass to the colon, which also has villi that allow the transport of the particles into the circulatory system as shown

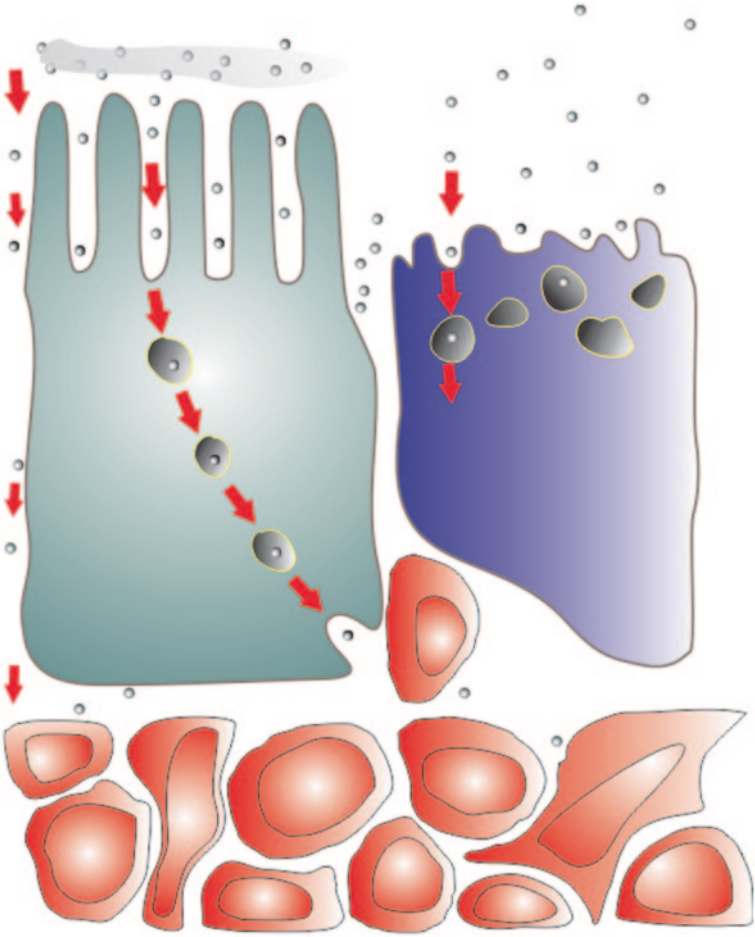

Fig. 15.2 Entry of the NP from the microvilli of the intestine into the bloodstream. When the NP (*gray spheres*) orally reach the small and large intestines, they can enter the bloodstream by three paths: **a** through the microvilli (*top fingerlike*), **b** by crossing the cell junctions (*spheres followed by small red arrows*), making them loose (transitosis), and **c** by natural killer cells (*thick red arrows*) invaginated NP (*gray spheres surrounded by black*) until the NP enter the bloodstream (*red area*) and are distributed throughout the body

in Fig. 15.2 (Jung et al. 2000). Some types of NPs which have been distributed through the blood vessels, liver, and lungs are able to penetrate cellular barriers such as the blood–brain and placental barriers (Gentile et al. 2008). In the case of mice, the immune cell profiles in response to a silver NP injection has been evaluated, and the authors concluded that the exposure can modulate the immune system in a dose-dependent mode, with smaller-size particles generating more severe effects (Zelikoff et al. 2013). The tissue distribution of NP depends on the physicochemical and morphological characteristics which could be associated

with inflammation, atherosclerosis, tumor growth, and metastasis (Hyung Joo et al. 2011); therefore, although it is known that NPs distribute and accumulate in the body, it is not easy to estimate the minimum time of exposure required to cause changes at the cellular and molecular levels, but there are recommendations on the time and exposure concentrations in each type of NP in particular. Such recommendations come from various institutes and agencies responsible for the security of NP in humans. For example, a recommended limit of exposure to the TiO_2 NP is 0.017 mg/m^3 (Stone et al. 2010), 0.3 mg/m^3 (NIOSH 2011), and 1.2 mg/m^3 (NEDO 2009) but without establishing a clear limit of occupational exposure due to the impracticality of some measurement techniques, the lack of adequate toxicological data, and the uncertainty of dose or exposure measures in investigations, among others (Gordon et al. 2014).

15.3 Life Cycle of NP

The NP life cycle begins with manufacturing, continues with transport and processing, transport of the finished product, consumption by humans or other living organisms, and ends with recycling or disposal of NP or the products in which they are present (Wang et al. 2013). It should be noted that given that NP are not biodegradable and accumulate in the environment if they are unintentionally released into environments dedicated to the production of human food commodities and water reservoirs, they may interact with the compounds of the ecosystem or consumed by organisms, thus causing a number of problems such as changes in the ecosystem or gene mutations (Wang et al. 2013). Consciousness must be induced in the use and proper handling of NP, and international standards must be established for its regulation (Fig. 15.3).

15.4 Regulation and Use of NP

It has been difficult to unify the criteria for handling the NP internationally. However, some rules have been developed to standardize NP handling and disposal, such as the International Organization for Standardization (ISO), in which 156 nations that provide regulatory standards for environmental and human risks in a variety of substances participate (Wang et al. 2013). On the other hand, the American Society of Testing Materials (ASTM) formed an international committee in 2005 to standardize and create a guide for handling nanomaterials, and the European Chemicals Agency (ECHA) established guidelines (derived no-effect levels, DNELs) that allow establishing chronic inhalation levels that do not cause side effects.

The Institute of Electrical and Electronics Engineers (IEEE) had an important role in the standardization of NP (Bergeson and Hester 2008). However, currently,

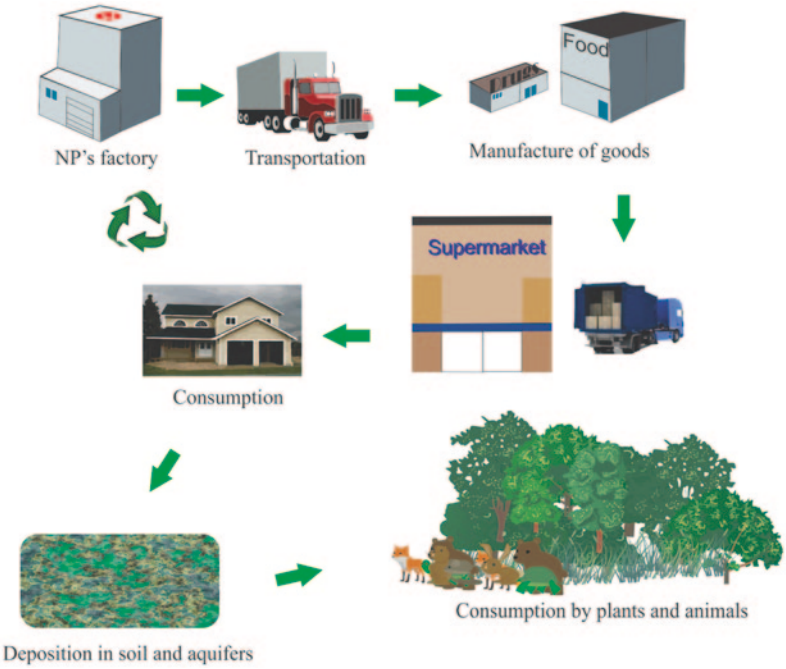

Fig. 15.3 Life cycle of the NP. The development of the NP continues with the transport of the same to the production lines to generate everyday products such as pharmaceuticals, cosmetics, and foods, among others. Later, they are transported to distribution centers, such as supermarkets, where they are purchased by consumers, whose waste is recycled or distributed in aquifers where they are accumulated by the organisms that inhabit them. This way, the NP only accumulates in the environment

we have not achieved an international consensus on the way NP should be handled to guarantee safe use. And the efforts to develop nanotechnology standards to maintain environmental and human safety over the unceasing development of nanotechnology will persist. In the USA, the Environmental Protection Agency (EPA) conducted an inventory of chemical substances that must be regulated by the Act to Control Toxic Substances (EPA 2011), while the Food and Drug Administration (FDA) has become increasingly involved in regulating nanotechnology products, because in the food industry, nanotechnology represents a significant and new line of research (Morris 2011). Besides, the European Food Safety Authority (EFSA) has been commissioned to provide recommendations on the use of NP in food for human and animal consumption, establishing criteria and limits on the use of additives in food. In addition, the International Agency for Research on Cancer (IARC) and the NIOSH have studied the evidence on the effects caused by exposure to NP and have established criteria and recommendations for the use of and exposure to NP, respectively (See Linsinger et al. 2013).

15.5 Use of NP in Food: Quality Versus Product Safety for Consumption

Nanotechnology has focused on the packing, processing, quality, safety, and nutraceutical and functional properties of the additives directly in food, packaging materials, and food supplements (Tiede et al. 2008), since the NP can be used as sensors for pollutants, antimicrobials, diffusion barriers, and changes in the nutritional quality of food, thus contributing to consumer safety (Weiss et al. 2006; Sanguansri and Augustin 2006; Corporate Watch 2007; Chaudhry et al. 2008). However, there are technological and economic implications within agrifood systems when changing the work techniques, increasing the lifetime of the products, and preventing pest attack, among others (Kalpana et al. 2012). It has been reported that there are about 200 companies worldwide involved in the processing of NP for food-related applications (Chau et al. 2007). In Mexico, some of the companies related to NP usage are Sensient Colors, Tate & Lyle, Ingredion, BASF, DSM, Fortitech, FX Morales, MF Powers, Naturex, Palsgaard, DuPont, and Sensient Flavors.

However, it should be noted that despite the increased number of publication of food production-related NP patents and the rapid rise in products that contain them, there is still no scientific evidence that demonstrates that its consumption is safe for humans, and the research on the toxicity of NP has not been in proportion to their development. A review in SCOPUS, until mid-2014, showed that while there are 2215 studies using the keyword "nanoparticles food," only 335 studies were reported using the keyword "food nanoparticles safety" and 35 studies using the keyword "food nanoparticles security." Therefore, although the use of nanotechnology has shown to favor the quality of foodstuffs, it must still be evaluated that these products do not threaten the integrity and health of consumers. Also, more emphasis is needed in the study of the risks and opportunities to avoid damaging the agricultural chain and not increasing the food prices (Kalpana et al. 2012).

15.5.1 Metal Oxides

The development and synthesis of NP such as titanium dioxide(TiO_2), zinc oxide (ZnO), silicium oxide (SiO_2), cupric oxide (CuO), cuprous oxide (Cu_2O), tin oxide(SnO_2), ferric oxide (Fe_2O_3), and cobalt oxide (Co_3O_4) have provided major advances in areas such as mechanical, optical, electrical, and chemical, in addition to other uses in food. However, nowadays, there are few studies on the effects of metal oxide NP on human and environment in relation to the number of studies for the synthesis of NP.

Metal oxides and metals may, accidentally, be in contact with foods such as TiO_2 (E 171), SiO_2 (E 551), Ag (E 174), ZnO (E6), and Co (E3), because they are part of food ingredients, or not incidentally as SnO_2 and Fe_2O_3, because they are acquired from the environment or through the packing materials or sensors.

15.5.2 Incidental and Not Incidental Food Additives

Incidental additives present in foods are due mainly to pesticides, herbicides, or chemicals which were in contact with the product during manufacturing or by contact with contaminated soil or containers used to transport food. On the other hand, not incidental additives are used to improve food quality.

15.5.2.1 Titanium Dioxide (Tio_2 Named as E 171)

Characterization and Identity

TiO_2 NP are synthetic particles forming a white, opaque powder with high photocatalytic activity formed at very high temperatures (>1000 °C) that come from rutile, anatase, and brookita (crystals are present in nature). The most commonly used material is the anatase form at 90 % purity. However, there is currently great interest in producing various structures, such as spheres, ribbons, floral arrangements with TiO_2 NP spheres or ribbons, which give different photocatalytic qualities to the TiO_2 NP (Li et al. 2013).

TiO_2 NP are present in various products such as sunscreens, toothpastes, vinyl paints, makeup and cosmetics, as carrier of drugs and in foods such as milk, ice cream, water flavoring powders, mozzarella cheese, preserved sweets, and chewing gums, among others, thus favoring the consumption of 1–2 mg of TiO_2 NP/kg per day (Weir et al. 2012).

Physicochemical Properties

There are works dealing with the physicochemical properties of the aggregates/agglomerates of TiO_2 NP in cell culture media such as Dulbecco's Modified Eagle's Medium (DMEM) and Roswell Park Memorial Institute Medium (RPMI) (Allouni et al. 2009; Zahoxia et al. 2010; Sekar et al. 2011). NP have also been characterized in H_2O, fetal bovine serum (FBS), phosphate-buffered saline (PBS), and human serum. However, there are only a few studies on the physicochemical properties of TiO_2 E 171. Table 15.1 presents some of the physicochemical characteristics of TiO_2 NP found by different authors.

Studies of In Vitro and In Vivo Effects

Authors have demonstrated the cytotoxic properties of TiO_2 NP where IC_{50} value for TiO_2 Degussa NP is 665 μg/cm^2 (Gramowski et al. 2010). There are also works in which it is reported that exposure to TiO_2 NP turns benign into malignant tumor cells through a process related to the production of reactive oxygen species (ROS) (Onuma et al. 2009). The increased production of ROS may be partly due

Table 15.1 Comparison of physicochemical properties of TiO_2 NP studied by several authors

Reference	Primary size	Hydrodynamic size (nm)	PDI	Zeta potential (mV)	pH
Allouni et al. 2009	–	348 ± 13	0.25 ± 0.01	−9 ± 1	NA
Sekar et al. 2011	–	650 ± 10	0.45 ± 0.08	−15 ± 1	7.8
Zahoxia et al. 2010	–	209 ± 9	0.035	30.2 ± 0.6	6.1

NA not available, *NP* nanoparticles, *PDI* polydispersity index

to mitochondrial dysfunction. The effect of TiO_2 NP on mitochondrial function was the decrease in membrane potential, where the rate of respiratory control and oxygen consumption is decreased, and the *P/O* ratio, repolarization, and phase lag increase. Together, these parameters showed that the TiO_2 NP disengage electron transport and ATP synthase activity (Freyre-Fonseca et al. 2011). It was also suggested that exposure to TiO_2 NP boosts a hypoxic environment since the results showed a decrease of 33 % in oxygen consumption during state III of the respiratory function.

It has also been reported (Weir et al. 2012) that there are various diseases associated with oral exposure of the TiO_2 NP, such as gastritis, colitis, and Crohn's disease (Lomer et al. 2004), but we have not found that these effects demonstrate under controlled conditions in vitro or in vivo. It has also been reported that TiO_2 NP have the ability to induce an increase in the expression of vascular endothelial growth factor (VEGF) (Onuma et al. 2009). VEGF, along with hypoxia inducible factor (HIF-1α), constitutes two of the most important factors involved in the process of generating new blood vessels from pre-existing vessels. This process is known as angiogenesis (Gui et al. 2011) and is usually involved in tumor formation. There are some in vivo and in vitro studies performed with anatase that evaluated the effects of TiO_2 NP on the skin and lungs; however, there are few studies performed with TiO_2 E 171 that evaluate their effects on the GI tract and circulatory system.

Conditions of Use and Regulation

The IARC classified TiO_2 NPs as possibly carcinogenic to humans (Group 2B) by inhalation. However, the FDA approved the use of TiO_2 NP classified in the group generally recognized as safe (GRAS). The EFSA classified these NP in the group E 171 for their use as additives (less than 1 % product weight) in food for humans and animals. In the USA, an adult can have exposures of up to 1 mg/kg/day of TiO_2 E 171. However, children could double the exposure of an adult per day (Weir et al. 2009). FDA has also approved the use of the combination of SiO_2 and TiO_2 NP in food to aid the solubility of TiO_2 NP in the food media (FDA CFR73.575 21).

15.5.2.2 Silver Zeolite (E 174)

Characterization and Identity

The silver zeolite A is a silver zinc sodium ammonium alumino silicate $M_{12}(2AlO_2 \bullet 2SiO_2)_6 \bullet 27H_2O$ (with M = Na^+, Ag^+, Zn^{2+}, NH_4^+). This compound (food grade) may have Ag contents above 5 % (w/w). The function of this substance is to preserve and control the growth of microorganisms in products. According to the demand, the silver zeolite A compound is not intended to have a technological effect in foods (EFSA 2011). Besides, Ag NP are used in cosmetics, electronic items, clothing, paints, sunscreens, bactericides, and for medical-related purposes (dental crowns and cancer treatments, among others; Römer et al. 2011).

Physicochemical Properties

Even up to date, no studies showing the physicochemical properties of silver-zeolite NP (E 174) have been found. However, there are few studies that analyze some of the physicochemical properties of silver NP. One concern on performing toxicological studies of NP is to know the effects when they are incorporated into the environment. In this regard, it has been shown that mobility, bioavailability, and toxicity of the NP of Ag are dominated by its colloidal stability in which the hydrodynamic diameter of the agglomerates of Ag NP had a dispersion of 27–42 nm and a zeta potential value varying from −40 to −46 mV when suspended in water (Römer et al. 2011).

In addition, studies were performed on protein corona covering Ag NP when the latter are suspended in different media, and it was found that the hydrodynamic diameter did not show significant differences when suspended in water and in a culture medium (Shannahan et al. 2013). However, the stability of the suspension decreased about 20 units. This is probably due to flocculation when in contact with biological environments.

Studies of In Vitro and In Vivo Effects

Various in vitro studies have indicated that Ag NP are toxic to mammalian cells, cells derived from skin, liver, lungs, brain, vascular system, and reproductive organs (Ahamed et al. 2010). It has been suggested that the toxicity was due to Trojan horse effects, when Ag^+ ions are released into the aqueous media once Ag NP is solubilized in biological media (Miura and Shinohara 2009). It has been found that exposure to Ag NP was associated with increased ROS, release of cytochrome C into the cytosol, and translocation of Bax protein in the mitochondria (Hsin et al. 2008). It was also found that exposure of Ag NP p53 by inducing apoptosis pathway, whereby these NP are used in chemotherapy (Gopinath et al. 2010). Also, it has been found that Ag NP can be translocated by blood circulation and can induce

the destruction of the blood–brain barrier and neuronal degeneration (Tang et al. 2009). Some immunological aspects were described before in this chapter (Zelikoff et al. 2013). Toxicological aspects of Ag NP were also evaluated by EFSA in 2005 (EFSA 2005). In this study, it was reported that a person consumes up to 10 g of Ag NP orally. Based on this information, a restriction of 0.005 mg/kg food with Ag NP could limit the intake to less than 13 %. Thus, an adult of 60 kg of body weight could be exposed to 0.044 mg Al/kg/week (EFSA 2011).

Conditions of Use and Regulation

Silver is ranked in the EFSA 3 Scientific Committee on Food (SCF) list, i.e., the group of additives for which there has not been established a daily intake recommendation, but their presence in food is accepted by restricting it to 0.05 mg Ag/kg food, based on the maximum concentration that causes no detectable adverse alterations in morphology, functional capacity, growth, development, or viability in humans (Non Observed Adverse Effects Level (NOAEL)). Over a lifetime, we ingest about 10 g of Ag in drinking water (EFSA 2011). Furthermore, Ag can favor the migration of Al in food. The potential exposure for a 60-kg adult can be estimated at a range of 4.4 % Training Within Industry (TWI) 1 mg/kg bw/week (EFSA 2008).

15.5.2.3 Zinc Oxide E6

Characterization and Identity

The ZnO (*Chemical Abstracts Service Number* (CAS No.) 1314-13-2, *Enzyme Commission Number* (EC Number) 215-222-5) is a water-insoluble material with ≥99.0 % purity. It is a semiconductor which use has increased given that it is a nontoxic biocompatible material showing good optical and mechanical properties (Cheng et al. 2009). It has been used in the rubber, pharmaceutical, and cosmetic industries; in photocatalysis; and also for therapeutic applications. Furthermore, ZnO is one of the most important trace elements in the organism of mammals and is present in the homeostasis, immune responses, oxidative stress, apoptosis, and aging. ZnO is added to many food products such as cereals and dietary supplements as a source of Zn.

Physicochemical Properties

A recent study showed that primary particles of ZnO having sizes of 30 ± 20 nm, 40 ± 20 nm, and 1024 ± 496 nm may form aggregates/agglomerates of sizes which hydrodynamic diameters vary from 70 to 150 nm, 90–160 nm, and 250–540 nm when suspended in water forming suspensions having zeta potential values of −14 ± 6 mV, 5 mV, and 19 ± 5±5 mV, respectively (Mu et al. 2014).

Table 15.2 In vivo and in vitro effects caused by exposure to ZnO NP

Reference	Model	Concentration	Conclusions
Mu et al. 2014	Epithelial cells	5.5 μg ZnO/ml	It is suggested that the dissolution and re-precipitation of uncovered ZnO NP cause cytotoxicity (MTT) and DNA damage
Polak N et al. 2014	*Caenorhabditis elegans* mutant Sylvester and triple knockout sensitive to metal (mtl-1, mtl-2, pcs-1) to ZnO NPs	0–50 mg ZnO/ml	It was observed that exposure to ZnO NP decreased the growth and development of reproductive capacity, and life expectancy effects were amplified in knockout mice
McCracken et al. 2013	C2BBe1 epithelial cell line, a clone of the Caco-2 cells		With ZnO NP in the same concentration, it was observed that medium toxicity in the Lactate Dehydrogenase (LDH) assay and mitochondrial activity decreased, but not the necrosis or apoptosis
Seok et al.2013	Sprague-Dawley rats	67.1, 134.2, 268.4, or 536.8 mg ZnO/kg for 13 weeks	Male and female rats had changes in hematological parameters related to anemia and pancreatitis
Sharma et al. 2012	Mice	300 mg ZnO/kg	The accumulation of ZnO NP induces liver cell damage after oral exposure for 14 consecutive days. ZnO NP also induces oxidative stress, which is indicated with the increment of lipoperoxidation

NP nanoparticles

Studies of In Vitro and In Vivo Effects

Solubility of ZnO in the stomach environment (pH 2.7) has a value of 98.5 % when the particles are smaller than 1 mm (Li et al. 2011). About 25 studies in vivo and in vitro were found in a search conducted in SCOPUS. These studies report the toxicity of the ZnO NP when used in foods (Table 15.2). In conjunction with the instability of the ZnO NP, the degree of solubility allows the oxidation and release of Zn^{+2} into the medium. It has been observed that the NP showing high solubility in a cell culture, such as ZnO NP exhibited higher toxicity in mammalian cell lines than those having low solubility, such as TiO_2 NP (Mu et al. 2014).

Likewise, in vitro studies with cells of Caco-2 colorectal adenocarcinoma and lung A549 cells showed that the size, surface charge, and the ligands and covers with surfactants may influence the permeability of the ZnO NP in the colorectal and lung areas (Hyung-Joo et al. 2011; Sahu et al. 2014). Another study reported that exposure to ZnO NP induced alterations in antioxidant parameters, the formation of 8-hydroxy-2 deoxyguanosine (8-OHdG) as an indicator of DNA damage and cell death (Syama et al. 2013).

Conditions of Use and Regulation

ZnO NP are classified as GRAS by the FDA (21CFR73.1991) and as an E6-safe additive by EFSA. Therefore, these NP are commercially produced and used as packing material and food additive (Hyung-Joo et al. 2011). In a study conducted by EFSA in 2012, it was considered that due to the high solubility of ZnO in the stomach environment, the physical and chemical specifications of ZnO (used in several toxicity studies) are incomplete and do not specify the purity/impurities ratio (EFSA 2012), so it was postulated by this body that the oral use of ZnO is safe.

15.5.2.4 Silicon Dioxide (SiO_2) E551

Characterization and Identity

Silicon dioxide (SiO_2), CAS No. 7631-86-9, is a fine-white powder with a high water absorption rate. It is insoluble in ethanol and water but forms a gel when combined with mineral acids. Particles of this compound are produced on an industrial scale as an additive for cosmetics, medicines, printing toners, and foods. In the biotechnology and biomedical areas, SiO_2 NP have been used as drug development systems, for example, in cancer therapy and in the immobilization of enzymes and DNA transfection (Izak-Nau et al. 2013).

SiO_2 NP are available in the market not as for their use in a specific function. They can have surfaces with positive, negative, or neutral charge and as monodisperse or in the form of aggregates (Izak-Nau et al. 2013). It has been observed that the industrially attractive physicochemical properties of SiO_2 NP can cause problems in human health (Chen and von Mikecz 2005; Ye et al.2010; Al-Rawi et al. 2011; McCracken et al. 2013).

Physicochemical Properties

There is little information on the physicochemical characteristics of SiO_2 NP probably because they are prepared according to the required functions. Examples of characterization studies performed with SiO_2 NP are shown in Table 15.3.

Table 15.3 Physicochemical properties including size, polidispersity index (PDI), zeta potential, pH, and shape of SiO_2 NP studied by different authors

Reference	Primary size	Hydrodynamic size (nm)	PDI	Zeta potential (mV)	pH	TEM
Izak-Nau et al. 2013	–	58.2 ± 2.6 nm	0.055	−41.71 ± 0.82	3.1	Sphere
Cho et al. 2012	6.2 ± 0.4	398.1 ± 24.8	–	–	–	–
McCracken et al. 2013	50	–	–	–	2	–

NP nanaoparticles, *TEM* transmission electron microscopy

Table 15.4 In vivo and in vitro effects caused by exposure to the SiO_2 NP

Reference	Model	Concentration	Conclusions
Chen and von Mikecz 2005			Formation of nucleoplasmic protein aggregates impairs nuclear function in response to SiO_2 NP
McCracken et al. 2013	C2BBe1 epithelial cells, a clone of Caco-2 cells	10 μg/cm^2	The treatment with silica and titanium with intestinal digestion simulating solution allowed a strong negative surface charge and particle sizes that approach to values similar to those found in the medium The C2BBe1 cells internalized TiO_2 and SiO_2 NP
Gehrke H et al. 2013	HT29 Cells	–	SiO_2 NP impact on the integrity of DNA in cells of human colon carcinoma (HT29). Stimulates the proliferation of HT29 cells. Interferes with the biosynthesis of glutathione
Al-Rawi et al. 2011	HELA cells. Primary SiO_2 NP of 70 nm and aggregates of 200–500 nm	SiO_2 NP of 70 nm and aggregates of 200–500 nm	Internalization and intracellular localization in mitochondria, endosomes, lysosomes, and nuclei were studied
Ye et al. 2010	L-02 liver cells	0.2, 0.4, and 0.6 mg/ml of colloids of SiO_2 (21, 48, and 86 nm) for 12, 24, 36, and 48 h	SiO_2 NPs cause different size, dose, and dependent time cytotoxicity. Also, they cause oxidative stress by ROS, activation of p53, and the regulation of the relation Bax/Bcl-2 involved in induction mechanisms of SiO_2 of 21 nm

NP nanaoparticle, *ROS* reactive oxygen species

Studies of In Vitro and In Vivo Effects

There are few studies on the toxicity of SiO_2 for food-related uses. While in the Pubmed database, 945 investigations conducted between 2000 and 2014 with the SiO_2 NP were found, only 10 of them were actually focused on safety aspects when used in food preparations. Some of the studies reviewed showed adverse effects on the GI system (Table 15.4).

Conditions of Use and Regulation

EFSA classified the SiO_2 as E 551. It is a substance recognized as GRAS by the FDA, and its use is permitted in the form of dry powders, salt (and their substitutes), food supplements, rice, and processed cheese. Also, it has been used as a carrier in

emulsifiers and colorants at levels reaching a maximum of 5 %. In flavoring, its use at levels of 50 g of SiO_2 NP/kg is allowed (EFSA 2009). Moreover, the FDA has authorized the use of the combination of $SiO_2 + TiO_2$ NP in food to aid solubility of TiO_2 NP (FDA CFR73.575 21).

15.5.2.5 Cobalt (III) Oxide (Co_2O_3) E3

Characterization and Identity

Cobalt oxide (Co_2O_3), CAS number 1308-04-09, is a black powder with molecular weight of 165.8646 g/mol. Its crystal structure is trigonal with a density of 5.18 g/cm^3. It is used as a trace element in animal food, and it has been reported to be used as an essential element in the human diet, and its applications likely to increase due to dietary supplements, occupation, and medical services (Paustenbach et al. 2013). It is used in electrochemical plants in colorants for ceramics and as a dryer in paints, varnishes, and inks (De Bie and Doyen 1962).

Physicochemical Properties

No reports on the physicochemical characteristics of Co_2O_3 NP were found. A work on spherical Co_3O_4 NP measuring 45 nm and tendency to form clusters with different shape and size up to 1000 nm was reported by Papis et al. (2009).

Studies of In Vitro and In Vivo Effects

Co_2O_3 NP accumulates in organisms when consumed and the tissues in which they are mainly found are those of liver, kidneys, bladder, blood, and lungs. This accumulation has been decreasingly observed in a dose–response manner (Naura 2009). In addition, the exposure to these NPs is associated with cardiomyopathies and vision and hearing damage when the concentration in cell culture tests is above 700 μg/L (8–40 weeks), whereas at 300 μg/L, hypothyroidism and polycythemia were reported. However, there has been observed that the use of these NP increased the risk of lung cancer induction.

In a monograph on the cobalt by the IARC (2006), it was reported that Moulin et al. 1993 studied mortality in a cohort of 1148 workers in an electrochemical cobalt plant, who worked exclusively in the maintenance section. The standardized mortality ratio (SMR) risk of lung cancer was 2.4, and for those employees who worked in other areas, the risk was 2.58. There is also evidence of increased risk in the group of workers employed for more than 10 years in the production of cobalt. In another study conducted on 874 women occupationally exposed and 520 unexposed, there was not found a relation regarding the duration or intensity of the exposure. Of the entire cohort, three lung cancer cases from a total of eight were related to Co exposure within 3 months (Tüchsen et al. 1996).

Furthermore, it was observed that the NP of Co_2O_3 can enter the cell cytoplasm in the form of vesicles and can increase the production of ROS (Papis et al. 2009) and together with TiO_2 NP is one of the metal compounds that can yield to photoinduced toxicity (Dasari et al. 2013).

Conditions of Use and Regulation

Authorized by the EFSA, the use in animal food and the FDA classifies it as GRAS substance (21 CFR 582.80). However, the exposure limits to Co NP are from 0.02 to 0.5 mg/m^3 (air space), although NIOSH recommends a maximum limit of 0.05 mg/m^3 (air space) by a working shift.

15.5.3 Incidental Food Compounds

15.5.3.1 Tin Dioxide (SnO_2) NP

Characterization and Identity

Tin dioxide (SnO_2), CAS number 18282-10-5, is a white powder soluble in water called cassiterite which is the most important chemical source of Sn. It is a colorless solid with a refractive index of 2.006. It crystallizes in the form of rutile, in which the Sn atoms have six coordinates and the oxygen atoms have three (Ginley et al. 2000). It is an attractive material for its use in gas biosensors (Tadeev et al. 1998) and solar cells (Omura et al. 1999), among others, because of their high transparency and electrical conductivity. SnO_2 NP have been used to develop semiconductor sensors that discriminate samples of virgin olive oil based on its organoleptic characteristics (Escuderos et al. 2013).

Physicochemical Properties

There are no studies yet regarding the physicochemical properties of the SnO_2 NP in the sensors used in food-related systems. There are also no studies analyzing the possible transport of SnO_2 NP in sensors to food.

Studies of In Vitro and In Vivo Effects

In a SCOPUS review, using the keyword "SnO_2," 16,500 studies from 2010 to 2014 were found, of which 4310 were devoted to the application of SnO_2 as a biosensor for food-related applications and only five studies on the toxicity of SnO_2 NP in food. Gambardella et al. (2014) reported that there is toxicity and alteration of the food chain when SnO_2 NP are disposed in the sea.

Furthermore, when the SnO_2 NP are used together with indium in a concentration of 90:10, a compound called indium tin oxide (ITO) is formed. A study showed that chronic and subchronic inhalation of this compound may cause lung toxicity in hamsters treated with 3 and 6 mg/kg of particles of ITO, twice a week for eight weeks (Tanaka et al. 2010). However, the effects of these NP when consumed orally by humans have not been analyzed.

Conditions of Use and Regulation

No regulations or recommendations by the IARC, NIOSH, FDA, or EFSA were found.

15.5.3.2 Iron (III) Oxide or Ferric Oxide

Characterization and Identity

Ferric oxide (Fe_2O_3), CAS number 309-37-1, is an odorless red solid. With insoluble rhomboid structure and 159.69 g/mol molecular mass, it is one of the main iron oxides. The mineral known as hematite, Fe_2O_3, is the major source of iron for the steel industry.

The magnetite γ-Fe_2O_3 NP is a cubic crystal that has gained great interest due to their super-paramagnetic properties and their applications in various fields such as catalysis, sensors, and magnetic resonance imaging (Hanini et al. 2011). These applications require that the NP are covered with agents such as acids and long-chain amines (Hanini et al. 2011).

Physicochemical Properties

The hydrodynamic diameter of the γ-Fe_2O_3 NP suspended in deionized water, DMEM, and PBS cell culture media, in the whole range of physiological pH values, was 2420, 90, and 204 nm, respectively, while zeta potential had values of +12.8, 9.1, and −23.6 mV, respectively (Hanini et al. 2011). Also, it has been found that Fe_2O_3 NP form individual aggregates having a diameter of 42.5 nm (TEM) and have a specific area of 34.39 ± 0.17 m^2/g (Gramowski et al. 2010) and 82.8 m^2/g when they have a hydrodynamic diameter of 957 nm and a zeta potential of −8.2 mV (Sun et al. 2011). It has also been reported that the IC_{50} of the Fe_2O_3 NP is 6.02 $\mu g/cm^2$ (Table 15.5) (Gramowski et al. 2010).

Also, a study performed using Wistar rats exposed to Fe_2O_3 NP included the characterization of the NP physicochemical properties in deionized water (Milli Q). The hydrodynamic diameter of the agglomerates (363 nm) was bigger than that measured by TEM, while the specific surface area was 38.02 m^2/g. The zeta potential was −18.6 mV (Table 15.5) (Singh et al. 2013).

Table 15.5 Physicochemical properties (size, zeta potential, pH, and shape) of Fe_2O_3 NP studied by different authors

Reference	Medium	Hydrodynamic diameter (nm)	Zeta potential (mV)	TEM diameter	pH	Specific area
Hanini et al. 2011	H_2O DMEM PBS	2420 90 204	+12.8 −9.1 −23.6	–	7.4	–
Gramowski et al. 2010	–	–	–	42.5	–	–
Sun et al. 2011	H_2O	957	−8.2	–	–	82.8
Singh et al. 2013	H_2O	363	−18.6	–	–	38.02

NP nanaoparticles, *TEM* transmission electron microscopy

Studies of In Vitro and In Vivo Effects

Regardless of that, until now the use of Fe_2O_3 NP directly in food had not been reported; there are reports that if for some reason these substances are released into the environment, they are able to modify ecosystems and to reach the products for human consumption such as vegetables and seafoods.

Frenk et al. (2013) studied the effects of $Fe_2O_3 < 50$ nm NP in two soil types to see the change in the activity of the bacterial community that made it up. In other works, the effect of Fe_2O_3 on watermelon has been evaluated, and it has been proved that these NP can be translocated by plant tissues causing significant physiological changes such as the activity of catalase, peroxidase, and superoxide dismutase; chlorophyll and malondialdehyde content; and the reduction of the ferric reductase activity (Li et al. 2013). In a study with crabs, the Fe_2O_3 transfer of the muddy sediment in Rhizophora leaves pellet was quantified, finding that the accumulation of metals in mangrove leaves and crabs reflected the chemical composition of the sediments, and that low levels of these compounds were transferred from the leaves and from the crabs to humans (Vilhena et al. 2013). These studies showed that Fe_2O_3 NP are able to pass through the food chain and reach humans through food. Currently, there are not enough studies on the effects that these NP may have on humans.

Terms of Use and Regulation

Organizations such as the IARC, FDA, and EFSA have not established exposure limits for the intake of these compounds. However, some exposure limits have been reported for the case of NP inhalation:

Occupational Safety and Health Administration (OSHA)—The exposure legal limit allowed in the air is 10 mg/m^3, average for an 8-h shift.

NIOSH—The exposure legal limit allowed in the air is 5 mg/m^3, average for a 10-h shift.

American Conference of Governmental Industrial Hygienists (ACGIH)—The exposure legal limit allowed in the air is 5 mg/m^3, average for an 8-h shift.

15.6 Conclusions

The use of NP in food is a common practice, since they aid in the preservation and improvement of food quality. There are different exposure pathways for the NP in foods: the exposure can be direct, through regulated additives, or indirectly, through the NP transport from biosensors, packaging, or through the food chain. The NP used to perform toxicological studies are, generally, free of impurities (99 %), while in foods, the use of mixes of these NP with others that help improve the characteristics of the product is frequent.

The effects that NP will cause to humans will depend on the physicochemical characteristics of the NP aggregates/agglomerates. NP form stable suspensions as measured by the zeta potential which values range from −20 to −45 mV. In the monographs by EFSA and FDA it is established that there is a risk when these products are consumed by humans. Some of these NP are only recommended for animal food.

Some of the NP previously classified as safe for human consumption by international organizations are, in fact, more dangerous than previously thought, causing effects such as increased ROS amounts and inflammation in cells. Currently, the development of new NP continues to grow rapidly, given the permitted limits established by these organizations.

There are possibilities of developing shapes, sizes, and compositions of many NPs that greatly increase their technological capabilities.

There is a need to establishing exposure limits for the NP; however, the lack of adequate toxicological data is the main barrier to developing maximum worker exposure to most NP. The second barrier is the lack of standardized and validated methods to monitor the concentrations of NP in the workplace. Furthermore, the occupational benchmark is based on a standard atmosphere for non-nanosized fine particles. In the report by Gordon et al. (2014), a group consensus failed to be reached on any of these points, but some recommendations were established such as the adoption of more effective hygiene measures to control occupational exposure to NP. There is also the need to implement quicker and more cost-effective methods to evaluate the toxicity of the new NP. Also, we must create predictive models to correlate the response of NP by using in vitro and in vivo models in the short and medium term (Gordon et al. 2014).

References

Allouni ZE, Cimpan MR, Høl PJ, Skodvin T, Gjerdet NR (2009) Agglomeration and sedimentation of TiO_2 nanoparticles in cell culture medium. Colloid Surface B 68(1):83–87

Al-Rawi M, Diabaté S, Weiss C (2011) Uptake and intracellular localization of submicron and nano-sized SiO_2 particles in HELA. Arch Toxicol 85(7):813–826

Arnall AH (2003) Future technologies, today's choices: nanotechnology, artificial intelligence and robotics; a technical, political and institutional map of emerging technologies. Greenpeace Environmental Trust, London

Bao YX, Cao Q, Yang Y, Mao R, Xiao L, Zhang H, Zhao HR, Wen H (2013) Expression and prognostic significance of Golgi glycoprotein 73 (GP73) with epithelial-mesenchymal transition (EMT) related molecules in hepatocellular carcinoma (HCC). Diagn Pathol 8:197

Baun A, Sorensen SN, Rasmussen RF, Hartmann NB, Koch CB (2008) Toxicity and bioaccumulation of xenobiotic organic compounds in the presence of aqueous suspensions of aggregates of nano-C(60). Aquat Toxicol 86:379–387

Brausch KA, Anderson TA, Smith PN, Maul JD (2010) Effects of functiolalized fullerenes on bifenthrin and tribufos toxicity to Daphia magna: survival, reproduction and growth rate. Environ Toxicol Chem 29:2600–2606

Bergeson LL, Hester T (2008) Nanotechnology deskbook. Environmental Law Institute, Eli Press, Washington, DC

Chau CF, Wu SH, Yen GC (2007) The development of regulations for food nanotechnology. Trends Food Sci Technol 18:269–280

Chaudhry Q, Aitken R, Scotter R, Blackburn J, Ross B, Boxall A, Castle L, Watkins R (2008) Applications and implications of nanotechnologies for the food sector. Food Addit Contam 25(3):241–258

Chen M, Von Mikecz A (2005) Formation of nucleoplasmic protein aggregates impairs nuclear function in response to SiO_2 nanoparticles. Exp Cell Res 305:51–62

Cheng X, Kan AT, Tomson MB (2004) Naphthalene adsorption and desorption from aqueous C60 fullerene. J Chem Eng Data 49:675–683

Cheng S, Yan D, Chen JT, Zhuo RF, Feng JJ, Li HJ, Feng HT, Yan PX (2009) Soft-template synthesis and characterization of ZnO_2 and ZnO hollow spheres. J Phys Chem C 113:13630–13635

Cho W-S, Duffin R, Bradley M, Megson IL, MacNee W, Howie1 SEM, Donaldson K (2012) NiO and Co_3O_4 nanoparticles induce lung DTH-like responses and alveolar lipoproteinosis. Eur Respir J 39:546–557

Dasari TP, Hwang HM (2013) Effect of humic acids and sunlight on the cytotoxicity of engineered zinc oxide and titanium dioxide nanoparticles to a river bacterial assemblage. J Environ Sci 25(9):1925–1935

De Bie E Doyen P (1962) Cobalt oxides and salts. Cobalt 15:3–13

EFSA (European Food Safety Authority) (2005) Opinion of the Scientific Panel of food additives, flavourings, processing aids and materials in contact with food on a request from the commission related to 2 Isopropyl thioxanthone (ITX) and 2 ethylhexyl-4-dimethylaminobenzoate (EHDAB) in food contact materials. The EFSA J 293:1–15

EFSA (2008) Opinion of the Scientific Panel on food additives, flavourings, processing aids and materials in contact with food (AFC) on safety of aluminium from dietary intake. EFSA J 754:1–34

EFSA (2009) Scientific Opinion of the Panel on Food Additives and Nutrient Sources added to Food. Calcium silicate and silicon dioxide/silicic acid gel added for nutritional purposes to food supplements. EFSA J 1132:1–24

EFSA (2011) Panel on food contact materials, enzymes, flavourings and processing aids (CEF). Scientific opinion on the safety evaluation of the substance, silver zeolite A (silver zinc sodium ammonium alumino silicate), silver content 2–5 %, for use in food contact materials. EFSA J 9(2):1999

EFSA (2012) Scientific Opinion on the use of animal-based measures to assess welfare in pigs. EFSA J 10(1):2512 [85 pp.]

Escuderos ME, García M, Jiménez A, Horrillo MC (2012) Edible and non-edible olive oils discrimination by the application of a sensory olfactory system based on tin dioxide sensors. Food Chem 136(3–4):1154–1159

Freyre-Fonseca V, Delgado-Buenrostro NL, Gutiérrez-Cirlos EB, Calderón-Torres CM, Cabellos-Avelar T, Sánchez-Pérez Y, Pinzón E, Torres I, Molina-Jijón E, Zazueta C, Pedraza-Chaverri J, García-Cuellar CM, Chirino YI (2011) Titanium dioxide nanoparticles impair lung mitochondrial function. Toxicol Lett 202(2):111–119

Gambardella C, Gallus L, Gatti AM, Faimali M, Carbone S, Antisari LV, Falugi C, Ferrando S (2014) Toxicity and transfer of metal oxide nanoparticles from microalgae to sea urchin larvae. Chem Ecol 30(4):308–316

Gentile F, Ferrari M, Decuzzi P (2008) The transport of nanoparticles in blood vessels: the effect of vessel permeability and blood rheology. Ann Biomed Eng 36(2):254–261

Ginley DS, Bright C (2000) Transparent conducting oxides. MRS Bull 25(15):15–18

Gordon SC, Butala JH, Carter JM, Elder A, Gordon T, Gray G, Sayre PG, Schulte PA, Tsai CS, West J (2014) Workshop report: strategies for setting occupational exposure limits for engineered nanomaterials. Regul Toxicol Pharm 68:305–311

Gopinath P, Gogoi SK, Sanpuic P, Paul A, Chattopadhyay A, Ghosh SS (2010) Signaling gene cascade in silver nanoparticle induced apoptosis. Colloid Surface B 77:240–245

Gui S, Zhang Z, Zheng L, Cui Y, Liu X, Li N, Sang X, Sun Q, Gao G, Cheng Z, Cheng J, Wang L, Tang M, Hong F (2011) Molecular mechanism of kidney injury of mice caused by exposure to titanium dioxide nanoparticles. J Hazard Mater 195(15):365–370

Gramowski A, Flossdorf J, Bhattacharya K, Jonas L, Lantow M, Rahman Q, Schiffmann D, Weiss DG, Dopp E (2010) Nanoparticles induce changes of the electrical activity of neuronal networks on microelectrode array neurochips. Environ Health Persp 118(10):1363–1369

Hanini A, Schmitt A, Kacem K, Chau F, Ammar S, Gavard J (2011) Evaluation of iron oxide nanoparticle biocompatibility. Int J Nanomed 6:787–794

Hsin YH, Chen CF, Huang S, Shih TS, Lai PS, Chueh PJ (2008) The apoptotic effect of nanosilver is mediated by a ROS- and JNK-dependent mechanism involving the mitochondrial pathway in NIH3T3 cells. Toxicol Lett 179:130–139

Hyun-Joo C, Sung-Wook C, Sanghoon K, Hyang-Sook C (2011) Effect of particle size of zinc oxides on cytotoxicity and cell permeability in Caco-2 cells. Int J Food Sci Nutr 16:174–178

Izak-Nau E, Voetz M, Eiden S, Duschl A, Puntes VF (2013) Altered characteristics of silica nanoparticles in bovine and human serum: the importance of nanomaterial characterization prior to its toxicological evaluation. Part Fibre Toxicol 10(1):56

Jing S, Shaochuang W, Dong Z, Hun FH, Lei W, Hui L (2011) Cytotoxicity, permeability, and inflammation of metal oxide nanoparticles in human cardiac microvascular endothelial cells. Cell Biol Toxicol 27:333–342

Jung T, Kamm W, Breitenbach A, Kaiserling E, Xiao JX, Kissel T (2000) Biodegradable nanoparticles for oral delivery of peptides: is there a role for polymers to affect mucosal uptake? Eur J Pharm Biopharm 50:147–160

Kalpana Sastry R Anshul S Rao NH (2012) Nanotechnology in food processing sector-An assessment of emerging trends. J Food Sci Technol 50(5):831–841

Li CH, Shen CC, Cheng YW, Huang SH, Wu CC, Kao CC, Liao JW, Kang JJ (2011) Organ biodistribution, clearance, and genotoxicity of orally administered zinc oxide nanoparticles in mice. Nanotoxicology 6(7):746–756

Li M, Jiang Y, Ding R, Song D, Yu H, Chen Z (2013) Hydrothermal synthesis of anatase TiO_2 nanoflowers on a nanobelt framework for photocatalytic applications, J Electr Mater 42(6):1290–1296

Linsinger TPJ, Chaudhry Q, Dehalu V, Delahaut P, Dudkiewicz A, Grombe R, Von der Kammer F, Larsen EH, Legros S, Loeschner K, Peters R, Ramsch R, Roebben G, Tiede K, Weigel S (2013) Validation of methods for the detection and quantification of engineered nanoparticles in food. Food Chem 138:1959–1966

Lomer MC, Hutchinson C, Volkert S, Greenfield SM, Catterall A, Thompson RP, Powell JJ (2004) Dietary sources of inorganic microparticles and their intake in healthy subjects and patients with Crohn's disease. Br J Nutr 92:947–955

McCracken C, Zane A, Knight DA, Dutta PK, Waldman WJ (2013) Minimal intestinal ephitelial cell toxicity in response to short and long term food relevant inorganic nanoparticle exposure. Chem Res Toxicol 26(10):1514–1525

Miura N, Shinohara Y (2009) Cytotoxic effect and apoptosis induction by silver nanoparticles in HeLa cells. Biochem Biophys Res Commun 390:733–737

Morris VJ (2011) Emerging roles of engineered nanomaterials in the food industry. Trends Biotechnol 29:509–516

Moulin JJ, Wild P, Mur JM, Fournier-Betz M, Mercier-Gallay M (1993) A mortality study of cobalt production workers: An extension of the follow-up. Am J Ind Med 23:281–288

Mu Q, David CA, Galceran J, Rey-Castro C, Krzemiński L, Wallace R, Bamiduro F, Milne SJ, Hondow N, Brydson RM, Vizcay-Barrena G, Routledge M, Jeuken LJ, Brown AP (2014) A systematic investigation of the physico-chemical factors that contribute to the toxicity of ZnO nanoparticles. Chem Res Toxicol 27:558–567

NIOSH (National Institute for Occupational Safety and Health) Department of health and human services. Centers for disease control and prevention. Occupational exposure to titanium dioxide. Bulletin 63:1–119

Naura AS, Sharma R (2009) Toxic effects of hexaammine cobalt(III) chloride on liver and kidney in mice: Implication of oxidative stress. Drug Chem Toxicol 32(3):293–299

Omura K, Veluchamy P, Tsuji M, Nishio T, Murojono D (1999) A SnO2 : F thin films from dimethyltin dichloride. J Electrochem Soc 146:2113–2116

Onuma K, Sato Y, Ogawara S, Shirasawa N, Kobayashi M, Yoshitake J, Yoshimura T, Iigo M, Fuji J, Okada F 2009. Nano-scaled particles of titanium dioxide convert bening mouse fibrosarcoma cells into aggressive tumor cells. Am J Pathol 175(5):2171–2183

Papis E, Rossi F, Raspanti M, Dalle-Donne I, Colombo G, Milzani A, Bernardini G, Gornati R (2009) Engineered cobalt oxide nanoparticles readily enter cells. Toxicol Lett 189:253–259

Paustenbach D, Tvermoes B, Unice K, Finley B, Kerger B (2013) A review of the health hazards posed by cobalt: potential importance of free divalent cobalt ion equilibrium in understanding systemic toxicity in humans. Crit Rev Toxicol 43:316–362

Polak N, Read DS, Jurkschat K, Matzke M, Kelly FJ, Spurgeon DJ, Stürzenbaum SR (2014) Metalloproteins and phytochelatin synthase may confer protection against zinc oxide nanoparticle induced toxicity in *Caenorhabditis elegans*. Compar Biochem Physiol C 160:75–85

Rocco MC (2005) Environmentally responsible development of nanotechnology. Environ Sci Technol 39:106A–112A

Römer I, White TA, Baalousha M, Chipman K, Viant MR, Lead JR (2011) Aggregation and dispersion of silver nanoparticles in exposure media for aquatic toxicity tests. J Chromatogr A 1218:4226–4233

Sahu D, Kannan GM, Vijayaraghavan R (2014) Size-dependent effect of zinc oxide on toxicity and inflammatory potential of human monocytes. J Toxicol Environ Health A 77(4):177–191

Sanguansri P, Augustin MA (2006) Nanoscale materials development: a food industry perspective. Trends Food Sci Technol 17:547–556

Sekar D, Falcioni ML, Barucca G, Falcioni G (2011) DNA damage and repair following *in vitro* exposure to two different forms of titanium dioxide nanoparticles on trout erythrocyte. Environ Toxicol 117–127

Seok SH, Cho WS, Park JS, Na Y, Jang A, Kim H, Cho Y, Kim T, You JR, Ko S, Kang BC, Lee JK, Jeong J, Che JH (2013) Rat pancreatitis produced by 13 week administration of zinc oxide nanoparticles: Biopersistence of nanoparticles and possible solutions. J Appl Toxicol 33(10):1089–1096

Shannahan JH, Lai X, Ke, PC, Podila R, Brown JM, Witzmann FA (2013) Silver nanoparticle protein corona composition in cell culture media. Plos One 8(9) e74001

Sharma V, Singh P, Pandey AK, Dhawan A (2012) Induction of oxidative stress, DNA damage and apoptosis in mouse liver after sub-acute oral exposure to zinc oxide nanoparticles. Mutat Res 745(1–2):84–91

Sompol P, Ittarat W, Tangpong J, Chen Y, Doubinskaia I, Batinic-Haberle I, Abdul HM, Butterfield DA, St Clair DK (2008) A neuronal model of Alzheimer's disease: an insight into the mechanisms of oxidative stress-mediated mitochondrial injury. Neuroscience 153(1):120–130

Smith MP, Wayne A (2007) Oxidative stress and dopamine depletion in an intrastriatal 6-hydroxydopamine model of Parkinson's disease. Neuroscience 144:1057–1066

Stone V, Nowack B, Baun A, Van den Brink N, Kammer F, Dusinska M, Handy R, Hankin S, Hassellöv M, Joner E, Fernandes TF (2010) Nanomaterials for environmental studies: classification, reference material issues, and strategies for physico-chemical characterisation. Sci Total Environ 408:1745–1754

Syama S, Reshma SC, Sreekanth PJ, Varma HK, Mohanan PV (2013) Effect of Zinc Oxide nanoparticles on cellular oxidative stress and antioxidant defense mechanisms in mouse liver. Toxicol Environ Chem 95(3):495–503

Tadeev AV, Delabouglise G, Labeau M (1998) Influence of Pd and Pt additives on the microstructural and electrical properties of SnO2-based sensors. Mater Sci Eng B 57(1):76–83

Tanaka A, Hirata M, Homma T, Kiyohara Y (2010) Chronic pulmonary toxicity study of indium-tin oxide and indium oxide following intratracheal instillations into the lungs of hamsters. J Occup Health 52:14–22

Tang J, Xiong L, Wang S, Wang S, Wang J, Liu L, Li J, Yuan F, Xi T (2009) Distribution, translocation and accumulation of silver nanoparticles in rats. J Nanosci Nanotechnol 9(8):4924–4932

Tiede K, Boxall BA, Tear SP, Lewis J, David H, Hassellov M (2008) Detection and characterization of engineered nanoparticles in food and the environment. Food Addit Contam A 25(7):795–821

Tuchsen F, Andersen O, Olsen J (1996) Referral bias among health workers in studies using hospitalization as a proxy measure of the underlying incidence rate. J Clin Epidemiol 49:791–794

United States Government Accountability Office (2010) Nanomaterials are widely used in commerce, but EPA faces challenges in regulating risk. GAO-10-549

Vilhena MS, Costa ML, Berredo JF (2013) Accumulation and transfer of Hg, As, Se, and other metals in the sediment-vegetation-crab-human food chain in the coastal zone of the northern Brazilian state of Pará (Amazonia). Environ Geochem Health 35(4):477–494

Wang J, Gerlach JD, Savage N, Cobb GP (2013) Necessity and approach to integred nanomaterial legislation and governance. Sci Total Environ 442:56–62

Weir A, Westerhoff P, Fabricious L, Von Goertz N (2012) Titanium dioxide nanoparticles in food and personal care products. Environ Sci Technol 46(4):2242–2250

Weiss J, Takhistov P, McClements J (2006) Functional materials in food nanotechnology. J Food Sci 71:R107–R116

World Health Organization International Agency for Research on Cancer (2006) Cobalt in hard metals and cobalt sulfate, gallium arsenide, indium phosphide and vanadium pentoxide. IARC Monog Eval Carc 86:68–73

World Health Organization International Agency for Research on Cancer (2010) Carbon black, titanium dioxide, and talc. IARC Monog Eval Carc 93:1–452

Ye Y, Liu J, Xu J, Sun L, Chen M, Lan M (2010) SiO_2 induces apoptosis vía activation of p53 and Bax mediated by oxidative stress in human hepatic cell line. Toxicol In Vitro 24(3):751–758

Zelikoff J, Willis D, Degheidy H, Zhang Q, Umbreit T, Goering P (2013) Immune cell profiles in response to silver nanoparticles associated with medical devices (P3357). J Immunol 190:202.1

Zhaoxia J, Xue J, Saji G, Tian X, Huan M, Xiang W, Suárez E, Zhang H, Hoek EM, Godwin H, Nel A, Zink JI (2010) Dispersion and stability optimization of TiO_2 nanoparticles in cell culture media. Environ Sci Technol 44:7309–7314

Chapter 16
Multiscale and Nanostructural Approach to Fruits Stability

Gabriela R. Cáez-Ramirez, Darío I. Téllez-Medina and Gustavo F. Gutierrez-López

16.1 Introduction

Biological systems are inherently dynamic and complex, and therefore, they are exposed to a progressive deterioration process. Stability of the fruits depends on the homeostatic ability of the system to retard changes caused by environmental factors. Fruits, whole fresh or minimally processed, are under the influence of biotic and abiotic stress factors. These factors induce ripening, dehydration, shrinkage, browning, and softening, all associated with poor quality attributes. Most of those alterations could be explained by morphostructural changes, such as those concerning cell morphology, cell adhesion, mechanical response, gas diffusion from respiration and physical integrity, among others.

Multiscale approach has been considered as a method to understand the relations among cells, organelles and the plant to get a unified description through combining macroscopic approach with molecular information by integrating mechanisms that occur at different temporal or spatial scales in terms of variables and relations of interest (Baldazzi et al. 2012). The tools of translational proteomics to identify and characterise genomic sequences are useful to improve the quality characteristics and the response of fruits against some biotic and abiotic factors (Agrawal et al. 2012). Molecular techniques reveal considerable information, which necessarily requires the intricate study of several parameters simultaneously to simplify a macro process explanation. However, vegetal material is a complex system since it is multi-functional, multi-compartmentalised, multi-component and multi-related. Hence, fruit structure is a fundamental issue to understand this complex system.

G. F. Gutierrez-López (✉) · D. I. Téllez-Medina
Departamento de Graduados e Investigación en Alimentos, Escuela Nacional de Ciencias Biológicas, Instituto Politécnico Nacional, Carpio y Plan de Ayala, México, 11340 México, DF, Mexico
e-mail: gusfgl@gmail.com

G. R. Cáez-Ramirez
Facultad de Ingeniería, Universidad de La Sabana, Chia, Colombia

© Springer Science+Business Media New York 2015

H. Hernández-Sánchez, G. F. Gutiérrez-López (eds.), *Food Nanoscience and Nanotechnology,* Food Engineering Series, DOI 10.1007/978-3-319-13596-0_16

The fruit structure is composed of fleshy vegetal material that is hierarchically composed of hydrated cells that exhibit turgor and are bound at their cell walls. Its elements are organised from molecules into assemblies, organelles, cells and tissues (Aguilera 2011). Those elements are linked by subsequent relationships at the micro- and nanoscales. Most information for quality control is gathered from the macroscale, from the entire fruit or its pieces, including colour, texture, size and shape (Fig. 16.1). Microscale takes into consideration single cells, their surroundings and organelles. Ultrastructural elements, such as the disposition of the cell walls and membranes, are related to mesoscale. Nanoscale elements include cellulose microfibril (~3–4 nm), cellulose macrofibril (~10–25 nm) (Gibson and Interface 2012), plasmodesmata (~40 nm), vesicles (~10–50 nm), thickness of extracellular matrix and cell membrane, starch granules and plastids, among others (Jeffery et al. 2012).

By taking into account that complexity increases geometrically along the scale, the advantage of this approach is to assess attributes that add knowledge in order to describe the phenomenon starting in the lowest complexity level (Mebatsion et al. 2008). However, in several studies of the changes at the nanoscale, phenomena are considered as isolated, even when most of the structural elements and the subsequent relationships occur at this level. Thus, any change at a nanostructural level, e.g. in microfibrils of cellulose affects cell wall integrity, water transportation, turgor diminish, tissue morphology variation, softening and finally poor quality. Hence, it is needed to establish the effect of changes at cell fruit nanostructures on the entire fruit appearance and its freshness.

The aim of this chapter is to explore the key elements in the study of fruit nanostructure and the information on the matter that could be analysed by considering the different scale levels of observation. It could be performed by means of two integration pathways: from micro- to nanoscales and from nano- to microscales, and by using property–structure–function relationships at multiscale. In this respect, this chapter explains why the analysis of the structure at different levels is a way to understand fruit stability by means of describing the general elements of a multiscale approach. Additionally, several examples of key elements needed to accomplish multilevel approach are presented, including cell and tissue morphology, the importance of the cell wall nanostructure and treatments of preservation processes at the nanoscale, as well as some applications at the nanometric scale. Finally, as an example, it is introduced the multiscale approach of the complex phenomena of senescence in papaya fruits (*Carica papaya* L.).

16.2 Fruits as Complex Systems

The maturation is a highly organised and genetically programmed process that induces an irreversible alteration leading to the development of softness and desirable edible quality attributes. This process involves changes in composition and organelles such as vacuole, chromoplasts and mitochondria (Perotti et al. 2014). The biochemical processes associated with increased respiratory rate, degradation of chlorophyll and biosynthesis of carotenes, anthocyanins and essential oils (the

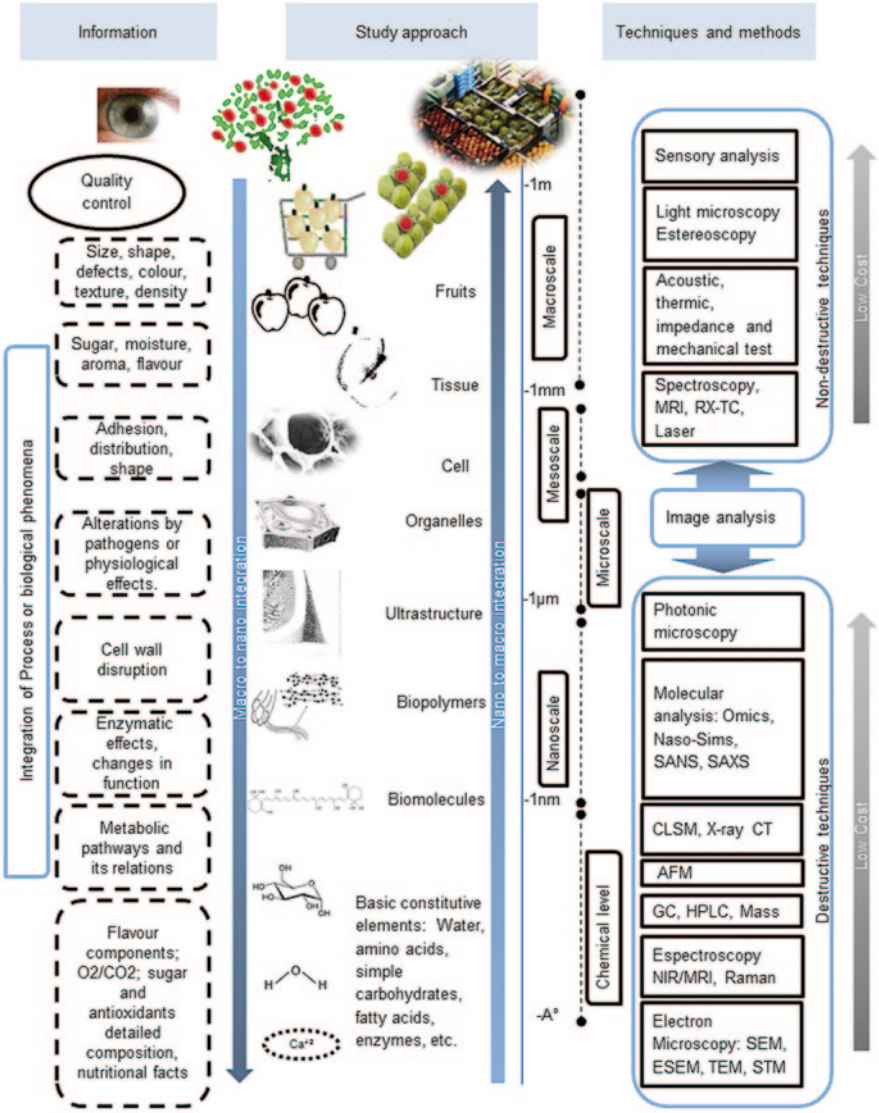

Fig. 16.1 Scheme guide of the elements and pathways to consider for a multiscale evaluation of fruits, generating a systemic integrated approach. *AFM* atomic force microscopy, *CLSM* confocal laser scanning microscopy, *SEM* scanning electron microscopy, *ESEM* environmental scanning electron microscopy, *STEM* scanning transmission electron microscopy, *STM* scanning tunneling microscopy, *X-ray CT* X-ray computed tomography, *nano-SIMS* nano-secondary ion mass spectrometry; *SANS* small-angle neutron scattering, *SAXS* small-angle X-ray scattering, *NIR* near infrared spectroscopy, *MIR* mid-infrared spectroscopy

components responsible for the flavour and aroma) increase the activity of enzymes degrading the cell wall and of those involved in ethylene production (Payasi et al. 2009). Physical changes related to maturation cause the maintenance of fruit structure are evidenced in firmness reduction of the edible portion of the fruit, associated with the degradation of cell wall polysaccharides, which consists of a complex structure of cellulose, hemicellulose and pectin that contributes to cell adhesion (Carpita and Gibeaut 1993).

Figure 16.1 shows the main parameters related to fruit stability, starting with freshness indicators of appearance, texture and sensory attributes, for instance, changes in colour, softening and sweet-acidity balance, that might be evaluated through different approaches, techniques and methods that come from chemical, physical and molecular causes (Ramos et al. 2013). As discussed above, it is easy to notice the great complexity of factors involved in fruit ripening; therefore, an integrated perspective from structure perspective is needed in order to study fruit stability and senescence.

16.3 Multiscale as a Way to Understand Fruit Instability

A multiscale approach implies not only the length interval division, the deep evaluation and observation of the system by balancing accuracy and complexity but also the totality of phenomena involved. Multiscale modelling to predict food parameters requires defining scale levels, whose physical properties reveal structural changes that might be compared with those reported in the current literature for the macroscale (Ho et al. 2013). However, a multiscale approach, in a context of fruit complexity, implies also a systematic problem divided by analysing cell relationships, intra- and intercellular, considering both integrative pathways, macro to nano and nano to macro. Figure 16.1 explains the procedure that might be followed in order to integrate a multiscale approach, including nanoscale evaluation by using different techniques with the purpose of achieving a deeper understanding of the fruit structure.

The nano- to macroscale pathway takes the structural arrangement of building blocks or key elements, across many hierarchical scales (Cranford and Buehler 2010). Hence, the nano to macro integrative pathway arises from detailed information; the relationships among the pre-existing nano elements are useful to understand the whole phenomenon. As an example of a nano to macro process, it is possible to self-assemble some mesoscopic structures, with sufficiently weak interactions, providing hydrophilic interactions that can increase the fruit structure stability (Van der Sman 2012).

In another work, tissues of vanilla fruit (*Vanilla planifolia*) were evaluated during the curing process by microstructural parameters in order to detect the main tissue changes corresponding to the highest concentration of vanillin (Tapia-Ochoategui et al. 2010). This approach has been useful to evaluate the effect of convective drying on total anthocyanin content, antioxidant activity and cell morphometric parameters of strawberry parenchymal tissue (*Fragaria x ananassa* Dutch) by following a micro to macro integrative analysis (Morales-Delgado et al. 2014).

The macro to nanoscale pathway implies an analytic thinking process to develop a detailed knowledge at each level from the general information. This uncommon integrative pathway implies the development of a generalised knowledge of the system and then to detail each level of analysis that is needed to understand certain phenomenon. A research on tomato internal compression damage, using nonlinear multiscale finite element model, concluded that the locular gel tissue displayed mechanical damage prior to the mesocarp and the exocarp tissues when an external loading force was applied to the tomatoes. This approach was useful to understand the effect on the stress distribution, deformation and mechanical damage of the tissues (Li et al. 2013a).

The understanding of fruit stability processes is determined by all existing relations among scale levels; those relationships determine structure, material properties and functionality of fruit (Seguí et al. 2010), which have been classified depending on the material and the attribute observed (Chung and McClements 2014). In the first place, those could come from the fruit structure–property relations, depending on composition and phase properties, processing conditions and interactions and physical properties (optical, rheological and structure stability). As well, the structure–function relationships are important, which depend on physiological activity, ripening rate, presence of ethylene, respiration rate, enzyme activity, nutritional and other interesting functions for consumers, and consumer perception of freshness related to appearance, flavour, mouth texture and storage stability.

The relationships within the system could be found if all those data coming from different scales are integrated by a unified approach and expressed in a unified relationship (Perrot et al. 2011). It can be useful to develop a new structure, keep its stability or restructure it in such a way that it acquires desirable functional and quality attributes at the macroscale (Trystram 2012). Therefore, it is possible to elucidate relationships to develop a better model for controlling undesirable changes caused by ripening or for guaranteeing freshness and quality attributes.

In a study at the micro-, ultra- and nanolevels of green grapefruits, *Vitis labrusca* L. treated with hydrogen peroxide, UV–C irradiation and ultrasound, authors reported that nanostructural and mechanical alterations occurred in the outer tangential epidermal cell wall (Fava et al. 2011). It was also reported in the same study that the green grapefruit colour, as a macroscale attribute, could help to identify alterations caused by treatments and to provide new insights for optimisation of disinfection processes. In another study, a multiscale modelling for apple ripening prevention was applied in controlled atmosphere storage to understand O_2/CO_2 diffusivity at macroscale, related to changes in the respiratory rate, by using R-X ray-computed tomography three-dimensional (CT 3D) image analysis (Herremans et al. 2014).

16.4 Main Topics Studied Around Fruit Nanostructure

Structural changes, reflected as significant defects of quality, could be analysed by taking into account nanoscale key elements. Considering the information collected from databases, those nanoelements have been grouped into three main items:

tissue, cell and organelles morphology; cell wall structure roll in fruit stability and nanoscale technologies to extend fruit stability.

Until February 2015, an increasing number of papers that take nanoscale elements in the evaluation of fruit stability into consideration can be found. A gathering information process, by using bibliographic databases around the world, has found several papers related to nanoscale and fruits and presented in three main categories: nanoscale and fruits, with 1259 papers; nanostructure and fruits, with 461 and multiscale modelling and fruits, with 465. Those papers are mainly associated with the cell wall, electron microscopy, nanotechnology, silver and gold nanoparticles, food packaging, carbon nanotubes as biosensors, delivering systems, multiscale modelling, biopolymers, films and food industry. However, such topics are no conclusive on interest areas. Structural changes, reflected in significant defects of quality, could be analysed by taking into account key elements that could be useful to describe changes in a multiscale approach, including tissue and cell morphology, cell wall structure, nanotechnology applications and processing effects, among others.

16.4.1 Tissue, Cell and Organelles Morphology

The knowledge of cell morphology and distribution in a tissue might be useful to create a porous structure. A fruit structure depends on the cellular random shape, intercellular spaces, architectural disposition and its turgor pressure. The virtual representation of a tissue, including its porosity, could be used to simulate gas or water transfer at nanoscale and also tissue damage by hydrostatic stress at storage and transportation (Abera et al. 2012). Moreover, nuclear magnetic resonance (NMR), magnetic resonance imaging (MRI) and x-ray tomography (XRT) analyses of the cell shape showed a possible explanation for the increasing of rehydration rate and loss of nutrients due to a blanching pretreatment for freeze-dried fruits (Van der Sman et al. 2014).

Physical accessibility of nutrients such as carotenoids was related to cell and organelles ultrastructure by analysing light microscopy and transmission electron microscopic (TEM) images of cell wall thickness, cell size, chromoplast, plastoglobules, membranes, tubules, vesicles, thylakoids and starch grains in several fruits and vegetables (mango (*Mangifera indica*), papaya (*Carica papaya*), tomato (*Solanum esculentum*), watermelon (*Citrullus lanatus*), red grapefruit (*Vitis vinífera*) and some vegetables such as carrot (*Daucus carota*), sweet potato (*Ipomoea batatas*) and butternut squash (*Cucurbita moschata*; Jeffery et al. 2012). Additionally, organelles architecture is responsible for some metabolic changes. Metabolic pathways generate important nutritional compounds such as carotenoids that depend on the organelle structure. It was found by several microscopy techniques laser scanning confocal microscopy (LSCM), scanning electron microscopy (SEM), TEM and hyperspectral confocal Raman microscopy) that there was a linkage between shape and size of chromoplast and type and quantity of carotenoids in *Capsicum annuum* fruit (Kilcrease et al. 2013).

16.4.2 Cell Wall Structure Roll in Fruit Instability

The fruit cell walls are significantly affected by ripening, something that has strong influence in maintaining the quality attributes, and studies on fruit structure are reported around several subjects (Table 16.1). The cell walls of edible portion, classified as primary, are composed of different polysaccharides and structural proteins, whose ratio depends on the cell type, the stage of development and constant remodelling ability (Lee et al. 2011). However, the biodiversity and changes in composition, which affect nanomechanical properties, might be studied under a multiscale approach, by new molecular assays, monoclonal antibodies (mAbs) and carbohydrate-binding modules (CBMs), in order to develop possible novel nanomaterials associated with biosynthetic genes (Fangel et al. 2012).

A balance between the symplast turgor pressure and the cell wall strength, which must have a controlled stiffness to allow cell growth, defines the cell shape. Control mechanisms are strongly related to the different steps of cellular remodelling; necessary signalling pathways involved are both between the apoplast and the cell wall and between the cell wall and the cytoplasm (Wolf, et al. 2012). A dynamic integration of the cell wall architectural study reveals similar principles of assembly and mechanisms of cell growth for all vegetal cells. Furthermore, cellulose synthesis and orientation of perturbation induce direct responses to signal transduction affecting other biosynthetic pathways that determine cell growth mechanism and control of anisotropic structuring (Benatti et al. 2012). Finally, methyl-esterification affects cellular adhesion and fruit ripening (Wolf et al. 2012).

Cell walls are constituted of complex arrays of a number of nanoelements and aim to be defence structures against biotic or abiotic stress, as for the case of pathogen threats, in which the cell walls are modified to counteract their harmful effects. Moreover, extracellular matrix structure of sweet oranges (*Citrus sinensis*) has been shown as a key element for a resistant answer to limit *Xanthomonas axonopodis* pathogens (Swaroopa Rani and Podile 2014). The monitoring process in every vegetal cell recognises whether the wall is necessary to produce more cellulose and induces an appropriate response, including the adjustment processes to phenomena of stress application and relaxation arise. However, the biological perspective of cell wall must be integrated to mechanical evaluation and other physical phenomena (Lee et al. 2011).

16.4.3 Nanoscale Technologies to Extend Fruit Stability

Several applications of nanostructures to preserve postharvested and fresh cut fruits have been reported, which are shown in Table 16.2. Most of those applications are related to nanopackaging materials, nanocoating materials, nanotechnology to macromolecular characterisation and pathogen detection. Diverse techniques

Table 16.1 Main topics studied around cell wall nanostructure

Topic studied	Vegetal material	Methodology	Relation	Information gathered from relations	Reference
Composition	*Solanum lycopersicum* L.	Raman micro-spectroscopy and image analysis	Structure–property	Localisation of the biopolymers in the primary cell wall	Chylińska et al. 2014
Cellulose	*Vitis vinifera* var. Chardonnay	FTIR, DSC, thermal gravimetric analysis (TGA), x-ray diffraction (XRD), scanning electron microscopy (SEM), TEM, AFM	Structure–property	Characterisation of cellulose structure	Lu and Hsieh 2012
Pectin	*Prunus persica* L.	AFM	Structure–function	Nanostructural degradation of water-soluble pectin	Zhang et al. 2012
Hemicellulose	*Prunus pseudocerasus* L.	AFM	Structure–property	The thickness of hemicellulose chains may be related to the textural differences observed in the cultivars of this fruit	Chen et al. 2009
Bioavailability of nutrients	*Diospyros kaki* L.	Cryo-SEM, light microscopy (LM) and CLSM	Structure– function	High hydrostatic pressure (HHP) treatment generates cell wall disruption and releases carotenoids from chromoplasts	Vázquez-Gutiérrez et al. 2011
Texture	*Malus* x *domestica* (Borkh)	AFM	Structure–property	Relation between texture and cell wall nanostructure	Cybulska et al. 2013
Water transport	Fruits tissue	Micro- and nano-modelled structure	Structure– property–function	Importance of the different microstructural features (intracellular space, cell wall, membrane and cytoplasm) for water transport	Fanta et al. 2013

AFM atomic force microscopy, *CLSM* confocal laser scanning microscopy, *DSC* differential scanning calorimetry, *FTIR* Fourier transform infrared spectroscopy, *HHP* high hydrostatic pressure *SEM* scanning electron microscopy, *TEM* transmission electron microscopy, *TGA* thermogravimetric analysis, *XRD* X-ray diffraction

Table 16.2 Nanoscale technology applications to fruits: some illustrative cases

General application	Vegetal material	Methodology	Advantage	Reference
Calcium treatment	*Fragaria chiloensis* L. Mill.	Molecular	Reduced cell wall-degrading genes after cold storage	Figueroa et al. 2012
	Fragaria annanassa Duch.	AFM	Slowed the breakdown of cell wall properties	Chen et al. 2011
	Prunus armeniaca L.	AFM	1 % of calcium-retarded depolymerisation and pectin solubilisation	Liu et al. 2009
	Solanum lycopersicum L.	Molecular, light microscopy and inductively coupled plasma-atomic emission spectroscopy (ICP-AES)	Controlled pectin-methyl-esterification, intercellular and tissue adhesion	Hyodo et al. 2013
	Cucumis melo L.	Texture, light microscopy and image analysis	Retarded depolymerisation. Cell morphology reflected the macroscale behaviour by image analysis	Casas-Forero and Caez-Ramirez 2011
Pathogen	*Carica papaya* L.	Molecular gene expression, colour and SEM	Hot water treatment induces resistance to anthracnose disease	Li et al. 2013a
Nanocoating	*Manguifera indica* var. Tommy Atkins	SEM, FTIR, zeta potential.	Gas flow reduction by a nanomultilayer coating of pectin and chitosan	Medeiros et al. 2012
Packaging and distribution	Nanosensors	Molecular, optical, spatial and bio-interaction, array nanosensors	It is possible to control information, storage conditions, labels, identification	Bowles and Lu 2014
Nutrient protection	β-carotene	TEM	Better bioaccesability depending on citric pectin concentration, methyl-esterification and the smallest size of droplets (15–16 μm)	Verrijssen et al. 2014
Processing	*Citrus* x *sinensis* juice	Composition and rheology	Destabilisation in frozen concentrate orange juice depends on the molecular structure of pectin	Galant et al. 2014

AFM atomic force microscopy, *FTIR* Fourier transform infrared spectroscopy, *ICP-AES* inductively coupled plasma atomic emission spectroscopy, *SEM* scanning electron microscopy, *TEM* transmission electron microscopy

and methodologies are reported to find interesting conclusions around nanoscale applications. Moreover, nanotechnology and nanomaterials have been applied for agricultural production to final products in order to improve process, quality, bioactivity and nutrition mostly evaluated at the molecular level (Cifuentes 2012). Nowadays, nanoagrochemicals for pest control, nanofertilisers and nanobiotechnology to increase production are widely employed to improve agricultural practices (Sekhon 2014). As other interesting applications, it is possible to introduce nanoparticles within organelles, such as chloroplast, to extend the photosynthetic activity, which could increase the rate of sugar production (Scholes and Sargent 2014). Those nanoparticle assemblies offer the opportunity to engineer plant functions by a nanobiotic approach (Giraldo et al. 2014).

16.4.4 Fruit Components Applied in Nanotechnology

Nanotechnology involves the design, synthesis and manipulation of structures in particles with dimension around 100 nm for specific functions. It is possible to develop some nanoparticles for specific applications from fruits. Some industrial nano applications of fruits include nutrient protection, nanocomposites and nanoemulsions. Silver nanoparticles could be developed from fruit elements of, for example, *Morinda citrofolia* L. that have inhibitory activity against human pathogens (Sathishkumar et al. 2012) or *Terminalia chebula* with reductive catalytic activity (Edison and Sethuraman 2012). Fruits of *Hovena dulcis*, tamarind and pear are useful to develop gold nanoparticles due to its optoelectric properties (Basavegowda et al. 2014; Ghodake et al. 2010).

Some nutrients have been nanoprotected. For example, antioxidants such as hesperetin from citric fruits in a lipid nanocarrier (Fathi and Varshosaz 2013), antioxidant extract of *Lagenaria siceraria* fruit (Kulkarni et al. 2014), betaxanthins from *Opuntia* fruits (Gandía-Herrero et al. 2010) and phenolic extract from sour cherry (*Prunus cerasus*) pomace (Luca et al. 2012). Other biocomponents of interest have been protected by microcapsules, such as chilli non-aqueous extracts due to their antibacterial, antioxidant and provitamin properties (Guadarrama-Lezama et al. 2012). Natural components are employed for other applications. For instance, it is possible to use an edible composite film of pectin/papaya puree/cinnamaldehyde nanoemulsion in order to reduce the growth of microbial pathogens (Otoni et al. 2014).

Finally, other study reported the development of nanocomposites that has been carried out in SiC nanowires produced by pyrolysing bunch fibres from oil-free palm fruits, infiltrated with tetraethyl orthosilicate. The amorphous nature of carbohydrate chains and the porous structure of the fibres were useful for this development (Chiew and Cheong 2012).

16.5 Case of Study: From Macro- to Nanoscale Integration to Understand the Senescence Process in Papaya (*Carica Papaya* L.)

Papaya consumption is interesting because of its content of several bioactive compounds. The structural matrix of the fruit is responsible for the assimilating rate of each component (Epriliati et al. 2009); thus, it is of great interest to study the relationship between structural and composition changes.

The complexity of the phenomenon of senescence in fresh pre-cut papaya is associated with the action of ethylene and with the ripening process, which prompt a cascade of enzymatic reactions of cell wall hydrolases and modify the tissue stability (Huerta-Ocampo et al. 2012). Changes in the composition of the carbohydrates during maturation provide important information about the patterns of the cell walls and may contribute to a better understanding of the role played by enzymatic processes in the softening of the papaya fruit (Shiga et al. 2009). Pectinases and their activity play a major role in metabolism and structural maintenance of fruit. Pectic substances yield effects on cell physiology and growth, intercellular adhesion, cell separation and rate of ripening (Duvetter et al. 2009).

It was evaluated the damage of fresh pre-cut papaya variety Tainung, stored at controlled conditions, by different microscopy methods, which are shown in Fig. 16.2. At macroscale, it was observed by stereoscopy the increasing roughness of the upper layer of the cut tissue as well as the colour changes. At the mesoscale, the tissue showed cell shape and size changes that revealed cell wall disruption. At microscale, the cell wall showed significant changes in the characteristic self-fluorescence of some of its components. The interaction at nanoscale was evaluated by environmental scanning electron microscopy (ESEM) and confirmed the cell wall disruption. Finally, it was obtained clear evidence of large damage due to time of storage after cutting. The studied pre-cut fresh papaya system shows that it is possible to find multiscale relations that contribute to explain the cellular changes through quantitative indicators of freshness in the tissue. The evaluation of the entire system showed that everything occurring at microscale is reflected at the macroscale as structural, mechanical and colour attributes. It is possible to find multiscale relations exhibiting the cellular changes through quantitative indicators of freshness in the tissue. The importance of this study is to contribute an alternative approach to fruit stability focused on minimising the causes of softening during storage of pre-cut fresh papaya.

16.6 Conclusions

Detailed analysis of the phenomena on a complex system at the nanoscale has allowed to improve the stability of fruits. Multiscale integration, including the nano approach, has revealed as key elements in evaluating the structural stability of the

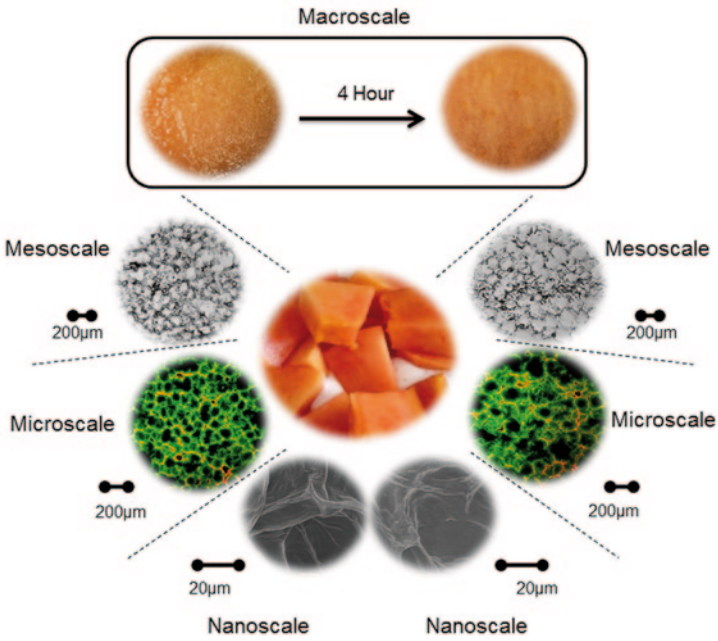

Fig. 16.2 Methodological approach to papaya senescence multiscale evaluation

fruit tissue, such as the shape and distribution of the cells, the cell wall that in association with the middle lamella creates a fundamental structural support and the use of associated preservation treatments. The most frequent pathway is oriented from nano to macro. However, both pathways, by using multi-level descriptors may find interesting relationships that lead to the understanding of complex phenomena that may have an influence in the retardation of senescence.

References

Abera MK, Fanta SW, Verboven P, Ho QT, Carmeliet J, Nicolai BM (2012) Virtual fruit tissue generation based on cell growth modelling. Food Bioprocess Tech 6(4):859–869

Agrawal GK, Pedreschi R, Barkla BJ, Bindschedler LV, Cramer R, Sarkar A, Renaut J, Job D, Rakwal R (2012) Translational plant proteomics: a perspective. J Proteomics 75(15):4588–4601

Aguilera JM (2011) Food microstructures for health, well-being, and pleasure. In: Aguilera JM, Simpson R (eds) Food engineering interfaces. Springer, New York, pp 577–588. ISBN 978-1-4419-7474-7

Baldazzi V, Bertin N, de Jong H, Génard M (2012) Towards multiscale plant models: integrating cellular networks. Trends Plant Sci 17(12):728–736

Basavegowda N, Idhayadhulla A, Lee YR (2014) Phyto-synthesis of gold nanoparticles using fruit extract of *Hovenia dulcis* and their biological activities. Ind Crops Prod 52:745–751

Benatti MR, Penning BW, Carpita NC, McCann MC (2012) We are good to grow: dynamic integration of cell wall architecture with the machinery of growth. Front Plant Sci 3:187

Bowles M, Lu J (2014) Removing the blinders: a literature review on the potential of nanoscale technologies for the management of supply chains. Technol Forecast Soc Chang 82:190–198

Carpita NC, Gibeaut DM (1993) Structural models of primary cell walls in flowering plants: consistency of molecular structure with the physical properties of the walls during growth. Plant J 3(1):1–30

Casas-Forero N, Caez-Ramirez G (2011) Morfometric and quality changes by application of three calcium sources under mild termal treatment in pre-cut fresh melon (*Cucumis melo* L.). Rev Mex Ing Quím 10(3):431–444

Chen F, Zhang L, An H, Yang H, Sun X, Liu H, Yao Y, Li L (2009) The nanostructure of hemicellulose of crisp and soft Chinese cherry (*Prunus pseudocerasus* L.) cultivars at different stages of ripeness. Lebenson Wiss Technol 42(1):125–130

Chen F, Liu H, Yang H, Lai S, Cheng X, Xin Y, Yang B, Hou H, Yao Y, Zhang S, Bu G, Deng Y (2011) Quality attributes and cell wall properties of strawberries (*Fragaria annanassa* Duch.) under calcium chloride treatment. Food Chem 126(2):450–459

Chiew YL, Cheong KY (2012) Growth of SiC nanowires using oil palm empty fruit bunch fibres infiltrated with tetraethyl orthosilicate. Physica E Low Dimens Syst Nanostruct 44(10):2041–2049

Chung C, McClements DJ (2014) Structure-function relationships in food emulsions: improving food quality and sensory perception. Food Struct 1(2):106–126

Chylińska M, Szymańska-Chargot M, Zdunek A (2014) Imaging of polysaccharides in the tomato cell wall with Raman microspectroscopy. Plant Methods 10(1):14

Cifuentes A (2012) Food analysis: present, future, and foodomics. ISRN Anal Chem 2012:1–16. doi:10.5402/2012/801607

Cranford S, Buehler MJ (2010) Materiomics: biological protein materials, from nano to macro. Nanotechnol Sci Appl 12(3):127–148

Cybulska J, Zdunek A, Psonka-Antonczyk KM, Stokke BT (2013) The relation of apple texture with cell wall nanostructure studied using an atomic force microscope. Carbohydr Polym 92(1):128–137

De Medeiros BG, Pinheiro AC, Carneiro-da-Cunha MG, Vicente AA (2012) Development and characterization of a nanomultilayer coating of pectin and chitosan—Evaluation of its gas barrier properties and application on Tommy Atkins mangoes. J Food Eng 110(3):457–464

Duvetter T, Sila DN, Van Buggenhout S, Jolie R, Van Loey A, Hendrickx M (2009) Pectins in processed fruit and vegetables: part I-stability and catalytic activity of pectinases. Compr Rev Food Sci Food Saf 8(2):75–85

Edison TJI, Sethuraman MG (2012) Instant green synthesis of silver nanoparticles using *Terminalia chebula* fruit extract and evaluation of their catalytic activity on reduction of methylene blue. Process Biochem 47(9):1351–1357

Epriliati I, D'Arcy B, Gidley M (2009) Nutriomic analysis of fresh and processed fruit products. 1. During *in vitro* digestions. J Agric Food Chem 57(8):3363–3376

Fangel JU, Ulvskov P, Knox JP, Mikkelsen MD, Harholt J, Popper ZA, Willats WG (2012) Cell wall evolution and diversity. Front Plant Sci 3:152

Fanta SW, Abera MK, Ho QT, Verboven P, Carmeliet J, Nicolai BM (2013) Microscale modeling of water transport in fruit tissue. J Food Eng 10:229–237

Fathi M, Varshosaz J (2013) Novel hesperetin loaded nanocarriers for food fortification: production and characterization. J Funct Foods 5(3):1382–1391

Fava J, Hodara K, Nieto A, Guerrero S, Alzamora SM, Castro MA (2011) Structure (micro, ultra, nano), color and mechanical properties of *Vitis labrusca* L. (grape berry) fruits treated by hydrogen peroxide, UV-C irradiation and ultrasound. Food Res Int 44(9):2938–2948

Figueroa CR, Opazo MC, Vera P, Arriagada O, Díaz M, Moya-León MA (2012) Effect of postharvest treatment of calcium and auxin on cell wall composition and expression of cell wall-modifying genes in the Chilean strawberry (*Fragaria chiloensis*) fruit. Food Chem 132(4):2014–2022

Galant AL, Widmer WW, Luzio GA, Cameron RG (2014) Characterization of molecular structural changes in pectin during juice cloud destabilization in frozen concentrated orange juice. Food Hydrocoll 41:10–18

Gandía-Herrero F, Jiménez-Atiénzar M, Cabanes J, García-Carmona F, Escribano J (2010) Stabilization of the bioactive pigment of opuntia fruits through maltodextrin encapsulation. J Agric Food Chem 58(19):10646–10652

Ghodake GS, Deshpande NG, Lee YP, Jin ES (2010) Pear fruit extract-assisted room-temperature biosynthesis of gold nanoplates. Colloids Surf B Biointerfaces 75(2):584–589

Gibson LJ, Interface JRS (2012) The hierarchical structure and mechanics of plant materials J R Soc Interface 9(76):2749–2766

Giraldo JP, Landry MP, Faltermeier SM, McNicholas TP, Iverson NM, Boghossian AA, Reuel NF, Hilmer AJ, Sen F, Brew JA, Strano MS (2014) Plant nanobionics approach to augment photosynthesis and biochemical sensing. Nat Mater 13(4):400–408

Guadarrama-Lezama AY, Dorantes-Alvarez L, Jaramillo-Flores ME, Pérez-Alonso C, Niranjan K, Gutiérrez-López GF, Alamilla-Beltrán L (2012) Preparation and characterization of non-aqueous extracts from chilli (*Capsicum annuum* L.) and their microencapsulates obtained by spray-drying. J Food Eng 112(1–2):29–37

Herremans E, Verboven P, Defraeye T, Rogge S, Ho QT, Hertog MLATM, Verlinden BE, Bongaers E, Wevers M, Nicolai BM (2014) X-ray CT for quantitative food microstructure engineering: the apple case. Nucl Instrum Methods Phy Res B 324:88–94

Ho QT, Carmeliet J, Datta AK, Defraeye T, Delele MA, Herremans E, Opara L, Ramon H, Tijskens E, Sman R, Liedekerke PV, Verboven P, Nicolaï BM (2013) Multiscale modeling in food engineering. J Food Eng 114(3):279–291

Huerta-Ocampo JÁ, Osuna-Castro JA, Lino-López GJ, Barrera-Pacheco A, Mendoza-Hernández G, De León-Rodríguez A, Barba de la Rosa AP (2012) Proteomic analysis of differentially accumulated proteins during ripening and in response to 1-MCP in papaya fruit. J Proteomics 75(7):2160–2169

Hyodo H, Terao A, Furukawa J, Sakamoto N, Yurimoto H, Satoh S, Iwai H (2013) Tissue specific localization of pectin-Ca^{2+} cross-linkages and pectin methyl-esterification during fruit ripening in tomato (*Solanum lycopersicum*). PloS One 8(11):e78949

Jeffery J, Holzenburg A, King S (2012) Physical barriers to carotenoid bioaccessibility. Ultrastructure survey of chromoplast and cell wall morphology in nine carotenoid-containing fruits and vegetables. J Sci Food Agric 92(13):2594–2602

Kilcrease J, Collins AM, Richins RD, Timlin JA, O'Connell MA (2013) Multiple microscopic approaches demonstrate linkage between chromoplast architecture and carotenoid composition in diverse *Capsicum annuum* fruit. Plant J 76(6):1074–1083

Kulkarni SD, Sinha BN, Kumar KJ (2014) Modified release and antioxidant stable *Lagenaria siceraria* extract microspheres using co-precipitated starch. Int J Biol Macromol 66:40–45

Lee KJD, Marcus SE, Knox JP (2011) Cell wall biology: perspectives from cell wall imaging. Mol Plant 4(2):212–219

Li Z, Li P, Yang H, Liu J (2013a) Internal mechanical damage prediction in tomato compression using multiscale finite element models. J Food Eng 116(3):639–647

Li X, Zhu X, Zhao N, Fu D, Li J, Chen W, Chen W (2013b) Effects of hot water treatment on anthracnose disease in papaya fruit and its possible mechanism. Postharvest Biol Technol 86:437–446

Liu H, Chen F, Yang H, Yao Y, Gong X, Xin Y, Ding C (2009) Effect of calcium treatment on nanostructure of chelate-soluble pectin and physicochemical and textural properties of apricot fruits. Food Res Int 42(8):1131–1140

Lu P, Hsieh YL (2012) Cellulose isolation and core–shell nanostructures of cellulose nanocrystals from chardonnay grape skins. Carbohydr Polym 87(4):2546–2553

Luca A, Cilek B, Hasirci V, Sahin S, Sumnu G (2012) Effect of degritting of phenolic extract from sour cherry pomace on encapsulation efficiency—production of nano-suspension. Food Bioprocess Technol 6(9):2494–2502

Mebatsion HK, Verboven P, Ho QT, Verlinden BE, Nicolaï BM (2008) Modelling fruit (micro) structures, why and how? Trends Food Sci Technol 19(2):59–66

Morales-Delgado DY, Téllez-Medina DI, Rivero-Ramírez NL, Arellano-Cárdenas S, López-Cortez S, Hernández-Sánchez H, Gutiérrez-López G, Cornejo-Mazón M (2014) Efecto del secado convectivo en el contenido total de antocianinas, actividad antioxidante y cambios morfométricos de células de parénquima de fresa (*Fragaria* X *ananassa* Dutch). Rev Mex Ing Quim 13(1):179–187

Otoni CG, De Moura MR, Aouada FA, Camilloto GP, Cruz RS, Lorevice MV, De Soares SFF, Mattoso LHC (2014) Antimicrobial and physical-mechanical properties of pectin/papaya puree/cinnamaldehyde nanoemulsion edible composite films. Food Hydrocoll 41:188–194

Payasi A, Mishra NN, Chaves ALS, Singh R (2009) Biochemistry of fruit softening: an overview. Physiol Mol Biol Plants 15(2):103–113

Perotti VE, Moreno AS, Podestá FE (2014) Physiological aspects of fruit ripening: the mitochondrial connection. Mitochondrion 17C:1–6

Perrot N, Trelea IC, Baudrit C, Trystram G, Bourgine P (2011) Modelling and analysis of complex food systems: state of the art and new trends. Trends Food Sci Technol 22(6):304–314

Ramos B, Miller FA, Brandão TRS, Teixeira P, Silva CLM (2013) Fresh fruits and vegetables—an overview on applied methodologies to improve its quality and safety. Innov Food Sci Emerg Technol 20:1–15

Sathishkumar G, Gobinath C, Karpagam K, Hemamalini V, Premkumar K, Sivaramakrishnan S (2012) Phyto-synthesis of silver nanoscale particles using *Morinda citrifolia* L. and its inhibitory activity against human pathogens. Colloids Surf B Biointerfaces 95:235–240

Scholes GD, Sargent EH (2014) Bioinspired materials: boosting plant biology. Nat Mater 13(4):329–331

Seguí L, Fito PJ, Fito P (2010) Analysis of structure-property relationships in isolated cells during OD treatments. Effect of initial structure on the cell behaviour. J Food Eng 99(4):417–423

Sekhon BS (2014) Nanotechnology in agri-food production: an overview. Nanotechnol Sci Appl 4(7):31–53

Shiga TM, Fabi JP, do Nascimento JR, Petkowicz CL, Vriesmann LC, Lajolo FM, Cordenunsi BR (2009) Changes in cell wall composition associated to the softening of ripening papaya: evidence of extensive solubilization of large molecular mass galactouronides. J Agric Food Chem 57(15):7064–7071

Swaroopa Rani T, Podile AR (2014) Extracellular matrix-associated proteome changes during non-host resistance in citrus- *Xanthomonas* interactions. Physiol Plant 150(4):565–579

Tapia-Ochoategui AP, Camacho-Díaz BH, Perea-Flores MJ, Ordóñez-Ruíz IM, Gutiérrez-López GF, Dávila-Ortiz G (2010) Morfometric changes during the traditional curing process of vanilla pods (*Vanilla planifolia*; Orchidaceae). Rev Mex Ing Quím 10(1):105–115

Trystram G (2012) Modelling of food and food processes. J Food Eng 110(2):269–277

Van der Sman, RGM (2012) Soft matter approaches to food structuring. Adv Colloid Interface Sci 176–177:18–30

Van der Sman RGM, Vergeldt FJ, Van As H, Van Dalen G, Voda A, Van Duynhoven JPM (2014) Multiphysics pore-scale model for the rehydration of porous foods. Innov Food Sci Emerg Technol 24:69–79

Vázquez-Gutiérrez JL, Quiles A, Hernando I, Pérez-Munuera I (2011) Changes in the microstructure and location of some bioactive compounds in persimmons treated by high hydrostatic pressure. Postharvest Biol Technol 61(2–3):137–144

Verrijssen TAJ, Balduyck LG, Christiaens S, Van Loey AM, Van Buggenhout S, Hendrickx ME (2014) The effect of pectin concentration and degree of methyl-esterification on the *in vitro* bioaccessibility of b-carotene-enriched emulsions. Food Res Int 57:71–78

Wolf S, Hématy K, Höfte H (2012) Growth control and cell wall signaling in plants. Annu Rev Plant Biol 63:381–407

Zhang L, Chen F, Yang H, Ye X, Sun X, Liu D, Yang B, An H, Deng Y (2012) Effects of temperature and cultivar on nanostructural changes of water-soluble pectin and chelate-soluble pectin in peaches. Carbohydr Polym 87(1):816–821

Chapter 17
Modulating Oxidative Stress: A Nanotechnology Perspective for Cationic Peptides

Anaid Hernández-Jabalera, Javier Vioque, Manuel Alaiz, Julio Girón-Calle, Cristina Megías, Cristian Jiménez-Martínez and Gloria Dávila-Ortíz

17.1 The Application of Nanotechnology for Human Health Improvement

Nanotechnology is recognized as an emerging and growing field that involves manufacturing, processing, and application of structures, devices, and systems to control shape and size at the nanometer scale (Bouwmeester et al. 2009).

The applications of nanotechnology cover a broad range of areas such as electronics, medicine, textiles, defense, food, agriculture, and cosmetics and allow integration between technology and biological systems not previously attainable (Chen et al. 2006; Bagchi et al. 2013).

The awareness that the nanoscale has certain properties appropriated to solve important medical challenges has promoted efforts directed to improve human health, such as the prevention or treatment of biological imbalance conditions like oxidative stress, which is closely related with the risk of developing several degenerative diseases (Sozer and Kokini 2009).

The materials and devices developed by nanotechnology can be designed to address many aspects, such as disease treatment, drug delivery systems, drug and food security, and diagnostic technologies, among others (Boddapati et al. 2005; Bouwmeester et al. 2009; Sozer and Kokini 2009). Moreover, nanotechnology is enthusiastically committed in refining the drawbacks underlying the assessment of the potential use of diet bioactive compounds for health improvement (Linazasoro 2008).

C. Jiménez-Martínez (✉) · A. Hernández-Jabalera · G. Dávila-Ortíz
Departamento Graduados e Investigación en Alimentos, Escuela Nacional de Ciencias Biológicas, Instituto Politécnico Nacional, Prol. Carpio y Plan de Ayala S/N, Col. Santo Tomás, 11340 México, DF, Mexico
e-mail: crisjm_99@yahoo.com

J. Vioque · M. Alaiz · J. Girón-Calle · C. Megías
Instituto de la Grasa, Consejo Superior de Investigaciones Científicas, 41012 Sevilla, Spain

© Springer Science+Business Media New York 2015

H. Hernández-Sánchez, G. F. Gutiérrez-López (eds.), *Food Nanoscience and Nanotechnology,* Food Engineering Series, DOI 10.1007/978-3-319-13596-0_17

This chapter addresses the contributions of some nanotechnologies to strength strategies directed to favorably modulate oxidative stress and thus to widely investigate associated opportunities for the improvement of the function of antioxidant peptides.

17.2 Modulating Oxidative Stress

Oxidative stress is a biological condition that occurs as a result of an imbalance between the production of oxidants and the ability of the antioxidant systems to neutralize the radicals, prevent, or partially repair the pathological processes associated with a number of serious diseases, such as cancer, coronary heart condition, Alzheimer's, neurodegenerative disorders, atherosclerosis, cataracts, and inflammation, among others (Halliwell 2011; Gruber et al. 2013).

In principle, oxidative stress can result from (i) diminished antioxidants, e.g., mutations affecting antioxidant defense enzymes or toxic agents that deplete such defenses or (ii) increased production of reactive species, e.g., as a consequence of the exposure to elevated levels of toxins or excessive activation of "natural" radicals-producing systems. Second mechanism is, probably, more relevant to human diseases than that described in (i) above and is frequently the target of attempted therapeutic schemes (Halliwell 2001). Radicals frequently generated include (i) reactive oxygen species (ROS) such as superoxide radical and hydroxyl radical, (ii) reactive nitrogen species (RNS), e.g., nitric oxide radical, and (iii) reactive nitrogen oxygen species such as peroxynitrite. Also other nonradical derivatives may contribute to oxidative stress as products of lipid peroxidation in membranes, e.g., hydrogen peroxide (H_2O_2) and unbound metal ions (Niki 2010).

The mechanisms involved in the accumulation of endogenous production of ROS are related to the mitochondria metabolism, the activity of xanthine oxidase and superoxide-dismutase enzymes, the activation of arachidonic acid metabolism, the metabolism of phosphoinositides, and the activity of Nicotinamide adenine dinucleotide/Nicotinamide adenine dinucleotide phosphate (NADH/NADPH) oxidase enzyme (Szeto 2006; Abuja and Albertini 2001; Alam et al. 2013). Among them, radicals generated in the mitochondria play an important role not only in ageing but also in apoptosis, cancer, neurodegeneration, and other age-related diseases; therefore, there is a great interest in strategies directed to protecting the mitochondria from ROS-mediated damage. However, antioxidants aimed to reach this organelle must meet with size requirements, in the order of the nanoscale preferentially and charge-hydrophobic balance that allow them to face the nature of mitochondrial membrane (Gruber et al. 2013).

An antioxidant has been defined as any substance that, when present at low concentrations compared with those of an oxidizable substrate, significantly delays or prevents the oxidation of that substrate (Halliwell 2001). The role and beneficial effects of antioxidants against radicals during oxidative stress have received much attention. Many types of antioxidants with different functions play their role in the defense network in vivo (Abuja and Albertini 2001).

Some antioxidants are proteins and enzymes, while others are natural or synthetic small molecules. From the mechanistic point of view, the antioxidants may be classified into the following groups: (i) preventive antioxidants, which suppress the formation of reactive oxygen and nitrogen by, e.g., reducing hydrogen peroxide and lipid hydroperoxides to water and lipid hydroxides or by sequestering metal ions such as iron and copper; (ii) antioxidants that avoid that radicals attack biologically essential molecules, e.g., scavenging antioxidants (many natural exogenous antioxidants use this mechanism); (iii) antioxidants that repair damages clearing the wastes and reconstituting the lost function, e.g., enzymes; and (iv) antioxidants that act as a cellular signaling messengers to regulate the level of antioxidant compounds and enzymes (Gruber et al. 2013).

So far, the use of antioxidants in the treatment of diseases associated with ROS has not had the expected success. Conventional antioxidants such as vitamins, polyphenols, or antioxidant peptides are susceptible to be metabolized or inactivated even before reaching their target sites. Additionally, many antioxidants can only quench a single free radical per molecule. Thus, in order to elicit detectable changes in ROS levels at the site of damage, continued and high dosing is required specially in cases where no efficient antioxidant recycling machinery exists (Elswaifi et al. 2009). Therefore, the commercial potential of compounds aimed to modulate oxidative stress is currently limited by the lack of a detailed demonstration of the in vitro/in vivo mechanisms of action along with their clinical relevance; however, important efforts from the nanotechnology standpoint have been carried out to overcome this major challenge (Gruber et al. 2013).

17.3 Antioxidant Peptides and Oxidative Stress Modulation

Most therapeutic peptides, antioxidants included, may be classified according to their origin by (i) synthesis, including natural peptides produced by plants, microorganisms, animals, or humans as vital compounds in their physiological functions; peptides isolated from genetic or recombinant libraries; and synthetic peptides discovered from chemical libraries (Latham 1999) and (ii) the fragmentation of larger proteins by enzymatic hydrolysis, fermentation, germination, gastrointestinal (GI) digestion, or chemical hydrolysis (Vlieghe et al. 2010). Moreover, the most suitable technology for the production of peptides is determined by their structural characteristics, size, and the aimed applications.

17.3.1 Synthetic Antioxidant Peptides

Some recognized families of small-peptide antioxidants have been developed mainly with a targeted delivery to the inner mitochondrial membrane, some of them with

a well-established efficacy in biological systems which have been characterized both in vitro and in vivo and are described in the following sections.

17.3.1.1 Szeto-Schiller Peptides

The Szeto-Schiller (SS) peptides are small peptides (approximately 10 amino acids) that possess a unique aromatic-cationic sequence, which alternates between aromatic and basic residues, and exhibit three positive charges at physiological pH. Studies with isolated cells showed that they may be rapidly internalized through the plasma membrane and accumulation in the mitochondria, where they bind to the inner membrane in an energy-independent and nonsaturable manner without the need for peptide transporters. The SS peptides are readily taken up by a wide variety of cell types, including neuronal, renal, epithelial, endothelial, and human embryonic kidney cells (Zhao et al. 2004). Once inside the cells, the SS peptides concentrate approximately 1000–5000-fold in the mitochondria where they migrate to the inner mitochondrial membrane. Their transport into the mitochondria is independent of the membrane potential and is not self-limiting because accumulation of the peptides does not decrease the mitochondrial membrane potential. Some studies on SS peptides containing a dimethyl tyrosine (Dmt) have demonstrated that the addition of this residue could certainly help scavenging hydroxyl radicals and peroxynitrite and possibly HOCl• and peroxyl radicals but are unlikely to react directly with superoxide or hydrogen peroxide (Gruber et al. 2013). Hence, such mitochondria-targeted antioxidants represent a promising nanotechnological approach in the therapy of neurodegenerative diseases (Zhao et al. 2004).

17.3.1.2 XJB Peptides

As detailed by Gruber et al. (2013), these are a family of hemigramicidin-TEMPO compounds composed of 4-NH_2-TEMPO, a stable nitroxide radical with in vitro antioxidant properties, conjugated to a pentapeptide fragment from gramicidin S, a natural antibiotic that localizes not only bacterial cell membranes but also mitochondrial membranes. This is probably due to its high affinity for the phospholipid cardiolipin in the inner mitochondrial membrane (Prenner et al. 1997; Wipf et al. 2005). Among the XJB peptides, those that have received more attention are XJB-5-131 and XJB-5-131 which have been shown to exert inhibition against the generation of actinomycin D-induced superoxide and cardiolipin peroxidation (Wipf et al. 2005; Cheng et al. 2010). XJB-5-131 was efficacious in a hemorrhagic shock rat model (Macias et al. 2007) and displayed anti-inflammatory properties in mice (Cheng et al. 2010). Recently, the XJB peptides have also been shown to protect cell cultures against radiation damage (Kanai et al. 2007; Rajagopalan et al. 2009; Cheng et al. 2010).

Common characteristics between design peptides aimed to target the mitochondria may include their incorporation as optimized arrays in dedicated nanostructures with high affinities for the different tissues that they need to reach and showing versatile transport properties.

17.3.2 Protein-Derived Antioxidant Peptides (Bioactive Peptides)

Bioactive peptides are amino acid residues encrypted within the sequence of a parent protein and may be released using exogenous or endogenous enzymes, food processing, or during microbial fermentation, as well as during GI digestion of food proteins (Korhonen and Pihlanto 2003). Unique intrinsic properties of bioactive peptides make them attractive agents able to promote health and reduce the risk of diseases, if regularly included in balanced diets (Chatterton et al. 2006; Smithers 2008).

These peptides may be obtained from several sources, although the most studied are derived from the proteins of milk (Kitts and Weiler 2003; Li and Li 2013; Power et al. 2014), fish and seafood (Ngo et al. 2011; Najafian and Babji 2012), and soybean (De Mejia and De Lumen 2006; Isanga and Zhang 2008; Wang et al. 2008b; García et al. 2013). Among them, raw materials in the form of processing by-products (Di Bernardini et al. 2011; Rustad et al. 2011; Soengas et al. 2012; Toldrá et al. 2012) or discards have gained much interest for their implications in the production costs. However, in most cases, bioactive peptides are produced along with a hundred or more inactive peptides in a complex mixture. Therefore, enrichment, fractionation, and purification strategies seem to be critical to obtain fractions that may achieve a good bioactivity (Butylina et al. 2006; Kapel et al. 2011).

Authors have reported membrane and chromatographic technologies as separation processes particularly suitable for such a purpose, and different criteria have been used to purify bioactive peptides. For food protein-derived antioxidant peptides, structure–function relationships are not well understood, but certainly, they depend on various characteristics such as amino acid sequence, molecular weight (MW), hydrophobicity, charge, and acid–base character. Functional properties of bioactive peptides are determined by its unique three-dimensional (3D) structure, and further, secondary structure rather than tertiary structure is the dominant factor affecting the binding characteristics of the peptides (Alaiz et al. 1992; Chan and Chen 2004; Elias et al. 2008). Consequently, the purification criteria proposed so far have included MW or content of hydrophobic or cationic residues as the key factors (Li and Leong 2011; Li et al. 2013).

17.3.2.1 Antioxidant Peptides Derived from Canola

The production of peptide fractions enriched with cationic peptides from canola proteins will be presented as an example of antioxidant activity improvement strategies.

Table 17.1 Amino acid composition of purified Canola peptide fractions (g/100er)>

Amino acid	Hydrolysate	F1	F2	F3	F4
Asp+Asn	10.66	12.73	10.78	11.52	9.47
Glu+Gln	21.07	12.38	13.57	17.24	13.67
Ser	5.85	2.79	3.93	2.53	3.94
Hys	1.92	4.15	14.75	10.04	17.08
Gly	6.96	4.79	5.14	3.46	5.14
Thr	3.97	3.15	3.56	3.63	2.84
Arg	6.22	11.07	7.38	7.65	6.76
Ala	5.97	3.09	2.88	2.39	2.90
Pro	5.98	1.62	2.21	3.03	1.50
Tyr	2.79	1.19	1.47	0.64	1.28
Val	3.11	5.08	4.95	5.19	4.70
Met	0.44	0.62	0.54	0.72	0.73
Cys	1.61	0.81	0.79	1.00	1.08
Ile	2.17	5.48	4.12	3.38	3.39
Trp	2.43	4.19	5.23	6.30	6.93
Leu	8.35	5.15	8.00	11.26	9.91
Phe	4.96	5.37	3.48	3.27	2.96
Lys	5.55	16.34	7.23	6.77	5.73

Rapeseed (*Brassica napus*) meal is an important industrial by-product of the oil extraction process. The antioxidant activity for protein hydrolysates obtained from these proteins has been previously reported (Cumby et al. 2008; He et al. 2013; Mäkinen et al. 2012). In this study, immobilized metal affinity chromatography (IMAC) was used to fractionate an Alcalase-prepared protein hydrolysate (60 min, 29.52 ± 0.24 % hydrolysis degree) under a cationic enrichment criterion in order to purify fractions with increased antioxidant activity. The proportion of rapeseed peptides with the ability to bind Cu^{2+} immobilized in the column accounts for the 22.46 % of total peptides in the original hydrolysate. These peptides were distributed in four fractions, namely F1 (12.21 %), F2 (2.27 %), F3 (3.195), and F4 (4.79) according to their elution order. The concentration of cationic peptides (%) in the purified fractions (Table 17.1) ranged from 1.7 to 2.3 times the original concentration in the hydrolysate. However, differences in the amount of each cationic amino acid were found. While for F1, the concentration of the amino acid Lys was the highest (16.34 %), and for the last three fractions, Hys was the amino acid with the greater increase, i.e., reaching 13.57, 17.24, and 13.67 % for F2, F3, and F4, respectively. The average molecular weight (AMW) distributions showed that most peptides or peptide aggregates in F1 had an AMW comprised between 2 and 9 kDa, size for most of peptides in the next two fractions diminished progressively, and most of peptides had a size comprised between 200 and 2 kDa; in the fraction F4, a major proportion of dipeptides and tripeptides were found but

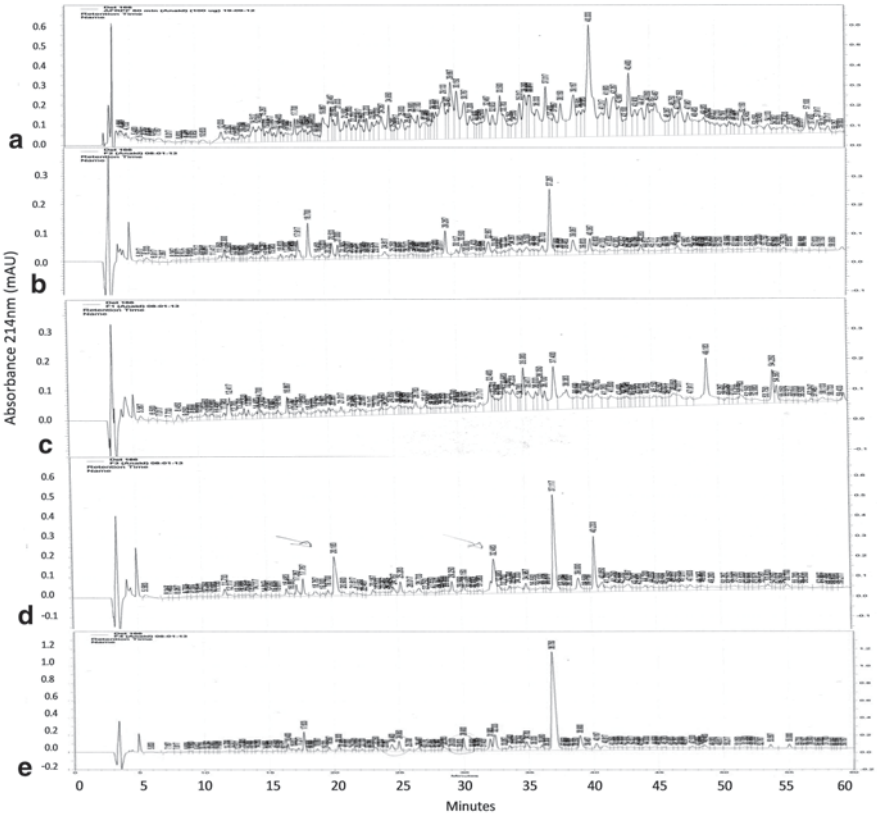

Fig. 17.1 Reversed-phase high-performance liquid chromatography (*RP-HPLC*) elution profiles for purified Canola peptide fractions. **a** Canola protein hydrolysate, **b** peptide fraction (F1), **c** peptide fraction (F2), **d** peptide fraction (F3), and **e** peptide fraction (F4)

also the highest amount of free amino acids. Reversed-phase (RP)-peptide profiles (Fig. 17.1) of purified fractions showed that peptides in purified fractions also contain hydrophobic regions.

The antioxidant activity of the fractions was evaluated in vitro in their radical scavenging activity against 2,2-diphenyl-1-picrylhydrazyl and 2,2'-azino-bis(3-ethylbenzothiazoline-6-sulphonic acid) (DPPH and $ABTS^{+}$) and capacity to inhibit β-carotene bleaching catalyzed by linoleic acid peroxidation products or Cu^{2+}; the antioxidant activity against intracellular radical species was also evaluated in the Caco-2 cell line using the 2′,7′-Dichlorofluorescin diacetate (DCFH-DA) assay (Wang and Joseph 1999, 2012). Results are presented in Fig. 17.2; the peptide fractions from F1 to F4 significantly improved ($P \leq 0.05$) their antioxidant activity in comparison with the original hydrolysate. Our results showed that the high cationic amino acid content and low MW allow these peptides to have antioxidant antiradical and activity against lipid peroxidation. Significant increase ($P \leq 0.05$) in cellular antioxidant activity was also found for purified fractions in comparison

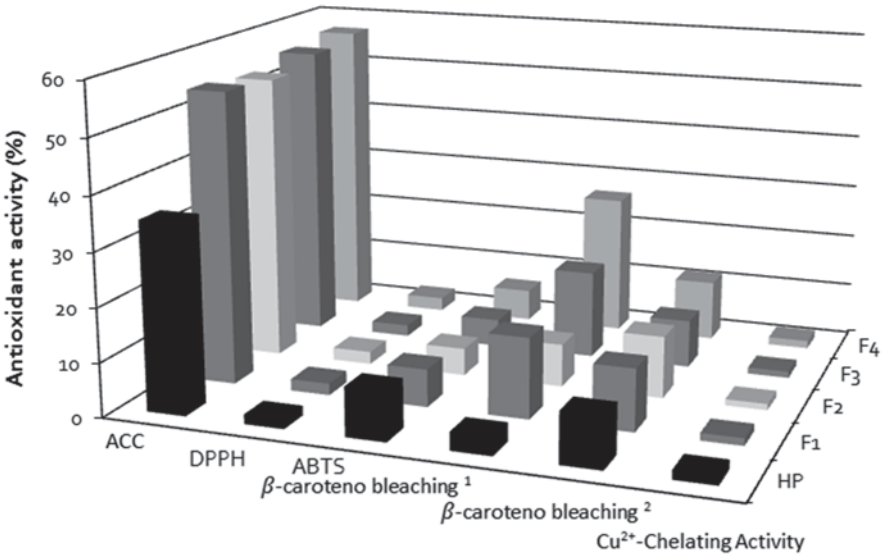

Fig. 17.2 Antioxidant activity of Canola peptide fractions. *ACC* cellular antioxidant activity (5 peptid, *DPPH* radical scavenging activity (1 peptid, *ABTS*$^{+}$ Trolox equivalent antioxidant capacity (TEAC) (mmTE/g) (0.2(0.2ven, β-carotene bleaching catalyzed by lipid peroxides (0.2y (1 pe, copper catalyzed by β-carotene bleaching (0.20.2y (1, and *Cu*^{2}+*chelating activity* (lmolEE/mg) (0.2activi)

with the raw hydrolysates; however, no significant difference ($P > 0.05$) could be found between fractions. According to these results, purified peptide fractions or fragments derived from their peptides may be able to pass through cell membrane and interact with intracellular radicals from cytosol or lipoperoxidation products from phospholipids from the cellular membrane (Fig. 17.3). Also, due to their particular cationic-hydrophobic character and their MW (200–2 kDa), which according to previous reports may correspond to a size in the order of ≤4 nm, they may be attractive as mitochondria-targeted antioxidants via integration into different types of nanoscale carriers. In agreement with the well-established approach to targeting small molecules to mitochondria, it is possible to take advantage of the negative charge of the mitochondrial matrix relative to the cytoplasm to facilitate accumulation of positively charged molecules (cations) in the mitochondrial matrix (Liberman et al. 1969). However, this is only possible if the cation is combined with a suitably bulky hydrophobic carrier that could allow the overall molecule to become sufficiently lipophilic to allow entry into the hydrophobic interior of biological membranes (Liberman et al. 1969; Murphy and Smith 2007). These results provide evidence consistent with the information suggesting an important involvement of cationic amino acids in the antioxidant activity of protein-derived peptides (Bou-

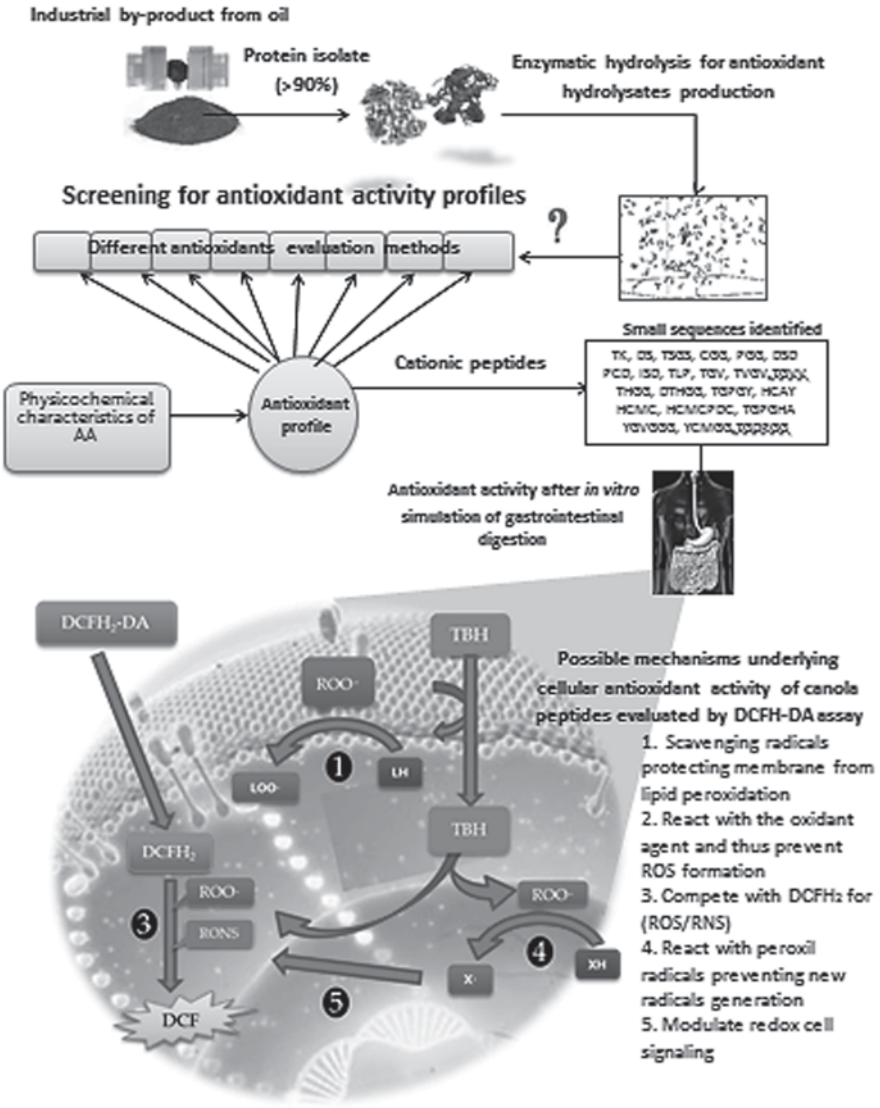

Fig. 17.3 Descriptive model for Canola peptide fraction preparation and possible antioxidant mechanisms

hallab et al. 1996; Gaberc-Porekar and Menart 2001; Iwaniak and Dziuba 2009; Pownall et al. 2011).

Major differences between synthetic and protein-derived antioxidant peptides can be attributed to their target application. Synthetic and recombinant antioxidant peptides are mainly produced for the pharmaceutical industry, for specific

applications as chemotherapy. Protein-derived antioxidant peptides have been studied mostly as bioactive compounds that may have physiological benefits or reduce the risks of diseases if consumed as part of regular diet in the so-called functional foods or as nutraceuticals (Chen et al. 2006).

Despite this fundamental difference, both types of antioxidant peptides face some of the same challenges, mainly those related to their bioavailability and biodistribution. These include absorption, transport, passage of biological membranes and cellular barriers, unfavorable biodistribution, low bioavailability, lack of water solubility, low therapeutic response despite high dosages, side effects, drug resistance, and toxicity. With a few exceptions, peptides composed of natural amino acids are not very good drug candidates because of their intrinsic physicochemical properties and pharmacokinetic profiles (Cho et al. 2008; Wang et al. 2008b; Heller et al. 2012). When compared with synthetic antioxidant peptides, food-derived peptides do have notable drawbacks: They generally have low stability in plasma, are sensitive to proteases, and can be cleared from circulation in a few minutes (Lipinski et al. 2012; Pillay et al. 2012)

As previously described in Sect. 17.2, the increased mitochondrial production of ROS and further damage of mtDNA and proteins may be closely related to developing neurodegenerative diseases, such as Parkinson's disease, Huntington's disease, and Alzheimer's disease (DiMauro et al. 2002); therefore, this organelle has become one of the most important targets in antioxidant therapy, and different strategies have being developed to targeting antioxidant to mitochondria (Heller et al. 2012).

Among them, the hydrophobic-cation targeting approach is one of the most successfully used in approaches to target mitochondria with synthetic peptides like the SS peptides, mitochondria-penetrating peptides (MPPs), cell-penetrating peptides (CPPs), manganese metalloporphyrin oligopeptide conjugates, tripeptide glutathione conjugates, or natural mitochondrial leading sequences (MLSs) (Pfanner and Geissler 2001; Horton et al. 2008; Szeto 2008; Yousif et al. 2009; Smith and Murphy 2011).

Furthermore, other approaches like chemical modification of sequences along with delivery with carriers have being explored. Nanotechnology is one of the most promising areas for these purposes (Gruber et al. 2013).

17.4 Nanotechnology Strategies for the Improvement of Antioxidants

The production of different nanosized antioxidant materials or antioxidant-loaded nanosystems may contribute with exogenous antioxidants to favorably modulate oxidative stress through different mechanisms (Heller et al. 2012).

Different structures, devices, and systems developed by nanotechnology have been used for targeting mitochondria with potential application in the improvement of antioxidants (Table 17.2).

Table 17.2 Nanosystems used for targeted mitochondria

Type	Structure	Reference
Polymer-based nanocarrier	Nanoparticles	US patent application number: US 201110111002
Lipid-based nanoencapsulators	Cationic liposomes	D'Souza and Weissig (2009)
Inorganic nanoparticles	DQAsomes	Weissig et al. (1998)
	Gold nanoparticles	Calin (2011)
	Titanium dioxide nanoparticles	Paunesku et al. (2003)
	Platinum nanoparticles	Hikosaka et al. (2008)
	Bimetallic nanoparticles	Durazo et al. (2011)
	MEND	Kinoshita and Hynynen (2005)
	Metal nanotubes	Sullivan et al. (2010)
Association colloids	Micelles	D'Souza et al. (2007)

MEND multifunctional envelope-type nano device

Among them, peptide nanoparticles are the most reported; they have been developed by adsorption on the nanocarrier surfaces, encapsulation in nanoparticles, and bioconjugation of nanoparticles and by molecular self-assembly of small peptides into nanoparticle size. This encapsulated protein on nanoparticles has great potential to enhance therapeutic activity of peptides by sustained and targeted delivery to the active site, improve stability, and better bioavailability (Pinto Reis et al. 2006). Only particles below 2 nm in diameter seem to be able to enter mitochondria, while bigger nanocarriers can target the proximity of mitochondria (Calin 2011).

Nanotubes have also been proposed as antioxidant enhancers due to their ability to "uncouple mitochondria" by acting as a proton channel when an unsafe membrane potential is reached (Sullivan 2010).

Combinations of nanocarrier-based strategies and targeting moieties are also being proposed. Reported combinations had included: conjugation of a cationic, lipophilic ligand to liposomes (TPP-modified fatty acid), stearyl triphenyl phosphonium (STPP) incorporated into liposomes, conjugates of TPP to gold nanoparticles, and quantum dots that are enfolded in micelles tied to a mitochondrial-targeting peptide (Boddapati et al. 2005; D'Souza et al. 2007; Hoshino et al. 2004).

According to Gruber et al. (2013), despite the growing interest in the field of nanotechnology, caution should be taken to provide clear evidence of (i) biocompatibility, in the long-term, including biodistribution and metabolism (if any) of these nanocarriers; (ii) fully standardized protocols for the preparation of the nano-DS, so that the results become more reproducible and comparable among different groups of research; and (iii) extensive in vitro and in vivo experiments that show safety and advantages over conventional approaches and comprehensive understanding of the intracellular trafficking and mechanisms of actions responsible for their antioxidant properties.

17.5 Final Remarks

Most of the important advances on targeted antioxidants for oxidative stress modulation through nanotechnology originated in the field of therapeutic antioxidants included cationic peptides. However, with the upcoming advances in both nanotechnology and antioxidant science, the technology transfer from pharmaceutical to food technology may be affordable for its application in the field dedicated to the functional foods development. Such advances must be directed to the elucidation of structure–activity relationships and in vivo fate of diet bioactive compounds and will aid toward a rational regulatory framework for these materials.

References

Abuja PM, Albertini R (2001) Methods for monitoring oxidative stress, lipid peroxidation and oxidation resistance of lipoproteins. Clin Chim Acta 306(1–2):1–17. doi:http://dx.doi.org/10.1016/S0009-8981(01)00393-X

Alaiz M, Navarro JL, Giron J, Vioque E (1992) Amino acid analysis by high-performance liquid chromatography after derivatization with diethyl ethoxymethylene malonate. J Chromatogr 591(1–2):181–186

Alam MN, Bristi NJ, Rafiquzzaman M (2013) Review on in vivo and in vitro methods of evaluation of antioxidant activity. Saudi Pharm J 21(2):143–152. doi:http://dx.doi.org/10.1016/j.jsps.2012.05.002

Bagchi D, Bagchi M, Moriyama H, Shahidi F (2013) Bioavailability and delivery of nutraceuticals and functional foods using nanotechnology. In: Yu H, Huang Q (eds) Bio-Nanotechnology. Blackwell, Oxford, pp 593–604

Boddapati SV, Tongcharoensirikul P, Hanson RN, D'Souza GG, Torchilin VP, Weissig V (2005) Mitochondriotropic liposomes. J Liposome Res 15(1–2):49–58. doi:10.1081/lpr-64958

Bouhallab S, Henry G, Boschetti E (1996) Separation of small cationic bioactive peptides by strong ion-exchange chromatography. J Chromatogr A 724(1–2):137–145. doi:http://dx.doi.org/10.1016/0021-9673(95)00928-0

Bouwmeester H, Dekkers S, Noordam MY, Hagens WI, Bulder AS, de Heer C, ten Voorde SE, Wijnhoven SW, Marvin HJ, Sips AJ (2009) Review of health safety aspects of nanotechnologies in food production. Regul Toxicol Pharmacol 53(1):52–62. doi:10.1016/j.yrtph.2008.10.008

Butylina S, Luque S, Nyström M (2006) Fractionation of whey-derived peptides using a combination of ultrafiltration and nanofiltration. J Memb Sci 280(1–2):418–426. doi:http://dx.doi.org/10.1016/j.memsci.2006.01.046

CalinViorel Pop (2011) Transport and delivery of glutathione into human cells using gold nanoparticles. US Patent 201110111002 A1, 12 May 2011

Chan R, Chen V (2004) Characterization of protein fouling on membranes: opportunities and challenges. J Memb Sci 242(1–2):169–188. doi:http://dx.doi.org/10.1016/j.memsci.2004.01.029

Chatterton DEW, Smithers G, Roupas P, Brodkorb A (2006) Bioactivity of β-lactoglobulin and α-lactalbumin—Technological implications for processing. Int Dairy J 16(11):1229–1240. doi:http://dx.doi.org/10.1016/j.idairyj.2006.06.001

Chen L, Remondetto GE, Subirade M (2006) Food protein-based materials as nutraceutical delivery systems. Trends Food Sci Technol 17(5):272–283. doi:http://dx.doi.org/10.1016/j.tifs.2005.12.011

Cheng S, Edwards SA, Jiang Y, Gräter F (2010) Glycosylation enhances peptide hydrophobic collapse by impairing solvation. Chemphyschem 11(11):2367–2374. doi:10.1002/cphc.201000205

Cho K, Wang X, Nie S, Chen ZG, Shin DM (2008) Therapeutic nanoparticles for drug delivery in cancer. Clin Cancer Res 14(5):1310–1316. doi:10.1158/1078-0432.ccr-07-1441

Cumby N, Zhong Y, Naczk M, Shahidi F (2008) Antioxidant activity and water-holding capacity of canola protein hydrolysates. Food Chem 109(1):144–148. doi:http://dx.doi.org/10.1016/j.foodchem.2007.12.039

D'Souza GG, Boddapati SV, Weissig V (2007) Gene therapy of the other genome: the challenges of treating mitochondrial DNA defects. Pharm Res 24(2):228–238. doi:10.1007/s11095-006-9150-y

D'Souza GG, Volkmar W (2009) Subcellular targeting: a new frontier for drug-loaded pharmaceutical nanocarriers and the concept of the magic bullet. Expert opinion on drug delivery 6(11):1135–1148

De Mejia E, De Lumen BO (2006) Soybean bioactive peptides: a new horizon in preventing chronic diseases. Sex Reprod Menopause 4(2):91–95

Di Bernardini R, Harnedy P, Bolton D, Kerry J, O'Neill E, Mullen AM, Hayes M (2011) Antioxidant and antimicrobial peptidic hydrolysates from muscle protein sources and by-products. Food Chem 124(4):1296–1307

DiMauro S, Tanji K, Bonilla E, Pallotti F, Schon EA (2002) Mitochondrial abnormalities in muscle and other aging cells: classification, causes, and effects. Muscle Nerve 26(5):597–607

Durazo S, Kadam R, Drechsel D, Patel M, Kompella U (2011) Brain mitochondrial drug delivery: influence of drug physiochemical properties. Pharm Res 28:2833–2847

Elias RJ, Kellerby SS, Decker EA (2008) Antioxidant activity of proteins and peptides. Crit Rev Food Sci Nutr 48(5):430–441. doi:10.1080/10408390701425615

Elswaifi SF, Palmieri JR, Hockey KS, Rzigalinski BA (2009) Antioxidant nanoparticles for control of infectious disease. Infect Disord Drug Targets 9(4):445–452

Gaberc-Porekar V, Menart V (2001) Perspectives of immobilized-metal affinity chromatography. J Biochem Biophys Methods 49(1–3):335–360

García MC, Puchalska P, Esteve C, Marina ML (2013) Vegetable foods: a cheap source of proteins and peptides with antihypertensive, antioxidant, and other less occurrence bioactivities. Talanta 106:328–349

Gruber J, Fong S, Chen CB, Yoong S, Pastorin G, Schaffer S, Cheah I, Halliwell B (2013) Mitochondria-targeted antioxidants and metabolic modulators as pharmacological interventions to slow ageing. Biotechnol Adv 31(5):563–592. doi:http://dx.doi.org/10.1016/j.biotechadv.2012.09.005

Halliwell B (2001) Free radicals and other reactive species in disease. eLS. Wiley. doi:10.1038/npg.els.0003913

Halliwell B (2011) Free radicals and antioxidants—quo vadis? Trends Pharm Sci 32(3):125–130. doi:http://dx.doi.org/10.1016/j.tips.2010.12.002

He R, Girgih AT, Malomo SA, Ju X, Aluko RE (2013) Antioxidant activities of enzymatic rapeseed protein hydrolysates and the membrane ultrafiltration fractions. J Funct Foods 5(1):219–227. doi:http://dx.doi.org/10.1016/j.jff.2012.10.008

Heller A, Brockhoff G, Goepferich A (2012) Targeting drugs to mitochondria. Eu J Pharm Biopharm 82(1):1–18. doi:http://dx.doi.org/10.1016/j.ejpb.2012.05.014

Hikosaka K, Kim J, Kajita M, Kanayama A, Miyamoto Y (2008) Platinum nanoparticles have an activity similar to mitochondrial NADH: ubiquinone oxidoreductase. Colloids and Surfaces B. Biointerfaces 66:195–200

Horton KL, Stewart KM, Fonseca SB, Guo Q, Kelley SO (2008) Mitochondria-penetrating peptides. Chem Biol 15(4):375–382. doi:10.1016/j.chembiol.2008.03.015

Hoshino A, Fujioka K, Oku T, Nakamura S, Suga M, Yamaguchi Y, Suzuki K, Yasuhara M, Yamamoto K (2004) Quantum dots targeted to the assigned organelle in living cells. Microbiol Immunol 48(12):985–994

Isanga J, Zhang GN (2008) Soybean bioactive components and their implications to health—a review. Food Rev Int 24(2):252–276

Iwaniak A, Dziuba B (2009) Motifs with potential physiological activity in food proteins—BIOPEP database. Acta Sci Pol Technol Aliment 8(3):59–85

Kanai A, Zabbarova I, Amoscato A, Epperly M, Xiao J, Wipf P (2007) Mitochondrial targeting of radioprotectants using peptidyl conjugates. Org Biomol Chem 5(2):307–309. doi:10.1039/b613334g

Kapel R, Klingenberg F, Framboisier X, Dhulster P, Marc I (2011) An original use of size exclusion-HPLC for predicting the performances of batch ultrafiltration implemented to enrich a complex protein hydrolysate in a targeted bioactive peptide. J Memb Sci 383(1–2):26–34. doi:http://dx.doi.org/10.1016/j.memsci.2011.08.025

Kinoshita M, Hynynen K (2005) A novel method for the intracellular delivery of siRNA using microbubble-enhanced focused ultrasound, Biochem. Biophys Res Commun 335:393–399

Kitts DD, Weiler K (2003) Bioactive proteins and peptides from food sources. Applications of bioprocesses used in isolation and recovery. Curr Pharm Des 9(16):1309–1323

Korhonen H, Pihlanto A (2003) Bioactive peptides: New challenges and opportunities for the dairy industry. Aust J Dairy Technol 58(2):129–134

Latham PW (1999) Therapeutic peptides revisited. Nat Biotechnol 17(8):755–757. doi:10.1038/11686

Li X, Leong SSJ (2011) A chromatography-focused bioprocess that eliminates soluble aggregation for bioactive production of a new antimicrobial peptide candidate. J Chromatogr A 1218(23):3654–3659

Li Y-W, Li B (2013) Characterization of structure–antioxidant activity relationship of peptides in free radical systems using QSAR models: key sequence positions and their amino acid properties. J Theor Biol 318:29–43. doi:http://dx.doi.org/10.1016/j.jtbi.2012.10.029

Li Z, Wang B, Chi C, Gong Y, Luo H, Ding G (2013) Influence of average molecular weight on antioxidant and functional properties of cartilage collagen hydrolysates from *Sphyrna lewini, Dasyatis akjei* and *Raja porosa*. Food Res Int 51(1):283–293. doi:http://dx.doi.org/10.1016/j.foodres.2012.12.031

Liberman EA, Topaly VP, Tsofina LM, Jasaitis AA, Skulachev VP (1969) Mechanism of coupling of oxidative phosphorylation and the membrane potential of mitochondria. Nature 222(5198):1076–1078

Linazasoro G (2008) Potential applications of nanotechnologies to Parkinson's disease therapy. Parkinsonism Relat Disord 14(5):383–392. doi:http://dx.doi.org/10.1016/j.parkreldis.2007.11.012

Lipinski CA, Lombardo F, Dominy BW, Feeney PJ (2012) Experimental and computational approaches to estimate solubility and permeability in drug discovery and development settings. Adv Drug Deliv Rev 64(Suppl):4–17

Macias CA, Chiao JW, Xiao J, Arora DS, Tyurina YY, Delude RL, Wipf P, Kagan VE, Fink MP (2007) Treatment with a novel hemigramicidin-TEMPO conjugate prolongs survival in a rat model of lethal hemorrhagic shock. Ann Surg 245:305–314

Mäkinen S, Johannson T, Vegarud Gerd E, Pihlava JM, Pihlanto A (2012) Angiotensin I-converting enzyme inhibitory and antioxidant properties of rapeseed hydrolysates. J Funct Foods 4(3):575–583. doi:http://dx.doi.org/10.1016/j.jff.2012.03.003

Murphy MP, Smith RA (2007) Targeting antioxidants to mitochondria by conjugation to lipophilic cations. Annu Rev Pharmacol Toxicol 47:629–656. doi:10.1146/annurev.pharmtox.47.120505.105110

Najafian L, Babji AS (2012) A review of fish-derived antioxidant and antimicrobial peptides: their production, assessment, and applications. Peptides 33(1):178–185. doi:http://dx.doi.org/10.1016/j.peptides.2011.11.013

Ngo DH, Wijesekara I, Vo TS, Van Ta Q, Kim SK (2011) Marine food-derived functional ingredients as potential antioxidants in the food industry: an overview. Food Res Int 44(2):523–529

Niki E (2010) Assessment of antioxidant capacity *in vitro* and *in vivo*. Free Radic Biol Med 49(4):503–515. doi:http://dx.doi.org/10.1016/j.freeradbiomed.2010.04.016

Paunesku T, Rajh T, Wiederrecht G, Maser J, Vogt S, Stojicevic N et al (2003) Biology of TiO2-oligonucleotide nanocomposites. Nat Mater 2(5):343–346

Pfanner N, Geissler A (2001) Versatility of the mitochondrial protein import machinery. Nat Rev Mol Cell Biol 2(5):339–349. doi:10.1038/35073006

Pillay J, Kamp VM, van Hoffen E, Visser T, Tak T, Lammers JW, Ulfman LH, Leenen LP, Pickkers P, Koenderman L (2012) A subset of neutrophils in human systemic inflammation inhibits T cell responses through Mac-1. J Clin Invest 122:327–336

Pinto Reis C, Neufeld RJ, Ribeiro AJ, Veiga F (2006) Nanoencapsulation II. Biomedical applications and current status of peptide and protein nanoparticulate delivery systems. Nanomedicine 2(2):53–65. doi:10.1016/j.nano.2006.04.009

Power O, Nongonierma AB, Jakeman P, Fitzgerald RJ (2014) Food protein hydrolysates as a source of dipeptidyl peptidase IV inhibitory peptides for the management of type 2 diabetes. Proc Nutr Soc 73(1):34–46

Pownall TL, Udenigwe CC, Aluko RE (2011) Effects of cationic property on the *in vitro* antioxidant activities of pea protein hydrolysate fractions. Food Res Int 44(4):1069–1074. doi:http://dx.doi.org/10.1016/j.foodres.2011.03.017

Prenner EJ, Lewis RN, Neuman KC, Gruner SM, Kondejewski LH, Hodges RS, McElhaney RN (1997) Nonlamellar phases induced by the interaction of gramicidin S with lipid bilayers. A possible relationship to membrane-disrupting activity. Biochemistry 36(25):7906–7916. doi:10.1021/bi962785k

Rajagopalan MS, Gupta K, Epperly MW, Franicola D, Zhang X, Wang H, Zhao H, Tyurin VA, Pierce JG, Kagan VE, Wipf P, Kanai AJ, Greenberger JS (2009) The mitochondria-targeted nitroxide JP4-039 augments potentially lethal irradiation damage repair. In Vivo 23(5):717–726

Rustad T, Storrø I, Slizyte R (2011) Possibilities for the utilisation of marine by-products. Int J Food Sci Technol 46(10):2001–2014

Smith RA, Murphy MP (2011) Mitochondria-targeted antioxidants as therapies. Discov Med 11(57):106–114

Smithers GW (2008) Whey and whey proteins—From 'gutter-to-gold'. Int Dairy J 18(7):695–704. doi:10.1016/j.idairyj.2008.03.008

Soengas P, Cartea ME, Francisco M, Sotelo T, Velasco P (2012) New insights into antioxidant activity of *Brassica* crops. Food Chem 134(2):725–733. doi:http://dx.doi.org/10.1016/j.foodchem.2012.02.169

Sozer N, Kokini JL (2009) Nanotechnology and its applications in the food sector. Trends Biotechnol 27(2):82–89. doi:http://dx.doi.org/10.1016/j.tibtech.2008.10.010

Sullivan SP, Koutsonanos DG, Martin MP, Lee JW, Zarnitsyn V, Choi SO, Murthy N, Compans RW, Skountzou I, and Prausnitz MR (2010) Dissolving polymer microneedle patches for influenza vaccination. Nat Med 16:915

Szeto HH (2006) Mitochondria-targeted peptide antioxidants: novel neuroprotective agents. AAPS J 8(3):E521–E531. doi:10.1208/aapsj080362

Szeto HH (2008) Cell-permeable, mitochondrial-targeted, peptide antioxidants. AAPS J 8 (2):E277–E283

Toldrá F, Aristoy MC, Mora L, Reig M (2012) Innovations in value-addition of edible meat by-products. Meat Sci 92(3):290–296

Vlieghe P, Lisowski V, Martinez J, Khrestchatisky M (2010) Synthetic therapeutic peptides: science and market. Drug Discov Today 15(1–2):40–56. doi:10.1016/j.drudis.2009.10.009

Wang H, Joseph JA (1999, 2012) Quantifying cellular oxidative stress by dichlorofluorescein assay using microplate reader. Free Radical Biology and Medicine 27(5–6):612–616

Wang W, Dia VP, Vasconez M, De Mejia EG, Nelson RL (2008b) Analysis of soybean protein-derived peptides and the effect of cultivar, environmental conditions, and processing on lunasin concentration in soybean and soy products. J AOAC Int 91(4):936–946

Wipf P, Xiao J, Jiang J, Belikova NA, Tyurin VA, Fink MP, Kagan VE (2005) Mitochondrial targeting of selective electron scavengers: synthesis and biological analysis of hemigramicidin-TEMPO conjugates. J Am Chem Soc 127(36):12460–12461. doi:10.1021/ja053679l

Yousif LF, Stewart KM, Horton KL, Kelley SO (2009) Mitochondria-penetrating peptides: sequence effects and model cargo transport. Chembiochem 10(12):2081–2088. doi:10.1002/cbic.200900017

Zhao K, Zhao GM, Wu D, Soong Y, Birk AV, Schiller PW, Szeto HH (2004) Cell-permeable peptide antioxidants targeted to inner mitochondrial membrane inhibit mitochondrial swelling, oxidative cell death, and reperfusion injury. J Biol Chem 279(33):34682–34690

Index

A
Alpha-Tocopherol 163, 169
Antibodies 215
Antioxidant peptides 285, 287
Antioxidants 292
Atomic Force Microscopy 21, 74, 132, 238

B
Beverages 53, 163, 211
Bioactive peptides 287
Bioavailability 274
Biosensors 33, 214–216

C
Calcium alginate 65
Canola 116, 287, 288
Capsaicin 192
Carbon nanotubes 232
Carrageenan 14, 65
Cavitation 147, 149, 150, 152, 156
Cell wall 64, 267, 268, 271–273, 277
Cellulose 64, 274
Chitosan 61, 62, 96, 107, 275
Confocal Laser Scanning Microscopy 10, 11
  applications of 13

D
Dark-Field Microscopy 9
Deterioration
  effects 189, 267
Dextran 61
Dispersion 168, 170, 171, 179, 244
DNA 215, 217
  detecting enzymatic activity 9
Dynamic Light Scattering 74, 102, 127, 190, 193

E
Egg albumin 74
Electron microscopy 16, 20, 235
Electrospinning 39–41, 48, 51
Electrospun polymers 47
Elongational stress 150
Emulsifiers 165, 178, 179

F
Filtration 51–53
Fluid microchannels 164
Fluorescence microscopy 9, 10
Food
  additives 250
  industry 243
  packaging 209
  safety 248
Foods 1, 14
Formulations 99, 114, 134, 177, 178
Free radicals 118
Freshness 225
Fruits 267, 268, 274, 276

G
Gelatin 33, 74
Gliadin 75

H
Hardness and elastic modulus 81, 85, 95, 96
Health improvement 283
High shear methods 145
Homogenizer 146, 149
Human Health 283
Hydrodynamics 169

© Springer Science+Business Media New York 2015

H. Hernández-Sánchez, G. F. Gutiérrez-López (eds.), *Food Nanoscience and Nanotechnology,* Food Engineering Series, DOI 10.1007/978-3-319-13596-0

I
Impact 32, 44, 121, 149, 154
Indentation Technique 81, 93

L
Legumin 75
Light microscopy 7, 102, 272
Lipid nanoparticles 114, 115, 121, 127, 183
Lipids 13
Liposomes 100, 103, 104, 106, 108, 110

M
MEMS 213
Metal oxides 40, 249
Micro and Nanotechnology 217
Microbial safety 50, 53
Microfluidics 111, 155, 156, 158, 163, 165
Microfluidization 124, 154, 156, 163, 165, 169
Microfluidizer 60, 157, 170
Micromirs 164
Microparticles 71, 188, 192, 199
Microscopy 5, 6, 8
Mitochondria 16, 268, 284, 292
Morphology 43
Multilayer emulsions 183
Multiple emulsions 183
Multiscale
approach 267, 268, 270

N
Nanoclay 206
platelets 206
Nanocomposites 205–207
Nanoelectromechanical systems (NEMS) 225
Nanoemulsions 50, 99, 164, 183
Nanoencapsulation 135
Nanofibers 40, 43, 47, 48, 50
Nanoliposomes 105, 184
Nanomembrane 39
Nanoparticles 2, 52, 59, 71, 75, 210, 244, 293
Nanoparticles characterization 243
Nano-sized foods 145
Nanosized systems 179–181, 183
Nanostructure 271
Nanostructured lipid carriers 114, 184
Nanostructuring 187
Nanotubes 2, 63, 71, 220, 293

O
Oxidative stress 253, 284, 285, 292
Oxygen barrier 209

P
Pectin 64, 274, 275
Photoelectron spectroscopy 235
Polymer packaging 211
Pressure 44, 54, 113, 149, 169–171
Proteins 21, 51, 69, 178, 188

R
Raman spectroscopy 235
Reactive oxygen species (ROS) 250, 285
Regulations 1
Residence Time Distribution 166, 170
Ripening 267, 271, 277

S
Scanning Electron Microscopy 16, 235, 244, 277
Senescence 270, 278
Serum albumin 65, 188, 189, 192
Silicates 207
Solid lipid nanocarriers (SLNs) 177
Starch 14, 33, 60, 166
Structure 6, 232, 274, 293
Structure-function 287
Surfactants 60, 92, 118, 127, 178–180, 183
Synthesis 233
Szeto-Schiller (SS) peptides 286

T
Toxicity 178, 240, 254, 261
Transmission Electron Microscopy 18, 244
Turbulence 147, 149, 171
Types 232

U
Ultrasound 151, 152

V
Viscoelastic behavior 81, 87, 89

Z
Zein 14, 51, 76, 96
α-lactalbumin 33
β-lactoglobulin 33